Harnessing boron reactivity for the synthesis of dynamic and reversible polymer networks

Juliette Brunet

N°d'ordre NNT : 2019LYS1198

THESE de DOCTORAT DE L'UNIVERSITE DE LYON
opérée au sein de
l'Université Claude Bernard Lyon 1

Ecole Doctorale N° 206
Ecole Doctorale de Chimie de Lyon

Spécialité de doctorat : Chimie
Discipline : Chimie des polymères

Soutenue publiquement le 04/10/2019, par :
Juliette Brunet

Harnessing boron reactivity for the synthesis of dynamic and reversible polymer networks

---

Devant le jury composé de :

Laurence Rozes	Professeure/Université Pierre et Marie Curie	Rapporteure
Renaud Nicolaÿ	Professeur/ESPCI Paris	Rapporteur
Catherine Journet-Gautier	Professeure des Universités/Université Lyon 1	Présidente du jury
Nicolas Seeboth	Docteur/Michelin (MFPM)	Examinateur
Jean Raynaud	Chargé de recherche/CNRS	Directeur de thèse
Damien Montarnal	Chargé de recherche/CNRS	Co-directeur de thèse
Emmanuel Lacôte	Directeur de recherche/CNRS	Invité
Fabrice Brunel	Maître de conférences/Université Lyon 1	Invité

UNIVERSITE CLAUDE BERNARD – LYON 1

Président de l'Université	**M. le Professeur Frédéric FLEURY**
Président du Conseil Académique	M. le Professeur Hamda BEN HADID
Vice-président du Conseil d'Administration	M. le Professeur Didier REVEL
Vice-président du Conseil Formation et Vie Universitaire	M. le Professeur Philippe CHEVALIER
Vice-président de la Commission Recherche	M. Fabrice VALLÉE
Directeur Général des Services	M. Alain HELLEU

COMPOSANTES SANTE

Faculté de Médecine Lyon Est – Claude Bernard	Directeur : M. le Professeur J. ETIENNE
Faculté de Médecine et de Maïeutique Lyon Sud – Charles Mérieux	Directeur : Mme la Professeure C. BURILLON
Faculté d'Odontologie	Directeur : M. le Professeur D. BOURGEOIS
Institut des Sciences Pharmaceutiques et Biologiques	Directeur : Mme la Professeure C. VINCIGUERRA
Institut des Sciences et Techniques de la Réadaptation	Directeur : M. le Professeur Y. MATILLON
Département de formation et Centre de Recherche en Biologie Humaine	Directeur : Mme la Professeure A-M. SCHOTT

COMPOSANTES ET DEPARTEMENTS DE SCIENCES ET TECHNOLOGIE

Faculté des Sciences et Technologies	Directeur : M. F. DE MARCHI
Département Biologie	Directeur : M. le Professeur F. THEVENARD
Département Chimie Biochimie	Directeur : Mme C. FELIX
Département GEP	Directeur : M. Hassan HAMMOURI
Département Informatique	Directeur : M. le Professeur S. AKKOUCHE
Département Mathématiques	Directeur : M. le Professeur G. TOMANOV
Département Mécanique	Directeur : M. le Professeur H. BEN HADID
Département Physique	Directeur : M. le Professeur J-C PLENET
UFR Sciences et Techniques des Activités Physiques et Sportives	Directeur : M. Y.VANPOULLE
Observatoire des Sciences de l'Univers de Lyon	Directeur : M. B. GUIDERDONI
Polytech Lyon	Directeur : M. le Professeur E.PERRIN
Ecole Supérieure de Chimie Physique Electronique	Directeur : M. G. PIGNAULT
Institut Universitaire de Technologie de Lyon 1	Directeur : M. le Professeur C. VITON
Ecole Supérieure du Professorat et de l'Education	Directeur : M. le Professeur A. MOUGNIOTTE
Institut de Science Financière et d'Assurances	Directeur : M. N. LEBOISNE

Remerciements

C'est non sans une certaine émotion que je conclus à présent ces trois années de doctorat au sein du laboratoire du C2P2. Il convient de remercier les personnes qui ont participé à mon évolution tant scientifique qu'humaine.

Tout d'abord, je tiens à remercier les membres du jury pour avoir accepté d'évaluer mon travail de thèse, en particulier Laurence Rozes et Renaud Nicolaÿ en leur qualité de rapporteurs. Je remercie également Nicolas Seeboth et Catherine Journet-Gautier pour leur présence en tant qu'examinateurs de mes travaux de thèse.

Cette thèse a été réalisée au laboratoire de Chimie, Catalyse, Polymères et Procédés (C2P2) et je remercie le directeur Timothy McKenna de m'avoir accueillie dans son laboratoire.

Ces travaux ont été conduits sous la supervision de quatre chercheurs auxquels j'adresse toute ma gratitude. Je commencerai donc par remercier Emmanuel Lacôte pour son apport scientifique sur la chimie du bore et Fabrice Brunel pour sa participation à ces travaux *via* les calculs DFT et pour sa sympathie.

Je remercie très sincèrement Damien Montarnal, mon co-directeur de thèse, pour tout ce qu'il m'a transmis scientifiquement. Même si les débuts ont pu être difficiles, c'était un plaisir pour moi d'apprendre à tes côtés. Merci de m'avoir transmis les secrets de la rhéologie (parfois de la soudure aussi…) et le goût de la construction des graphes sur Origin (je ne saurais m'en passer à présent) ! Tu transmets ta passion à merveille et on peut se considérer chanceux d'avoir un encadrant comme toi, toujours à l'écoute, de bonne humeur et disponible (même dans les moments de rush). J'espère vivement avoir l'opportunité de retravailler avec toi un jour.

Mes travaux de thèse ont été dirigés par Jean Raynaud et notre collaboration fut particulièrement enrichissante pour moi. Merci d'avoir partagé avec moi l'étendu de ton savoir. Grâce à toi, je maîtrise (mieux) la chimie. Au-delà de l'aspect purement scientifique de notre collaboration, je me souviendrai longtemps de nos conversations animées où ton optimisme débordant contrebalançait avec ma vision désabusée. Merci pour toutes les découvertes musicales que tu m'as partagées (ce qui fait de toi un directeur de thèse d'exception) ! J'ai beaucoup d'estime et de respect pour toi et j'espère sincèrement que nous resterons amicalement en contact.

Ces travaux de thèse sont également le fruit de nombreuses collaborations scientifiques. A ce titre, je remercie successivement Lionel Perrin pour les calculs DFT, Matthieu Humbert et David

Gajan pour la RMN du solide, Kaï Szeto pour la DRIFT, Anne Baudouin pour la DOSY du fluor et Christine Lucas pour les suivis de réaction par RMN à haute température. Je remercie tout particulièrement Franck Collas pour les études DSC de mes polymères qui furent de grands pas en avant pour le projet. Un remerciement chaleureux à l'attention de Sébastien Norsic qui facilite la vie au laboratoire de tous les doctorants et qui m'a enseigné l'utilisation d'un réacteur sous pression (je ne désespère pas d'être un jour plus rapide que toi aux mots fléchés !).

De façon générale, je remercie l'ensemble des permanents du laboratoire pour les discussions enrichissantes que nous avons pu avoir au cours de ces trois années ainsi que pour votre sympathie. Un remerciement plus spécifique à Nathalie Jouglard, qui est bienveillante à l'égard de tous les étudiants du laboratoire. Je remercie également Pierre-Yves Dugas, impressionnant de par l'étendue de sa culture, pour nos discussions ainsi qu'Edgar Espinosa pour sa gentillesse et sa générosité. Je tiens à remercier Vincent Monteil pour ses conseils concernant mon futur parcours professionnel (et allez l'ASM !).

La thèse est une aventure humaine extraordinaire où nous nous retrouvons embarqués sur des montagnes russes avec une succession de bons et de mauvais moments. De bons amis sont nécessaires autant dans ces périodes de liesse que de découragement.

Mes premiers remerciements vont à Douriya, fraîchement arrivée à la fin de ma première année avec sa philosophie très sartrienne. Tu as été le soleil de ma thèse avec tes rires communicatifs. Merci pour tous les moments que nous avons partagés et pour le soutien mutuel dans les galères que nous avons parfois traversées. Et le rendez-vous est pris pour une soirée Aligot dans mon pays !

Mes pensées vont ensuite à Magali que je remercie chaleureusement pour tous les moments que nous avons passés ensemble, le thé de 16h10 avec son lot de potins étant un rendez-vous quotidien immanquable. Merci pour toutes nos discussions, pour ton oreille attentive et tes nombreux conseils.

Mes remerciements vont ensuite à deux personnes indissociables pour moi : Aurélien et Cédric. Même si un certain nombre d'années nous sépare, j'ai énormément apprécié nos soirées tous les trois à refaire le monde qui restent pour moi de précieux moments.

Mathieu, je me suis énormément retrouvée dans ta personnalité, impulsif et excessif, mais ô combien sensible (même sous tes airs de métalleux…). Merci pour tous les verres que nous avons partagés, en espérant qu'ils soient encore nombreux. Nous partons à présent dans la même galère donc bon courage pour la suite et je te donne rendez-vous en Auvergne pour quelques belles randos !

Les soirées et autres évènements sont nombreux au laboratoire du C2P2 et ce fut un plaisir de partager cela avec les autres doctorants et post-doctorants. Une pensée affective pour James (co-bureau pour quelques mois, ce fut un plaisir de te découvrir davantage), Rémi (nous avons formé un joli trio avec Doudou), Priscilla, Amel et les derniers arrivés Florian et Paul. Je n'oublie pas les doctorants de ma « promotion », Cédric (mon coloc temporaire du JEPO), Astrid, Yashmin (ma co-bureau aux bras ouverts dans les moments difficiles) et Matthieu, je vous souhaite de belles réussites.

Ma vie ne se limitant pas à la thèse, je tenais à remercier quelques personnes qui comptent pour moi et qui ont indirectement mais certainement contribué à cette aventure.

Je remercie chaleureusement (et immanquablement) Morgane, que je connais depuis huit ans maintenant et qui m'a toujours soutenue (surtout ces dernières années…). On a partagé beaucoup de choses ensemble, la moto, l'escalade et les verres (de faro) dans les bars de Clermont. Que cela dure encore longtemps !

Ma famille a toujours été d'un soutien indéfectible dans mes études. Ainsi, je remercie mes grands-parents d'avoir été présents en ce jour si particulier pour moi. Je vous remercie aussi pour tout votre amour et votre ouverture d'esprit. Une pensée également à mes oncles, tantes et cousines pour le soutien que vous m'avez apporté, même de loin.

Je remercie également ma grande sœur, Audrey, d'être présente en ce jour de soutenance et plus généralement dans ma vie. Pour mon grand bonheur, nos chemins se croisent de nouveau. Je suis très fière de toi (et de nous deux) dans tes réalisations professionnelles et personnelles.

C'est avec la plus vive émotion que j'adresse mes remerciements à mes parents. Je vous remercie pour votre soutien sans faille au travers de ce parcours, dans les succès comme dans les échecs. Merci pour toutes les valeurs que vous m'avez transmises. Je vous dois absolument tout, tant professionnellement que personnellement. Les mots me manquent pour vous exprimer (pudiquement) toute ma gratitude et tout mon amour. J'espère vous rendre fiers. La boucle est ainsi bouclée, nous sommes à présent quatre Dr. Brunet.

Mes derniers mots vont à Océane, sans qui rien ne serait possible. Merci pour tous ces moments hors du temps que j'ai vécu à tes côtés, pour ta douceur et ta bienveillance infinies. Merci d'avoir toujours su rallumer la lumière, même dans les moments les plus difficiles. J'ai confiance en l'avenir en espérant qu'il soit davantage commun pour nous deux.

« Ce qui compte c'est se libérer soi-même, découvrir ses propres dimensions, refuser les entraves. »

Virginia Woolf

« Apprenez à aimer vos échecs, Marcus, car ce sont eux qui vous bâtiront. Ce sont vos échecs qui donneront toute leur saveur à vos victoires. »

Joël Dicker

Résumé

Ces travaux de thèse portent sur l'élaboration et l'étude des propriétés thermomécaniques de polymères dynamiques incorporant des dérivés borés. Tout en appliquant ce concept à une variété d'architectures macromoléculaires : copolymères fonctionnels, briques di- et tri-fonctionnelles, deux réactivités distinctes du bore ont été étudiées et exploitées. Une large gamme de méthodes de caractérisation a été utilisée pour mener à bien ce projet : spectroscopies FTIR in-situ et RMN (liquide et solide), ainsi que de nombreuses analyses thermiques et mécaniques.

Dans un premier temps, nous avons considéré la formation de paires de Lewis frustrées entre des acides de Lewis (organoboranes) et des bases de Lewis (amines et phosphines) stériquement encombrés, cette interaction pouvant être fortement modulée par la participation d'un troisième composé tel que des molécules de gaz. Ainsi, nous avons été capables de former des réseaux dynamiques réticulables de façon réversible avec le dioxyde de carbone.

Dans un second temps, nous avons mis en évidence une nouvelle réactivité des esters boroniques cycliques impliquant une ouverture de cycle à haute température, assistée par la présence de nucléophiles. Cette réaction a été mise à profit pour former des polymères réticulés dynamiquement, pouvant atteindre des températures de transition vitreuse jusqu'à 220°C et dé-réticulables par dilution avec un bon solvant du polymère (apolaire). Cette réactivité a été mise en évidence pour une variété de polymères accessibles par copolymérisation radicalaire (styrène, éthylène, acétate de vinyle, acrylate de butyle) ou par post-fonctionnalisation de polymères commerciaux (polybutadiène).

Mots–clés : polymères organoborés, paires de Lewis, réseaux dynamiques, réticulation réversible, propriétés thermiques et mécaniques.

Abstract

This thesis focuses on the development and study of thermomechanical properties of dynamic polymers incorporating borylated derivatives. While applying this concept to a variety of macromolecular architectures: functional copolymers, di- and tri-functional bricks, two distinct reactivities of boron have been explored. A wide range of characterization methods has been used to carry out this project: in-situ FTIR and NMR spectroscopies (liquid and solid), as well as thermal and mechanical analyses.

In a first step, we considered the formation of Frustrated Lewis Pairs between Lewis acids (organoboranes) and Lewis bases (amines and phosphines) sterically hindered, as this interaction can be strongly modulated by the participation of a third compound such as gas molecules. Thus, we have been able to form dynamic networks reversibly crosslinkable with carbon dioxide.

In a second step, we demonstrated a new reactivity of cyclic boronic esters involving a ring opening at high temperature, assisted by the presence of nucleophiles. This reaction has been used to form dynamically crosslinked polymers, which can reach glass transition temperatures up to 220°C and de-crosslinkable by dilution in a good (apolar) polymer solvent. This reactivity has been exemplified through a variety of polymers accessible by radical copolymerization (styrene, ethylene, vinyl acetate, butyl acrylate) or by post-functionalization of commercial polymers (polybutadiene).

Keywords: organoboron polymers, Lewis pairs, dynamic networks, reversible crosslinking, thermal and mechanical properties.

List of abbreviations

(S)-DTBM-SEGPHOS: (S)-(+)-5,5′-Bis[di(3,5-di-tert-butyl-4-methoxyphenyl)phosphino]-4,4′-bi-1,3-benzodioxole

A1: Monofunctional molecule bearing a Lewis acid group

A2: Difunctional molecule bearing two Lewis acid groups

ADMET: Acyclic Diene Metathesis

AIBN: Azobisisobutyronitrile

ATRP: Atom Transfer Radical Polymerization

B1: Monofunctional molecule bearing a Lewis base group

B2: Difunctional molecule bearing two Lewis base groups

BPin: boronic acid, pinacol ester

BPO: Benzoyl peroxide

CANs: Covalent Adaptable Networks

CLP: Classical Lewis Pair

Đ: Dispersity

DFT: Density Functional Theory

DMC: Dimethyl carbonate

DMF: N,N'-dimethylformamide

DRIFT: Diffuse Reflectance Infrared Fourier Transform Spectroscopy

DSC: Differential Scanning Calorimetry

e. g.: exempli gratia

FLP: Frustrated Lewis Pair

FRP: Free Radical Polymerization

G': Storage modulus

G'': Loss modulus

i. e.: id est

M_n: Number average molar mass

mol %: molar percent

M_w: Mass average molar mass

n-BA: n-butyl acrylate

NMR: Nuclear Magnetic Resonance

P4VP: Poly(4-vinylpyridine)

PB: Polybutadiene

PBA-SBPin – x %: Poly(4-vinylphenylboronic acid, pinacol ester-co-n-butyl acrylate) with x % molar of 4-vinylphenylboronic acid, pinacol ester

PBPin: Poly(vinylboronic acid, pinacol ester)

Poly(A): Polymer functionalized with lateral Lewis acid groups

Poly(B): Polymer functionalized with lateral Lewis base groups

ppm: part per million

PS: Polystyrene

PS-$B(OH)_2$ – x %: Poly(styrene-co-4-vinylboronic acid) with x % molar of 4-vinylphenylboronic acid

PS-BPin - x %: Poly(4-vinylphenylboronic acid, pinacol ester-ran-styrene) with x % molar of 4-vinylphenylboronic acid, pinacol ester

PSBPin: Poly(4-vinylphenylboronic acid, pinacol ester)

PS-PPh_2 – x %: Poly(styrene-co-4-styryldiphenylphosphine) with x % molar of 4-styryldiphenylphosphine

PVac-VBPin – x %: Poly(4-vinylboronic pinacolate-co-vinyl acetate) with x % molar of 4-vinylphenylboronic pinacolate

PVBPin: poly(vinylboronic pinacolate)

R.T.: Room Temperature

RAFT: Reversible Addition-Fragmentation chain Transfer

ROMP: Ring-Opening Metathesis Polymerization

sc CO_2: Supercritical CO_2

SEC: Size-exclusion Chromatography

ss-NMR: Solid-state Nuclear Magnetic Resonance

T_g: Glass transition temperature

TGA: Thermal Gravimetric Analysis

THF: Tetrahydrofuran

TPBPin; 1,3,5-phenyltriboronic acid, tris(pinacol) ester

VAc: Vinyl acetate

VBPin: Vinylboronic pinacolate

wt %: weight percent

Résumé en français

L'utilisation de polymères borés au sein du laboratoire du C2P2 a démarré par la thèse d'Audrey Ledoux (2012-2015), afin d'exploiter les propriétés de briques amines-boranes pour le relargage contrôlé d'hydrogène. [1] Dans ces travaux, la réactivité des amines-boranes de type RNH_2-BH_2R' a été développée tandis que cette thèse s'appuie davantage sur la réactivité de groupements organoboranes fonctionnalisés de type BR_2 avec R choisis en fonction des applications visées.

Ces dernières années, les polymères hybrides combinant des éléments du groupe principal sur des architectures polymères conventionnelles ont montré un grand intérêt applicatif. [2], [3] Parmi eux, les polymères contenant des atomes de bore sont une classe importante de matériaux à la frontière entre les chimies inorganique et organique. Ces polymères ont de nombreuses applications grâce à la nature intrinsèque de l'atome de bore qui possède une lacune électronique permettant un grand nombre de réactions chimiques. [4] Ainsi, ils sont utilisés en tant que réactifs ou catalyseurs supportés, [5] détecteurs, [6] polymères répondant à des stimuli [7] ou moyens de séparations [8] grâce à leur capacité à réagir avec des nucléophiles. La littérature relate aussi de nombreux exemples d'utilisation de ces polymères dans des systèmes dynamiques. [9]

L'introduction de bore sur un squelette polymère est également une plateforme compatible avec de nombreuses techniques de copolymérisation et de post-fonctionnalisation. Ainsi, il est possible d'ajuster l'acidité de Lewis de la fonction borée par un choix de groupements adaptés. [10], [11] Il a été démontré dans la littérature que les acides de Lewis fortement encombrés ne forment pas d'adduits avec des bases de Lewis encombrées stériquement. C'est ainsi qu'est défini le concept de paires de Lewis frustrées a contrario des paires de Lewis classiques formant des adduits. [12], [13] De plus, suivant l'énergie associée à la liaison dative, un large spectre de réactivité est possible dû à une dynamique associée à l'équilibre entre forme complexée et libre.

Dans la littérature, les paires de Lewis frustrées (ou non) ont été largement étudiées pour leur capacité à activer de façon hétérolytique des petites molécules comme le dihydrogène [14] ou d'autres molécules de gaz. [15] Cette dernière caractéristique a été exploitée dans ces travaux de thèse. Ainsi, nous nous sommes intéressés à la capture réversible de dioxyde de carbone par des paires de Lewis à base de groupements acides de Lewis borés dont de nombreux exemples sont présents dans la bibliographie. [16]–[23]

Plusieurs stratégies ont alors été adoptées pour la synthèse de systèmes supramoléculaires « tricomposants » en gardant les polymères comme matrices de capture du dioxyde de carbone.

Principalement, nous nous sommes concentrés sur l'interaction entre des acides et des bases de Lewis difonctionnels formant des polymères supramoléculaires par polyaddition capables de réagir avec une molécule de CO_2 à chaque point d'interaction acide-base entre les monomères. Cette stratégie est représentée par le système A de la Figure 1. Egalement, à partir de polymères portant des groupes bases de Lewis pendants en interaction avec des molécules difonctionnelles bases de Lewis, nous avons pu créer des systèmes tridimensionnels. Dans ce cas, le polymère est réticulé de façon supramoléculaire par des interactions acide-base puis par l'ajout de dioxyde de carbone. Cette deuxième stratégie est représentée par le système B de la Figure 1.

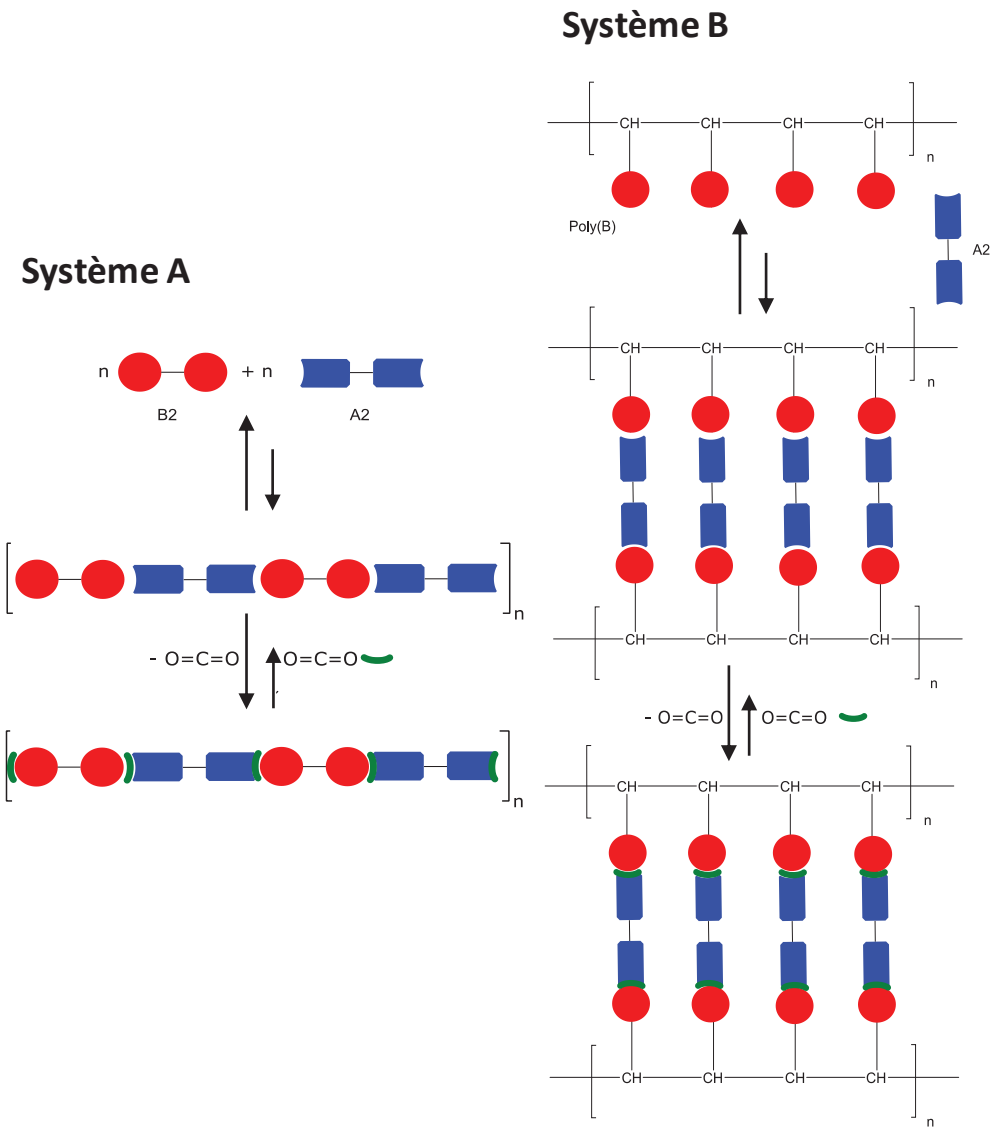

Figure 1 : Stratégies d'interaction utilisées pour la capture réversible de CO_2 par des paires de Lewis frustrées. Système A : Interaction entre des molécules difonctionnelles bases et acides de Lewis B2 et A2. Système B : Interaction entre un polymère fonctionnalisé par des groupes bases de Lewis poly(B) et des molécules difonctionnelles acides de Lewis A2.

Une partie importante du travail concernant les paires de Lewis a été dédiée à la synthèse des molécules et polymères fonctionnalisés. Du côté des acides de Lewis, nous nous sommes intéressés à la synthèse d'aryl boranes et quant aux bases de Lewis, notre choix s'est porté sur

des molécules ou polymères phosphorés ou azotés. Les différents systèmes étudiés sont représentés en Figure 2.

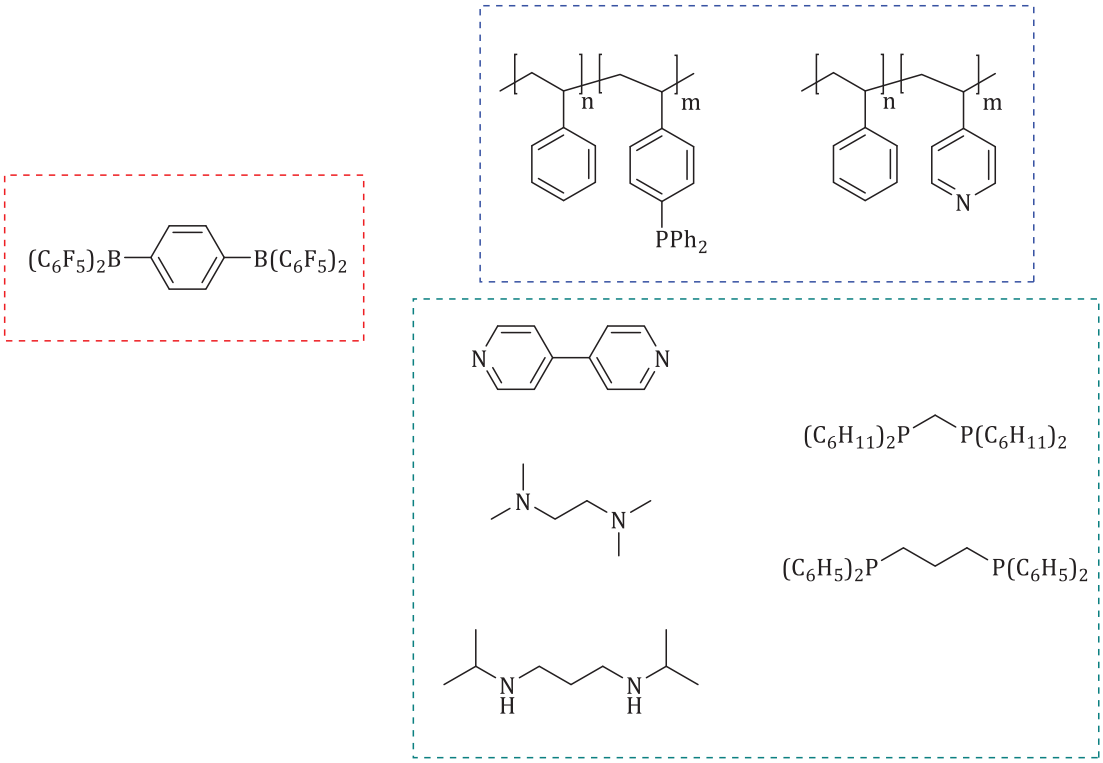

Figure 2 : Structures chimiques des systèmes étudiés. Encart rouge : Molécule difonctionnelle acide de Lewis. Encart bleu : Polymères fonctionnalisés bases de Lewis. Encart vert : Molécules difonctionnelles commerciales bases de Lewis.

Au travers de méthodes spectroscopiques et rhéologiques, nous avons mis en évidence la capture partiellement réversible du dioxyde de carbone par des paires de Lewis bore-phosphore, principalement *via* la stratégie B de la Figure 1. En effet, l'utilisation de bases de Lewis comprenant des atomes d'azote n'a pas été concluante pour la capture du dioxyde de carbone car ces bases ne présentaient pas une dynamique satisfaisante (ou une proportion de paires ouvertes suffisante). De plus, certains composés aminés sont capables de capturer directement le CO_2 par la formation de carbonates et carbamates.

Au cours de ces travaux de recherche, et au gré de nouveaux travaux concurrents publiés dans la littérature au cours de la thèse ainsi que d'observations expérimentales surprenantes, un second axe de recherche s'est dégagé concernant l'étude des comportements dynamiques exhibés par les polymères comprenant des unités esters boroniques cycliques. Diverses structures de ces types de polymères ont été synthétisées et étudiées grâce à une gamme de méthodes analytiques (spectroscopies RMN et IR, DSC, ATG, DMA, rhéologie, chromatographie d'exclusion stérique) avec des collaborations scientifiques de haut niveau en RMN du solide du bore, DOSY du fluor et modélisation DFT.

Les polymères organoborés que nous avons étudiés comportent des groupements d'esters boroniques pendants sur des structures vinyliques ou styréniques. Dans un premier temps, l'homopolymère du 4-vinylphenylboronic pinacolate - dont la synthèse par polymérisation radicalaire libre a été optimisée - nous a permis d'établir un mécanisme de réactivité des fonctions d'esters boroniques.

Grâce à des méthodes spectroscopiques et rhéologiques, nous avons suspecté une réticulation dynamique entre les chaînes de polymères par ouverture de cycle de l'ester boronique. Celle-ci serait provoquée par une attaque nucléophile sur la lacune électronique du bore sur une plage de température qui conduirait à la formation de l'alkoxyde libre pendant. Ce dernier attaquerait donc la lacune électronique d'un autre groupement d'ester boronique créant un pontage entre deux chaînes. Le nucléophile pourrait être un reste de pinacol dû à la synthèse du monomère ou bien des molécules d'eau absorbées par le matériau. Expérimentalement, il a été également observé que cette réticulation est réversible par simple dilution dans un solvant apolaire tel que le toluène. En effet, la forme de cycle fermé intramoléculaire à 5 atomes est favorisée entropiquement. Des calculs DFT ont confirmé ce mécanisme décrit en Figure 3.

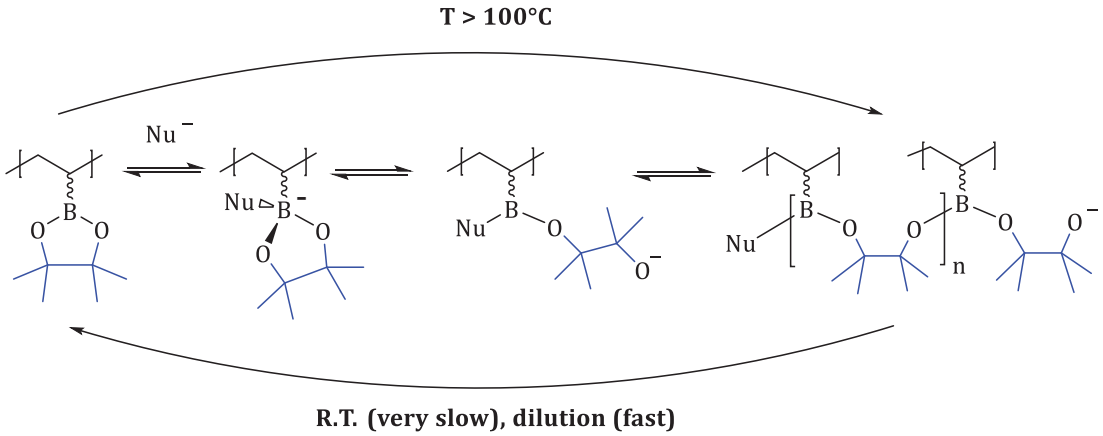

Figure 3 : Mécanisme d'ouverture de cycle et réticulation assistées par une attaque nucléophile.

Ce mécanisme a permis alors d'expliquer les phénomènes observés en calorimétrie différentielle à balayage qui révélait une augmentation de la température de transition vitreuse après une rampe de température. Nous avons ainsi obtenu des polymères organoborés avec des températures de transition vitreuse jusqu'à 220°C. Le résultat de l'analyse en calorimétrie différentielle est indiquée en Figure 4.

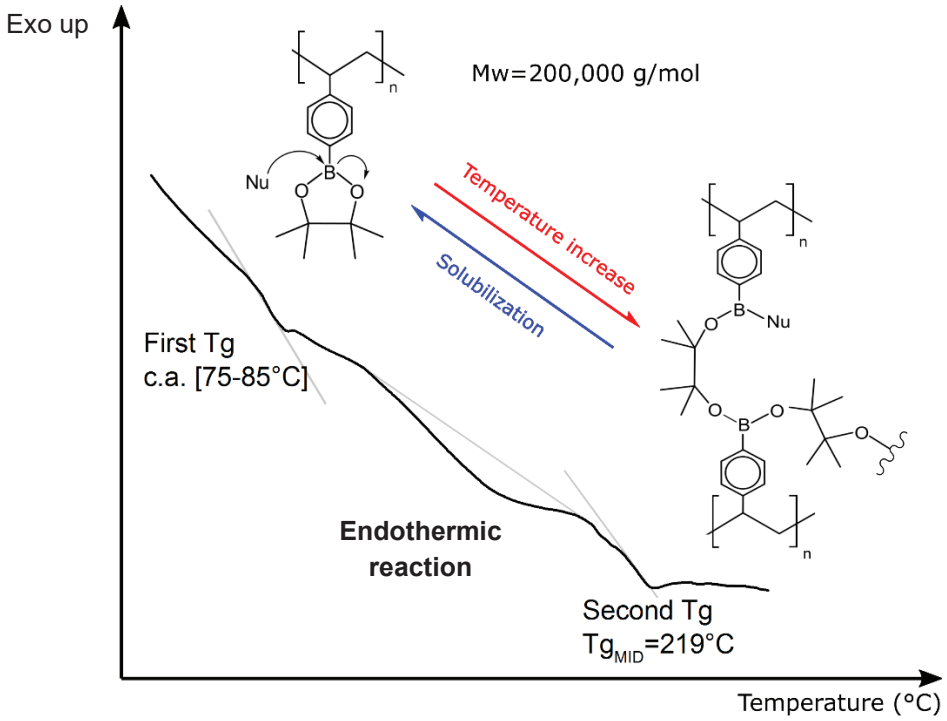

Figure 4 : Résultat de la calorimétrie différentielle à balayage avec les structures associées.

Il est intéressant de noter que ces systèmes se distinguent des vitrimères et des réseaux covalents adaptables (CANs) qui ont respectivement des densités de réticulation constantes ou diminuant continument avec la température. [24], [25] En effet, les polymères portant des groupements d'esters boroniques constitueraient le premier exemple de réseaux dynamiques avec une densité de réticulation augmentant avec la température, ou du moins sur une certaine gamme de température.

Cette réactivité, mise en évidence par différentes méthodes analytiques, ouvrirait la voie au design de matériaux de hautes transitions vitreuses reprocessables en se basant sur l'ouverture de cycle des esters boroniques. Ceci pourrait constituer une voie de réticulation alternative aux voies classiques.

A la suite de ces travaux, nous avons donc souhaité approfondir notre compréhension du phénomène observé en exemplifiant avec différentes structures de polymères comprenant des esters boroniques. Ainsi, nous avons synthétisé une variété de (co)polymères fonctionnalisés par des esters boroniques en chaînes pendantes vinyliques ou styréniques. Pour ce faire, nous avons utilisé des copolymérisations radicalaires ou des post-fonctionnalisations de polymères commerciaux par catalyse homogène. Sur ce dernier point, nous avons concentré nos efforts sur l'hydroboration de polybutadiène de hautes masses molaires avec des groupements d'esters pinacoliques par catalyse au cuivre ou au fer. L'ensemble des systèmes borés à ce jour étudiés sont décrits sur la Figure 5.

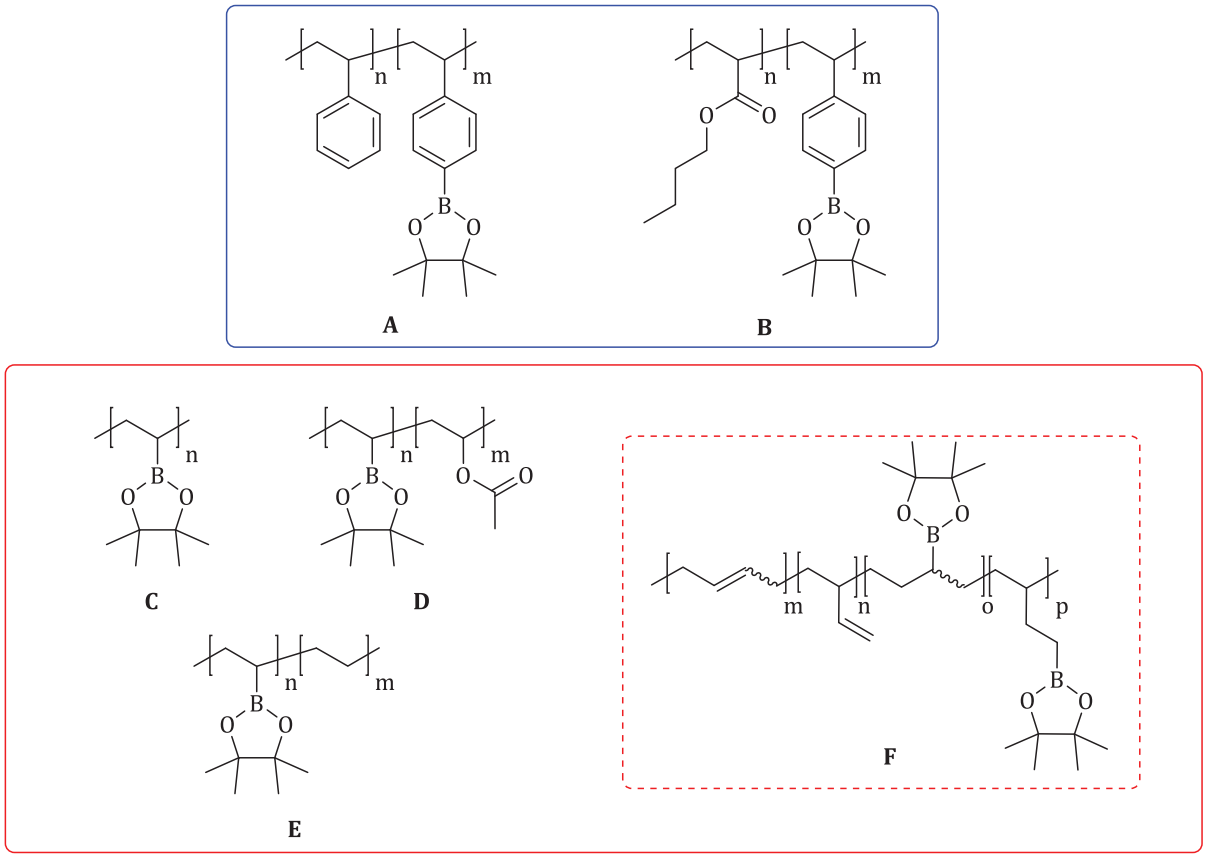

Figure 5 : Polymères organoborés étudiés. Encadrement bleu : Systèmes styréniques. Encadrement rouge : Systèmes vinyliques. Trait plein : Polymères organoborés obtenus par voie radicalaire. Trait pointillé : Fonctionnalisation de polybutadiène commercial.

Les différentes analyses réalisées sur l'ensemble de ces systèmes ont révélé la présence de réticulation dynamique due à la présence d'esters boroniques sur les chaînes polymères. Des comportements variables ont cependant été détectés selon les squelettes étudiés.

Conformément à l'homopolymère du 4-vinylphenylboronic pinacolate, les copolymères stryrène/4-vinylphenylboronic pinacolate (**A**, Figure 5) présentent des températures de transition vitreuse augmentant avec la quantité de monomère boré, confirmant l'implication de ces groupements dans les phénomènes de réticulation observés. La même tendance a été également détectée dans les copolymères acrylate de butyle/4-vinylphenylboronic pinacolate (**B**, Figure 5), avec toutefois la présence d'une séparation de phase entre les domaines riches et pauvres en 4-vinylphenylboronic pinacolate impactant les propriétés mécaniques du matériau.

L'homopolymère vinylique synthétisé à partir du vinylboronic acid pinacolate (**C**, Figure 5) a manifesté une réticulation dynamique dans une certaine gamme de températures allant de 60°C à 80°C avec l'inversion des modules G' et G'' mesurés par rhéologie comme décrit en Figure 6. De plus, un comportement d'élastomères a été mis en évidence dans cette gamme de températures avec la présence d'un plateau caoutchoutique. Cette polymérisation radicalaire fut également un challenge de synthèse. En effet, les radicaux de l'amorceur radicalaire utilisé (peroxyde de

benzoyle dans notre étude) attaquent également l'atome de bore déficitaire en électrons plus vulnérable dans le cas de la forme vinylique du monomère. Nous avons choisi de bloquer la lacune électronique de l'atome de bore par un ajout contrôlé de tétrahydrofurane, base de Lewis.

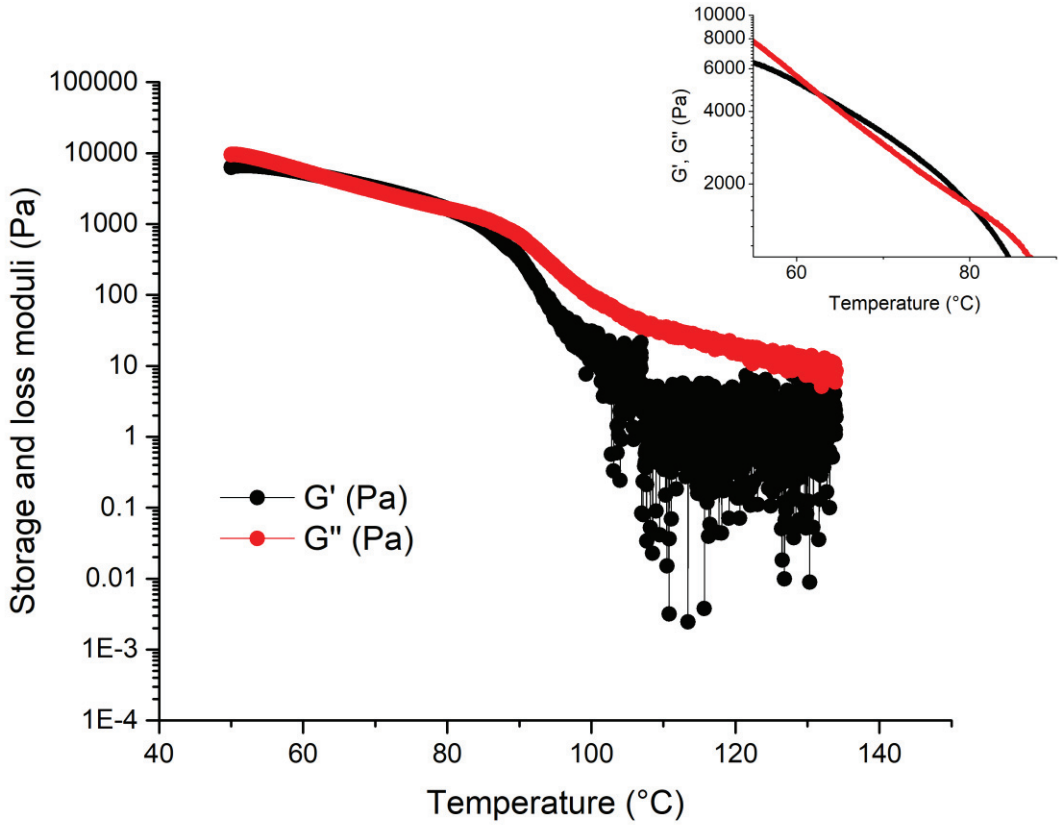

Figure 6 : Suivi des modules G' et G'' entre 50°C et 150°C. Zoom sur les températures entre 55°C et 90°C.

Par la suite, nous avons souhaité copolymériser ce monomère vinylique avec des co-monomères d'intérêt industriel tels que l'acétate de vinyle (**D**, Figure 5) ou l'éthylène (**E**, Figure 5). Concernant le copolymère avec l'acétate de vinyle, une augmentation de la température de transition vitreuse a été détectée par calorimétrie différentielle à balayage. Pour l'éthylène, les phénomènes de réactivité et de fusion se sont superposés et la contribution de la réactivité des esters boroniques impliquant une réticulation a été difficile à décorréler. Nous nous contenterons de confirmer la perturbation des phénomènes de fusion et de cristallisation habituellement observés dans le polyéthylène par la présence de groupements d'esters boroniques. Ceci est représenté par les thermogrammes obtenus en Figure 7. Cette copolymérisation fut également réalisée aussi bien dans le carbonate de diméthyle que dans le dioxyde de carbone supercritique, solvant vert plébiscité par la recherche ces dernières années.

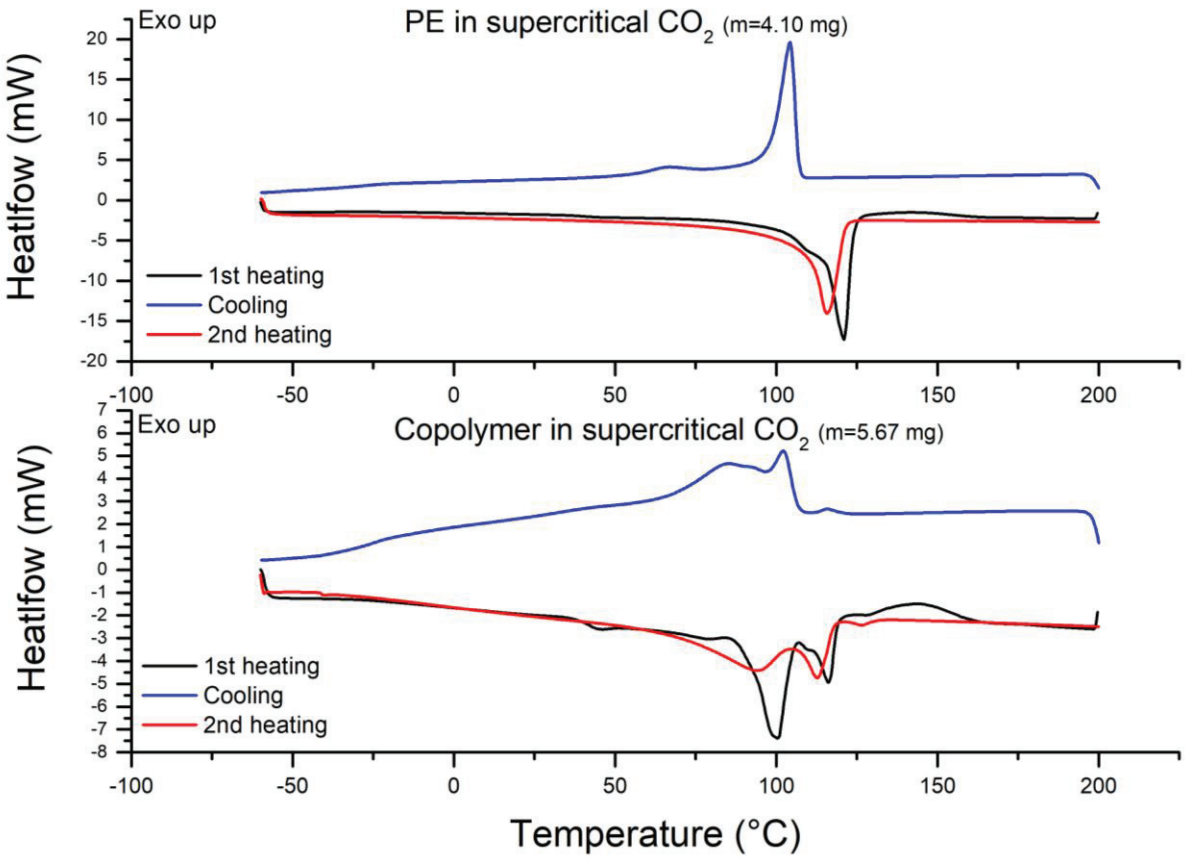

Figure 7 : Allure des thermogrammes obtenus par calorimétrie différentielle à balayage avec la présence ou non d'esters boroniques dans le polymère étudié.

Dans une optique différente, nos travaux de recherche nous ont amené à nous pencher sur la fonctionnalisation d'élastomères afin de proposer une nouvelle voie de réticulation réversible du polybutadiène. Deux voies de synthèse ont été exploitées pour permettre l'hydroboration, et ainsi l'installation de groupements d'esters boroniques, par deux catalyses homogènes schématisées en Figure 8.

La catalyse au cuivre (voie A, Figure 8) a permis la fonctionnalisation par les esters boroniques sur les liaisons diéniques mais nous avons eu à faire face à des problèmes de réticulation par ponts covalents induits par la catalyse utilisée (couplages oxydants). La contribution des esters boroniques pour une réticulation dynamique est donc négligeable par rapport au réseau covalent formé.

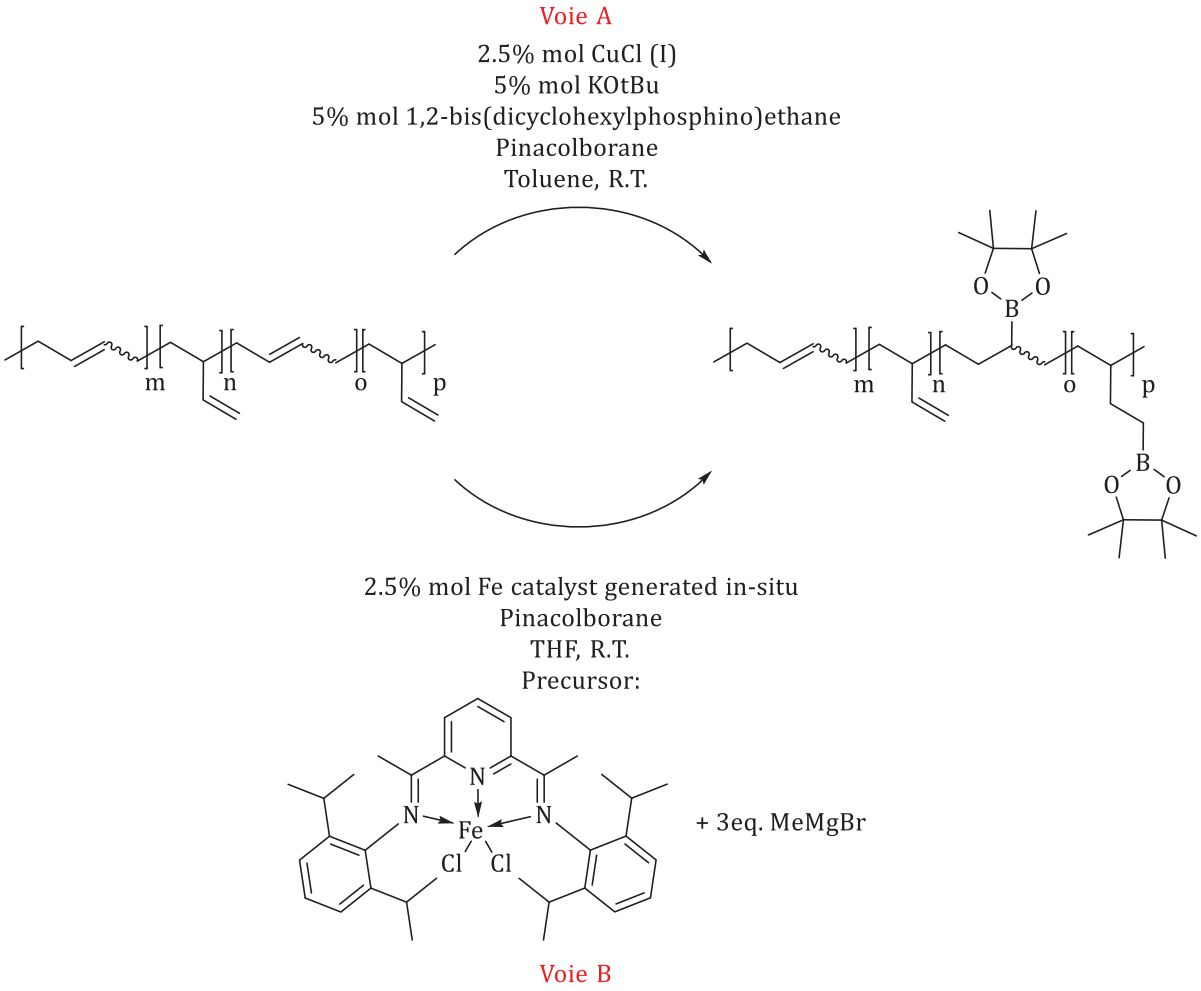

Figure 8 : Voies d'hydroboration du polybutadiène.

Les résultats ont été nettement plus concluants dans le cas de l'hydroboration par catalyse au fer (voie B, Figure 8). Dans ce cas, nous avons mis en évidence une séparation de phase entre les phases riches et pauvres en esters boroniques. La réticulation dynamique par ouverture de cycle des esters boroniques a donc été étudiée par rhéologie et a montré un réel impact sur les propriétés mécaniques du polymère avec l'augmentation des modules mesurés et la présence d'un plateau caoutchoutique plus large. La présence de relaxation mécanique témoigne du caractère dynamique de cette réticulation qui se produit uniquement dans les phases riches en esters boroniques. L'expérience illustrée en Figure 9 est représentative des comportements mécaniques mis en évidence avant et après réactivité des esters boroniques sur la matrice de polybutadiène.

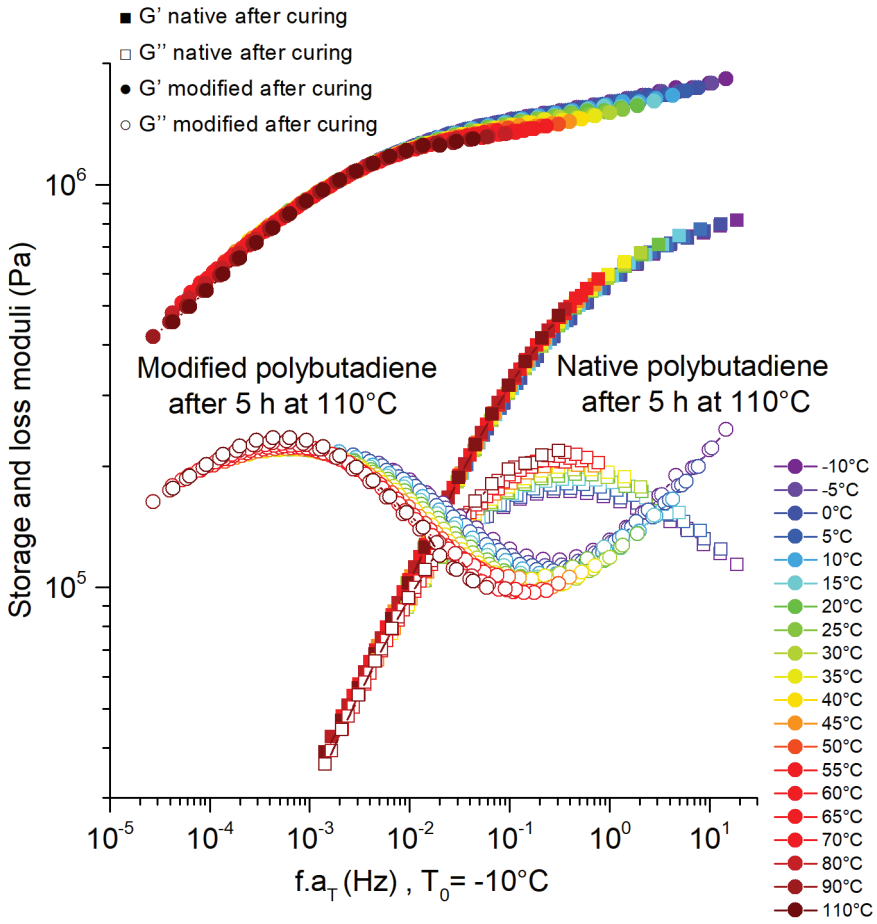

Figure 9 : Courbes maîtresses du polybutadiène natif (carrés) et modifié (cercles) après 5 h à 110°C.

Une étude plus fondamentale a été réalisée sur une molécule trifonctionnelle portant trois groupements esters boroniques. En s'appuyant sur la réactivité des esters boroniques, nous avons cherché à construire un réseau tridimensionnel non recristallisable qui conduirait à une verre hybride organique/inorganique. Ainsi, nous avons choisi un polyalcool induisant l'ouverture de cycle des esters boroniques à l'état fondu (hauts et proches points de fusion des deux molécules) et créant ainsi des pontages entre les molécules trifonctionnelles d'esters boroniques. Le refroidissement du matériau conduit à un verre transparent s'avérant être soluble dans des solvants tels que le tétrahydrofurane. Une étude par calorimétrie différentielle à balayage a de plus montré l'augmentation progressive de la température de transition vitreuse au cours de la réaction. Elle atteint son maximum pour une ratio O/B de 3.2 suggérant la pyramidalisation du bore ($sp^2 \rightarrow sp^3$). De plus, des analyses par RMN du solide du bore ont mis en évidence la présence de plusieurs espèces borées après une rampe de température confirmant la présence d'une réaction chimique au sein du matériau. Les espèces et les mécanismes réactionnels hypothétiques sont représentés en Figure 10. Ces expériences sont prometteuses mais demandent des investigations supplémentaires pour expliciter les mécanismes de réaction.

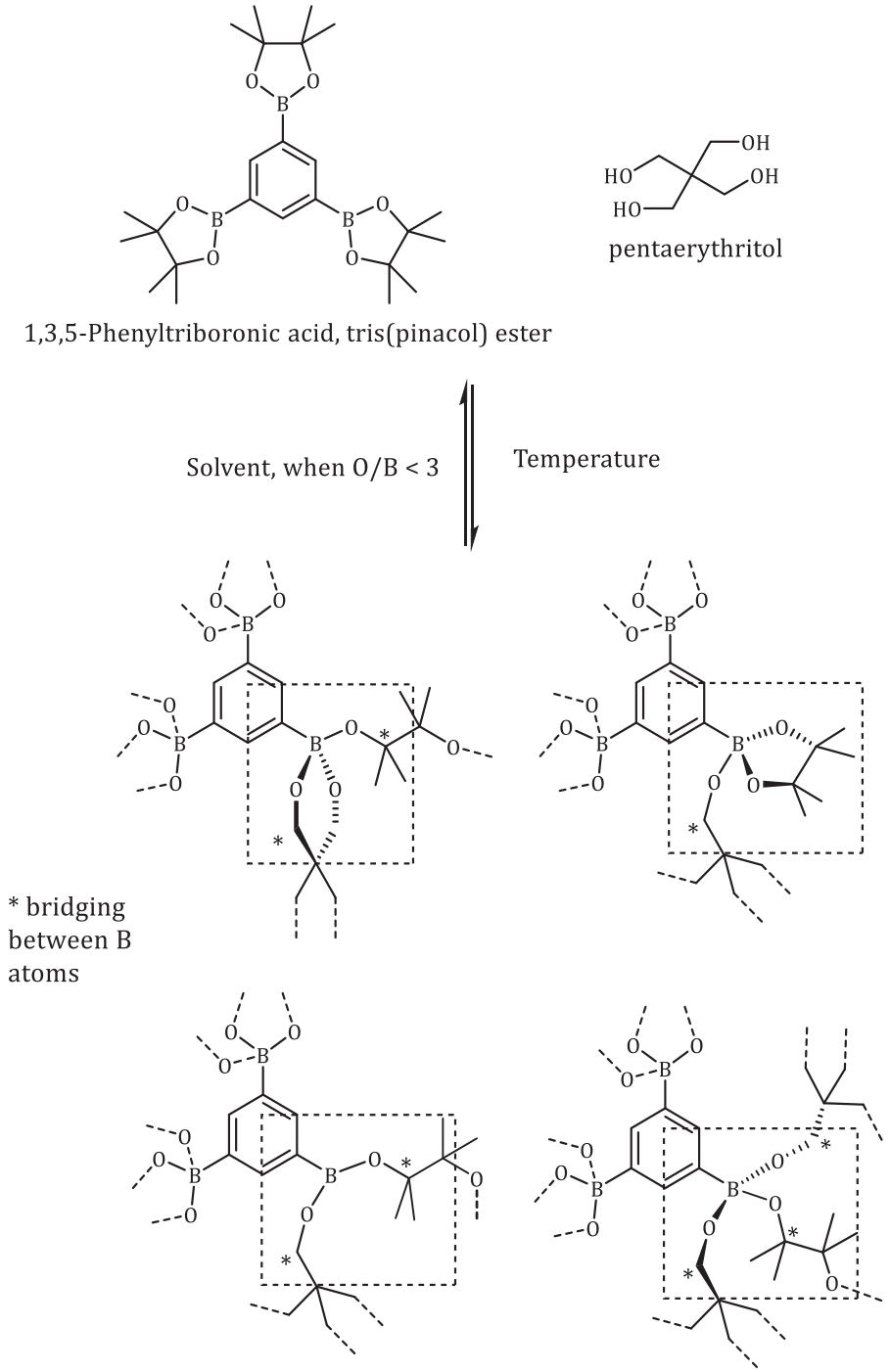

Figure 10 : Système étudié et hypothèses de mécanismes réactionnels.

Pour conclure, nous avons synthétisé et étudié des systèmes polymères capables de capter de façon réversible du dioxyde de carbone. Cette réversibilité a été démontrée par des analyses spectroscopiques UV ou par rhéologie. Par l'étude de polymères organoborés, nous avons également mis en évidence l'importance de la réactivité des esters boroniques pour la formation de polymères réticulés de façon dynamique par assistance nucléophile sur une certaine gamme de température. Nous avons exploité cette réactivité en étendant ces concepts à une variété de

polymères par copolymérisation radicalaire ou par post-modification de polymères diéniques. Des comportements similaires ont été observés dans chaque cas avec une augmentation de la température de transition vitreuse induite par la réticulation due à l'ouverture de cycle des esters boroniques. Cette réactivité ouvre la voie à la possibilité d'ajuster la température de transition vitreuse d'une large gamme de polymères utilisés en industrie par une réaction simple et robuste. De nouveaux réseaux dynamiques et réversibles sont donc accessibles à la frontière entre les vitrimères et les réseaux covalents adaptables.

Références

[1] A. Ledoux, "Polymères contenant des paires de Lewis de type amine-borane , en tant que réservoirs d'hydrogène : relation structure / activité," Université de Lyon, **2016**.

[2] A. S. Abd-El-Aziz, "Journal of inorganic and organometallic polymers: Preface," *Journal of Inorganic and Organometallic Polymers*, vol. 10, no. 4, pp. 157–158, **2000**.

[3] F. Kato, "Inorganic and organometallic polymers," *Annu. Rep. Prog. Chem., Sect. A Inorg. Chem.*, vol. 109, pp. 277–298, **2013**.

[4] F. Jäkle, "Borylated polyolefins and their applications," *J. Inorg. Organomet. Polym.*, vol. 15, no. 3, pp. 293–307, **2005**.

[5] C. Schunicht, A. Biffis, and G. Wulff, "Microgel-supported oxazaborolidines: Novel catalysts for enantioselective reductions," *Tetrahedron*, vol. 56, pp. 1693–1699, **2000**.

[6] A. Sundararaman, M. Victor, R. Varughese, and F. Jäkle, "A family of main-chain polymeric Lewis acids: Synthesis and fluorescent sensing properties of boron-modified polythiophenes," *J. Am. Chem. Soc.*, vol. 127, pp. 13748–13749, **2005**.

[7] K. Shiomori, A. E. Ivanov, I. Y. Galaev, Y. Kawano, and B. Mattiasson, "Thermoresponsive Properties of Sugar Sensitive Copolymer of N-Isopropylacrylamide and 3-(Acrylamido)phenylboronic Acid," *Macromol. Chem. Phys.*, vol. 205, no. 1, pp. 27–34, **2004**.

[8] S. Senel, "Boronic acid carrying (2-hydroxyethylmethacrylate)-based membranes for isolation of RNA," *Colloids Surfaces A Physicochem. Eng. Asp.*, vol. 219, no. 1–3, pp. 17–23, **2003**.

[9] W. L. A. Brooks and B. S. Sumerlin, "Synthesis and Applications of Boronic Acid-Containing Polymers : From Materials to Medicine," *Chem. Rev.*, vol. 116, pp. 1375–1397, **2016**.

[10] A. Sundararaman, R. A. Lalancette, L. N. Zakharov, A. L. Rheingold, and F. Jäkle, "Structural diversity of pentafluorophenylcopper complexes. First evidence of π-coordination of unsupported arenes to organocopper aggregates," *Organometallics*, vol. 22, pp. 3526–3532, **2003**.

[11] A. Sundararaman and F. Jäkle, "A comparative study of base-free arylcopper reagents for the transfer of aryl groups to boron halides," *J. Organomet. Chem.*, vol. 681, pp. 134–142, **2003**.

[12] H. C. Brown, H. I. Schlesinger, and S. Z. Cardon, "Studies in Stereochemistry. I. Steric Strains as a Factor in the Relative Stability of Some Coordination Compounds of Boron," *J. Am. Chem. Soc.*, vol. 64, no. 2, pp. 325–329, **1942**.

[13] G. Wittig and E. Benz, "Über das verhalten von dehydrobenzol gegenüber nucleophilen und elektrophilen reagenzien," *Chem. Ber.*, vol. 92, pp. 1999–2013, **1959**.

[14] G. C. Welch and D. W. Stephan, "Facile heterolytic cleavage of dihydrogen by phosphines and boranes," *J. Am. Chem. Soc.*, vol. 129, pp. 1880–1881, **2007**.

[15] D. W. Stephan and G. Erker, "Frustrated Lewis pair chemistry of carbon, nitrogen and sulfur oxides," *Chem. Sci.*, vol. 5, no. 7, p. 2625, **2014**.

[16] C. M. Mömming *et al.*, "Reversible metal-free carbon dioxide binding by Frustrated Lewis Pairs," *Angew. Chemie - Int. Ed.*, vol. 48, pp. 6643–6646, **2009**.

[17] I. Peuser *et al.*, "CO_2 and formate complexes of phosphine/borane Frustrated Lewis Pairs," *Chem. - A Eur. J.*, vol. 17, pp. 9640–9650, **2011**.

[18] M. Harhausen, R. Fröhlich, G. Kehr, and G. Erker, "Reactions of modified intermolecular frustrated P/B lewis pairs with dihydrogen, ethene, and carbon dioxide," *Organometallics*, vol. 31, no. 7, pp. 2801–2809, **2012**.

[19] W. S. Siebert, M. Hildenbrand, P. Hornbach, G. Karger, and H. Pritzkow, "1,2- and 1,1-Diborylalkene," *Naturforsch*, vol. 44, pp. 1179–1186, **1989**.

[20] X. Zhao and D. W. Stephan, "Bis-boranes in the frustrated Lewis pair activation of carbon dioxide," *Chem. Commun.*, vol. 47, no. 6, p. 1833, **2011**.

[21] M. J. Sgro, J. Dömer, and D. W. Stephan, "Stoichiometric CO_2 reductions using a bis-borane-based frustrated Lewis pair," *Chem. Commun.*, vol. 48, p. 7253, **2012**.

[22] M. Feroci, I. Chiarotto, S. Vecchio Ciprioti, and A. Inesi, "On the reactivity and stability of electrogenerated N-heterocyclic carbene in parent 1-butyl-3-methyl-1H-imidazolium tetrafluoroborate: Formation and use of N-heterocyclic carbene-CO_2 adduct as latent catalyst," *Electrochim. Acta*, vol. 109, pp. 95–101, **2013**.

[23] J. D. Holbrey *et al.*, "1,3-Dimethylimidazolium-2-carboxylate: the unexpected synthesis of an ionic liquid precursor and carbene-CO_2 adduct," *Chem. Commun.*, vol. 347, no. 1, pp. 28–29, **2003**.

[24] D. Montarnal, M. Capelot, F. Tournilhac, and L. Leibler, "Silica-Like Malleable Materials from Permanent Organic Networks," *Science (80-.).*, vol. 334, pp. 965–969, **2011**.

[25] C. N. Bowman and C. J. Kloxin, "Covalent Adaptable Networks : Reversible Bond Structures Incorporated in Polymer Networks," *Angew. Chemie - Int. Ed.*, vol. 51, pp. 4272–4274, **2012**.

Outline

General introduction

Polymers, also referred abusively as “plastics” in common language, are ubiquitous in our day-to-day life and essential in a wide range of applications from commodity uses in automotive, building, packaging to specific applications such as encapsulation and delivery of active chemicals in cosmetics and pharmacy. Nature gave us numerous examples of polymers such as natural rubber, polysaccharides or proteins. Synthetic polymer materials have yet undergone a huge development and diversification over almost a century and therefore are an important pan of research in chemistry, due to their main advantages: lightweight, various possible architectures and physical properties, chemical inertness and good thermal insulation.

The thermomechanical properties of polymers are determined by the chemical nature of the selected monomers and their macromolecular architectures. Most polymers can be classified in two main groups: thermoplastics and thermosets. Thermoplastics are long, often entangled polymeric chains that are processable by simple increase of the temperature above the melting temperature or the glass transition temperature. Thermosets contain permanent crosslinks between the polymer chains that highly affect the thermomechanical properties of the polymer. In this case, due to the presence of bonds tying them together, the chains can no longer flow as they form a tridimensional network even at high temperatures. These polymers exhibit a thermal stability and solvent resistance that are very useful in many applications. Among them, elastomers are a particular case of thermosets as they present additional properties such as super elasticity and resilience. One of the main drawbacks of thermosets and elastomers, inherent to their crosslinked nature, is the difficulty to recycle them due to the irreversible chemical bonds contrary to thermoplastics that can be processed repetitively bearing in mind oxidative degradation. Thus, researchers have focused their efforts on combining the advantages of thermoplastics and crosslinked polymers by introducing dynamical and reversible bonds between polymer chains with the main examples of vitrimers and covalent adaptable networks (CANs). [1]–[12]

The development of hybrid polymers combining main groups’ elements with typical structures has been of growing interest for material science in the last few years. [13], [14] Polymers containing boron atoms are an important class of materials at the border between inorganic and organic chemistries. They have many applications due to the intrinsic nature of the boron atom as it gives a binding platform to nucleophiles and opens a path to a wide range of chemical reactions. [15] Besides, it confers organoboron polymers a dynamic character and reactivity

thanks to the many possible reactions on the tunable electronic vacancy. These polymers have already been used in dynamic networks mainly through the reactivity of boronic acid groups. [16]

The introduction of boron-based groups on polymer backbones also allows for the tuning of the Lewis acidity by post-functionalization. This feature is used for the introduction of aryl groups of boron halides with arylcopper reagents providing highly Lewis acidic organoboron polymers. [17], [18]

Highly Lewis acidic groups can be involved in Frustrated Lewis Pairs (FLPs) with steric hindrance precluding the dative bond of the Classical Lewis Pairs (CLPs). Indeed, a bulky Lewis base combined with a bulky electrophilic Lewis acid does not undergo self-quenching and thus does not form a dative adduct in common sense. [19], [20] Therefore, this interaction is part of supramolecular chemistry between a host and a guest that can be tuned by different stimuli such as temperature, ionic force, pH or solvation.

Consequently, integrating such supramolecular units into polymeric backbones leads to responsive materials with tunable structures and physical properties, with growing fields of application. In this thesis work, we propose a breakthrough concept in supramolecular chemistry in which the interaction between host and guest (acid and base) is adjustable not only globally *via* an environmental parameter but locally using a third component such as a gas or a small molecule that inserts within the host-guest complex. New applications could range from gas sensors to membranes with adaptive selectivity.

Chapter 1 presents the chemistry of boron-based polymers with their syntheses and applications relying on the types of bonds studied: boron-carbon, boron-nitrogen and boron-oxygen. The latter will be further discussed with the last updates on this subject. Frustrated Lewis Pairs (FLP) and concepts related are described and the combination between FLP and polymers is also investigated.

Chapter 2 is dedicated to the synthesis of Lewis-functionalized molecular bricks or polymers comprising Lewis acid or base functionalities. The interactions are studied between Lewis acid and base harnessing the concept of Frustrated Lewis Pairs with the addition of a small molecule (in this work, carbon dioxide).

Chapter 3 reports the study of the dynamic character of organoboron polymers carrying boronate esters on styrenic backbones with the use of a wide range of analytical methods. From these data, mechanism explaining the dynamic crosslinking of these polymers is proposed.

Chapter 4 describes the extension of the concepts established in Chapter 3 to a wide variety of copolymers. Styrenic-based organoboron monomers are copolymerized with acrylates, while vinylic-based organoboron monomers are homopolymerized and copolymerized with vinyl acetate or ethylene. Hydroboration of polybutadiene is also presented for the introduction of boronate ester on pre-synthesized polymers. A breakthrough concept is also investigated with the design of an organic/inorganic hybrid system based a trifunctional boronate ester small molecule that induces the creation of glasses. All (co)polymers are studied through spectroscopic and mechanical analyses.

Experimental Section contains all the experimental data related to the trials presented in the main text with analyses performed.

References

[1] C. N. Bowman and C. J. Kloxin, "Covalent Adaptable Networks: Reversible Bond Structures Incorporated in Polymer Networks," *Angew. Chemie - Int. Ed.*, vol. 51, pp. 4272–4274, **2012**.

[2] T. Maeda, H. Otsuka, and A. Takahara, "Dynamic covalent polymers: Reorganizable polymers with dynamic covalent bonds," *Prog. Polym. Sci.*, vol. 34, no. 7, pp. 581–604, **2009**.

[3] R. J. Wojtecki, M. A. Meador, and S. J. Rowan, "Using the dynamic bond to access macroscopically responsive structurally dynamic polymers," *Nat. Mater.*, vol. 10, pp. 14–27, **2011**.

[4] Y. Zhang, A. A. Broekhuis, and F. Picchioni, "Thermally self-healing polymeric materials: The next step to recycling thermoset polymers?," *Macromolecules*, vol. 42, no. 6, pp. 1906–1912, **2009**.

[5] X. Chen *et al.*, "A Thermally Re-mendable Cross-Linked Polymeric Material," *Science (80-.).*, vol. 295, pp. 1698–1703, **2002**.

[6] P. Reutenauer, E. Buhler, P. J. Boul, S. J. Candau, and J. M. Lehn, "Room temperature dynamic polymers based on Diels-Alder chemistry," *Chem. - A Eur. J.*, vol. 15, no. 8, pp. 1893–1900, **2009**.

[7] T. F. Scott, A. D. Schneider, W. D. Cook, and C. N. Bowman, "Photoinduced plasticity in cross-linked polymers," *Science (80-.).*, vol. 308, no. 5728, pp. 1615–1617, **2005**.

[8] Y. Amamoto, J. Kamada, H. Otsuka, A. Takahara, and K. Matyjaszewski, "Repeatable photoinduced self-healing of covalently cross-linked polymers through reshuffling of trithiocarbonate units," *Angew. Chemie - Int. Ed.*, vol. 50, no. 7, pp. 1660–1663, **2011**.

[9] D. Montarnal, F. Tournilhac, M. Hidalgo, J. L. Couturier, and L. Leibler, "Versatile one-pot synthesis of supramolecular plastics and self-healing rubbers," *J. Am. Chem. Soc.*, vol. 131, no. 23, pp. 7966–7967, **2009**.

[10] B. Ghosh and M. B. Urban, "Self-Repairing Oxetane-Substituted Polyurethane Networks," *Science (80-.).*, vol. 323, pp. 1458–1460, **2009**.

[11] R. Nicolaÿ, J. Kamada, A. Van Wassen, and K. Matyjaszewski, "Responsive gels based on a dynamic covalent trithiocarbonate cross-linker," *Macromolecules*, vol. 43, no. 9, pp. 4355–4361, **2010**.

[12] D. Montarnal, M. Capelot, F. Tournilhac, and L. Leibler, "Silica-Like Malleable Materials from Permanent Organic Networks," *Science (80-.).*, vol. 334, pp. 965–969, **2011**.

[13] A. S. Abd-El-Aziz, "Journal of inorganic and organometallic polymers: Preface," *Journal of Inorganic and Organometallic Polymers*, vol. 10, no. 4, pp. 157–158, **2000**.

[14] F. Kato, "Inorganic and organometallic polymers," *Annu. Rep. Prog. Chem., Sect. A Inorg. Chem.*, vol. 109, pp. 277–298, **2013**.

[15] F. Jäkle, "Borylated polyolefins and their applications," *J. Inorg. Organomet. Polym.*, vol. 15, no. 3, pp. 293–307, **2005**.

[16] W. L. A. Brooks and B. S. Sumerlin, "Synthesis and Applications of Boronic Acid-Containing Polymers : From Materials to Medicine," *Chem. Rev.*, vol. 116, pp. 1375–1397, **2016**.

[17] A. Sundararaman, R. A. Lalancette, L. N. Zakharov, A. L. Rheingold, and F. Jäkle, "Structural diversity of pentafluorophenylcopper complexes. First evidence of π-coordination of unsupported arenes to organocopper aggregates," *Organometallics*, vol. 22, pp. 3526–3532, **2003**.

[18] A. Sundararaman and F. Jäkle, "A comparative study of base-free arylcopper reagents for the transfer of aryl groups to boron halides," *J. Organomet. Chem.*, vol. 681, pp. 134–142, **2003**.

[19] H. C. Brown, H. I. Schlesinger, and S. Z. Cardon, "Studies in Stereochemistry. I. Steric Strains as a Factor in the Relative Stability of Some Coördination Compounds of Boron," *J. Am. Chem. Soc.*, vol. 64, no. 2, pp. 325–329, **1942**.

[20] G. Wittig and E. Benz, "Über das verhalten von dehydrobenzol gegenüber nucleophilen und elektrophilen reagenzien," *Chem. Ber.*, vol. 92, pp. 1999–2013, **1959**.

Chapter 1:

Bibliographical review

Chapter 1 presents the chemistry of boron-based polymers with their syntheses and applications relying on the types of bonds studied: boron-carbon, boron-nitrogen and boron-oxygen. The latter will be further discussed with the last updates on this subject. Frustrated Lewis Pairs (FLP) and concepts related are described and the combination between FLP and polymers is also investigated.

Table of contents

I. Introduction

The development of hybrid polymers (organic/inorganic) combining main group elements with typical organic polymers is showing an increasing interest over the last few years. [1], [2] In particular, organoboron polymers are a growing field of research due to their interesting properties associated with the electron-deficient nature of many boron compounds. [3] Firstly set aside due to the hydrolytic and oxidative sensitivity of many boron-containing molecules, [4] it was demonstrated that organoboron polymers can be obtained in high molar masses and that many of them are perfectly stable for extended periods of time under ambient or even demanding conditions. [5]

Polymers containing boron atoms are an important class of materials at the frontier between inorganic and organometallic chemistry. They have many applications due to the intrinsic electron deficient nature of the boron atom as it gives a binding platform for nucleophiles and opens a path to a wide range of chemical reactions. [6] Such polymers have applications in supported reagents and immobilized catalysts, [7] sensors, [8] stimuli responsive polymers [9] and separation media [10] for their ability to bind nucleophiles. Besides, they are also used as intermediates in the synthesis of functionalized polymers and as polymeric electrolytes for batteries, [11] flame retardants [12] and preceramic materials. [13]

The intrinsic reactivity of the boron atom also confers a dynamic character to organoboron polymers thanks to the possible reactions harnessing the electronic vacancy. From this postulate, this PhD work hopes to deepen the understanding of the reactivity governing the dynamics of organoboron polymers.

The objective of this bibliographical part is to present an overview of new developments concerning organoboron polymers. These polymers will be studied according to the chemistry and the nature of the boron-Ƶ bond, mainly boron-carbon, boron-nitrogen and boron-oxygen linkages. A deeper focus will be made on this latter class of polymers featuring B-O bonds, as they are an excellent entry point to introduce boron in macromolecular architectures and can be further derivatized into a wide range of organoboron hybrid materials.

Besides, within these organoboron polymers, a distinction can be done between two main types of organoboron polymers depending on the position of the boron-containing group. Hence, organoboron polymers can exhibit boron atoms in main-chain functionalized conjugated or non-conjugated polymers and side-chain functionalized conjugated or non-conjugated polymers, as illustrated in Figure I. 1. Each polymer types will be described in the following parts.

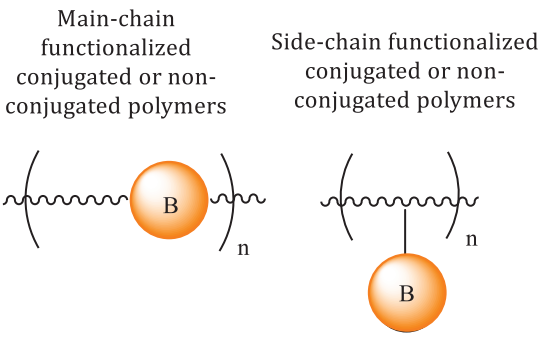

Figure I. 1: Main types of organoboron polymers.

Different sorts of bonds between the boron atom and another atom in boron-containing polymers are explored through examples in the next three parts. Firstly, the polymers with boron-carbon bonds will be investigated. Secondly, polymers comprising boron-nitrogen linkages will be presented. In a third part, polymers containing boron-oxygen bonds will be detailed.

Focusing on responsive materials, we will also present how Lewis acid/base chemistry can be involved in such systems arising from polymers harnessing the Lewis acid character of boron moieties. In this optic, the last part of this bibliographical review will be dedicated to the presentation of the specificities of Frustrated Lewis Pairs' chemistry and how it was recently involved in dynamic organoboron polymer networks.

II. Synthesis of polymers containing Boron-Carbon bonds

Boron-carbon bonds are introduced in the main chain or in the side chain of functionalized polymers. The introduction of boron in π-conjugated polymers is one of the approach used to modify the electronic properties. Besides, boron is an attractive platform for post-functionalization with nucleophiles. Chain polymerization methods, coupling reactions and post-modifications of existing polymers are the main strategies to afford such polymers.

A. Main-chain functionalized polymers with boron-carbon bonds

Chujo and Matsumi pioneered the functionalization of organic polymers containing boron in the polymer backbone. [14], [15] They synthesized a variety of π-conjugated organoboron polymers, presented in Figure I. 2, having a high stability under air and moisture and exhibiting properties such as fluorescence emission, n-type electrochemical activity, electrical conductivity, third order non-linear optical property and anion sensing ability.

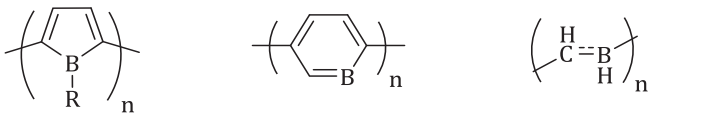

Polyborole Poly(borabenzene) Poly(bora-acetylene)

Figure I. 2: Potential π-conjugated organoboron polymers presented by Chujo and Matsumi in 2008. [14]

In addition to chain polymerization methods, they were able to use several methods of coupling: polycondensation with Grignard reagent, [16] Sonogashira-type polycondensation [17] and polycondensation *via* tin-boron exchanges. [8] Transition metal-catalyzed coupling procedures have been successfully conducted more recently with nickel, palladium or copper-based catalysts for instance. [18]–[20] This method is well-suited for the polymerization of boron monomers in which boron is stabilized by tetracoordination and incorporated into a cyclic system. [21]

Thanks to its π-acceptor character in conjugated organic molecules, main chain-type organoboron polymers are used in optoelectronic devices (OLEDs, FETs, photovoltaics) and in sensory applications. [6], [22]

Hydroboration is a smart strategy for the introduction of boron in functionalized polymers and will be used in this PhD work. Siebert, Corriu and Douglas first reported in 1998 the formation of conjugated main chain organoboron polymers as shown in Figure I. 3. They were obtained by the hydroboration of 2,5-diethynylthiophene derivatives with BCl_3/Et_3SiH mixture. Interestingly, the polymers presented different colors depending on the substituents on the alkynyl groups and the

boron center itself. However, the high sensitivity to moisture and oxygen hindered further analysis. [23]

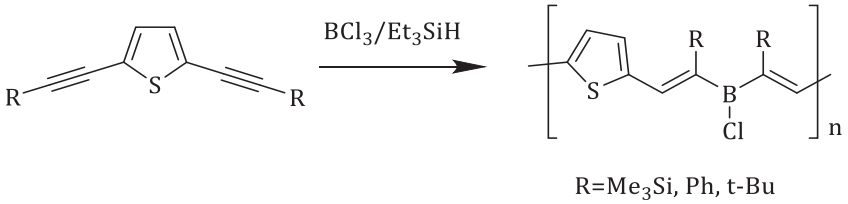

Figure I. 3: First conjugated main-chain organoboron polymers. [23]

At the same time, Chujo and co-workers presented a breakthrough in the development of isolable and well-characterized conjugated organoboron polymers. More stable polymers, as boron atoms are only involved in boron-carbon bonds, were synthesized by hydroboration polymerization [16], [24] *via* the facile preparation and selective reactivity of sterically hindered arylboranes $ArBH_2$ (Ar=Mes (mesityl, 2,4,6-trimethylphenyl), Tip (2,4,6-triisopropylphenyl)). [25], [26] (Figure I. 4)

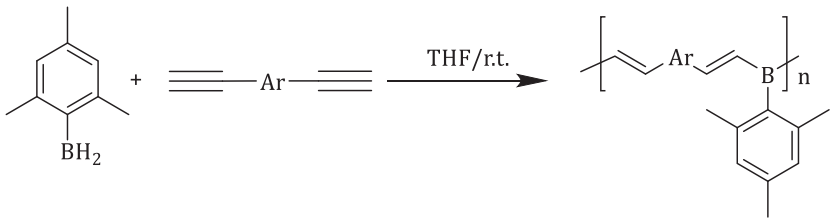

Figure I. 4: Hydroboration polymerization of aromatic diynes using mesitylborane (Ar=aryl). [16]

The bulky aryl groups hinder attack of nucleophiles at boron and thus affect high stability to oxygen and moisture. These polymers are soluble in common organic solvents allowing to easily estimate the molar masses by size exclusion chromatography (SEC) versus polystyrene (PS) standards. An average of 41 repeating units has been measured for the polymer obtained in Figure I. 4 with Ar=Phenyl corresponding to M_n=10,500 g/mol. For a series of aryl groups, ^{11}B NMR chemical shifts of ≈31 ppm were recorded.

Wagner, Holthausen, Jäkle and co-workers studied conjugated polymers with 9,10-dihydro-9,10-diboraanthracene as a building block. The latter was synthesized by reaction between 9,10-diboromo-9,10-dihydro-9,10-diboraanthracene and an excess of $HSiEt_3$ under ultra-sonication. This polymerization path is described in Figure I. 5. [27]

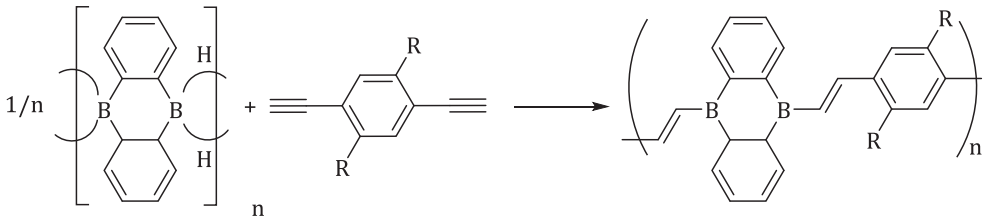

Figure I. 5: Hydroboration polymerization of 1 4-diethynylbenzenes with 9,10-dihydro-9,10-diboraanthracene. R=H: C_6H_6, R.T.; R=OC_6H_{13}: Toluene or THF, R.T. [27]

In order to maximize π-overlap between boron and the aromatic substituents, and to ensure stability by incorporation of boron into a ring system, the rigid and planar diboraanthracene was the perfect candidate. The diboraanthracene precursor is interesting on its own right because it adopts a polymeric structure in the solid state as a result of two-electron-three-center B-H-B bridges. [27]

Jäkle and co-workers took an interest on tin-boron exchange reactions as a potentially milder and more selective polymerization method. [8] In this research, the polycondensation process occurs between a bifunctional haloborane and a ditin species as presented in Figure I. 6.

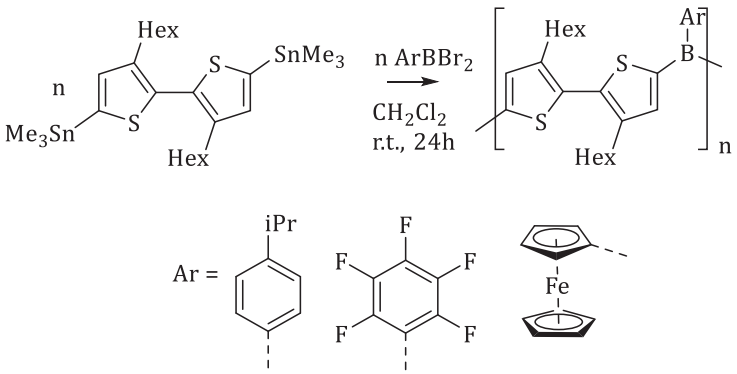

Figure I. 6: Synthesis of Boron-Modified Polythiophenes by Jäkle. [8]

One main advantage of these polymerizations is the possible use of non-coordinating solvents such as dichloromethane or toluene, avoiding the need of ether solvents that tend to react with highly Lewis acidic borane centers through Lewis pair interactions or cationic polymerization (for instance, ring-opening polymerization of tetrahydrofuran). This strategy was also studied by Jia and co-workers using the diboron building block 9,10-dibromo-9-10-dihydro-9,10-dibromaanthracene in combination with phenylene or perfluorophenylene bridging moieties as shown in Figure I. 7. [28]

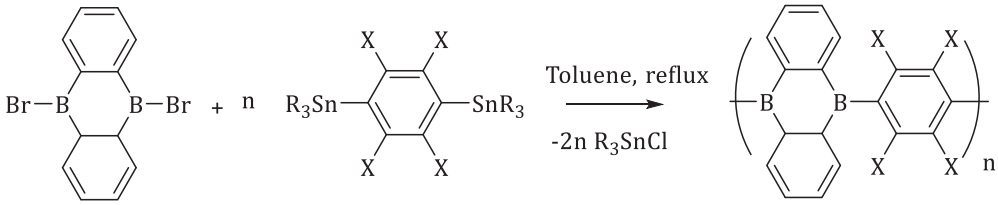

Figure I. 7: Polycondensation studied by Jia and co-workers. X=H or F. [28]

Bonifácio and co-workers presented a complete different strategy of synthetizing those polymers. They first prepared the organoboron monomers, which were then copolymerized with 2,7-dibromo-9,9-di-n-octylfluorene presented in Figure I. 8. SEC analysis showed high molar masses of M_n=22,900 g/mol relative to PS standards. The response of these copolymers toward a series of anions was evaluated in photoluminescence quenching measurements. [19]

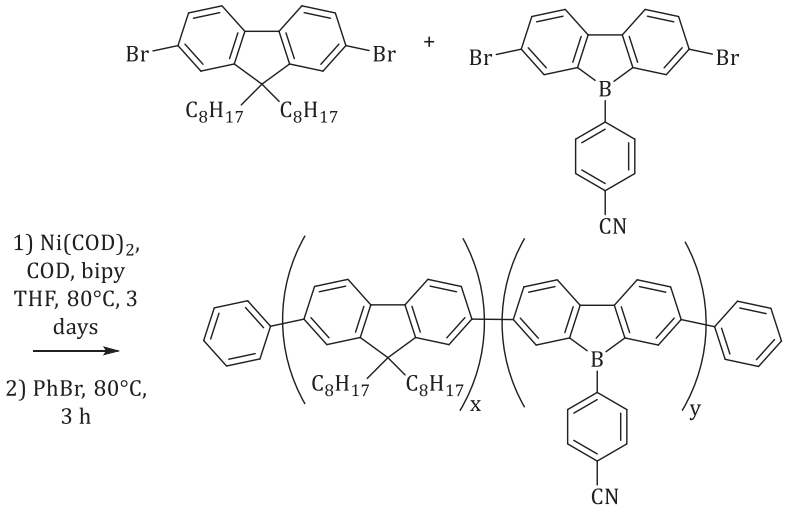

Figure I. 8: Synthesis of random flurorene/dibenzoborole copolymer by Bonifácio and co-workers. [19]

B. Side-chain functionalized polyolefins with boron-carbon bonds

Side-chain functionalized organoboron polymers are prepared through a variety of polymerization techniques such as free radical polymerization, metathesis polymerization or Ziegler-Natta polymerization. Anionic polymerization is generally not used for the polymerization of organoboron monomers since the initiators and propagating species tend to react through nucleophilic attack at the empty p-orbital on boron.

a. Ziegler-Natta polymerization

Chung and co-workers used Ziegler-Natta procedures to obtain homopolymers and random copolymers from boron-functionalized monomers. [29]–[34] Ziegler-Natta catalysts are normally incapable of incorporating functional group because of catalyst poisoning. A new approach for the synthesis of functionalized polyolefins has been investigated *via* borane-containing polymers.

The chemistry of Chung and co-workers has focused on the direct copolymerization of borane monomers and α-olefins with Ziegler-Natta catalysts taking advantage of the stability of the borane groups to transition metal catalysts. Indeed, the linker between the double bonds and the boron-based group is used to space out the functionality away from the active polymerization center. In addition, the borane monomers and thus polymers are soluble in hydrocarbon solvents. This allows for the formation of high molar masses copolymers.

The study presented the copolymerization between 5-hexenyl-9-BBN (BBN=9-borabicyclo(3.3.1)nonane) and propylene under inert atmosphere at ambient temperature using $TiCl_3$ and $Al(Et)_2Cl$. The polymerization was started by the addition of the heterogeneous catalyst mixture to the solution of the two monomers in toluene, as presented in Figure I. 9. 5-hexenyl-9-BBN reactivity was found to follow the same trend as high α-olefins in heterogeneous Ziegler-Natta polymerization: the smaller the size, the higher the reactivity is. However, propylene was preferentially polymerized in the first stages of the copolymerization conducting to a monomer-feed gradient over time. [32]

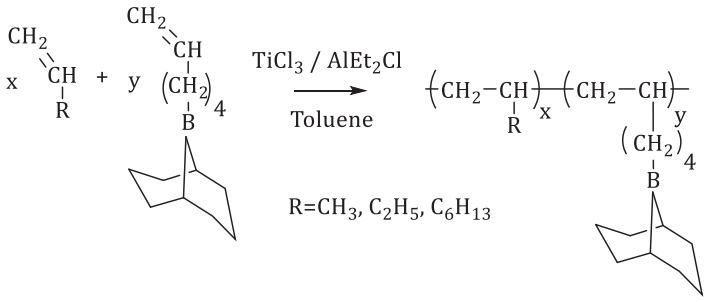

Figure I. 9: Copolymerization of 5-hexenyl-9-BBN and α-olefins by Ziegler-Natta procedure. [32]

b. Metathesis polymerization

Chung and co-workers studied the first ring-opening metathesis polymerization (ROMP) of boron-containing monomers. The monomer exo-B-5-norborn-2-enyl-9-BBN was synthesized by selective hydroboration of 2,5-norboradiene with 9-BBN. The polymerization was then carried out at room temperature in the presence of WCl_6/Me_4Sn with a 2 M monomer solution in toluene during 2 h (Figure I. 10). The ratio used was WCl_6:2 Me_4Sn:100 monomer. [35] Boron-functionalized poly(octadiene) was prepared in a similar way by ROMP of 1,5-cyclooctadiene with $WCl_6/SnMe_4$ in the presence of 1,10-bis(9-BBN)-5-decene used as a chain-stopper agent. [36]

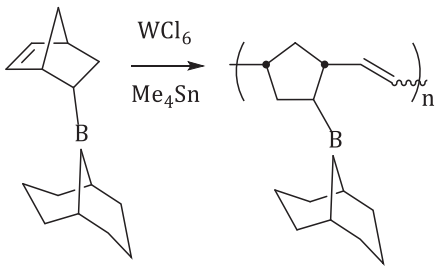

Figure I. 10: Ring-opening polymerization of 9-BBN-norborene. [35]

First and second-generation Grubbs-type Ru catalysts were also used by Sneddon for the ROMP of 6-(norbornenyl)decaborane and 6-(cyclooctenyl)decaborane as depicted in Figure I. 11. Because of their air stability and tolerance to functional groups, Grubbs-type ROMP catalysts are perfect for the synthesis of boron-containing polymers. Polymerization reactions of decaboranyl-substituted norborene and cyclooctene monomers were carried out at room temperature for 1 h in dichloromethane with between 1 and 2 mol % of Grubbs catalyst. Size exclusion chromatography in THF showed M_n of 30,000 g/mol compared to PS standards and $Đ$ between 1.1 and 1.8 typical for ROMP. DSC studies gave glass transition temperatures of polymers in the range of 65-70°C making these polymers excellent candidates for applications requiring molten processing. [37]

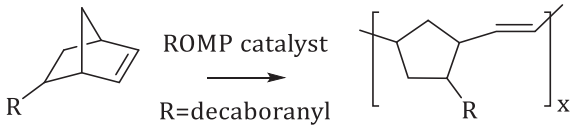

Figure I. 11: ROMP of decaboranyl-substituted norbornene monomers. [37]

c. Post-modification of existing polymers

i. From unfonctionalized polyolefins

Paetzold first studied the path from unfunctionalized polyolefins to organoboron-functionalized polymers. The direct borylation of polystyrene/divinylbenzene resin with the haloborane Br_2BH occurs only under forcing conditions (120-140°C) and is limited by relatively low selectivity. [38]

More recently, Hartwig and Hillmyer reported transition metal catalyzed borylation of polyolefins to obtain boronate-functionalized polymers in a one-step process. A selective functionalization of polyolefins would bypass the challenge of developing highly active polymerization catalysts that incorporate polar monomers. The polymer functionalization was conducted on a model polyolefin (polyethylethylene) with 5 mol % $[Cp^*RhCl_2]_2$ and a 0.25:1 ratio of diboron reagent B_2Pin_2 to polymer for 36 h at 150°C to reach complete conversion with HBPin as side product. The reaction was conducted on neat polymer substrates, which are fluid at the reaction temperatures. The

functionalization is described in Figure I. 12 and is subsequently followed by the oxidation of the boronate ester group to obtain a pendent alcohol group. [39]

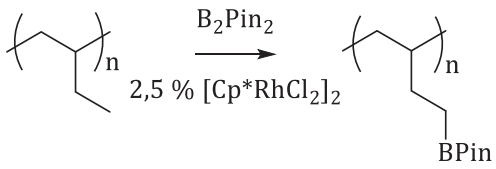

Figure I. 12: Catalytic modification of polyolefins. [39]

ii. From polyolefins containing olefinic groups

Ramakrishnan showed that the borylation of ROMP polymers is possible in the presence of an excess of 9-BBN-H and a tungsten-based catalyst in THF at 50-70°C for 18-24 h. (Figure I. 13) The yield in all cases is greater to 95 %. In the C12 case, higher temperature was used to ensure that the polymer was completely soluble in the beginning. [40]

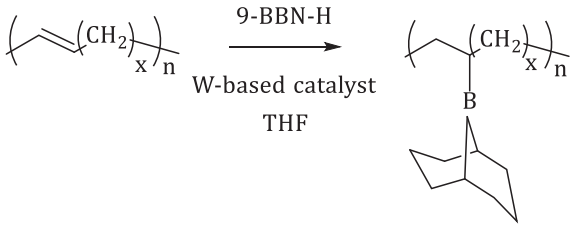

Figure I. 13: Borylation of ROMP polymers in presence of 9-BBN. [40]

Similarly, Chung used butyl rubber as a precursor to boron-functionalized polymers through hydroboration with 9-BBN-H. Hydroboration was carried out by adding 9-borabicyclononane into a polymer solution in THF as described in Figure I. 14. Owing to the good solubility of borane reagents and borane containing polymers, the hydroboration reaction of the polymer is very similar to those of small organic compounds. To ensure complete hydroboration, the reaction was run at 65°C for 5 h. The reaction is quite effective and the concentration of borane groups in the polymer can be controlled by the quantity of borane reagents used. This strategy was subsequently followed by the selective oxidation of the hydroborated product. The final grafted copolymers were used as compatibilizers in polyisobutylene blends. [41]

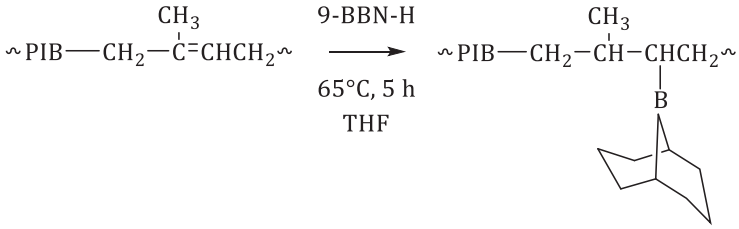

Figure I. 14: Hydroboration of butyl rubber conducted by Chung and co-workers. [41]

Hydroboration chemistry has also received attention for chain-end functionalization. Chujo and co-workers showed that the hydroboration of the terminal double bond of styryl-terminated polystyrene with thexylborane gives a polymer with an organoboron unit at the center of the polymer. Thexylborane was reacted with two molar equivalents of styryl ether as described in Figure I. 15. The resulting organoboron polymers showed unimodal distribution of chain length by SEC. The same result was demonstrated from the reaction between 1-decene and thexylborane. [42] Besides, Chung used the hydroboration path on vinyl-terminated polypropylene with 9-BBN-H in THF allowing for high degrees of functionalization. [43] Ganesan and co-workers recently reported the preparation of polymer-supported 9-BBN from a high-loading Merrifield resin. [44]

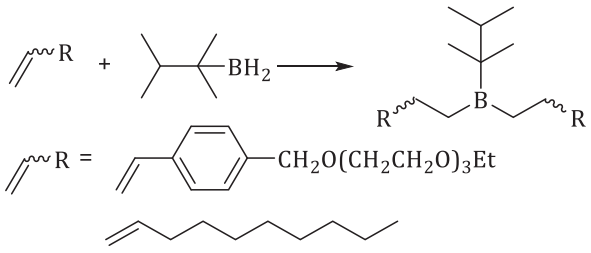

Figure I. 15: Hydroboration of styryl terminated polystyrene. [42]

Hydroboration was also applied to polydienes such as polybutadiene and polyisoprene for instance in the work of Pinazzi and co-workers. They reported the treatment of these polymers with an excess of bis-boracyclanes (i.e. disiamylborane, 9-BBN, dis(dimethyl-3,5-borinane), bis(dimethyl-3,6-borepane), bis-borinane) in THF. A quasi-selective conversion of 1,4-polydienes has been obtained contrary to 1,2- and 3,4-polydienes with a selectivity lower than 50 %. The hydroborated polymers were then converted to functionalized polymers by oxidation. [45], [46] In another study by Chung *et al.*, they described the preparation of homogeneously functional polymers with narrow molecular weight distribution involving the hydroboration of polydienes, especially 1,2-polybutadiene. The reaction was performed under vacuum at -10°C for 1 h with 9-BBN as the hydroboration agent. They established in this work the order of hydroboration activity as 1,2-polybutadiene > 1,4-polybutadiene > 1,4-polyisoprene. As well as previously, the modified polymers were also oxidized to obtain a variety of functional polymers. [47]

Furthermore, Smith *et al.* reacted a brominated polystyrene with n-BuLi in benzene followed by addition of the bulky fluoroborane $Trip_2BF$ (Trip=2,4,6-tri-isopropylphenyl) in THF as presented in Figure I. 16. The resulting triarylborane-functionalized polymer was converted to the lithium hydroborate resin with t-BuLi for use in the stereoselective reduction of ketones. [48]

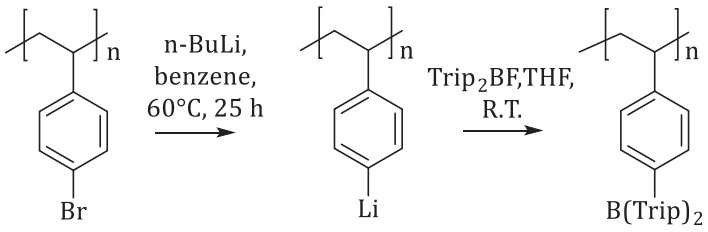

Figure I. 16: Functionalization of polystyrene with triarylborane. [48]

Another path of incorporation of borane moieties into polymers is through boron-oxygen and boron-nitrogen bonds. These polymers can be synthesized by polycondensation or by polymerization of boron-containing monomers. The possibility of reversible formation of polymeric materials *via* dynamic covalent bonds is one aspect that hooked scientific attention in the past few years.

III. Synthesis of polymers containing Boron-Nitrogen bonds

In this part, polymers containing boron-nitrogen bonds in the main chain or in the side chain are described. On the one hand, the boron atom is willingly introduced to modify the electronic properties of π-conjugated polymers thanks to its electronic vacancy. On the other hand, boron-nitrogen bonds-containing polymers harness the Lewis acid-base interactions and dynamics implied.

A. Main-chain functionalized polymers with boron-nitrogen bonds

Incorporation of B-N linkages into a heterocyclic ring-system is attractive due to the stabilizing effect. Polymers containing diazaborole units in the main chain are the earliest examples of boron-containing polymers and were first reported by Marvel and co-workers in 1962. The polymers were obtained by condensation of aromatic diboronic esters with 3,3'-diaminobenzidine, presented in Figure I. 17. The high thermal stability up to 500-600°C for the phenylene derivative is remarkable. Nevertheless, these polymers were sensitive to hydrolytic degradation and were not further investigated. [49]

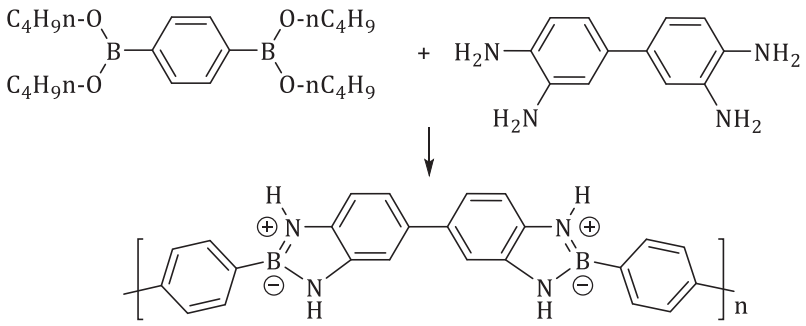

Figure I. 17: Synthesis of polymer systems containing B-N linkage into a heterocyclic ring. [49]

Transition metal-catalyzed coupling procedures have been successfully conducted more recently. [18], [20] This method is applicable to the polymerization of boron monomers in which boron is stabilized by tetracoordination and incorporated into a cyclic system. [21] As an example, Yamaguchi *et al.* obtained oligomers comprising a recurring benzodiazaborole unit by the Pd-complex-catalyzed polycondensation in Figure I. 18 with bis(tributyltin) and bis(tributylstannyl)acetylene. UV-visible spectroscopy proved the expansion of the electron system through the B-C and B-N bonds of the oligomers. The polymers were synthesized in high yields with molar masses of M_n=5,560 g/mol relative to PS standards and were stable up to 355°C according to TGA measurements under nitrogen atmosphere. [50]

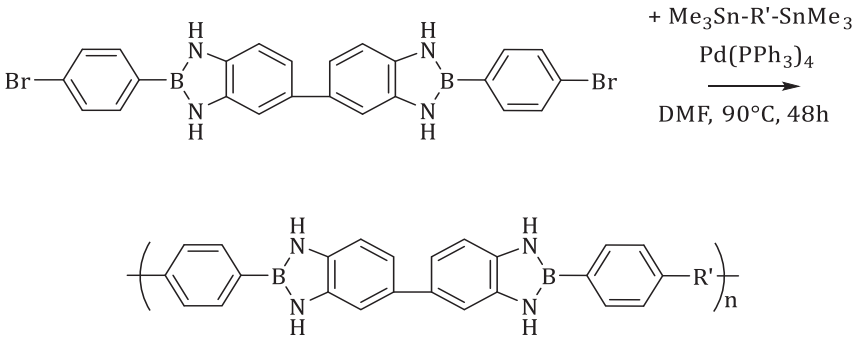

Figure I. 18: Synthesis of bisbenzodiazaborole oligomers by Yamaguchi et al. [50]

Similarly to conjugated main chain-type organoboron polymers with B-C bonds, conjugated main chain-type organoboron polymers with B-N linkages are used in optoelectronic devices (OLEDs, FETs, photovoltaics) and in sensory applications. [22]

The incorporation of tetracoordinate boron in the main chain can be advantageous for improved stability of the resulting polymer thanks to the chelating effect and electronic saturation of Lewis-base interaction. Interesting photophysical properties are obtained when a donor-acceptor structure is formed with an alternance of chromophores and organic π-systems.

Pyrazaboroles are an important class of boron-nitrogen heterocycles and they are known for their high stability. Wagner and co-workers have explored them as building blocks of supramolecular structures. [51]–[53] Chujo worked on the synthesis and properties of polymers that contain pyrazabole moieties in the main chain by Sonogashira-Hagihara coupling polymerization between iodo-functionalized pyrazaborole and di-alkyne monomers. (Figure I. 19) [54]

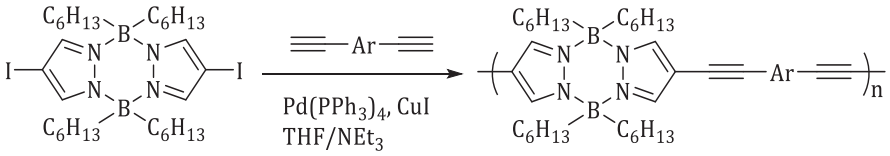

Figure I. 19: Polymers containing pyrazaborole studied by Chujo. [54]

Relatively high molar masses were achieved with M_n up to 34,000 g/mol relative to PS standards. However, no significant red shift in the UV-vis absorption was obtained compared to the molecular analogue. This result was consistent with a lack of extension of π-conjugation *via* the pyrazabole moiety due to tetracoordinate boron centers. It was possible in some extent to tune the UV emission by incorporating different groups into the polymer. These polymers are thus expected as new optical materials with near-UV emissions. [54]

Jäkle and his team used polymer modification to incorporate an organoboron quinolate moiety into a polymer main chain. In their work, they treated a bromoborane polymer precursor with methyl-protected quinolato ligands under mild conditions. This strategy allows for the control of

the molar masses predetermined by the number of repeating units of the prepolymer. For the synthesized polymer represented in Figure I. 20, M_n varied between 7,900 and 10,800 g/mol compared to PS standards depending on the nature of the R group. The 4-dimethylaminophenyl pendent group leads to a strong bathochromic shift resulting in a very weak red emission. [55]

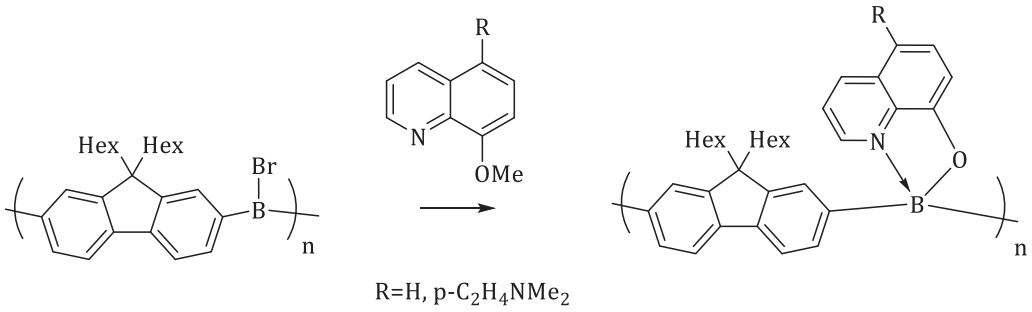

Figure I. 20: Post-modification of a bromoborane polymer with a quinolate moiety. [55]

The same team introduced another method for the preparation of polymer comprising boron and quinolate moieties in the main chain *via* polycondensation involving boron-induced ether cleavage between methyl-protected bifunctional hydroxylquinolate ligands and a bifunctional bromoborane. This polymerization was found to be spontaneous under mild conditions without the need of any catalyst with methyl bromide as a side product. The nature of the linker Ar (Figure I. 21) modifies the photophysical properties of the polymer. For instance, with a highly delocalized Th-C_6H_4-Th linker, the lowest energy absorption corresponds to intramolecular charge transfer from this conjugated linker to the pyridyl moiety. In the case of the less delocalized diphenyl linker, intramolecular charge transfer occurs from the fluorene moiety of the diboron monomer to the pyridyl rings and the resulting polymer shows a strong yellow-green emission. [55], [56]

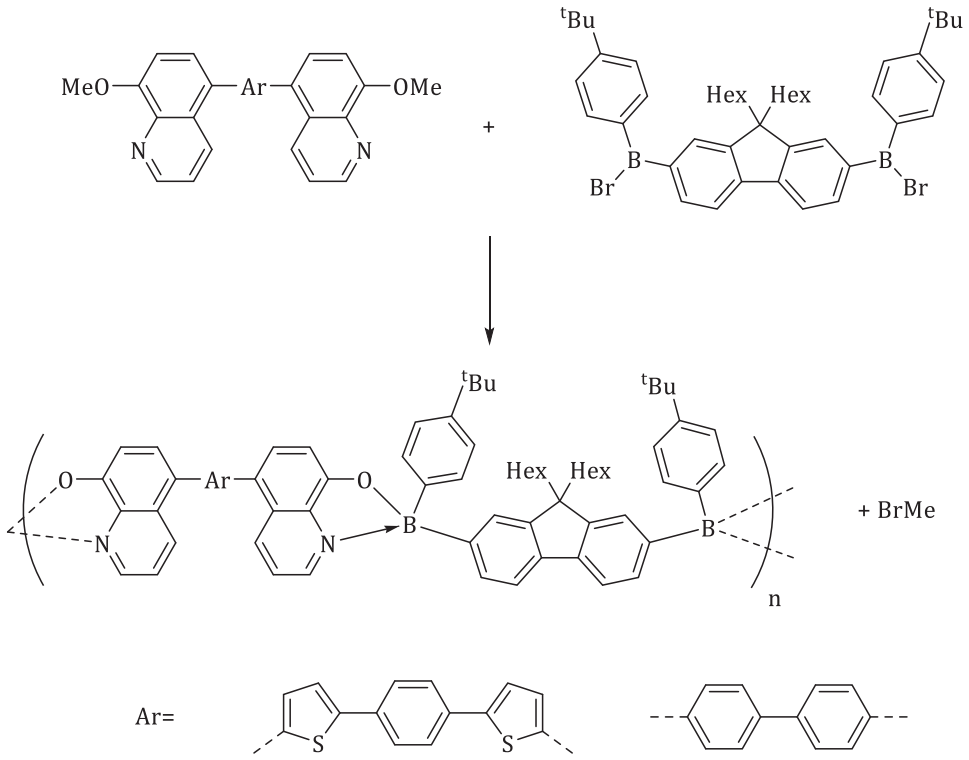

Figure I. 21: Spontaneous polycondensation of bifunctional hydroxyquinolate and bifunctonal bromoborane. [56]

Li and co-workers reported the incorporation of 4,4-difluoro-4-bora-3a,4a-diaza-s-indacene (BODIPY), a boron-based chromophore, into a phenylene ethylnylene conjugated polymers *via* Sonogshira-Hagihara couplings as illustrated in Figure I. 22. [57] BODIPY is widely used thanks to its high stability under ambient conditions, its strong luminescence and the possible tuning of the emission color through substituents on either boron or the pyrrolic ring systems. The molar masses obtained were quite low M_n=1,700-6,000 g/mol compared to PS standards. Concerning the photophysical properties, the resulting polymers exhibit red emissions attributed to BODIPY-centered π-π* transitions that are strongly red-shifted due to the extension of π-conjugation at the pyrrolic 2,6-positions. Besides, the exact emission color depends on the electronic structure of the conjugated dialkyne precursor studied that affects the extension of the conjugation. [58]

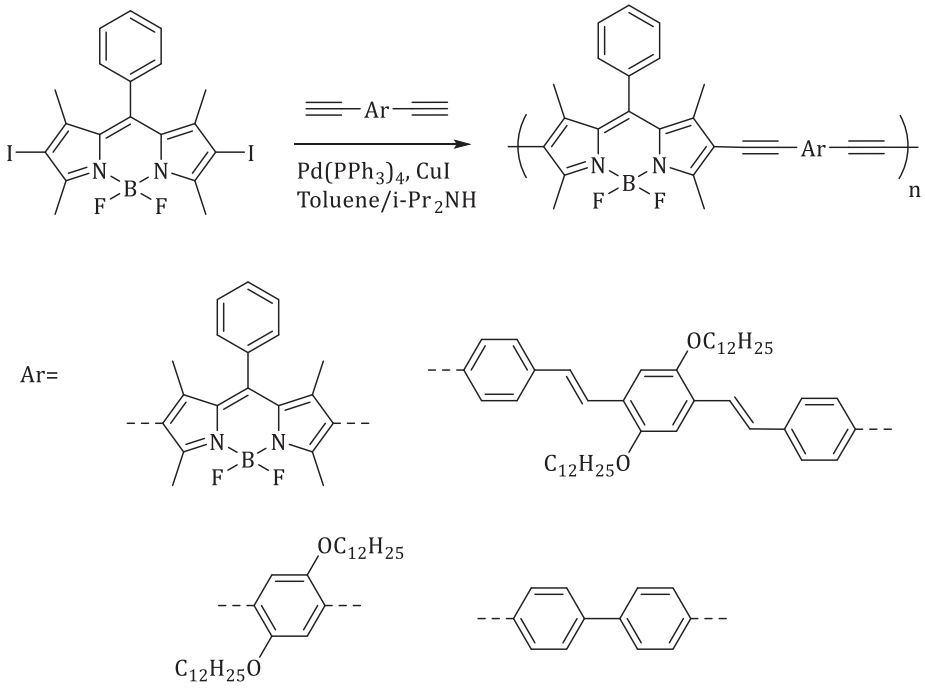

Figure I. 22: Incorporation of BODIPY moieties into conjugated polymers by Li and co-workers. [57]

Harnessing the Lewis acid properties of boron, Manners and co-workers reported the synthesis of high molar masses boron-nitrogen macromolecules, isosters of polyolefins and commonly called polyaminoboranes. They used iridium-catalyzed dehydrocoupling of aminoboranes or N-alkyl amine-boranes analogues, using the Brookhart's Ir(III) pincer complex IrH_2POCOP as a precursor. (Figure I. 23) Indeed, a recent focus in amine-boranes as hydrogen-storage materials shows a growing interest conducting to the developments of improved dehydrocoupling catalysts. [59]

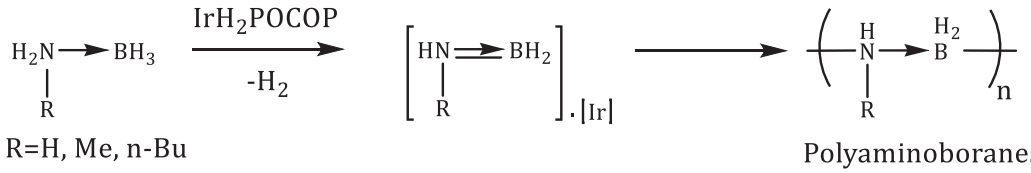

Figure I. 23: Synthesis of polyaminoboranes from amine-boranes by Iridium catalysis. [59]

Raynaud and Lacôte recently described the one-step polycondensation of diamines and diboranes comprising bis-hydrogenated nitrogen and boron atoms by the in-situ deprotonation of the diammonium salts and concomitant reduction of bisboronic acids with $LiAlH_4$. This reaction leads to the assembly of polymer chains through Lewis pairs in their backbone. These polymers, whose structures are represented in Figure I. 24, were investigated as reactive materials in hydrogen-transfer reactions based on ammonia-borane chemistry. Thus, they were found to hydrogenate imines, aldehydes and ketones under mild conditions and perform better than their molecular analogues. [60], [61]

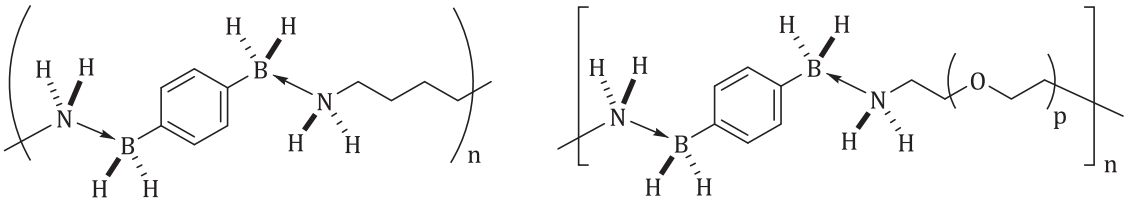

Figure I. 24: Polyboramines synthesized by Raynaud and Lacôte. [61]

Chujo and Matsumi studied polymers with aminoboranes in the main chain taking advantage of alkoxyboration of aliphatic or aromatic diisocyanate derivatives with dialkoxyborane species, firstly described by Cragg, Lappert and Tilley to form a special analogue of polyurethane. [62] As an example, in Figure I. 25, reaction of mesityldimethoxyborane with 1,6-hexamethylene diisocyanate in bulk at 140°C resulted in a soluble polymer with M_n=6,700 g/mol relative to PS standards. The bulky mesityl group on the boron atom proved critically important for the successful preparation of soluble polymers and their hydrolytic stability. [63]

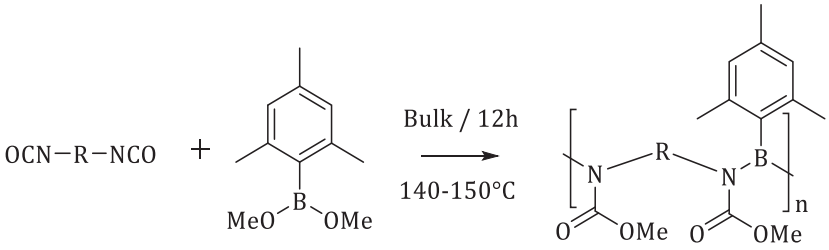

Figure I. 25: Synthesis of aminoborane polymers by Chujo and Matsumi. [63]

Wagner and co-workers presented one example of polymers bearing boron-nitrogen heterocycles in the main chain in the 1990's with the preparation of a series of ferrocene-containing B-N macrocycles. The incorporation of transition metal complexes into conjugated organoboron polymers is exciting due to the additional d_π-p_π conjugation and the possibility for redox tuning of the properties of the conjugated polymers. They demonstrated that donor-acceptor reactions could form dynamic boron-based polymers, which is very relevant to the use of Lewis pairs to structure macromolecular architectures. [51], [64] This postulate constitutes the premises of this PhD work. Equimolar reaction of 1,1'-bis(dimethylboryl) ferrocene with aromatic diamines, such as pyridine or 4-4'-dipyridine, led to spontaneous and reversible formation of one-dimensional coordination polymers, as demonstrated in Figure I. 26.

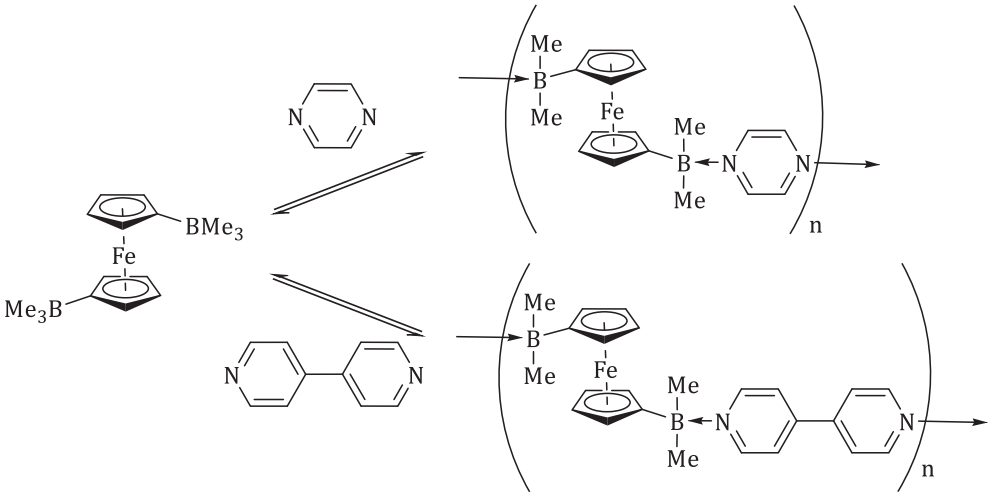

Figure I. 26: Coordination poly(ferrocene)s bridged by pyridine and bipyridine. [64]

The intense colors of the polymers in Figure I. 26 arise from charge transfer processes from the electron-rich ferrocene to the electron-deficient boron bound heterocycles. In solution, equilibrium takes place and complete dissociation occurs at temperatures above 85°C in toluene. [64] Other examples of organoboronate polymers from donor-acceptor reactions with 4,4'-bipyridine can be found in the work of Severin *et al.* [65]

In another fashion for the incorporation of transition metal complexes into conjugated organoboron polymers, Manners and Braunschweig synthesized ferrocenylborane polymers *via* ring-opening polymerization of boron-bridged ferrocenophanes in Figure I. 27. However, the solubility of such polymers is moderate in usual solvents such as benzene. [66]

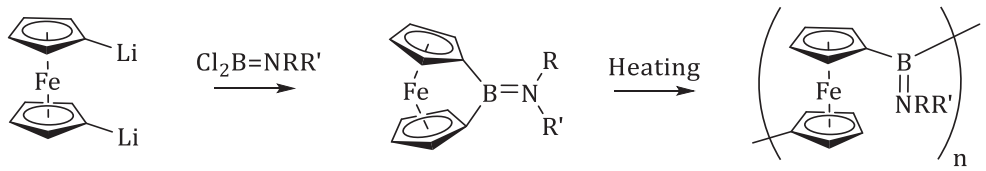

Figure I. 27: Synthesis of ferrocenylborane polymers by Manners and Braunschweig. [66]

B. Side-chain functionalized polyolefins with boron-nitrogen bonds

In literature, monomers functionalized with functional groups bearing boron-nitrogen bonds were also polymerized such as vinylborazines, vinylphenylborazines and vinyl-functionalized boranes. Several examples are discussed in this part.

Pellon *et al.* pioneered the polymerization of vinyl monomers containing boron with a first example in 1961 focusing on B-trivinyl-N-triphenylborazine and B-triallyl-N-triphenylborazine. Free radical polymerization was used for the polymer syntheses and gelation was observed due to the vinyl polyfunctionality of the monomers. [67]

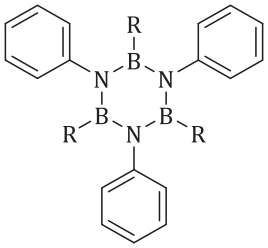

R=-$CH_2CH=CH_2$ B-triallyl-N-triphenylborazine (TAB)
R=-$CH=CH_2$ B-trivinyl-N-triphenylborazine (TVB)

Figure I. 28: Structure of vinyl borazine monomers studied by Pellon et al. [67]

In following studies, Sneddon and co-workers reported the syntheses and properties of poly(B-vinylborazine). B-vinylborazine has been found to polymerize in solution *via* free radical polymerization using AIBN as initiator at 80°C to afford soluble polymers in usual solvents. A small fraction of the high molar masses polymers consisted of branched or lightly cross-linked polymer chains that were assumed to result from dehydrocoupling on the borazine ring as illustrated in Figure I. 29. Applying the same method, copolymers from styrene and B-vinylborazine have also been prepared and exhibited branchings between the polymer chains due to the presence of B-vinylborazine. The latter was thus categorized as a branching agent by the authors. [68], [69]

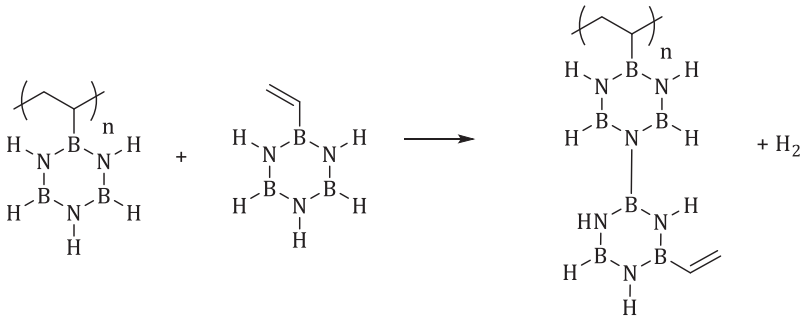

Figure I. 29: Polymers based on B-vinylborazines and branching due to dehydrocoupling reactions. [68], [69]

In the same years, Jackson and Allen presented the preparation [70] and the homo- and copolymerization of vinylphenylborazines focusing on p-vinylphenylcyclotriborazine monomers. [71] They used free radical polymerization with 2 % of AIBN as initiator and benzene as solvent at 60°C. In this study, they also identified a crosslinking involving alkylborazines that hindered the preparation of linear polymers with pendent organoborazine rings.

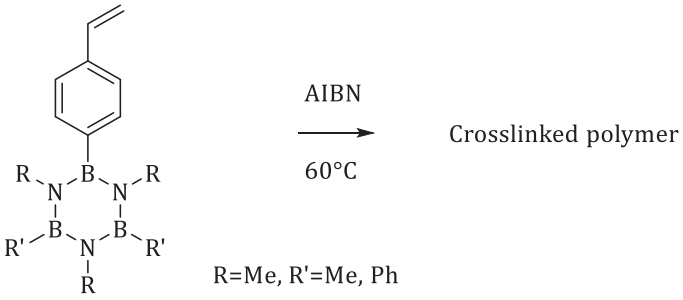

Figure I. 30: Polymerization of vinylphenylborazines studied by Jackson and Allen. [71]

As aforementioned in the case of main-chain organoboron polymers, polymers functionalized with chromophores are attractive due to optic and electronic properties. With the strategy of designing the monomers with convenient functions, BODIPY dyes have been incorporated into polyolefins by attachment to methacrylate groups and subsequent copolymerizations with other monomers. In this fashion, the same Chujo and co-workers reported the homo- and copolymerization of a methacrylate monomer derived from a luminescent difluoro- or dialkynyl-BODIPY derivative. RAFT polymerization was performed to control the molar masses of the resulting functionalized poly(methyl methacrylate) in the first step and then the second styrene block was added to the copolymer. The synthetic path is presented in Figure I. 31. The final copolymer showed a molar masses of M_n=59,300 g/mol with a dispersity ($Đ$) of 1.41. [72]

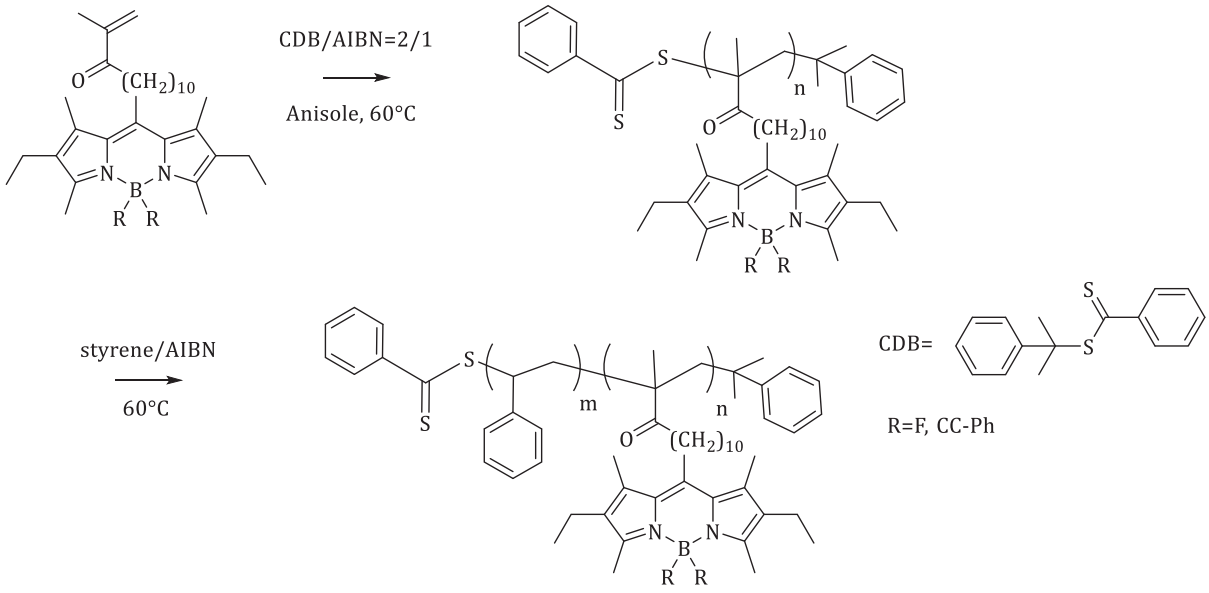

Figure I. 31: RAFT copolymerization of BODIPY-functionalized methacrylate monomer with styrene. [72]

To afford such polymers, post-modification by substitution reactions to install quinolate moieties on pre-synthesized polymers were widely used by Jäkle and co-workers. For instance, they firstly reported the preparation of quinolate-functionalized organoboron polymers *via* alcoholysis of B-aryl substituents on pendent groups of polyolefins (Route A, Figure I. 32). [73] In a second study, they took advantage of the high selectivity of Sn/B exchange reactions of aryldibromoboranes

with phenyl trimethyltin derivatives to synthesize quinolate-functionalized organoboron polymers (Route B, Figure I. 32). [74] These methods allow for the formation of high molar masses organoboron polymers almost fully functionalized (> 95 %) that are highly soluble in organic solvents. Besides, the emission characteristics of these polymers are tunable by varying the substituent R. They were thus able to cover almost the entire visible spectrum from blue to red emission. [73], [74] Another path was chosen by Weck and co-workers to afford side-chain functionalized quinolate polymers *via* the treatment of hydroquinoline-functionalized polymers with triphenylborane. [75]

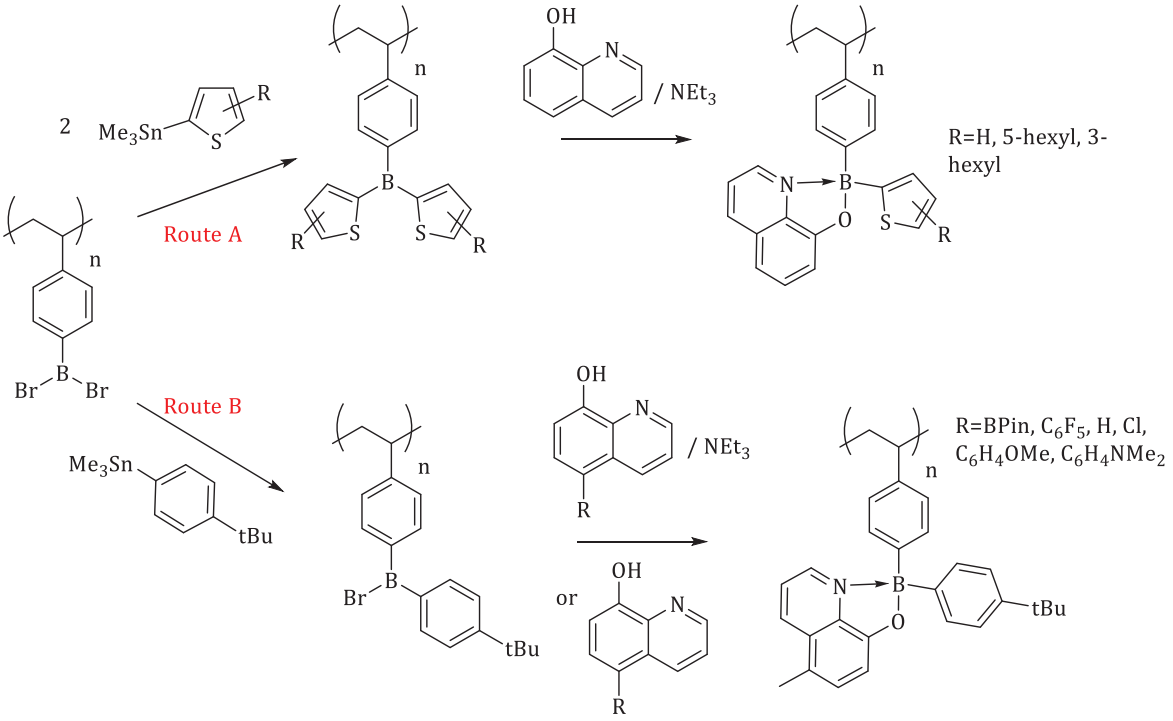

Figure I. 32: Post-modification of dibromoborane polymers for the preparation of quinalote-functionalized organoboron polymers. [73], [74]

Concerning the polymers containing boron-carbon or boron-nitrogen bonds, two main approaches have been adopted in the results reported above. On the one hand, boron has been introduced in macromolecular architectures through ring-opening polymerization or coupling reactions to afford π-conjugated polymers. The deficient nature of the boron atom induces modification of the electronic properties of the materials. This feature has been harnessed to obtain optoelectronic devices. On the other hand, synthesizing boron-based polymers has been a platform for the post-modification of polymers by nucleophilic attack and thus has opened the path to a wide variety of polymers. In recent works, it has also been demonstrated that polymers with boron-nitrogen bonds in the main chain can arise dynamic networks through donor-acceptor interactions. A huge variety of structures has been assessed in literature to find new properties of these attractive hybrid organic/inorganic materials.

IV. Synthesis and applications of polymers containing Boron-Oxygen bonds

This part will be further developed as it is at the heart of the research reported in this manuscript. The interests in incorporating boron-oxygen bonds will be discussed in terms of reactivity of the functional groups studied. Then, the syntheses of polymers comprising boron-oxygen linkages will be described. In a last part, the applications of these polymers, especially in chemo-sensing, will be illustrated.

A. Interests of boron-oxygen bonds in polymers

a. Boronic acid reactivity

Boronic acids feature trivalent boron atom bonded to alkyl or aryl substituent and two hydroxyl groups R-B(OH)$_2$. [76] They can be formed by the successive hydrolysis of a borane [77] as depicted in Figure I. 33.

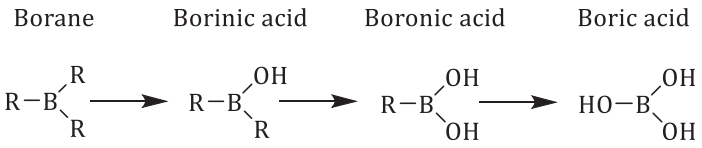

Figure I. 33: Boronic acid from hydrolysis of borane. [77]

Boronic acids can as well be prepared by transmetallation, metal-halogen exchange, transition-metal-catalyzed direct boronylation and coupling of diboronyl species with aryl halides. [76]

Boronic acids exhibit a trigonal planar sp^2-hybridized boron atom with six valence electrons. Boronic acid can suffer oxidation to afford boric acid. In solid state, boronic acid can reorganize into trimer to form the anhydride boroxine, the cyclotrimeric form of boronic acids. (Figure I. 34) They are easily produced by the simple dehydration of boronic acids forming six-member cycles in a very stable form. However, they are rarely used as synthetical products. [78] One of the rare examples of their application is the formation of boroxine cross-linkages to immobilize blue-light emitting oligo-fluorene diboronic acids. [79] In the same fashion, borinic acids can form anhydride dimers called diboroxanes. (Figure I. 34)

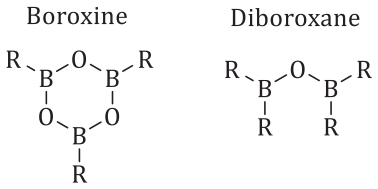

Figure I. 34: Products of trimerization of boronic acid and dimerization of borinic acid. [77]

Boronic acid reactivity is taking advantage of the empty p-orbital of the boron atom resulting in Lewis acidity. Consequently, they form complexes with Lewis bases while the hybridization of the boron center shifts from sp^2 to sp^3 with the boronic acid becoming an anionic and tetrahedral hydroxyl coordinate moiety. [77] In aqueous media, boronic acids are in equilibrium between an undissociated neutral trigonal form and a dissociated anionic tetrahedral form. The reaction of the anionic boronate anion with a diol leads to stable boronate esters. Adding diols to boronic acids in aqueous media shifts the equilibrium to anionic forms. This behavior is useful for diol-responsive materials. The pK_a of boronic acids can range from 4.0 to 10.5. (Figure I. 35) [80], [81]

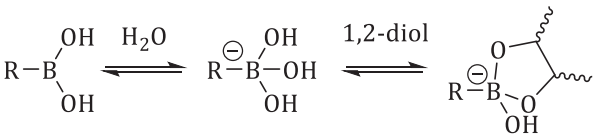

Figure I. 35: Equilibrium of boronic acids in aqueous media. [80], [81]

In biomedical applications, the most used boronic acids are arylboronic acids; nonetheless, a variety of boronic acids can be obtained by tuning the aromatic ring and the associated substituents. Indeed, these modifications affect the pK_a of the boronic acid and the efficiency of ester formation. As an example, benzoxaboroles are cyclic analogues of boronic acids and react similarly toward diols but have lower pK_a values. It can be explained by the release of the ring strain within the B-O heterocycle during the sp^3 hybridization. This work by Benkovic in 2012 is illustrated in Figure I. 36 (a). [82] Wulff and co-workers designed *o*-(dimethylaminomethyl)phenylboronic acid (Figure I. 36 (b)), a boronic-type acid where a nitrogen center adjacent to boron was added and was found to facilitate the formation of boronate esters due to the B-N dative bond. [83] In the same way, a carbonyl adjacent to the boron atom facilitates boron ester formation through an intramolecular B-O-coordinated interaction. In this context, Lowe *et al.* synthesized 2-acrylamidophenylboronate as represented in Figure I. 36 (c) and used it for its ability to bind to glucose. [84] To conclude, these substituents extend the sugar binding properties of the boronic acids to a wide range of pH conditions. [77]

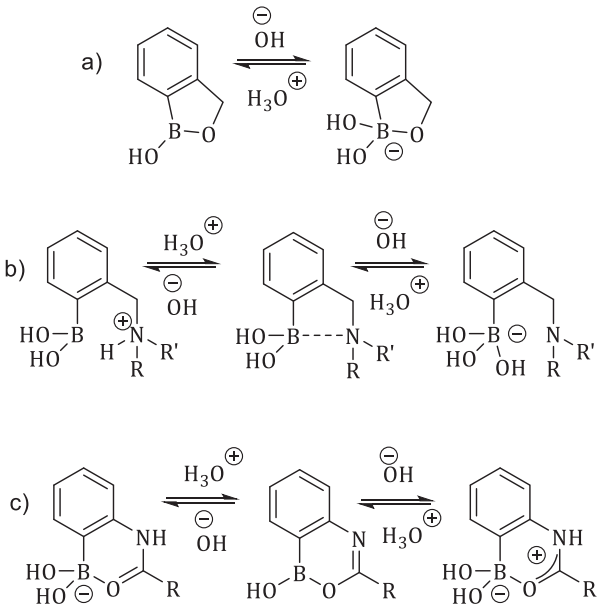

Figure I. 36: Variety of design of boronic acids found in literature. [77]

b. Main boronic acid derivatives: boronate esters

As ester formation can be very efficient, multifunctional boronic acids and diols allows for the synthesis of a wide variety of architectures. The esters formed from the neutral version of boronic acids are less hydrolytically stable than those formed from the boronate species due to the accessibility of the electronic vacancy of the boron atom. [77] These compounds can serve as protecting groups to manage the reactivity of B-C bonds. The synthesis of the boronate esters between boronic acids and diols is described below in Figure I. 37. The process is an equilibrium and the ester formation can be driven by the use of a Dean-Stark apparatus or a desiccant agent in the reaction media. [78]

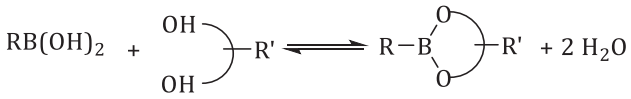

Figure I. 37: Formation of boronate esters from boronic acids and diols. [78]

Boronate esters can be synthesized by transesterification of smaller dialkyl esters with distillation of the volatile alcohol by-product. Besides, cyclic esters from air-sensitive alkylboronic acids can be formed by treatment of a diol with lithium trialkylborohydrides. [85] In 1953, Kuivila and co-workers reported one of the first preparation of boronate esters from diols and polyols. They worked on phenylboronic acid with sugars, such as mannitol and sorbitol, and 1,2-diols like catechol and pinacol. The boronate esters were found to precipitate upon cooling the solution. However, 1,2-cyclohexanediol did not provide the corresponding boronate ester due to the unfavorable geometry. They concluded that, whereas the two diols are not oriented in the same plane in the chair conformation, they adopt a favorable orientation only in the boat conformation,

which is thermodynamically unfavored. [86] These geometric constraints have to be taken into account for the design of reactive moieties.

Moreover, diethanolamine boronate esters represent a useful class of boronate esters. They can be formed in high yields without the need of any dehydration techniques. [87] Weidmann and Zimmerman presented the synthesis of other boronate esters with N-substituted diols. The internal coordination between the nitrogen lone pair and boron vacancy makes the hydrolysis of these compounds less favorable and stabilizes the boron atom against oxidation. [88]

The stability of boronate esters and boronic acids is thermodynamically comparable, thus, hydrolysis can occur in water or by atmosphere exposure. This phenomenon is very rapid for acyclic boronate esters and for less sterically-demanding ones (from ethylene or propylene glycol). [89] On the contrary, hydrolysis can be considerably slowed by hindered cyclic aliphatic esters such as pinacol (Figure I. 38) that is a widely used protecting group to isolate and purify boronic acids being a workhorse of organic chemistry. [86]

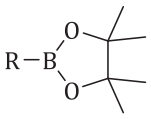

Figure I. 38: Common boronate esters from pinacol.

To have more insights in the chemistry of boronic acid and derivatives, I would recommend the book chapter by Dennis Hall published in 2006. [78]

B. Synthesis of main-chain functionalized polymers with boron-oxygen bonds

In the 1970's, Gerwarth studied the formation of boronate polymers *via* polycondensation of phenylboronic acid and aliphatic diols. He showed that the special characteristic of R-B(OR')$_2$ is the reversible formation and cleavage of the boron-oxygen bonds in the presence of trace amounts of water shown in Figure I. 39. High molar masses polymers could not be obtained, but equilibria involving cyclic species were evident. [90] One can reasonably question this metathesis mechanism from evident steric considerations and the very uncomfortable four-atom transition state postulated.

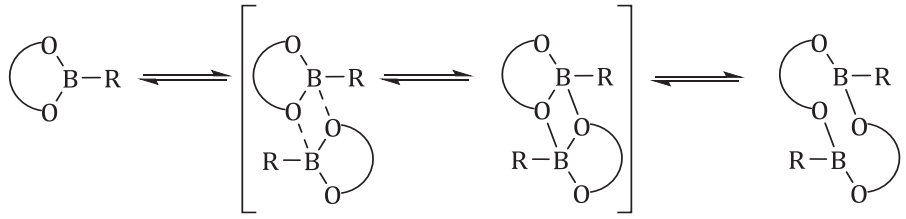

Figure I. 39: Proposed mechanism of reversible cleavage of B-O bonds. [90]

Wagener and co-workers emitted similar observations while studying the polymerization of boronate monomers by acyclic diene metathesis (ADMET). They used molybdenum and ruthenium catalysis to afford ADMET polymers under bulk conditions. However, they faced issues due to ligand-exchange reactions within the boronate moiety that drastically affected the long-term stability and solution characterization of the polymers. They thus assumed the existence of a competition between the metathesis polymerization and the ligand-exchange reaction. This competition is represented in Figure I. 40. [91]

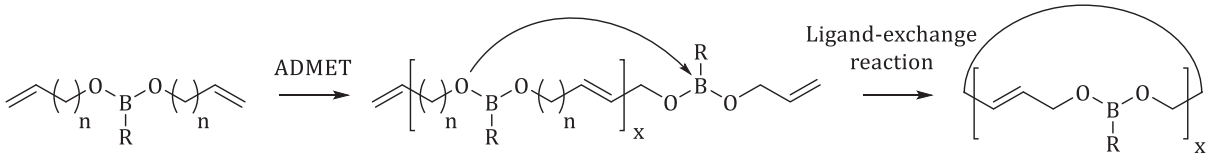

Figure I. 40: Representation of the metathesis polymerization followed by ligand-exchange reactions. [91]

These mechanisms will be further discussed in the Chapter 3 focused on dynamic organoboron polymers that harness the reactivity of boronate esters. We will present an alternative to the metathesis mechanism and subsequent creation of reversibly crosslinked networks. Indeed, we will focus on how the dynamic character is linked to the mechanism since there is then a way to tune the dynamics knowing the key parameter.

The dynamic covalent assembly of boronate polymers structures has been extensively studied ranging from macrocycles to linear polymers and 3-dimensional networks. These polymers are used for the preparation of covalent organic frameworks (COFs) for applications in gas storage and separation. [92]–[95]

Lavigne and co-workers used 9,9-dihexylfluorene-2,7-diboronic acid as a building block for the preparation of organoborate polymers by condensation in Figure I. 41. They used the ability of boronic acids to form boroxines at high temperature. Molar masses of M_n=10,000-11,000 g/mol versus PS standards were obtained. [96]

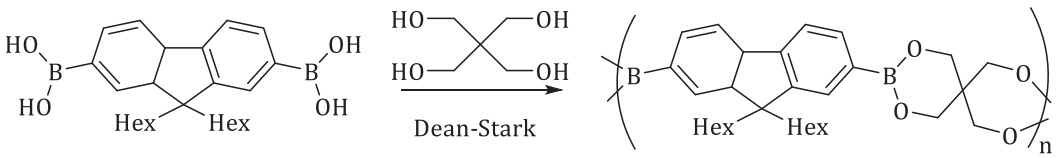

Figure I. 41: Synthesis of organoborate polymers by Lavigne and co-workers in 2005. [96]

In 2008, Trogler and Sanchez used the boronate transesterification to synthesize a borylated fluorescein derivative into a dynamic covalent polymer network in Figure I. 42. The molar masses obtained was M_n=6,700 g/mol relative to PS standards. [97]

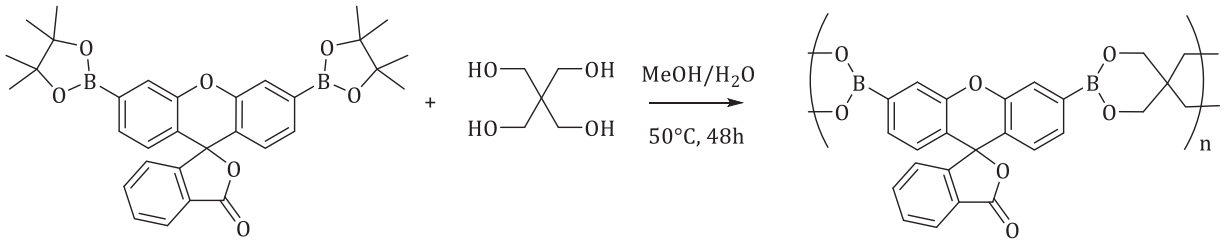

Figure I. 42: Synthesis of poly-3',6'-bis(1,3,2-dioxaborinane)fluoran by double transesterification. [97]

C. Synthesis of side-chain functionalized polyolefins with boron-oxygen bonds

This part focuses on the side-chain functionalized classical polymers including boron-oxygen bonds and how it can be involved in dynamic systems. Several strategies can be used for the synthesis of such compounds: polymerization of classical functionalized monomers or post-modification of existing polymers to staple on boron moieties.

a. Free radical polymerization

Vinylphenylboronic acid, vinylphenylboronic esters and boronate-functionalized acrylamides are polymerized by free radical polymerization thermally induced by AIBN, BPO or potassium persulfate. [98]–[100] 4-vinylphenylboronic acid derivatives [101]–[106] and 3-acrylamidophenylboronic acid [107], [108] can be copolymerized with a variety of other monomers such as styrene, vinylpyrrolidone, acrylonitrile, maleic and citraconic anhydride, N-phenyl maleimide and acryl amides. (Figure I. 43) Some reactivity ratios of boron-based monomers involved in copolymerizations with common monomers are indicated in Table I. 1.

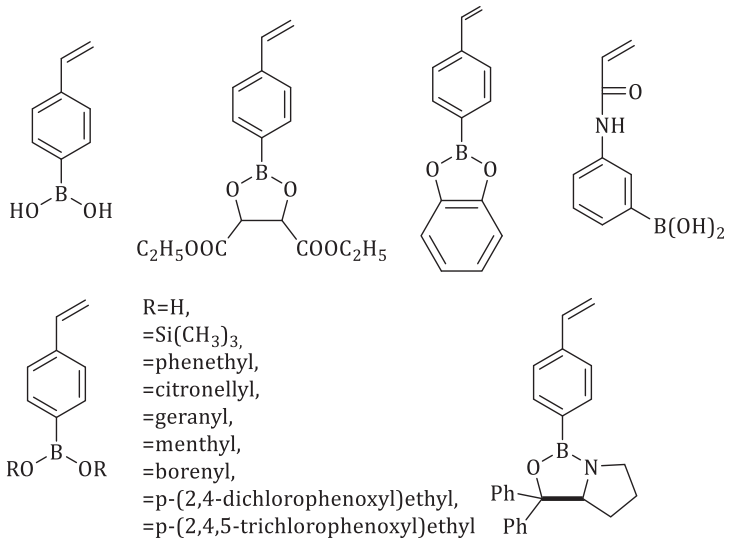

Figure I. 43: Variety of 4-vinylphenylboronic acid derivative monomers successfully (co)polymerized in literature. [102], [107], [108]

Table I. 1: Reactivity ratios from literature of boron-based monomers involved in copolymerizations with classical monomers. [102], [107], [108]

Monomer 1	Monomer 2	Reactivity ratio 1	Reactivity ratio 2
4-vinylphenylboronic acid	Styrene	0.28	0.83
Bis(trimethylsilyl) p-vinylphenylboronate ester	Styrene	0.28	0.87
3-acrylamidophenylboronic acid	N,N'-dimethylacrylamide	0.65	0.54
N-acryloyl-m-aminophenylboronic acid	N,N'-dimethylacrylamide	2.2	0.84

Boronic-acid carrying telomers with sulphide termini were prepared by telomerisation of N,N'-dimethylacrylamide and 3-acrylamidophenylboronic acid using a disulphide species as iniferter (acting as initiator, transfer agent and terminator) under photoirradiation at 365 nm as presented in Figure I. 44. [109]

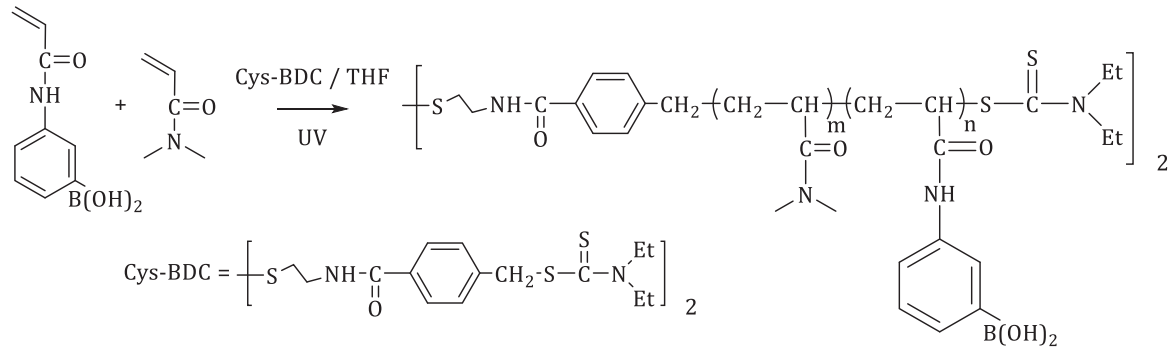

Figure I. 44: Telomerisation of 3-acrylamidophenylboronic acid using an iniferter. [109]

Taking advantage of controlled radical polymerization, Jäkle was able to synthesize boron-containing polymers with defined molar masses. In this optic, Jäkle and co-workers prepared a boron-functionalized block copolymer using atom transfer free radical polymerization (ATRP) from an organoboron monomer. Chain extension of the borylated polymer with styrene gave a block copolymer with borylated PS and unfunctionalized PS. The polymerization conditions were optimized by varying monomer concentration, temperature, initiator-to-catalyst ratio and ligand-to-catalyst ratio. The best results were obtained with a ratio of monomer: initiator: catalyst: ligand of 100:1:2:4 at 90°C. The organoboron monomer reactivity was found to be similar to that of styrene with reactivity ratio close to 1. At higher conversion, deviations from ideal behavior were observed due to increase of chain transfer events. Moreover, the molar masses increases linearly with conversion up to 60%, while *Đ* stays low. In a same way, deviations from linearity were noticed at higher conversions with values of the number-average molar masses (M_n) lower than expected but with slightly higher *Đ*. To conclude, the polymerization of this organoboron monomer can be considered as a controlled process until 60% conversion. [110] (Figure I. 45)

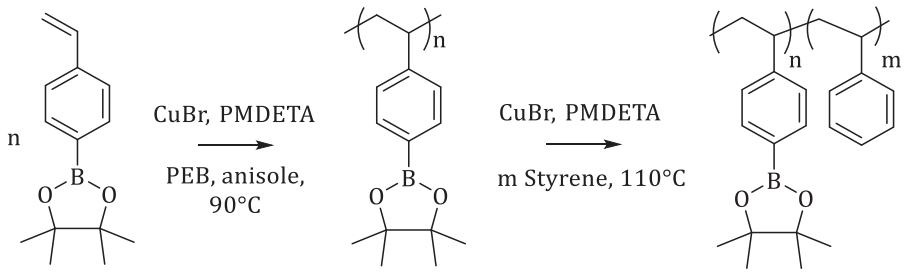

Figure I. 45: Synthesis of the organoboron block copolymer PSBPin-b-PS (PEB=phenylethyl bromide and PMDETA=N,N',N',N'',N''-pentamethyldiethylenetriamine). [110]

Oxazaborolidine-modified polymer microgels have also been described and used as new catalyst support for the enantioselective reduction of prochiral ketones. The preparation of these polymers, based on the monomers in Figure I. 46, was conducted by solution polymerization (5 wt % monomer in THF) at 64°C for four days. The approach implied the synthesis of microgels

bearing free boronic acid functionalities followed by their conversion into oxazaborolidines by treatment with chiral aminoalcohols. [7]

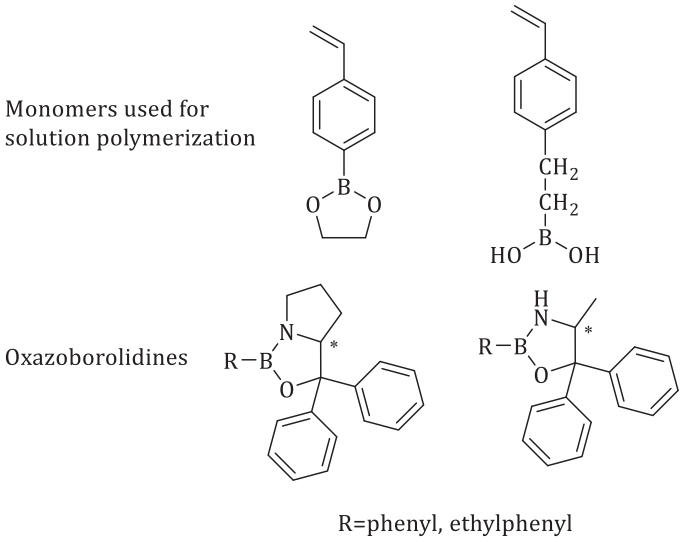

Figure I. 46: Synthesis of polymerized oxaborolidines. [7]

In 2017, at the beginning of this thesis work, Leibler and his team designed copolymers containing pendent dioxaborolane groups and they evidenced a dynamic behavior of these copolymers exhibiting a vitrimer character through metathesis of the dioxaborolanes. They synthesized copolymers from methyl methacrylate or styrene with functionalized monomers carrying dioxaborolane moieties by controlled radical polymerization as illustrated in Figure I. 47. They reported the metathesis of dioxaborolanes taking place without the addition of catalyst at temperatures above 60°C. Through this reaction, the molecules reversibly exchange diols groups, which allows for the synthesis of vitrimers from polymers containing only C-C bonds in their backbones by addition of a bis-dioxaborolane compound as represented in Figure I. 47. [111]

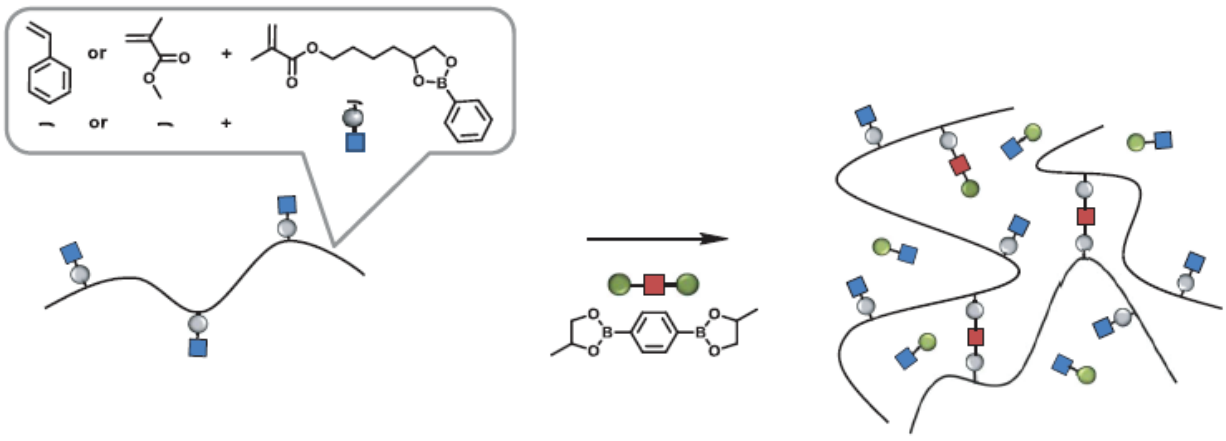

Figure I. 47: Crosslinking of functional polymers with pendent dioxaborolane groups through metathesis with a bis-dioxaborolane. From [111]*. Reprinted with permission from AAAS.*

This article is of high interest and particularly relevant to our work on the synthesis of dynamic organoboron polymers and will thus be further discussed in Chapter 3.

b. Post-functionalization of existing polymers

Post-functionalization is an attractive path for the synthesis of organoboron polymers. It allows for the control of molar masses and degrees of functionalization. These boron-based polymers can be obtained from a variety of polymers that are presented in the following sections.

i. From lithiated polystyrene and poly(methylstyrene)

High degree functionalized polymers with boronic acid can be obtained through Fréchet's three step reaction involving bromation, lithiation and quenching with electrophiles. (Figure I. 48) [112] This method has been widely used in the functionalization of styrenic resins. [113]–[116]

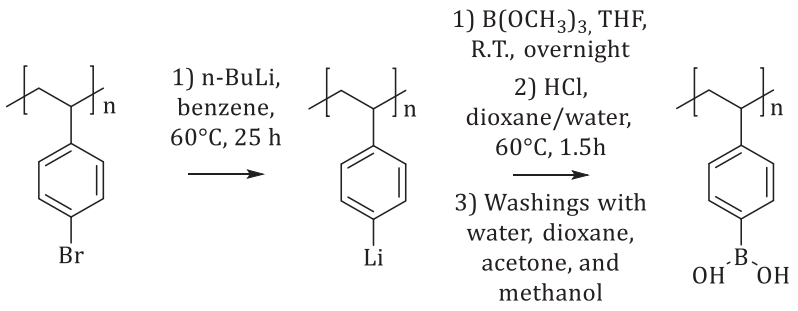

Figure I. 48: Functionalization of stryrenic resins by Fréchet. [112]

In some cases, the polystyrene boronic acid intermediate can be transformed into oxazaborolidines that are used as catalysts in organic reactions. The reaction is conducted by addition of diols in toluene. [106], [113], [117], [118] Nevertheless, if this method is applied to the preparation of soluble organoboron polymers, significant crosslinking is commonly observed probably due to the formation of a small amount of diarylborane residues during the borane treatment. [117] Another possibility inducing the crosslinking could be the dehydration and subsequent formation of boronixes. The polymerization of organoboron monomers can be advantageous to avoid this issue as seen in Figure I. 49. [106]

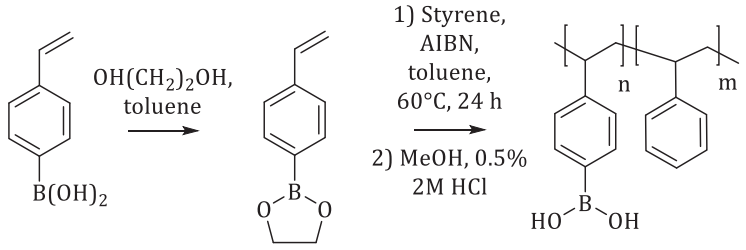

Figure I. 49: Transformation of polystyrene boronic acid into oxazaborolidines followed by polymerization of organoboron monomers. [106]

ii. From mercuriated polystyrene

Thorpe and co-workers converted mercuriated polystyrene **1** [119], [120], polythiophenes **2** [121], poly(N-vinylcarbazole)s **3** [122] and poly(acenaphthylene)s **4** [123] to the respective boronic acid-appended polymers. The mercuriated group is used to do the C-H bond activation; however, this can be considered as nasty chemistry with the use of mercuriated salts. All those modifications are related in Figure I. 50.

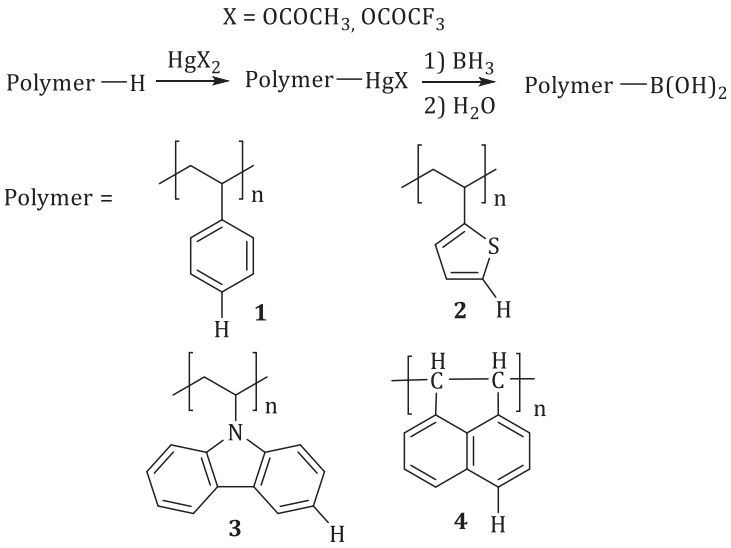

Figure I. 50: Post-functionalization of mercuriated polymers. [119]-[123]

iii. From silylated polystyrene

Jäkle and his team have recently demonstrated a new procedure providing access to well-defined soluble organoboron polymers and copolymers of controlled architecture, molar masses and degree of functionalization. The substituents on the boron can be easily exchanged and thus the Lewis acidity can be tuned. The path has been described in three steps: the living (co)polymerization of the silylated functional monomer, the exchange of the functional groups for Lewis acidic boron centers and the tuning of the Lewis acidity of the individual boron centers through high yield substituent exchange reactions. This strategy avoids the issues of the boron

reactivity interference with radicals that tends to limit the molar masses through recombination. [124], [125]

For the preparation of the trimethylsilyl-functionalized polymer, atom transfer radical polymerization (ATRP) is used conducting to a controlled molar masses polymer (**1**, Figure I. 51). [126] 4-Trimethylsilylstyrene was polymerized in anisole with 2 mol % 1-phenylethylbromide as an initator and catalyzed by CuBr/pentamethyldiethylenetriamine. They obtained a 68.5 % conversion within 5 h at 110°C. The molar masses of **1**, Figure I. 51 was M_w=6,500 relative to PS standards and $Đ$=1.13. This approach can be applied to the synthesis of random copolymers, end-functionalized polymers, and block copolymers containing silyl groups at defined positions on the polymer chain.

In the second step, the silylated polymer previously obtained is treated with an excess of BBr_3, a strong Lewis acid which is known to cleave Si-C(sp^2), to form highly Lewis acidic polymer (**2**, Figure I. 51). [124], [125] The reaction was conducted under mild conditions (ambient temperature) with nearly quantitative yields and high selectivity over a period of 12 h in a 12% yield. This procedure represents an exceptionally simple route to boron-functionalized polystyrene avoiding the use of toxic metals and providing selectivity without apparent cross-linking of the polymer chain. However, the length of polymer chains obtained is quite limited and waste is obvious (Me_3SiBr, HBr).

The bromine substituents were then displaced through another set of high yield substituent reactions with nucleophiles (**3**, Figure I. 51). [125] A large variety of reagents has been explored for the introduction of π-donating alkoxy substituents on boron including alcohols, ethers and silylethers with centers of moderate Lewis acidity.

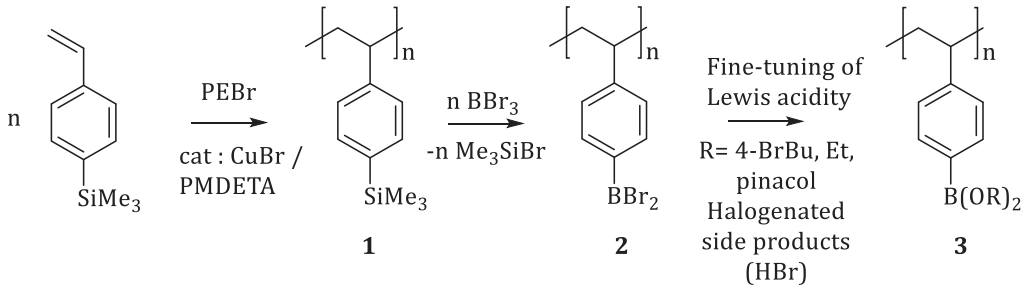

Figure I. 51: Modification of silylated polymers conducting to organoboron polymers by Jäkle and co-workers. [125]

High Lewis acidic triarylborane polymers with thiophene or similar aryl substituents are accessible with stannylated reagents such as trimethylstannylthiophene or 2-trimethylstannyl-5,5'-bithiophene. [5] An alternative synthetic method is applied for the introduction of aryl groups of boron halides with arylcopper reagents providing highly Lewis acidic organoboron polymers. [127], [128]

iv. From polyethylene

Following the work of Röttger *et al.* [111], Leibler and Tournilhac presented in 2018 the synthesis of functionalized polyethylenes grafted with dioxaborolane maleimide groups that behave like vitrimers through metathesis reactions between dioxaborolane moieties. Reactive extrusion technique was used to obtain the targeted networks. Dioxaborolane maleimide was first grafted onto a polyethylene backbone and subsequently crosslinked by the addition of a bis-dioxaborolane. The scheme of reaction is described in Figure I. 52. The system exhibited a phase separation induced by the difference of polarity between the polymer chains and the dioxaborolane maleimide groups. They evidenced that the crosslinking does not rearrange this phase separation. This last feature will be further discussed in Chapter 4. [129]

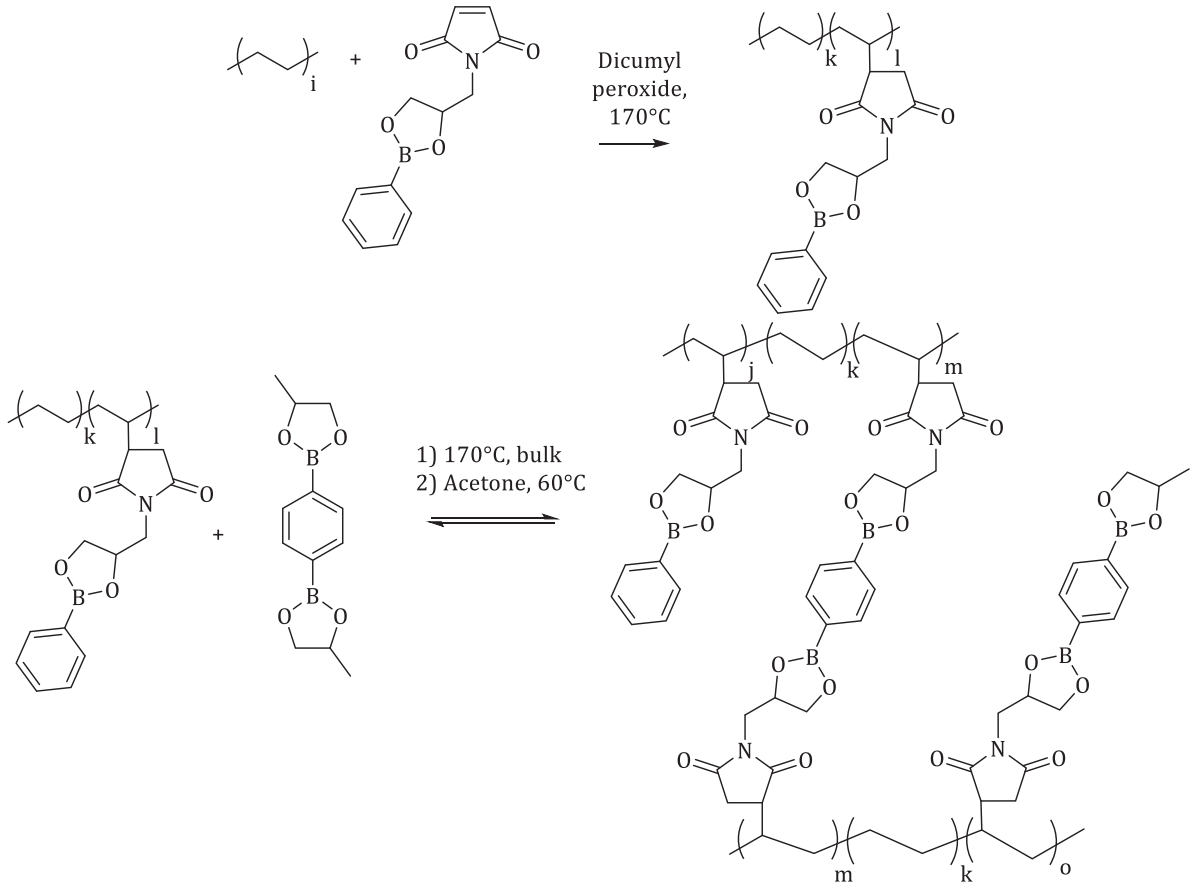

Figure I. 52: Synthesis of grafted polyethylene and subsequent crosslinking by metathesis of dioxaborolanes. [129]

Nicolaÿ and co-workers recently reported the functionalization of polyethylene by nitroxide radical coupling of a bis-dioxaborolane using reactive extrusion. [130] As already discussed sooner, these polymers exhibit a dynamic crosslinking and are qualified as vitrimers thanks to metathesis reactions occurring between dioxaborolane groups. [111] Concerning the vitrimer synthesis, they introduced different routes conducting to crosslinked networks. Firstly, a two-step process was presented involving the grafting of a TEMPO-boronate ester radical on a polymer chain and

subsequent crosslinking through metathesis. A second route implied the use of a bis-TEMPO-boronate ester that yields vitrimers in a single step process. The two routes are explained in Figure I. 53. [130]

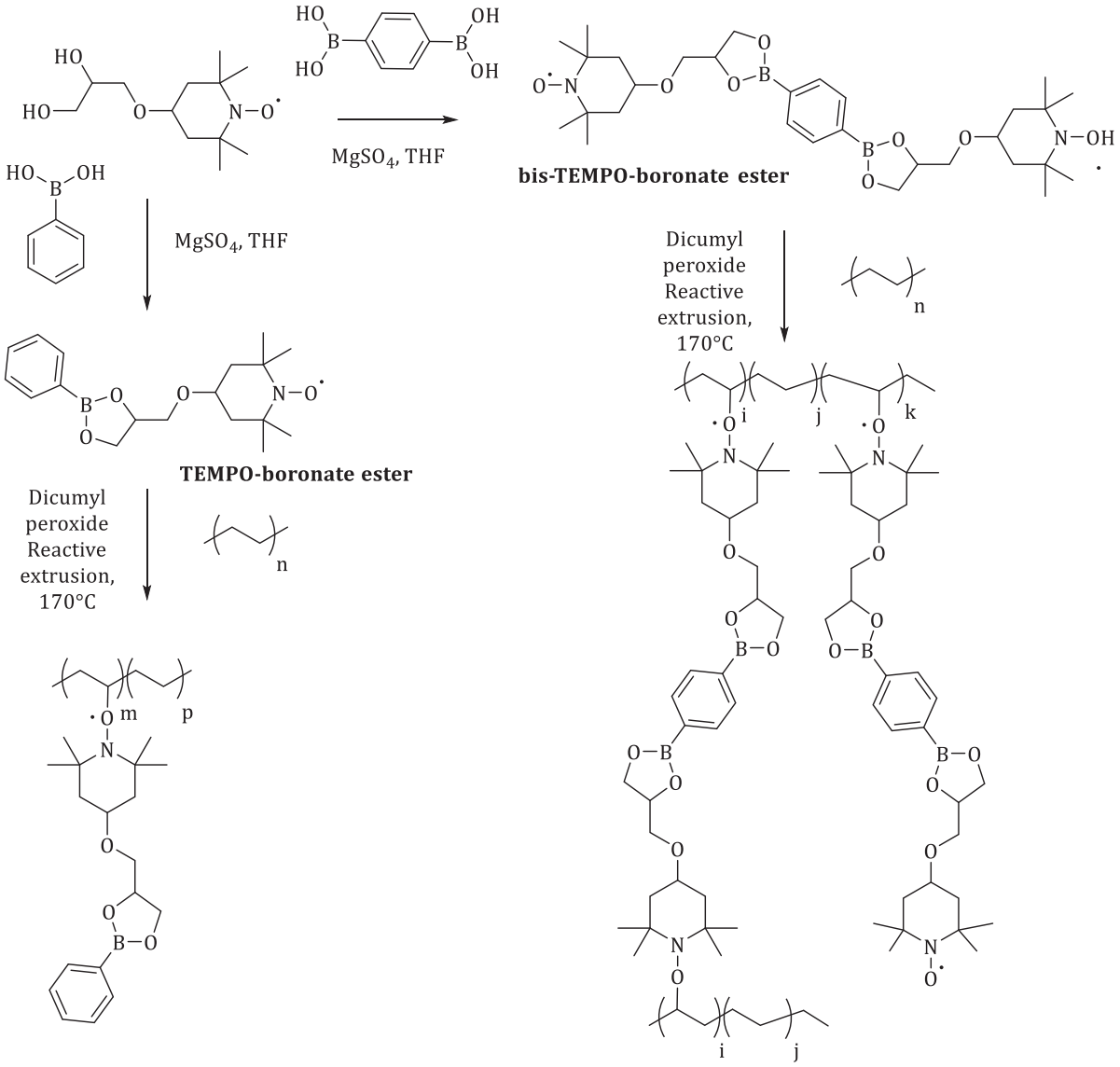

Figure I. 53: Synthesis of grafting agents TEMPO-boronate ester and bis-TEMPO-boronate ester and subsequent preparation of grafted polyethylene and polyethylene vitrimer by reactive extrusion. [130]

D. Synthesis of side-chain functionalized conjugated organoboron polymers with boron-oxygen groups

The functionalization of conjugated organic polymers with Lewis acidic boron groups provides a tuning of the photophysical and electrical properties of the conjugated polymer chain through binding of Lewis bases to the boryl groups.

a. Electrochemical polymerization

Fabre and Freund's groups have considered the electropolymerization of boron-functionalized thiophene, pyrrole and aniline derivatives to develop boronate-functionalized conjugated polymers. [131]–[133] An example is described in Figure I. 54.

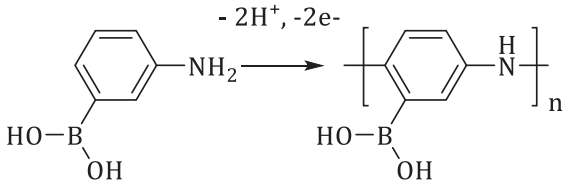

Figure I. 54: Electropolymerization of boron-functionalized thiophene by Freund and co-workers. [131]

b. Chemical polymerization

Following the work of Wolfbeis on this subject, [134] Freund *et al.* demonstrated that the oxidative polymerization of the fructose complex of aniline boronic acid with ammonium persulfate in the presence of fluoride leads to poly(aniline boronic acid) (Figure I. 55). The polymerization of the fructose complex was carried out under ambient conditions with the addition of ammonium persulfate to oxidize conducting to a water soluble and self-doped polymer. [135]

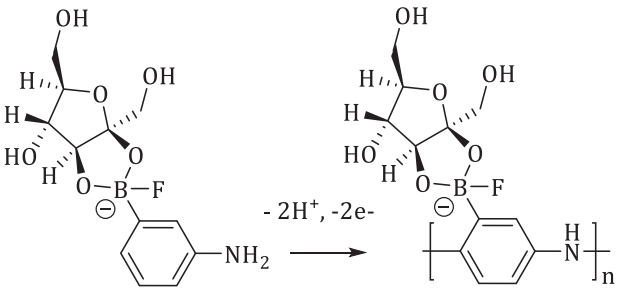

Figure I. 55: Oxidation polymerization of the fructose complex of aniline boronic acid. [135]

E. Applications of boronic acid-containing polymers

In recent times, macromolecules bearing boronic acid groups found uses in a variety of applications such as dynamic covalent materials, thermo- and saccharide-responsive hydrogels, sensors and nanomaterials. Thus, they are perfect candidates for biomedical applications for example in the detection of type-1 diabetes due to their ability to bind with saccharides. Moreover, they can be used as HIV barriers, separations and chromatography, cell capture and culture, enzymatic inhibition and in site-specific radiation therapy. [77]

As the applications of poly(boronic acid) and derivatives are numerous, we will focus on hydrogels, nanomaterials and molecular sensing applications with examples related to the thesis

subject, especially harnessing transesterification reactions. For more information, the review of 2015 by Sumerlin and co-workers covers a large spectrum of poly(boronic acid) applications. [77]

a. Hydrogels from boronic acid-functionalized macromolecules

i. Dynamic covalent boronate ester cross-linked hydrogels

Boronate and boronic esters are categorized as "dynamic covalent" structures thanks to their facile exchange between bound and free species. [136], [137] This feature leads to unique mechanical properties. Actually, hydrogels crosslinked *via* boronate esters are not permanently rigid but flow under their own weight. This results from the rearrangement of boronate esters in which the esters dissociate by hydrolysis to yield the free boronic acids and diols before forming boronate ester crosslinks with newly acids and diols. In this fashion, boronate esters crosslinked hydrogels exhibit a self-healing behavior.

In the literature, these boronate ester networks have been prepared *via* a variety of methods. Willner and his team used the mixing of polymeric boronic acids with polymeric diols or the mixing of multifunctional small molecules with a counter-functionalized polymer support. [138] Similarly, borax, a tetrahydroxy boron species, can be used in addition with diol-functional polymers to afford boronate ester gels. [139] Sumerlin also investigated crosslinking of multifunctional small molecules to form a macroscopic network. [136]

The same group recently published hydrogels that are able to self-heal at both neutral and acidic pH. To do so, they synthesized copolymers of 2-acrylamidophenyboronic acid (2-APBA) and N,N-dimethylacrylamide (DMA) and gels were formed by the mixing of these two previous compounds with poly(vinyl acetate) (PVA) or a dopamine-modified polymer (P(DOPAAm-*co*-DM)) as depicted in Figure I. 56. The boron exists as tetrahedral boronates species over a wide range of pH as the carbonyl oxygen of the amide group is in a position to coordinate with the boron center. The stability of these hydrogels make them suitable for applications in gastrointestinal medicine. [140]

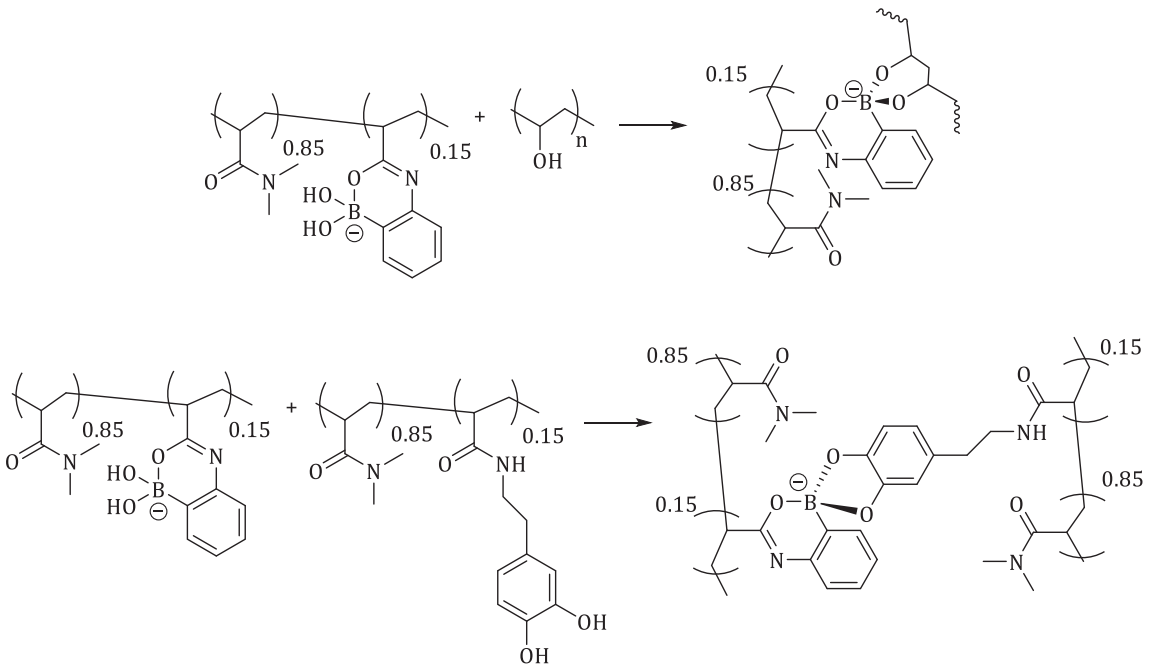

Figure I. 56: Hydrogel formation between P(2-APBA-co-DMA) (15 mol % 2APBA) with PVAc and P(DOPAAm-co-DMA) (15 mol % DOPAAm) at neutral pH. [140]

Auzély-Velty and co-workers prepared dynamic covalent hydrogels by mixing polysaccharides bearing carboxylates such as hyaluronic acid or carboxymethylcellulose modified with phenylboronic acid and maltose moieties. The hydrogels formed are pH-dependent self-healing materials featuring viscoelastic properties. They can be used in soft matrices for neuronal regeneration. The structure of the prepared system is presented in Figure I. 57. [141]

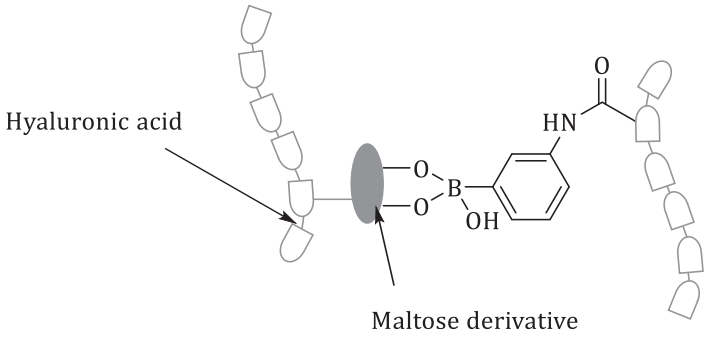

Figure I. 57: Dynamic covalent hydrogels based on hyaluronic acid crosslinked with boronate ester bonds. [141]

ii. Responsive hydrogels

The properties of the boronic acid-based hydrogels have been recently combined to stimuli-responsive compounds to afford multiresponsive materials. Poly(N-isopropylacrylamide) (PNIPAM) is perfectly suitable for coupling properties with boronic acids according to its Lewis base character able to interact with the electron vacancy of boron atoms. Besides, PNIPAM exhibits a lower critical solution temperature (LCST) which means that the polymer is soluble in water below a specific temperature. For these polymers, the volume phase transition temperature

(VPTT) can be tuned by copolymerization with hydrophobic or hydrophilic monomers. As previously described, boronic acids exist as either hydrophobic below pK_a or hydrophilic above pK_a or upon complexation (for example with glucose). The VPTT of thermoresponsive materials based on boronic acids are a function of glucose concentration and pH.

Kataoka and co-workers are pioneers in boronic acid-modified thermoresponsive materials under glucose concentration and pH. Indeed, from 1996, they explored the copolymerization of NIPAM and 3-APBA or 2-APBA. The resulting gels contained 10 mol % of boronic acids. In an aqueous media, the phenylboronic acids are in equilibrium between the associated and the dissociated form. In the last anionic form, complexation with glucose is possible and forms a stable complex. As a result, an increase of the concentration of glucose induces the increase of the concentration of the borate anions and a decrease of the concentration of the associated form as illustrated in Figure I. 58. The complexation of glucose on the borate anions drastically changes the solubility of the copolymer composed of PNIPAM and phenylboronic acid based co-monomer. In other words, increasing glucose concentration induced the increase of the VPTT. This technology is used in the controlled delivery of insulin from the gel depending on its solubility. [142]–[144]

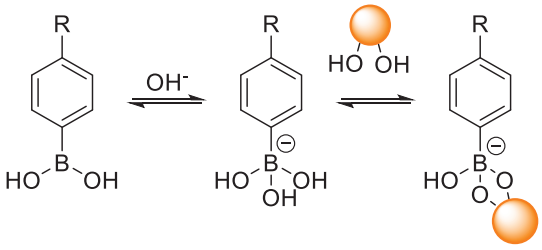

Figure I. 58: Equilibrium between phenylboronic acid moiety and glucose in aqueous media described by Kataoka. [144]

Zhou and co-workers presented an alternative to these hydrogels with the involvement of acrylic acid in copolymers with NIPAM and MBA. The microgels were then functionalized by introducing hydrophobic phenylboronic acid (PBA) groups. This resulted in the decrease of the VPTT, thus the P(NIPAM-PBA) microgels bearing 10 mol % of PBA are in collapsed state at room temperature. In a same way that previously depicted, the addition of glucose to the aqueous media makes the microgels drastically swell. Indeed, the glucose sensitivity of the boronic acid groups based on the stabilization of the phenylborate ions converts hydrophobic PBA groups to hydrophilic phenylborate groups. [145], [146] In a more recent study, the same group synthesized copolymer from NIPAM and 2-acrylamidophenylboronic acid (2-AAPBA) which exhibits a different behavior in presence of glucose. Actually, the microgel collapses instead of swelling thanks to the configuration of 2-AAPBA allowing for an intramolecular B-O coordinated interaction stabilizing the tetrahedral form of PBA (Figure I. 59). In this specific case and contrary to the previous studies, the glucose addition shifts the VPTT to lower temperatures. This is presented in the literature as

the new contraction-type glucose-sensitive microgels also expected to have applications in self-regulated insulin release and glucose sensing. [147]

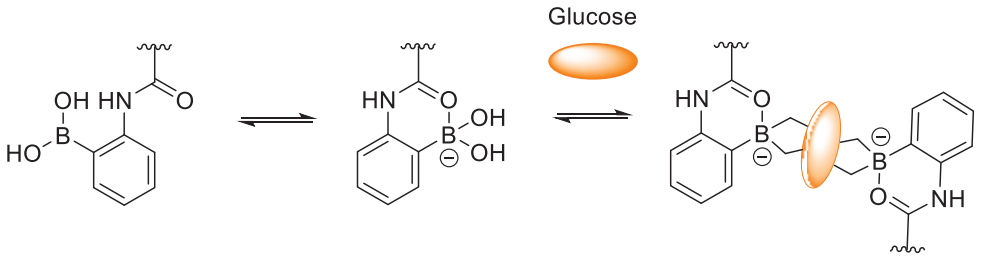

Figure I. 59: Contraction of the glucose-borate complex in the microgel. [147]

Zhang and co-workers reported the synthesis of random copolymer of NIPAM and phenylboronic acid (PBA) followed by the introduction of an amino-reactive function such as N-hydroxysuccidinic (NHS) ester. This newly introduced group has the ability to react with amino groups of a protein or peptide through click chemistry with NHS. The studied copolymer has both pH and glucose responsiveness thanks to the PBA groups. It was grafted to the surface of M13 viruses *via* the presence of NHS groups resulting in a hybrid virus-polymer bio-conjugate. By combining the different properties of the reactive groups involved in the copolymer, they were able to observe a reversible gelation behavior regulated by temperature, pH or glucose. Thus, bioactive species can be loaded inside the viral hydrogel depending on the media conditions. These newly formed bio-conjugates can be used in biomaterials. [148]

Jay *et al.* presented a pH-sensitive hydrogel based on phenylboronic acid (PBA) and diol-containing salicylhydroxamic acid (SHA). They took advantage of the condensation reaction of boronic acids with 1,2- or 1,3-diols forming five- or six-membered cyclic esters. This reaction is reversible and highly influenced by the pH. The PBA-SHA complex, represented in Figure I. 60, will exist predominantly upon neutralization in the tetrahedral conformation forming a densely crosslinked elastic gel. Conversely, at acidic pH, few crosslinks exist resulting in a low viscosity gel. This pH-responsive complex has potential to act as a barrier to HIV-1. [149]

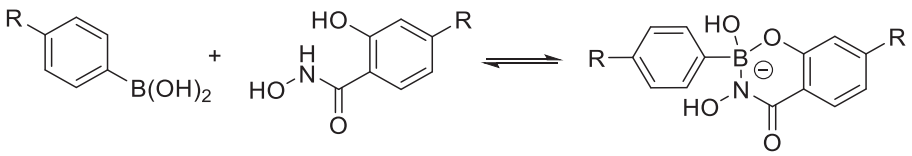

Figure I. 60: Equilibrium between PBA and SHA groups and PBA-SHA complex. [149]

b. Nanomaterials including boronic acid groups

i. Boronic acid-containing block copolymers

Several groups focused on the ability of boronic acid-containing block copolymers to self-assemble under different stimuli to form a variety of different nanostructures from micelles to vesicles. Indeed, these copolymers can find applications in drug delivery by encapsulating drugs in the nanoparticles.

In the previous parts, we presented the synthesis of copolymers performed by Jäkle's team involving 4-vinylphenylboronic acid and styrene. In other papers, they found out that these materials presented self-assembled morphologies depending on the solution pH and the choice of organic co-solvent. In this optic, the morphology can range from micelles to worm-like aggregated structures. [150] Well-defined copolymers of ethylene glycol and 4-vinylphenylboronic acid were also prepared by another group and it was demonstrated that the micellization behavior was dependent of the pH and of the glucose presence. Thanks to the hydrophobicity of the boronic acid segment at $pH<pK_a$, the polymer undergoes self-assembly in water to form nanostructures smaller than 100 nm. [151]

Sumerlin and co-workers studied poly(3-acrylamidophenylboronic acid)-*b*-poly-(N,N'-dimethylacrylamide) in aqueous solution. The presence of free boronic acid moieties confers the copolymer a pH-responsive behavior as a result of the Lewis acidic boron center that is able of reacting to yield negatively charged boronate species (See previous part on the reactivity of boronic acids). This specific copolymer exhibits a pK_a around 10 and the boronic acid is insoluble below this value. Thus, the block copolymers were able to dynamically self-assemble in micelles with the pH as the driven force. In this fashion, the dissociation of the aggregates was induced by raising the pH above the pK_a to form unimers. The aggregates were found to swell as the hydrophilicity of the core increased due to the gradual ionization of the boronic acid residues until the interior portion of the aggregates became hydrophilic enough to reach a complete dissolution. The dissociation can also be initiated by adding sugars, such as fructose or glucose, capable of forming boronate esters. This last feature is reversible thanks to the dynamic-covalent nature of the boronic acid-diol complexes. [152]

The same team combined the pH- and sugar-responsive character of polymers bearing boronic acid moieties with the thermosponsiveness of NIPAM. On the one hand, at high pH and low temperature, the polymers exist as unimers. On the other hand, high pH and high temperature led to nanoparticle formation with a PNIPAM core, while low temperature and low pH led to nanoparticle conduct to nanoparticle with 3-acrylamidophenylboronic acid. The action of the pH can also be replaced by the addition of a sugar such as glucose. [153]

In another paper, they harnessed the ability of boronic acid to form boronic esters by reacting with 1,2- or 1,3-diols to afford macromolecular stars with reversible boronic esters linkages. Firstly, homopolymers of 3-acrylamidophenylboronic acid conduct to macroscopic dynamic-covalent networks when crosslinked with multifunctional diols. However, the addition of diol crosslinkers to block copolymers of poly(N,N'-dimethylacrylamide)-*b*-poly(3-acrylamidophenylboronic acid) forms multi-arm stars with boronic ester cores. Due to the dynamic character of the boronate ester formation, the stars dissociate *via* competitive exchange reactions. The star formation-dissociation was shown to be repeatable. [154]

ii. Boronate ester-stabilized nanoparticles

In the same fashion, boronate esters have been used to stabilize nanoparticles. As an example, Lam and co-workers reported the synthesis of dual-responsive boronate cross-linked micelles for drug delivery. Their work is based on the self-assembly of polymers containing boronic acid moieties and polymers bearing catechol groups. To reach this goal, they used polyethylene glycol (PEG) and dendritic cholic-acid block copolymers. The boronic acid (nitrophenyl boronic acid or phenylboronic acid) and catechol groups are then introduced on the block copolymers by post-functionalization. The resulting boronate esters obtained by complexation of boronic acid and catechol on different block copolymers conduct to the self-assembly of the polymers into micelles by crosslinking. The crosslinked groups are illustrated in Figure I. 61. The complexation was found to be stable at physiological pH; however, it dissociates when the pH was reduced to 5.0 or upon addition of mannitol (sugar alcohol) by a competition mechanism between the catechol and the newly introduced polyol in the reaction media. [155]

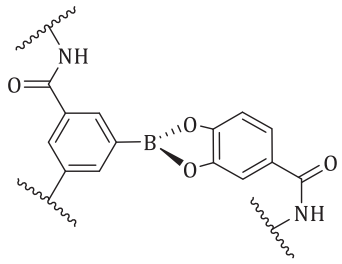

Figure I. 61: Cross-linking involved in the self-assembly of micelles described by Lam and co-workers. [155]

In another paper by Zhao *et al.* from 2014, they presented the nanoparticles based on dextran copolymers. Indeed, poly(dextran-*b*-*DL*-lactide) were prepared and then the dextran block on one part of the copolymers was functionalized with 3-carboxy-5-nitrophenylboronic acid group resulting in a self-assembly between the unmodified dextran and the modified dextran of the block copolymers. In neutral conditions, the modified copolymers form shell-crosslinked micelles by transesterification reaction with the unmodified copolymers that enables the loading of doxorubicin. Nevertheless, under acidic conditions, the boronate esters formed hydrolyse and the

micelles are de-crosslinked to release the doxorubicin (chemotherapy agent for cancer treatments) as described in Figure I. 62. [156]

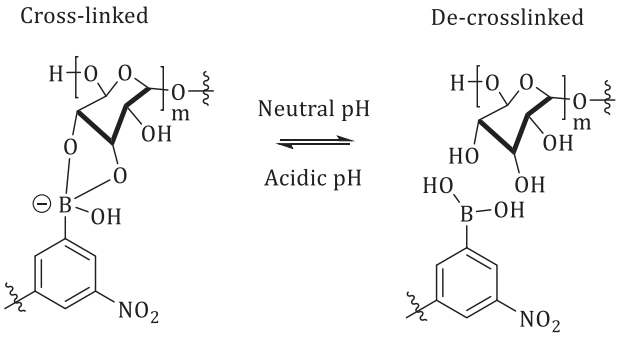

Figure I. 62: Boronic acid-dextran pH sensitive crosslinking described by Zhao et al. [156]

c. Molecular sensing

Many applications of boronic acids in molecular sensing are related in the literature and only a few representative examples will be described in this part.

i. Electrochemical sensing

Glucose-sensing electrode were prepared in 1996 by Okano and co-workers by casting a polymer gel containing phenylboronic acid on a platinum electrode. They prepared a copolymer from N,N'-dimethylacrylamide, (N,N'-dimethylamino)propylacrylamide, 3-methylacrylamidophenylboronic acid and butyl methacrylate. This contains both boronic acid and tertiary amine groups that form a stable complex with poly(vinyl alcohol) by interaction between the boronic acid moieties and the hydroxyl groups. The copolymer-polymer complex changes its swelling degree depending on the glucose concentration due to the competition between the interaction of boronic acid with hydroxyl groups from poly(vinyl alcohol) or from glucose. This swelling was found to result in a measurable increase of the current conducting to a glucose sensor. Indeed, the swelling of the polymer complex allows for a more facile electron transfer whereas, upon the removal of glucose, the resistance increases. [157]

Freund and co-workers investigated the coupling of the properties of a highly conductive polymer such as poly(aniline) with boronic acid complexation ability. In this optic, they synthesized a poly(aniline) carrying boronic acid groups and they studied the complexation of the newly poly(aniline boronic acid) with saccharides (Figure I. 63) by potentiometric measurements. The transduction mechanism is based on the change of pK_a from the complexation and the resulting change in the electrochemical potential. In the pH range of 6-10, the complexation of saccharides by the boronic acid groups is stable. Based on this electrochemical study, the optimum pH values for polymer-fructose and polymer-glucose complexation were found to be respectively 7.4 and 9.0 according to the maximum open circuit voltage. [158]

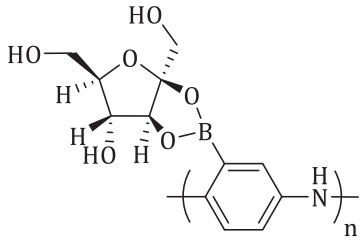

Figure I. 63: Complexation of poly(aniline boronic acid) with saccharides investigated by Freund and co-workers. [158]

Molecular imprinted polymer (MIP) sensor for dopamine were designed based on 3-acrylamidophenyl boronic acid with N,N'- methylenebisacrylamide and acrylamide. The polymer was synthesized by electrochemical polymerization on the surface of a gold electrode in the presence of dopamine in water. The resulting electrochemical sensor is selectively sensitive to dopamine by reversible complexation between the polymer and dopamine. The reactive pathway is described in Figure I. 64. [159]

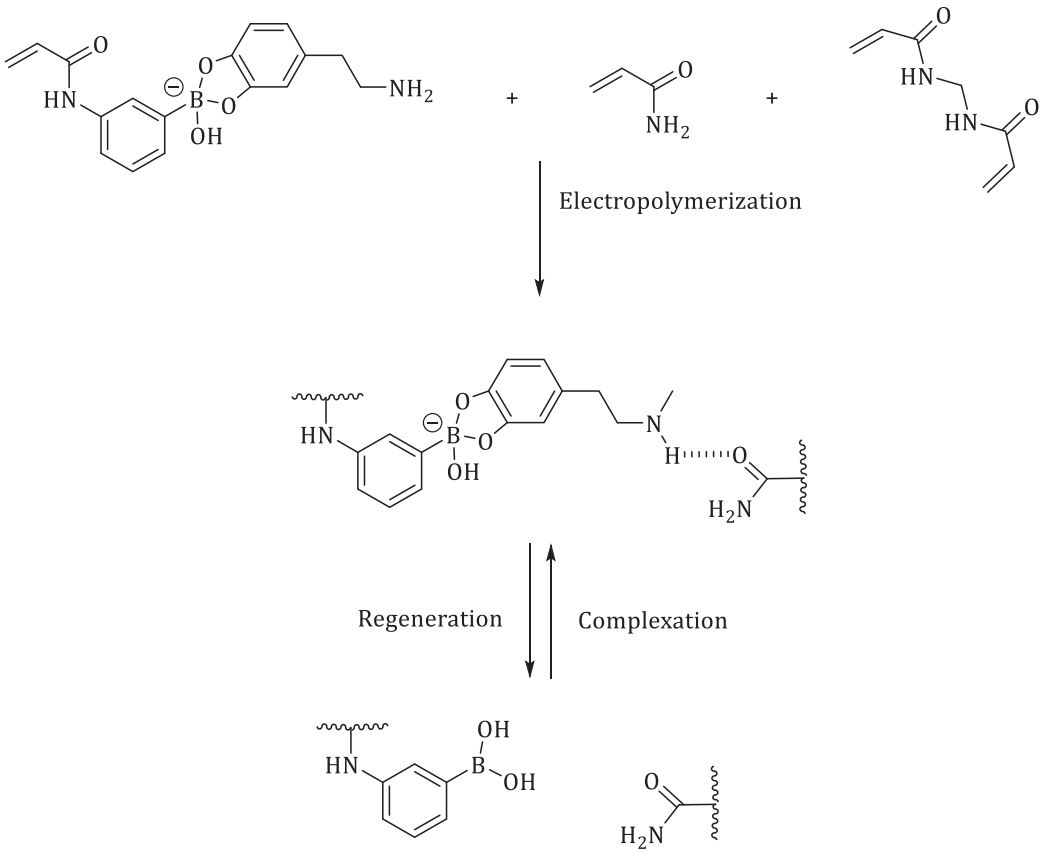

Figure I. 64: Formation of a molecularly imprinted polymer sensor for dopamine. [159]

Sugnaux and Klok described glucose-sensitive QCM-sensors by using direct surface RAFT polymerization. They synthesized polymers from 3-methacrylamido phenylboronic acid by RAFT polymerization resulting to a coating on the silica surface of the QCM sensor as depicted in Figure I. 65. This path allows for the controlled growth of poly(3-methacrylamido phenylboronic acid) brushes with thicknesses up to 20 nm without the need of additional post-polymerization

modifications. The modified QCM sensor by the polymer brushes responds with a linear change in the shift of the fundamental resonance frequency over a range of glucose concentration but is insensitive toward the presence of fructose. This paper validated the potential of these polymer brushes as glucose sensitive coatings that could find applications in diabetes detectors. [160]

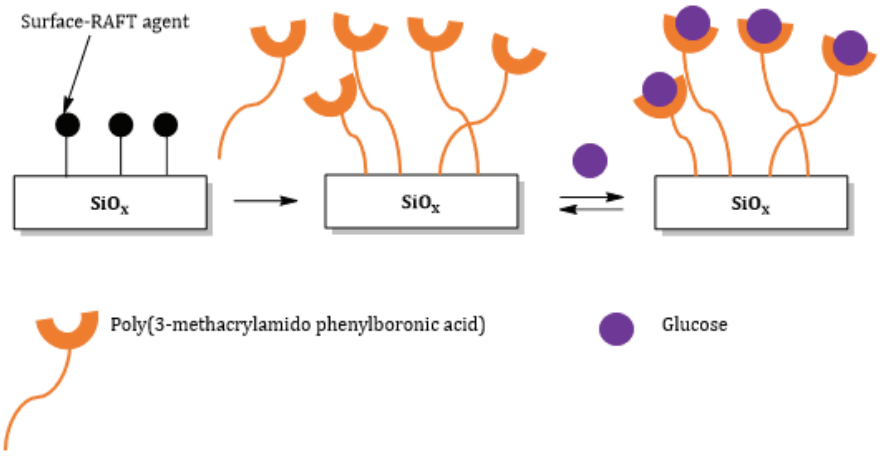

Figure I. 65: Functionalization of the surface of QCM-sensor to afford glucose-sensitive sensor. [160]

In another approach, pressure-transducer sensors were prepared by Lin *et al*. from crosslinked hydrogels containing 3-acrylamidophenylboronic acid and N,N'-dimethylaminopropylacrylamide. The synthesized hydrogels were introduced between a pressure transducer and a semipermeable membrane. They were found to shrink in presence of glucose due to the crosslinks formed with glucose. However, the hydrogels swell while increasing the fructose concentration. Moreover, the resulting pressure changes are reversible over various cycles. [161]

ii. Optical sensing

Many examples of the use of polymers containing boronic acid groups are related in literature with applications in surface plasmon resonance and reflectance spectroscopies, holographic devices, fluorescence and absorbance sensors and in polymerized crystalline colloidal arrays. In this part, only few examples taken from the literature will be described.

Willner studied the effect of glucose on the swelling of a copolymer made from m-acrylamidophenylboronic acid and acrylamide by surface plasmon resonance. This technique is extremely sensitive to the refractive index of layers present in the interfacial region. In this approach, the shifting of reflectance minimum is an indicator of the presence of glucose. After immersion of the copolymer hydrogel in a glucose solution, they found that the reflectance minimum shifts by an angle of 0.6° corresponding to a thickness increase of 100 nm. [162] In another paper, the same principle was harnessed and the refractive index was calculated from the

changes in the film thickness, however, they employed thiol-functional homopolymers of vinylphenylboronic acid. [163]

In another optic, a new type of holographic sensor has been developed by the modification of silver holographic films with hydrogels from 3-acrylamidophenylboronic acid or 2-acrylamido-5-fluorophenylboronic acid. Thanks to the binding of glucose on the boronic acid groups, the color of the hologram was found to red-shift to longer wavelengths due to volume expansion of the hydrogels. This subsequent change of color is thus used to identify glucose concentration. [164]

In 1995, poly(L and D-lysine)s were modified with boronic-acid moieties and a cyanine dye was found to be reoriented in the presence of sugars. Indeed, the complexation of sugars to the boronic acids induces the formation of an anionic sp^3-hybridized boron that affects the electrostatic interaction between the polymer and the cyanine dye. The structures of the reactant are presented in Figure I. 66. Thus, the complexation shifts the absorption spectrum of the dye to shorter wavelengths. This change of wavelengths is followed to measure the sugar concentration. [165]

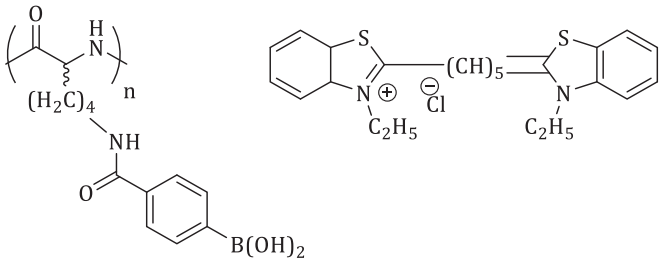

Figure I. 66: Modified poly(L- and D-lysine)s (left) and cyanine dye (right). [165]

Other systems used the same absorbance shift strategy with boronic-acid substituted azobenzenes. In the work of Egawa, a boronic acid-appended azobenzene dye was attached to poly(ethyleneimine). They studied the effect of the addition of glucose and demonstrated that this induces a significant change in the UV-visible absorption spectra of the polymer solution. They assumed that sugar binding decreases pK_a of boronic acid to accelerate the coordination with OH^- ions, which results in a cleavage of the B-N bond and an increase of the absorbance around 400 nm. This work harnesses the Lewis pair interaction between azobenzene and boronate ester groups. [166] In Chapter 2, we will deepen this concept with the introduction of Lewis pairs in polymer networks.

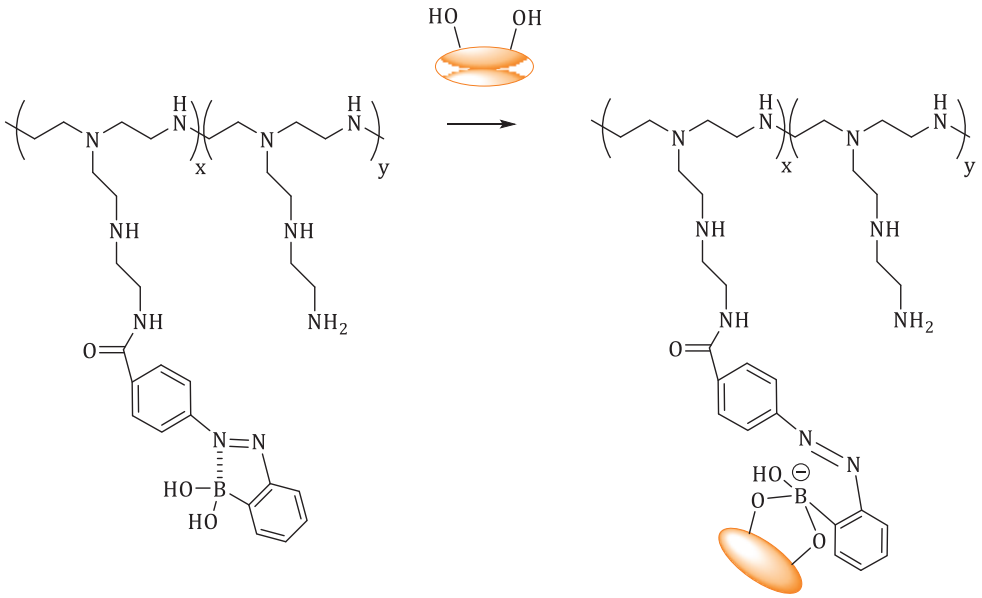

Figure I. 67: Structural changes in the polymer in the presence of sugars. [166]

Asher and co-workers combined the polymerized crystalline colloidal arrays (PCCA) with pendent boronic groups. PCCA consist of colloidal particles packed in a crystalline order at the size scale of the light wavelength (400-800 nm). Thus, they can diffract light in accordance with the Bragg law. Changes in the spacing of the particles affect the diffraction and shift the wavelength of iridescent light. 3-acrylamidophenylboronic acid-modified polystyrene particles were added to a polystyrene matrix. The presence of glucose results in the formation of boronate anions that induces electrostatic repulsion between the negatively charged boron atoms. Thus, the hydrogel swells and the materials exhibits a red shift in the diffraction wavelength. [167]

In this another way, a fluorescent anionic dye and a viologen bearing boronic acid moieties have been synthesized and immobilized into a poly(2-hydroethyl methacrylate) hydrogel. The fluorescence is controlled by the quenching efficiency of the viologen receptor. The complexation between the two species is facilitated by electrostatic attraction and the quenching is due to the electron-receiving ability of the viologen. When glucose is added, the boronic acid turns into anionic boronate esters weakening the electrostatic attraction between the dye and the quencher. Thus, a loss in the quenching efficiency was evidenced as the increase of the fluorescence intensity as described in Figure I. 68. [168]

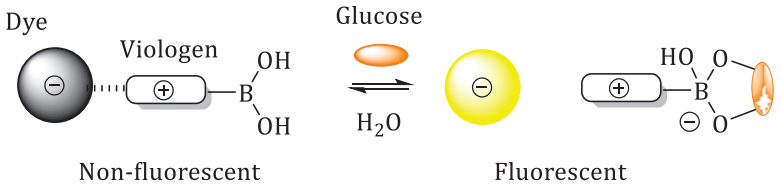

Figure I. 68: Fluorescent sensing of glucose via *boronic acid groups.* [168]

To conclude, a wide range of boron-based moieties is accessible through a variety of reaction paths such as polymerization of functionalized monomers or post-functionalization of existing polymers. In boronic acids and boronate esters researches, the formation of dynamic and reversible polymer networks is accentuated. Polymers functionalized with boron-based groups are very useful to design new vitrimers or covalent adaptable networks. In this PhD work, two Chapters (3 & 4) will be fully dedicated to this topic on the synthesis and characterization of a new type of dynamic polymer networks harnessing boronate ester reactivity.

V. The chemistry of Frustrated Lewis Pairs

This last part relates on the concept of the chemistry of Frustrated Lewis Pairs and the application of this specific chemistry in the design of dynamic polymer networks that constitute a burning topic in nowadays polymer chemistry. The introduction of bonds with tuneable energy between a weak bond of several kcal/mol (1-3 kcal/mol) and a strong bond close to a covalent bond (30-60 kcal/mol) is an interesting strategy to form such networks.

A. Generalities on Frustrated Lewis Pairs

In 1923, Gilbert Lewis described the behavior of electron-pair-donor and electron-pair-acceptor known as Lewis acid and Lewis base usually forming strong adducts. [169] He drew an analogy to the H_3O^+/OH^- neutralization reaction in Brønsted acid/base chemistry. Indeed, Lewis pair exhibits chemistry that is different from the components separately. However, it has been reported that all Lewis acid/Lewis base pairs do not form strong adducts.

Brown *et al.* showed that lutidine forms an adduct with BF_3 but not with the less acidic and bulkier $B(CH_3)_3$. [170] Consequently, Wittig and co-workers described the 1,2-addition reaction of the PPh_3/BPh_3 pair to benzyne and that the $[CPh_3]^-$ anion/BPh_3 pair adds to butadiene. [171] These observations demonstrated that the combination of a bulky Lewis base with a bulky electrophilic Lewis acid does not undergo self-quenching. These new pairs are called Frustrated Lewis Pairs and will be noted FLP in the following of this document. Varying the groups on the Lewis acid and the Lewis base is tuning the energy of the supramolecular bond formed.

Two main sorts of FLPs are described in the literature: intermolecular Lewis acid/Lewis base pair where the Lewis acid and the Lewis base are two separated molecules and react with added substrates in bimolecular reactions, and intramolecular Lewis acid/Lewis base pair which is only one molecule carrying the two reactive groups forming the FLP. Several reports presented the combinations in Figure I. 69 that has been used as ambiphilic ligands in metal coordination chemistry.

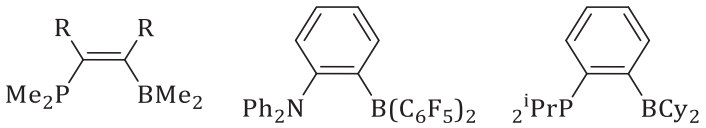

Figure I. 69: Examples of intramolecular FLP. Cy=cyclohexyl. [172], [173]

One of the main feature of FLP is their ability to polarize and desymmetrize to finally split dihydrogen. Thus, they contribute to metal-free catalytic hydrogenations. As an example, Stephan and co-workers reported that combinations of bulky phosphines with $B(C_6F_5)_3$ provided intermolecular systems that cleaved H_2 as shown in Figure I. 70 [174] while Erker group studied the intramolecular ethylene-bridged phosphine/borane as a highly active non-metallic system for the activation of dihydrogen. [175] There are plenty of studies on the characteristics of the FLPs but they will not be detailed in this thesis document. One can refer to Stephan and Erker review on the development and perspectives of FLP chemistry. [176]

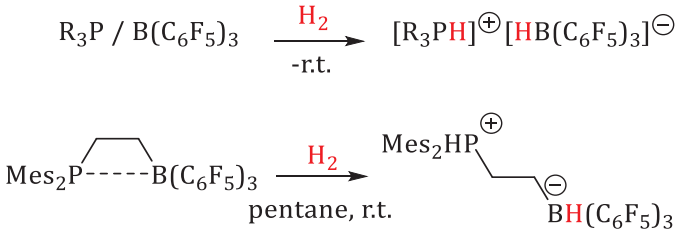

Figure I. 70: Examples of FLP cleavage of dihydrogen. (Mes=mesityl, R=^{t}Bu, Mes) [174], [175]

Recently, FLP chemistry expanded due to the great variability of the cooperative reactions of FLPs with a variety of substrates, leading to small-molecule binding and activation *via* polarization of symmetric molecules. FLP chemistry is a new and exciting area of chemistry providing many possibilities in organic, inorganic and polymer chemistries. In the next part, a focus will be done on the interaction of FLP with small molecules, especially gases, which is the subject of this PhD work.

B. Reactions of CO_2 with FLPs

a. Capture of CO_2

The capture of CO_2 by inter- and intramolecular P/B FLPs was firstly reported in 2009 by Stephan and Erker. [177] It was observed that a solution of $B(C_6F_5)_3$ and P^tBu_3 covered by an atmosphere of carbon dioxide provided the immediate precipitation of a white solid corresponding to the capture of CO_2 between the Lewis acid and the Lewis base (Figure I. 71). Similarly, pressurizing a pentane solution of the intramolecular FLP $(Me_3C_6H_2)_2PCH_2CH_2B(C_6F_5)_3$ with 2 bars CO_2 resulted in the formation of a white solid. An interesting feature of the two described reactions is the reversibility in the capture of CO_2 depending on external parameters such as temperature or pressure detailed in Figure I. 71.

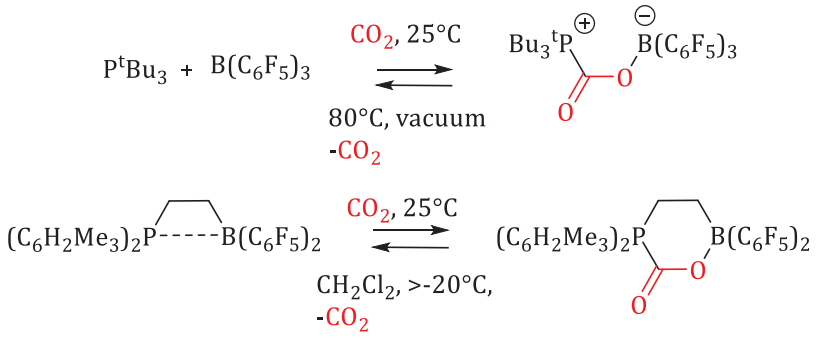

Figure I. 71: Reversible capture of CO_2 by frustrated phosphine-borane Lewis pairs demonstrated by Stephan and Erker. [177]

Stephan and Erker teams worked subsequently on this topic and proved that FLPs derived from $B(C_6F_4H)_3$ and $^iPr_3P$, or $^tBu_3P$, bind to CO_2 conducting to the formation of species $R_3P(CO_2)B(C_6F_4H)_3$ (R=^{i}Pr, ^{t}Bu). In the same manner, the boranes $RB(C_6F_5)_2$ (R= hexyl, Cy, nornobornyl), $ClB(C_6F_5)_2$ or $PhB(C_6F_5)_2$ and $^tBu_3P$ and CO_2 reversibly produce $^tBu_3P(CO_2)BR(C_6F_5)_2$ depending on temperature or pressure. These compounds are described in Figure I. 72. [178], [179]

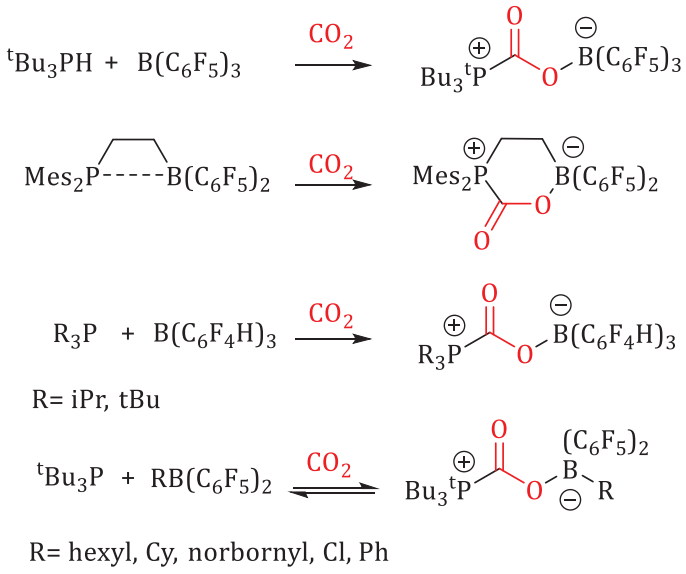

Figure I. 72: Synthesis of CO_2-products through FLP capture. [178], [179]

The capture of CO_2 by bis-boranes and phosphines has been explored by Siebert and Stephan. The combination of $Me_2C{=}C(BCl_2)_2$ [180] with $^tBu_3P$ and 1 atm CO_2 resulted in the formation of the product $Me_2C{=}C(B(Cl_2)_2O_2CP^tBu_3$ as presented in Figure I. 73. [181] In a similar way, the analogue complex $Me_2C{=}C(B(C_6F_5)_2)_2O_2CP^tBu_3$ was also prepared (Figure I. 73). More recently, the reaction of bis-borane $C_6H_4(B(Cl_2)_2)$ with $^tBu_3P$ and CO_2 has been reported (Figure I. 73). [182] However, contrary to the precedent products, it binds to CO_2 through a single boron center while a Cl atom bridges to the second B atom affording $C_6H_4[BCl_2(Cl)BCl(O_2CP^tBu_3)]$. This species is thermally robust at 80°C during 24h. [182]

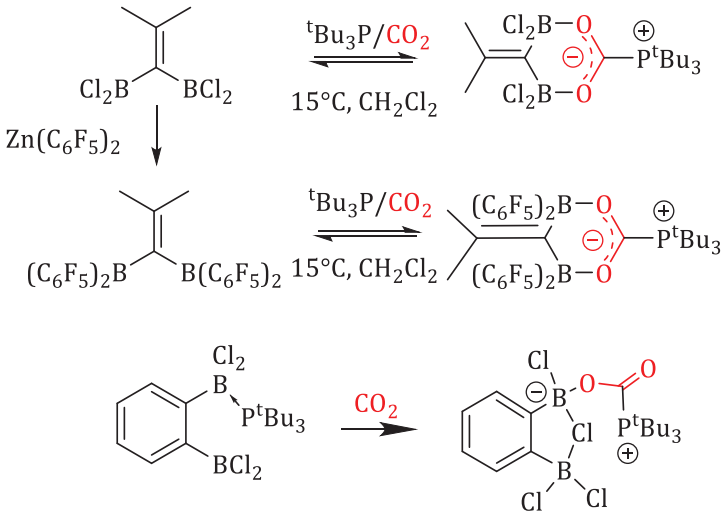

Figure I. 73: Bis-boranes and phospines capture of CO_2. [180]–[182]

Similarly to phosphines, N-heterocyclic carbenes (NHC) as Lewis bases have been investigated to bind and react with CO_2 to form zwitterionic adducts. [183], [184] Tamm and co-workers have reported the carbene-borane adduct $C_3H_2(N^tBu)_2/B(C_6H_3(CF_3)_2)_3$ that behaves as an FLP reacting with CO_2 as shown in Figure I. 74. [185] Similarly, $C_3R_2(N^tBu)_2/B(C_6F_5)_3$ with R=H, Me affords synthetic routes to $C_3R_2(N^tBu_2)CO_2B(C_6F_5)_3$. [186] Moreover, computational studies proved that these products are more thermodynamically stable than the carbene-CO_2 adducts which tend to reversibility at high temperatures.

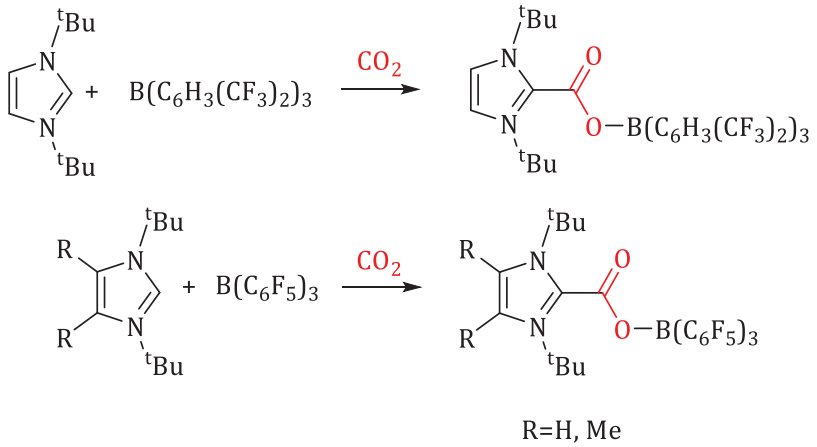

Figure I. 74: Reactions of carbene-borane FLPs with CO_2. [185]

Likewise, primary and secondary amines are known to react with CO_2 in order to form carbamates. [187], [188] However, $PhCH_2NMe_2$ is unreactive to CO_2 [189]–[191] but the FLP $(PhCH_2NMe_2)B(C_6F_5)_3$ reversibly forms the $PhCH_2NMe_2(CO_2)B(C_6F_5)_3$ adduct that releases CO_2 at temperature higher than -20°C in dichloromethane. [192] Thus, sterically hindered amines can be used as Lewis bases in FLP chemistry. Besides, N-isopropyl aniline and $B(C_6F_5)_3$ give $PhHNiPrCO_2B(C_6F_5)_3$ reacting with CO_2 in a non-reversible way. In addition, phosphinimine Lewis

bases $Ph_3PN(R)$ and $B(C_6F_5)_3$ also bind to CO_2 to form $Ph_3PN(R)CO_2B(C_6F_5)_3$ with R= Ph, C_6F_5. [193] FLP including amines are described in Figure I. 75. It is noteworthy that the reversibility of the CO_2 capture depends on the strength of the interaction between the Lewis acid and the Lewis base used. In other words, bulkier Lewis acid and base provide low energy supramolecular bonds and thus reversible character of CO_2 capture.

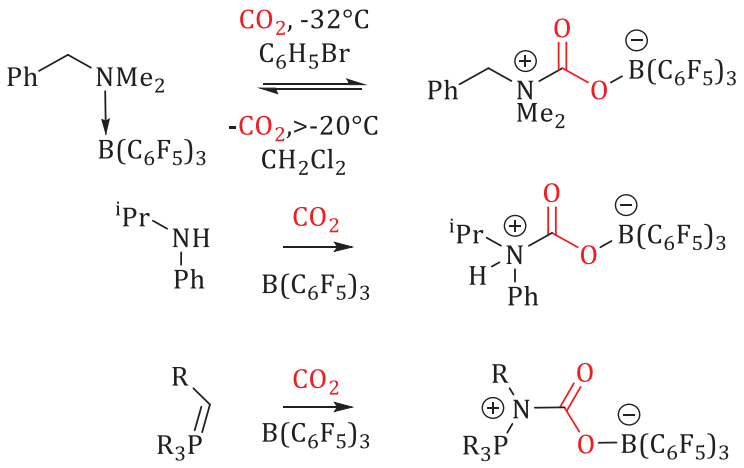

Figure I. 75: Reactions of N-bases, $B(C_6F_5)_3$ and CO_2. [192], [193]

Tamm studied the ability of the pyrazole-borane $(C_3H^tBu_2N_2)B(C_6F_5)_2$ presented in Figure I. 76 to capture CO_2 conducting to intramolecular bound CO_2 adduct. The product obtained is thermally stable under vacuum at high temperature and no sign of CO_2 release was observed. Indeed, the formation of this product was found to be strongly exothermic (ΔE=-29.8 kcal/mol) which is in agreement with the irreversible CO_2 fixation. [194]

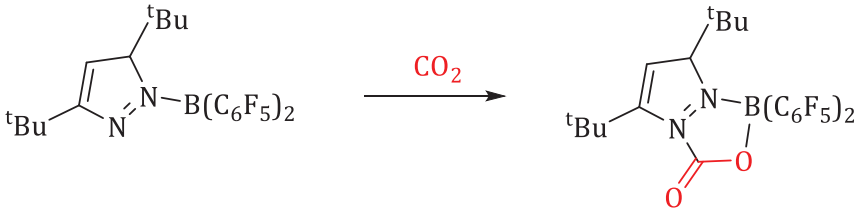

Figure I. 76: Tamm's work on the reactions of pyrazole-borane with CO_2. [194]

A variety of Lewis bases and Lewis acids has been investigated to capture CO_2 efficiently. As an example, FLPs based on Al-Lewis acids have led to CO_2 capture as studied by Uhl and co-workers. They showed that intramolecular Al-P systems react with CO_2 to afford the five-membered ring in which CO_2 is C-bound to P and O-bound to Al in the species $Mes_2PC(CHR')AlR_2(CO_2)$ with R=R'=^{t}Bu, Ph, R=$CH_2{}^t$Bu or R'=^{t}Bu, Ph (**1**, Figure I. 77). [195] Müller and his team have described reactions of FLPs derived from silylium cation $[(C_6Me_5)_3Si][B(C_6F_5)_4]$ with phosphines binding to CO_2 (**2**, Figure I. 77). [196] An alternative approach with Lewis acidic metal centers based on zirconium has been used by Wass and co-workers (**3**, Figure I. 77). [197] More recently, transition metal species

as bases in FLP-type capture of CO_2 have been studied such as ruthenium (**4**, Figure I. 77), [198] phosphorus (**5**, Figure I. 77) [199] or hafnium centers (**6**, Figure I. 77). [200]

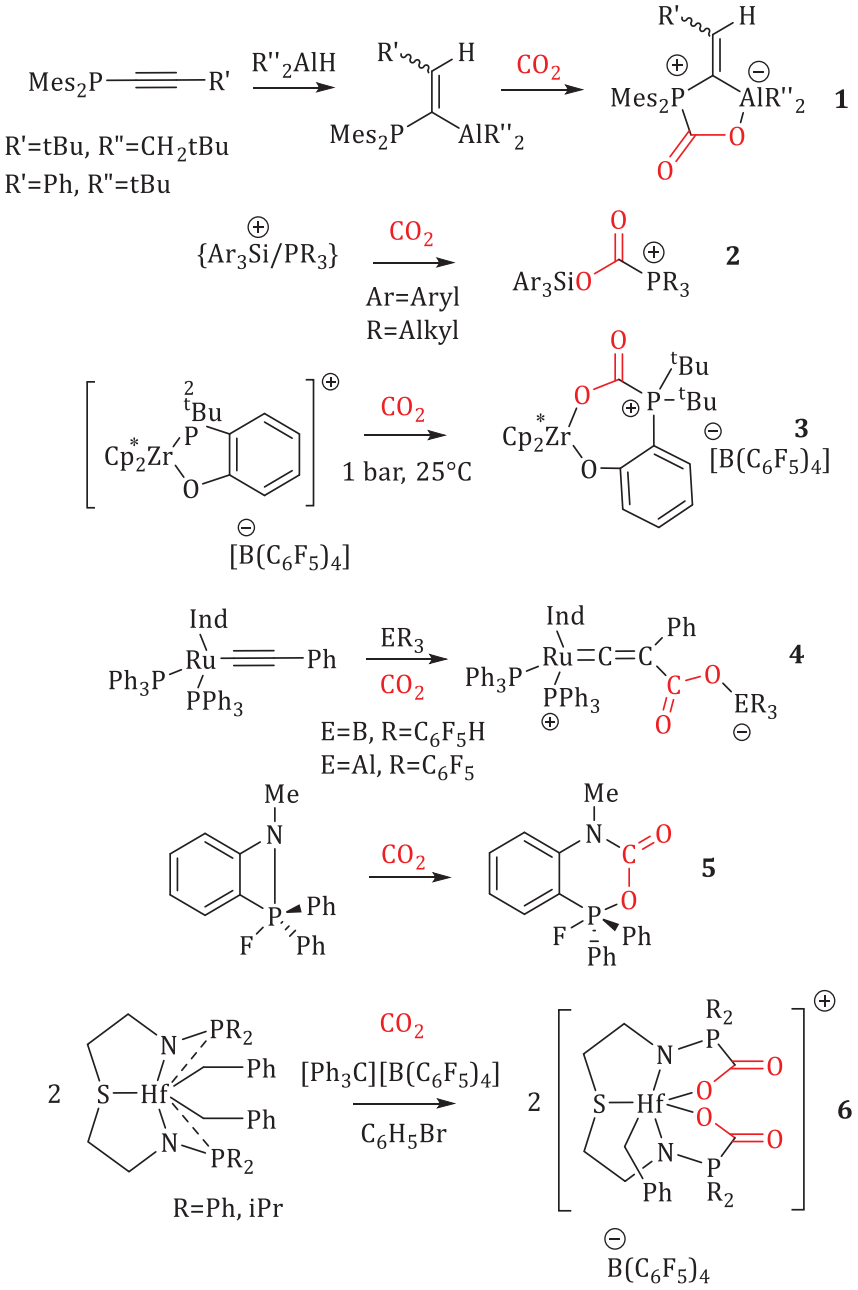

Figure I. 77 : Variety of FLPs investigated for CO_2 capture.

To conclude, FLP has the ability to polarize and disymmetrize CO_2 that is a very stable molecule due to its oxygenated and symmetric character. FLP can thus activate this gas molecule and capture in a reversible path CO_2. This last feature is useful to re-use CO_2 that is a platform for many compound syntheses such as alcohols, ethers or ketones creating an alternative to petrochemistry. The variety of chemical products that can be synthesize from CO_2 is represented in Figure I. 78. It is important to note that reduction is one of the main path to obtain other products. In this fashion, the reduction of CO_2 will be presented in the next part.

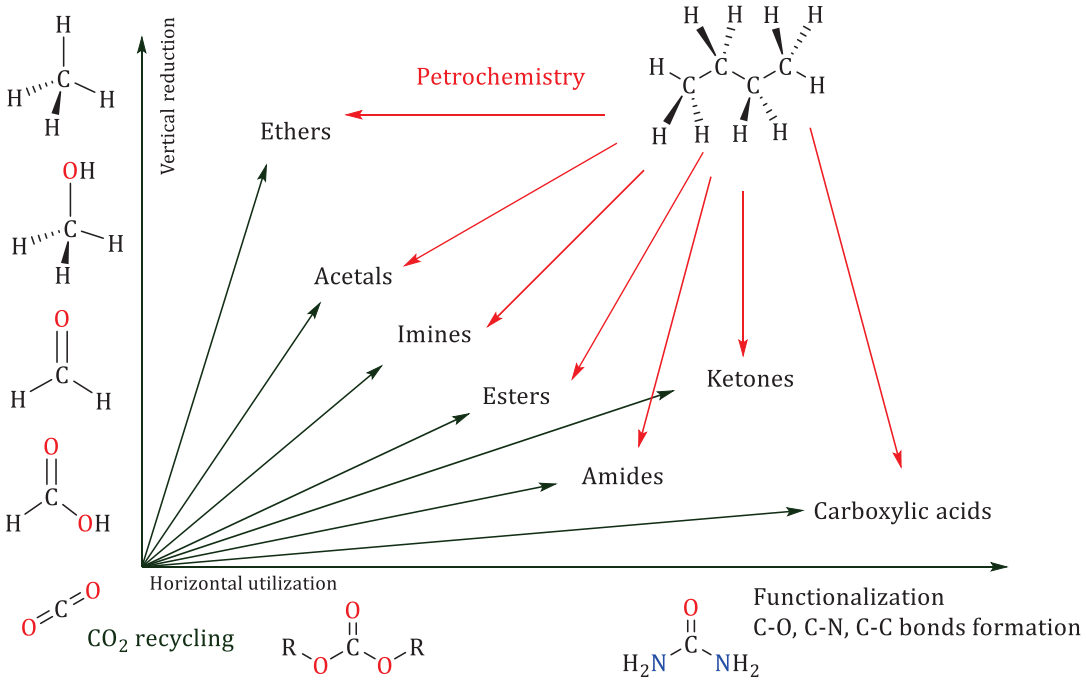

Figure I. 78: CO_2 as a platform for variety of chemical products. [201]

b. CO_2 reductions

i. Stoichiometric reactions of CO_2 with FLPs

In 2009, O'Hare and Ashley proved that addition of CO_2 to a 1:1 mixture of tetramethylpiperidine (TMP)-$B(C_6F_5)_3$ in toluene under a H_2 atmosphere turns to the quantitative conversion into $CH_3OB(C_6F_5)_3$ after 6 days at 160°C, as described in Figure I. 79. This reduction was found to be reversible by heating up to 110°C. [202]

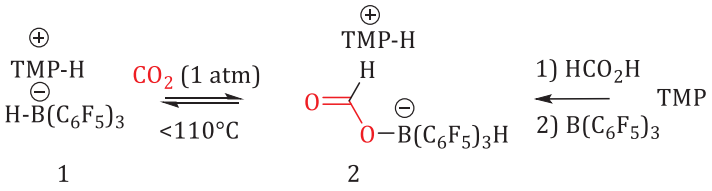

Figure I. 79: Reversible reduction of CO_2 to formate 2 with H_2 activated by a FLP 1. [202]

As shown in Figure I. 80, Piers and co-workers proved that TMP and $B(C_6F_5)_3$ activates CO_2 and in the presence of triethylsilane, affords a silyl carbamate and [TMPH]-[$HB(C_6F_5)_3$] subsequently converted to the formate [TMPH]-[$HCO_2B(C_6F_5)_3$]. [203]

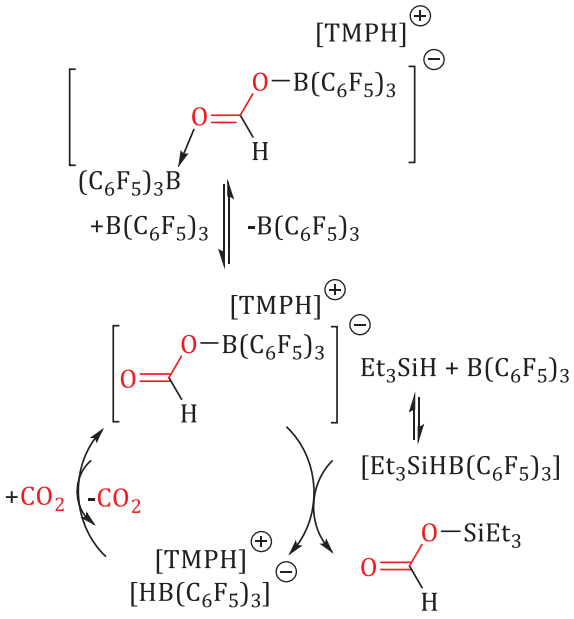

Figure I. 80: Activation of CO_2 by TMP and $B(C_6F_5)_3$ in presence of triethylsilane. [203]

At this stage of the bibliographical review, it is worth mentioning that $B(C_6F_5)_3$ is mainly used instead of other boranes such as Piers' borane $HB(C_6F_5)_2$ or $RB(C_6F_5)_2$ with R=Ph for instance. Indeed, in such compounds, ligand exchanges on the boron atom are possible *via* bent bonds (also known as banana bonds) that induce a loss of boron active species. This phenomenon hinders the activation of small molecules like CO_2.

Stephan reported in 2012 the first example of a sequential two-step double CO_2 activation using a phosphine/borane FLP presented in Figure I. 81. Indeed, the $(Me_3Si)_3P$-$B(p\text{-}C_6F_4H)_3$ mixture reacted with CO_2 to give $((Me_3Si)_3P\text{-}C(OSiMe_3)O)B(p\text{-}C_6F_4H)_3$ (**2**, Figure I. 80) which acts as an intermediate for further reaction with CO_2 affording the bis-insertion product $((Me_3SiO)C{=}P\text{-}C(OSiMe_3){=}O)B(p\text{-}C_6F_4H)_3$ (**3**, Figure I. 81). Compounds **2** and **3** in Figure I. 80 can reversibly rearrange in compounds **2'** and **3'**. [204]

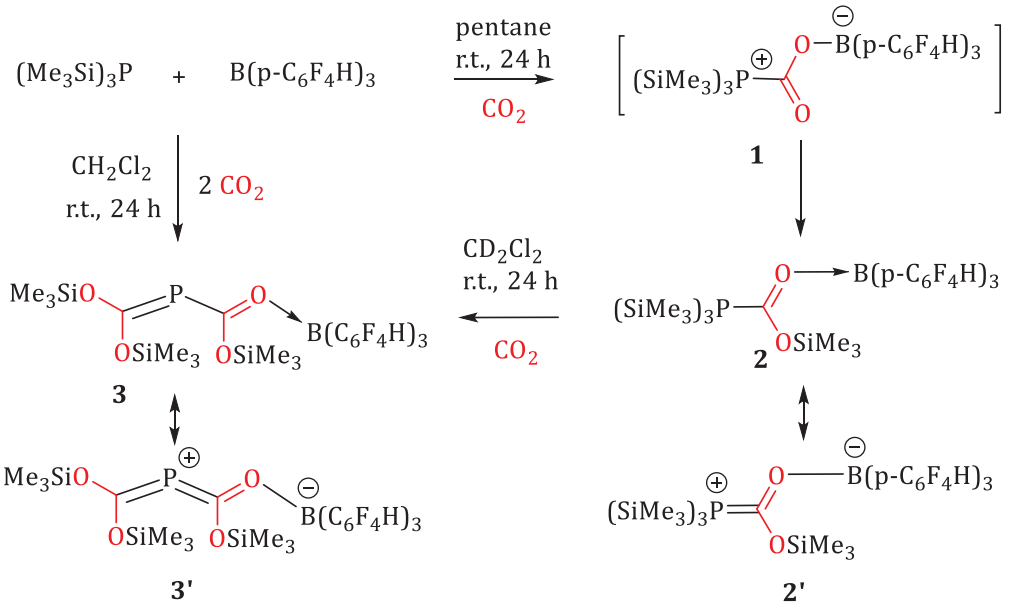

Figure I. 81: Sequential two-step double CO_2 activation using a phosphine/borane FLP demonstrated by Stephan and co-worker. [204]

P/Al FLPs can be used for the stoichiometric reductions of CO_2 by FLP systems. It has been proved, as shown in Figure I. 82, that 1:2 mixtures of Mes_3P-AlX_3 (X=Cl, Br, I) reacting with CO_2 give $Mes_3P(CO_2)(AlX_3)_2$. Both oxygen atoms of CO_2 are bound to AlX_3 units. [205] Contrary to P/B CO_2 complexes, P/Al CO_2 complexes are stable and do not undergo CO_2 loss even on heating up to 80°C under vacuum.

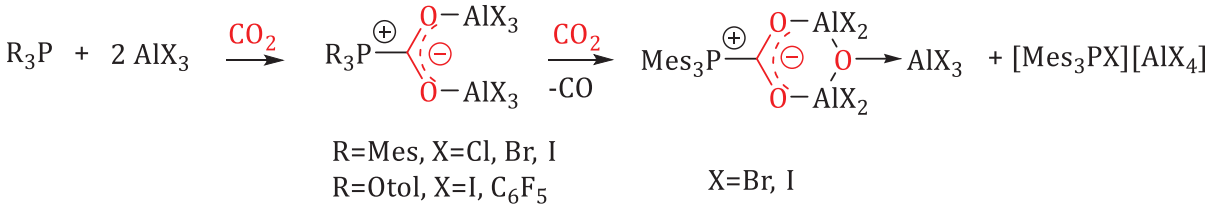

Figure I. 82: Reductions of CO_2 with Al/P FLP systems. [205]

ii. *Catalytic reductions of CO_2 with FLPs*

In order to develop a catalytic reduction of CO_2, FLP system including less oxophilic Lewis acids has been explored to harness the reversible character of CO_2 capture.

Dobrovetsky and Stephan described in 2013 the reduction of CO_2 to CO using CH_2I_2 to generate the catalytically species, $Et_3P{=}C{=}PEt_3$ in situ. The (bis)ylide reacts with CO_2 eliminating phosphine oxide and generating the transient phosphaketene. This reaction is accelerated by the presence of catalytic $ZnBr_2$ while the zinc ion and phosphine act on phosphaketene to regenerate the (bis)ylide, with concurrent CO elimination. The reaction path is described is Figure I. 83. [206] One can evoke that the oxidation of a phosphine giving a side product in this catalytic cycle is remaining costly and is a sacrifice of one equivalent of the phosphorus-based molecule. In a

similar fashion, ruthenium/phosphine combinations have been used to capture CO_2 between the phosphine fragment and the metal center. These species were found to reduce CO_2 in the presence of an excess of HBPin generating MeOBPin and $O(BPin)_2$. [207]

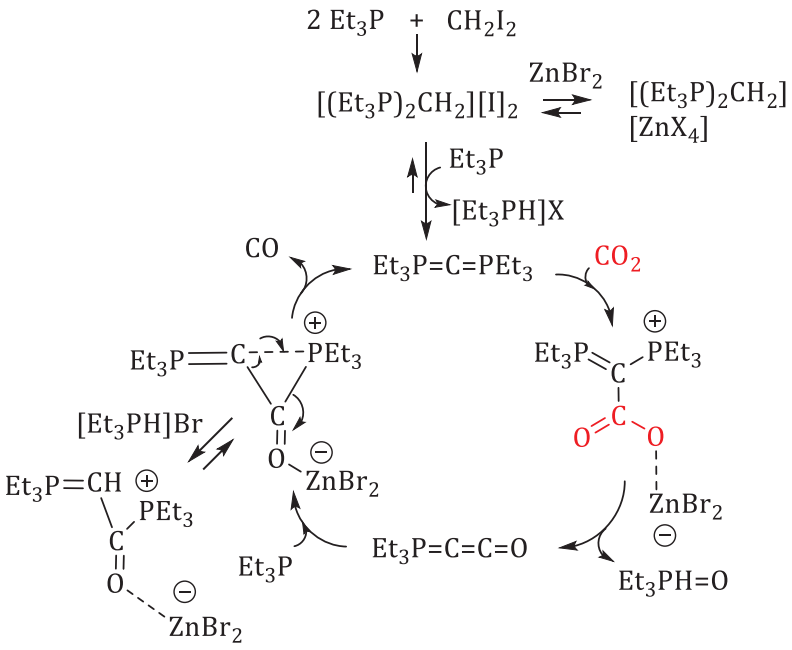

Figure I. 83: Catalytic reduction of CO_2 by phosphine/zinc combinations [206]

Fontaine and co-workers reported that intramolecular FLP 1-Bcat-2-PPh_2-C_6H_4 acts as an ambiphilic metal-free system organocatalyst for the reduction of carbon dioxide in presence of hydroboranes (HBR_2=HBcat, HBPin, 9-BBn, BH_3·SMe_2 and BH_3·THF) to generate CH_3OBR_2 or $(CH_3OBO)_3$ products that can be hydrolysed to methanol. (Figure I. 84) [208]

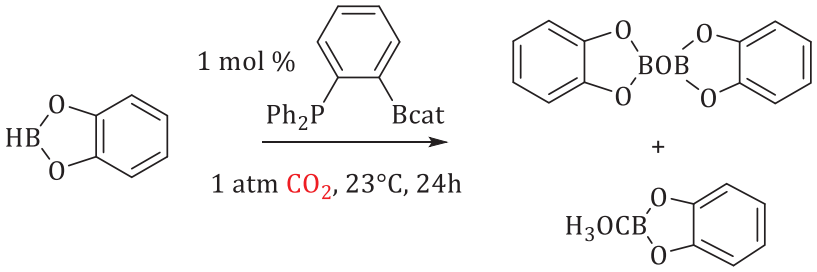

Figure I. 84: Reduction of CO_2 in presence of HBcat and P/B FLP. [208]

C. Reactions of SO_2 with FLPs

The reactions of FLPs with CO_2 opened a new path for the ability of FLPs to activate other small molecules such as SO_2. SO_2 is part of the sulfur oxides gases abbreviated as SO_x but the other gases in the group are less common in the atmosphere. The largest source of this gas is the burning of fossil fuels by power plants and industrial facilities. Important exposures to SO_2 can harm the human respiratory system and induce health problems. It can also harm trees and plants by

damaging foliage and decreasing growth and it contributes to acid rain. [209] It is thus environmentally challenging to capture such compounds.

Erker and co-workers described some addition products of phosphorus/boron FLPs and SO_2. FLP made from $^tBu_3P$ and $B(C_6F_5)_3$ reacts with sulphur dioxide at room temperature in bromobenzene to give the product of addition. The corresponding ^{11}B NMR signal is at δ=0.3 ppm, typical of a four-coordinate boron. It was proved by X-ray crystal structure analysis that the FLP **1** in Figure I. 85 had undergone 1,2-addition to S=O bond of SO_2 to form the zwitterion $^tBu_3$-P(S(O)O)$B(C_6F_5)_3$. In a same way, the FLPs **2** and **5** also add SO_2 rapidly in pentane at -78°C to yield respectively **4** and **6**. The configurations obtained by addition were confirmed by NMR signals and X-ray crystal structure analysis. [210]

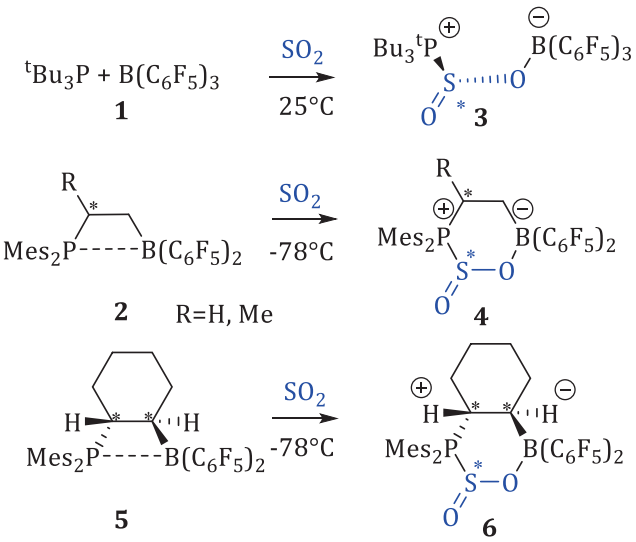

Figure I. 85: Synthesis of FLP-SO_2 complexes. [210]

D. Reactions of N_2O with FLPs

Similarly to SO_2, N_2O is part of nitrous oxides gases also known as NO_x and is a highly greenhouse gas. N_2O emissions are related to agricultural and industrial activities. [211] The same idea of capture is also interesting in this case.

Stephan and co-workers demonstrated the FLP binding of N_2O and described the first crystallographic characterizations of bound N_2O species. The reaction of an equimolar mixture of $^tBu_3P$ and $B(C_6F_5)_3$ with 1 bar of N_2O in bromobenzene results in the precipitation of a white solid. The observed ^{11}B resonances of δ=0.4 ppm indicates a four-coordinate boron center. ^{15}N NMR signals at 566.6 and 381.7 ppm and $^1J_{NN}$=15.6 Hz establishes the presence of two inequivalent nitrogen atoms. A crystal structure analysis confirmed the formulation of a N_2O molecule bridging the P and B fragments in a 1,3-mode. Heating an NMR sample in C_6D_5Br at 135°C for 44 h of this

product conducts to the liberation of N_2 and to the formation of the Lewis adduct $(^tBu_3P{=}O)B(C_6F_5)_3$ as the main product. A dependence on the combined Lewis acidity and basicity has been previously observed in the interaction of small molecules with FLPs. As an example, FLP $(o\text{-tolyl})_3P/B(C_6F_5)_3$ does not react with N_2O whereas $^tBu_3P/B(C_6F_5)_2Ph$, with a less acidic borane, reacts with N_2O. This demonstrated that the Lewis acidity at B has a bigger impact on the remote N-N and P-N interactions without a dramatic effect on the B-O bond. The reaction is described in Figure I. 86. [212]

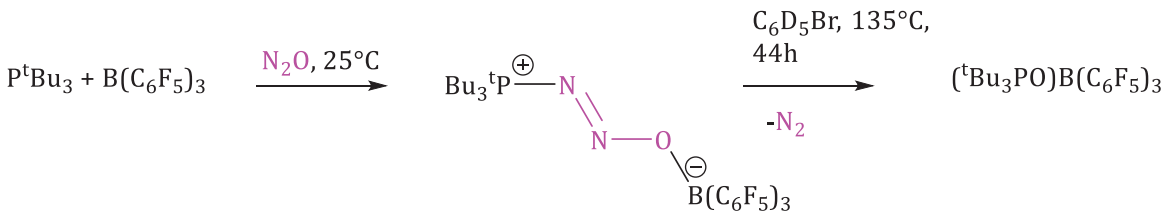

Figure I. 86: Reaction of P/B FLP with N_2O. [212]

The ability of these N_2O-FLP compounds to tolerate weaker Lewis acids prompted an examination of exchange reactions. Stephan explored the reaction of $^tBu_3PN_2OB(C_6H_4F)_3$ with $Zn(C_6F_5)_2$ that forms the centrosymmetric dimer $[^tBu_3PN_2OZn(C_6F_5)_2]_2$. By adjusting the stoichiometry to 1:1.5 $^tBu_3PN_2OB(C_6H_4F)_3$:$Zn(C_6F_5)_2$, $(^tBu_3PN_2OZn(C_6F_5)_2)_2Zn(C_6F_5)_2$ was obtained while the 1:2 ratio gave $^tBu_3PN_2O(Zn(C_6F_5)_2)_2$ (Figure I. 87). These compounds were the first metal complexes in which binding mode of N_2O was established without ambiguity. [213]

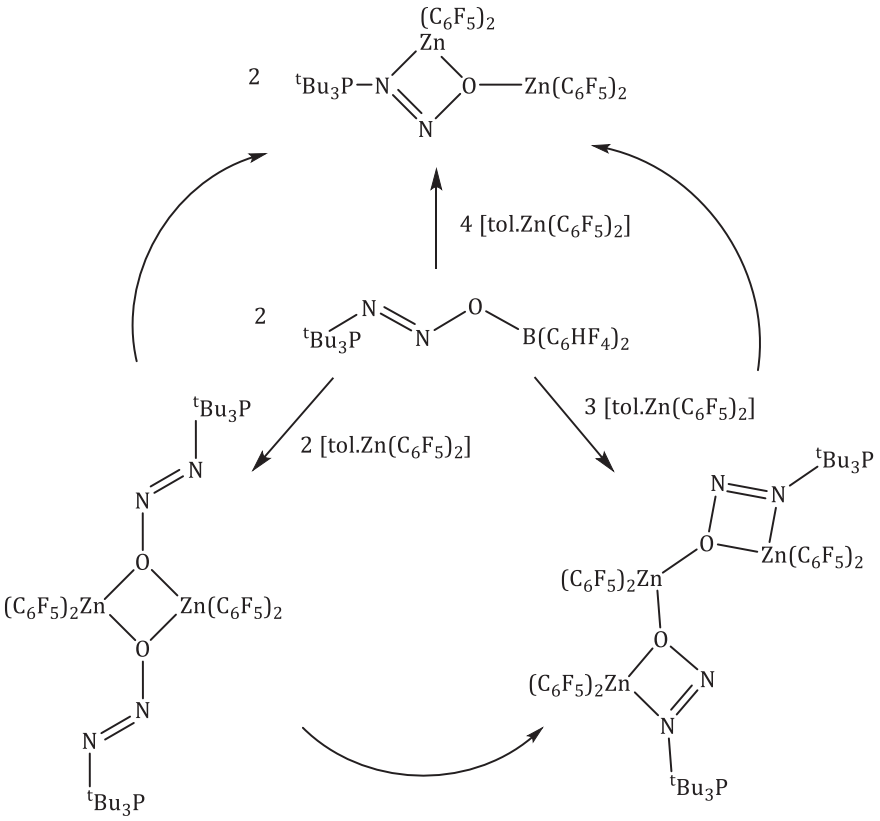

Figure I. 87: Reaction of $^{t}Bu_3PN_2OB(C_6H_4F)_3$ with $Zn(C_6F_5)_2$ depending on the ratio explored by Stephan. [213]

E. Applications of FLP in dynamic polymer networks

In another fashion, researchers recently focused on introducing Frustrated Lewis Pairs into polymers. The goal is to report dynamic networks by reaction of Lewis acid and Lewis base groups. In some cases, they harnessed the ability of FLP to reversibly bind small molecules.

Shaver and his team depicted FLP polymers as responsive self-healing gels harnessing the interesting properties of FLP in polymer matrices. To reach this goal, they synthesized a macromolecular FLP from linear copolymers bearing bulky Lewis acidic and basic pendent groups. They prepared copolymers from styrene and B- and P-functionalized monomers *via* RAFT polymerization as represented in Figure I. 88. [214]

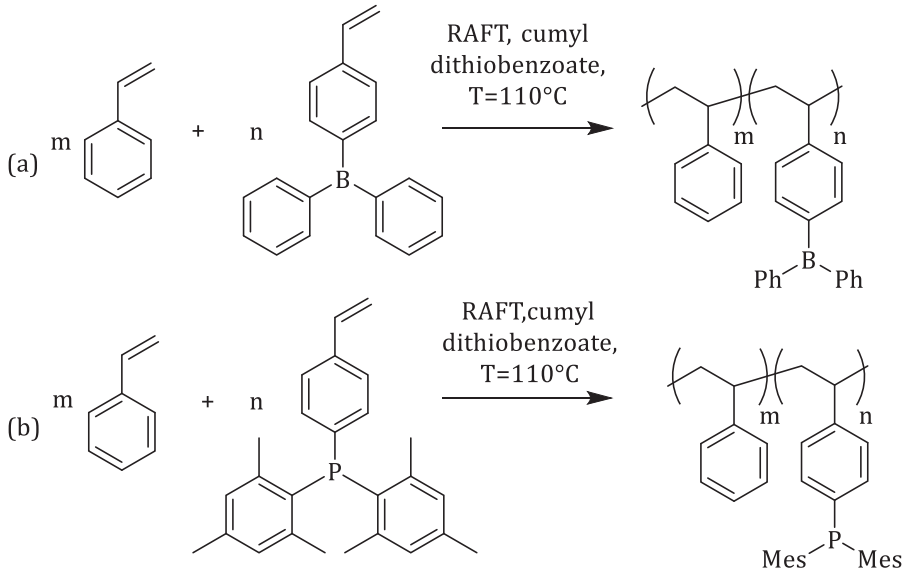

Figure I. 88: Self-initiated RAFT copolymerization of styrene with B- and P-functionalized monomers using cumyl dithiobenzoate as RAFT agent at 110°C. [214]

The reactivity of the macromolecules was explored but no interaction was observed for mixtures of the two copolymers as the bulky environments of the B and P inhibit any reactivity. Though, the addition of a small molecule, in this case diethyl azodicarboxylate, rapidly leads to a network and yields crosslinked polymer chains as described in Figure I. 89. The gel studied was found to be dynamic and thermally responsive. Indeed, heating the swollen gel to 100°C provokes gel rupture and dissolution of the polymer chains. Lower temperatures can also break the network but on much longer times. Besides, the addition of diethyl azocarboxylate initially reacts locally with boron and phosphorus centers forming a temporarily set gel. As the crosslinks are exchangeable, they continue to equilibrate and conduct to a stable gel structure over time. [214]

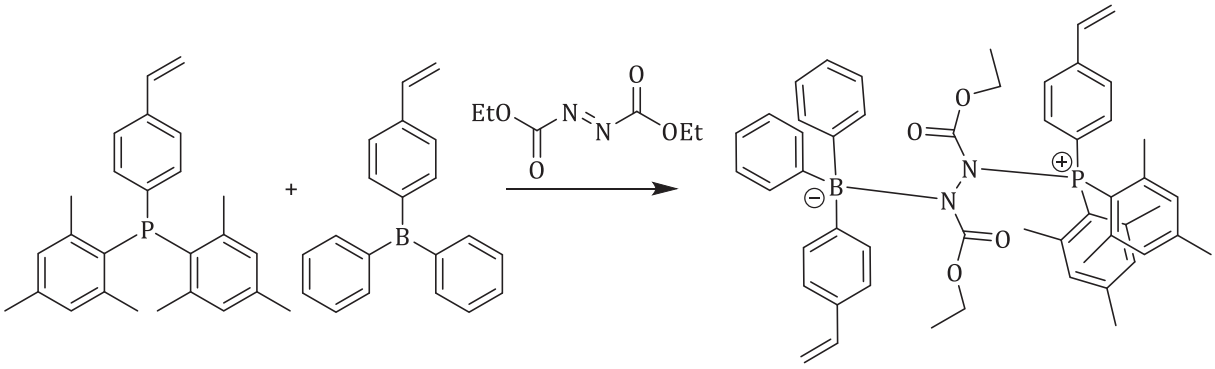

Figure I. 89: Reaction occurring between Lewis acid and base bearing bulky groups in presence of diethyl azodicarboxylate. [214]

Trunk *et al.* described the use of semi-immobilized FLP in microporous polymer networks for the room-temperature activation of hydrogen. They synthesized porous polymer networks based on sterically encumbered triphenylphosphine groups in order to mimic the basic sites presents in FLP chemistry. The synthesis of the phosphine polymers were carried out *via* Yamamoto

polymerization from tri(p-bromophenyl)phosphine derivatives with increasing steric hindrance around the phosphorus atoms. The polymerization occurred with $Ni(COD)_2$ in a mix of DMF and THF at room temperature for 22 h. The networks obtained were purified *via* Soxlhet extraction with methanol. They impregnated these networks with $B(C_6F_5)_3$ conducting to the formation of a semi-immobilized FLP. The resulting system is illustrated in Figure I. 90. They proved that this combination was able to cleave dihydrogen heterolytically at ambient temperature and low dihydrogen pressure. [215]

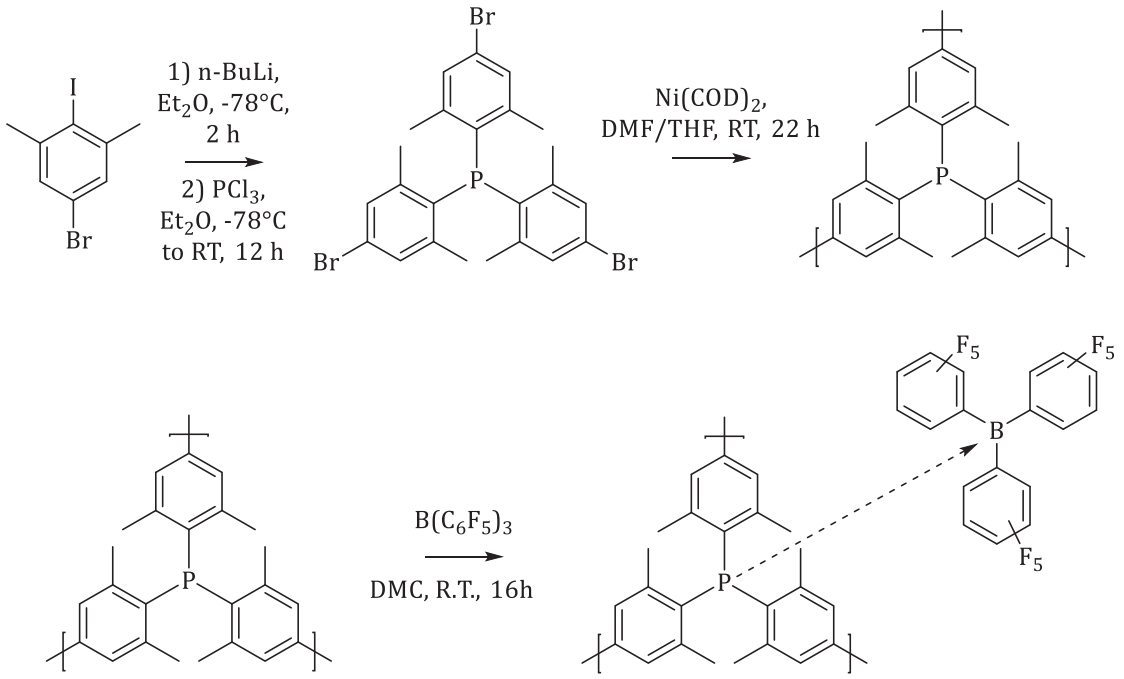

Figure I. 90: Synthesis of semi-immobilized FLP in polymer networks. [215]

Similarly, Rose and co-workers reported the use of solid FLP in a polyamine organic framework for the catalytic hydrogenation of alkenes. In this work, they synthesized a solid FLP by combination of polyamine presenting tertiary amine groups as the Lewis bases and $B(C_6F_5)_3$ as the strong Lewis acid. The polyamine network was synthesized by a n-alkylation of p-xylylenediamine with 1,4-bis(dibromomethyl)benzene (Figure I. 91) and was then impregnated with $B(C_6F_5)_3$. This system was used for the catalytic hydrogenation of diethyl benzylidenemalonate as model reaction. [216]

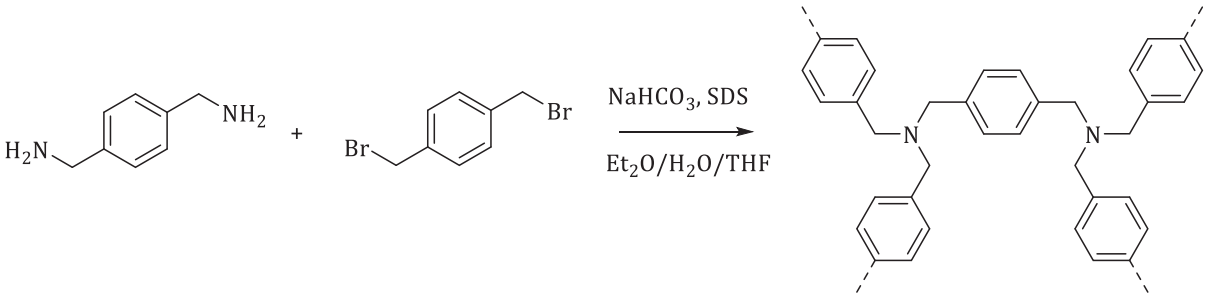

Figure I. 91: Synthesis of the polyamine organic frameworks. [216]

Recently, Yan and co-workers reported a hybrid system between FLP and polymers in order to synthesize gas-responsive materials. In this case, they synthesized two complementary Lewis acidic and basic block copolymers carrying respectively bulky borane and phosphine groups. They noticed that the mixing of equimolar amounts of the two functionalized copolymers in toluene (0.6 mM) did not show any significant reaction. However, this system was submitted to CO_2 stimuli (1.0 atm, flow rate = 0.1 ml/s) and the copolymers binded CO_2, as shown in Figure I. 92, conducting to the self-assembly of the polymers in a micellar formation proved by DLS and TEM analyses. The reaction is also evidenced by the visual change of the solution from transparent to semiopaque. Closer inspection of this organization showed that they are core-corona micelles where the core comprises the crosslinked FLP-bearing block chains while the polystyrene block chains are surrounding outside as the corona. This binding was found to be reversible when heating to 60°C where the micelles can entirely dissociate. They used these systems to afford nanocatalysts for recyclable C1 catalysis and they applied it to the catalytic formylation of N-H bonds toward a variety of amine substrates. They opened a route for a sustainable conversion of CO_2. [217]

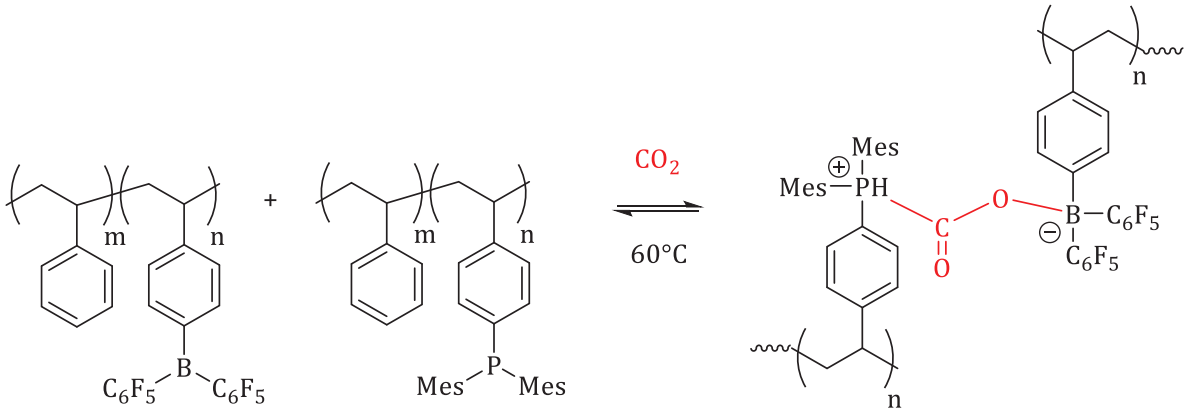

Figure I. 92: Reversible binding of CO_2 between two Lewis acidic and basic block copolymers. [217]

VI. Conclusion

This bibliographical part provides an overview of the state of the art on organoboron polymers bearing different types of linkages: B-C, B-N or B-O. Through this study, we determined that conjugated organoboron polymers presenting B-C and B-N bonds are mainly used for optoelectronic applications thanks to the electronic effects correlated to their structures. More interestingly, one can harness the reactivity surrounding boron to advantageously design dynamic polymer networks.

Concerning the organoboron polymers featuring B-O bonds, the syntheses have been widely investigated and the related literature will be the basis of the work presented in this thesis manuscript to afford organoboron polymers. Moreover, it was interesting to be aware of the utilization of these polymers for the design of dynamic networks and the different hypotheses related to the exchange mechanisms. This feature will be of great interest in the context of our research and we will present breakthrough concepts in the formation of dynamic boron-based polymers with the B-O linkages as the driving force of the dynamic character.

Once we control the reactivity of boron, we are able to tune its inherent Lewis acidity by specific functional groups attached to the boron center. Thus, it is possible to go further with the chemistry of Frustrated Lewis Pairs. This attractive chemistry contributes to the establishment of new dynamic systems relying on supramolecular chemistry and involving three-component interactions with various polymer architectures derived from organoboron polymers. Numerous third components have been examined through interaction with FLP such as gas molecules. The recent studies presented in this bibliographical part reported the possibility of reversibly capturing carbon dioxide. This constitutes a hot topic in the actual context and therefore will be a challenge for us in this thesis work.

VII. References

[1] A. S. Abd-El-Aziz, "Journal of inorganic and organometallic polymers: Preface," *Journal of Inorganic and Organometallic Polymers*, vol. 10, no. 4, pp. 157–158, **2000**.

[2] F. Kato, "Inorganic and organometallic polymers," *Annu. Rep. Prog. Chem., Sect. A Inorg. Chem.*, vol. 109, pp. 277–298, **2013**.

[3] John Emsley, *The Elements*. Calendron Press, **1998**.

[4] P. T. K. Lee and L. Rosenberg, "Scope and selectivity of $B(C_6F_5)_3$-catalyzed reactions of the disilane $(Ph_2SiH)_2$," *J. Organomet. Chem.*, vol. 809, pp. 86–93, **2016**.

[5] Y. Qin, G. Cheng, K. Parab, A. Sundararaman, and F. Jäkle, "Lewis acidic organoboron polymers," *Macromol. Symp.*, vol. 196, pp. 337–345, **2003**.

[6] F. Jäkle, "Borylated polyolefins and their applications," *J. Inorg. Organomet. Polym.*, vol. 15, no. 3, pp. 293–307, **2005**.

[7] C. Schunicht, A. Biffis, and G. Wulff, "Microgel-supported oxazaborolidines: Novel catalysts for enantioselective reductions," *Tetrahedron*, vol. 56, pp. 1693–1699, **2000**.

[8] A. Sundararaman, M. Victor, R. Varughese, and F. Jäkle, "A family of main-chain polymeric Lewis acids: Synthesis and fluorescent sensing properties of boron-modified polythiophenes," *J. Am. Chem. Soc.*, vol. 127, pp. 13748–13749, **2005**.

[9] K. Shiomori, A. E. Ivanov, I. Y. Galaev, Y. Kawano, and B. Mattiasson, "Thermoresponsive Properties of Sugar Sensitive Copolymer of N-Isopropylacrylamide and 3-(Acrylamido)phenylboronic Acid," *Macromol. Chem. Phys.*, vol. 205, no. 1, pp. 27–34, **2004**.

[10] S. Senel, "Boronic acid carrying (2-hydroxyethylmethacrylate)-based membranes for isolation of RNA," *Colloids Surfaces A Physicochem. Eng. Asp.*, vol. 219, no. 1–3, pp. 17–23, **2003**.

[11] W. Xu, X. Sun, and C. A. Angell, "Anion-trapping and polyanion electrolytes based on acid-in-chain borate polymers," *Electroanalysis*, vol. 48, pp. 2255–2266, **2003**.

[12] S. Lu and I. Hamerton, "Recent developments in the chemistry of halogen-free flame retardant polymers," vol. 27, pp. 1661–1712, **2002**.

[13] A. Müller, A. Zern, P. Gerstel, J. Bill, and F. Aldinger, "Boron-modified poly(propenylsilazane)-derived Si-B-C-N ceramics: preparation and high temperatures properties," *J. Eur. Ceram. Soc.*, vol. 22, pp. 1631–1643, **2002**.

[14] N. Matsumi and Y. Chujo, "π-Conjugated Organoboron Polymers *via* the Vacant p-Orbital of the Boron Atom," *Polym. J.*, vol. 40, no. 2, pp. 77–89, **2008**.

[15] Y. Chujo, "Hydroboration, haloboration and phenylboration polymerizations," *Macromol. Symp.*, vol. 118, pp. 111–116, **1997**.

[16] N. Matsumi, K. Naka, and Y. Chujo, "Extension of π-conjugation length *via* the vacant p-orbital of the boron atom. Synthesis of novel electron deficient π-conjugated systems by hydroboration polymerization and their blue light emission," *J. Am. Chem. Soc.*, vol. 120, pp. 5112–5113, **1998**.

[17] N. Matsumi and Y. Chujo, "Synthesis of π-Conjugated Poly(cyclodiborazane)s by Organometallic Polycondensation," *Macromolecules*, vol. 33, no. 22, pp. 8146–8148, **2000**.

[18] C. H. Zhao, A. Wakamiya, and S. Yamaguchi, "Highly emissive poly(aryleneethynylene)s

containing 2,5-diboryl-1,4-phenylene as a building unit," *Macromolecules*, vol. 40, pp. 3898–3900, **2007**.

[19] V. Bonifacio, J. Morgado, and U. Scherf, "Polyfluorenes with On-Chain Dibenzoborole Units — Synthesis and Anion-induced photoluminescence quenching," *J. Polym. Sci. Part A Polym. Chem.*, vol. 46, pp. 2878–2883, **2008**.

[20] D. Reitzenstein and C. Lambert, "Localized versus Backbone Fluorescence in N-p-(Diarylboryl) phenyl-substituted 2,7- and 3,6-linked polycarbazoles," *Macromolecules*, vol. 42, pp. 773–782, **2009**.

[21] A. Nagai, J. Miyake, K. Kokado, Y. Nagata, and Y. Chujo, "Highly Luminescent BODIPY-Based Organoboron Polymer Exhibiting Supramolecular Self-Assemble Structure," *J. Am. Chem. Soc.*, vol. 130, pp. 15276–15278, **2008**.

[22] C. D. Entwistle and T. B. Marder, "Applications of three-coordinate organoboron compounds and polymers in optoelectronics," *Chem. Mater.*, vol. 16, no. 23, pp. 4574–4585, **2004**.

[23] R. J.-P. Corriu, T. Deforth, W. E. Douglas, G. Guerrero, and W. S. Siebert, "Unsaturated polymers containing boron and thiophene units in the backbone," *Chem. Commun.*, vol. 9, pp. 963–964, **1998**.

[24] N. Matsumi, M. Miyata, and Y. Chujo, "Synthesis of organoboron π-conjugated polymers by hydroboration polymerization between heteroaromatic diynes and mesitylborane and their light emitting properties," *Macromolecules*, vol. 32, pp. 4467–4469, **1999**.

[25] K. Smith, A. Pelter, and Z. Jin, "Synthesis and properties of 2,4,6-trimethylphenylborane (mesitylborane), a stable alternative to thexylborane," *Angew. Chemie - Int. Ed.*, vol. 33, no. 8, pp. 851–853, **1994**.

[26] A. Pelter, K. Smith, D. Buss, and Z. Jin, "Hindered organoboron groups in organic synthesis. 17. Synthesis of 2,4,6-triisopropylphenylborane $(TripBH_2)_2$, a useful alternative to thexylborane," *Heteroat. Chem.*, vol. 3, no. 3, pp. 275–277, **1992**.

[27] A. Lorbach *et al.*, "9,10-Dihydro-9,10-diboraanthracene: Supramolecular structure and use as a building block for luminescent conjugated polymers," *Angew. Chemie - Int. Ed.*, vol. 48, pp. 4584–4588, **2009**.

[28] J. Chai, C. Wang, L. Jia, Y. Pang, M. Graham, and S. Z. D. Cheng, "Synthesis and electrochemical properties of a new class of boron-containing n-type conjugated polymers," *Synth. Met.*, vol. 159, no. 14, pp. 1443–1449, **2009**.

[29] S. Ramakrishnan, E. Berluche, and T. C. Chung, "Functional Group Containing Copolymers Prepared by the Ziegler-Natta Process," *Macromolecules*, vol. 23, pp. 378–382, **1990**.

[30] T. C. Chung and D. Rhubright, "Synthesis of Functionalized Polypropylene," *Macromolecules*, vol. 24, no. 4, pp. 970–972, **1991**.

[31] T. C. Chung and G. J. Jiang, "Synthesis of poly(1-octene-g-methyl methacrylate) copolymers," *Macromolecules*, vol. 25, no. 18, pp. 4816–4818, **1992**.

[32] T. C. Chung and D. Rhubright, "Kinetic Aspects of the Copolymerization between alpha-Olefins and Borane Monomer in Ziegler-Natta Catalyst," *Macromolecules*, vol. 26, no. 12, pp. 3019–3025, **1993**.

[33] T. C. Chung, D. Rhubright, and G. J. Jiang, "Synthesis of Polypropylene-graft-poly(methyl methacrylate) Copolymers by the Borane Approach," *Macromolecules*, vol. 26, no. 14, pp. 3467–3471, **1993**.

[34] T. C. Chung and D. Rhubright, "Polypropylene-graft-Polycaprolactone: Synthesis and Applications in Polymer Blends," *Macromolecules*, vol. 27, no. 6, pp. 1313–1319, **1994**.

[35] S. Ramakrishnan and T. C. Chung, "Poly(exo-5-hydroxynorbornene): a functional polymer using metathesis polymerization of an organoborane derivative," *Macromolecules*, vol. 22, no. 7, pp. 3181–3183, **1989**.

[36] T. C. Chung, "Synthesis of functional metathesis catalysts polymers *via* borane monomers and metathesis catalysts," *J. Mol. Catal.*, vol. 76, pp. 15–31, **1992**.

[37] X. Wei, P. J. Carroll, and L. G. Sneddon, "New Routes to Organodecaborane Polymers *via* Ruthenium-Catalyzed Ring-Opening Metathesis Polymerization," *Organometallics*, vol. 23, pp. 163–165, **2004**.

[38] P. Paetzold and J. Hoffmann, "Eine neue Methode zur Borylierung von Alkylbenzol und Polystyrol," *Chem. Ber.*, vol. 113, pp. 3724–3733, **1980**.

[39] Y. Kondo, D. García-Cuadrado, J. F. Hartwig, N. K. Boaen, N. L. Wagner, and M. A. Hillmyer, "Rhodium-catalyzed, regiospecific functionalization of polyolefins in the melt," *J. Am. Chem. Soc.*, vol. 124, no. 7, pp. 1164–1165, **2002**.

[40] S. Ramakrishnan, "Well-Defined Ethylene-Vinyl Alcohol Copolymers *via* Hydroboration: Control of Composition and Distribution of the Hydroxyl Groups on the Polymer Backbone," *Macromolecules*, vol. 24, pp. 3753–3759, **1991**.

[41] T. C. Chung *et al.*, "Butyl rubber graft copolymers: synthesis and characterization," *Polymer (Guildf).*, vol. 36, no. 18, pp. 3565–3574, **1995**.

[42] Y. Chujo, I. Tomita, T. Asano, and T. Saegusa, "Hydroboration of styryl-terminated polystyrene with bifunctional thexylborane," *Polym. Bull.*, vol. 30, pp. 215–222, **1993**.

[43] B. Lu and T. C. Chung, "Maleic Anhydride Modified Polypropylene with Controllable Molecular Structure: New Synthetic Route *via* Borane-Terminated Polypropylene," *Macromolecules*, vol. 31, pp. 5943–5946, **1998**.

[44] J. D. Revell, B. Dörner, P. D. White, and A. Ganesan, "PS-COD and PS-9-BBN: Polymer-supported reagents for solution-phase parallel synthesis," *Org. Lett.*, vol. 7, no. 5, pp. 831–833, **2005**.

[45] C. P. Pinazzi, P. Guillaume, and D. Reyx, "Fixation de microchaînons carbonyles sur des polyisoprènes et polybutadiènes par hydroboration. Réaction sur modèles macromoléculaires.," *J. Polym. Sci. Symp.*, vol. 47, no. 1, pp. 167–178, **1974**.

[46] C. P. Pinazzi, P. Guillaume, and D. Reyx, "Gamma-oxoalkylation de polyalcadiènes à structures-1,4 predominantes par reaction couplée à l'hydroboration," *Eur. Polym. J.*, vol. 13, no. 9, pp. 707–711, **1977**.

[47] T. C. Chung, M. Raate, E. Berluche, and D. N. Schulz, "Synthesis of functional hydrocarbon polymers with well-defined molecular structures," *Macromolecules*, vol. 21, no. 7, pp. 1903–1907, **1988**.

[48] K. Smith, G. A. El-Hiti, D. Hou, and G. A. DeBoos, "Preparation and use of sterically hindered organobis(2,4,6-triisopropylphenyl)hydroborates and their polystyrene derivatives for the diastereoselective reduction of ketones," *J. Chem. Soc. Perkin Trans. 1*, pp. 2807–2812, **1999**.

[49] J. E. Mulvaney, J. J. Bloomfield, and C. S. Marvel, "Polybenzborimidazolines," *J. Polym. Sci. Part A Polym. Chem.*, vol. 62, pp. 59–72, **1962**.

[50] I. Yamaguchi, T. Tominaga, and M. Sato, "Pd-complex-catalyzed synthesis of oligomers

having a recurring benzodiazaborole unit in the main chain," *Polym. Int.*, vol. 58, pp. 17–21, **2009**.

[51] M. Grosche, E. Herdtweck, F. Peters, and M. Wagner, "Boron–Nitrogen Coordination Polymers Bearing Ferrocene in the Main Chain," *Organometallics*, vol. 18, pp. 4669–4672, **1999**.

[52] E. Herdtweck, F. Jäkle, and M. Wagner, "Ferrocenophanes with Interannular Boron - Phosphorus Bridges : Synthesis, Structure, and Reactivity toward Nitrogen Bases," *Organometallics*, vol. 16, pp. 4737–4745, **1997**.

[53] K. Ma, M. Scheibitz, S. Scholz, and M. Wagner, "Applications of boron-nitrogen and boron-phosphorus adducts in organometallic chemistry," *J. Organomet. Chem.*, vol. 652, pp. 11–19, **2002**.

[54] F. Matsumoto, Y. Nagata, and Y. Chujo, "Synthesis of novel poly(pyrazabole)s with electron-withdrawing structure in their main chain," *Polym. Bull.*, vol. 53, pp. 155–160, **2005**.

[55] H. Li and F. Jäkle, "Universal scaffold for fluorescent conjugated organoborane polymers," *Angew. Chemie - Int. Ed.*, vol. 48, no. 13, pp. 2313–2316, **2009**.

[56] Y. Cui and S. Wang, "Diboron and triboron compounds based on linear and star-shaped conjugated ligands with 8-hydroxyquinolate functionality: Impact of intermolecular interaction and boron coordination on luminescence," *J. Org. Chem.*, vol. 71, no. 17, pp. 6485–6496, **2006**.

[57] M. Zhu *et al.*, "Effecient Tuning Nonlinear Optical Properties: Synthesis and Characterization of a series of Novel Poly(aryleneethylene)s co-containing BODIPY," *J. Polym. Sci. Part A Polym. Chem.*, vol. 46, no. 22, pp. 7401–7410, **2008**.

[58] G. Ulrich, R. Ziessel, and A. Harriman, "The chemistry of fluorescent bodipy dyes: Versatility unsurpassed," *Angew. Chemie - Int. Ed.*, vol. 47, no. 7, pp. 1184–1201, **2008**.

[59] A. Staubitz, A. P. Soto, and I. Manners, "Iridium-catalyzed dehydrocoupling of primary amine-borane adducts: A route to high molecular weight polyaminoboranes, boron-nitrogen analogues of polyolefins," *Angew. Chemie - Int. Ed.*, vol. 47, no. 33, pp. 6212–6215, **2008**.

[60] A. Ledoux, "Polymères contenant des paires de Lewis de type amine-borane , en tant que réservoirs d'hydrogène : relation structure / activité," Université de Lyon, **2016**.

[61] A. Ledoux, P. Larini, C. Boisson, V. Monteil, J. Raynaud, and E. Lacôte, "Angewandte Polyboramines for Hydrogen Release : Polymers Containing Lewis Pairs in their Backbone," *Angew. Chemie - Int. Ed.*, vol. 54, pp. 15744–15749, **2015**.

[62] R. H. Cragg, M. F. Lappert, and B. P. Tilley, "Chloroboration and Allied Reactions of Unsaturated Compounds. Part III. Aminoboration and Alkoxyboration of Isocyanates and Isothiocyanates.," *J. Chem. Soc.*, pp. 2108–2115, **1964**.

[63] N. Matsumi and Y. Chujo, "Alkoxyboration Polymerization. Synthesis of Novel Poly(boronic carbamate)s," *Macromolecules*, vol. 31, pp. 3802–3806, **1998**.

[64] M. Fontani, F. Peters, W. Scherer, W. Wachter, M. Wagner, and P. Zanello, "Adducts of Ferrocenylboranes and Pyridine Bases: Generation of Charge-Transfer Complexes and Reversible Coordination Polymers," *Eur. J. Inorg. Chem.*, pp. 1453–1465, **1998**.

[65] N. Christinat, E. Croisier, R. Scopelliti, M. Cascella, U. Röthlisberger, and K. Severin, "Formation of boronate ester polymers with efficient intrastrand charge-transfer transitions by three-component reactions," *Eur. J. Inorg. Chem.*, no. 33, pp. 5177–5181,

2007.

[66] H. Braunschweig *et al.*, "Incorporation of a first row element into the bridge of a strained metallocenophane: synthesis of a boron-bridged ferrocenophane," *Angew. Chem. Int. Ed. Engl.*, vol. 36, no. 21, pp. 2338–2340, **1997**.

[67] J. Pellon, W. G. Deichert, and W. M. Thomas, "Polymerization of vinyl monomers containing boron I. p-vinylphenylboronic acid," *J. Polym. Sci.*, vol. 55, pp. 153–160, **1961**.

[68] K. Su, E. E. Remsen, H. M. Thompson, and L. G. Sneddon, "Syntheses and Properties of Poly(B-vinylborazine) and Poly(styrene-*co*-B-vinylborazine) Copolymers," *Macromolecules*, vol. 24, pp. 3760–3766, **1991**.

[69] A. T. Lynch and L. G. Sneddon, "Transition-Metal-Promoted Reactions of Boron Hydrides. 12. Syntheses, Polymerizations, and Ceramic Conversion Reactions of B-Alkenylborazines," *J. Am. Chem. Soc.*, vol. 111, no. 16, pp. 6201–6209, **1989**.

[70] L. A. Jackson and C. W. Allen, "Organoborazines. Part 2. Synthesis of alkenyltriborazines," *J. Chem. Soc. Dalt. Trans.*, vol. 12, p. 2423, **1989**.

[71] L. A. Jackson and C. W. Allen, "Organoborazines. III. Homo- and copolymerization of p-vinylphenylcyclotriborazines," *J. Polym. Sci. Part A Polym. Chem.*, vol. 30, pp. 577–581, **1992**.

[72] A. Nagai, K. Kokado, J. Miyake, and Y. Chujo, "Highly luminescent nanoparticles: Self-assembly of well-defined block copolymers by π-π stacked BODIPY dyes as only a driving force," *Macromolecules*, vol. 42, no. 15, pp. 5446–5452, **2009**.

[73] Y. Qin, C. Pagba, P. Piotrowiak, and F. Jäkle, "Luminescent organoboron quinolate polymers," *J. Am. Chem. Soc.*, vol. 126, no. 22, pp. 7015–7018, **2004**.

[74] Y. Qin, I. Kiburu, S. Shah, and F. Jäkle, "Luminescence tuning of organoboron quinolates through substituent variation at the 5-position of the quinolato moiety," *Org. Lett.*, vol. 8, no. 23, pp. 5227–5230, **2006**.

[75] X. Y. Wang and M. Weck, "Poly(styrene)-supported Alq_3 and BPh_2q," *Macromolecules*, vol. 38, no. 17, pp. 7219–7224, **2005**.

[76] D. G. Hall, *Boronic Acids: Preparation and Applications in Organic Synthesis and Medicine*. Wiley-VCH Verlag GmbH & Co. KGaA, **2006**.

[77] W. L. A. Brooks and B. S. Sumerlin, "Synthesis and Applications of Boronic Acid-Containing Polymers : From Materials to Medicine," *Chem. Rev.*, vol. 116, pp. 1375–1397, **2016**.

[78] D. G. Hall, *Structure , Properties , and Preparation Of Boronic Acid Derivatives . Overview of Their Reactions and Applications*. Wiley-VCH Verlag GmbH & Co, **2005**.

[79] Y. Li, J. Ding, M. Day, Y. Tao, J. Lu, and D. Marie, "Novel Stable Blue-Light-Emitting Oligofluorene Networks Immobilized by Boronic Acid Anhydride Linkages," *Chem. Mater.*, vol. 15, no. 4, pp. 4936–4943, **2003**.

[80] J. N. Cambre and B. S. Sumerlin, "Biomedical applications of boronic acid polymers," *Polymer (Guildf).*, vol. 52, no. 21, pp. 4631–4643, **2011**.

[81] G. Springsteen and B. Wang, "A detailed examination of boronic acid-diol complexation," *Tetrahedron*, vol. 58, pp. 5291–5300, **2002**.

[82] J. W. Tomsho, A. Pal, D. G. Hall, and S. J. Benkovic, "Ring Structure and Aromatic Substituent Effects on the pK_a of the Benzoxaborole Pharmacophore," *ACS Med. Chem. Lett.*, vol. 3, pp. 48–52, **2012**.

[83] G. Wulff, M. Lauer, and H. Böhnke, "Rapid Proton Transfer as Cause of an Unusually Large Neighboring Group Effect," *Angew. Chemie - Int. Ed. English*, vol. 23, pp. 741–742, **1984**.

[84] X. Yang, M. Lee, F. Sartain, X. Pan, and C. R. Lowe, "Designed Boronate Ligands for Glucose-Selective Holographic Sensors," *Chem. - A Eur. J.*, vol. 12, pp. 8491–8497, **2006**.

[85] L. Garlaschelli, G. Mellerio, and G. Vidari, "High Yield Preparation of Boronic Esters of 1,2-Diols with Lithium Trialkylborohydrides," *Tetrahedron Lett.*, vol. 30, no. 5, pp. 597–600, **1989**.

[86] H. G. Kuivila, A. H. Keough, and E. Soboczenski, "Areneboronates from diols and polyols," *J. Org. Chem.*, vol. 19, no. 5, pp. 780–783, **1952**.

[87] R. L. Letsinger and N. Remes, "Organoboron Compounds. V. The Preparation of an Unsymmetrical Diarylborinate," *J. Am. Chem. Soc.*, vol. 77, no. 9, pp. 2489–2491, **1955**.

[88] H. Zimmerman and H. Weidmann, "Borsäure-ester von N-Substituierten Aminoalkoholen," *European J. Org. Chem.*, vol. 619, no. 1, pp. 28–35, **1959**.

[89] R. Haruta, M. Ishiguro, N. Ikeda, and H. Yamamoto, "Chiral Allenylboronic Esters: A Practical Reagent for Enantioselective Carbon-Carbon Bond Formation," *J. Am. Chem. Soc.*, vol. 104, no. 24, pp. 7667–7669, **1982**.

[90] U. Gerwarth, "Rearrangements of medium sized O-B-O heterocycles to cyclic oligomers," *Naturforsch*, vol. 32b, pp. 1408–14145, **1977**.

[91] P. S. Wolfe and K. B. Wagener, "Investigation of organoboronates in metathesis polymerization," *Macromolecules*, vol. 32, no. 24, pp. 7961–7967, **1999**.

[92] M. Mastalerz, "The next generation of shape-persistant zeolite analogues: Covalent Organic Frameworks," *Angew. Chemie - Int. Ed.*, vol. 47, pp. 445–447, **2008**.

[93] N. Fujita, S. Shinkai, and T. D. James, "Boronic acids in molecular self-assembly," *Chem. - An Asian J.*, vol. 3, no. 7, pp. 1076–1091, **2008**.

[94] K. Severin, "Boronic acids as building blocks for molecular nanostructures and polymeric materials," *Dalt. Trans.*, p. 5254, **2009**.

[95] A. L. Korich and P. M. Iovine, "Boroxine chemistry and applications: A perspective," *Dalt. Trans.*, vol. 39, pp. 1423–1431, **2010**.

[96] W. Niu, C. O'Sullivan, B. M. Rambo, M. D. Smith, and J. J. Lavigne, "Self-repairing polymers: poly(dioxaborolane)s containing trigonal planar boron," *Chem. Commun.*, p. 4342, **2005**.

[97] J. C. Sanchez and W. C. Trogler, "Polymerization of a boronate-functionalized fluorophore by double transesterification: applications to fluorescence detection of hydrogen peroxide vapor," *J. Mater. Chem.*, vol. 18, p. 5134, **2008**.

[98] A. K. Hoffmann and W. M. Thomas, "The Synthesis of p-Vinylphenylboronic Acid And Some of Its Derivatives," *J. Am. Chem. Soc.*, vol. 81, no. 3, pp. 580–582, **1959**.

[99] R. L. Letsinger and S. B. Hamilton, "Organoboron Compounds. X. Popcorn Polymers And Highly Cross-Linked Vinyl Polymers Containing Boron," *J. Am. Chem. Soc.*, vol. 81, no. 12, pp. 3009–3012, **1959**.

[100] W. J. Lennarz and H. R. Snyder, "Arylboronic Acids. III. Preparation and Polymerization of p-Vinylbenzeneboronic Acid," *J. Am. Chem. Soc.*, vol. 82, pp. 2169–2171, **1960**.

[101] J. Pellon, L. H. Schwind, M. J. Guinard, and W. M. Thomas, "Polymerization of vinyl monomers containing boron II. p-vinylphenylboronic acid," *J. Polym. Sci.*, vol. 55, pp. 161–167, **1961**.

[102] M. Hartmann, H. Carlsohn, and J. Pauls, "Über Copolymere der p-Vinylbenzolboronsaure mit Styrol," *Die Makromol. chemie*, vol. 177, pp. 131–144, **1976**.

[103] H. Kamogawa and S. Shiraki, "Effect of Pendant Functional Alcohol Residues of (p-Vinylphenyl)borate Copolymers on Hydrolysis," *Macromolecules*, vol. 24, pp. 4224–4226, **1991**.

[104] B. B. De, S. Sivaram, and P. K. Dhal, "An Unequivocal Approach to Ascertain Asymmetric Induction in the Polymer Main Chain during Enantioselective Copolymerization of 1,2-Disubstituted Olefins," *Macromolecules*, vol. 29, no. 1, pp. 468–470, **1996**.

[105] R. Hu and T. C. Chung, "Poly(acrylonitrile-*co*-vinylcatecholborane): A new precursor for carbon containing B/C, B/N and B/O species," *Carbon N. Y.*, vol. 34, no. 5, pp. 595–600, **1996**.

[106] G. Giffels, J. Beliczey, M. Felder, and U. Kragl, "Polymer enlarged oxazaborolidines in a membrane reactor: Enhancing effectivity by retention of the homogeneous catalyst," *Tetrahedron: Asymmetry*, vol. 9, pp. 691–696, **1998**.

[107] T. Ikeya, K. Kataoka, T. Okano, and Y. Sakurai, "Selective adhesion of rat lymphocyte subpopulation on the polymer surface with phenylboronic acid moieties: evaluation by field-flow fractionation/adhesion chromatography (FFF/AC) method," *React. Funct. Polym.*, vol. 37, pp. 251–261, **1998**.

[108] A. E. Ivanov, H. Larsson, I. Y. Galaev, and B. Mattiasson, "Synthesis of boronate-containing copolymers of N,N-dimethylacrylamide, their interaction with poly(vinyl alcohol) and rheological behaviour of the gels," *Polymer (Guildf).*, vol. 45, pp. 2495–2505, **2004**.

[109] H. Kitano, S. Morokoshi, K. Ohhori, M. Gemmei-Ide, Y. Yokoyama, and K. Ohno, "Accumulation of phenyl boronic acid-carrying telomers on a gold surface," *J. Colloid Interface Sci.*, vol. 273, pp. 106–114, **2004**.

[110] Y. Qin, V. Sukul, D. Pagakos, C. Cui, and F. Jäkle, "Preparation of organoboron block copolymers *via* ATRP of silicon and boron-functionalized monomers," *Macromolecules*, vol. 38, no. 22, pp. 8987–8990, **2005**.

[111] M. Röttger, T. Domenech, R. van der Weegen, A. Breuillac, R. Nicolaÿ, and L. Leibler, "High-performance vitrimers from commodity thermoplastics through dioxaborolane metathesis," *Science (80-.).*, vol. 356, no. 6333, pp. 62–65, **2017**.

[112] M. J. Farrall and J. M. J. Fréchet, "Bromination and Lithiation: Two Important Steps in the Functionalization of Polystyrene Resins," *J. Org. Chem.*, vol. 41, no. 24, pp. 3877–3882, **1976**.

[113] C. Franot, G. B. Stone, P. Engeli, C. Spöndlin, and E. Waldvogel, "A polymer-bound oxazaborolidine catalyst: Enantioselective borane reductions of ketones," *Tetrahedron: Asymmetry*, vol. 6, no. 11, pp. 2755–2766, **1995**.

[114] G. Belogi, T. Zhu, and G.-J. Boons, "Polymer-supported oligosaccharide synthesis by a loading–release–reloading strategy," *Tetrahedron Lett.*, vol. 41, pp. 6969–6972, **2000**.

[115] G. Belogi, T. Zhu, and G.-J. Boons, "Polystyrylboronic acid as a reusable polymeric support for oligosaccharide synthesis," *Tetrahedron Lett.*, vol. 41, no. 36, pp. 6965–6968, **2000**.

[116] D. Crich and M. Smith, "Solid-phase synthesis of β-mannosides," *J. Am. Chem. Soc.*, vol. 124, no. 30, pp. 8867–8869, **2002**.

[117] C. Caze, N. El Moualij, P. Hodge, C. Lock, and J. Ma, "Some enatioselective borane reductions of prochiral ketones catalysed by polymer-supported oxazaborolidines bound *via* the

boron atom," *J. Chem. Soc. Perkin Trans. 1*, pp. 345–349, **1995**.

[118] C. Caze, N. Moualij, P. Hodge, and C. J. Lock, "Chiral oxazaborolidines bound *via* the boron atom to polymers prepared using 2-vinylthiophene: polymer-supported catalysts for the enantioselective reduction of prochiral ketones by borane," *Polymer (Guildf).*, vol. 36, no. 3, pp. 621–629, **1995**.

[119] N. Bullen, P. Hodge, and G. Thorpe, "Mercuriation and thalliation of polystyrene: conversion of the products into polystyrenes containing iodobenzene, phenylboronic acid, and phenol residues," *J. Chem. Soc. Perkin Trans. 1*, pp. 1863–1867, **1981**.

[120] S. A. El-Assiery, K. A. Dillingham, A. Ponsonby, F. G. Thorpe, and R. S. Wareham, "Reactions of mercuriated polystyrenes with boron hydrides," *Eur. Polym. J.*, vol. 29, no. 2/3, pp. 443–447, **1993**.

[121] A. A. H. A. Al-kadhumi, P. Hodge, and F. G. Thorpe, "Mercuriation and Thalliation of Polymers Prepared Using 2-Vinylthiophene: Conversion of Products into Polymers Containing Thienylboronic Acid Residues," *Br. Polym. J.*, vol. 16, pp. 225–230, **1984**.

[122] A. A. H. A. Al-kadhumi, P. Hodge, and F. G. Thorpe, "Lithiation , Mercuriation , and Thalliation of Poly (N-vinylcarbazole): Chemical Transformations of the Products," *Br. Polym. J.*, vol. 19, pp. 325–331, **1987**.

[123] A. A. H. A. Al-kadhumi, P. Hodge, B. J. Hunt, and F. G. Thorpe, "Chemical modification *via* mercuriation and thalliation of crosslinked polymers prepared from acenaphthylene: preparation of polymers containing iodo, phenolic, or boronic acid residues," *React. Funct. Polym.*, vol. 7, pp. 15–23, **1987**.

[124] Y. Qin, G. Cheng, A. Sundararaman, and F. Jäkle, "Well-defined boron-containing polymeric Lewis acids," *J. Am. Chem. Soc.*, vol. 124, no. 43, pp. 12672–12673, **2002**.

[125] Y. Qin, G. Cheng, O. Achara, K. Parab, and F. Jäkle, "A new route to organoboron polymers *via* highly selective polymer modification reactions," *Macromolecules*, vol. 37, no. 19, pp. 7123–7131, **2004**.

[126] K. Matyjaszewski and J. Xia, "Atom transfer radical polymerization," *Chem. Rev.*, vol. 101, pp. 2921–2990, **2001**.

[127] A. Sundararaman, R. A. Lalancette, L. N. Zakharov, A. L. Rheingold, and F. Jäkle, "Structural diversity of pentafluorophenylcopper complexes. First evidence of π-coordination of unsupported arenes to organocopper aggregates," *Organometallics*, vol. 22, pp. 3526–3532, **2003**.

[128] A. Sundararaman and F. Jäkle, "A comparative study of base-free arylcopper reagents for the transfer of aryl groups to boron halides," *J. Organomet. Chem.*, vol. 681, pp. 134–142, **2003**.

[129] R. G. Ricarte, F. Tournilhac, and L. Leibler, "Phase Separation and Self-Assembly in Vitrimers: Hierarchical Morphology of Molten and Semicrystalline Polyethylene/ Dioxaborolane Maleimide Systems," *Macromolecules*, vol. 52, pp. 432–443, **2019**.

[130] F. Caffy and R. Nicolaÿ, "Transformation of polyethylene into a vitrimer by nitroxide radical coupling of a bis-dioxaborolane," *Polym. Chem.*, p. Advance Article, **2019**.

[131] E. Shoji and M. S. Freund, "Poly(aniline boronic acid): A new precursor to substituted poly(aniline)s," *Langmuir*, vol. 17, no. 23, pp. 7183–7185, **2001**.

[132] M. Nicolas, B. Fabre, G. Marchand, and J. Simonet, "New Boronic-Acid-and Boronate-Substituted Aromatic Compounds as Precursors of Fluoride-Responsive Conjugated

Polymer Films," *European J. Org. Chem.*, pp. 1703–1710, **2000**.

[133] B. Fabre, "Synthesis of a boron-containing conducting polymer from the anodic oxidation of Tris(pyrrolyl)borane," *Synth. Met.*, vol. 129, pp. 309–314, **2002**.

[134] E. Pringsheim, E. Terpetschnig, S. A. Piletsky, and O. S. Wolfbeis, "A Polyaniline with Near-Infrared Optical Response to Saccharides," *Adv. Mater.*, vol. 11, no. 10, pp. 865–868, **1999**.

[135] B. A. Deore, I. Yu, and M. S. Freund, "A Switchable Self-Doped Polyaniline: Interconversion between Self-Doped and Non-Self-Doped Forms," *J. Am. Chem. Soc.*, vol. 126, no. 1, pp. 52–53, **2004**.

[136] J. J. Cash, T. Kubo, A. P. Bapat, and B. S. Sumerlin, "Room-Temperature Self-Healing Polymers Based on Dynamic-Covalent Boronic Esters," *Macromolecules*, vol. 48, pp. 2098–2106, **2015**.

[137] A. P. Bapat, D. Roy, J. G. Ray, D. A. Savin, and B. S. Sumerlin, "Dynamic-Covalent Macromolecular Stars with Boronic Ester Linkages," *J. Am. Chem. Soc.*, vol. 133, pp. 19832–19838, **2011**.

[138] V. Heleg-Shabtai, R. Aizen, R. Orbach, M. A. Aleman-garcia, and I. Willner, "Gossypol-Cross-linked Boronic acid-modified hydrogels: A Functional Matrix for the Controlled Release of an Anticancer Drug," *Langmuir*, no. 31, pp. 2237–2242, **2015**.

[139] L. He, D. Szopinski, Y. Wu, G. A. Luinstra, and P. Theato, "Toward Self-Healing Hydrogels Using One-Pot Thiol-Ene Click and Borax-Diol Chemistry," *ACS Macro Lett.*, vol. 4, pp. 673–678, **2015**.

[140] C. C. Deng, W. L. A. Brooks, K. A. Abboud, and B. S. Sumerlin, "Boronic acid-based hydrogels undergo self-healing at neutral and acidic pH," *ACS Macro Lett.*, vol. 4, pp. 220–224, **2015**.

[141] D. Tarus, E. Hachet, L. Messager, B. Catargi, V. Ravaine, and R. Auzély-velty, "Readily Prepared Dynamic Hydrogels by Combining Phenyl Boronic Acid- and Maltose-Modified Anionic Polysaccharides at Neutral pH," *Macromol. Rapid Commun.*, vol. 35, pp. 2089–2095, **2014**.

[142] T. Aoki *et al.*, "Glucose sensitive lower critical solution temperature changes of copolymers composed of N-isopropylacrylamide and phenylboronic acid moities," *Polym. J.*, vol. 28, no. 4, pp. 371–374, **1996**.

[143] K. Kataoka, H. Miyazaki, and M. Bunya, "Totally Synthetic Polymer Gels Responding to External Glucose Concentration: Their Preparation and Application to On-Off Regulation of Insulin Release," *J. Am. Chem. Soc.*, vol. 120, no. 13, pp. 12694–12695, **1998**.

[144] A. Matsumoto, K. Yamamoto, R. Yoshida, K. Kataoka, T. Aoyagi, and Y. Miyahara, "A totally synthetic glucose responsive gel operating in physiological aqueous conditions," *Chem. Commun.*, vol. 46, pp. 2203–2205, **2010**.

[145] Y. Zhang, Y. Guan, and S. Zhou, "Synthesis and Volume Phase Transitions of Glucose-sensitive Microgels," *Biomacromolecules*, vol. 7, pp. 3196–3201, **2006**.

[146] Y. Zhang, Y. Guan, and S. Zhou, "Permeability Control of Glucose-Sensitive Nanoshells," *Biomacromolecules*, vol. 8, pp. 3842–3847, **2007**.

[147] Z. Tang, Y. Guan, and Y. Zhang, "Concentration-type glucose-sensitive microgel functionalized with a 2-substituted phenylboronic acid ligand," *Polym. Chem.*, vol. 5, pp. 1782–1790, **2014**.

[148] J. Cao, S. Liu, Y. Chen, and Z. Zhang, "Synthesis of end-functionalized boronic acid containing copolymers and their bioconjugates with rod-like viruses for multiple responsive," *Polym.*

Chem., vol. 5, pp. 5029–5036, **2014**.

[149] B. J. I. Jay *et al.*, "Modulation of Viscoelasticity and HIV Transport as a Function of pH in a Reversibly Crosslinked Hydrogel," *Adv. Funct. Mater.*, vol. 19, pp. 2969–2977, **2009**.

[150] C. Cui, E. M. Bonder, Y. Qin, and F. Jäkle, "Synthesis and Solvent-Dependent Micellization of the Amphiphilic Block Copolymer Poly (styreneboronic acid)-block-Polystyrene," *J. Polym. Sci. Part A Polym. Chem.*, vol. 48, pp. 2438–2445, **2010**.

[151] S. Maji, G. Vancoillie, L. Voorhaar, Q. Zhang, and R. Hoogenboom, "RAFT Polymerization of 4-Vinylphenylboronic Acid as the Basis for Micellar Sugar Sensors," *Macromol. Rapid Commun.*, vol. 35, pp. 214–220, **2014**.

[152] J. N. Cambre, D. Roy, and B. S. Sumerlin, "Tuning the Sugar-Response of Boronic Acid Block Copolymers," *J. Polym. Sci. Part A Polym. Chem.*, vol. 50, pp. 3373–3382, **2012**.

[153] S. D. Roy, J. N. Cambre, and B. S. Sumerlin, "Triply-responsive boronic acid block copolymers: solution self-assembly induced by changes in temperature, pH, or sugar concentration," *Chem. Commun.*, pp. 2106–2109, **2009**.

[154] A. P. Bapat, D. Roy, J. G. Ray, D. A. Savin, and B. S. Sumerlin, "Dynamic-Covalent Macromolecular Stars with Boronic Ester Linkages," *J. Am. Chem. Soc.*, vol. 133, pp. 19832–19838, **2011**.

[155] Y. Li *et al.*, "Well-Defined, Reversible Boronate Crosslinked Nanocarriers for Targeted Drug Delivery in Response to Acidic pH Values and cis-Diols," *Angew. Chemie - Int. Ed.*, vol. 51, pp. 2864–2869, **2012**.

[156] Z. Zhao, X. Yao, Z. Zhang, L. Chen, C. He, and X. Chen, "Boronic Acid Shell-Crosslinked Dextran-b-PLA Micelles for Acid-Responsive Drug Delivery," *Macromol. Biosci.*, vol. 14, pp. 1609–1618, **2014**.

[157] A. Kikuchi *et al.*, "Glucose-Sensing Electrode Coated with Polymer Complex Gel Containing Phenylboronic Acid," *Anal. Chem.*, vol. 68, no. 5, pp. 823–828, **1996**.

[158] B. A. Deore, M. D. Braun, and M. S. Freund, "pH Dependent Equilibria of Poly(anilineboronic acid)-Saccharide Complexation in Thin Films," *Macromol. Chem. Phys*, vol. 207, pp. 660–664, **2006**.

[159] S. Hong, L. Yoon, S. Lee, M. So, and K. Wong, "A Dopamine Electrochemical Sensor Based on Molecularly Imprinted Poly(acrylamidophenylboronic acid) Film," *Electroanalysis*, vol. 25, no. 4, pp. 1085–1094, **2013**.

[160] C. Sugnaux and H. Klok, "Glucose-Sensitive QCM-Sensors *Via* Direct Surface RAFT Polymerization," *Macromol. Rapid Commun.*, vol. 35, pp. 1402–1407, **2014**.

[161] G. Lin *et al.*, "Osmotic Swelling Pressure Response of Smart Hydrogels Suitable for Chronically-Implantable Glucose Sensors," *Sens Actuators B Chem.*, vol. 144, no. 1, pp. 1–14, **2010**.

[162] R. Gabai, N. Sallacan, V. Chegel, T. Bourenko, E. Katz, and I. Willner, "Characterization of the Swelling of Acrylamidophenylboronic Acid-Acrylamide Hydrogels upon Interaction with Glucose by Faradaic Impedance Spectroscopy, Chronopotentiometry, Quartz-Crystal Microbalance (QCM), and Surface Plasmon Resonance (SPR) Experiments," *J. Phys. Chem. B*, vol. 105, pp. 8196–8202, **2001**.

[163] F. S. H. Krismastuti, W. L. A. Brooks, M. J. Sweetman, B. S. Sumerlin, and N. H. Voelcker, "A photonic glucose biosensor for chronic wound prognostics," *J. Mat B*, vol. 2, pp. 3972–3983, **2014**.

[164] S. Kabilan *et al.*, "Holographic glucose sensors," *Biosens. Bioelectron.*, vol. 20, pp. 1602–1610, **2005**.

[165] T. Kimura, M. Takeuchi, T. Nagasaki, and S. Shinkai, "Sugar-Induced Color and Orientation Changes in a Cyanine Dye Bound to Boronic-Acid-Appended Poly(L-lysine)," *Tetrahedron Lett.*, vol. 36, no. 4, pp. 559–562, **1995**.

[166] Y. Egawa, R. Gotoh, T. Seki, and J. Anzai, "Sugar response of boronic acid-substituted azobenzene dye-modi fied polymer," *Mater. Sci. Eng. C*, vol. 29, no. 1, pp. 115–118, **2009**.

[167] S. A. Asher *et al.*, "Photonic Crystal Carbohydrate Sensors: Low Ionic Strength Sugar Sensing," *J. Am. Chem. Soc.*, vol. 125, no. 5, pp. 3322–3329, **2003**.

[168] S. Gamsey, J. T. Suri, R. A. Wessling, and B. Singaram, "Continuous Glucose Detection Using Boronic Acid-Substituted Viologens in Fluorescent Hydrogels: Linker Effects and Extension to Fiber Optics," *Langmuir*, vol. 22, no. 28, pp. 9067–9074, **2006**.

[169] R. J. Gillespie and E. A. Robinson, "Gilbert N. Lewis and the chemical bond: The electron pair and the octet rule from 1916 to the present day," *J. Comput. Chem.*, vol. 28, no. 1, pp. 87–97, **2007**.

[170] H. C. Brown, H. I. Schlesinger, and S. Z. Cardon, "Studies in Stereochemistry. I. Steric Strains as a Factor in the Relative Stability of Some Coördination Compounds of Boron," *J. Am. Chem. Soc.*, vol. 64, no. 2, pp. 325–329, **1942**.

[171] G. Wittig and E. Benz, "Über das verhalten von dehydrobenzol gegenüber nucleophilen und elektrophilen reagenzien," *Chem. Ber.*, vol. 92, pp. 1999–2013, **1959**.

[172] S. Bontemps, G. Bouhadir, K. Miqueu, and D. Bourissou, "On the versatile and unusual coordination behavior of ambiphilic ligands o-$R_2P(Ph)BR'_2$," *J. Am. Chem. Soc.*, vol. 128, no. 37, pp. 12056–12057, **2006**.

[173] R. Roesler, W. E. Piers, and M. Parvez, "Synthesis, structural characterization and reactivity of the amino borane 1-(NPh_2)-2-$[B(C_6F_5)_2]C_6H_4$," *J. Organomet. Chem.*, vol. 680, no. 1–2, pp. 218–222, **2003**.

[174] G. C. Welch and D. W. Stephan, "Facile heterolytic cleavage of dihydrogen by phosphines and boranes," *J. Am. Chem. Soc.*, vol. 129, pp. 1880–1881, **2007**.

[175] P. Spies *et al.*, "Rapid intramolecular heterolytic dihydrogen activation by a four-membered heterocyclic phosphane–borane adduct," *Chem. Commun.*, p. 5072, **2007**.

[176] D. W. Stephan and G. Erker, "Frustrated Lewis Pair Chemistry: Development and Perspectives," *Angew. Chemie Int. Ed.*, vol. 54, pp. 6400–6441, **2015**.

[177] C. M. Mömming *et al.*, "Reversible metal-free carbon dioxide binding by Frustrated Lewis Pairs," *Angew. Chemie - Int. Ed.*, vol. 48, pp. 6643–6646, **2009**.

[178] I. Peuser *et al.*, "CO_2 and formate complexes of phosphine/borane Frustrated Lewis Pairs," *Chem. - A Eur. J.*, vol. 17, pp. 9640–9650, **2011**.

[179] M. Harhausen, R. Fröhlich, G. Kehr, and G. Erker, "Reactions of modified intermolecular frustrated P/B lewis pairs with dihydrogen, ethene and carbon dioxide," *Organometallics*, vol. 31, no. 7, pp. 2801–2809, **2012**.

[180] W. S. Siebert, M. Hildenbrand, P. Hornbach, G. Karger, and H. Pritzkow, "1,2- and 1,1-Diborylalkene," *Naturforsch*, vol. 44, pp. 1179–1186, **1989**.

[181] X. Zhao and D. W. Stephan, "Bis-boranes in the frustrated Lewis pair activation of carbon dioxide," *Chem. Commun.*, vol. 47, no. 6, p. 1833, **2011**.

[182] M. J. Sgro, J. Dömer, and D. W. Stephan, "Stoichiometric CO_2 reductions using a bis-borane-based frustrated Lewis pair," *Chem. Commun.*, vol. 48, p. 7253, **2012**.

[183] M. Feroci, I. Chiarotto, S. Vecchio Ciprioti, and A. Inesi, "On the reactivity and stability of electrogenerated N-heterocyclic carbene in parent 1-butyl-3-methyl-1H-imidazolium tetrafluoroborate: Formation and use of N-heterocyclic carbene-CO_2 adduct as latent catalyst," *Electrochim. Acta*, vol. 109, pp. 95–101, **2013**.

[184] J. D. Holbrey *et al.*, "1,3-Dimethylimidazolium-2-carboxylate: the unexpected synthesis of an ionic liquid precursor and carbene-CO_2 adduct," *Chem. Commun.*, vol. 347, no. 1, pp. 28–29, **2003**.

[185] E. L. Kolychev, T. Bannenberg, M. Freytag, C. G. Daniliuc, P. G. Jones, and M. Tamm, "Reactivity of a frustrated Lewis pair and small-molecule activation by an isolable arduengo carbene-B{3,5-$(CF_3)_2C_6H_3$}$_3$ complex," *Chem. - A Eur. J.*, vol. 18, pp. 16938–16946, **2012**.

[186] E. Theuergarten *et al.*, "Computational and experimental investigations of CO_2 and N_2O fixation by sterically demanding N-heterocyclic carbenes (NHC) and NHC/borane FLP systems," *Dalt. Trans.*, vol. 43, pp. 1651–1662, **2014**.

[187] Y. Liu, P. Jessop, M. Cunningham, C. Eckert, and C. Liotta, "Switchable Surfactants," *Science (80-.).*, vol. 313, pp. 958–960, **2006**.

[188] D. A. Dickie, M. V. Parkes, and R. A. Kemp, "Insertion of carbon dioxide into main-group complexes: Formation of the $[N(CO_2)_3]_3$- ligand," *Angew. Chemie - Int. Ed.*, vol. 47, pp. 9955–9957, **2008**.

[189] F. Fichter and B. Becker, "Über die bildung ysmmetrisch dialkylierter harnstoffe durch erhitsen der entsprechenden carbaminate," *Berichte d. Dtsch. Chem. Gesellschaft. Jahrg*, vol. 44, pp. 3481–3485, **1911**.

[190] E. A. Werner, "Constitution of Carbarnides. Part XI. The mechanism of the synthesis of urea from ammonium carbamate. The preparation of certain mixed tri-substituted carbamates and dithiocarbamates.," *J. Chem. Soc. Trans.*, vol. 117, pp. 1046–1053, **1920**.

[191] D. Belli Dell'Amico, F. Calderazzo, L. Labella, F. Marchetti, and G. Pampaloni, "Converting Carbon Dioxide into Carbamato Derivatives," *Chem. Rev.*, vol. 103, no. 10, pp. 3857–3897, **2003**.

[192] T. Voss *et al.*, "Frustrated Lewis Pair Behavior of Intermolecular Amine/$B(C_6F_5)_3$ Pairs," *Organometallics*, vol. 31, no. 6, pp. 2367–2378, **2012**.

[193] C. Jiang and D. W. Stephan, "Phosphinimine–borane combinations in frustrated Lewis pair chemistry," *Dalt. Trans.*, vol. 42, no. 3, pp. 630–637, **2013**.

[194] E. Theuergarten *et al.*, "Fixation of carbon dioxide and related small molecules by a bifunctional frustrated pyrazolylborane Lewis pair," *Dalt. Trans.*, vol. 41, p. 9101, **2012**.

[195] C. Appelt *et al.*, "Geminal phosphorus/aluminum-based frustrated lewis pairs: C-H versus C≡C activation and CO_2 fixation," *Angew. Chemie - Int. Ed.*, vol. 50, no. 17, pp. 3925–3928, **2011**.

[196] M. Reißmann, A. Schäfer, S. Jung, and T. Müller, "Silylium Ion/Phosphane Lewis Pairs," *Organometallics*, vol. 32, pp. 6736–6744, **2013**.

[197] A. M. Chapman, M. F. Haddow, and D. F. Wass, "Frustrated Lewis Pairs beyond the Main Group : Cationic Zirconocene-Phosphinoaryloxide Complexes," *J. Am. Chem. Soc.*, vol. 133, pp. 18463–18478, **2011**.

[198] M. P. Boone and D. W. Stephan, "Ancillary metal centers in frustrated lewis pair chemistry: Ruthenium acetylide as a lewis base in the activation of CO_2, aldehyde, and alkyne," *Organometallics*, vol. 33, no. 1, pp. 387–393, **2014**.

[199] L. J. Hounjet, C. B. Caputo, and D. W. Stephan, "Phosphorus as a lewis acid: CO_2 sequestration with amidophosphoranes," *Angew. Chemie - Int. Ed.*, vol. 51, pp. 4714–4717, **2012**.

[200] M. J. Sgro and D. W. Stephan, "Activation of CO_2 by phosphinoamide hafnium complexes," *Chem. Commun.*, vol. 49, p. 2610, **2013**.

[201] G. Kerlero de Rosbo, L. Rakotojaona, and J. De Bucy, "Valorisation chimique du CO_2 : Etat des Lieux - Quantification des bénéfices énergétiques et environnementaux et évalution économique de trois voies chimiques," **2014**.

[202] A. E. Ashley, A. L. Thompson, and D. O'Hare, "Non-metal-mediated homogeneous hydrogénation of CO_2 to CH_3OH," *Angew. Chemie - Int. Ed.*, vol. 48, no. 52, pp. 9839–9843, **2009**.

[203] A. Berkefeld, W. E. Piers, and M. Parvez, "Tandem Frustrated Lewis Pair/Tris(pentafluorophenyl)borane-Catalyzed Deoxygenative Hydrosilylation of Carbon Dioxide," *J. Am. Chem. Soc.*, vol. 132, pp. 10660–10661, **2010**.

[204] K. Takeuchi and D. W. Stephan, "Silyl-migrations in frustrated Lewis pair chemistry: reactions of $((CH_3)_3Si)_3P$ and $B(C_6F_4H)_3$ with H_2 and CO_2," *Chem. Commun.*, vol. 48, p. 11304, **2012**.

[205] G. Ménard and D. W. Stephan, "Room Temperature Reduction of CO_2 to Methanol by Al-Based Frustrated Lewis Pairs and Ammonia Borane," *J. Am. Chem. Soc.*, vol. 132, pp. 1796–1797, **2010**.

[206] R. Dobrovetsky and D. W. Stephan, "Catalytic reduction of CO_2 to CO by using zinc(II) and in situ generated carbodiphosphoranes," *Angew. Chemie - Int. Ed.*, vol. 52, pp. 2516–2519, **2013**.

[207] M. J. Sgro and D. W. Stephan, "Frustrated lewis pair inspired carbon dioxide reduction by a ruthenium tris(aminophosphine) complex," *Angew. Chemie - Int. Ed.*, vol. 51, pp. 11343–11345, **2012**.

[208] M. A. Courtemanche, M. A. Légaré, L. Maron, and F. G. Fontaine, "A highly active phosphine-borane organocatalyst for the reduction of CO_2 to methanol using hydroboranes," *J. Am. Chem. Soc.*, vol. 135, pp. 9326–9329, **2013**.

[209] E. P. A. of the U. States, "Sulfur Dioxide (SO_2) Pollution." [Online]. Available: https://www.epa.gov/so2-pollution/sulfur-dioxide-basics#effects.

[210] M. Sajid *et al.*, "Reactions of phosphorus/boron frustrated Lewis pairs with SO_2," *Chem. Sci.*, vol. 4, pp. 213–219, **2013**.

[211] A. de l'Environnement et de la M. de l'Energie (ADEME), "Le protoxyde d'azote - N_2O." [Online]. Available: https://www.ademe.fr/entreprises-monde-agricole/reduire-impacts/reduire-emissions-polluants/dossier/protoxyde-dazote-n2o/definition-sources-demissions-impacts-protoxyde-dazote.

[212] E. Otten, R. C. Neu, and D. W. Stephan, "Complexation of Nitrous Oxide by Frustrated Lewis Pairs," *J. Am. Chem. Soc.*, vol. 131, pp. 9918–9919, **2009**.

[213] R. C. Neu, E. Otten, and D. W. Stephan, "Bridging binding modes of phosphine-stabilized nitrous oxide to $Zn(C_6F_5)_2$," *Angew. Chemie - Int. Ed.*, vol. 48, pp. 9709–9712, **2009**.

[214] M. Wang, F. Nudelman, R. Matthes, and M. P. Shaver, "Frustrated Lewis Pair Polymers as

Responsive Self-Healing Gels," *J. Am. Chem. Soc.*, vol. 139, no. 40, pp. 14232–14236, **2017**.

[215] M. Trunk, J. F. Teichert, A. Thomas, and S. Juni, "Room-Temperature Activation of Hydrogen by Semi-immobilized Frustrated Lewis Pairs in Microporous Polymer Networks," *J. Am. Chem. Soc.*, vol. 139, pp. 3615–3618, **2017**.

[216] A. Willms *et al.*, "Solid Molecular Frustrated Lewis Pairs in a Polyamine Organic Framework for the Catalytic Metal-free Hydrogenation of Alkenes," *ChemCatChem*, vol. 10, pp. 1835–1843, **2018**.

[217] L. Chen, R. Liu, and Q. Yan, "Polymer meets Frustrated Lewis Pair: Second-generation CO_2-responsive nanosystem for sustainable CO_2 conversion," *Angew. Chemie - Int. Ed.*, vol. 57, no. 30, pp. 9336–9340, **2018**.

Chapter 2:

Reactive networks based on Lewis pairs

Chapter 2 is dedicated to the synthesis of Lewis-functionalized molecular bricks or polymers comprising Lewis acid or base functionalities. The interactions are studied between Lewis acids and bases harnessing the concept of Frustrated Lewis Pairs with the addition of a small molecule (in this work, carbon dioxide).

Table of contents

I. Introduction and strategies targeted

In a classical Lewis pair (CLP), a mutual quenching and neutralization occur between an electron-pair-donor and an electron-pair-acceptor respectively called Lewis acid and Lewis base, resulting in the formation of strong adducts. This concept was first described in 1923 by Gilbert Lewis. [1] On the other hand, some Lewis acids and bases are found to break this rule as no mutual quenching occurs when the two compounds are in presence of each other. Indeed, these Lewis acids and bases present steric and electronic frustrations that impedes the dative bond. [2] These new pairs are named as Frustrated Lewis Pairs and will be further abbreviated as FLPs. Figure II. 1 illustrates the difference between CLPs and FLPs.

Figure II. 1: Schematic difference between classical Lewis pair (CLP) and Frustrated Lewis pair (FLP).

In the bibliographical part (Chapter 1), we widely described the chemistry of these well-known FLPs such as their ability to split dihydrogen and thus their contribution to metal-free catalytic hydrogenations. [3], [4] In this present thesis work, we focused on the small-molecule binding by FLP which is a new and exciting area of chemistry that provides many possibilities in organic, inorganic and, in our subject of interest, polymer chemistry.

Indeed, FLPs present a reactivity with a large variety of small molecules: reactions with alkynes, dienes, alkenes, cyclic ethers and numerous gases such as CO, CO_2, NO, N_2O, SO_2, and also have an effect on the opening of cyclic molecules: tetrahydrofuran, cyclopropranes, cyclic ethers or even lactides. [5]

Following our reasoning, we decided to work on the capture of CO_2 by FLPs in a green chemistry optic. Undeniably, CO_2 is one of the major reason of climate warming due to the human and industrial development over the past hundred years that caused an increase of atmospheric CO_2 concentration. CO_2 emissions doubled over two decades from 0.65 tons in 1950 to 1.2 tons in 1970 and have remained stable since. In order to solve the CO_2 emissions problem, many scientists have proposed the large-scale sequestration of CO_2 from our atmosphere by geological storage, ocean storage, and mineral carbonation or by biomass and soil. [6] This idea of sequestration of CO_2 poses many challenges for researchers and faces many economic and ethical issues.

Moreover, captured CO_2 can be used in many valorization pathways and commercial applications, for instance in organic chemistry, hydrogenation, thermochemistry, photoelectrocatalysis, ex-situ mineralization and dried reforming. Two main paths can be adopted for converting CO_2 in another molecule: the functionalization with groups of interest or the reduction to higher states of energy. In this fashion, CO_2 can be the source for the formation of ethers, acetals, esters, amides, imines, carboxylic acids or still ketones. [7] CO_2 could be become an abundant, inexpensive, low toxic and renewable source of carbon for the synthesis of widely used organic molecules (Figure II. 2). This is also detailed in Chapter 1.

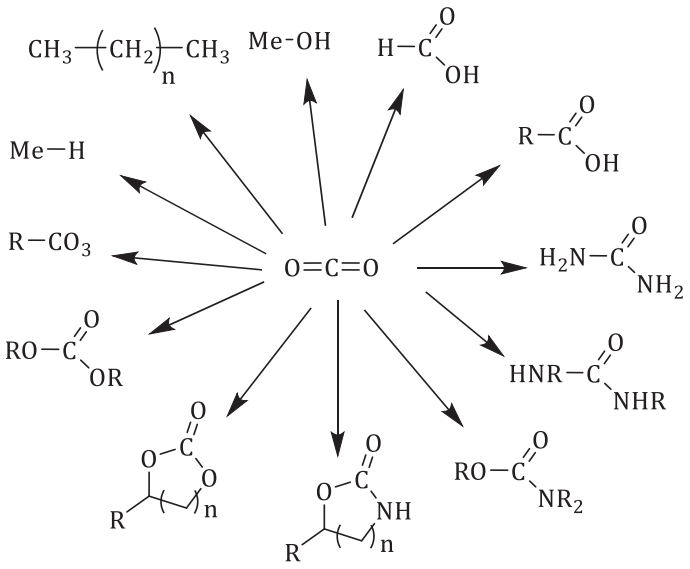

Figure II. 2: CO_2 as a source of a wide range of organic molecules.

Nevertheless, the efficient reduction of CO_2 to important molecules is hampered by its high thermodynamic stability as well as kinetic inertness towards reduction. [8] This drawback arises from the symmetric and stable nature of CO_2. To counteract this issue, efficient reduction catalysts are needed to synchronize C-O bond cleavage with C-H and C-C bond formation at a high kinetic rate and with a low energy demand. Over the last decades, CO_2 activation and reduction at a metal center has been widely investigated. [9]–[13] On the other hand, the activation of CO_2 by organic systems remains underexplored. It relies on the formation of stable adducts with organic Lewis bases such as guanidines or N-heterocyclic carbenes (NHCs). [14]–[16] Most progress has been gained *via* the synergistic action of Lewis pairs, able to coordinate both the C and O centers of CO_2. [8]

With the concept of FLP introduced by Stephan and Erker [17], [18] and as presented in the bibliographical chapter, several CO_2 adducts have been isolated in which the C atom is attached to a C, N, or P donor while one or two O atoms coordinate a group XIII Lewis base (B or Al). [5], [19]–[28] In most papers, FLP-CO_2 adducts are used as catalytic intermediates in the reduction of CO_2 with

hydrosilanes or hydroboranes. [29]–[33] Activation of CO_2 by FLP is thus an interesting path for the metal-free catalytic reduction reactions.

One advantage of the use of FLP chemistry in the capture of CO_2 is the reversibility of the sequestration reaction meaning that CO_2 could be recycled and used for another application with capital gain. Considering our skills panel, we were willing to combine polymer and FLP chemistries in the same research area in order to form polymers able to reversibly capture CO_2. The capture of CO_2 could thus induce a change of the mechanical properties by crosslinking between the functionalized polymer chains under gas stimulus. Subsequent catalysis chemistry could then be harnessed to give an elegant path for reduction reactions and modifications of mechanical properties, possibly used in actuators to store mechanical energy.

In this fashion, the main idea of this Chapter is to synthesize networks integrating FLP units able to interact reversibly with a third component such as a gas or a small molecule in a host-guest complex. Several strategies have been reported and are discussed in this chapter. Indeed, we can create networks relying on different interaction models: between difunctional molecules, between a difunctional molecule and a functionalized polymer or between two functionalized polymers.

In the following chapter, the systems will be abbreviated as:

- A1 for monofunctionalized molecule carrying one Lewis acid group,
- B1 for monofunctionalized molecule carrying one Lewis base group,
- A2 for difunctional molecule carrying two Lewis acid groups,
- B2 for difunctional molecule carrying two Lewis base groups,
- Poly(A) for a Lewis acid functionalized polymer,
- Poly(B) for a Lewis base functionalized polymer.

As reported in the literature, Lewis acids can be boron- and aluminum-based whereas Lewis bases can be phosphines, primary and secondary amines or even N-heterocyclic carbenes. These compounds do not show the same acidity or basicity strength and this will be further discussed in this part, especially through NMR studies. Besides, based on our work about boron-based polymers, we started from organoboron polymers that are smart platforms for a wide variety of functionalization thanks to the electronic vacancy on the boron atom.

The first route consisted on the investigation of the interaction between two difunctional small molecules, respectively bis(Lewis acid) (A2) and bis(Lewis base) (B2), without and with CO_2 addition. In this fashion, a supramolecular polymer could be formed by poly(Lewis addition)

between the difunctional molecules simply through Lewis interaction. This path can be illustrated in Figure II. 3.

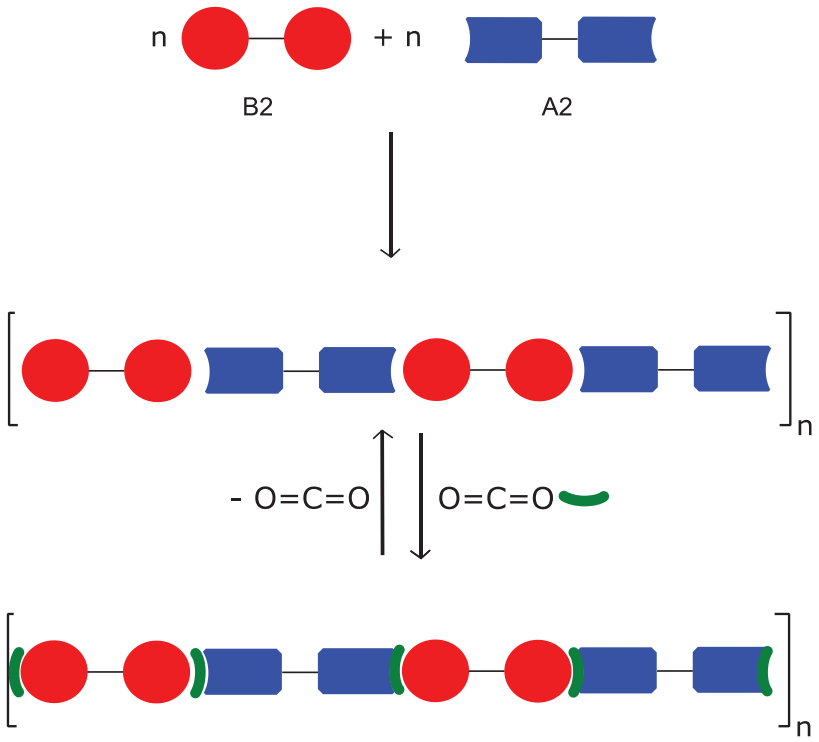

Figure II. 3: A2+B2 strategy of interaction.

The second route studied is focusing on the interaction between a difunctional molecule carrying two Lewis acidic moities interacting with a polymer functionalized by pendent Lewis bases without and with CO_2. The interactions and supramolecular self-assembly structures expected are represented in Figure II. 4. A tridimensional supramolecular network, with rather low energy interactions depending on frustration, is thus targeted with a difunctional Lewis acid as linker. Subsequently CO_2 could promote the formation of stronger dynamic network with dative Lewis bonds.

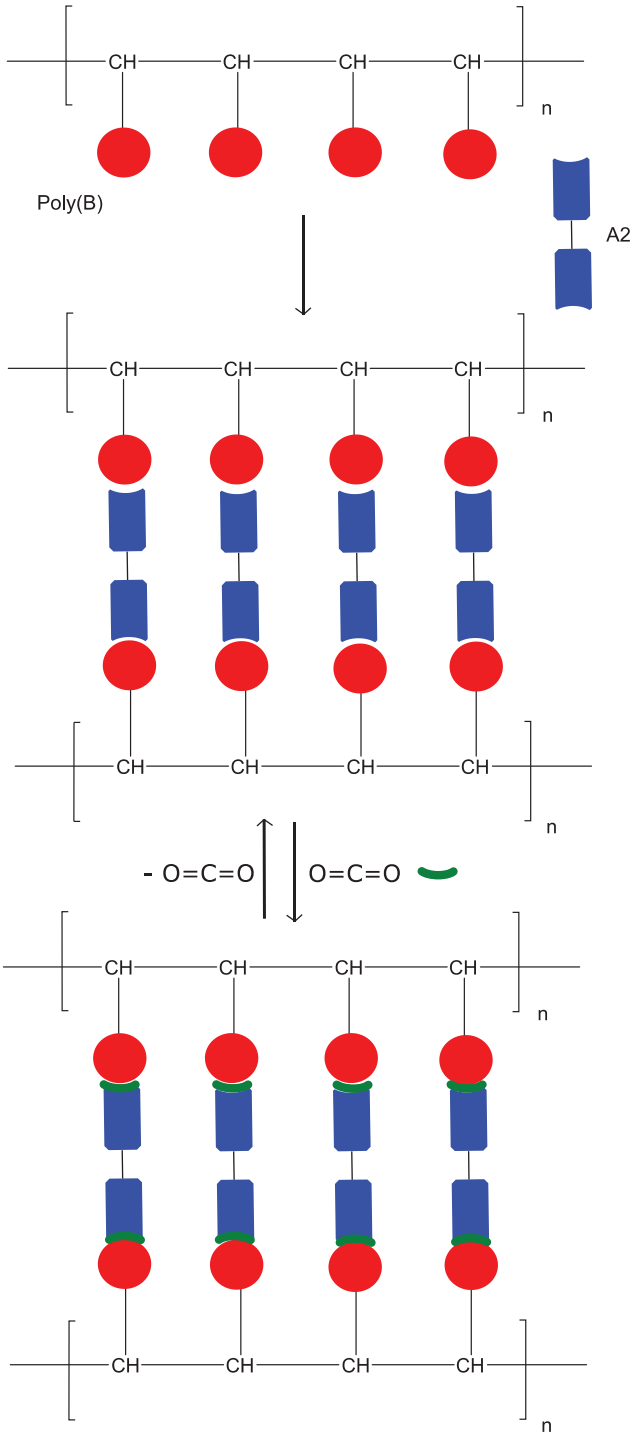

Figure II. 4: Poly(B)+A2 strategy of interaction.

The last strategy investigated is the supramolecular interaction between two polymers as symbolized in Figure II. 5 that could form a crosslinked network *via* the addition of CO_2. Nonetheless, during our research, works about functionalized Lewis acid- and base-functionalized polymers interacting with CO_2 were reported and took the wind out of one's sails thus we did not focused that much on this last route. The details of their researches are presented in Chapter 1 and will be discussed in this Chapter as well.

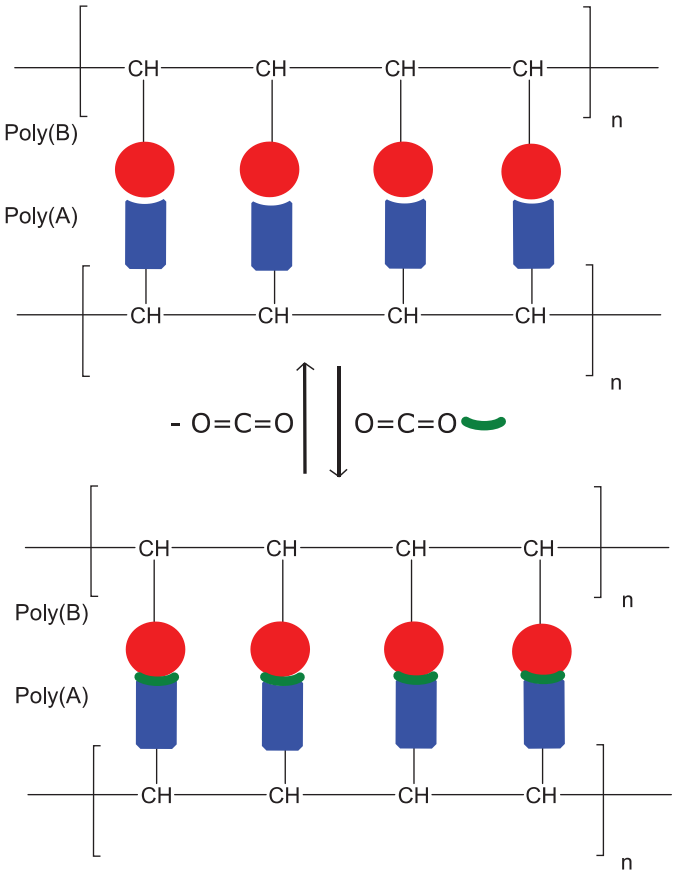

Figure II. 5: Poly(A)+Poly(B) strategy of interaction.

Based on these various designs, the first part of this chapter will be dedicated to the syntheses of difunctionalized molecules, namely A2 and B2. This will be followed by the syntheses of the functionalized polymers, poly(A) and poly(B). In a third part, the interactions between monofunctionalized model molecules, A1 and B1, will be assessed. Next, A2+B2 route will be investigated followed by A2+poly(B) and lastly, poly(A) and poly(B) will be discussed briefly. Each system will be studied by different techniques such as spectroscopies (NMR or UV) and rheology.

II. Syntheses of difunctionalized molecules

A. Synthesis of difunctional Lewis acid A2

Tris(pentafluorophenyl)borane is a well-known activator in homogenous metallocene and post-metallocene catalytic polymerization thanks to its Lewis acidity. [34] It is also used in catalysis directly as an organocatalyst. [35]–[38] Thanks to its attractive properties in terms of reactivity and stability, we focused on the synthesis of a polyfunctional perfluoroarylborane to have the best chance at evidencing some supramolecular phenomena.

Multifunctional compounds with two or more Lewis acid sites available for Lewis bases binding are rarer than monofunctional compounds and are also harder to study. However, due to their potential in supramolecular chemistry, polyfunctional perfluoroaryl boranes (mostly bifunctional) have been of growing interest over the past 5-10 years and in particular, compounds of general formula $(F_5C_6)_2B$-linker-$B(C_6F_5)_2$. [39], [40]

The first insights in the chemistry of bidentate Lewis acid were conducted by Shriver and Billas in 1967 with a bidentate version of the boron-based Lewis acid (BF_3) with an alkyl linker ($F_2BCH_2CH_2BF_2$). However, this compound was not found to readily chelate neutral bases. Besides, even if the structure of this bidendate Lewis acid is simple at first look, the difficulties in preparing and handling this compound was quite deceiving and slowed down research in this area. [41]

Luckily, more recently, papers related the synthesis of bifunctional perfluoroaryl boranes with $B(C_6F_5)_2$ units bridged by one [42]–[44], two [45]–[53], three atoms or more [54], [55]. Some examples from literature of difunctional perfluoroaryl boranes are illustrated in Figure II. 6.

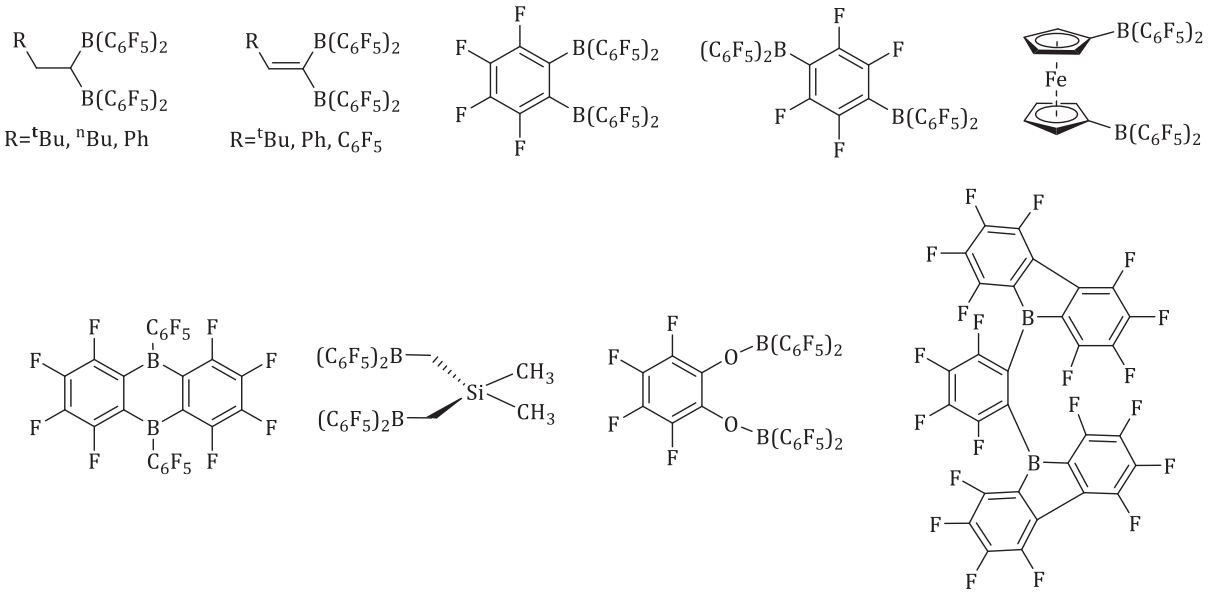

Figure II. 6: Examples of difunctional perfluoroaryl boranes from litterature. [39], [40]

It is interesting to integrate 1,2-phenylene-type linkers in difunctional perfluoroaryl boranes since they bring rigidity to the system and possible conjugation through the unsaturated bonds that could enhance the Lewis acid properties of the compound. Obviously, a system with a fully fluorinated phenylene linker would be more attractive owing to the increased Lewis acidity of the boron centers. However, the synthesis would be harder and more side products would be obtained.

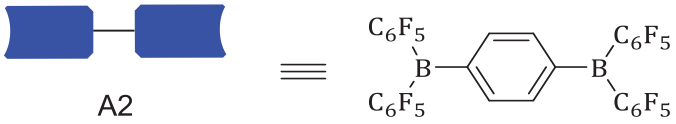

Figure II. 7: Structure targeted for the A2 difunctionalized molecule.

From these constatations and focusing on the difunctionalized Lewis acid A2 (Figure II. 7), we targeted the synthesis of an aromatic ring carrying two $B(C_6F_5)_2$ groups in para positions with enhanced Lewis acidity thanks to possible conjugation. Besides, as far as we know, the synthesis of this specific compound has not yet been reported in the literature. The path used was a two-step synthesis as illustrated below in Figure II. 8:

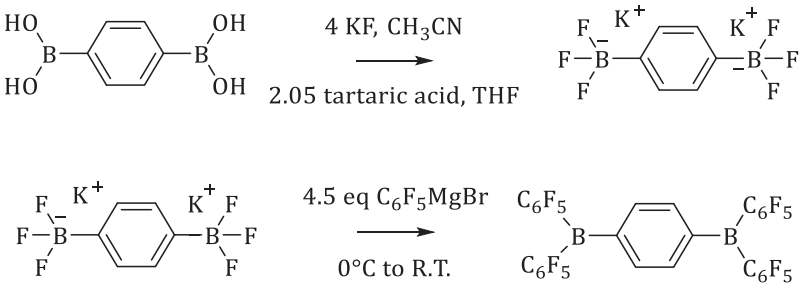

Figure II. 8: Two-step reaction path for the synthesis of A2.

Starting from a commercial molecule, the first step allows for the formation of a difunctionalized molecule bearing two BF_3^- moieties ligand-exchanged using a Grignard reagent in the second step. The first step relies on the work of Lennox and Jones that they applied to the monofunctionalization of a boronic acid molecule. [56] We simply transferred the method reported to a difunctional molecule adapting the quantities of reactants used. In the same manner, benzene-1,4-diboronic acid was treated with potassium fluoride in presence of tartaric acid in a mixture of water, acetonitrile and tetrahydrofuran to install BF_3K groups on each side of the aromatic ring. The characterization of the product is detailed in the Experimental Section. The white powder produced was correctly identified by NMR spectroscopy, but the yield remained quite low due to the difficulty of separation of the product from the salts.

Then, it was treated with the chosen Grignard reagent to install the pentafluoroaryl groups on the boron atom and thus to tune the Lewis acidity of the molecule A2. This second step was quite

challenging as the molecule and the salts obtained from the reaction with the Grignard are difficult to separate (filtrations under argon using cannula technique or sintered glass, extractions with solvents) and we considered the challenging synthesis of this difunctional molecule as a notable success by itself. All the NMR spectra are detailed in the Experimental Section from Figure V. 2 to V. 10. The product was a sand color powder, slightly soluble in THF but unfortunately, the yield remained quite low (close to 15 %). However, we managed to study this compound in interaction with other functionalized molecules, polymers and gases.

B. Synthesis of difunctional Lewis base B2

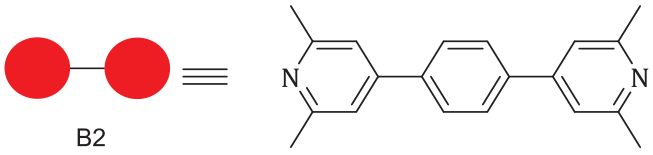

Figure II. 9: Structure targeted for the B2 difunctionalized molecule.

For the synthesis of the difunctional molecule carrying two lutidine groups in para positions on a central phenyl linker (Figure II. 9), we relied on the work of Hayashi. [57] Indeed, they reported the synthesis of linear-extended bipyridines *via* a three-step path. The first step of the reaction involves dihydropyridine synthesis *via* the widely described Hantzsch method. [58], [59] It is followed by a subsequent oxidative aromatization with molecular oxygen in presence of activated carbon. The last step is a decarboxylation process at high temperature in presence of CaO. The total reaction path is depicted in below Figure II. 10.

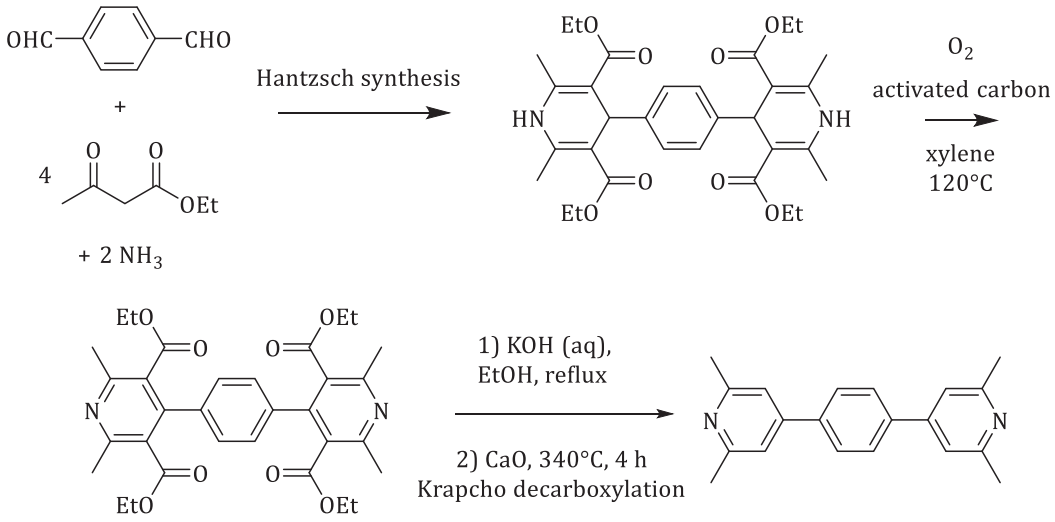

Figure II. 10: Three-step synthesis of the difunctional molecule B2. [57]

During the first step, the treatment of the selected dialdehydes (terephtaldehyde) with ethyl acetoacetate and ammonium in ethanol at reflux gave the corresponding 1,4-dihydropyridine (tetraethyl-4,4'-(1,4-phenylene)bis(2,6-dimethyl-1,4-dihydropyridine-3,5-dicarboxylate)) with a

high yield (≈97 %). Then, the oxidative aromatization in presence of O_2 and activated carbon at 120°C in xylene afforded the corresponding pyridine (tetraethyl-4,4'-(1,4-phenylene)bis(2,6-dimethylpyridine-3,5-dicarboxylate)) in a yield around 60 %. Besides, this process is environmentally friendly, economically and simple to operate. The characterization of the products are detailed in the Experimental Section, especially the NMR spectra of each intermediate product (Figures V. 12 to V. 15).

Unfortunately, the last step presented several issues, as we were not able to run the decarboxylation of the product of the second step. The decarboxylation procedure is first conducted by hydrolysis with KOH in ethanol and then by the addition of CaO and heating at 340°C for several hours. After several trials, we were not able to synthesize the targeted product without degradation but we only afforded the second-step product. The issues encountered might be solved by a better control of the temperature, by a homogeneous heating or by changing the base used in the first step.

III. Syntheses of functionalized polymers

A. Synthesis of Lewis acid functionalized polymers (polyA)

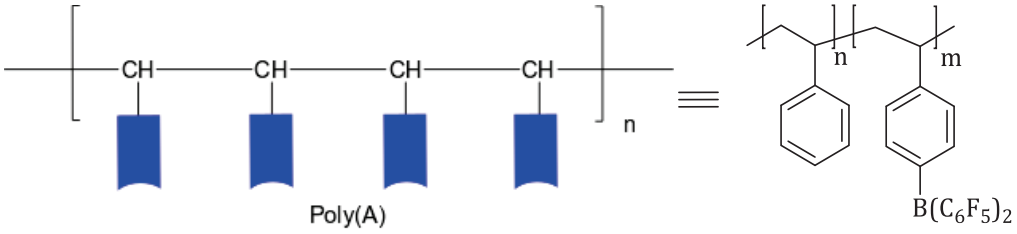

Figure II. 11: Structure targeted for poly(A) functionalized by Lewis acid groups.

Several strategies could be adopted for the synthesis of Lewis acid functionalized (co)polymers (Figure II. 11). Indeed, the boron moieties targeted can be inserted prior to the polymerization or by a post-functionalization method. The choice of the functionalization strategy depends on parameters such as the sensitivity of the boron function targeted and the solubility of the polymer. In this part, we chose a post-functionalization path starting from (co)polymers containing 4-vinylphenylboronic acid monomer to turn it in the desired boron pendent moiety. This strategy gives access to boron-based (co)polymers where the Lewis acidity can be finely tuned.

It is compulsory to mention at this step the versatile route reported by Jäkle and co-workers for the introduction of Lewis acidic boron centers into the side chains of organic polymers. Their methodology consists of three successive steps involving firstly the controlled (co)polymerization of a silylated monomer with a co-monomer such as styrene. Then, the silyl pendent groups on the polymers backbone are exchanged with BBr_3 to give dibromoborane-functionalized (co)polymers that constitutes a particularly versatile platform for post-functionalization. It is then easy to finely tune the Lewis acidity of the pendent groups through substituent-exchange reactions with nucleophiles. In their research, they treated the dibromoborane-functionalized (co)polymers with pentafluorophenylcopper to yield the corresponding well defined highly Lewis acidic triarylborane polymer. [60] In another work, they performed the synthesis of the monomer 4-styryl-di(pentafluorophenyl) borane that was then polymerized *via* RAFT polymerization. [61] However, it is quite surprising that this monomer undergoes clean radical polymerization since the Lewis acidic boron can intercept the growing polymer chain leading to transfer reaction.

In our work, we were willing to avoid the use of BBr_3 in our experiments due to its inherent toxicity and the difficulty to handle it.

Concerning polymer syntheses, we investigated (co)polymers with pendent Lewis acid groups that are boron-based ($B(C_6F_5)_2$). We relied on the reaction path already described in the last part used for the synthesis of functionalized small molecules. [56] In this fashion, we firstly synthesized

(co)polymers from styrene and 4-vinylphenylboronic acid (4-VBP) with controlled ratio. The reactivity ratios of the radical solution copolymerization for this monomer combination were estimated by Hartmann and co-workers as 0.83 for styrene and 0.28 for 4-vinylphenylboronic acid. [62] The copolymers tends to present polystyrene blocks and it could be difficult to incorporate the boron-based monomer. Then, the boronic acid moieties were transformed in BF_3K and subsequently in $B(C_6F_5)_2$ by addition of a selected Grignard agent (C_6F_5MgBr). The reaction path is indicated in Figure II. 12.

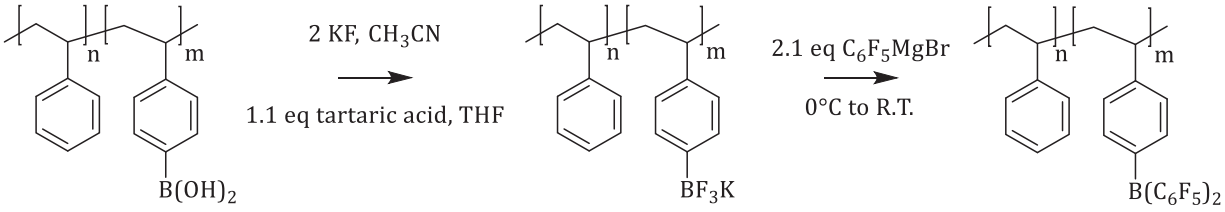

Figure II. 12: Reaction path for the synthesis of poly(A).

In a first step, poly(styrene-*co*-4-vinylphenylboronic acid)s were synthesized with different ratios of the two monomers through free radical polymerization at 60°C in THF using benzoyl peroxide as initiator. [63] We summarized in Table II. 1 the data on the copolymers obtained and the NMR spectra are available from Figures V. 17 to V. 19:

Table II. 1: Experimental data of the poly(styrene-co-4-vinylphenylboronic acid)s synthesized from styrene and 4-vinylphenylboronic acid. [1] Molar ratios determined by ^1H NMR spectroscopy. [2]Values *determined by SEC-THF using PS standards and conventional calibration.*

Entry	***Theoretical 4-VPB ratio (%)[1]***	***Experimental 4-VPB molar ratio (%)[1]***	***M_n[1](g/mol)***	***M_w[1] (g/mol)***	***Dispersity Đ***	***Yield***
1	30	20	20 300	121 100	5.9	91 %
2	50	40	25 000	94 000	3.8	89 %
3	100	100	12 500	32 900	2.6	92 %

The post-functionalizations were then realized for several copolymers. The first step involving the treatment with KF was successful in each case as observed by NMR spectroscopies (Figures V. 20 to V. 25 in the Experimental Section). However, the functionalization with the Grignard agent was proved to be more difficult. The main issue of this latter step was the purification process to separate the functionalized polymer from the salts obtained from the Grignard reaction and it made it difficult to correctly identify the product desired. The experiments were repeated several times with different strategies of purification (filtrations under argon using cannula technique or

sintered glass, extractions with solvents), but the products remained impure with resulting salts. Notwithstanding, we obtained the corresponding ^{19}F NMR spectrum is depicted in Figure II. 13.

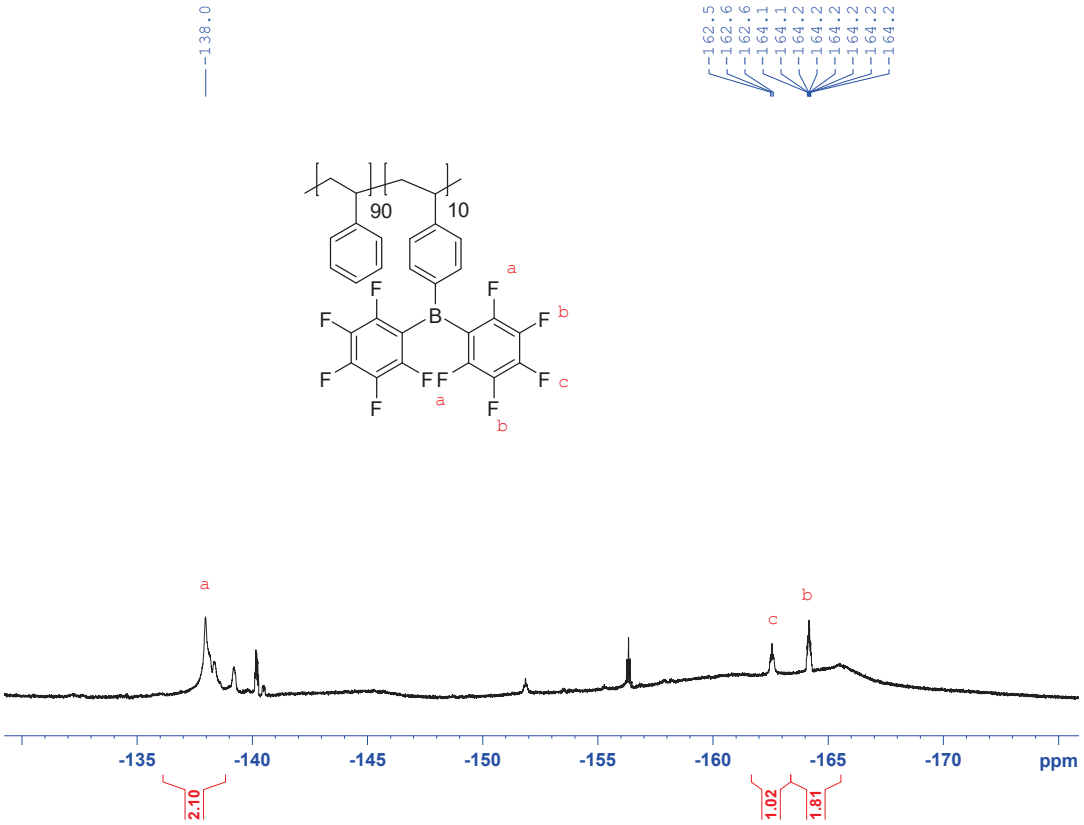

Figure II. 13: ^{19}F NMR spectrum of a functionalized copolymer bearing $B(C_6F_5)_2$ pendent groups in THF-d_8.

Unfortunately, due to the issues encountered during the syntheses, no interaction test was further conducted with the polymers synthesized in this manner.

B. Syntheses of Lewis base functionalized polymers (polyB)

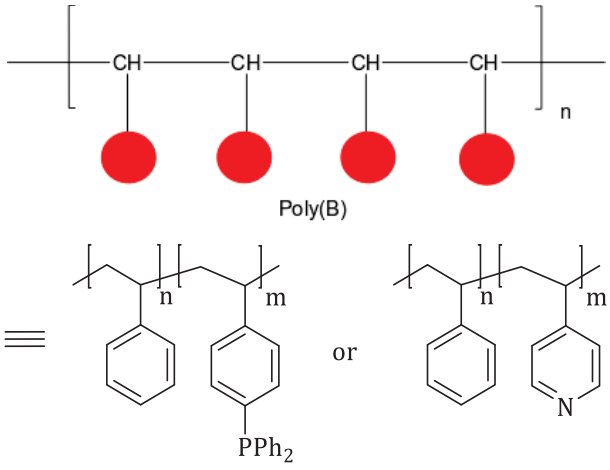

Figure II. 14: Structures targeted for poly(B)s functionalized by Lewis base groups.

In this part, the syntheses of polymers carrying pendent base groups such as phosphines and N-heterocycles are described (Figure II. 14). The steric hindrance and the electronic effects around the phosphorus or nitrogen atoms were harnessed to tune the Lewis basicity of the pendent moieties.

Indeed, the bulky phenyl groups on the phosphorus atoms are conferring a higher Lewis basicity to the functionalized copolymers than in the case of copolymers having N-heterocyclic pendent groups. The PPh_2 groups could be involved in FLP thanks to its hindrance contrary to pyridine groups which have the tendency to react in CLP. [17]

a. Polymers functionalized by phosphine groups

Firstly, we got interested in the copolymerization of styrene with 4-styryldiphenylphosphine (Figure II. 15) relying on the work of Choi *et al.* Indeed, they reported the radical copolymerization of this phosphorus-based monomer with styrene to afford a polystyrene functionalized with controlled amounts of diphenylphosphine pendent groups. These polymers are already used in Mitsunobu and alcohol bromination reactions. In their work, copolymers were obtained by free radical polymerization at 85°C with AIBN as initiator in toluene. [64]

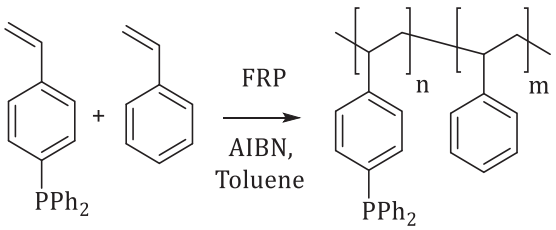

Figure II. 15: Copolymerization of styrene and 4-styryldiphenylphosphine.

It has to be noted that the homopolymerization of 4-styryldiphenylphosphine is not possible due to steric hindrance brought by the phenyl groups that hampered the monomers to be attached to one another. Thus, we applied this strategy of copolymerization to afford copolymers with different monomers ratios and besides we tried to optimize the copolymerization parameters in order to obtain high molar masses, especially M_w, that will improve the mechanical properties of the networks formed from these copolymers. Besides, we targeted copolymers with low contents of phosphorus-based monomer in order to facilitate the incorporation of this bulky monomer. The results of the experiments are summarized in Table II. 2. NMR spectra are described from Figures V. 28 to 32 as well as the chromatograms in THF are represented in Figure V. 33 in the Experimental Section.

Table II. 2: Experimental data of the copolymers synthesized from styrene and 4-styryldiphenylphosphine. [1]Molar ratios determined by NMR spectroscopy, [2]Values determined by SEC-THF using PS standards and conventional calibration.

Entry	Theoretical ratio[1]	Experimental ratio[1]	[Initiator] (mol eq.)	T (°C)	M_n[2] (g/mol)	M_w[2] (g/mol)	Dispersity Đ	Yield
1	20	21.3	0.02	90	2 100	4 800	2.3	75%
2	20	23.3	0.02	80	2 500	5 400	2.2	88%
3	20	23.5	0.02	70	2 600	5 150	2	71%
4	20	23.4	0.01	90	2 100	5 100	2.4	66%
5	20	24.5	0.01	80	4 300	5 900	1.4	51%
6	20	28.9	0.01	70	5 200	6 500	1.3	33%
7	20	25.7	0.01	70	8 300	9 200	1.1	55%
8	20	24.1	0.01	70	9 100	11 400	1.2	99%
9	20	23.8	0.01	70	10 100	11 700	1.2	61%
10	50	35.6	0.02	90	1 700	2 000	1.3	81%

Decreasing the temperature at 70°C and the amount of initiator to 0.02 molar equivalent of initiator compared to the total quantity of monomers was found to be a strategy to increase the molar masses. Nonetheless, they remained not as high as we expected but the copolymers will still be used in interaction tests.

b. Polymers functionalized by pyridine groups

Secondly, we focused on the synthesis of copolymers bearing pyridine lateral groups that could play the role of Lewis base in interaction studies. In the rest of the examination, two batches of polymers were used: a commercial homopolymer from 4-vinylpyridine supplied by Sigma-Aldrich and a synthesized copolymer from styrene and 4-vinylpyridine.

The copolymer batch was produced by free radical polymerization at 70°C with benzoyl peroxide as initiator. The copolymer is represented in Figure II. 16.

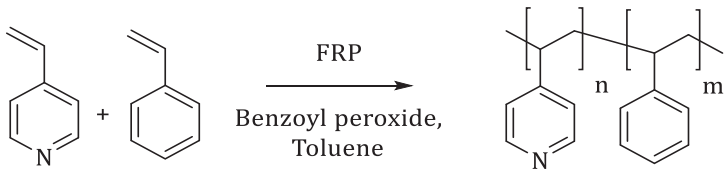

Figure II. 16: Copolymerization of styrene and 4-vinylpyridine.

The data of the (co)polymers used are detailed below in Table II. 3 and the NMR spectra are illustrated in Figures V. 35 and V. 36 in the Experimental Section while Figure V. 37 represents the chromatogram in THF.

Table II. 3: Experimental data of the copolymers synthesized from styrene and 4-vinylpyridine. [1]Molar ratios of 4-vinylpyridine determined by NMR spectroscopy, [2]Values determined by SEC-THF using PS standards and conventional calibration. Entry 2 corresponds to a commercial poly(4-vinylpyridine) from Sigma Aldrich.

Entry	***Theoretical ratio[1]***	***Experimental ratio[1]***	***[Initiator] (mol eq.)***	***T (°C)***	***M_n[2] (g/mol)***	***M_w[2] (g/mol)***	***Dispersity Đ***	***Yield***
1	20	18	0.01	70	22 500	39 400	1.8	75%
2	100	100	-	-	-	160 000	-	-

These polymers exhibit interesting molar masses to present good mechanical properties related to entanglements, meaning segments of random-coil chains are long enough to form one loop on themselves. Indeed, in presence of high molar masses, the interpenetration of the polymer induces entanglements that are important in determining rheological, dynamic and fracture properties. For instance, at low molar masses, the zero shear viscosity behaves as a simple Rouse fluid with $\eta_0 \approx M_w$ whereas at higher molar masses $\eta_0 \approx M_w^{3.4}$. It was established by previous work that entanglements occur when $M_w \approx 3M_c$ with M_c the critical entanglement molecular weight. [65], [66]

Thus, these polymers will be studied in the following work under gas stimuli. It should also be noted that the homopolymer from 4-vinylpyridine is found to be only soluble in chloroform while the copolymer from styrene and 4-vinylpyridine is soluble in toluene.

Table II. 4 sums up the compounds A1, B1, A2, B2, poly(A) and poly(B) that are used in this chapter. They can be commercially purchased or synthesized during this work.

Table II. 4: Summary of the compounds commercially purchased and synthesized that are used in the following study.

Compounds	Commercially purchased	Synthesized
A1	$B(C_6F_5)_3$	-
B1	PPh_3 C_5H_5N	-
A2	-	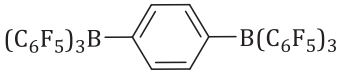
B2	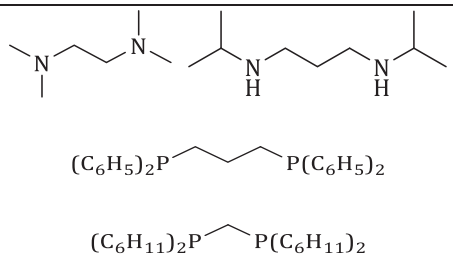	-
Poly(A)	-	-
Poly(B)	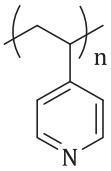	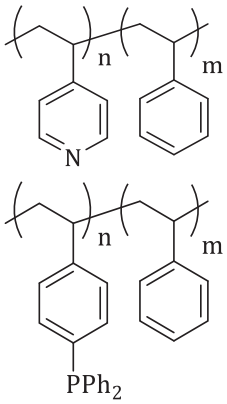

IV. NMR spectroscopy study on model molecules (A1+B1)

Prior to work on the functionalized polymers or polyfunctionalized small molecules, we investigated the interactions between selected model molecules offering the similar structures and functional groups.

A. Interaction between monofunctional molecules: $B(C_6F_5)_3$ (A1) and PPh_3 (B1)

In this optic, the selected monofunctionalized Lewis acid A1 was tris(pentafluorophenyl)borane $B(C_6F_5)_3$ that was put in interaction with a phosphine Lewis base, namely triphenylphosphine PPh_3 (B1) (Figure II. 17). The two compounds mimic the reactive pendent groups of respectively poly(styrene-*co*-bis(perfluorophenyl)(4-vinylphenyl)borane) and poly(styrene-*co*-4-styryldiphenylphosphine). Tris(pentafluorophenyl)borane $B(C_6F_5)_3$ was firstly synthesized in 1964 by Stone, Massey and Park [67] and is now available commercially with high purity, herein furnished by Alfa Aesar.

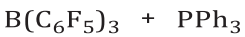

Figure II. 17: Lewis pair between tris(pentafluorophenyl)borane and triphenylphosphine.

The two molecules were mixed in controlled amounts in a Young tube to cover a range of molar ratios and thus to see the influence of the experimental ratios on the FLP formed. The blends studied are detailed in Table II. 5. A1 was firstly dissolved in toluene-d_8 and then the B1 compound was added. Surprisingly, we observed a direct precipitation of the FLP complex formed even at low proportions of PPh_3. In order to be able to study the complex obtained by liquid NMR spectroscopy, a small amount of THF was added to the system, which allows for the solubilization of the product. However, it could also induce a change in the complexation and in the thermodynamics of the system studied, as THF is in competition with PPh_3 for the complexation of the electronic vacancy of the boron atom.

Table II. 5: Molar ratios studied by NMR spectroscopy for the FLP formed from $B(C_6F_5)_3$ (A1) and PPh_3 (B1).

Entry	***Ratio A1:B1***
1	1:0.38
2	1:0.62
3	1:0.94
4	1:1.52

Adducts of $B(C_6F_5)_3$ and Lewis bases are often studied by NMR spectroscopies either in solution or in solid state. Indeed, the ^{11}B NMR chemical shift [67] and the separation between the resonances for the meta and para fluorine atoms in ^{19}F NMR spectrum [68] are quite sensitive to the changes around the boron center and the strength of the adduct interaction associated to electronic and steric effects.

For the analysis of the products, we relied on the NMR spectroscopies of clue nucleus that are highly influenced in this complex and easily investigated. In this fashion, ^{19}F, ^{11}B and ^{31}P NMR spectroscopies were conducted respectively in Figure II. 18, Figure II. 20 and Figure II. 21 and will be further discussed.

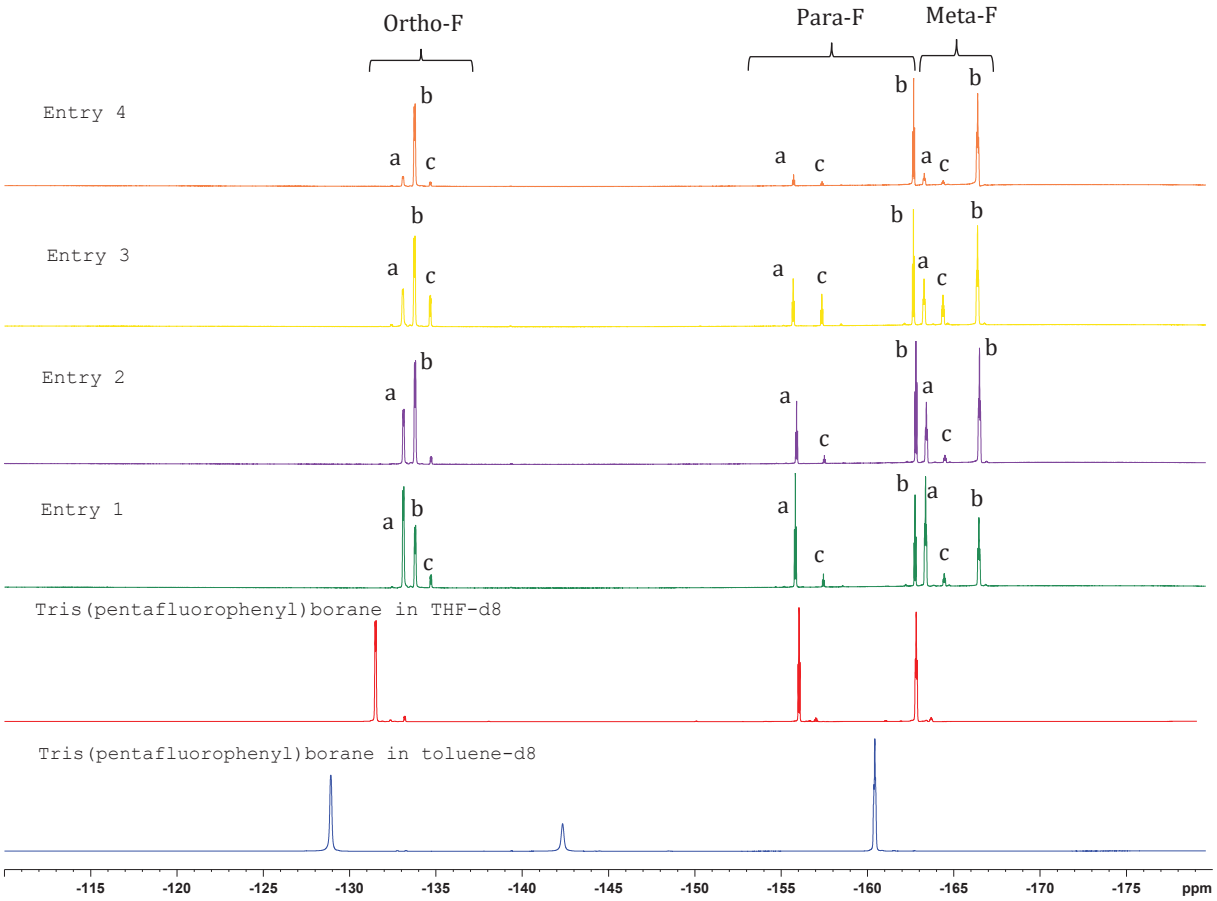

Figure II. 18: ^{19}F NMR spectra of mixtures between tris(pentafluorophenyl)borane and triphenylphosphine in various ratios.

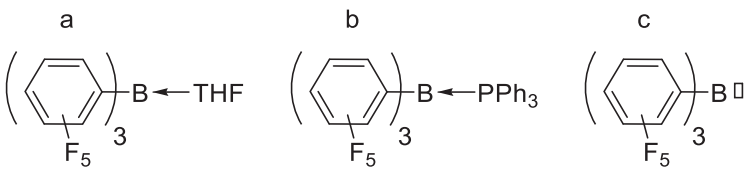

Figure II. 19: Structures identified by NMR spectroscopy.

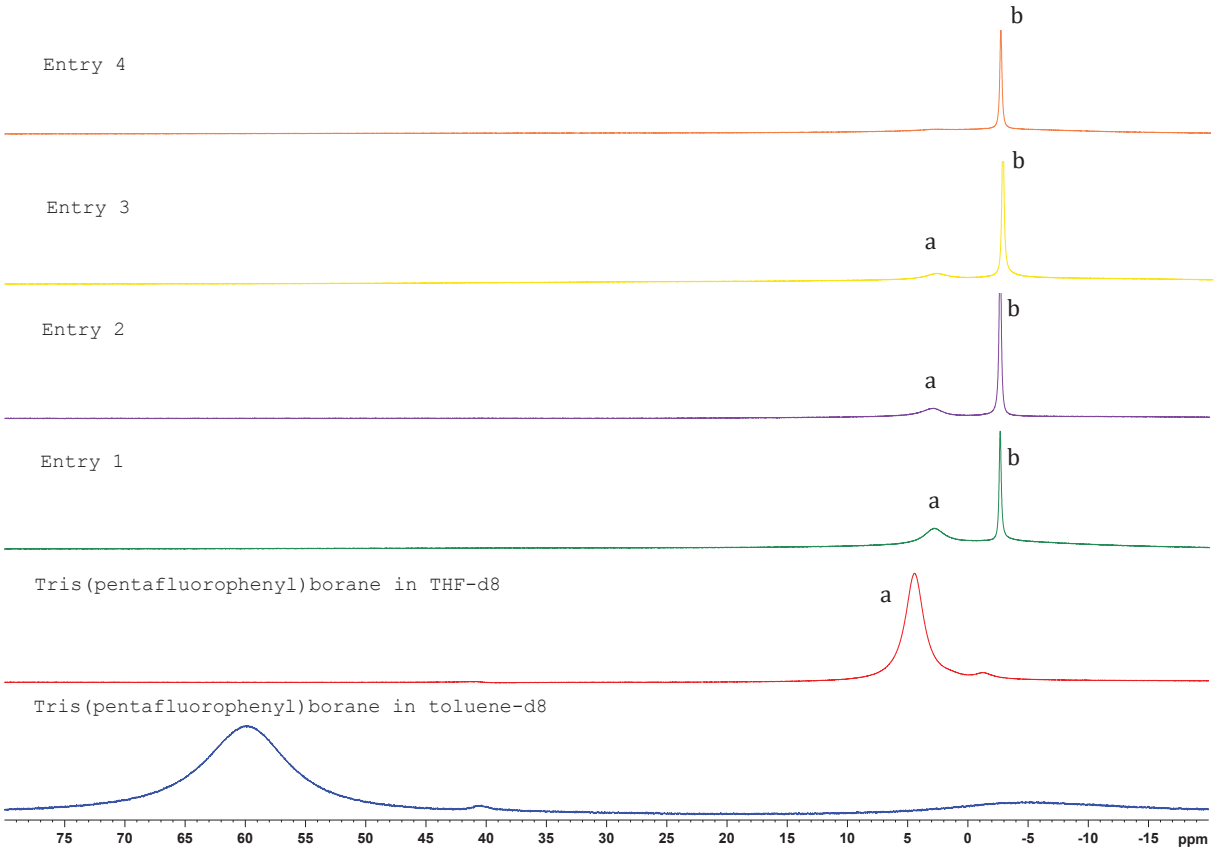

Figure II. 20: ^{11}B NMR spectra of mixtures between tris(pentafluorophenyl)borane and triphenylphosphine in various ratios.

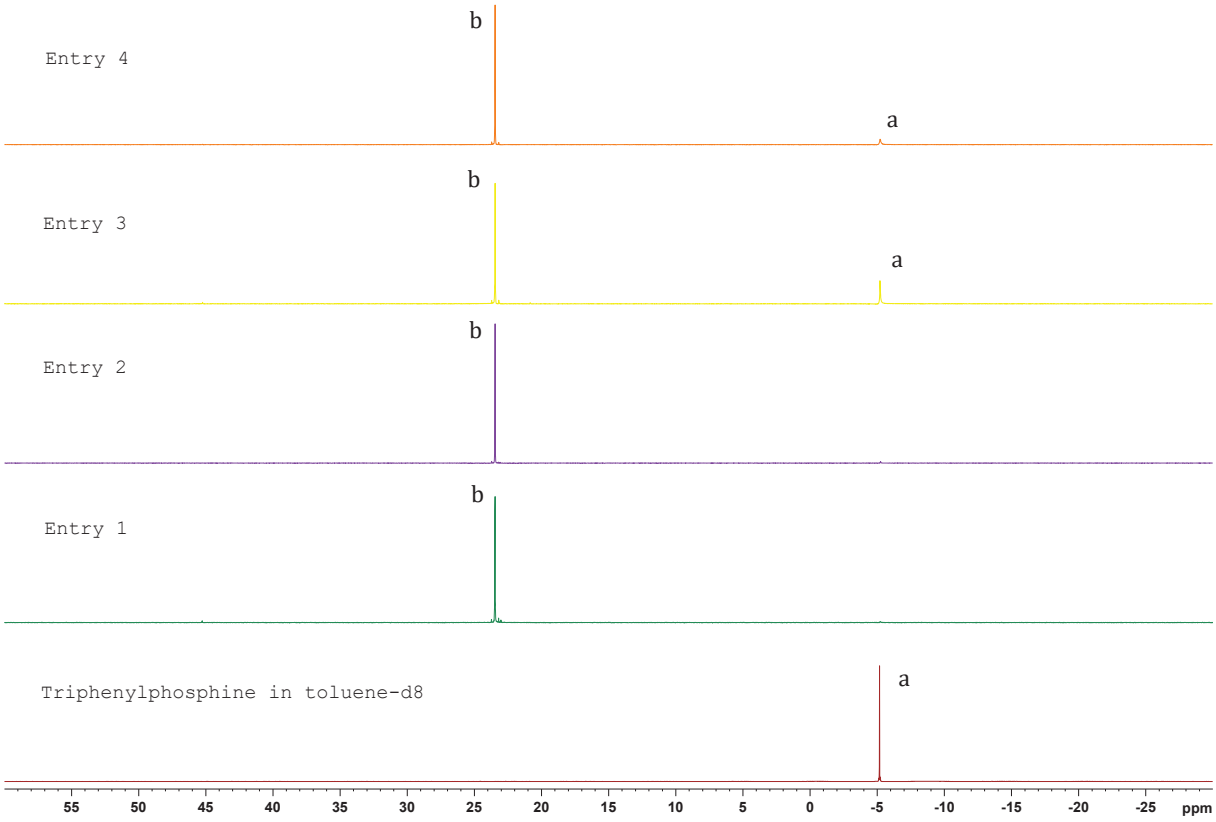

Figure II. 21: ^{31}P NMR spectra of mixtures between tris(pentafluorophenyl)borane and triphenylphosphine mixtures in various ratios.

Firstly, ^{19}F spectra in Figure II. 18 shows the difference between tris(pentafluorophenyl)borane analyzed in toluene (blue) or in THF (red). In THF, the respective chemical shifts of the ortho, para and meta fluorine atoms from left to right (Figure II. 18) are shifted as the borane forms a complex with THF that is a coordinating solvent complexing the electronic vacancy of the boron atom impacting the geometric structure from trigonal to pyramidal of the strong Lewis acid. The addition of a small part of triphenylphosphine (Entry 1, Table II. 5, Figure II. 18) evidenced the influence of the addition of the Lewis base in the system with the appearance of new signals of fluorine atoms at -133.8 ppm, -162.7 ppm and -166.47 ppm and the shifts of the signal of the tris(pentafluorophenyl)borane coordinated by THF at -133.1 ppm (previously at -131.8 ppm), -155.8 ppm (previously at 156.4 ppm) and -163.4 ppm (previously at -163.3 ppm). A coexistence between the complex $B(C_6F_5)_3$---THF and $B(C_6F_5)_3$---PPh_3 is thus highlighted. The increase of the molar ratio of Lewis base in the system enhances the signals of the new chemical shifts attributed to the phosphine-borane complex that predominates in the solution (Entries 2 and 3, Table II. 5, Figure II. 18). In excess of phosphine, only the borane-phosphine complex is observed in the spectrum (Entry 4, Table II. 5, Figure II. 18) with fluorine atoms in ortho positions at -133.7 ppm, in para positions at -162.7 ppm and in meta positions at -166.1 ppm. From these spectra, it was possible to attribute each signal to the corresponding fluorine-based species that are the following depending on the complexation on the boron atom: THF-complexed $B(C_6F_5)_3$, PPh_3-complexed $B(C_6F_5)_3$ and free $B(C_6F_5)_3$. The signals corresponding are respectively indicated by **a**, **b** and **c** letters on Figure II. 18 and represented in Figure II. 19.

From ^{19}F spectroscopy, we were willing to calculate the complexation constant at each ratio studied to deepen our understanding of the Lewis pair formed from $B(C_6F_5)_3$ and PPh_3. To reach this goal, we relied on the work of Fielding. [69] In this case of slow exchanges, the bound and free species gave rise to discrete NMR signals that can be integrated to determine K.

Table II. 6: Estimation of the complexation constant K for each ratio based on ^{19}F spectroscopy.

Entry	*Experimental ratio A1:B1*	*K (L/mol)*
1	1:0.38	509
2	1:0.62	non reliable
3	1:0.94	88
4	1:1.52	619

From the results in Table II. 6, it is possible to confirm that the complexation constant between $B(C_6F_5)_3$ and PPh_3 is around $10^{2\text{-}3}$ L/mol.

In the second time, the different mixtures were compared by ^{11}B NMR spectroscopy and the spectra are depicted in Figure II. 20. The first finding that can be done is the difference of the chemical shift related to the boron atom of the tris(pentafluorophenyl)borane between the free form and the THF-complexed one from 60.3 ppm to 4.7 ppm. At the addition of triphenylphosphine (Entry 1, Table II. 5, Figure II. 20), a newly boron-based species is detected that is the result between the complexation between the borane and the phosphine. The equilibrium between $B(C_6F_5)_3$---THF (**a** signal, Figure II. 19, Figure II. 20) and $B(C_6F_5)_3$---PPh_3 (**b** signal, Figure II. 19, Figure II. 20) is favorable to the phosphine-borane interaction upon addition of phosphine as the THF-based complex tends to disappear completely close to equivalence and above (Entries 2, 3 and 4, Table II. 5, Figure II. 19, Figure II. 20).

Lastly, ^{31}P spectra give the same information about the formation of the complex. Indeed, the triphenylphosphine chemical shift is directly shifted in presence of an excess of tris(pentafluorophenyl)borane (Entries 1 and 2, Table II. 5, Figure II. 21) from -4.4 ppm to 23.9 ppm. At equimolarity and in excess of triphenylphosphine, the system exhibits a coexistence between the free triphenylphosphine (**a** signal, Figure II. 19, Figure II. 21) and the complex phosphine-borane (**b** signal, Figure II. 19, Figure II. 21).

This NMR spectroscopy study showed that the equilibrium between borane-phosphine and borane-THF is favorable to the borane-phosphine complex. This highlights the fact that the Lewis pair is not so frustrated and behaves more as a CLP.

B. Interaction between monofunctional molecules: $B(C_6F_5)_3$ (A1) and C_5H_5N (B1)

In a second study, the monofunctionalized Lewis acid A1 selected was tris(pentafluorophenyl)borane $B(C_6F_5)_3$ that was put in interaction with pyridine (C_5H_5N) that is a non-sterically hindered Lewis base (B1). They both mimic the reactive pendent groups of respectively poly(styrene-*co*-bis(perfulorophenyl)(4-vinylphenyl)borane) and poly(styrene-*co*-4-vinylpyridine).

The two molecules were mixed in controlled amounts in a Young tube to cover a range of molar ratios and thus to see the influence of the respective concentrations on the FLP formed. The blends studied are detailed in Table II. 7. A1 was firstly dissolved in toluene-d_8 and then the B1 compound was added. The complex formed was slightly soluble in toluene allowing for a convenient analysis by liquid NMR spectroscopy.

Table II. 7: Molar ratios studied by NMR spectroscopy for the FLP formed from $B(C_6F_5)_3$ (A1) and C_5H_5N (B1).

Entry	***Molar ratio A1:B1***
1	1:0.3
2	1:0.6
3	1:1
4	1:1.5

For the analysis of the products, we relied on the NMR spectroscopies of clue nucleus that are highly influenced in this complex and easily investigated. In this fashion, ^{19}F and ^{11}B NMR spectroscopies were conducted, respectively observable in Figure II. 22 and Figure II. 23.

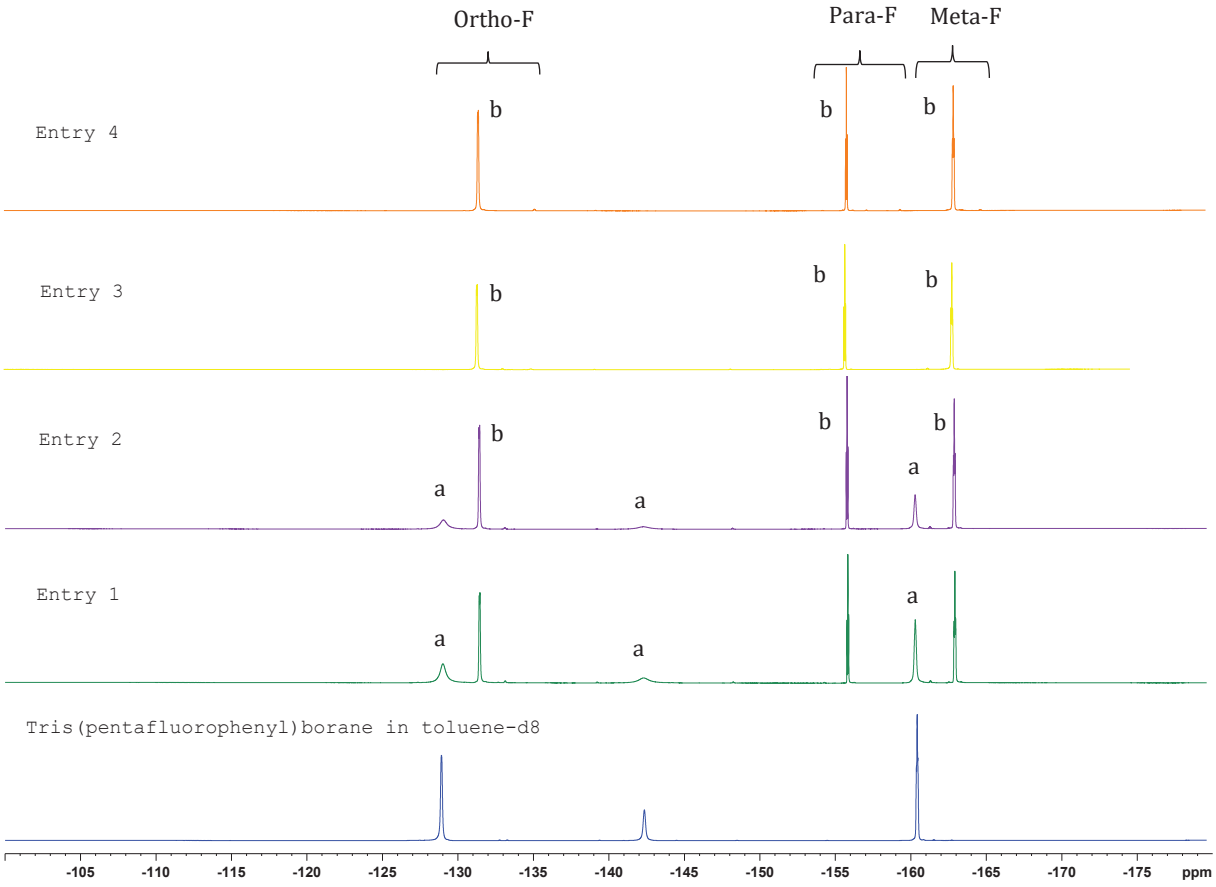

Figure II. 22: ^{19}F NMR spectra of mixtures between tris(pentafluorophenyl)borane and pyridine in various ratios.

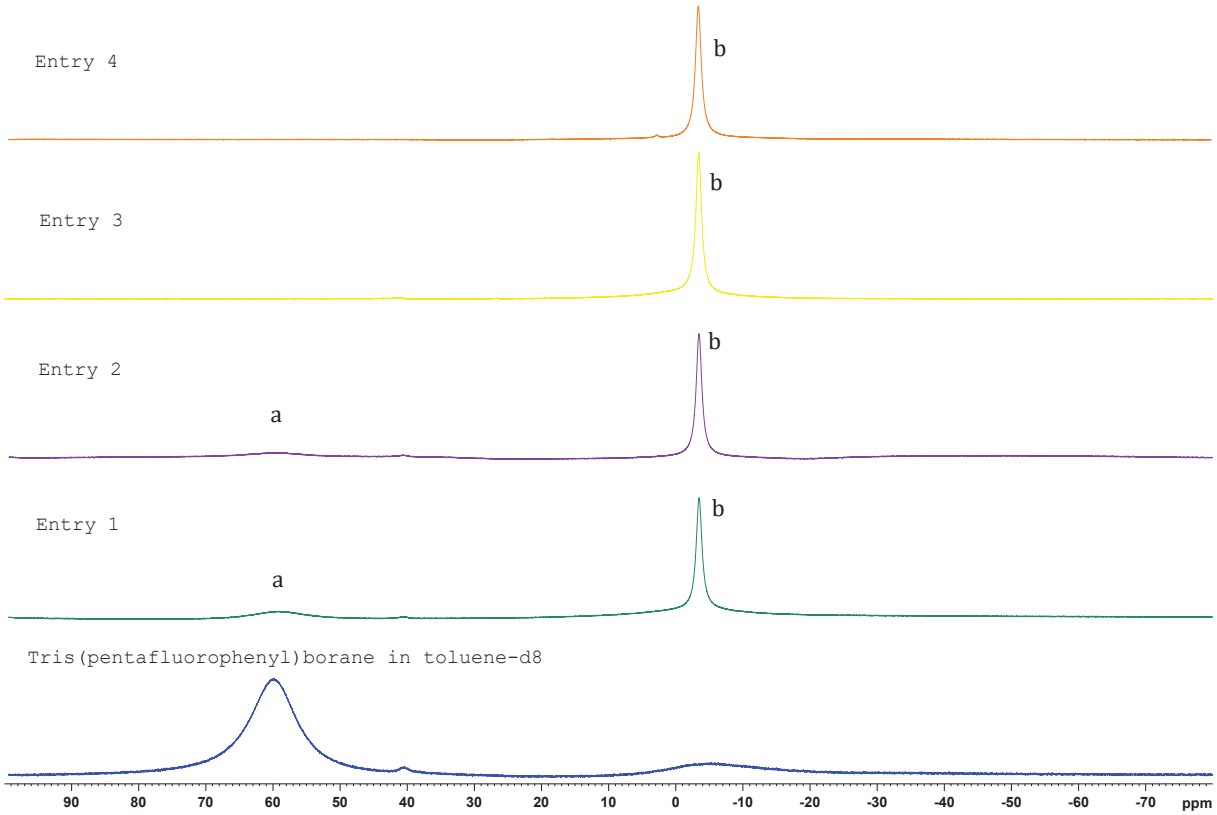

Figure II. 23: ^{11}B NMR spectra of mixtures between tris(pentafluorophenyl)borane and pyridine in various ratios.

Firstly, the different mixtures were examined through the scope of ^{19}F spectroscopy and it was observed at the addition of low amounts of pyridine the appearance of a new species resulting from the Lewis acid-base interaction between the boron and the nitrogen atoms (Entries 1 and 2, Table II. 7, Figure II. 22). The chemical shifts of this new species are -131.4 ppm for the fluorine atoms in ortho positions, -155.7 ppm in para positions and -162.8 ppm in meta positions. Until the equimolarity, there is coexistence of the free tris(pentafluorophenyl)borane (signals **a**, Figure II. 22) and the complexed version with pyridine (signals **b**, Figure II. 22). At the ratio 1:1 and above between the Lewis acid and the Lewis base, the free tris(pentafluorophenyl)borane completely disappears in favor of the Lewis pair (Entries 3 and 4, Table II. 7, Figure II. 22). The same observations can be made for ^{11}B NMR spectroscopy in Figure II. 23.

From ^{19}F spectroscopy, we were not able to estimate complexation constants between $B(C_6F_5)_3$ and C_5H_5N but the complexation seems to be quantitative as the complexed species are directly formed at the addition of pyridine. The complexation constant is supposed to be high in this case ($>10^{5\text{-}6}$ L/mol). Indeed, K above 10^5 L/mol become too steep to measure with this NMR method and more sensitive NMR probes should be used. [69] In this case, the pair formed between $B(C_6F_5)_3$ and C_5H_5N behaves as a CLP as the interaction is very strong.

C. Conclusions from NMR spectroscopy analyses

It was not surprising that $B(C_6F_5)_3$ formed rapidly strong adducts with Lewis bases such as triphenylphosphine and pyridine, even with a precipitation that occurs in the case of interaction with triphenylphosphine. Indeed, it has been demonstrated by the NMR method of Childs that $B(C_6F_5)_3$ is a slightly stronger Lewis acid than BF_3. [70], [71]

One of the main drawbacks of the Lewis concept is the incapacity to establish any universal scale of Lewis acid and base strength, as it can be easily done for the Brønsted acids and bases with the well-known pK_a scale. Actually, there is no single reference that can be definitely chosen and thus there are virtually as many Lewis acid and base scales than possible references. [72]–[79]

Borane derivatives are perfect Lewis acids owing to the electron deficiency of the central boron atom with a vacant p-orbital (Figure II. 24). In the field of boranes, many attempts have been made to quantify the Lewis acidity of compounds *via* thermodynamic data such as the adduct formation enthalpy, chemical reactivity or spectroscopic analysis. [72], [80] Independently of the method, it is admitted that a stronger coordinate covalent bond is due to the increased Lewis acidity when the Lewis base is constant. However, some contradictions have been found in literature. [81], [82] Pearson has established the Hard and Soft Acids and Bases principle (HSAB) that relates that hard acids prefer to bind to hard bases whereas soft acids prefer to bind to soft bases. In his work, small acceptor atoms that exhibit outer electrons not easily excited and that bear considerable positive charge characterize hard acids. On the other hand, soft acids have acceptor atoms with lower positive charge, large size and easily excited outer electrons. He introduced the notion of polarizable Lewis pair. [83] Nonetheless, this principle does not give basis for quantitative classification of Lewis acids. [84] In fact, in the case of boranes, Lewis acidity should be quantified *via* the ability of boron to accept an electron pair or vertical electron affinity. [84], [85]

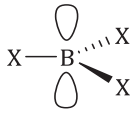

Figure II. 24: Boron atom structure and representation of vacant p-orbital.

Triarylboranes are ideal candidates for providing strong Lewis acids as the simple modification of the aromatic backbone adjusts their Lewis acidity. Indeed, the introduction of electron-withdrawing groups on the aromatic rings increases the Lewis acidity of the boron atom whereas electron-donating substituents decrease the Lewis acidity. [84] From these observations, the Lewis acid strength of $B(C_6F_5)_3$ is much higher than the one of $B(C_6H_5)_3$ thanks to the pentafluorophenyl groups. [34] Tris(pentafluorophenyl)borane can be considered as the perfect boron-based Lewis acid due to its high Lewis acidity as well as thermal and hydrolytic stabilities. [39], [86] Increasing

the fluorination of the aryl groups increases the Lewis acidity of triarylboranes and it is thus possible to construct the following scale of Lewis acidity based on the Gutmann-Beckett method:

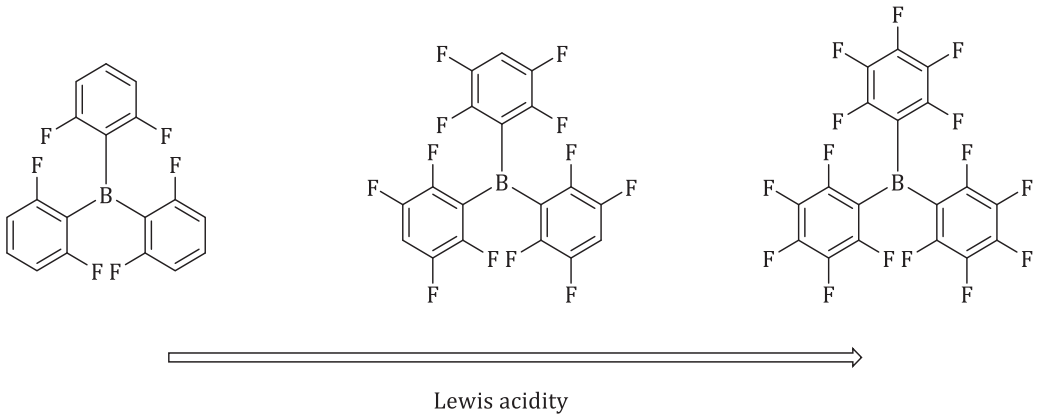

Figure II. 25: Lewis acidity scale of some fluorinated triarylboranes determined by Gutmann-Beckett scale. [87], [88]

The Gutmann-Beckett method relies on the change of the ^{31}P NMR chemical shift of Et_3PO upon complexation with a Lewis acid. [89], [90]

Apart from the effects of withdrawing substituents on the aryl groups, an important factor in the Lewis acid-base complex formation is the reorganization energy of the acceptor molecule. Indeed, the formation of a Lewis acid-base complex requires a change of the geometry of the Lewis acid from trigonal planar to pyramidal geometry. Energies of reorganization of acceptors centers have been estimated for BH_3 (56 kJ/mol), BF_3 (86 kJ/mol) and $B(C_6F_5)_3$ (75-100 kJ/mol). The compounds with a pre-organized acceptor center possessing a pyramidal structure should be stronger Lewis acids. [84]

Thanks to its reported properties, tris(pentafluorophenyl)borane forms stable and isolable adducts with many Lewis bases. This can be represented below in Figure II. 26:

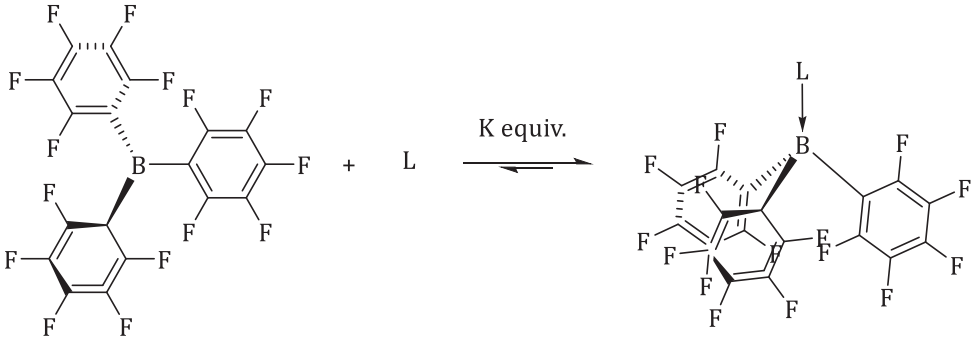

Figure II. 26: Equilibrium between free Lewis acid and base and adduct and representation of the geometric change between trigonal form borane and pyramidalized borane. [39]

Although thermodynamically favored, kinetically these adducts are quite labile with rapid exchanges with free ligands. This is consistent with the observed exchanges between $B(C_6F_5)_3$--THF and $B(C_6F_5)_3$--PPh_3.

To compare the different adducts formed in these experiments, we relied on the differences in the chemical shifts measured by ^{11}B NMR spectra and between the meta and para fluorine atom shifts in ^{19}F NMR spectra as well as the association constants K. The results are summarized in Table II. 8:

Table II. 8: Summary of the differences observed in NMR spectroscopies for three Lewis bases. [a]Referenced for tris(pentafluorophenyl)borane in toluene-d_8. [b]Difference of chemical shift between the meta and para fluorine atoms in the ^{19}F NMR spectra. [c]Calculated from ^{19}F spectra.

Entry	*Lewis base*	*δ ^{11}B (ppm)[a]*	*$\Delta\delta_{m,p}$ (ppm)[b]*	*K (L/mol)[c]*
1	THF	55.8	6.6	not measured
2	PPh_3	61.2	3.7	10^{2-3}
3	C_5H_5N	63.5	7.1	10^{5-6}

With each of the Lewis bases, $B(C_6F_5)_3$ forms strong adducts that is translated by the direct change of the chemical shift in ^{11}B NMR spectra and the apparition of precipitate from the solution. It is also observed that PPh_3 disrupts the most the structure of the borane as the chemical shifts of the meta and para fluorine atoms are closer in this case (Entry 2, Table II. 8). The complexation constants also indicated that $B(C_6F_5)_3/C_5H_5N$ has a strong interaction and thus does not exhibit any FLP behavior. In the case of $B(C_6F_5)_3/PPh_3$ pair, the complexation constant is lower indicating that the interaction between the Lewis acid and base is more frustrated. We can conclude from these NMR experiments that the Lewis pairs studied behave as CLP with varying bond strength instead of being FLP. Interestingly, we were able to evidence a reactivity of the $B(C_6F_5)_3/PPh_3$ pair with CO_2. To tune the Lewis basicity of PPh_3, phenyl groups could be replaced by mesityl groups to increase the steric hindrance. One can mention that the calculations of complexation constants should be done with higher dilutions to afford more precise results.

V. NMR spectroscopy investigation of system based on difunctional Lewis acid (A2) and base (B2)

A. Pairs relying on diamine Lewis base

Several studies were also performed on difunctional molecules carrying two acidic or basic Lewis groups. NMR spectrum were acquired respectively without and with addition of CO_2 in the medium and we tried to distinguish capture of the gas molecule by the Lewis pair formed. This capture is highly dependent of the base used as it modifies the frustrated character of the Lewis pair studied. The Lewis dibase studied chosen were diamines or diphosphines. Concerning the Lewis diacid, we always relied on the synthesized bis borane $B(C_6F_5)_2$-Ph-$B(C_6F_5)_2$ described in the first part.

Firstly, the interaction between commercial 4,4'-bipyridine and synthesized $B(C_6F_5)_2$-Ph-$B(C_6F_5)_2$ was attempted as illustrated in Figure II. 27.

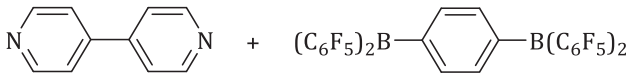

Figure II. 27: Lewis pair between 4,4'-dipyridine and $B(C_6F_5)_2$-Ph-$B(C_6F_5)_2$.

However, we faced precipitation issues and were not able to perform NMR spectroscopies in liquid state on this Lewis pair that is not frustrated enough to form a FLP.

In a second approach, the interaction between N,N,N′,N′-tetramethylethylenediamine (tertiary amine) and $B(C_6F_5)_2$-Ph-$B(C_6F_5)_2$ as illustrated below in Figure II. 28.

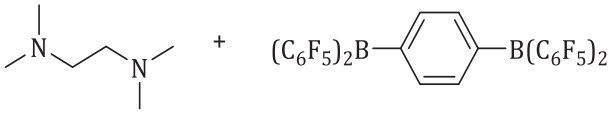

Figure II. 28: Lewis pair between N,N,N′,N′-tetramethylethylenediamine and $B(C_6F_5)_2$-Ph-$B(C_6F_5)_2$.

The interactions between the two compounds only and then under CO_2 were investigated by NMR spectroscopies of ^{1}H, ^{19}F and ^{11}B. We compared the acquired spectra on Figure II. 29 for ^{1}H, Figure II. 30 for ^{19}F, Figure II. 31 for ^{11}B spectroscopies.

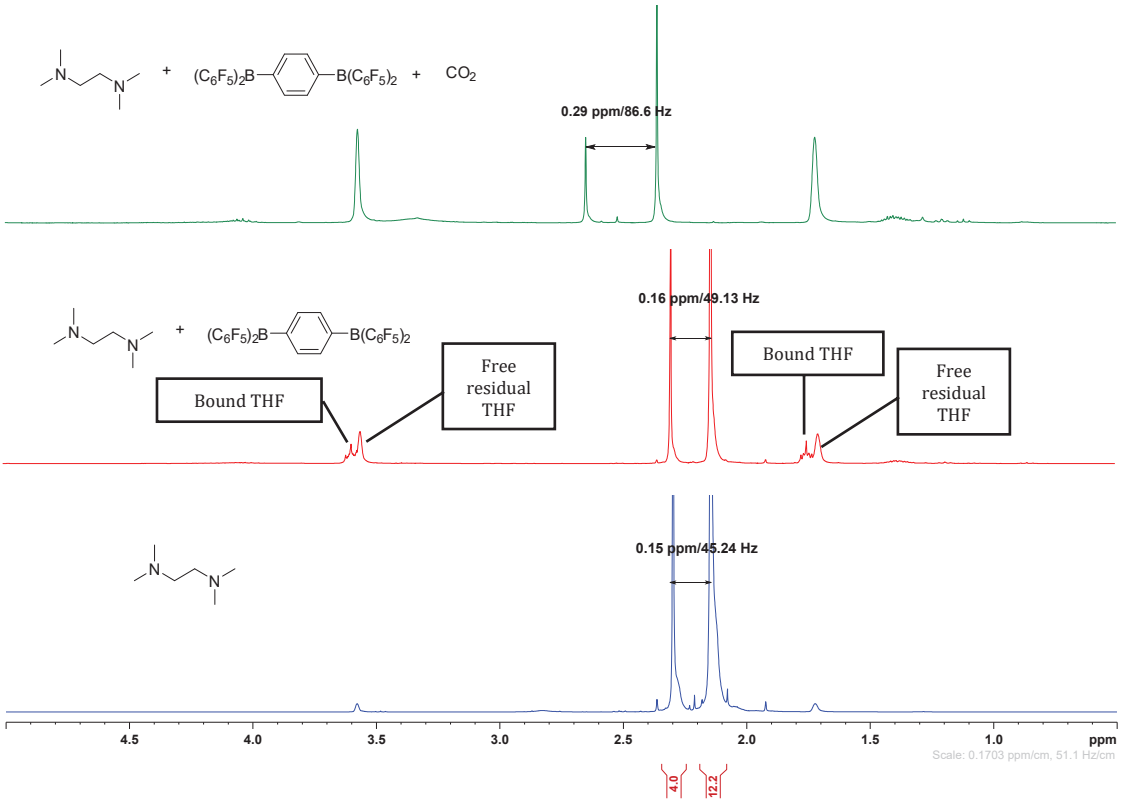

Figure II. 29: ^{1}H NMR spectra of N,N,N′,N′-tetramethylethylenediamine in blue, N,N,N′,N′-tetramethylethylenediamine and $B(C_6F_5)_2$-Ph-$B(C_6F_5)_2$ in red and N,N,N′,N′-tetramethylethylenediamine and $B(C_6F_5)_2$-Ph-$B(C_6F_5)_2$ and CO_2 in green in THF-d_8.

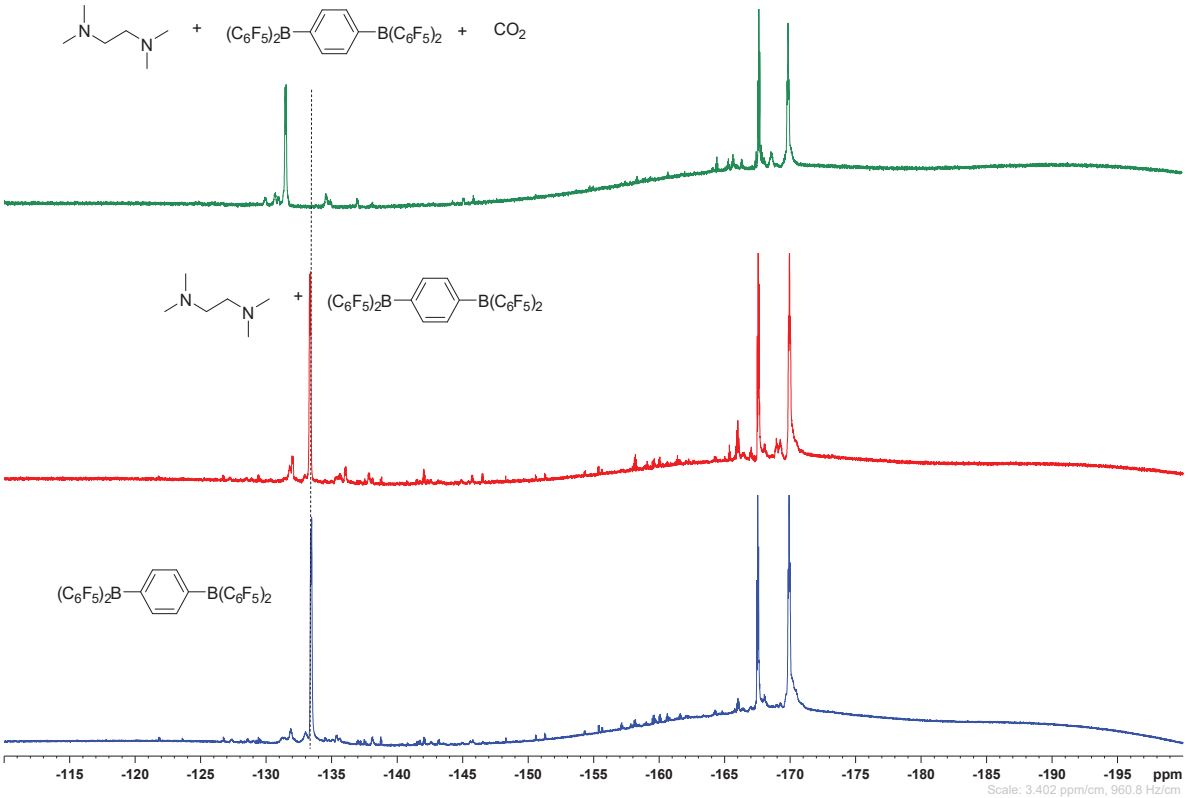

Figure II. 30: ^{19}F NMR spectra of N,N,N′,N′-tetramethylethylenediamine in blue, N,N,N′,N′-tetramethylethylenediamine and $B(C_6F_5)_2$-Ph-$B(C_6F_5)_2$ in red and N,N,N′,N′-tetramethylethylenediamine and $B(C_6F_5)_2$-Ph-$B(C_6F_5)_2$ and CO_2 in green in THF-d_8.

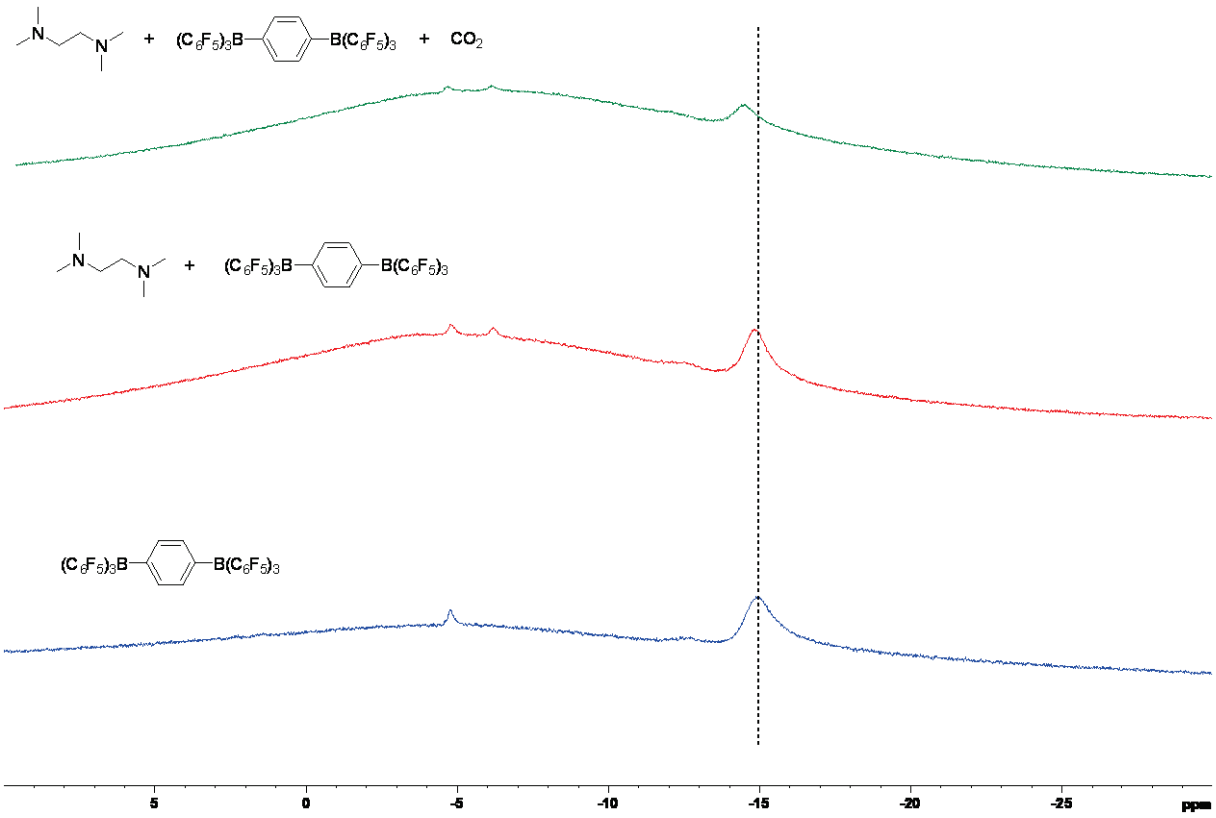

Figure II. 31: ^{11}B NMR spectra of N,N,N′,N′-tetramethylethylenediamine in blue, N,N,N′,N′-tetramethylethylenediamine and $B(C_6F_5)_2$-Ph-$B(C_6F_5)_2$ in red and N,N,N′,N′-tetramethylethylenediamine and $B(C_6F_5)_2$-Ph-$B(C_6F_5)_2$ and CO_2 in green in THF-d_8.

On Figure II. 29, the ^1H spectra of N,N,N',N'-tetramethylethylenediamine in blue, the mixture between $B(C_6F_5)_2$-Ph-$B(C_6F_5)_2$ and N,N,N',N'-tetramethylethylenediamine in red and then the mixture after being exposed to CO_2 in green are represented. On the first spectrum, we can clearly distinguish the CH_2 and CH_3 protons of the diamine at 2.4 ppm and 2.25 ppm in THF-d_8. Besides, residual THF from deuterated solvent can be distinguished with signals at 1.72 ppm and 3.58 ppm. Then, at the addition of the difunctional pentafluoroaryl borane, we can see the addition on multiplets corresponding to THF bound to the difunctional pentafluoroaryl borane. This indicates that the difunctional amine has difficulty to displace THF from the electronic vacancy of the bis borane. Thus, the pair formed is more likely to be frustrated as the amine and the borane studied in this case exhibit a weak interaction. Moreover, the two signals corresponding to the diamine molecule at 2.1 ppm and 2.3 ppm are more spread. After the Young tube being connected to CO_2 for approximately 20 minutes, it was analyzed once more and we found that only free forms of THF residual from the deuterated solvent subsists in the media. Moreover, the interval between the CH_2 and CH_3 signals of the diamine are importantly shifted and spreaded (from 0.16 ppm of interval to 0.29 ppm) indicating changes in the structure of the constituents of the pair.

In the ^{19}F NMR spectra of Figure II. 30, it is possible to detect some new small signals at the mixing of the Lewis base and Lewis acid on the red spectrum, for instance at -131 ppm and -168 ppm.

However, it is difficult to confirm that this is the result of the interaction between the borane and amine compounds. The lack of evident changes in the resulting spectra shows that the pair studied behaves as a FLP. After the incorporation of CO_2 in the Young tube, the ^{19}F spectrum gives more information as depicted on the green spectrum. When calibrating the meta and para fluorines signals on those of the starting fluorinated molecule, we clearly perceive that the ortho fluorines signal is shifted of approximately 2 ppm. It is thus possible to confirm that there is an effect of CO_2 on the Lewis pair.

The ^{11}B spectra were then examined through Figure II. 31 and the addition of diamine to $B(C_6F_5)_2$-Ph-$B(C_6F_5)_2$ induces the creation of a new species whose ^{11}B signal is at -7.9 ppm as visible on the red spectrum. After the addition of CO_2, it is possible to distinguish a shift of the signal from -14.9 ppm to -14.37 ppm showing the impact of CO_2 on the FLP studied. The difference can be easily followed thanks to the black dashed line in Figure II. 31.

Thanks to all these NMR data, we assumed that a supramolecular interaction is happening between the borane and the amine groups when the two compounds are mixed, provoking the creation of a new species as seen by ^{11}B NMR, which constitutes an example of Frustrated Lewis pair. Besides, ^{19}F and ^{1}H NMR spectroscopies evidenced the influence of CO_2 on the pair newly formed and relying on the literature presented on Chapter 1, we herein admit that the capture of CO_2 by this specific pair is efficient and conducts to a new species illustrated below in Figure II. 32:

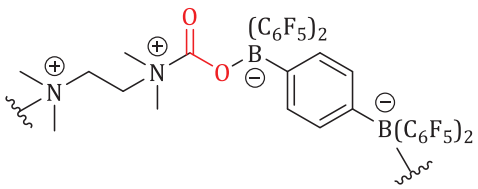

Figure II. 32: CO_2 capture by N,N,N′,N′-tetramethylethylenediamine and $B(C_6F_5)_2$-Ph-$B(C_6F_5)_2$.

It is difficult to discuss whether the complexation forms a polymer or oligomer that could have been induced by the CO_2 capture as no evident broadening of the observed NMR signals was detected.

Secondly, we focused on the interaction between a secondary amine, namely N,N′-diisopropyl-1,3-propanediamine and $B(C_6F_5)_2$-Ph-$B(C_6F_5)_2$ as illustrated below in Figure II. 33.

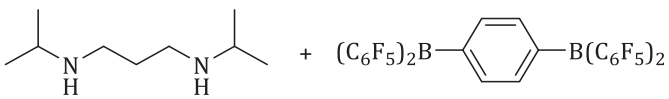

Figure II. 33: Lewis pair between N,N′-diisopropyl-1,3-propanediamine and $B(C_6F_5)_2$-Ph-$B(C_6F_5)_2$.

As previously, we obtained different NMR spectra that were compared on Figure II. 34 for ^{1}H, Figure II. 35 for ^{19}F, Figure II. 36 for ^{11}B:

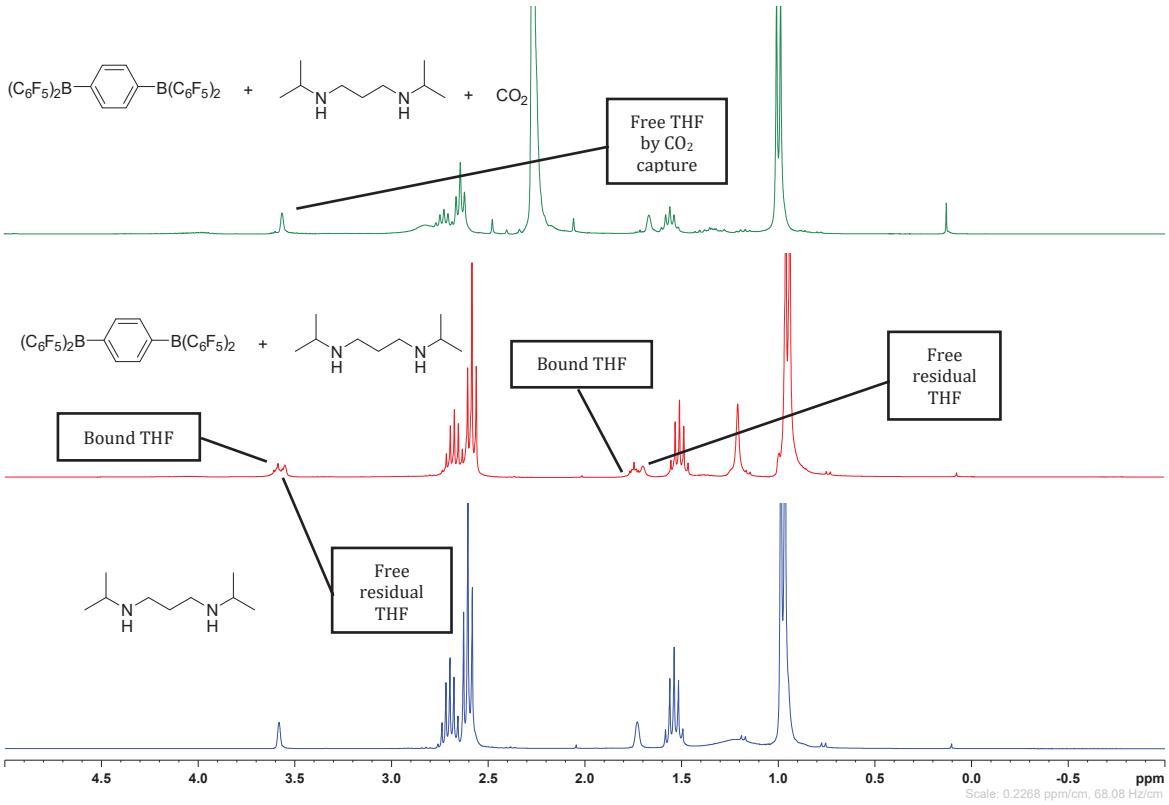

Figure II. 34 ^{1}H NMR spectra of N,N′-diisopropyl-1,3-propanediamine in blue, N,N′-diisopropyl-1,3-propanediamine and $B(C_6F_5)_2$-Ph-$B(C_6F_5)_2$ in red and N,N′-diisopropyl-1,3-propanediamine and $B(C_6F_5)_2$-Ph-$B(C_6F_5)_2$ and CO_2 in green in THF-d_8.

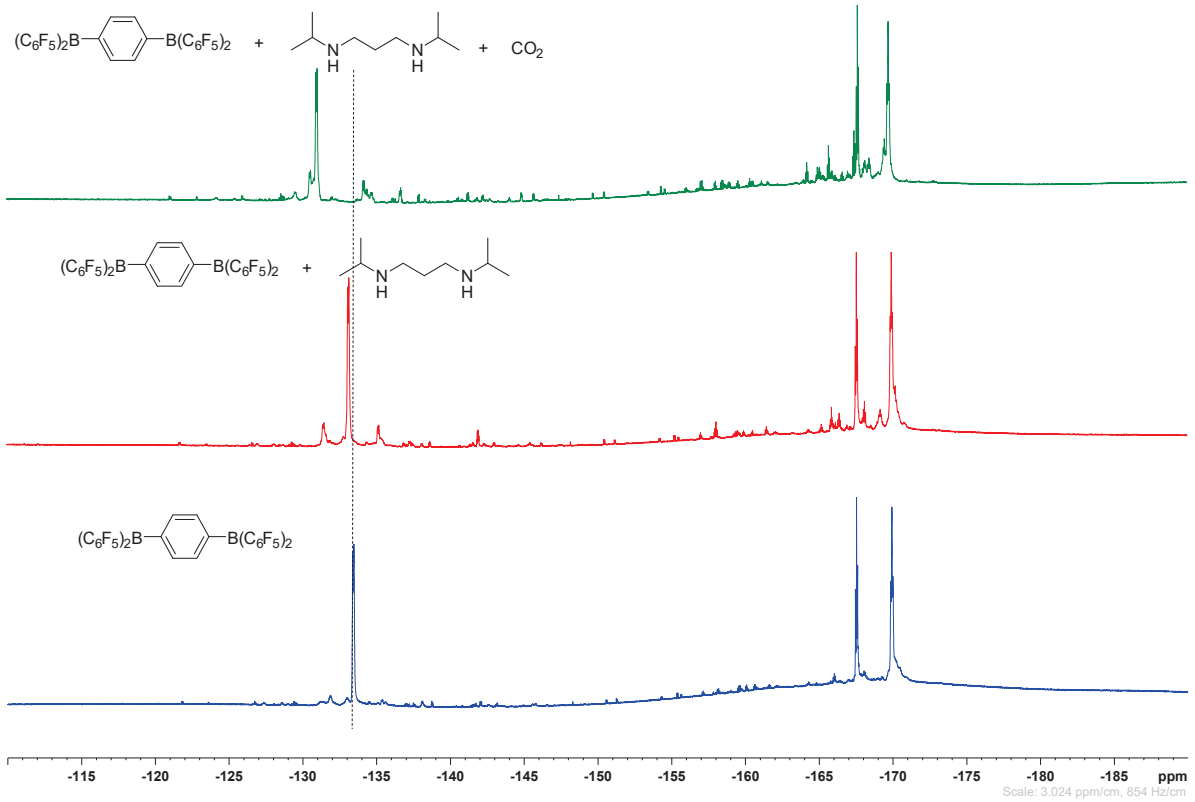

Figure II. 35: ^{19}F NMR spectra of $B(C_6F_5)_2$-Ph-$B(C_6F_5)_2$ in blue, N,N′-diisopropyl-1,3-propanediamine and $B(C_6F_5)_2$-Ph-$B(C_6F_5)_2$ in red and N,N′-diisopropyl-1,3-propanediamine and $B(C_6F_5)_2$-Ph-$B(C_6F_5)_2$ and CO_2 in green in THF-d_8.

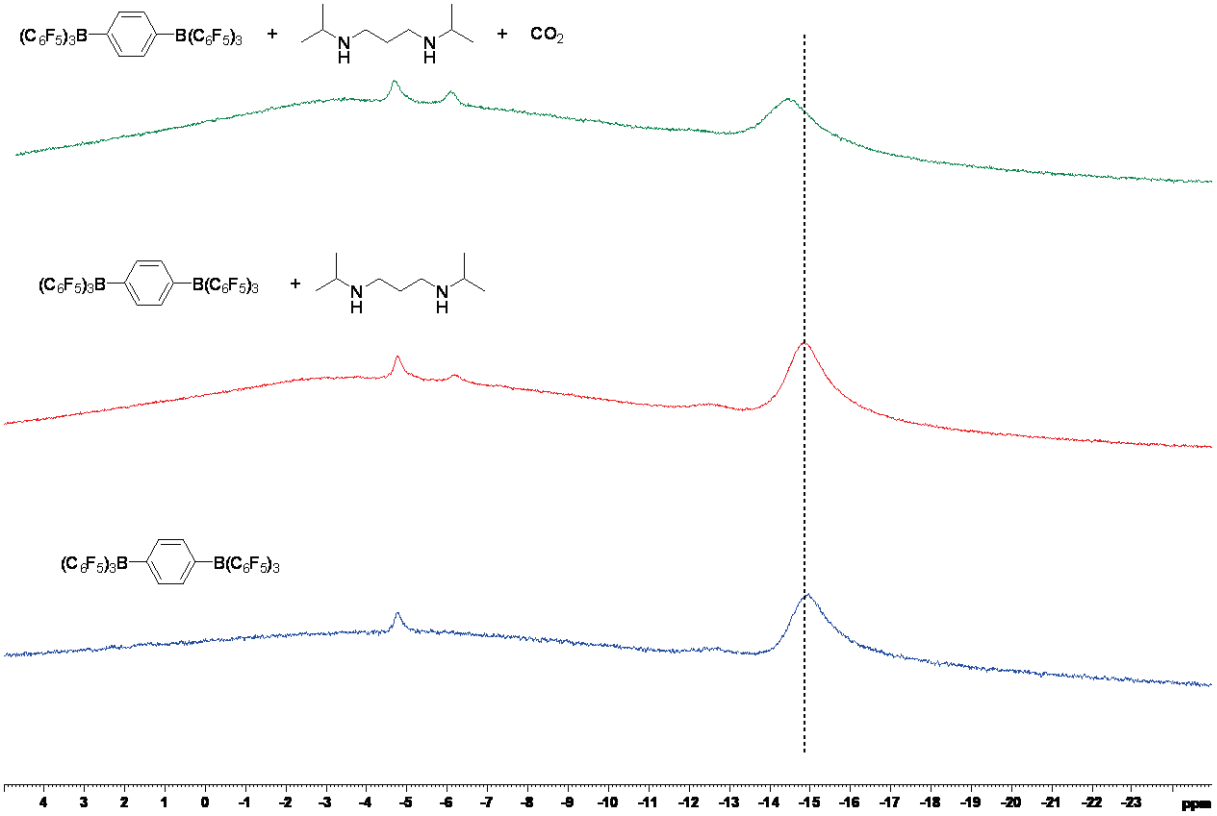

Figure II. 36: ^{11}B NMR spectra of $B(C_6F_5)_2$-Ph-$B(C_6F_5)_2$ in blue, N,N′-diisopropyl-1,3-propanediamine and $B(C_6F_5)_2$-Ph-$B(C_6F_5)_2$ in red and N,N′-diisopropyl-1,3-propanediamine and $B(C_6F_5)_2$-Ph-$B(C_6F_5)_2$ and CO_2 in green in THF-d_8.

On Figure II. 34, we compared the spectra of the secondary diamine in blue, the mixture between the difunctional borane and the secondary diamine in red and lastly, the impact of CO_2 in green on the NMR spectra. Between the blue and red spectra, it is possible to detect that the amine is in constraint form due to the singlet signal of the NH proton contrary to the large signal seen on the red spectra around 1.2 ppm. This clear interaction indicates that the Lewis pair studied is not frustrated. Moreover, it is possible to detect residual THF from the synthesis of the difunctional borane thanks to the presence of multiplets at 3.62 ppm and 1.79 ppm. In this case, THF is bound to the electronic vacancies of boron atoms. At the addition of CO_2, only the residual free THF from deuterated solvent is visible at 3.58 ppm and 1.72 ppm indicating that the possible interaction between the difunctional amine, the difunctional borane and CO_2 is more favorable than the interaction between the bis-borane and THF. In this case, THF is completely removed from the electronic vacancies of boron atoms. Besides, the NH signal is not sharp meaning that the diamine is not constrained anymore by its Lewis pair interaction with the difunctional pentafluroaryl borane. We can also detect water at 2.46 ppm that could arise from the addition of CO_2 in the medium.

Figure II. 35 evidences that new fluorine signals appears at the equivalence between the difunctionalized pentafluoroaryl borane and N,N'-diisopropyl-1,3-propanediamine, especially two signals on each side of the ortho fluorine signal at -134 ppm. When adding CO_2 to the media, the ortho fluorines signal is thus shifted of 2.12 ppm but the two small signals observed on the red spectrum remained the same, corresponding to species that did not react with CO_2.

The last NMR spectra comparison of ^{11}B in Figure II. 36 shows the apparition of a new specie at -7.9 ppm resulting from the Lewis interaction between the borane and amine groups. Besides, the incorporation of CO_2 provokes the shift of the signal from -14.9 ppm to -14.1 ppm as it can be easily followed with the dark dashed line in Figure II. 36.

In this part, we suspected that the secondary diamine used was able to capture CO_2 by itself and thus hindered the capture of CO_2 by the total Lewis pair. Indeed, this phenomenon was already reported in literature. [91] Besides, thanks to ^{19}F NMR spectroscopy, we were able to detect the signals testifying the interaction between borane and amine groups and hence that they remained constant at the addition of CO_2 contrary to the shifted signal of the ortho fluorines of the difunctionalized pentafluoroaryl borane. This could indicate that the result of the capture of CO_2 by the secondary diamine interacts with the pentafluoroarylborane and coexists with the Lewis pair formed in the reaction medium. Moreover, a clear interaction between the Lewis base and Lewis acid occurs indicating that the Lewis pair studied is not frustrated and might not capture CO_2 by itself.

In order to differentiate the effect of CO_2 on the Lewis pair from the effect of CO_2 on the diamine, the NMR spectra of N,N'-diisopropyl-1,3-propanediamine were probed under an atmosphere of CO_2 through ^{1}H and ^{13}C nucleus studies respectively in Figure II. 37 and Figure II. 38.

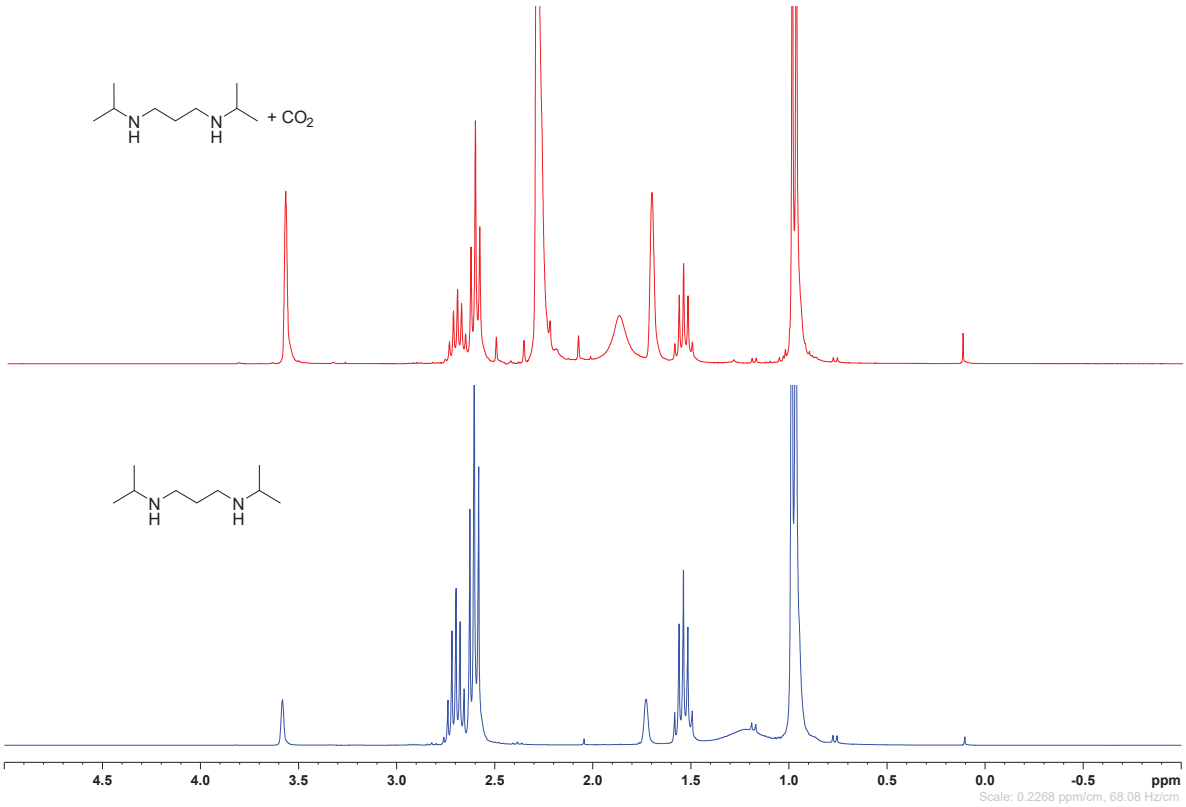

Figure II. 37: ^{1}H NMR spectra of N,N'-diisopropyl-1,3-propanediamine in blue and N,N'-diisopropyl-1,3-propanediamine under CO_2 in red in THF-d_8.

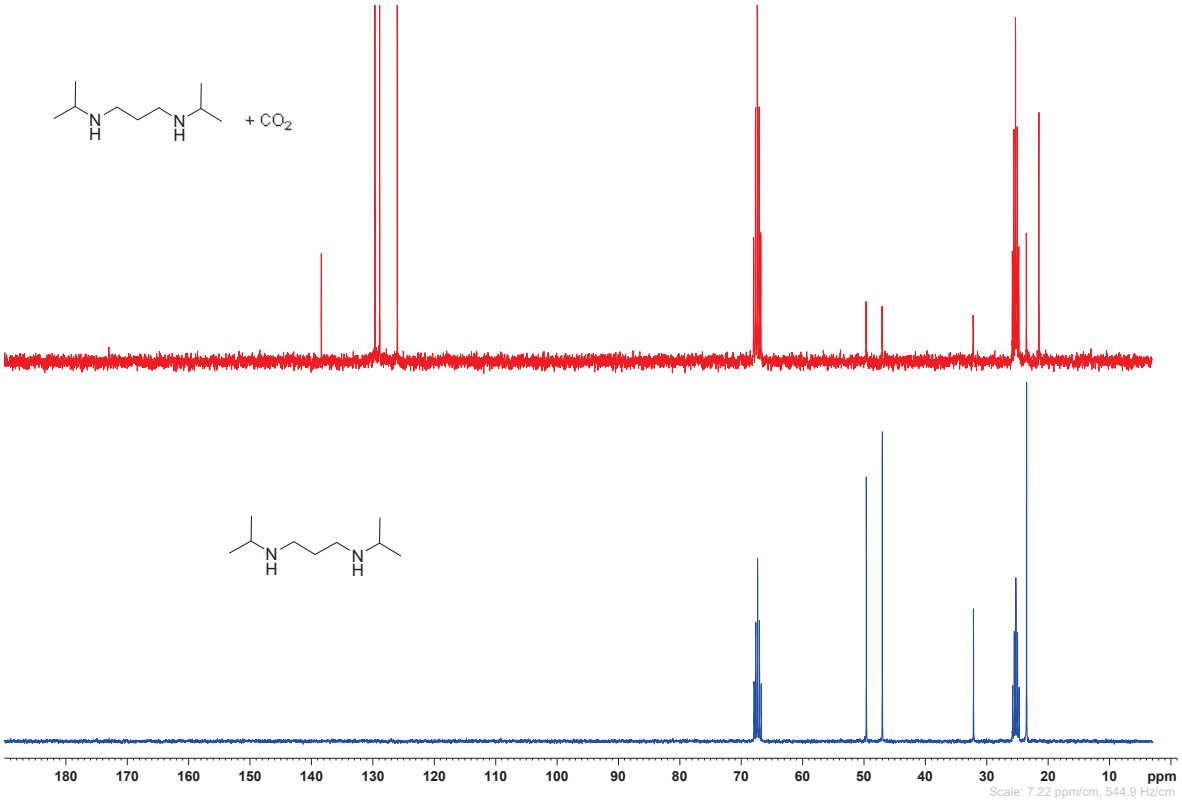

Figure II. 38: ^{13}C NMR spectra of N,N'-diisopropyl-1,3-propanediamine in blue and N,N'-diisopropyl-1,3-propanediamine under CO_2 in red in THF-d_8.

In Figure II. 37, it is clear that new signals at 1.9 ppm and 2.3 ppm are appearing after the presence of CO_2 on N,N'-diisopropyl-1,3-propanediamine that could correspond to protons in RC**H**-RC=O and 2RCH-N**H$_2$** forms. Like previously, the addition of CO_2 provokes the introduction of water in the medium at 2.46 ppm.

Besides, in Figure II. 38, new signals can also be detected at 21.5 ppm that might correspond to **C**-C(=O)-R, 126 ppm (CO_2), 129 ppm, 130 ppm (hydrogenocarbonates) and 137 ppm that could arise from R-**C**ONR$_2$. A small signal at 173 ppm can be distinguished and be related to carbamates compounds.

Relying on the work of Yang *et al.*, the following equilibrium equations can be written in Figure II. 39. [91] In equation (1), the amine reacts with CO_2 *via* a nucleophilic reaction to generate carbamate derivatives. These compounds formed in this reaction may also generate carbonate or bicarbonate *via* hydrolysis (equations (3) and (4)) if water is present in the media that seems to be our case. Carbamates are thermally more stable than bicarbonates and consume higher energy of desorption. [91]

The NMR spectra above are consistent with the suspected carbamate formation while reacting with CO_2.

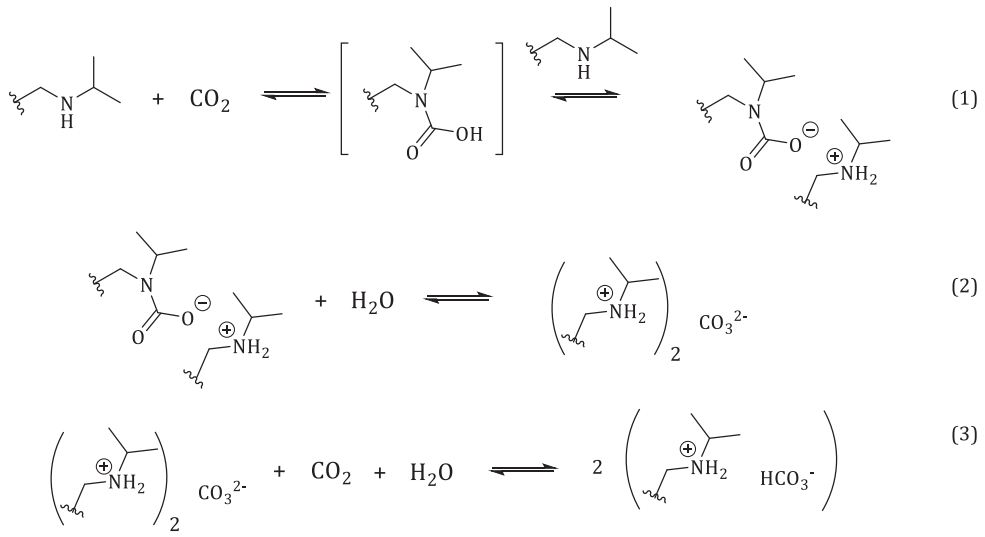

Figure II. 39: Suspected reactivity of N,N'-diisopropyl-1,3-propanediamine and CO_2.

Besides, it was experimentally observed that the capture of CO_2 had the effect of forming precipiates (whitening) I, the amine liquid as illustrated on the left side for the capture of CO_2 by N,N'-diisopropyl-1,3-propanediamine (Figure II. 40). It was also possible to attest that N,N,N′,N′-tetramethylethylenediamine does not react in presence of CO_2 (Figure II. 40).

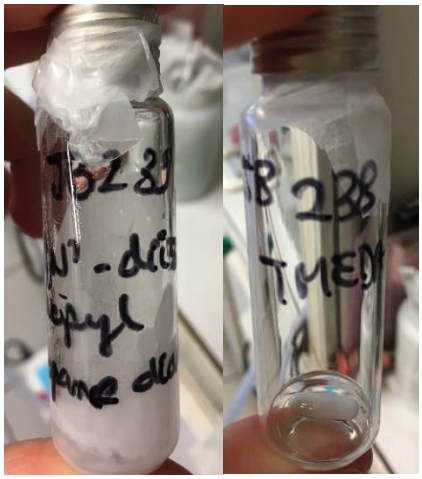

Figure II. 40: Visual aspects of N,N'-diisopropyl-1,3-propanediamine and N,N,N′,N′-tetramethylethylenediamine with CO_2.

To complete this study, the influence of CO_2 on the Lewis diacid $B(C_6F_5)_2$-Ph-$B(C_6F_5)_2$ was probed by NMR spectroscopies. The NMR spectra showed a small shift of 0.74 ppm for the ortho fluorine signal in Figure II. 42 and of 1.34 ppm for the boron atom signal after the addition of CO_2 in Figure II. 43. In this case, we assumed that the lone pairs of the oxygen atoms of CO_2 might coordinate the electronic vacancies of the boron atoms on the Lewis diacid through η_1 coordination *via* oxygen atoms (Figure II. 41), but CO_2 is not readily captured by the Lewis diacid itself.

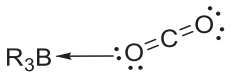

Figure II. 41: Representation of η_1 coordination via *oxygen atoms on boron atoms.*

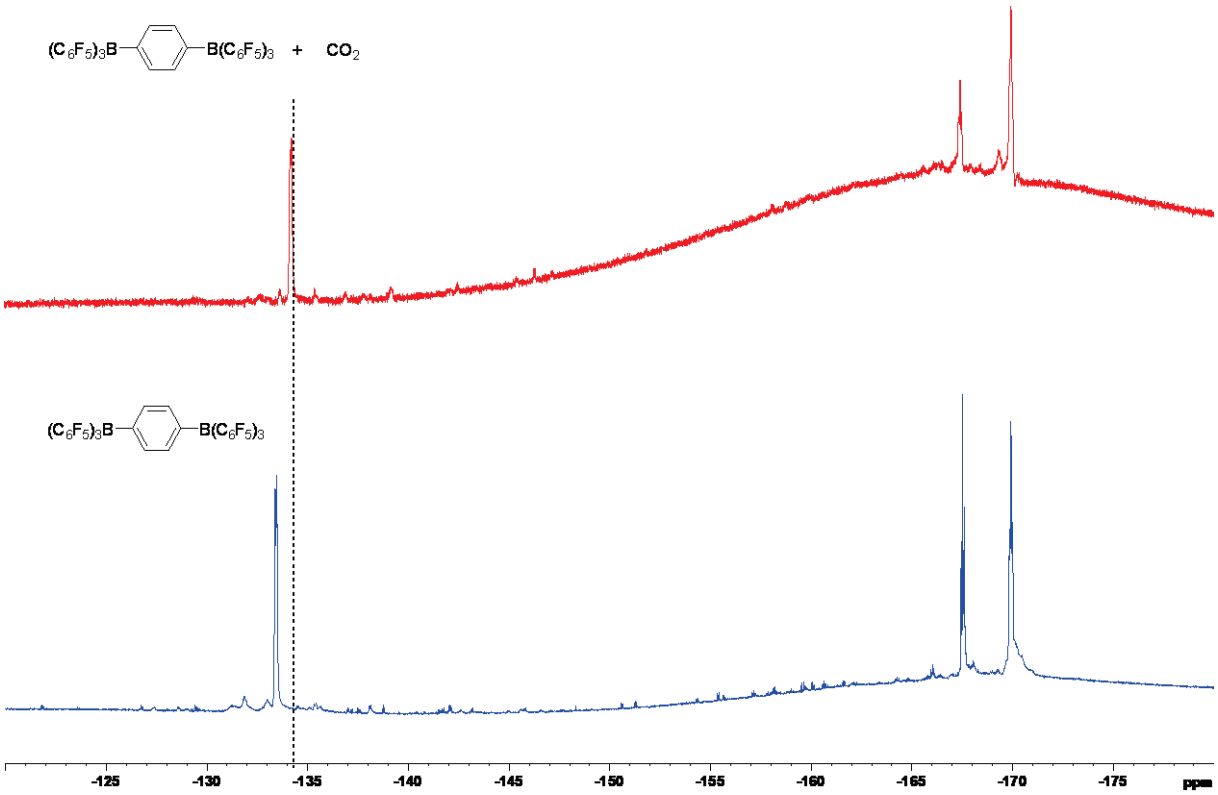

Figure II. 42: ^{19}F NMR spectra of $B(C_6F_5)_2$-Ph-$B(C_6F_5)_2$in blue and $(B(C_6F_5)_2)_2$-Ph-$(B(C_6F_5)_2)_2$ under CO_2 in red in THF-d8.

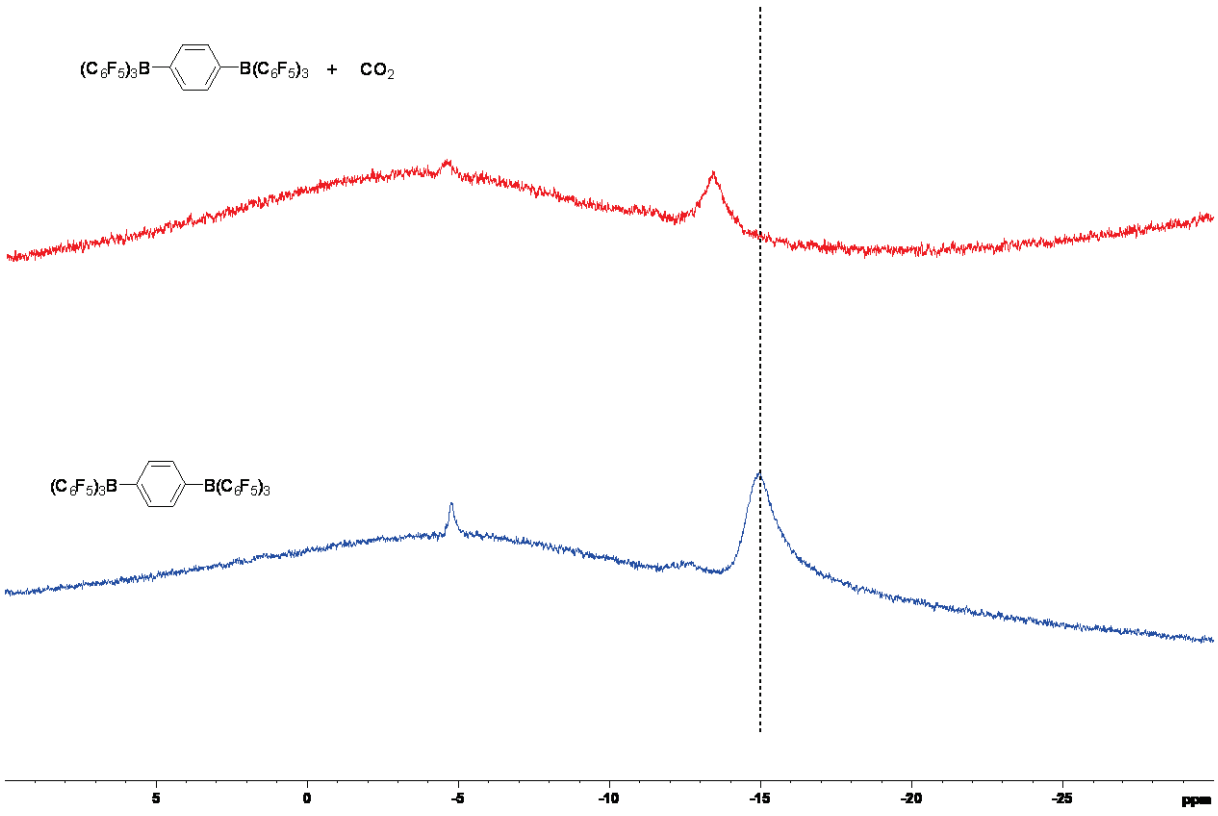

Figure II. 43: ^{11}B NMR spectra of $B(C_6F_5)_2$-Ph-$B(C_6F_5)_2$ in blue and $(B(C_6F_5)_2)_2$-Ph-$(B(C_6F_5)_2)_2$ under CO_2 in red in THF-d_8.

To conclude, two pairs were studied in this part: N,N,N',N'-tetramethylethylenediamine with $B(C_6F_5)_2$-Ph-$B(C_6F_5)_2$ and N,N'-diisopropyl-1,3-propanediamine with $B(C_6F_5)_2$-Ph-$B(C_6F_5)_2$. Concerning the first pair, it was difficult to clearly visualize the influence of the Lewis dibase on the Lewis diacid. However, it was clear that this pair is able to capture CO_2, especially through ^1H and ^{11}B experiments. We can conclude that this pair behaves as a FLP. On the other hand, an obvious interaction between N,N'-diisopropyl-1,3-propanediamine and $B(C_6F_5)_2$-Ph-$B(C_6F_5)_2$ was observed, classifying this pair as a CLP. In addition, we faced some issues with this secondary amine that can capture CO_2 by itself *via* the formation of carbamate derivatives. Astonishingly, CO_2 can also have an influence of $B(C_6F_5)_2$-Ph-$B(C_6F_5)_2$ *via* the coordination of the oxygen lone pairs on the boron atoms. It was thus difficult to decorrelate the role of each compounds separately and of the Lewis pair.

B. Pairs relying on diphosphine Lewis base

In a third experiment, we switched to a diphosphine Lewis base and we investigated the interaction between 1,3-bis(diphenylphosphino)propane and $B(C_6F_5)_2$-Ph-$B(C_6F_5)_2$ as illustrated in Figure II. 44.

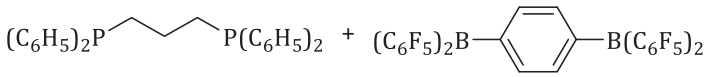

Figure II. 44: Lewis pair between 1,3-bis(diphenylphosphino)propane and $B(C_6F_5)_2$-Ph-$B(C_6F_5)_2$.

The ^1H, ^{19}F and ^{11}B NMR spectra were obtained as indicated below, respectively in Figure II. 45, Figure II. 46 and Figure II. 47.

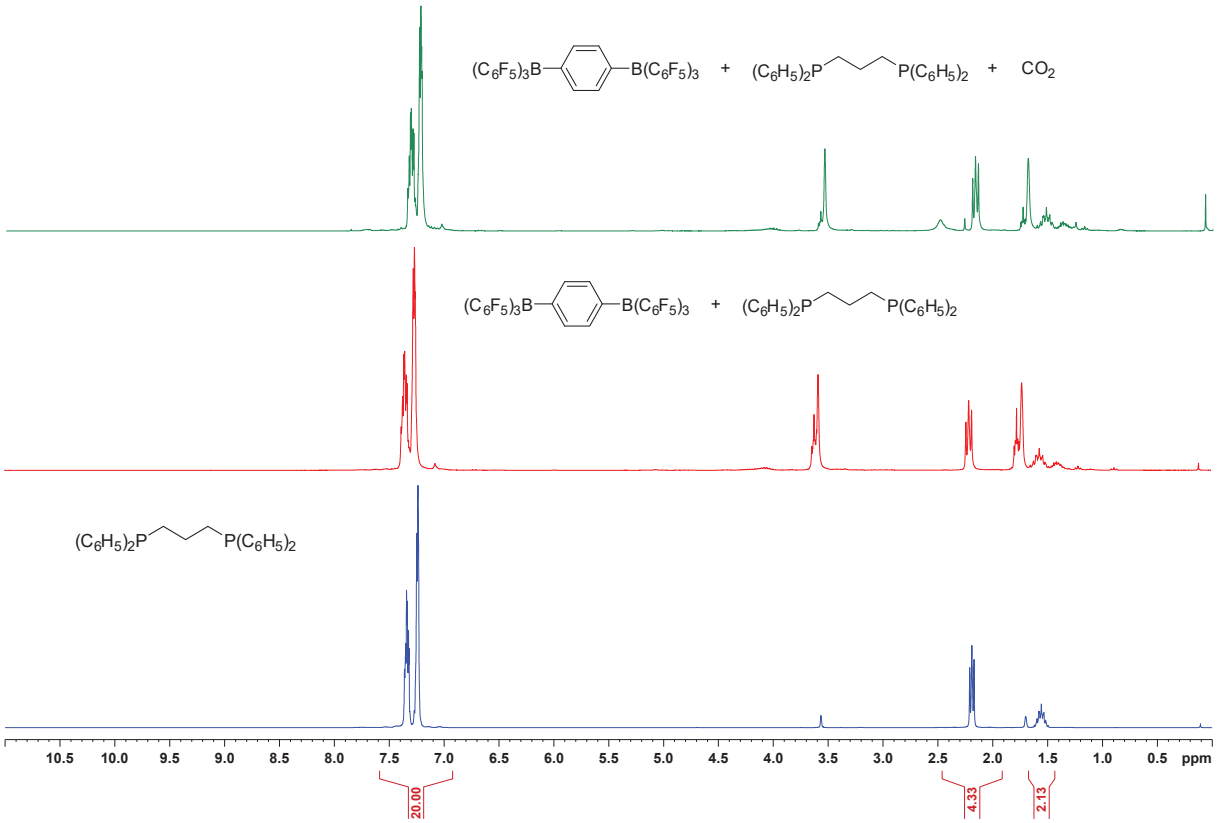

Figure II. 45: ^{1}H NMR spectra of 1,3-bis(diphenylphosphino)propane in blue, 1,3-bis(diphenylphosphino)propane and $B(C_6F_5)_2$-Ph-$B(C_6F_5)_2$ in red and 1,3-bis(diphenylphosphino)propane and $B(C_6F_5)_2$-Ph-$B(C_6F_5)_2$ and CO_2 in green in THF-d_8.

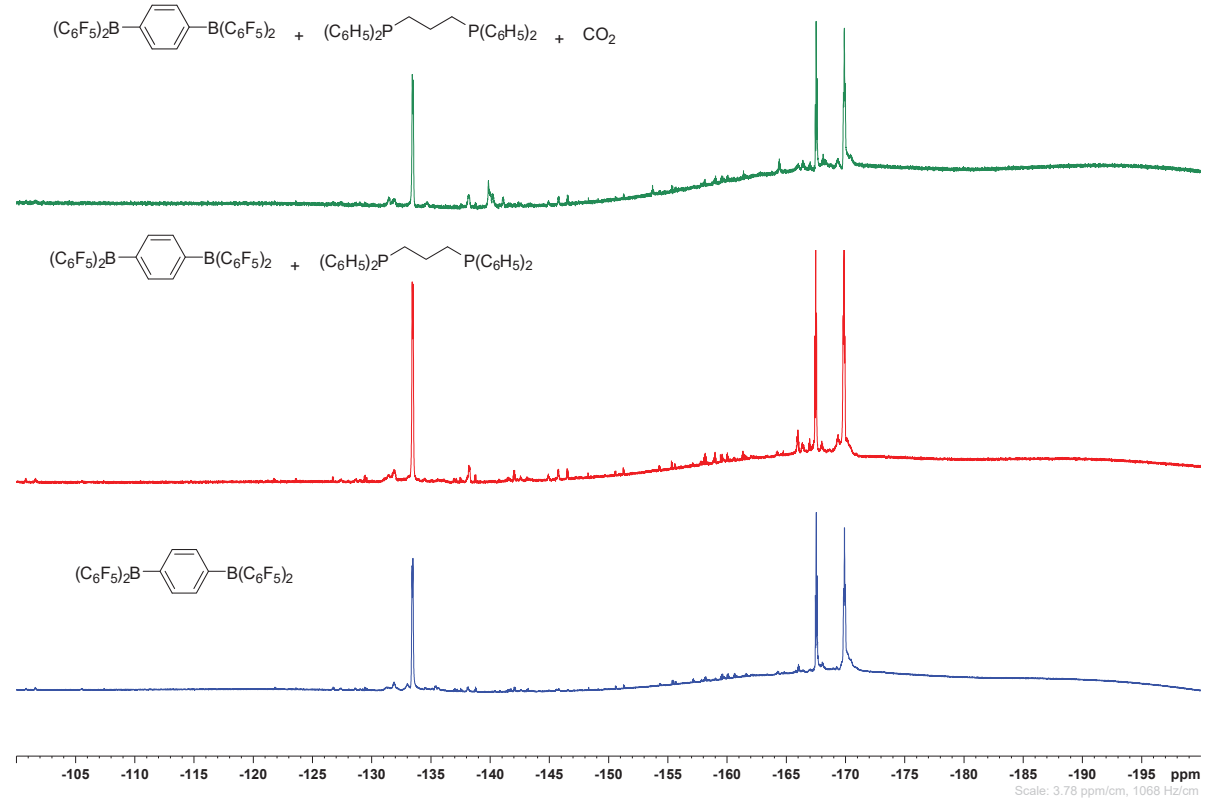

Figure II. 46: ^{19}F NMR spectra of $B(C_6F_5)_2$-Ph-$B(C_6F_5)_2$ in blue, 1,3-bis(diphenylphosphino)propane and $B(C_6F_5)_2$-Ph-$B(C_6F_5)_2$ in red and 1,3-bis(diphenylphosphino)propane and $B(C_6F_5)_2$-Ph-$B(C_6F_5)_2$ and CO_2 in green in THF-d_8.

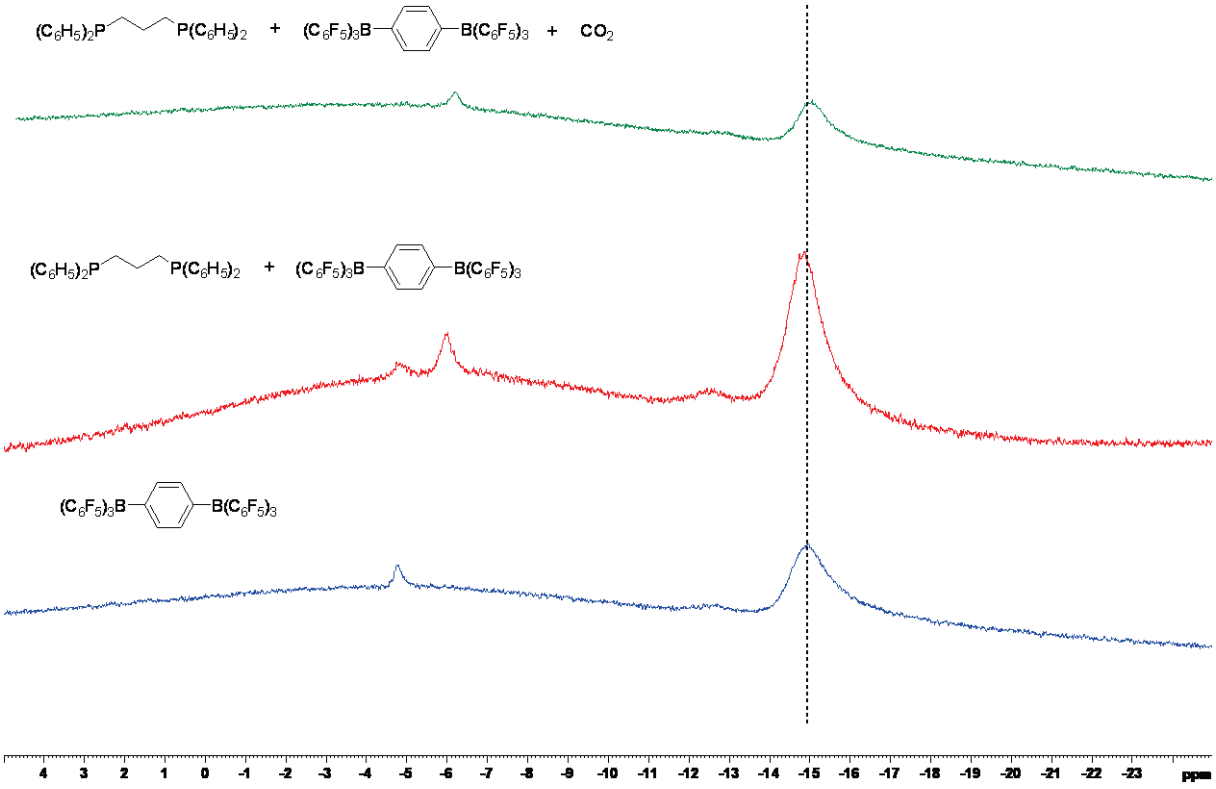

Figure II. 47: ^{11}B NMR spectra of $B(C_6F_5)_2$-Ph-$B(C_6F_5)_2$ in blue, 1,3-bis(diphenylphosphino)propane and $B(C_6F_5)_2$-Ph-$B(C_6F_5)_2$ in red and 1,3-bis(diphenylphosphino)propane and $B(C_6F_5)_2$-Ph-$B(C_6F_5)_2$ and CO_2 in green in THF-d_8.

Firstly, Figure II. 45 compares the ^1H spectra of 1,3-bis(diphenylphosphino)propane in blue, 1,3-bis(diphenylphosphino)propane and $B(C_6F_5)_2$-Ph-$B(C_6F_5)_2$ in red and 1,3-bis(diphenylphosphino)propane and $B(C_6F_5)_2$-Ph-$B(C_6F_5)_2$ and CO_2 in green. The initial product is easily identified by ^1H NMR with the correct integrals. At the addition of the difunctionalized pentafluoroaryl borane, the first difference is the splitting of the signals corresponding to the THF solvent indicating that two forms of THF are coexisting in the media: free and complexed forms by the boron atoms. However, no changes are visible concerning the formation of a Lewis pair. This could indicate that the pair studied is more frustrated. Besides, the addition of CO_2 does not bring any modification, except a supplementary signal distinguishable at 2.5 ppm that could arise from the capture of CO_2 by the FLP newly formed.

Secondly, ^{19}F in Figure II. 46 shows that the addition of phosphine to the borane does not provoke an overlap of the ortho fluorine signals. However, the incorporation of CO_2 in the medium brought new signals between -138 and -142 ppm as illustrated in the green spectra.

The last spectra studied are the ^{11}B NMR ones superimposed in Figure II. 47. An obvious new signal is brought from the Lewis pair interaction at -5.9 ppm on the red spectrum that coexists with the difunctional pentafluoroaryl borane at -4.9 ppm. The addition of CO_2 induces the

disappearance of the initial signal at -4.9 ppm in favor of the signal at -5.9 ppm. Besides, the signal at -14.9 ppm is shifted to -14.57 ppm.

The structure of the new species formed from the interaction between the pair and CO_2 can be represented in Figure II. 48.

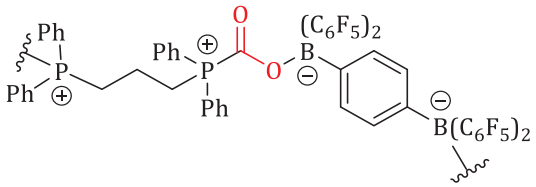

Figure II. 48: CO_2 capture by 1,3-bis(diphenylphosphino)propane and $B(C_6F_5)_2$-Ph-$B(C_6F_5)_2$.

In another system, $B(C_6F_5)_2$-Ph-$B(C_6F_5)_2$ was studied through the interaction with another diphosphine: bis(dicyclohexylphosphino)methane (Figure II. 49) by NMR spectroscopy.

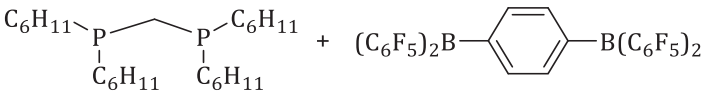

Figure II. 49: Lewis pair between bis(dicyclohexylphosphino)methane and $B(C_6F_5)_2$-Ph-$B(C_6F_5)_2$.

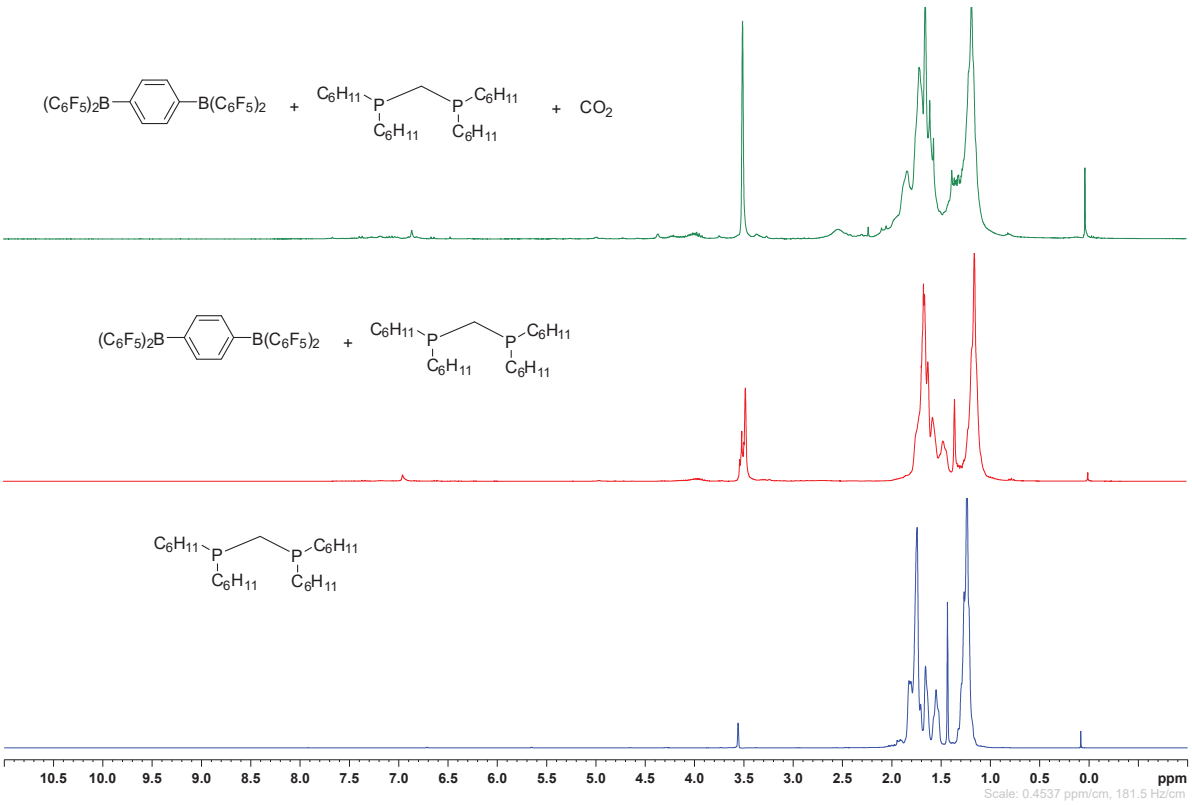

Figure II. 50: ^1H NMR spectra of bis(dicyclohexylphosphino)methane in blue, bis(dicyclohexylphosphino)methane and $B(C_6F_5)_2$-Ph-$B(C_6F_5)_2$ in red and bis(dicyclohexylphosphino)methane and $B(C_6F_5)_2$-Ph-$B(C_6F_5)_2$ and CO_2 in green in THF-d_8.

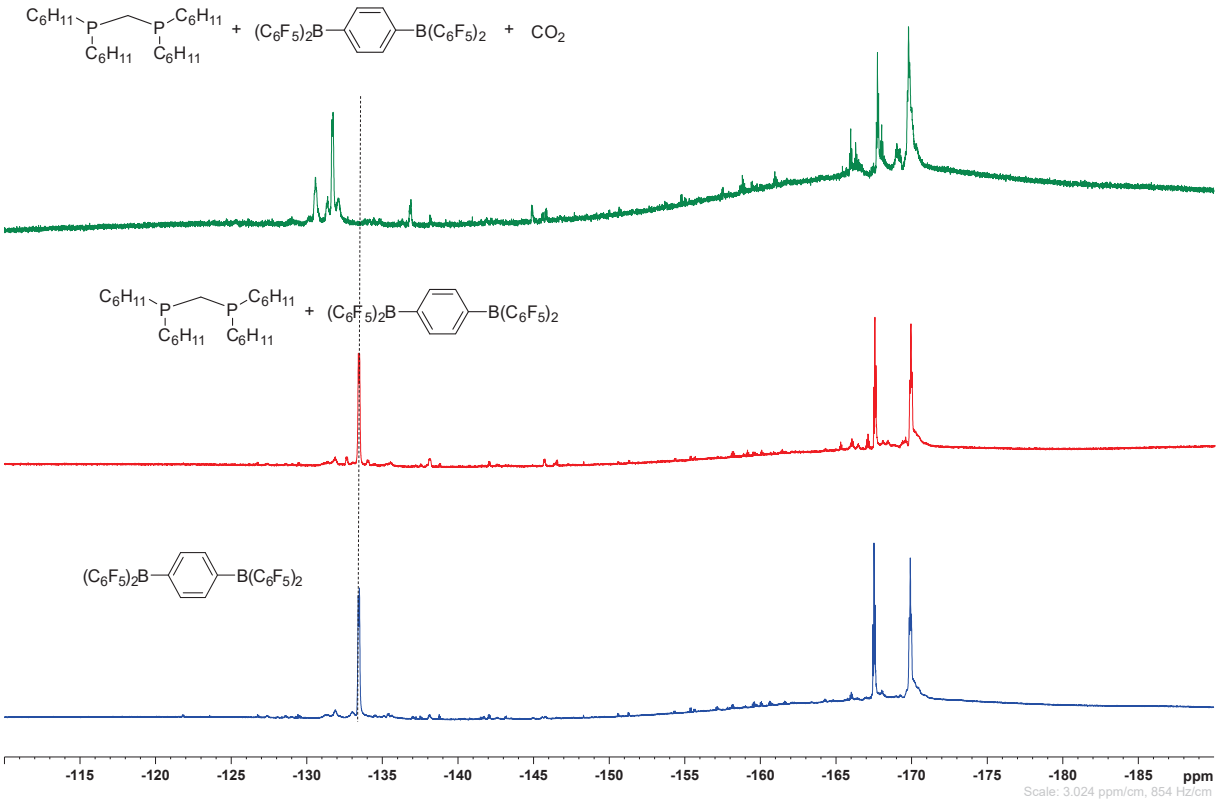

Figure II. 51: ^{19}F NMR spectra of B(C6F5)2-Ph-B(C6F5)2 in blue, bis(dicyclohexylphosphino)methane and $B(C_6F_5)_2$-Ph-$B(C_6F_5)_2$ in red and bis(dicyclohexylphosphino)methane and $B(C_6F_5)_2$-Ph-$B(C_6F_5)_2$ and CO_2 in green in THF-d_8.

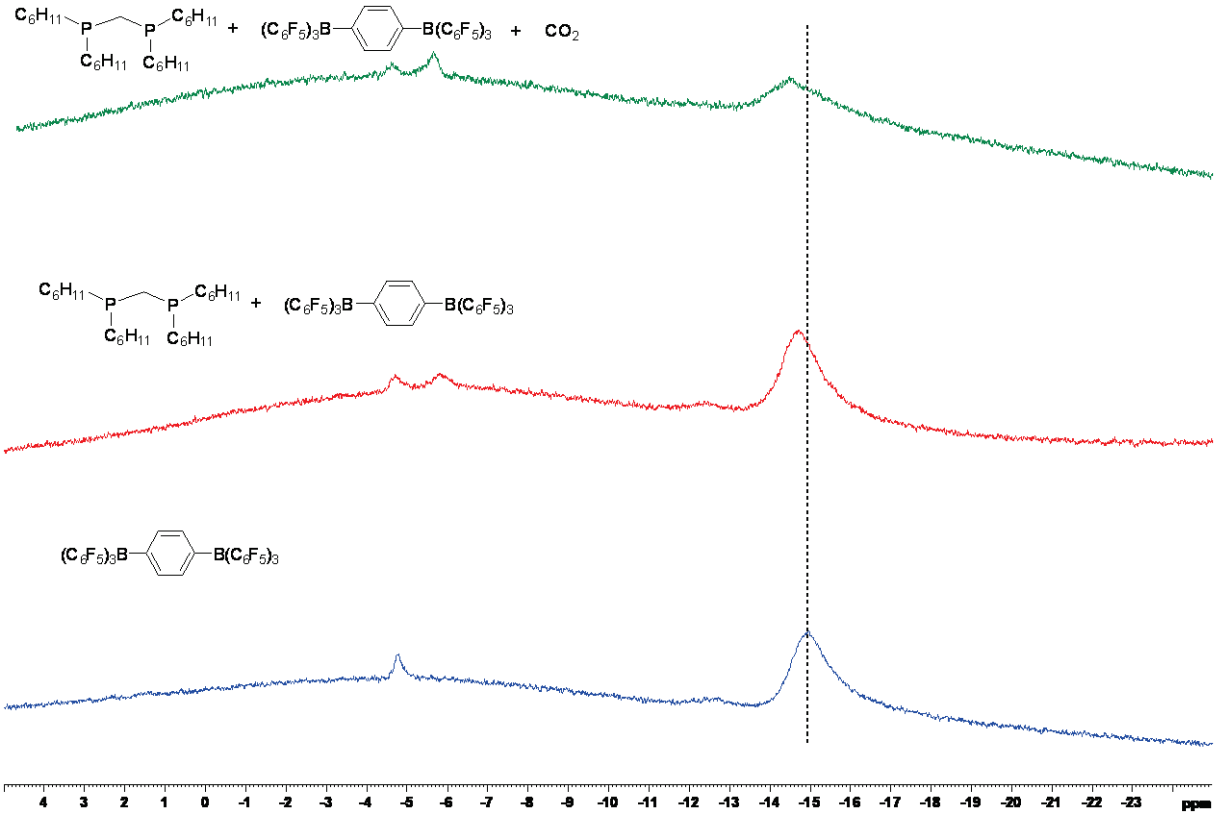

Figure II. 52: ^{11}B NMR spectra of $B(C_6F_5)_2$-Ph-$B(C_6F_5)_2$ in blue, bis(dicyclohexylphosphino)methane and $B(C_6F_5)_2$-Ph-$B(C_6F_5)_2$ in red and bis(dicyclohexylphosphino)methane and $B(C_6F_5)_2$-Ph-$B(C_6F_5)_2$ and CO_2 in green in THF-d_8.

Figure II. 50 relates the evolution of the ^{1}H NMR spectrum of bis(dicyclohexylphosphino)methane in blue, in presence of $B(C_6F_5)_2$-Ph-$B(C_6F_5)_2$ in red and with both $B(C_6F_5)_2$-Ph-$B(C_6F_5)_2$ and CO_2 in green. At the addition of the pentafluoroaryl bisborane, the signals for THF solvent are split but it is difficult to see further differences. The lack of differences could come from the frustration of the Lewis pair studied. After the introduction of CO_2 in the reaction medium, a new signal is detected at 2.25 ppm arising from the presence of a carbonyl that results from the capture of CO_2 by the FLP formed.

In Figure II. 51, we compared the ^{19}F spectra for the same experiments as before. The addition of difunctional phosphine to pentafluoroaryl borane induces a small shift in the signal of the ortho fluorine atoms of the Lewis acid. Secondly, CO_2 induces a larger shift of this same signal of 1.81 ppm and the apparition of new signals at -131 ppm, -138 ppm and -171 ppm that might arise from the capture of CO_2 but that could also be due to the oxidation of the bis borane (air contamination).

Figure II. 52 shows the evolution in terms of ^{11}B NMR spectroscopy. An obvious new signal is brought from the Lewis pair interaction at -5.9 ppm on the red spectrum that coexists with the difunctional pentafluroroaryl borane at -4.9 ppm. The addition of CO_2 induces the predominance of the -5.9 ppm signal compared to the initial -4.9 ppm. Besides, the signal in blue at -14.9 ppm is shifted of 0.88 ppm after addition of CO_2.

The resulting species from the capture of CO_2 by the newly synthesized pair can be represented as below in Figure II. 53.

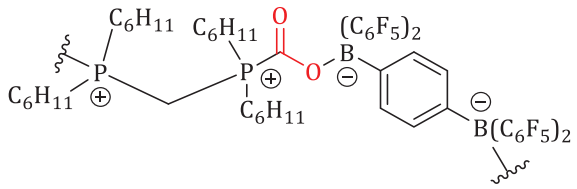

Figure II. 53: CO_2 capture by bis(dicyclohexylphosphino)methane and $B(C_6F_5)_2$-Ph-$B(C_6F_5)_2$.

To conclude on this part, we studied the interactions by NMR spectroscopies of two Lewis pairs: 1,3-bis(diphenylphosphino)propane and $B(C_6F_5)_2$-Ph-$B(C_6F_5)_2$ and bis(dicyclohexylphosphino)-methane and $B(C_6F_5)_2$-Ph-$B(C_6F_5)_2$. Concerning the first one, it was quite difficult to probe the influence of the Lewis dibase on the Lewis diacid suggesting the FLP nature of this pair. Small changes in the NMR spectra after the addition of CO_2 could indicate CO_2 capture but it was not that obvious. On the other hand, it was also difficult to perceive the influence of bis(dicyclohexylphosphino)methane on $B(C_6F_5)_2$-Ph-$B(C_6F_5)_2$ but more important changes in the NMR spectra after the addition of CO_2 were detected. This could confirm the ability of this FLP to capture CO_2.

VI. System based on difuctional Lewis acid A2 and Lewis base-functionalized (co)polymer (polyB)

In this part, the behavior of Lewis pairs from difunctional Lewis acid and Lewis base-functionalized polymers will be investigated. A first part will be dedicated to nitrogen-based polymers and a second part to phosphorus-based polymers.

A. Nitrogen-based polymers as Lewis-base functionalized (co)polymer (polyB)

a. Macroscopic observations

Firstly, we tried to figure out the interaction between Lewis acid and Lewis base through simple macroscopic observations. We studied the reaction between the synthesized $B(C_6F_5)_2$-Ph-$B(C_6F_5)_2$ and the commercial poly(4-vinylpyridine) (P4VP) from Sigma Aldrich (M_w=160,000 g/mol), as described in Figure II. 54.

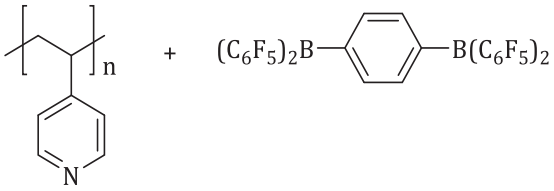

Figure II. 54: Lewis pair between $B(C_6F_5)_2$-Ph-$B(C_6F_5)_2$ and poly(4-vinylpyridine).

P4VP was solubilized in chloroform (5 wt % solution) and then the Lewis diacid was added to the solution. Chloroform was the only solvent found to dissolve the homopolymers from 4-vinylpyridine. A high increase of the viscosity in the medium was observed at this point (Figure II. 55).

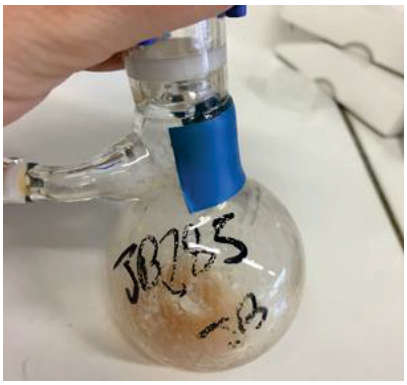

Figure II. 55: Increase of viscosity observed at the mix of poly(4-vinylpyridine) and $B(C_6F_5)_2$-Ph-$B(C_6F_5)_2$ in chloroform.

The interaction between pyridine and pentafluoroaryl borane was really fast and gave rise to a high viscosity testifying that linkages between the polymer chains are created thanks to the difunctional Lewis acid. The exchanges are fast between the B-N linkages allowing for the

reorganization of the network formed that tends to be more homogenous over time. The drying of the gel obtained formed a solid that can no longer be resolubilized. (Figure II. 56).

Figure II. 56: Visual after drying of the poly(4-vinylpyridine) and $B(C_6F_5)_2$-Ph-$B(C_6F_5)_2$ mix.

To facilitate the control of this increase of viscosity of the solution mixture, it was decided to complex the boron electronic vacancies of the difunctional Lewis acid with two molar equivalents of triethylamine. The reaction was reproduced in the same conditions and it was found that the viscosity does not increase as fast as previously. The solution seemed to be also more homogenous in this case, as illustrated in Figure II. 57.

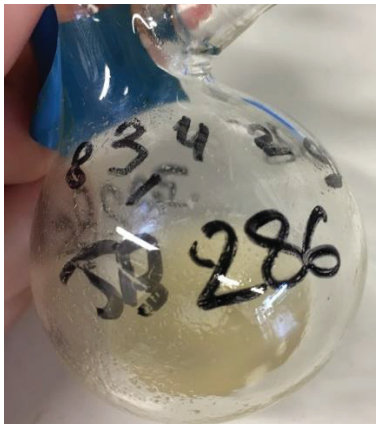

Figure II. 57: Increase of viscosity observed at the mix of poly(4-vinylpyridine) and $B(C_6F_5)_2$-Ph-$B(C_6F_5)_2$ with 2 molar equivalents of triethylamine in chloroform.

The creation of the network in this case is slowed down by the presence of triethylamine. Indeed, the borane groups can not interact directly with the pendent pyridine groups, but need first to displace of triethylamine before being able of complexing the pyridine groups. The interaction between pyridine and borane is more favorable than the interaction between triethylamine and borane evidencing competition between the Lewis bases. The drying of the solution put in evidence the presence of gels when triethylamine was evaporated as represented in Figure II. 58. Furthermore, the addition of toluene had the effect of swelling the gel parts instead of solubilizing it proving the efficiency of the interaction B--N.

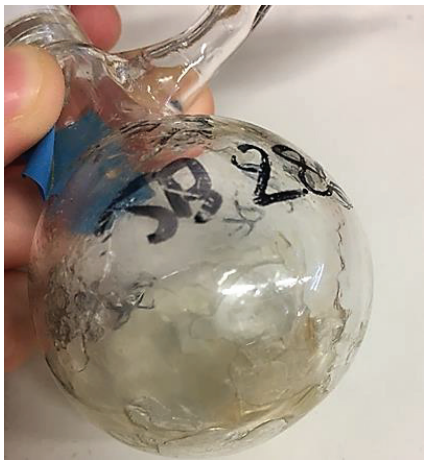

Figure II. 58: Recovery of gel after drying of the solution of poly(4-vinylpyridine) and $B(C_6F_5)_2$-Ph-$B(C_6F_5)_2$ in chloroform.

Lutidine can also be used instead of triethylamine to complex the boron vacancy of the difunctional Lewis diacid. In the same conditions, a small change of the viscosity was observed (Figure II. 59).

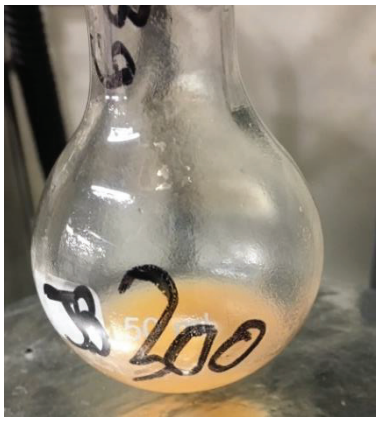

Figure II. 59: Small increase of viscosity observed at the mix of poly(4-vinylpyridine) and $B(C_6F_5)_2$-Ph-$B(C_6F_5)_2$ with 2 molar equivalents of lutidine in chloroform.

To deepen the control of the increase of viscosity of the solution, a copolymer with a controlled amount of 4-vinylpyridine was used. Poly(styrene-*co*-4-vinylpyridine) containing 18 % molar of 4-vinylpyridine was dissolved in dried toluene as well as the difunctional Lewis diacid was solubilized in toluene with 2 molar equivalents of triethylamine. The solutions were mixed to reach a ratio B:N of 1.

The addition of the borane provokes a rapid increase of the viscosity in the medium as illustrated in Figure II. 60.

Figure II. 60: Increase of viscosity observed at the mix of poly(styrene-co-4-vinylpyridine) and $B(C_6F_5)_2$-Ph-$B(C_6F_5)_2$ with 2 molar equivalents of triethylamine in toluene.

The aspect of the solution after the addition of the borane testifies the efficiency of the interaction between the Lewis acid and base groups respectively carried by the difunctional molecule and the copolymer.

In order to check if the increase of viscosity was not only due to phase separation, the same reaction was conducted with the monofunctionalized Lewis acid $B(C_6F_5)_3$ instead of the difunctional one. This compound was added to a 5 wt % solution of poly(4-vinylpyridine) dissolved in chloroform with the addition of one molecule of $B(C_6F_5)_3$ every 40 monomer units. In this case, no increase of the viscosity was observed and the Lewis pairs remained fully soluble in the solvent.

This constitutes a counter-example proving that the aforementioned increase of viscosity in the case of difunctional Lewis acid is only due to the Lewis interaction between the borane and pyridine groups and cannot be attributed to phase separation.

Rheology experiments could not be carried out because of lack of time but need to be done in the future to confirm the observations done visually and to deepen the understanding of the Lewis pair studied.

b. NMR spectroscopy

To complete this study, the reaction presented previously through the visual prism was probed by NMR spectroscopy relying on the interaction between poly(styrene-*co*-4-vinylpyridine) and tris(pentafluorophenyl) borane with a ratio B:N 1. The monofunctional Lewis acid was chosen in this case to avoid gelation in the NMR tube (Figure II. 61) and allow for the correct acquisition of NMR spectra.

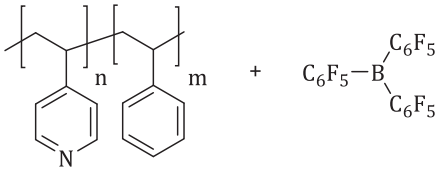

Figure II. 61: Interaction between poly(styrene-co-4-vinylpyridine) and tris(pentafluorophenyl)borane studied by NMR spectroscopy.

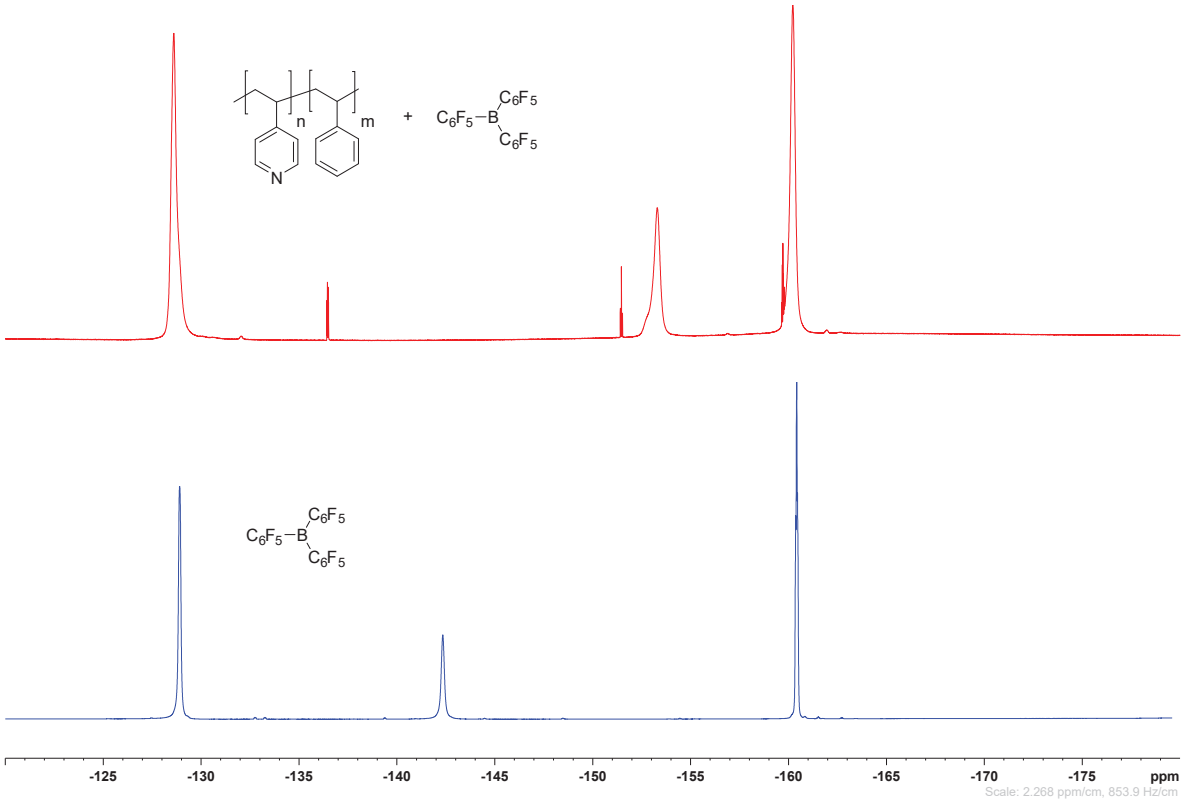

Figure II. 62: ^{19}F NMR spectra of $B(C_6F_5)_3$ in blue and poly(styrene-co-4-vinylpyridine) and $B(C_6F_5)_3$ in red in toluene-d_8.

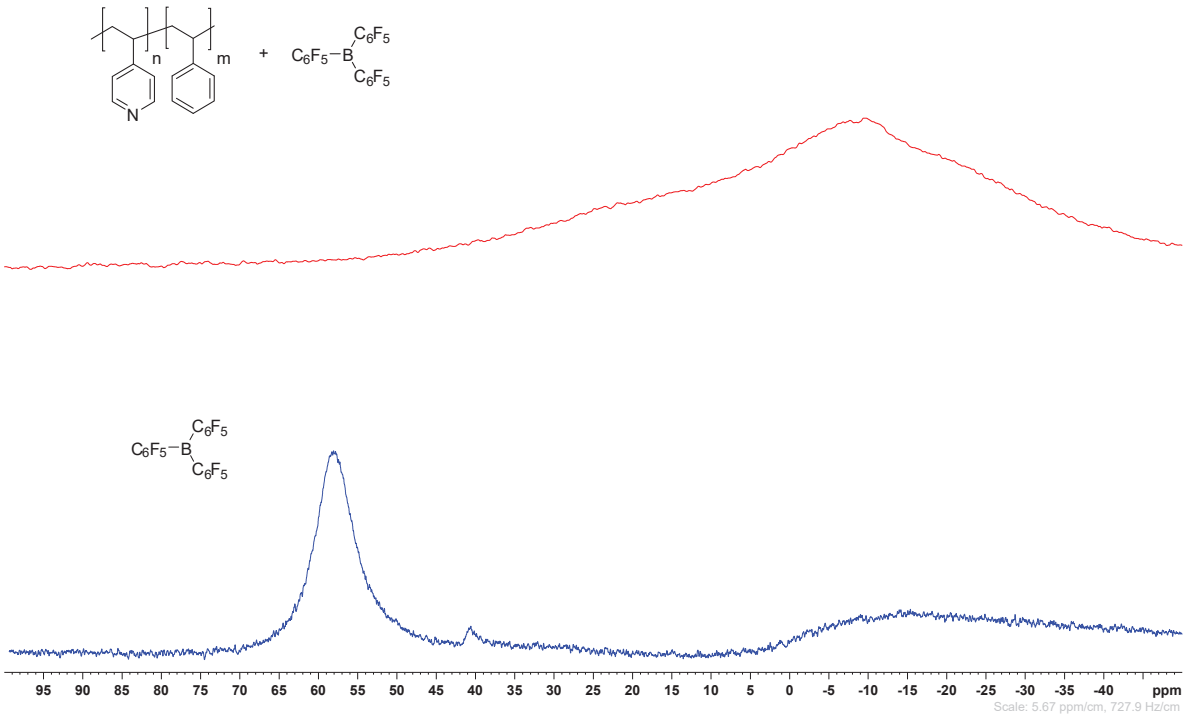

Figure II. 63: ^{11}B NMR spectra of $B(C_6F_5)_3$ in blue and poly(styrene-co-4-vinylpyridine) and $B(C_6F_5)_3$ in red in toluene-d_8.

In Figure II. 62, we compared the acquired ^{19}F NMR spectrum of the tris(pentafluorophenyl)borane in blue to the spectrum of the blend between tris(pentafluorophenyl)borane and poly(styrene-*co*-4-vinylpyridine) in red. There is a clear shift of the para fluorine atom signals from -146 ppm to -165 ppm as well as a clear broadening of the signals observed, due to interactions implying a polymer.

Thanks to ^{11}B spectra in Figure II. 63, an important shift of the boron atom signal from 57 ppm to -10 ppm testifies the Lewis pair formation between the borane and pyridine groups.

In this specific case, we are in presence of a classical Lewis pair as the compounds, especially the Lewis base, namely the pyridine groups, are not that much sterically hindered. The interaction is thus easily probed by NMR spectroscopy and a mutual quenching (Figure II. 64) is occurring between the Lewis acid and base groups. The broadening of the fluorine signals can also indicated that the borane is reacting with all the pendent pyridine groups carried by the polymer.

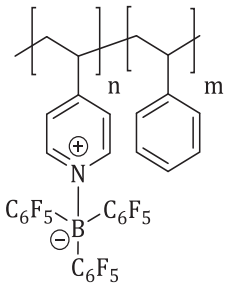

Figure II. 64: Mutual quenching between pyridine and borane groups.

This Lewis pair was not studied under CO_2 flux as it does not exhibit the FLP properties and thus ability to capture CO_2.

c. Rheological study

Nevertheless, to carry on the evaluation of this Lewis pair, we chose to probe the mechanical behavior of the system based on a poly(B) and A2 interaction from poly(styrene-*co*-4-vinylpyridine) and $B(C_6F_5)_2$-Ph-$B(C_6F_5)_2$ (Figure II. 65).

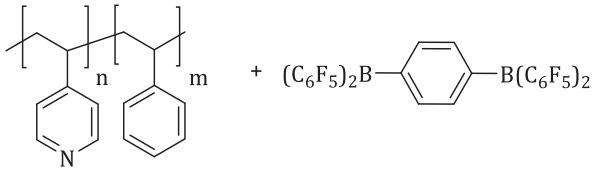

Figure II. 65: Lewis pair from poly(styrene-co-4-vinylpyridine) and $B(C_6F_5)_2$-Ph-$B(C_6F_5)_2$.

Rheology is the macroscopic method of choice to detect physical changes in a material as well as in a solution. Thus rheology measurements were performed on a 10 wt % solution of poly(styrene-*co*-4-vinylpyridine) in toluene at ambient temperature that was followed by the addition of a 20 wt % solution of difunctional pentafluoroaryl borane with triethylamine to easily handle the synthesized compound. The ratio B:N was close to one. A Couette cell equipped with a Pelletier was used to conduct this experiment, ensuring a temperature of 25°C through the experiment.

As illustrated in Figure II. 66, the addition of $B(C_6F_5)_2$-Ph-$B(C_6F_5)_2$ induced the rise of the moduli of the solution. This low but significant increase was attributed to the formation of Lewis pairs in the solution between the pendent pyridine groups of the styrenic polymer and the difunctional borane molecule.

The low concentration of the solution and the subsequent low density of crosslinking, could explain the low moduli measured and the absence of gel point; however, we were constrained by the availability of the compounds, especially $B(C_6F_5)_2$-Ph-$B(C_6F_5)_2$ that is quite difficult to synthesize as already mentioned in the first part of this Chapter.

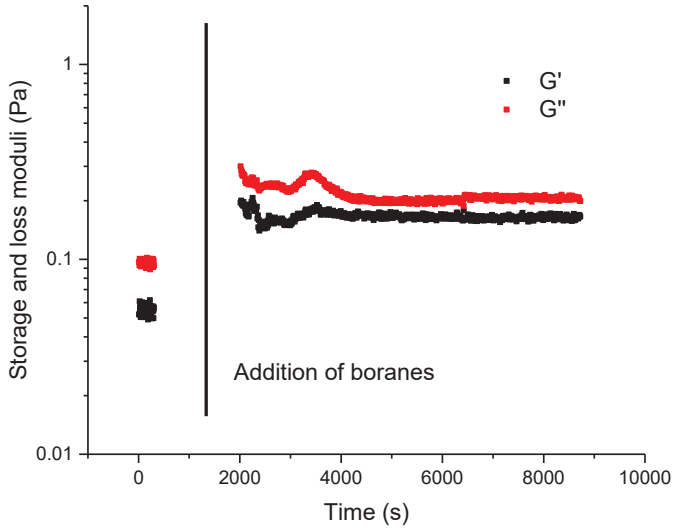

Figure II. 66: Oscillation time before and after the interaction between poly(styrene-co-4-vinylpyridine) and $B(C_6F_5)_2$-Ph-$B(C_6F_5)_2$.

In order to decorrelate the effect of the difunctional Lewis acid mocule $B(C_6F_5)_2$-Ph-$B(C_6F_5)_2$ to the effect that could have a monofunctionalized Lewis acid molecule $B(C_6F_5)_3$, we probed in a same manner, the evolution of the storage and loss moduli of a 10 wt % solution of poly(styrene-*co*-4-vinylpyridine) in toluene at ambient temperature in which we added a 20 wt % solution of tris(pentafluorophenyl)borane complexed by triethylamine to reach the equivalence between B and N atoms.

The experiment is transcribed in Figure II. 67 that shows that the moduli did not increase only by using monofunctionalized Lewis acid. Thus, the increase of moduli previously observed is not due to electronic effects related with the creation of Lewis pair, but attributed to the difunctional character of the Lewis acid.

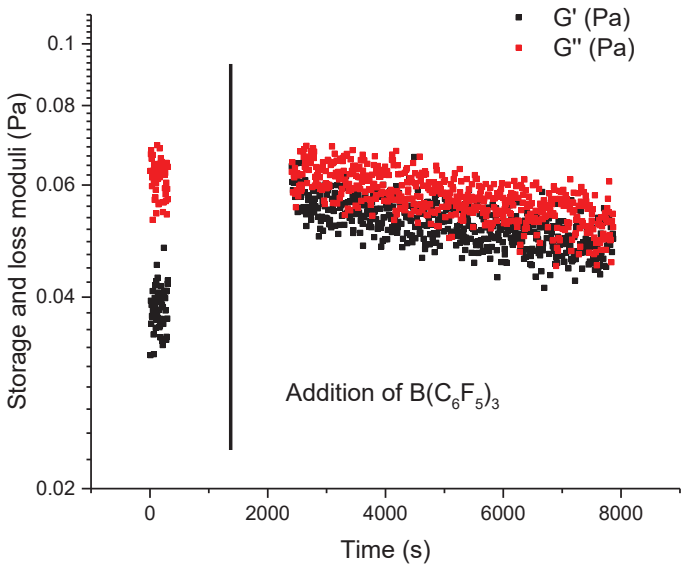

Figure II. 67: Oscillation time of interaction before and after the addition of $B(C_6F_5)_3$ in a solution of poly(styrene-co-4-vinylpyridine).

From these rheology results, we assumed that the aforementioned increase of the storage and loss moduli is due to the Lewis pair interaction between the pendent pyridine groups and the two pentafluoroaryl borane groups in para position on a phenylene linker. In this fashion, we confirmed the creation of a Lewis pair in solution between poly(B) and A2 that results in the increase of the viscosity. Unfortunately, the low concentrations (and low density of crosslinking) studied in the rheometer did not allow for the observation of a gel point.

Future works could be dedicated to the improvement of this rheological study using more concentrated solutions in order to easily probe the phenomenon observed so far.

B. Phosphorus-based polymers as Lewis-base functionalized (co)polymer (polyB)

a. Macroscopic observations

Firstly, interaction between a phosphorus-based copolymer as polyfunctional Lewis base and difunctional Lewis acid was investigated by simple macroscopic observations. We studied the reaction between $B(C_6F_5)_2$-Ph-$B(C_6F_5)_2$ and poly(styrene-*co*-4-styryldiphenylphosphine), as described in Figure II. 68.

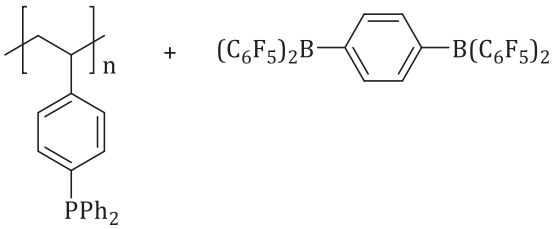

Figure II. 68: Lewis pair between $B(C_6F_5)_2$-Ph-$B(C_6F_5)_2$ and poly(styrene-co-4-styryldiphenylphosphine).

The two compounds were solubilized in toluene and triethylamine was added as previously to complex the electronic vacancies of the difunctionalized Lewis acid. The ratios were maintained to reach B:P 1. The borane solution was then added on the polymer solution.

At first sight, the viscosity seemed to increase quickly and then decreased to homogenize the solution leaving the solution more viscous than before the addition of the borane as showed in Figure II. 69.

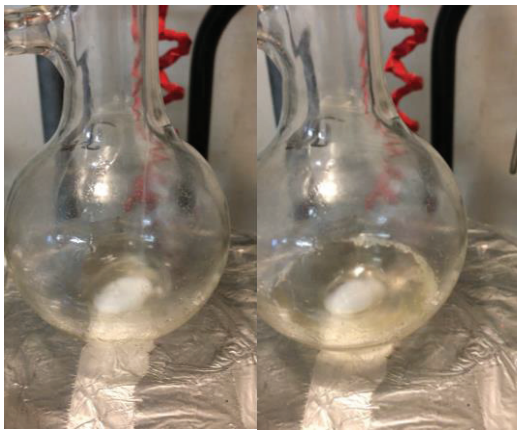

Figure II. 69: Increase of viscosity observed at the mix of poly(styrene-co-4-styryldiphenylphosphine) and $B(C_6F_5)_2$-Ph-$B(C_6F_5)_2$ with 2 molar equivalents of triethylamine in toluene. Left: Beginning of the reaction. Right: After homogenization.

At this stage, we hypothesized that the interaction between the hindered boranes and phosphines in the system poly(B) and A2 conducts to a supramolecular network arising from the FLP interaction. This could explain the reported increase of viscosity in the solution.

b. NMR spectroscopy

To complete this study, the reaction presented previously was probed by NMR spectroscopy relying on the interaction between poly(styrene-*co*-4-styryldiphenylphosphine) and tris(pentafluorophenyl) borane (Figure II. 70). The monofunctional Lewis acid was chosen in this case to avoid gelation in the NMR tube and allow for the correct acquisition of ^{19}F, ^{31}P and ^{11}B NMR spectra.

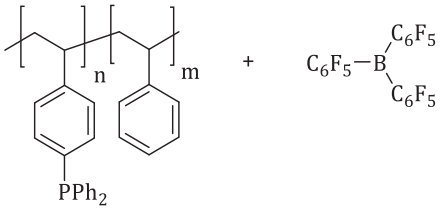

Figure II. 70: Interaction between poly(styrene-co-4-styryldiphenylphosphine) and tris(pentafluorophenyl)borane studied by NMR spectroscopy.

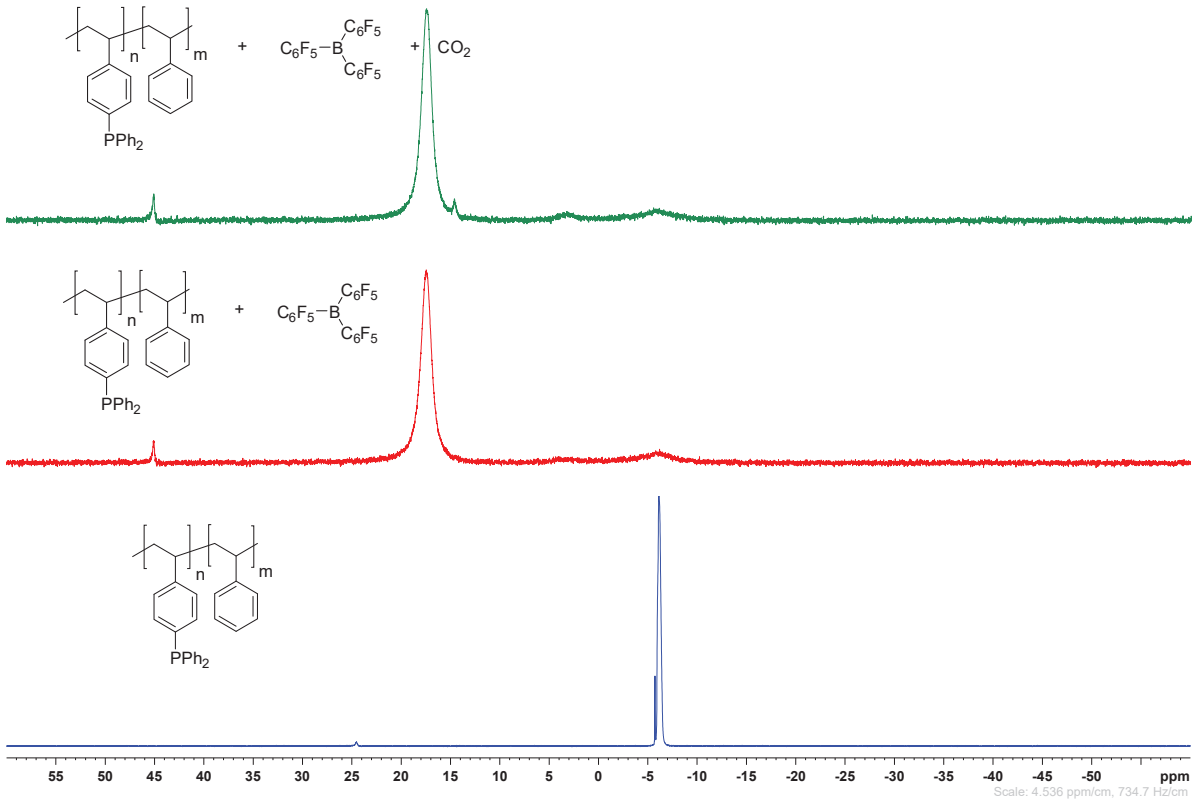

Figure II. 71: ^{31}P NMR spectra of poly(styrene-co-4-styryldiphenylphosphine) in blue and poly(styrene-co-4-styryldiphenylphosphine) and $B(C_6F_5)_3$ in red and poly(styrene-co-4-styryldiphenylphosphine) and $B(C_6F_5)_3$ and CO_2 in green in toluene-d_8.

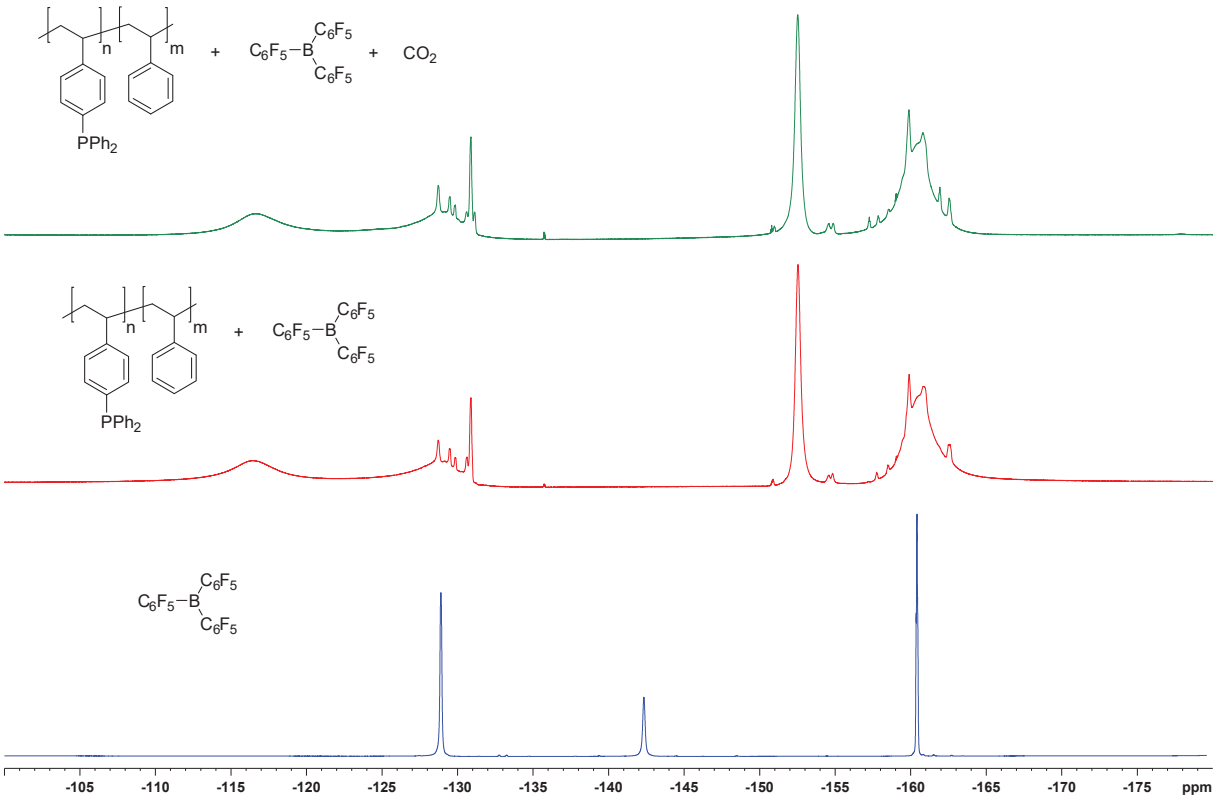

Figure II. 72: ^{19}F NMR spectra of $B(C_6F_5)_3$ in blue and poly(styrene-co-4-styryldiphenylphosphine) and $B(C_6F_5)_3$ in red poly(styrene-co-4-styryldiphenylphosphine) and $B(C_6F_5)_3$ and CO_2 in green in toluene-d_8.

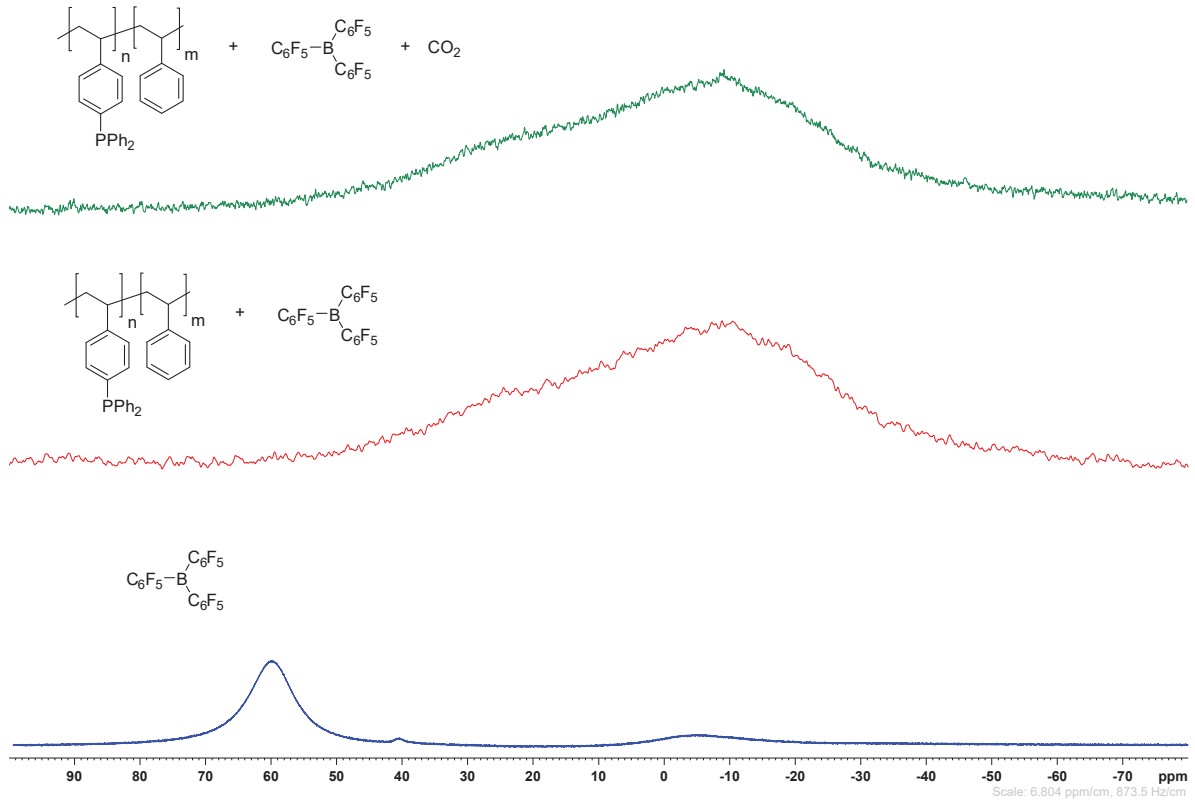

Figure II. 73: ^{11}B NMR spectra of $B(C_6F_5)_3$ in blue and poly(styrene-co-4-styryldiphenylphosphine) and $B(C_6F_5)_3$ in red poly(styrene-co-4-styryldiphenylphosphine) and $B(C_6F_5)_3$ and CO_2 in green in toluene-d_8.

Figure II. 71 relates the evolution of the ^{31}P of poly(styrene-*co*-4-styryldiphenylphosphine) in blue, then after addition of $B(C_6F_5)_3$ in red and lastly after being exposed to CO_2 in green. In blue, we can only distinguish the signal at -6 ppm corresponding to the pendent phosphine groups carried by the copolymer. The oxidized form is present with a small signal at 24.5 ppm. At the addition of borane, this signal is shifted and broadened to reach 17 ppm indicating the efficient interaction between the borane and phosphine groups from the polymer. The oxidized form is as well shifted to reach 46 ppm. A large signal is still present at -6 ppm due to the residual free phosphine groups that did not interact with boranes. Lastly, the addition of CO_2 does not induce important changes in the ^{31}P NMR spectrum only a small signal appears at 15 ppm that could correspond to the CO_2-capture species. Higher pressure of CO_2 and longer times of exposure (herein, 5-10 min) should be required to obtain a more important signal.

In Figure II. 72, we compared the ^{19}F spectrum of $B(C_6F_5)_3$ in blue, of the blend between poly(styrene-*co*-4-styryldiphenylphosphine) and $B(C_6F_5)_3$ in red and after the absorption of CO_2 by the reaction media in green. Firstly, the red spectrum undergoes important changes: the high shift of the para fluorine atoms signals that testifies the interaction of the Lewis pair; the broadening of the signals that shows that the interaction is occurring on a polymer; the unexplained presence of a large signal around -114 ppm. However, the addition of CO_2 does not affect the ^{19}F NMR spectrum.

The same comparison are conducted in Figure II. 73 and we mainly note the huge shift and broadening of the boron signal for 60 ppm to -5 ppm related to the FLP formation. After the exposition to CO_2, a small shouldering can be distinguished at 25 ppm that could arise from the CO_2 capture by the newly FLP.

We could also suggest performing solid-state NMR spectroscopy to see the interaction between the different compounds without the influence of solvent.

c. Rheological study

To carry on the evaluation of this Lewis pair, we chose to probe the mechanical behavior of the system based on a poly(B) and A2 interaction from poly(styrene-*co*-4-styryldiphenylphosphine) and $B(C_6F_5)_2$-Ph-$B(C_6F_5)_2$ (Figure II. 74).

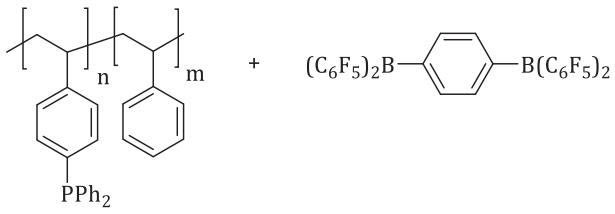

Figure II. 74: Lewis pair from poly(styrene-co-4-styryldiphenylphosphine) and tris(pentafluorophenyl)borane.

Rheology is the macroscopic method of choice to detect physical changes in a material as well as in a solution. Thus rheology measurements were performed on a 25 wt % solution of poly(styrene-*co*-4-styryldiphenylphosphine) in toluene at ambient temperature that was followed by the addition of a 20 wt % solution of difunctional pentafluoroaryl borane with triethylamine to easily handle the synthesized compound. The ratio B:P was close to one. A Couette cell equipped with a Pelletier was used to conduct this experiment, controlling the temperature along the experiment.

In a first experiment, we checked the constancy of the storage and loss moduli of the starting solution of copolymer as illustrated in Figure II. 75.

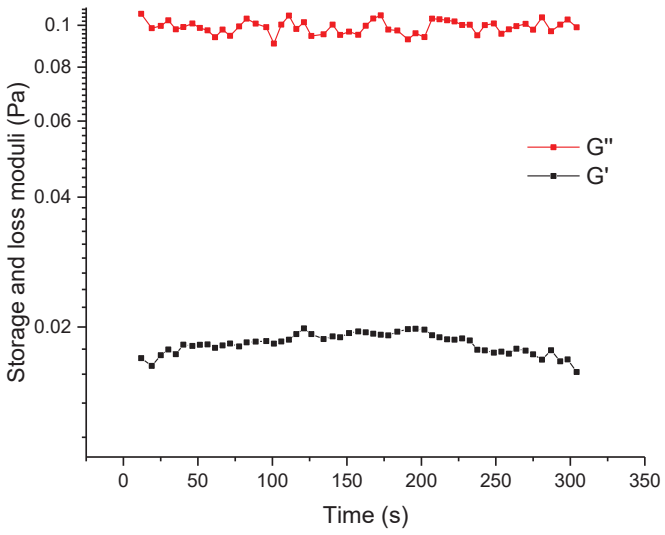

Figure II. 75: Monitoring of the storage and loss moduli of the initial solution of polymer.

In a second step was added the solution containing the difunctional pentafluoroaryl borane and an important increase of the moduli were remarked as shown in Figure II. 76.

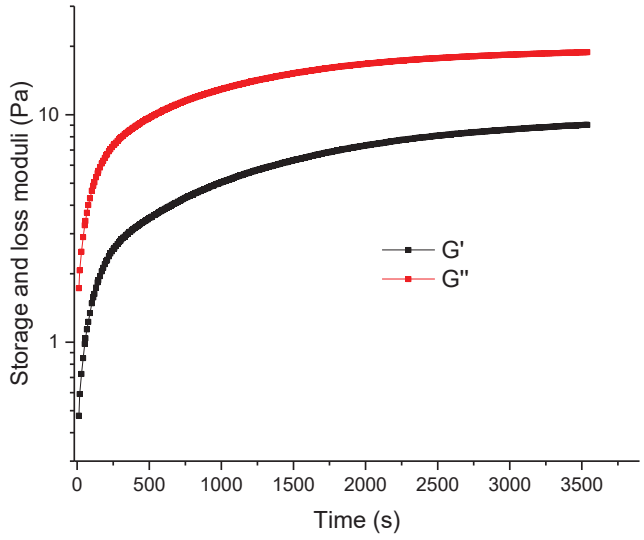

Figure II. 76: Oscillation time at the addition of the difunctional Lewis acid.

A CO_2 bottle was then joined to the rheometer, the solution was thus exposed to CO_2 atmosphere during several hours, and the storage and loss moduli were monitored through this time. A general increase of G' and G'' was observed until the observation of a gel point translated by the visual cross of the two moduli, as represented in Figure II. 77. This gel point testifies for the formation of a 3D network that is induced by the capture of the CO_2 by the FLP.

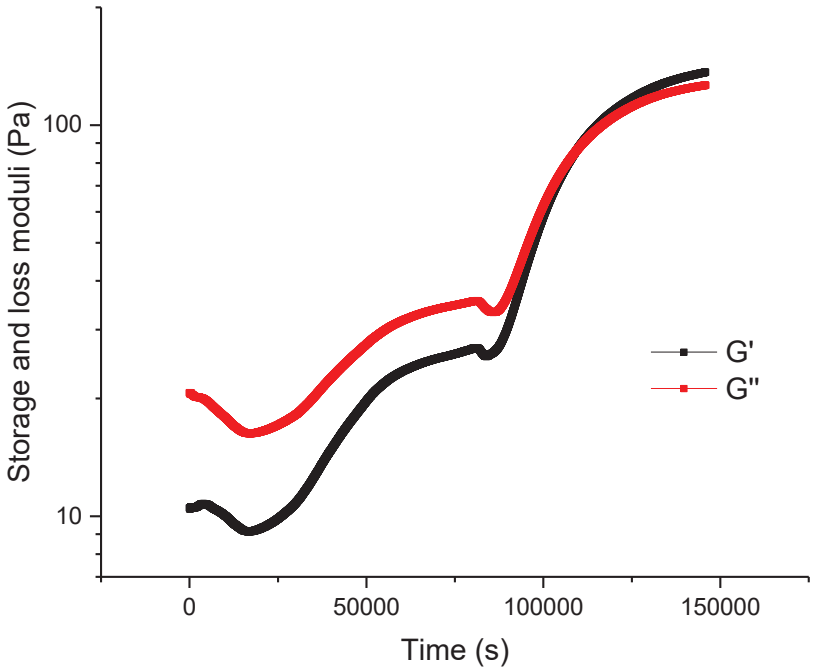

Figure II. 77: Oscillation time after opening of the CO_2 flux at 25 °C.

As aforementioned in Chapter 1 and in the introduction of this Chapter 2, it was reported that the capture of CO_2 by FLP was found to be a reversible process. [61] In the work of Yan, it was also assumed that increasing the temperature provokes desorption of CO_2 from the FLP.

In this fashion, we were willing to probe the reversible character of the CO_2 capture observed above. Hence, we followed the evolution of the storage and loss moduli over a temperature ramp from 20°C to 70°C (Figure II. 78).

A reverse gel point was detected quickly indicating the breaking of the network previously formed. Besides, G' and G'' kept on decreasing as the network constantly de-crosslinked.

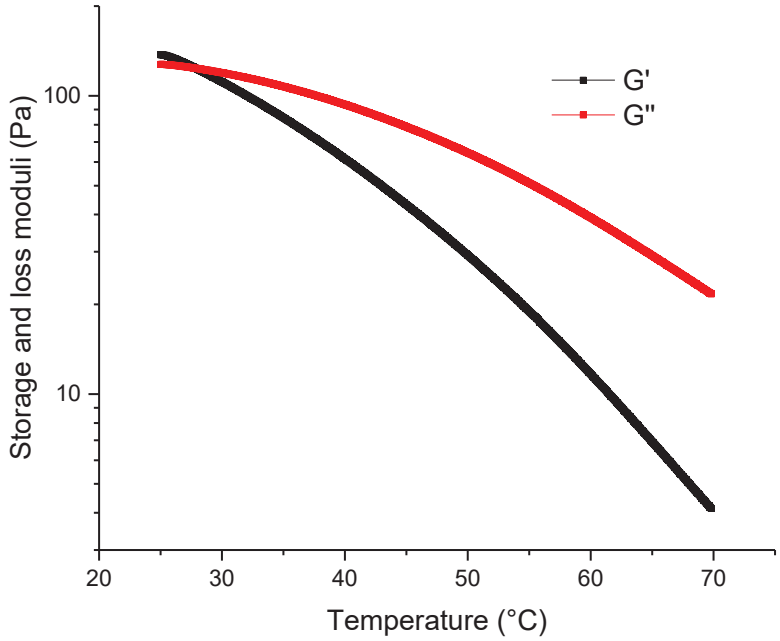

Figure II. 78: Monitoring of the storage and loss moduli on a temperature ramp from 20°C to 70°C.

The solution was then cooled to 25°C and the storage and loss moduli were found to increase until a plateau (Figure II. 79). No gel point was detected in this case, which means that the 3D network was efficiently broken by the CO_2 desorption. However, the G' and G'' did not reach their initial values. Higher temperature or longer times might be required to completely release CO_2.

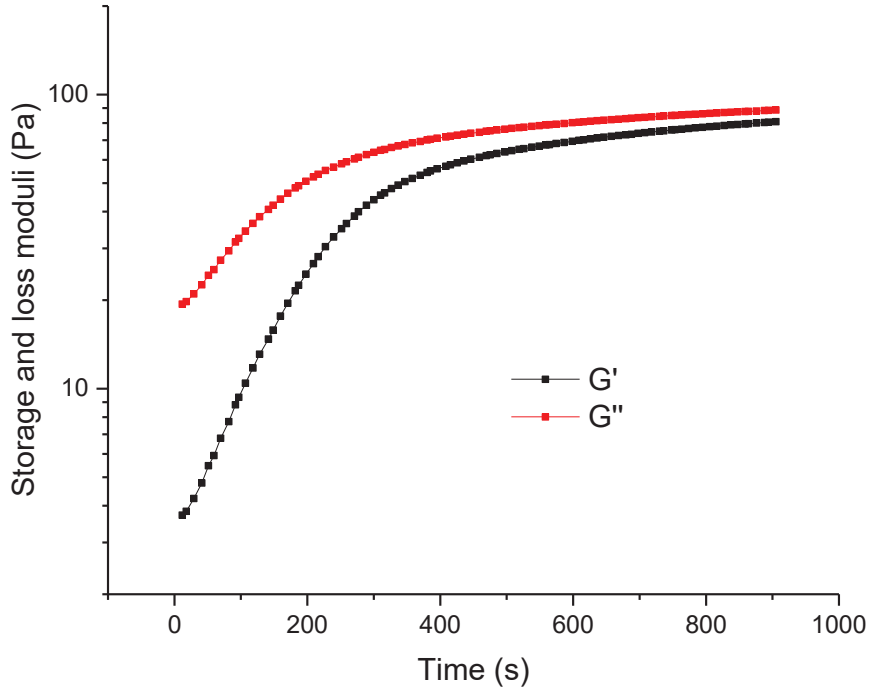

Figure II. 79: Oscillation time at 25°C after heating ramp.

To probe the reproducibility of the capture of CO_2, the solution was once more exposed to CO_2 atmosphere and the storage and loss moduli were monitored as depicted in Figure II. 80. More rapidly this time, we reached a gel point confirming the formation of the covalent network arising from the CO_2 capture by the FLP solution.

We assumed that the desorption of CO_2 was not complete during the heating ramp which causes a faster crosslinking in this latter case and could as well explain the non-recovery of the initial moduli.

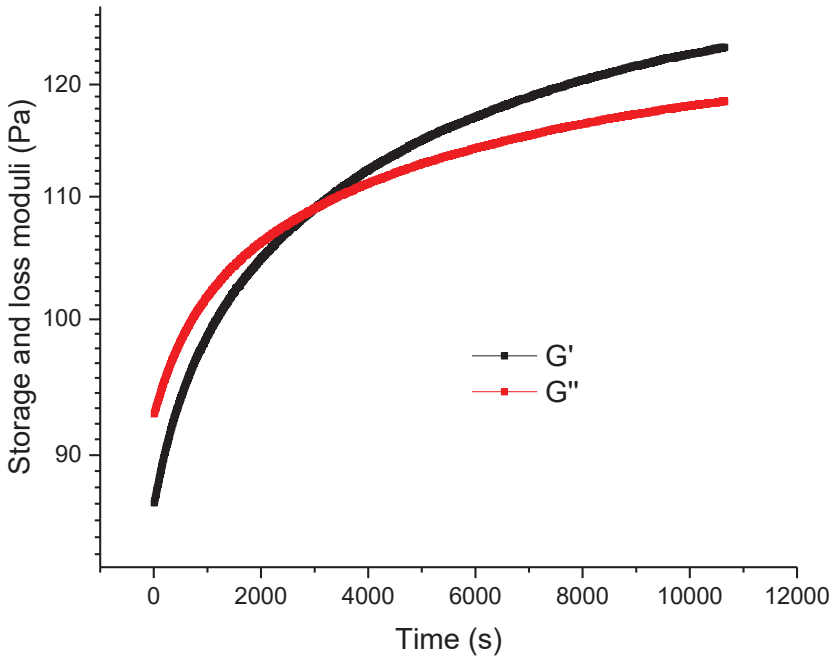

Figure II. 80: Monitoring of the storage and loss moduli at 25°C after reopening of CO_2 flux.

To sum it up, the storage and loss moduli are compiled in Figure II. 81 to have an overview of the different behaviors measured with different conditions of temperature and pressure of CO_2.

To complete this rheological study, the profiles of frequency sweeps at each step of the experiment were acquired and compared in Figure II. 82. The frequency sweeps were acquired at different times indicated on Figure II. 81 by the blue letters A, B, C and D, respectively for the initial solution, after the addition of the Lewis diacid, after the addition of CO_2 and after the heating ramp from 25°C to 70°C.

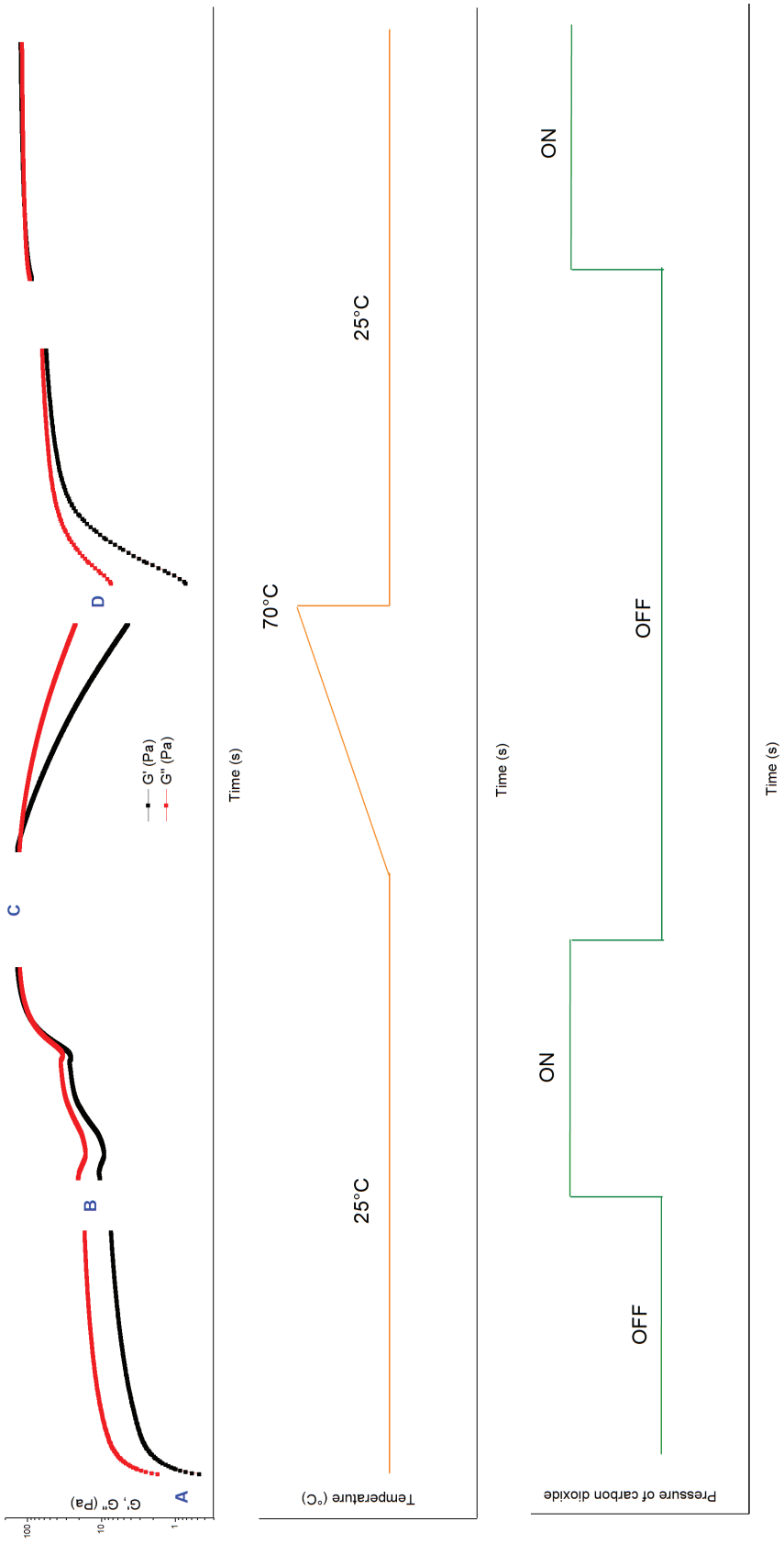

Figure II. 81: Evolution of the storage and loss moduli over time with different conditions of temperature and pressure of CO_2. Time scale is omitted for clarity.

At first sight, it is obvious that the addition of the Lewis diacid to the initial polymer solution induced the increase of the G' and G'' moduli. For the initial solution, G' is omitted due to the lack of reliability of very low values (inertia issue related to the rheometer). After the exposition of CO_2, the moduli were once more increased and the crosslinked character was visible with a certain relaxation time. The exchange dynamic is slowed down by the interaction of CO_2. It is also possible to compare the relaxation time τ^* before and after the introduction of CO_2 in the system. It can be calculated with the following equation involving the frequency at the crossing point f_c:

$$\tau^* = {}^1/_{2\pi f_c}$$

In this manner, we obtained two different relaxation times from the blue and red curves in Figure II. 82: 0.025 s before the capture of CO_2 and 0.16 s after the capture of CO_2. This result confirmed the slow-down of the exchanges dynamic *via* the introduction of covalent bonds resulting from the capture of CO_2 by the Lewis pair.

The last curve acquired after the heating ramp shows that the system was not anymore crosslinked and that no relaxation time was thus observed in this latter case. The moduli were also decreased and close to the ones before CO_2 exposition confirming the reversible character of the CO_2 capture by our system poly(B) and A2.

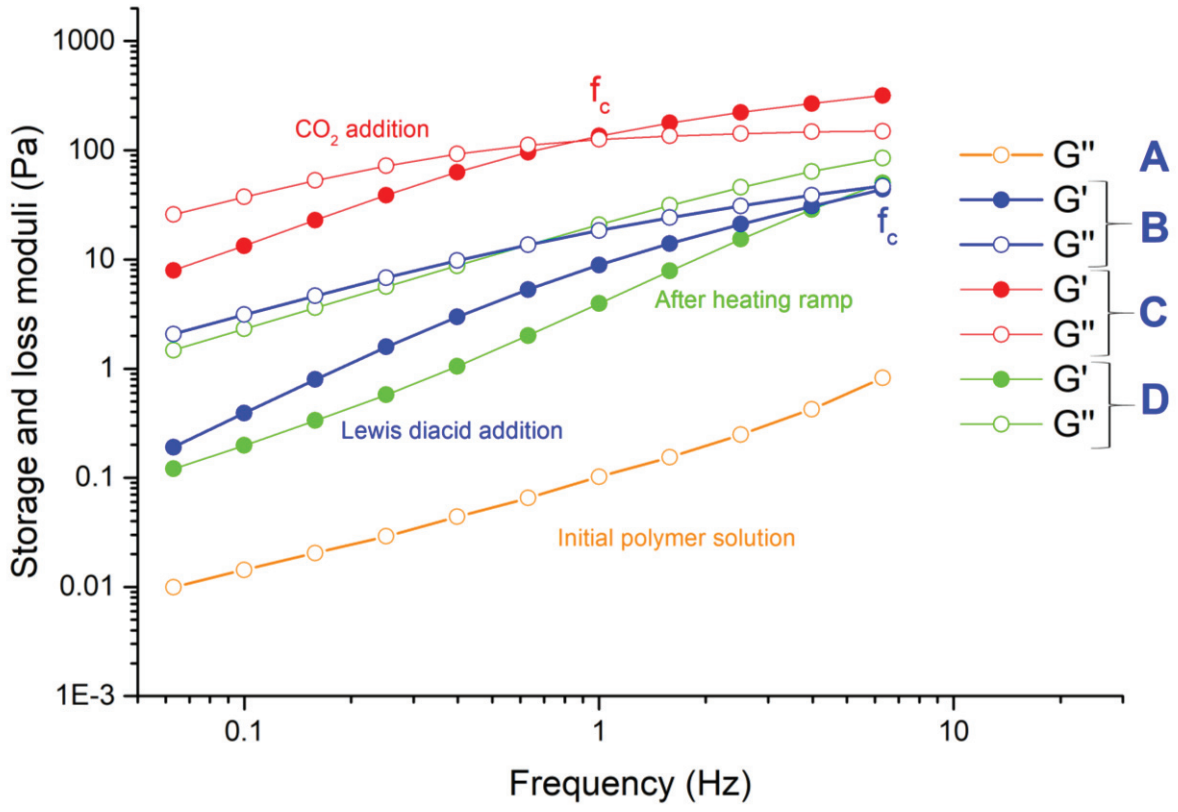

Figure II. 82: Comparison of frequency sweep profiles at each step of the experiment A, B, C and D.

d. UV spectroscopy

As reported in literature, the capture of CO_2 by FLP has the effect to induce turbidity in a solution by changing the solubility of the compounds in the solvent. [61] Thus, the monitoring of this turbidity can be used to determine the efficiency of the capture and its reversibility. In this fashion, the reversible character of the CO_2 capture can be probed by UV spectroscopy through the absorbance measure. Indeed, the absorbance is herein due to the turbidity present in the solution and is the signature of the CO_2 capture. Besides, it was also reported that the desorption of CO_2 is occurring with an increase of the temperature in the medium. [61]

In this optic, we decided to follow the evolution of the absorbance of a solution containing the Lewis pair formed from poly(styrene-*co*-4-styryldiphenylphosphine) and $B(C_6F_5)_2$-Ph-$B(C_6F_5)_2$, that was subjected to a flux of CO_2 and sealed, while increasing the temperature at a specified wavelength. This curve was compared to the data obtained from the same experiments with, on the one hand, a solution of $B(C_6F_5)_2$-Ph-$B(C_6F_5)_2$ and, on the other hand, a solution of poly(styrene-*co*-4-styryldiphenylphosphine). The different curves during heating and cooling are plotted in Figure II. 83.

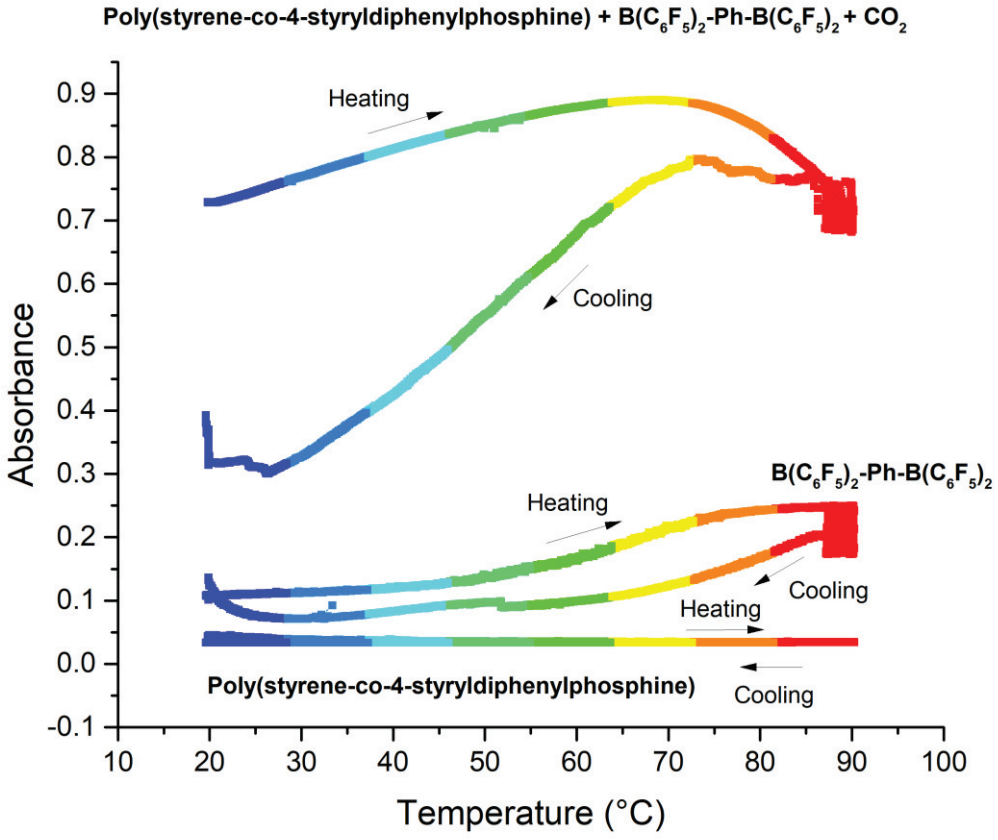

Figure II. 83: Comparison of the absorbance of three solutions over temperature: solution of poly(styrene-co-4-styryldiphenylphosphine) and $B(C_6F_5)_2$-Ph-$B(C_6F_5)_2$ under CO_2 in toluene, solution of $B(C_6F_5)_2$-Ph-$B(C_6F_5)_2$ under CO_2 in toluene and solution of poly(syrene-co-4-styryldiphenylphosphine) under CO_2 in toluene.

Firstly, on the absorbance curve corresponding to the solution of poly(styrene-*co*-4-styryldiphenylphosphine) and $B(C_6F_5)_2$-Ph-$B(C_6F_5)_2$, an increase of the absorbance was observed between 20°C and 75°C. This was followed by a decrease the absorbance after this temperature and thus a decrease of the turbidity that could be explained by the desorption of the gas from the FLP. During the cooling segment, the turbidity of the solution kept decreasing but did not totally disappear.

In order to decorrelate the evolution of the turbidity from other phenomenon that could arise from the reactants, solutions of $B(C_6F_5)_2$-Ph-$B(C_6F_5)_2$ and poly(styrene-*co*-4-styryldiphenylphosphine) were probed by UV spectroscopy to monitor the evolution of the absorbance, and thus turbidity, over the temperature ramp applied to the previous sample. Concerning the difunctional pentafluoroaryl borane, the solution had an inherent absorbance that was due to the yellow coloration of the solution. In addition, the absorbance responds to the Beer-Lambert law expressed as $A = \varepsilon lc$ with ε the molar absorption coefficient, l the path length and c the molar concentration. Among these parameters, ε is dependent of the temperature of measurement. [92] This could also explain the variations observed of the absorbance for this experiment in addition to the color of the solution. Indeed, the absorbance slightly increased during the heating segment and slightly decreased during the cooling segment. These tendencies could explain also the unexplained increase of the turbidity during the heating segment of the previous experiment.

In a same manner, a solution of poly(styrene-*co*-4-styryldiphenylphosphine) in toluene was probed by UV-spectroscopy but was not found to exhibit any absorbance along the temperature ramp from 20 to 90°C.

From these observations, we can conclude that the release of the CO_2 can be simply followed by a measure of the turbidity of a solution. However, it was found that the bis borane brought an inherent absorbance due to its coloration. Besides, the capture of CO_2 is not totally reversible by the simple increase of the temperature in the medium as we do not recover a null absorbance. Besides, vacuum should be applied to pull off the released CO_2; this could constitute the object of further experiment.

VII. Systems based on Lewis acid (polyA) and base-functionalized (polyB) polymers

The last strategy investigated was the interaction between two polymers as symbolized in Figure II. 5. Unfortunately, during our research, works about functionalized-Lewis acid and base polymers interacting with CO_2 were reported and took the wind out of our's sails thus we did not focused on this last route. Besides, the issues faced for the synthesis of polymer carrying pendent Lewis acid groups hindered our progress for this path.

Indeed, in the Chapter 1, we reported the last insights in this strategy where the polymer and the FLP chemistries were gathered to obtain networks able to capture reversibly CO_2 gas.

Recently, Yan and co-workers reported a hybrid system between FLP and polymers in order to synthesize gas-responsive materials. In this case, they synthesized two complementary Lewis acidic and basic block copolymers carrying respectively bulky borane phosphine groups as we targeted during my thesis work without success. In their study, they chose mesityl groups carried by phosphines and pentafluorophenylborane groups in copolymers with styrene.

They used a different path for the synthesis of the Lewis acid functionalized polymer *via* RAFT method starting from the already functionalized monomer 4-styryl-di(pentafluorophenyl)borane. This method seems to be more straightforward than the one chosen in our research where the post-modification strategy was preferred.

This system was subjected to CO_2 stimuli and the copolymers bind CO_2 conducting to a micellar organization of the copolymers as shown in Figure II. 84. This binding was found to be reversible when heating to 60°C. In their case, lower temperatures were needed to obtain the desorption of CO_2. This could arise from the more frustrated character of the Lewis pair that they studied in this paper. They used these systems to afford nanocatalysts for recyclable C1 catalysis. They opened a route for a sustainable conversion of CO_2. [61]

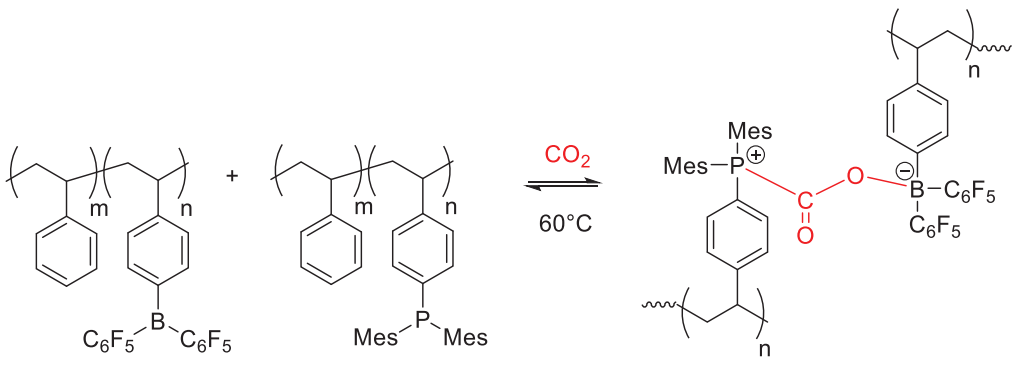

Figure II. 84: Reversible binding of CO_2 between two Lewis acidic and basic block copolymers. [61]

VIII. Conclusion

The capture of CO_2 is a challenging topic in the actual context of global warming and is a highly exploited subject for many research teams around the world. Besides, the capture is one thing but the storage presented other issues as described in the introduction of this Chapter. In this fashion, the ability to reuse the captured gas by desorption of the gas molecules is a supplementary challenge as many organic compounds can be synthesized from CO_2. This could conduct to a path for the utilization of CO_2 as a C1-building block.

The chemistry of Frustrated Lewis Pairs opened new paths for the reversible capture of small molecules such as common gas at normal conditions of temperature and pressure. This idea of this Chapter was to combine this last feature with our main research area: polymer chemistry. In this manner, different systems of interactions were studied with always the concept of designing a network able to capture CO_2 in a reversible way. These networks are thus based on Lewis moieties that are able to interact to form FLP or CLP.

We started with the innovative synthesis of a new difunctional pentafluoroaryl borane with a phenylene linker that was not reported in literature as far as we know. The two Lewis acid groups probably interacting could constitute platforms for the creation of networks. Unfortunately, we were not able to synthesize the difunctional Lewis base carrying two lutidine groups that could have played the role of co-monomers for supramolecular polyaddition between the two difunctional small molecules.

Issues were also faced in the synthesis of functionalized (co)polymer with pendent pentafluoroaryl boranes *via* post-functionalization of organoboron copolymers. This path was not the best choice to straightforward afford these polymers. This could be a new axis of exploration for further investigation in this interesting area.

On the other hand, the synthesis of copolymers from styrene and 4-vinylpyridine was already reported and a mastered part for affording Lewis-base functionalized polymers. However, the Lewis basicity of pyridine groups does not revet a Frustrated character due to the lack of steric hindrance. Thus, this functionalized polymer could not be used in the capture of CO_2 as it does not present FLP properties. In a same manner, copolymers from styrene and 4-styryldiphenylphosphine were synthesized with controlled amounts of phosphine groups. The diphenylphosphine groups exhibit enough steric hindrance to be used in FLP in face of pentafluoroaryl borane moieties and thus this system could then been used in the reversible CO_2 capture.

The Lewis interaction respectively between nitrogen and boron based pairs and phosphorus and boron based pairs were investigated by spectroscopic techniques on model molecules (aka monofunctional) and difunctional molecules.

In our study, we favored the system based on the difucntionalized pentafluoroaryl borane with a phenylene linker interacting with poly(styrene-*co*-4-styryldiphenylphosphine). We evidenced the capture of CO_2 by NMR spectroscopy as well as rheology. The reversible character of this capture was also probed by rheology and UV spectroscopy. The main result is the non-total desorption of CO_2 from the FLP system at 70°C.

It would also have been interesting to work with copolymers functionalized with tertiary amine as we showed that the N,N,N',N'-tetramethylethylethylenediamine and $B(C_6F_5)_2$-Ph-$B(C_6F_5)_2$ behaves as a FLP through the spectroscopic study. In this fashion, it would be possible to open new path for the synthesis of dynamic networks responsive to CO_2.

The grail in terms of mechanical properties was not achieved with the interaction between two functionalized polymers and many researchers are currently working on this topic. This last route could be a perspective for this work.

IX. References

[1] R. J. Gillespie and E. A. Robinson, "Gilbert N. Lewis and the chemical bond: The electron pair and the octet rule from 1916 to the present day," *J. Comput. Chem.*, vol. 28, no. 1, pp. 87–97, **2007**.

[2] H. C. Brown, H. I. Schlesinger, and S. Z. Cardon, "Studies in Stereochemistry. I. Steric Strains as a Factor in the Relative Stability of Some Coordination Compounds of Boron," *J. Am. Chem. Soc.*, vol. 64, no. 2, pp. 325–329, **1942**.

[3] G. C. Welch and D. W. Stephan, "Facile heterolytic cleavage of dihydrogen by phosphines and boranes," *J. Am. Chem. Soc.*, vol. 129, pp. 1880–1881, **2007**.

[4] D. W. Stephan and G. Erker, "Frustrated lewis pairs: metal-free hydrogen activation and more," *Angew. Chemie - Int. Ed.*, vol. 49, no. 1, pp. 46–76, **2010**.

[5] D. W. Stephan, "Frustrated Lewis Pairs," *J. Am. Chem. Soc.*, vol. 137, no. 32, pp. 10018–10032, **2015**.

[6] E. H. Oelkers and D. R. Cole, "Carbon Dioxide Sequestration: A solution to a Global Problem," *Elements*, vol. 4, no. 5, pp. 305–310, **2008**.

[7] G. Kerlero de Rosbo, L. Rakotojaona, and J. De Bucy, "Valorisation chimique du CO_2 : Etat des Lieux - Quantification des bénéfices énergétiques et environnementaux et évalution économique de trois voies chimiques," **2014**.

[8] N. Von Wolff, G. Lefèvre, J. C. Berthet, P. Thuéry, and T. Cantat, "Implications of CO_2 Activation by Frustrated Lewis Pairs in the Catalytic Hydroboration of CO_2: A View Using N/Si + Frustrated Lewis Pairs," **2016**.

[9] M. Aresta, C. F. Nobile, V. G. Albano, E. Forni, and M. Manassero, "New nickel-carbon dioxide complex: synthesis, properties and crystallographic characterization of (carbon dioxide)-bis(tricyclohexylphosphine)nickel," *J. Chem. Soc., Chem. Commun.*, pp. 636–637, **1975**.

[10] W. Leitner, "The coordination chemistry of carbon dioxide and its relevance for catalysis: A critical survey," *Coord. Chem. Rev.*, vol. 153, pp. 257–284, **1996**.

[11] D. Walther, M. Ruben, and S. Rau, "Carbon Dioxide and Metal Centres: From Reactions Inspired by Nature to Reactions in Compressed Carbon Dioxide as Solvent," *Coord. Chem. Rev.*, vol. 182, pp. 67–100, **1999**.

[12] F. J. Fernández-Alvarez, A. M. Aitani, and L. A. Oro, "Homogeneous catalytic reduction of CO_2 with hydrosilanes," *Catal. Sci. Technol.*, vol. 4, pp. 611–624, **2014**.

[13] L. Vaska, "Catalytic activation of carbon dioxide by metal complexes," *J. Mol. Catal.*, vol. 47, pp. 381–388, **1988**.

[14] N. Kuhn, M. Steimann, and G. Weyers, "Synthesis and properties of 1,3-diisopropyl-4,5-dimethylimidazolium-2-carboxylate. A stable carbene adduct of carbon dioxide.," *Z. Naturforsch*, vol. 54b, pp. 427–433, **1999**.

[15] C. Villiers, J.-P. Dognon, R. Pollet, P. Thuéry, and M. Ephritikhine, "An isolated CO_2 adduct of a nitrogen base: Crystal and electronic structures," *Angew. Chemie - Int. Ed.*, vol. 49, no. 20, pp. 3465–3468, **2010**.

[16] L. J. Murphy, K. N. Robertson, R. A. Kemp, H. M. Tuononen, and J. A. C. Clyburne, "Structurally simple complexes of CO_2," *Chem. Commun.*, vol. 51, pp. 3942–3956, **2015**.

[17] D. W. Stephan, "Frustrated Lewis pairs: a new strategy to small molecule activation and

hydrogenation catalysis," *Dalt. Trans.*, pp. 3129–3136, **2009**.

[18] G. Erker, "Frustrated Lewis pairs: Reactions with dihydrogen and other 'small molecules,'" *Comptes Rendus Chim.*, vol. 14, no. 9, pp. 831–841, **2011**.

[19] M.-A. Courtemanche, A. P. Pulis, É. Rochette, M.-A. Légaré, D. W. Stephan, and F.-G. Fontaine, "Intramolecular B/N frustrated Lewis pairs and the hydrogenation of carbon dioxide," *Chem. Commun.*, vol. 51, no. 48, pp. 9797–9800, **2015**.

[20] B. R. Barnett, C. E. Moore, A. L. Rheingold, and J. S. Figueroa, "Frustrated Lewis pair behavior of monomeric (boryl)iminomethanes accessed from isocyanide 1,1-hydroboration," *Chem. Commun.*, vol. 51, pp. 541–544, **2015**.

[21] C. M. Mömming *et al.*, "Reversible Metal-Free Carbon Dioxide Binding by Frustrated Lewis Pairs," *Angew. Chemie Int. Ed.*, vol. 2, pp. 6643–6646, **2009**.

[22] E. Theuergarten *et al.*, "Computational and experimental investigations of CO_2 and N_2O fixation by sterically demanding N-heterocyclic carbenes (NHC) and NHC/borane FLP systems," *Dalt. Trans.*, vol. 43, pp. 1651–1662, **2014**.

[23] G. Ménard, T. M. Gilbert, J. A. Hatnean, A. Kraft, I. Krossing, and D. W. Stephan, "Stoichiometric Reduction of CO_2 to CO by Phosphine/AlX_3-Based Frustrated Lewis Pairs," *Organometallics*, vol. 32, no. 15, pp. 4416–4422, **2013**.

[24] A. L. Travis, S. C. Binding, H. Zaher, T. A. Q. Arnold, J.-C. Buffet, and D. O'Hare, "Small molecule activation by frustrated Lewis pairs," *Dalt. Trans.*, vol. 42, no. 7, pp. 2431–2437, **2013**.

[25] C. Appelt *et al.*, "Geminal phosphorus/aluminum-based frustrated lewis pairs: C-H versus C≡C activation and CO_2 fixation," *Angew. Chemie - Int. Ed.*, vol. 50, no. 17, pp. 3925–3928, **2011**.

[26] G. Ménard and D. W. Stephan, "Room Temperature Reduction of CO_2 to Methanol by Al-Based Frustrated Lewis Pairs and Ammonia Borane," *J. Am. Chem. Soc.*, vol. 132, pp. 1796–1797, **2010**.

[27] F. Bertini *et al.*, "Preorganized Frustrated Lewis Pairs," *J. Am. Chem. Soc.*, vol. 134, no. 1, pp. 201–204, **2012**.

[28] C. Das Neves Gomes, E. Blondiaux, P. Thuéry, and T. Cantat, "Metal-free reduction of CO_2 with hydroboranes: Two efficient pathways at play for the reduction of CO_2 to methanol," *Chem. - A Eur. J.*, vol. 20, no. 23, pp. 7098–7106, **2014**.

[29] M. A. Courtemanche, M. A. Légaré, L. Maron, and F. G. Fontaine, "A highly active phosphine-borane organocatalyst for the reduction of CO_2 to methanol using hydroboranes," *J. Am. Chem. Soc.*, vol. 135, pp. 9326–9329, **2013**.

[30] T. Wang and D. W. Stephan, "Carbene-9-BBN ring expansions as a route to intramolecular frustrated lewis pairs for CO_2 reduction," *Chem. - A Eur. J.*, vol. 20, no. 11, pp. 3036–3039, **2014**.

[31] R. Declercq *et al.*, "Hydroboration of Carbon Dioxide Using Ambiphilic Phosphine-Borane Catalysts: On the Role of the Formaldehyde Adduct," *ACS Catal.*, vol. 5, no. 4, pp. 2513–2520, **2015**.

[32] Z. Lu, H. Hausmann, S. Becker, and H. A. Wegner, "Aromaticity as stabilizing element in the bidentate activation for the catalytic reduction of carbon dioxide," *J. Am. Chem. Soc.*, vol. 137, no. 16, pp. 5332–5335, **2015**.

[33] A. Berkefeld, W. E. Piers, and M. Parvez, "Tandem Frustrated Lewis Pair/Tris(pentafluorophenyl)borane-Catalyzed Deoxygenative Hydrosilylation of Carbon

Dioxide," *J. Am. Chem. Soc.*, vol. 132, pp. 10660–10661, **2010**.

[34] G. Erker, "Tris(pentafluorophenyl)borane: a special boron Lewis acid for special reactions," *Dalt. Trans.*, pp. 1883–1890, **2005**.

[35] J. R. Lawson and R. L. Melen, "Tris(pentafluorophenyl)borane and Beyond: Modern Advances in Borylation Chemistry," *Inorg. Chem.*, vol. 56, no. 15, pp. 8627–8643, **2017**.

[36] C. R. Reddy, G. Rajesh, S. V. Balaji, and N. Chethan, "Tris(pentafluorophenyl)borane: a mild and efficient catalyst for the chemoselective tritylation of alcohols," *Tetrahedron Lett.*, vol. 49, no. 6, pp. 970–973, **2008**.

[37] A. Antiñolo *et al.*, "Tris(pentafluorophenyl)borane as an efficient catalyst in the guanylation reaction of amines," *Dalt. Trans.*, vol. 45, no. 26, pp. 10717–10729, **2016**.

[38] D. Zhou and Y. Kawakami, "Tris(pentafluorophenyl)borane as a superior catalyst in the synthesis of optically active SiO-containing polymers," *Macromolecules*, vol. 38, no. 16, pp. 6902–6908, **2005**.

[39] W. E. Piers, "The Chemistry of Perfluoroaryl Boranes," *Adv. Organomet. Chem.*, vol. 52, no. 04, pp. 1–76, **2005**.

[40] W. E. Piers, G. J. Irvine, and V. C. Williams, "Highly Lewis acidic bifunctional organoboranes," *Eur. J. Inorg. Chem.*, no. 10, pp. 2131–2142, **2000**.

[41] D. F. Shriver and M. J. Biallas, "Observation of the Chelate Effect with a Bidentate Lewis Acid, $F_2BCH_2CH_2BF_2$," *J. Am. Chem. Soc.*, vol. 89, no. 5, pp. 1078–1081, **2005**.

[42] L. Jia, X. Yang, C. Stern, and T. J. Marks, "Cationic d°/f° Metallocene Catalysts . Properties of Binuclear Organoborane Lewis Acid Cocatalysts and Weakly Coordinating Counteranions Derived Therefrom," *Organometallics*, vol. 13, pp. 3755–3757, **1994**.

[43] H. Schulz, H. Pritzkow, and W. Siebert, "Umsetzung von Bis(trimethylgermyl)acetylen und Bis(trimethylstannyl)acetylen mit Diboran(4)-Derivaten," *Zeitschrit für Naturforsch.*, vol. 48b, no. 719–722, pp. 4–7, **1993**.

[44] J. R. Galsworthy, M. L. H. Green, C. V Williams, and A. N. Chernega, "Syntheses and Characterisation of Amino(pentafluorophenyl) boranes. Crystal Structure of $I(Me_3Si NB(C_6F_5)_2]$," *Polyhedron*, vol. 17, no. 1, pp. 119–124, **1998**.

[45] R. Kösters, G. Seidel, K. Wagner, and B. Wrakmeyer, "Organosubstituierte cis-1,2-diborylalkene aus elecktrophile chelatbildner," *Chem. Ber.*, vol. 126, pp. 305–317, **1993**.

[46] W. Siebert, M. Hildenbrand, P. Hornbach, G. Karger, and H. Pritzkow, "1,2- and 1,1-Diborylalkenes," *Zeitschrift für Naturforsch. B*, vol. 44b, pp. 1179–1186, **1989**.

[47] W. Schacht and D. Kaufmann, "Thermolyse von Arylhalogenboranen; Synthese von 1,3-Dibora- und 1,3-Borasilaindanen," *J. Organomet. Chem.*, vol. 331, pp. 139–152, **1987**.

[48] D. Kaufmann, "Synthese und Reaktionen silylierter dihalogenphenylborane," *Chem. Ber.*, vol. 120, pp. 901–905, **1987**.

[49] D. J. Parks, R. E. Spence, and W. E. Piers, "Bis(pentafluorophenyl)borane: Synthesis, Properties, and Hydroboration Chemistry of a Highly Electrophilic Borane Reagent," *Angew. Chemie - Int. Ed. English*, vol. 34, no. 7, pp. 809–811, **1995**.

[50] V. C. Williams, W. E. Piers, W. Clegg, M. R. J. Elsegood, S. Collins, and T. B. Marder, "New Bifunctional Perfluoroaryl Boranes. Synthesis and Reactivity of the ortho-Phenylene-Bridged Diboranes 1,2-$[B(C_6F_5)_2]_2C_6X_4$ (X=H, F)'," *J. Am. Chem. Soc.*, vol. 121, pp. 3244–3245, **1999**.

[51] M. V. Metz, D. J. Schwartz, C. L. Stern, P. N. Nickias, and T. J. Marks, "Organo-Lewis Acid Cocatalysts in Single-Site Olefin Polymerization-A Highly Acidic Perfluorodiboraanthracene," *Angew. Chemie - Int. Ed.*, vol. 39, no. 7, pp. 1312–1316, **2000**.

[52] R. D. Chambers and T. Chivers, "Polyfluoroaryl Organometallic Compounds. Part I. Pentafluorophenyl Derivatives of Tin," *J. Am. Chem. Soc.*, pp. 4782–4790, **1964**.

[53] P. Surtori and M. Weidenbruch, "Darstellung und Eigenschaften von Pentafluorbenzoesaure-Derivaten," *Chem. Ber.*, vol. 100, pp. 3016–3023, **1967**.

[54] L. H. Doerrer, A. J. Graham, D. Haussinger, and M. L. H. Green, "Electrophilic addition reactions of the Lewis acids $B(C_6F_5)_2R$ [R=C_6F_5, Ph, H or Cl] with the metallocene hydrides $[M(C_5H_5)_2H_2]$ (M=Mo or W), $[Re(C_5H_5)_2H]$ and $[Ta(C_5H_5)_2H_3]$," *Dalt. Trans.*, pp. 813–820, **2000**.

[55] G. E. Herberich and A. Fischer, "Borylcyclopentadienides," *Organometallics*, vol. 15, pp. 58–67, **1996**.

[56] A. J. J. Lennox and G. C. Lloyd-Jones, "Preparation of Organotrifluoroborate Salts: Precipitation-Driven Equilibrium under Non-Etching Conditions," *Angew. Chemie Int. Ed.*, vol. 51, pp. 9385–9388, **2012**.

[57] Z. Gan, A. Okui, Y. Kawashita, and M. Hayashi, "Convenient Synthesis of Linear-extended Bipyridines Involving a Central Phenyl Linking Group," *Chem. Lett.*, vol. 37, no. 12, pp. 1302–1303, **2008**.

[58] A. Hantzsch, "Condensationsprodukte aus Aldehydammoniak und ketonartigen Verbindungen," *Berichte d. Dtsch. Chem. Gesellschaft. Jahrg*, vol. 14, pp. 1637–1638, **1881**.

[59] A. Hantzsch, "Ueber die Synthese pyridinartiger Verbindungen aus Acetessigäther und Aldehydammoniak," *Ann. der Chemie*, vol. 215, pp. 1–81, **1892**.

[60] Y. Qin, G. Cheng, O. Achara, K. Parab, and F. Jäkle, "A new route to organoboron polymers *via* highly selective polymer modification reactions," *Macromolecules*, vol. 37, no. 19, pp. 7123–7131, **2004**.

[61] L. Chen, R. Liu, and Q. Yan, "Polymer meets Frustrated Lewis Pair: Second-generation CO_2-responsive nanosystem for sustainable CO_2 conversion," *Angew. Chemie - Int. Ed.*, vol. 57, no. 30, pp. 9336–9340, **2018**.

[62] M. Hartmann, H. Carlsohn, and J. Pauls, "Über Copolymere der p-Vinylbenzolboronsaure mit Styrol," *Die Makromol. chemie*, vol. 177, pp. 131–144, **1976**.

[63] A. Ledoux, "Polymères contenant des paires de Lewis de type amine-borane , en tant que réservoirs d'hydrogène : relation structure / activité," Université de Lyon, **2016**.

[64] M. Kwok Wai Choi, H. He Song, and P. H. Toy, "Direct Radical Polymerization of 4-Styryldiphenylphosphine: Preparation of Polystyrene Polymers," *J. Org. Chem.*, vol. 68, no. 17, pp. 9831–9834, **2003**.

[65] Pierre-Gilles de Gennes, *Scaling concepts in Polymer Physics*. Cornell University Press, **1979**.

[66] P. Wool, Richard, "Polymer Entanglements," *Macromolecules*, vol. 26, pp. 1564–1569, **1993**.

[67] A. G. Massey and A. J. Park, "Perfluorophenyl derivatives of the elements. I. Tris(pentafluorophenyl)borane," *J. Organomet. Chem.*, vol. 2, pp. 245–250, **1964**.

[68] A. D. Horton and J. De With, "Controlled Alkene and Alkyne Insertion Reactivity of a Cationic Zirconium Complex Stabilized by an Open Diamide Ligand," *Organometallics*, vol. 16, pp. 5424–5436, **1997**.

[69] L. Fielding, "Determination of Association Constants (K_a) from Solution NMR data," *Tetrahedron*, vol. 56, no. 536, pp. 6151–6170, **2000**.

[70] H. Jacobsen, H. Berke, S. Döring, G. Kehr, G. Erker, and O. Meyer, "Lewis Acid Properties of Tris(pentafluorophenyl)borane. Structure and Bonding in L-B(C_6F_5)$_3$ Complexes," *Organometallics*, vol. 18, no. 6, pp. 1724–1735, **1999**.

[71] R. F. Childs, L. D. Mulholland, and A. Nixon, "The Lewis acid complexes of unsaturated carbonyl and nitrile compounds. A nuclear magnetic resonance study," *Rev. Can. Chim.*, vol. 60, no. 6, pp. 801–808, **1982**.

[72] C. Laurence, J. Graton, and J.-F. Gam, "An Overview of Lewis Basicity and Affinity Scales," *J. Chem. Educ.*, vol. 88, pp. 1651–1657, **2011**.

[73] R. F. W. Bader, *Atoms in Molecules: A quantum theroy*. Clarendon Press, **1994**.

[74] C. Laurence and J. F. Gal, *Lewis basicity and affinity scales: data and measurement*. John Wiley & Sons, Inc, **2001**.

[75] V. Gutmann, *The donor-acceptor approach to molecular interactions*. Springer US, **1978**.

[76] P. C. Maria and J. F. Gal, "A Lewis basicity scale for nonprotogenic solvents: Enthalpies of complex formation with boron trifluoride in dichloromethane," *J. Phys. Chem.*, vol. 89, no. 7, pp. 1296–1304, **1985**.

[77] C. Laurence, K. A. Brameld, J. Graton, J.-Y. Le Questel, and E. Renault, "The pK(BHX) Database: Toward a Better Understanding of Hydrogen-Bond Basicity for Medicinal Chemists," *J. Med. Chem.*, vol. 52, no. 14, pp. 4073–4086, **2009**.

[78] C. Laurence *et al.*, "An enthalpic scale of hydrogen-bond basicity. 4. Carbon π bases, oxygen bases, and miscellaneous second-row, third-row, and fourth-row bases and a survey of the 4-fluorophenol affinity scale," *J. Org. Chem.*, vol. 75, no. 12, pp. 4105–4123, **2010**.

[79] P. Metrangolo, F. Meyer, T. Pilati, G. Resnati, and G. Terraneo, "Halogen bonding in supramolecular chemistry," *Angew. Chemie - Int. Ed.*, vol. 47, no. 33, pp. 6114–6127, **2008**.

[80] G. A. Olah, S. G. K. Prakash, A. Molnar, and J. Sommer, *Superacid chemistry*. John Wiley & Sons, Inc, **2009**.

[81] T. D. Coyle, H. D. Kaesz, and F. G. A. Stone, "Molecular Addition Compounds of Boron. II. Thiophane-Borane and related adducts," *J. Am. Chem. Soc.*, vol. 81, no. 12, pp. 2989–2994, **1959**.

[82] B. D. Rowsell, R. J. Gillespie, and G. L. Heard, "Ligand Close-Packing and the Lewis Acidity of BF_3 and BCl_3," *Inorg. Chem.*, vol. 38, no. 6, pp. 4659–4662, **1999**.

[83] R. G. Pearson, "Hard and soft acids and bases - The evolution of a chemical concept," *Coord. Chem. Rev.*, vol. 100, pp. 403–425, **1990**.

[84] I. B. Sivaev and V. I. Bregadze, "Lewis acidity of boron compounds," *Coord. Chem. Rev.*, vol. 270–271, pp. 75–88, **2014**.

[85] J. A. Plumley and J. D. Evanseck, "Periodic Trends and Index of Boron Lewis Acidity," *J. Phys. Chem. A*, vol. 113, pp. 5985–5992, **2009**.

[86] W. E. Piers and T. Chivers, "Pentafluorophenylboranes: from obscurity to applications," *Chem. Soc. Rev.*, vol. 26, pp. 345–354, **1997**.

[87] M. Ullrich, A. J. Lough, and D. W. Stephan, "Dihydrogen Activation by B(p-C_6F_4)$_3$ and Phosphines," *Organometallics*, vol. 29, no. 21, pp. 3647–3654, **2010**.

[88] L. Greb, C. Daniliuc, K. Bergander, and J. Paradies, "Functional-Group Tolerance in Frustrated Lewis Pairs : Hydrogenation of Nitroolefins and Acrylates," *Angew. Chemie Int. Ed.*, vol. 52, pp. 5876–5879, **2013**.

[89] U. Mayer, V. Gutmann, and W. Gerger, "The Acceptor Number - A Quantitative Empirical Parameter for the Electrophilic Properties of Solvents," *Monatshefte für Chemie*, vol. 106, pp. 1235–1257, **1978**.

[90] M. A. Beckett, G. C. Strickland, J. R. Holland, and S. K. Varma, "A Convenient NMR method for the measurement of Lewis acidity at boron centres: correlation of reaction rates of Lewis acid initiated epoxide polymerizations with Lewis acidity," *Polymer (Guildf).*, vol. 37, no. 20, pp. 4629–4631, **1996**.

[91] Q. Yang, M. Bown, A. Ali, D. Winkler, G. Puxty, and M. Attalla, "A Carbon-13 NMR Study of Carbon Dioxide Absorption and Desorption with Aqueous Amine Solutions," *Energy Procedia*, vol. 1, no. 1, pp. 955–962, **2009**.

[92] R. C. Dennis, *Dictionary of Spectroscopy*. John Wiley & Sons, NY, **1982**.

Chapter 3:

Dynamic polymers harnessing the boronate esters reactivity

Chapter 3 reports the study of the dynamic character of organoboron polymers carrying boronate esters on styrenic backbones with the use of a wide range of analytical methods. From these data, mechanism explaining the dynamic crosslinking of these polymers is proposed.

Table of contents

I. Introduction

Polymers bearing boronate ester groups have been a growing field of research due to their unique properties associated with the electron deficiency located at boron, and conferring reactivity harnessed *via* post-polymerization for instance. [1] In addition, these polymers have also received recent attention focusing on the covalent or dynamic crosslinking that can result from reactions between boronic/boronate groups or interactions with other reactants. This topic was covered in the bibliographical part in Chapter 1. [2]

One of the main advantages of these boron-containing polymers is the access to a wide variety of derivatizations they offer simply based on ligand-exchange occurring *via* tetrahedralization/pyramidalization of trigonal planar boron environment through nucleophilic coordination at the boron vacancy, and subsequent formation of borate intermediates. This feature offers the possibility to finely tune the reactivity of nucleophilic aryl/alkyl boronates involved in most C-C cross couplings. For instance, one can hydrolyze boronate esters, using either acidic or basic conditions and a nucleophilic attack on the boron vacancy is involved in both cases. [3]–[7]

Based on the same principle, in the presence of 1,2- or 1,3-diols, boronic acids readily form boronate esters at room temperature. This reaction is quantitative with the help of a desiccant to absorb the generated water. This reactivity has been exploited in numerous applications, as detailed in Chapter 1. pH-dependent complexation between boronic acid-containing polymers and various carbohydrates such as sugars has thus proven useful in the field of responsive polymers for a variety of molecular recognition or chemosensing applications [8] such as pH-dependent complexation of various carbohydrates [9] or smart drug delivery systems with integrated glucose sensing [10]. Following similar approaches, covalent dynamic crosslinking of organoboron polymers is receiving a growing interest in the context of materials with high mechanical performances and facilitated recycling or processing. [11], [12]

Such crosslinks with externally adjustable dynamics (e.g. using temperature or light) are sought-after as they confer both the benefits of thermosets in conditions of slow dynamics (e.g. creep and stress-cracking resistance) and malleability, plasticity, weldability or recyclability in conditions of fast dynamics. A distinction can be made between dynamic polymer networks featuring a constant crosslink density but faster crosslink reshuffling upon heating (vitrimers) [13]–[15] and networks featuring both a decreased crosslink density and shorter crosslink-bond lifetimes upon heating or UV-irradiation (covalent adaptable networks (CANs)). [16]–[20]

Concerning vitrimers, they were first described by Leibler and co-workers in 2011 as epoxy networks that can rearrange and thus can be processable contrary to permanently crosslinked materials. The concept highlighted by the authors was to allow reversible exchange reactions by transesterification rearranging the network while keeping constant the total number of links in the material. In this paper, the system studied behaves like a classical hard epoxy resin with a glass transition around 80°C and a modulus about 1.8 GPa. However, contrary to classical epoxy resins, transesterification reaction allows the networks to completely relax and flow and thus behaves as a viscoelastic fluid at higher temperatures. The networks are permanent as they only swell in solvent but do not dissolve. [13]

Based on both the transesterification equilibrium and the aforementioned reactivity at boron, CANs gels in toluene have been obtained by adding bis(boronate ester) crosslinkers in polycyclooctene containing vicinal diol moieties. The exchanges can be tuned by strategically positioning secondary amines in the vicinity of the boron atoms, which greatly accelerates the exchange dynamics. [21] Recently, Nicolaÿ, Leibler and co-workers disclosed fascinating covalent exchangeable vitrimer networks crosslinked by dynamic exchanges of boronate ester linkages *via* metathesis of boronates esters. However, the actual exchange mechanism remains unsolved and we were willing to focus on this aspect in this Chapter. [22]

To the best of our knowledge, none of the dynamic crosslinked materials described so far reached the very high glass transition temperatures (T_g above 200°C) required for adhesives, protective coatings, low-wear or low-friction materials when exposed to high temperatures (contact with hot parts, composites for aerospace, electronics, bearings…). For such demanding applications, only a few thermoplastics constituted of very rigid segments, but with various degree of processability are commercially available (such as polyaryletherketones, polyethersulfones, polyaramides, polyetherimides or polybenzimidazoles). [23] Alternatively, one can use non-reprocessable, very densely crosslinked thermosetting resins such as maleimide or phenolic formaldehyde, or specialty epoxies with T_gs that can reach 400°C. [24]

Table III. 1: Examples of high-T_g thermoplastics. [23]

Polymer	*Glass transition temperature (°C)*
Polyether etherketone	143
Polyetherketone	153
Polybenzimidazole	410
Polyimide	250
Polyetherimide	217
Polysulfone	193
Polyether sulfone	237
Polyphenyl sulfone	220
Polyamide imide	275
Liquid crystal polymers	110

All vitrimers disclosed so far have moderate crosslink densities and exhibit therefore two clearly distinguishable relaxations: the conventional glass-to-rubber transition involving cooperative mobility at the scale of polymer segments (conventional T_g) and a second rubber-to-liquid transition related to crosslink exchanges and dynamic rearrangements of the network topology at the scale of the network mesh. Although the rubber-to-liquid transition can occur at very high temperatures in systems with sluggish exchange kinetics, the glass-to-rubber transition is contingent on the rigidity of the backbone in-between crosslinks and was not reported so far beyond 166°C. [25] Some CANs feature very rigid and densely crosslinked backbones, but their T_g is limited by de-crosslinking of the network at elevated temperatures: rigid furan-maleimide networks undergo a unique glass-to-liquid transition around 120°C. [17]

This part focuses on the synthesis and characterization of poly(4-vinylphenylboronic pinacolate) (PSBPin) which exhibits a very high T_g (up to ~220°C). Although the bulky pinacol ester group is expected to reduce the chain mobility in comparison to polystyrene, the rigidity in the structure of the polymer and the polar interactions cannot account for such a high T_g and compelled us to further explore the dynamics of this polymer connected to the reactivity of the pendent cyclic boronate.

Firstly, the optimization of the (co)polymer synthesis will be presented followed by a differential scanning calorimetry (DSC) investigation that evidenced a reactivity within the (co)polymers at higher temperatures. This prompted us to the use of spectroscopic methods and rheology in the

next parts to gather proofs about the hypothetic reactivity mechanism expressed. DFT calculations and NMR study on model molecules in the last part allowed the establishment of the putative mechanism leading to the high glass transition temperature of our material. This mechanism will be fully described and discussed.

II. Synthesis of organoboron polymers

A. Case of poly(4-vinylphenylboronic acid, pinacol ester)

To obtain boron-containing polymers, different strategies can be adopted: the direct polymerization of boron-containing monomer or the post-modification of already existing polymers.

In early years, Letsinger and Hamilton polymerized 4-vinylphenylboronic pinacolate (or 4-vinylphenylboronic acid, pinacol ester) by seeding method. [26] In this paper, they polymerized organoboron monomers *via* the addition of a copolymer from styrene and divinylbenzene at 80°C used as a seed for the polymerization process. The molar masses were not indicated so we were not able to make any comparison at this point.

Jäkle previously reported a highly versatile multi-step synthesis of the poly(4-vinylphenylboronic acid, pinacol ester) already described in the bibliographical review in Chapter 1. It consists in the (co)polymerization by ATRP of 4-trimethylsilylstyrene monomer to afford a silyl functionalized (co)polymer. Then, the silyl group is readily exchanged to a dibromoboryl moiety using boron tribromide to yield a dibromoborane-functionalized (co)polymer that constitutes a platform for post-modification. Although this last method opens routes to well-defined structures such as block copolymers with narrow polydispersity and fixed-length blocks, the molar masses remain relatively modest (M_n below 10 kg/mol). [27]

In order to maximize the mechanical properties, we targeted higher molar masses to achieve higher entanglement. We thus decided to optimize the free radical polymerization of this boronate styrenic-based monomer to aim at higher M_w in particular. Indeed, we faced many issues concerning the brittleness of the polymer studied and its molding was found to be impossible without optimization of the molar masses that guarantee the integrity of the material. Homopolymers of polystyrene are reported to be highly brittle in the literature and we can consider that the same characteristic is present in our polymer. [28] A lot of time was thus dedicated to the increase of the molar masses of the polymer synthesized.

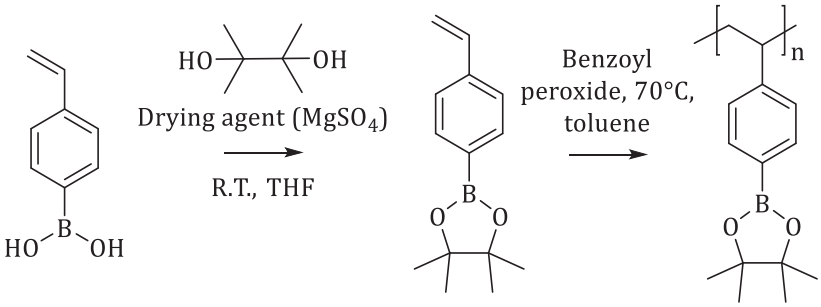

Figure III. 1: Synthesis of poly(4-vinylphenylboronic pinacolate) (PSBPin).

The organoboron monomers containing boronate ester pendent groups were synthesized *via* condensation reaction between 4-vinylphenylboronic acid and pinacol according to established methods. [29] It was observed that the monomers synthesized by this method always contained minute amounts of pinacol as observed by ^{1}H NMR. This amount was estimated under 1 % mol in the final compound. The ^{1}H, ^{13}C and ^{11}B spectra are respectively searchable in Figures V. 38, V. 39 and V. 40 of the Experimental Section.

However, we carried polymerizations without further purification. This contamination will be further discussed within the core of the proposed mechanism, as a putative source of nucleophilic assistance to the observed dynamic crosslinking behavior of the polymer. The synthetic path is illustrated in Figure III. 1.

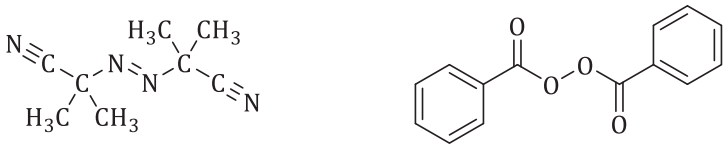

Figure III. 2: Structures of initiators commonly used in radical polymerization.

The most common initiators are diazo compounds such as azobisisobutyronitrile or organic peroxides such as benzoyl peroxide. [30] In our study, the monomers were then polymerized by free radical polymerization involving benzoyl peroxide (BPO, Figure III. 2) as the initiator. It was preferred as an initiator in order to minimize any residual functionality from more conventional azobis-based initiators. Azobisisobutyronitrile (AIBN, Figure III. 2) was avoided as the initiator due to its nitrile moieties that could for instance be involved in Lewis pairs with the boronate side-chain moiety or that could lead to the thermal degradation of the polymer.

In typical polymerization, the reaction was conducted in a weakly complexing organic solvent such as toluene in a Schlenk vessel with 0.01 or 0.02 molar equivalent of benzoyl peroxide at a temperature ranging from 70 to 90°C. NMR data are visible in Figures V. 41, V. 42 and V. 43 of the Experimental Section.

B. Optimization of polymerization parameters by size-exclusion chromatography study

Parameters including temperature, quantity of initiator, and nature of the solvent were varied and their impact on the molar masses were assessed. The goal was to be able to synthesize polymers with sufficiently high molar masses to have processable materials for mechanical tests. A representative part of the results obtained is presented in Table III. 2 below.

Table III. 2: Synthesis optimization of poly(4-vinylphenylboronic pinacolate). [1]Values determined by SEC-THF using PS standards and conventional calibration.

Entry	***Solvent***	***[Benzoyl peroxide] (mol eq.)***	***T (°C)***	***M_n (g/mol)[1]***	***M_w (g/mol)[1]***	***Dispersity Đ***	***Yield***
1	Toluene	0.01	80	25 000	39 000	1.6	60 %
2	Anisole	0.01	90	20 000	36 000	1.8	21 %
3	Dimethyl carbonate	0.01	80	12 000	17 000	1.4	20 %
4	Toluene	0.02	80	17 000	31 000	1.8	24 %
5	Toluene	0.02	70	42 000	230 000	5.4	75 %
6	Toluene	0.02	60	38 000	121 000	3.2	56 %
7	Toluene	0.02	80	25 000	44 000	1.7	60 %
8	Toluene	0.01	80	23 000	35 000	1.5	47 %

Polymerizations were conducted at different temperatures: 60°C, 70°C and 80°C (Entries 4, 5 and 6, Table III. 2) and the size exclusion traces were compared. Size exclusion chromatography in THF gave us the molar masses through the volume of elution compared to PS standards. Conducting the polymerization at the temperature of 70°C leads to the highest molar masses despite the larger dispersity. Most part of the chains are thus terminated by a disproportionation step where one radical transfers a hydrogen atom to the other to form two stable macromolecules yielding the main population on the size-exclusion chromatography traces. The higher molar masses are reached due to the recombination of polymer chains where two growing chain radicals form a covalent bond in a single stable macromolecule. This leads to a small proportion of highest

molar masses chains in the final polymer. However, even in a low proportion, the presence of longest chains can have a high impact on the mechanical properties and counteract the issues of the brittleness observed in the material. These results are illustrated by the chromatograms in Figure III. 3 (a).

The polymerization was then performed in three solvents: toluene, anisole and dimethyl carbonate (Entries 1, 2 and 3, Table III. 2). Higher molar masses with acceptable dispersity were obtained in the case of toluene. Thus, the latter was chosen as the polymerization solvent for the rest of the study. Moreover, toluene as an apolar solvent does not have any effect of complexation on the boron vacancy and thus is a good candidate for the polymerization of boron-based monomer. For the synthesis of high molar masses organoboron polymers, the strategy is to avoid transfer reactions that are decreasing the molar masses. The use of a low-transferring solvent such as toluene was preferable in this case. [31] The chromatograms are compared in Figure III. 3 (b).

The quantity of initiator has also an influence on the molar masses of the polymer and higher molar masses were achieved with increasing the quantity of initiator. (Entries 7 and 8, Table III. 2 and Figure III. 3 (c))

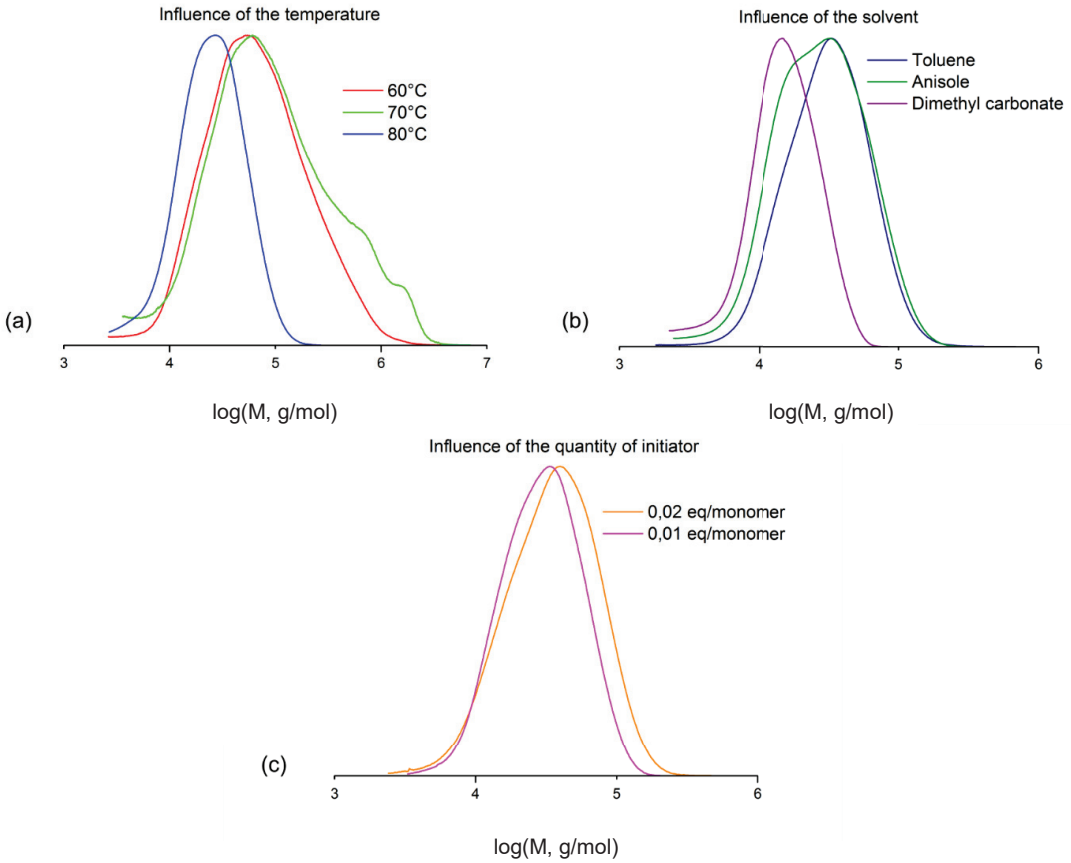

Figure III. 3: Influence of synthesis parameters on the molar masses of poly(4-vinylphenylboronic pinacolate) by free radical polymerization. (a) Study of the influence of the polymerization temperature, (b) Study of the influence of the polymerization solvent and (c) influence of the quantity of initiator used.

After these optimizations, the polymerization was conducted at the temperature of 70°C in toluene with 0.02 molar equivalent of benzoyl peroxide compared to the quantity of monomer. Eventually, poly(4-vinylphenylboronic pinacolate)s featuring M_w up to 230,000 g/mol compared to PS standards could be obtained, which were further assessed in the rest of this study.

The kinetic of hopolymerization has also been studied by size-exclusion chromatography to monitor the evolution of the molar masses as a function of time. This could indicate the profile of the polymerization kinetic. The conversion can also be evaluated by NMR spectroscopy but the results are not presented in this case, as the determination of the integrals of polymer and monomer are quite difficult to separate especially at the beginning of the reaction. For your information, the ^1H spectra are available in Figure V. 44 in the Experimental Section.

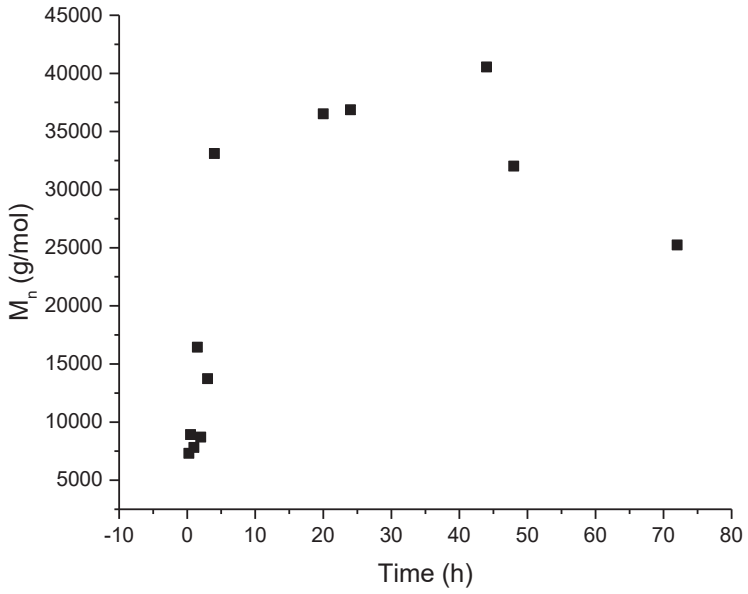

Figure III. 4: Monitoring of the molar masses during polymerization.

The growth of the chains is rapid during the first hours of the polymerization process and the final molar masses are reached after 15 h of reaction (Figure III. 4).

It is also possible to directly compare the chromatograms during the homopolymerization which indicate the evolution of the molar masses (Figure III. 5). They increase during the first hours and are close to their maximum values after 4 h of polymerization. After this time, it is possible to distinguish new populations of chains exhibiting even higher molar masses. We assumed that recombinations are responsible for these longer polymer chains. Besides, this can be a benefit to counter the brittleness of the polymer.

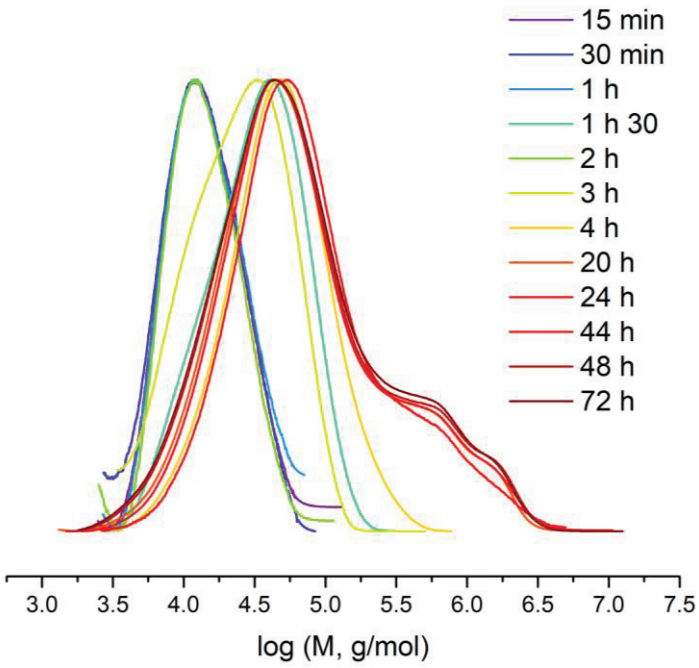

Figure III. 5: Monitoring of the homopolymerization of 4-vinylphenylboronic pinacolate by size-exclusion chromatography.

C. Synthesis of random copolymers and reactivity ratios

Copolymers involving 4-vinylphenylboronic pinacolate monomer and usual comonomers such as styrene, vinylpyrrolidone, acrylonitrile, maleic anhydride and others have been reported in the literature. [26], [32]–[35]

In our research, poly(4-vinylboronic pinacolate-*co*-styrene)s were produced using the same procedure than for homopolymers of 4-vinylphenylboronic pinacolate. We were then able to determine the reactivity ratios of each monomer respectively by Fineman-Ross and Mayo-Lewis equations. The reactivity ratio for each propagating chain is defined as the ratio of the rate constant for addition of a monomer of the species already at the chain end to the rate constant for addition of the other monomer. [36] Thus, the reactivity ratios are defined as r_1 and r_2 respectively the reactivity ratios of styrene and 4-vinylphenylboronic pinacolate:

$$r_1 = {}^{k_{11}}/_{k_{12}} \text{ and } r_2 = {}^{k_{22}}/_{k_{21}}$$

with k_{11} (and k_{22}) the rate constants for addition of styrene (4-vinylboronic pinacolate) to a styrene (respectively 4-vinylboronic pinacolate) chain end and k_{12} (and k_{21}) the rate constants for addition of styrene (4-vinylboronic pinacolate) to a 4-vinylphenylboronic pinacolate (respectively styrene) chain end.

In the Mayo-Lewis linear equation established in 1944 [37], the reactivity ratios r_1 and r_2 of each monomer are linked through this form of equation for a copolymer from monomer 1 and 2:

$$r_2 = \frac{f_1}{f_2}\left[\frac{F_2}{F_1}\left(1 + \frac{f_1 r_1}{r_2}\right) - 1\right]$$

with f_1 and f_2 the initial mole fractions of monomers in the reaction and F_1 and F_2 the mole fraction of each monomer in the copolymer. This method is usually applied to copolymerizations at low conversions; however, it has been proved to this equation can be used to high-conversion copolymerization of styrene and methylmethacrylate for instance. [38] The different compositions used are listed in Table III. 3 and were calculated from NMR spectra in Figures V. 48 to V. 61 in the Experimental Section.

Table III. 3: Compositions of the copolymers studied for the calculation of reactivity ratios of styrene and 4-vinylphenylboronic pinacolate. f_1 and f_2 the initial mole fractions respectively of styrene and 4-vinylphenylboronic pinacolate in the reaction and F_1 and F_2 the mole fractions respectively of styrene and 4-vinylphenylboronic pinacolate in the copolymer.

Entry	***f_1***	***f_2***	***F_1***	***F_2***
1	0.9	0.1	0.88	0.12
2	0.8	0.2	0.82	0.18
3	0.8	0.2	0.74	0.26
4	0.7	0.3	0.69	0.31
5	0.6	0.4	0.70	0.30
6	0.4	0.6	0.44	0.56
7	0.3	0.7	0.4	0.6
8	0.2	0.8	0.23	0.77
9	0.1	0.9	0.03	0.97

For each composition, plots are generated with arbitrary r_2 values from the experimental data. The intersection of the lines gives the r_1 and r_2 values for the system studied. Following this method, we obtained the graphic in Figure III. 6 with a straight line for each f_1/f_2 couple. We found r_1=0.87 and r_2=0.8 for styrene and 4-vinylphenylboronic pinacolate monomers respectively.

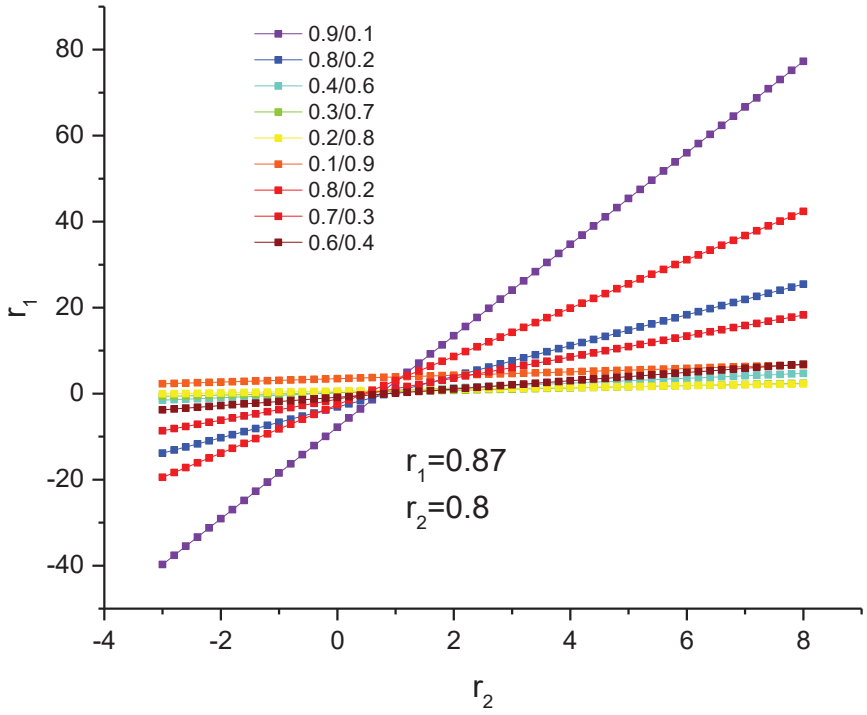

Figure III. 6: Reactivity ratio determination by Mayo-Lewis equation for each f_1/f_2 couple.

To confirm our calculation by the Mayo-Lewis equation, we also used the Fineman-Ross method to verify our reactivity ratio values of styrene and 4-vinylphenylboronic pinacolate in a copolymer. In this way, Fineman and Ross rearranged the Mayo-Lewis equation into a linear form. [39]

The relation between the reactivity is then expressed as below:

$$A = Br_1 + r_2$$

$$\text{with } A = \frac{f_1(2F_1-1)}{(1-f_1)F_1} \text{ and } B = \frac{{f_1}^2(1-F_1)}{(1-f_1)^2F_1}$$

The plot of A versus B yields a straight line with slope r_1 and intercept r_2 as showed in Figure III. 7. This conducted to the following reactivity ratios: r_1=1 and r_2=0.82 respectively for the styrene comonomer and the 4-vinylphenylboronic pinacolate comonomer in the copolymer synthesized by free radical polymerization.

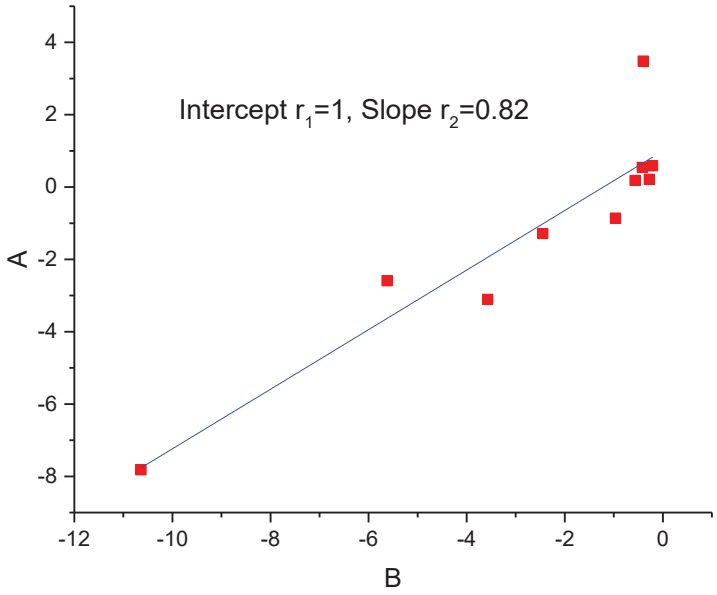

Figure III. 7: Reactivity ratio determination by Fineman-Ross equation.

The two calculation methods used conducted to very near results validating the final values of the reactivity ratios. The results obtained prompted us to conclude that the copolymers synthesized are more likely to form statistical copolymers since they present close reactivity ratios.

In order to obtain more precise results concerning the reactivity ratios, the experiments should have been stopped at lower conversions. However, only a slight deviation between the theoretical and experimental ratios has been observed at lower conversion (Table III. 4) thus validating our hypothesis.

To sum it up concerning the copolymers synthesized, we obtained the following results concerning the incorporation ratios of each monomer, the molar masses and the reaction yields obtained. All the data are collected in Table III. 4.

We can see that the yields obtained for the following copolymerizations are really disparate and do not follow any rational law. However, for each copolymerization, we are closed to the ratios targeted thanks to the close reactivity ratios of the two monomers. The molar masses and dispersities follow the same trends for each copolymer. We were only able to reach high molar masses for the homopolymers of 4-vinylphenylboronic pinacolate. The chromatograms of the copolymers are gathered in Figure V. 69 in the Experimental Section.

Table III. 4: Experimental data of the copolymers synthesized from styrene and 4-vinylphenylboronic pinacolate. [1]Molar ratio of 4-vinylphenylboronic pinacolate monomer. [2]Values determined by SEC-THF using PS standards and conventional calibration.

Entry	***Theoretical ratio[1]***	***Experimental ratio[1]***	***M_n[2] (g/mol)***	***M_w[2] (g/mol)***	***Dispersity Đ***	***Yield***
1	20	26	23 000	40 000	1.7	40%
2	30	31	18 000	36 000	2	75%
3	40	38	20 000	42 000	2.2	39%
4	50	44	21 000	43 000	2.1	70%
5	60	44	18 000	33 000	1.8	37%
6	70	60	19 000	30 000	1.7	31%
7	80	77	20 000	42 000	2.1	91%
8	90	97	29 000	59 000	2	40%
9	100	100	42 000	230 000	5.4	75%

III. Differential scanning calorimetry investigation

A. Analyses on homopolymers

After drying process under vacuum, the synthesized organoboron polymers were characterized by differential scanning calorimetry (DSC) and an unusual yet interesting thermal behavior was detected.

Firstly, Figure III. 8 shows DSC analysis performed in standard 40 µL aluminum capsules with pierced caps, which allow the evaporation of volatile residues.

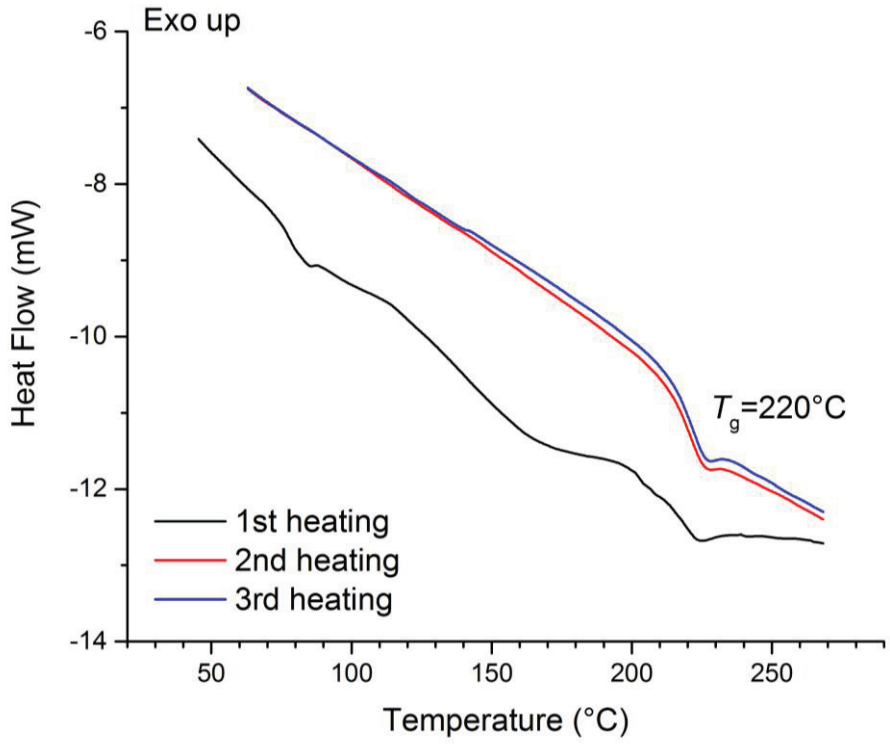

Figure III. 8: DSC thermograms of homopolymer PSBPin in 40 µL pierced alumina pans.

During the first heating, an initial thermal event could be attributed to a glass transition temperature around 80°C. Then, another thermal event around 150°C was evidenced but solely during the first heating segment. This endothermic phenomenon was first attributed to evaporation of remaining polymerization/precipitation solvent and adsorbed moisture but could conceal an underlying chemical reaction.

At the end of the first heating segment, a second glass transition temperature appeared at temperature ranging from 210°C to 220°C, depending on the M_w of the poly(pinacol 4-vinylphenylboronate ester)s used. The second heating segment as well as all other subsequent heating segments revealed the same position for the second glass transition temperature. This

higher glass transition temperature is therefore reproducible over at least 5 heating/cooling cycles, and independent of the heating segment, apart from the first one.

This thermal behavior and the ultimately high glass transition temperature evidenced prompted us to investigate further to comprehend this phenomenon. For this purpose, complementary differential scanning measurements in middle pressure capsules were undertaken as shown in Figure III. 9. In these capsules, the evaporation phenomenon was indeed not measured and different thermal events occurring at high temperatures were observed. Blank experiments were conducted using middle-pressure capsules containing only water or only toluene and no endotherms could be observed.

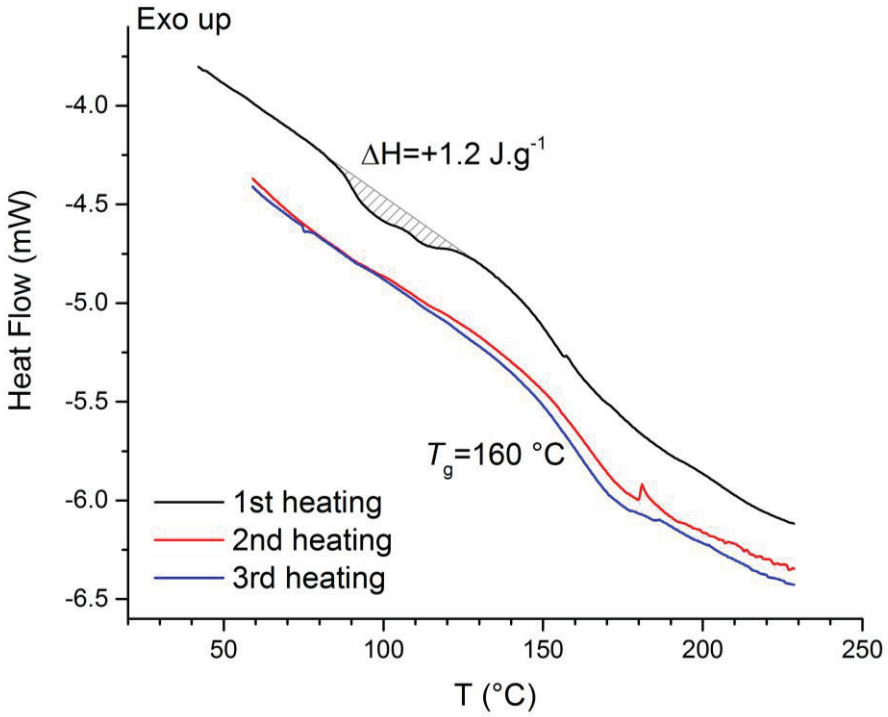

Figure III. 9: DSC curves of poly(4-vinylphenylboronic pinacolate) in 100 µL medium pressure alumina crucible.

In this sealed case study, the same kind of phenomenon with the first glass transition temperature around 90°C was observed, followed by an endotherm between 90°C and 130°C during the first heating segment. It leads to the second glass transition temperature at 160°C at the end of the first heating segment. This glass transition temperature was also detected during the second heating segment, and subsequent heating cycles after that. The final glass transition temperature was lower in this case than in standard 40 µL aluminum capsules with pierced caps. As explained in the latter part of the main text, we believe that in this case, adventitious water adsorbed on the polymer is not removed during the heating/cooling cycles. It may act to some extent as a plasticizer and thus contribute to the decrease of the glass transition temperature.

At this point, a hypothesis involving the creation of linkages between the boron atoms *via* interconnected pinacolate moieties effectively crosslinking the polymer chains was formulated. This bridging phenomenon could involve the ring-opening of the phenylboronic pinacolate, and subsequent reformation of new intermolecular boronates thus explaining the slightly endothermic reaction observed. These linkages would conduct to a lower mobility of the polymer chains and thus to a higher glass transition temperature.

B. Thermal analysis of copolymers

In order to exemplify our hypothesis, we decided to evidence the same phenomena in copolymers of styrene and 4-vinylphenylboronic pinacolate. The quantity of boronate esters in the polymer was varied by copolymerization with styrene and to determine the influence on the thermal behaviors and associated glass transition temperatures.

Differential scanning calorimetry measurements were carried out and are depicted from Figures V. 63 to V. 68 in the Experimental Section. Nearly identical, yet temperature-shifted, thermal behaviors were observed (Figure III. 10): a first glass transition then an unusual yet less pronounced thermal event and a subsequent second glass transition, again reproducibly observable at all incremental heating cycles. Interestingly, an increase of the second glass transition temperature with increasing boronate monomer content was observed, which means that the high T_g phenomenon can be finely tuned by adjusting the boronate content.

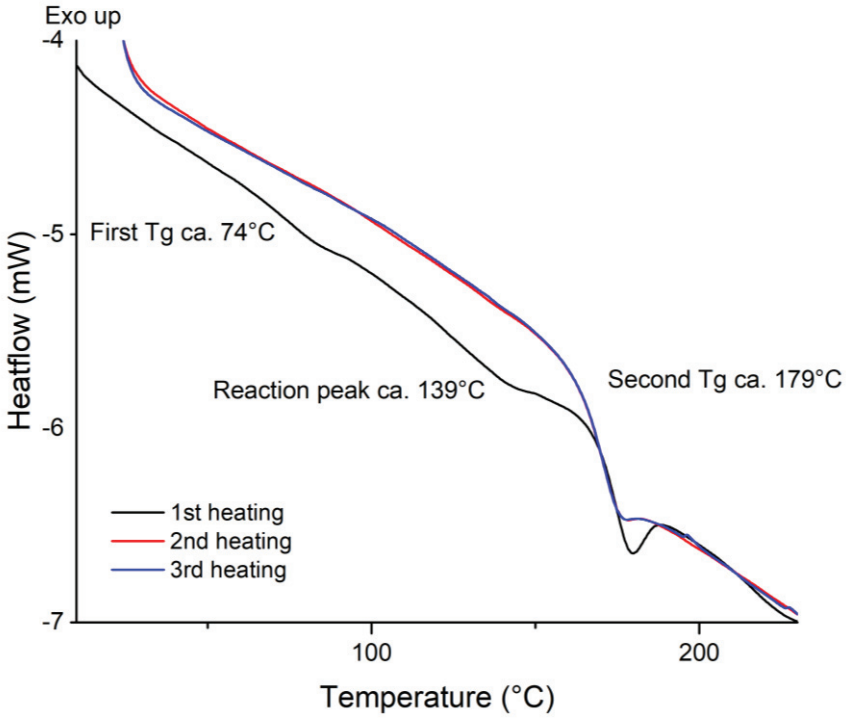

Figure III. 10: Thermograms of a copolymer with 50 mol % of boronate ester monomers in 40 µL pierced aluminum pans.

Gordon and Taylor have proposed in 1952 a model for the prediction of the glass transition temperature for copolymers from the properties of the pure compounds. [40] The equation related is expressed as followed:

$$T_g = \frac{[\omega_1 T_{g,1} + K\omega_2 T_{g,2}]}{[\omega_1 + K\omega_2]}$$

with $T_{g,1}$ and $T_{g,2}$ the glass transition temperature of homopolymers from the monomers 1 and 2, ω_1 and ω_2 the mass fraction of each monomer in the copolymer and K an adjustable fitting parameter.

This equation is applicable for fitting the glass transition temperature of many copolymers and it can be used to describe the composition dependence of miscible polymer blends exhibiting negative and position deviation if K is treated as an adjustable parameter. However, the Gordon-Taylor equation should only be applied to blends and mixtures with relative weak specific intermolecular interactions.

The Gordon-Taylor equation (Figure III. 11) successfully fits the evolution of the glass transition temperature with K=0.6 since both polymers have similar structural groups and no specific interactions are present.

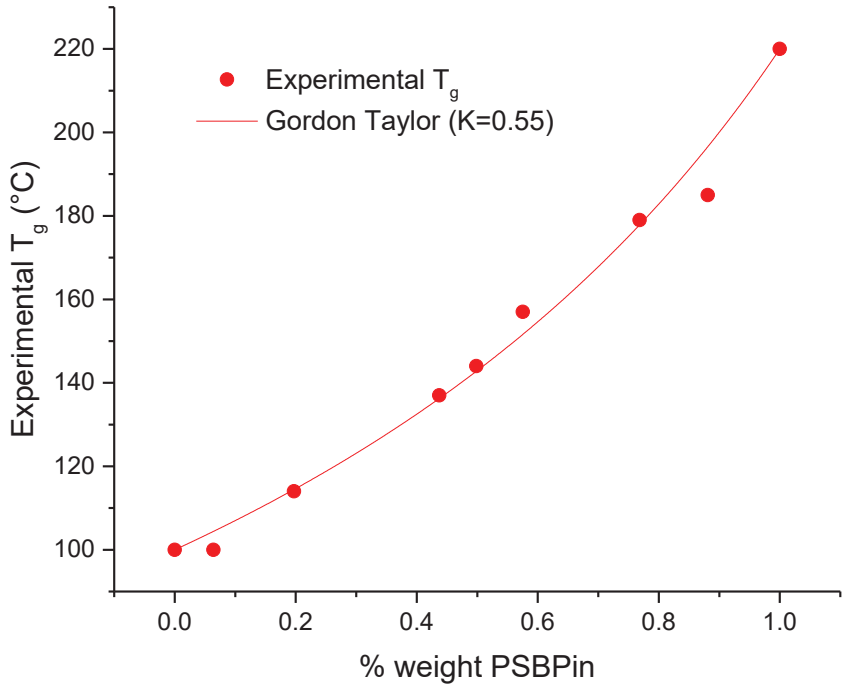

Figure III. 11: Evolution of the second glass transition temperature with the increase of molar proportion of 4-vinylphenylboronic pinacolate monomer and Gordon-Taylor fit.

C. First conclusions from the DSC study

After characterizing the macromolecular features of our boron-containing polymers, we realized that the unusual thermal patterns could conceal an overlooked reactivity, undisclosed when these polymers were first reported and characterized by Jäkle *et al*. [41] In particular, the two observable glass transition events flanking the "reactivity" event, determined as endothermic in pressured DSC capsules (to differentiate from any remaining solvent evaporation which is also endothermic).

Interestingly, it was possible to re-dissolve the capsule-contained polymer in toluene, even after multiple heating/cooling cycles. This could indicate that if linkages are involved, they are somehow reversible, and thus we would be in the presence of dynamic crosslinks.

All the primary characterizations of our homo- and copolymers of 4-vinylphenylboronic pinacolate thus suggested a reactivity of our chains allowing a second glass transition to occur at higher temperature in bulk. In order to assess this reactivity, we resorted to methods of characterization at the molecular level such as spectroscopic methods developed in the next part.

IV. Spectroscopic methods on the homopolymer

A. DRIFT spectroscopy on the homopolymer

Temperature-resolved Diffuse Reflectance Infrared Fourier Transform spectroscopy (DRIFT) was performed on homopolymer powder with no preparation. Diffuse reflectance was developed for facile analysis of powders in their neat state. The most widely used model for diffuse reflectance was established by Kubelka-Munk, which condensed the geometric particularities of an inhomogeneous material into one single parameter: the scattering coefficient, s (cm^{-1}). [42] Indeed, the reflection of radiant energy at boundary surfaces induces multiple reflections at surfaces of small particles and the reflecting power is called reflectance. The diffuse reflectance is given as:

$$R_\infty = 1 + \frac{k}{s} - \sqrt{\frac{k}{s}\left(2 + \frac{k}{s}\right)}$$

with k (cm^{-1}) the absorption coefficient of the sample directly related to the material.

The equation can then be re-written in a simplest form yielding the Kubelka-Munk transformation:

$$\frac{k}{s} = \frac{(1 - R_\infty)^2}{2R_\infty}$$

R_∞ was defined as the rate between the experimental intensity obtained from the sample and the intensity obtained from a reference sample (KBr in this case) at the same temperatures. For K → 0 meaning no absorption, R_∞ → 1 where all the light is reflected by the sample. For S → 0 meaning no scattering, R_∞ → 0 where all light is transmitted or absorbed.

The sample of poly(4-vinylphenylboronic pinacolate) was heated in a special cell equipped with an reflectance IR probe, device which permitted to accumulate successive IR spectra at increasing temperature with a controlled heating rate. The Kubelka-Munk model was calculated for each temperature and some noticeable differences appeared in between the spectra, in the 1700-500 cm^{-1} wavenumber region (Figure III. 12).

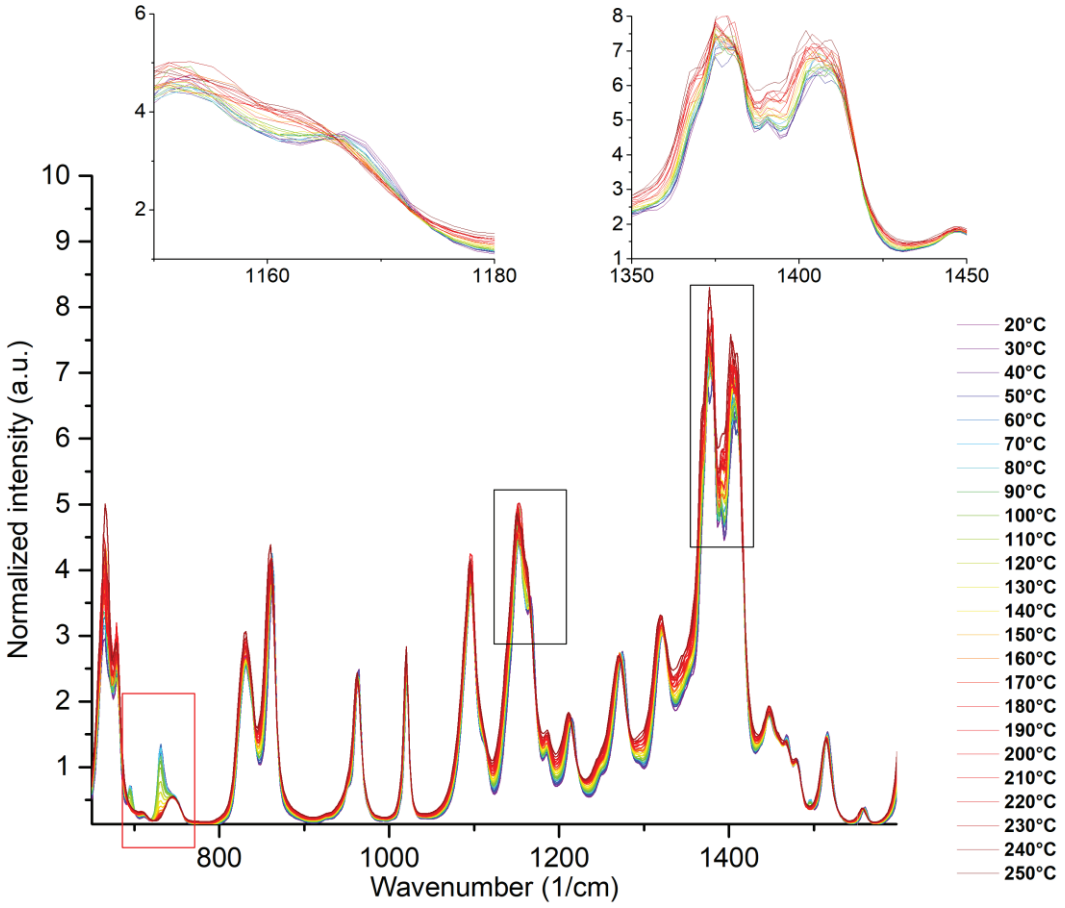

Figure III. 12: Superposition of IR spectra at each temperature between 20°C and 250°C and zooms on the regions of interest in black boxes. Red box corresponding to the loss of solvent (toluene).

In Figure III. 12, the black boxes pointed out the changes occuring while the temperature increases. These data were compared to DFT calculations performed by Lionel Perrin. Density functional theory (DFT) is a computational quantum modelling method to investigate the electronic structure of atoms and molecules. Different hydrid functions can be used to solve the calculations such as B3LYP or M06/def2TZVP that gather different theories and are consistent with the experimental results.

It was found that the differences observed experimentally are in accordance with changes of environments around the boron atom for the bands between 1350 cm^{-1} and 1400 cm^{-1} and of the structure of the pinacol for the band around 1170 cm^{-1} as identified in Figure III. 13. However, the main difference in the red box was due to the loss of toluene in the sample.

Nevertheless some additional noticeable differences could be further assigned to the vibration modes comprised of torsions/elongations of the O–B–O (1357.3 cm^{-1} and 1383.1 cm^{-1} calculated by DFT) as well as C–O (1174.8 cm^{-1} calculated by DFT) bonds of the pinacol motif in our model compound of phenyl pinacol boronate (Figure III. 13).

Remarquable frequencies with respective (relative intensities) were found by DFT calculations:

- 1174.8 cm^{-1} (316)
- 1357.3 cm^{-1} (169)
- 1383.1 cm^{-1} (599)

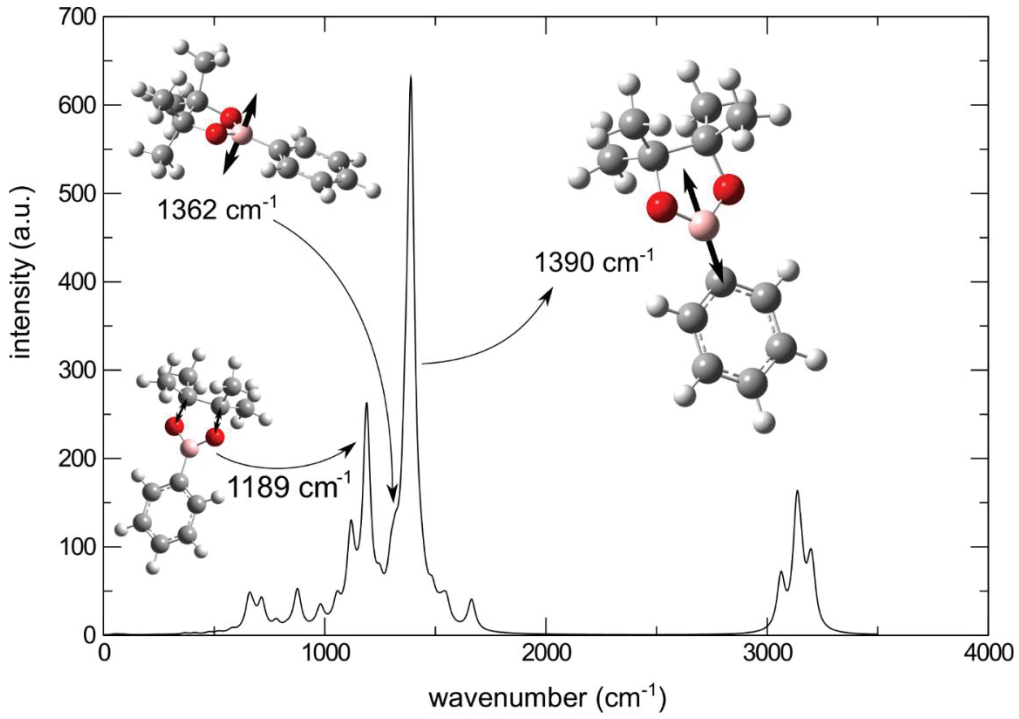

Figure III. 13: Simulated spectrum of the pendent group of the polymer and identified characteristic bands (using B3LYP/6-31G(d)). The values were later confirmed and refined to 1174.8 cm^{-1} (relative intensity: 316); 1357.3 cm^{-1} (relative intensity: 169); and 1383.1 cm^{-1} (relative intensity: 599), using M06/def2TZVP level of theory for optimization and frequency calculation.

B. Solid-State NMR spectroscopy

Solid-state boron NMR (^{11}B ss-NMR) spectroscopy was used to detect differences in the environment of the boron atom before and after heating treatment, to further understand the increase of glass transition temperature in the material. ^{11}B ss-NMR of boron is not an obvious method at first sight due to the difficulty of interpretation from the quadrupolar nature of the nucleus (spin 3/2). Besides, the solid state hindered the mobility inside the material and the observed large signals are due to the anisotropic (directionally dependent) interactions.

When comparing signals in Figure III. 14, one cannot conclude from the maximum of intensity of the observable massif but should rather get interested in the δ_{iso} (isotropic chemical shift), the ηQ values (asymmetry parameter of the quadrupolar interaction) and observe the relative asymmetries/anisotropies of the signals.

In our case, the two signals when superimposed are distinct, thus the polymer is different before and after thermal treatment. In particular, the shape of the massif is different, suggesting an altered boron environment once the poly(4-vinylphenylboronic pinacolate) is exposed to high temperature.

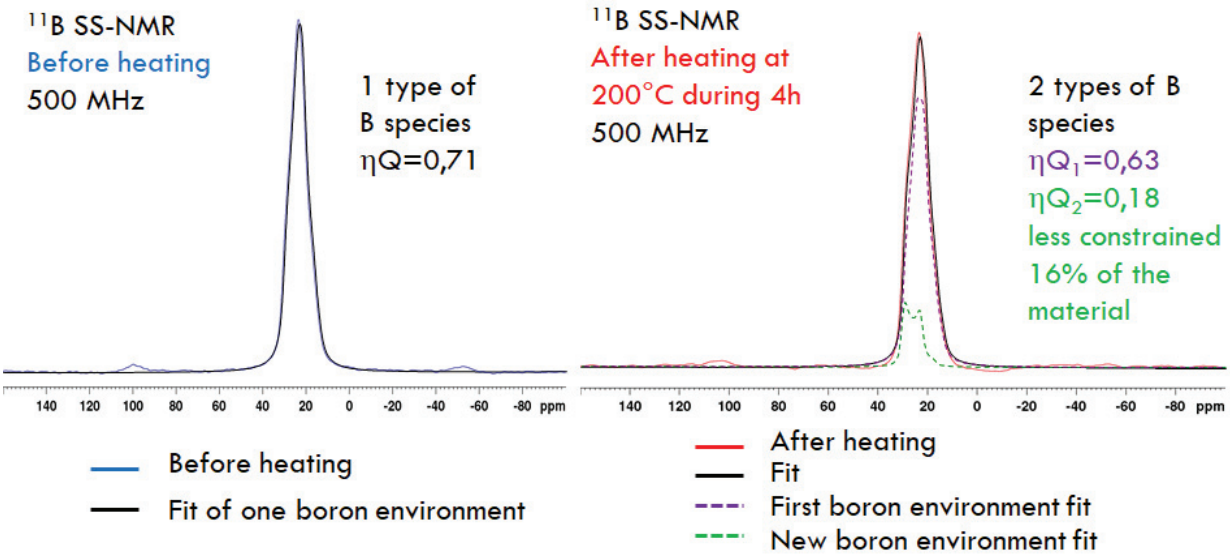

Figure III. 14: Solid-state ^{11}B NMR study of poly(vinylphenylboronic pinacolate). Left: superposition of the experimental signal in blue and the fit in black before thermic treatment; Right: superposition of the experimental signal in red, the total fit in black, the first boron environment fit in dashed purple and the second boron environment fit in dashed green after thermic treatment.

Indeed, such asymmetry suggests the presence of two types of environment surrounding the boron atoms after heating treatment. Simulations are mandatory to evaluate the presence of only one or several types of boron chemical environments. The "dmfit" program was developed to account for quadrupolar couplings and render easy such simulations of spectra obtained from combination of discrete species. [43]

When fitting the signal before heating treatment, one type of boron is sufficient and the simulation perfectly matches the experimental spectrum. On the contrary, when fitting the signal after heating treatment, two types of boron are necessary to achieve perfect match between the simulation and the experimental spectrum. Simulations using the "dmfit" program therefore allowed us to unveil a new boron environment after heating, displaying more symmetrical features, in particular quadrupolar couplings (lower ηQ value, Figure III. 14), with a different δ_{iso} of 32.5 ppm.

This particular boron environment, with enhanced mobility (symmetry of the computed signal and low ηQ value) could be the signature of boronates with intermolecular bridging pinacolates. The main constrained environment, common to the sample before and after heating, with a δ_{iso} of 30.5 before (and 30 after) and similar relatively high ηQ values (0.71 and 0.63 respectively)

consistent with a fixed geometry, was attributed to native phenyl boronate pinacol cyclic species. Interestingly, the low value of ηQ for the new species is not consistent with the formation of boroxine moieties (δ_{iso}≈25 ppm) as they typically display much higher ηQ values (> 0.7), characteristic of constrained geometries around boron. [44], [45]

The slight differences can be attributed to solvent evaporation (toluene leftovers, adsorbed moisture that are no longer present after heating for 4 h at 200°C). Our investigation was then one-step further into confirming our original hypothesis of ring opening of cyclic pinacol boronates.

V. Rheological investigation

After characterizing our systems using molecular and thermic techniques, we decided to assess the macroscopic behavior of poly(4-vinylphenylboronic pinacolate) by rheological measurements.

In order to better characterize the polymer after the heating step, we investigated its viscoelastic properties from 230 to 260°C by shear rheology, using small amplitude oscillations. Frequency-dependent storage and loss moduli at different temperatures were shifted by conventional time-temperature superposition in order to build a master curve using 230°C as reference temperature (Figure III. 15). The proximity to the glass transition was evidenced by the strong increase of G' and G" at high frequencies, while the upturn of G' at lower frequencies suggested the presence of entanglements or crosslinks.

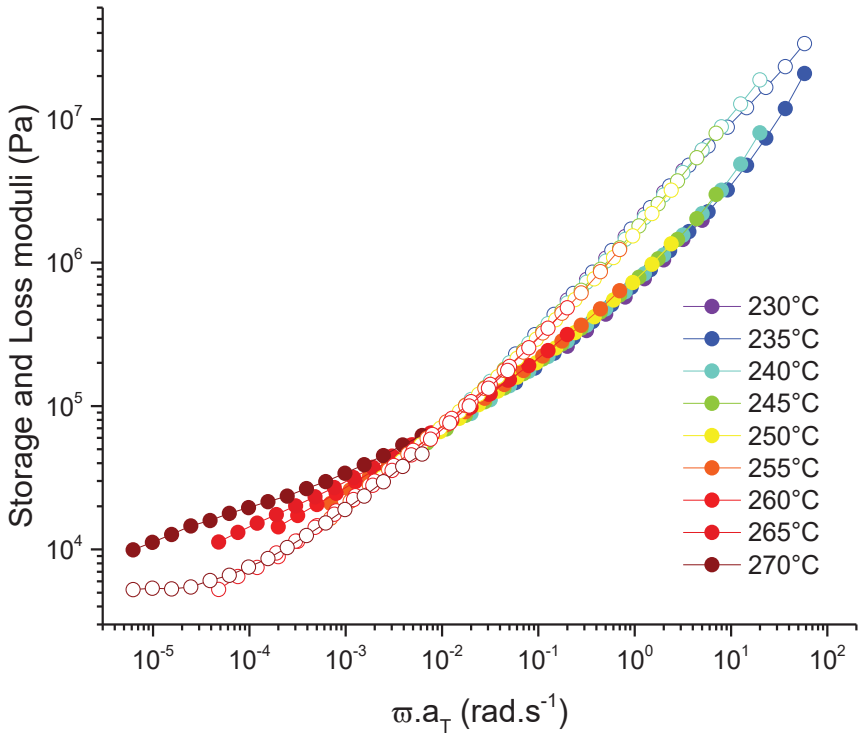

Figure III. 15: Master curve of dynamic storage and loss moduli of PSBPin in bulk, referenced at 230°C. G' in closed circles and G" in opened circles.

The temperature dependency of the shift factors determined from the time-temperature superposition (TTS) of frequency sweeps and referenced at T_0=230°C is plotted in semi-log plot in Figure III. 16.

The Williams-Landel-Ferry (WLF) equation is an empirical equation associated with the time-temperature superposition. [46] The equation is used to fit the shift factors a_T to the temperature. The superposition parmeters a_T follow the equation:

$$\log(a_T) = \frac{-C_1(T - T_0)}{C_2 + (T - T_0)}$$

where T is the temperature, T_0 the reference temperature used for the determination of the superposition parameters and C_1 and C_2 empirical constants to fit the values of a_T. The behavior of conventional polymers is well represented by WLF.

We plotted in red the WLF law using the so-called "universal constants" for T_0=230°C thus yielding C_1=10.7 and C_2=70°C, and in blue the best fit when using C_2=50+T_0-T_g in Figure III. 16. [46]

The apparent linear dependence of log(a_T) (black line) with temperature observed can only be fitted with very high C_2 parameters (C_2 >> T_g) which is unrealistic from a physical standpoint.

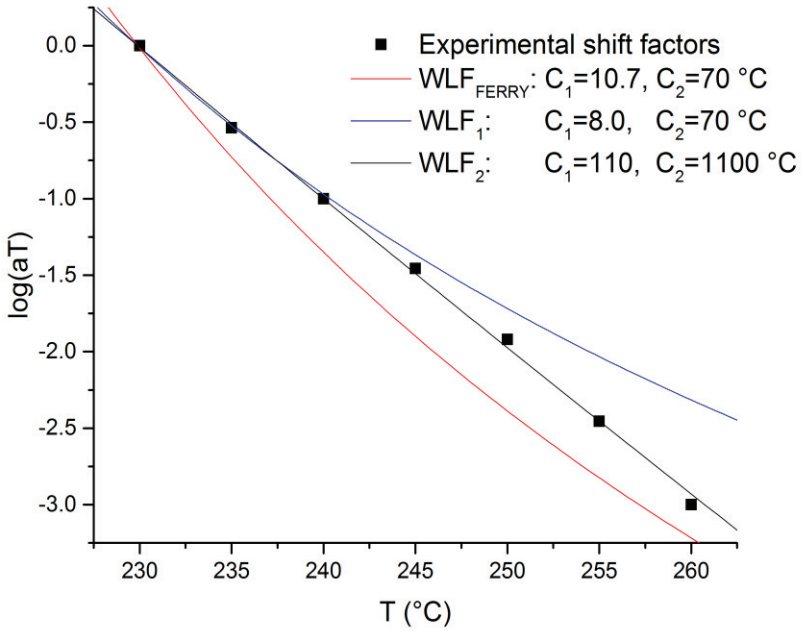

Figure III. 16: WLF profiles with different values of C_1 and C_2 constants.

The dependency of the shift factors with temperature could not be fitted with the classical Williams-Landel-Ferry model but followed instead an Arrhenius model (Figure III. 18): $a_T = e^{-E_a/RT}$. The Arrhenius law describes the temperature dependency of reaction rates. It is used in many thermally-induced reactions or processes. [47]

Capelot and Leibler showed that, when the dynamics of covalent networks are controlled by chemical exchanges, the temperature dependency of viscosities follows an Arrhenius law rather than a WLF law (Figure III. 17). [48], [49]

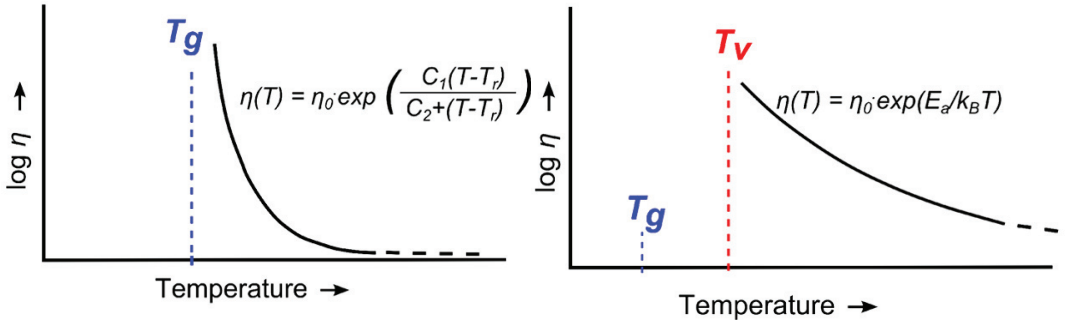

Figure III. 17: Left: Viscosity follows a WLF law with temperature for a thermoplastic polymer. Right: Viscosity follows an Arrhenius law for a network comprising dynamic covalent exchanges. Adapted with permission from [48]. Copyright 2012 American Chemical Society.

It is possible to reach the activation energy of the reaction by plotting $\ln(a_T)$ depending on the temperature presented in Figure III. 18. The slope obtained by a linear fitting equation is directly linked to the activation energy taking into account the R factor. This allowed us to find a very high activation energy about 500 kJ/mol for the reaction studied.

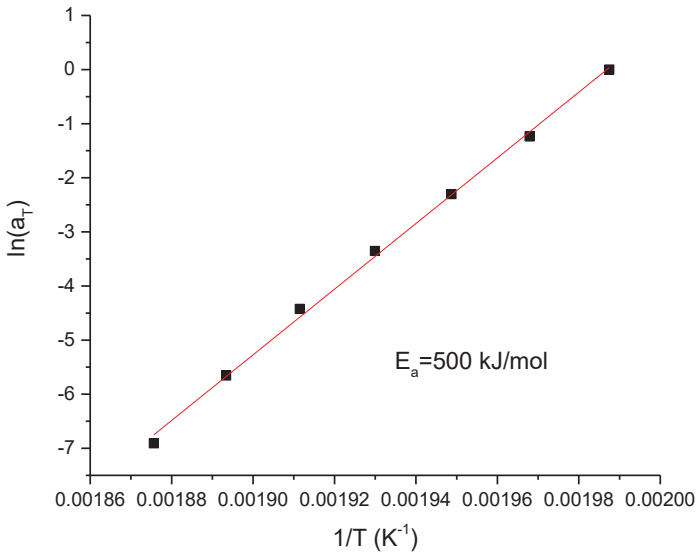

Figure III. 18: Arrhenius-like dependency of the shift factors.

Judging from the very high viscous flow activation energies measured by rheology, it is likely that the dynamic network is not purely driven by associative exchanges like vitrimers, but undergoes depolymerization like CANs. Indeed, in the case of vitrimers, the flow activation energy is only due to associative exchanges and is around 150 kJ/mol for classic vitrimers. [49] In our case, the flow

activation energy is much higher and we assumed that it does not contain only the contribution of exchanges but also depolymerization processes.

The very fact that bridging between boron atoms lead to high glass transition temperatures in our system and subsequently froze the depolymerisation kinetics was critical in evidencing these dynamic crosslinking phenomena. When comparing our system to vitrimers and CANs, that have either constant crosslinking densities or continuously decreasing crosslinking densities with temperature, it is exciting to note that polymers bearing cyclic boronate esters may constitute the first example of a distinct class of dynamic networks, with a crosslinking density increasing with temperature, at least within a defined temperature range.

As lower frequencies could not be probed because of degradations starting to occur above 260°C, we rather chose to further study highly plasticized PSBPin as a 50 wt% solution in xylenes (bp ≈ 140°C). For these experiments, xylene was preferred to toluene thanks to its higher boiling point (140°C vs. 110°C) preventing the solution from drying during the experiment. Monitoring in-situ the viscoelastic properties of this solution by small amplitude oscillations at 100°C indicated initially a low-viscosity, followed by a strong increase in viscosity after about 10 h. Upon shearing with large deformations, the viscosity suddenly dropped but grew again within 4 h, showing this time a clear gelation with G'/G" crossover and an elastic modulus increasing up to 50 kPa. (Figure III. 19) The slow and reversible build-up of elasticity rather indicates a reversible crosslinking phenomenon than entanglement.

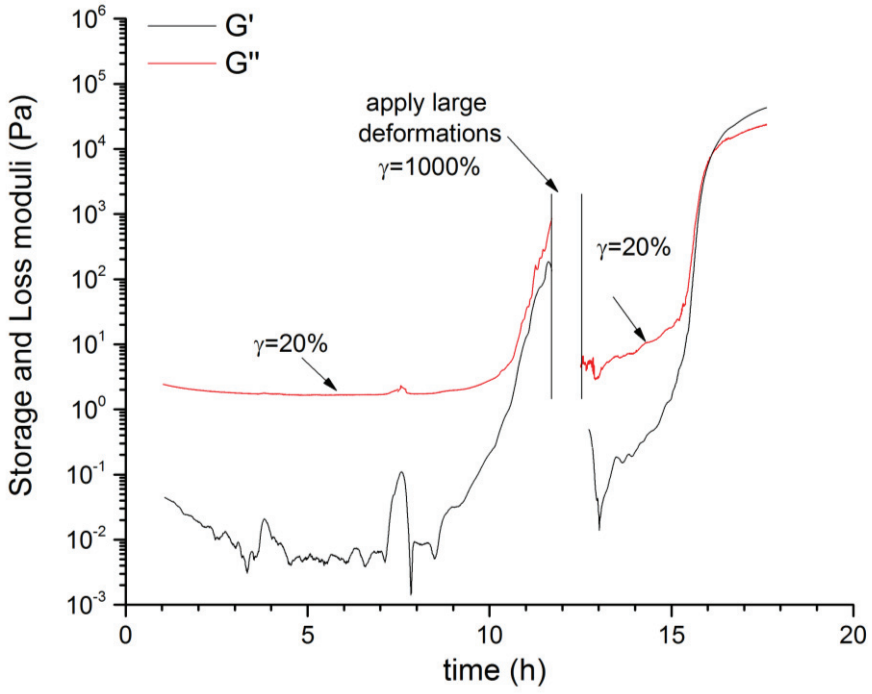

Figure III. 19: Time monitoring of storage and loss moduli of PSBPin at 50 wt% in xylenes.

This increase of viscosity observed could thus be attributed to an efficient reversible crosslinking between the polymer chains, not only favorable in bulk conditions but also possible in concentrated solutions. The chains must be close to one another to enable the crosslinking reaction, entropically disfavored, but that remains statistically feasible. This explains also why we need around 16 h to be able to detect a gel point in the concentrated solution.

The combination of DSC and rheology experiments thus indicates a dynamic crosslinking of PSBPin occurring very slowly in plasticized PSBPin at 100°C. The presence of an endothermic reaction points towards an analogous, faster crosslinking in bulk in the 130-180°C range. However, complete characterization of the dynamic-crosslinking density is not possible as the transition associated to chemical exchanges appears coincident with the segmental glass transition.

VI. Putative mechanism involved in the boronate esters reactivity

A. Liquid-State NMR spectroscopy: Study of mechanism on model molecules

In order to verify the possibility of a ring-opening of pinacol boronate esters, followed by subsequent bridging between two boron atoms, potentially carried by different polymer strands, we resorted to the study of model molecules, to further investigate what could cause such ring-openings.

We realized that an exchange reaction in between boronate esters could be evidenced by appropriately selecting our model substrates. If a ring-opening of boronates was occurring at temperatures higher than 100°C for poly(4-vinylphenylboronic pinacolate) in bulk, we should be able to evidence it by working with phenyl boronates bearing two different 1,2-diols and a specific nucleus-tag to advantageously use NMR spectroscopy to quantify the repartition of our evolving substrates.

Nicolaÿ and Leibler studied similar exchanges between two boronate esters carrying different diols at 60°C by a more indirect method, namely gas chromatography. The results of their experiments are illustrated in Figure III. 20. They highlighted a metathesis between the boronate esters groups to explain the exchanges observed. [22]

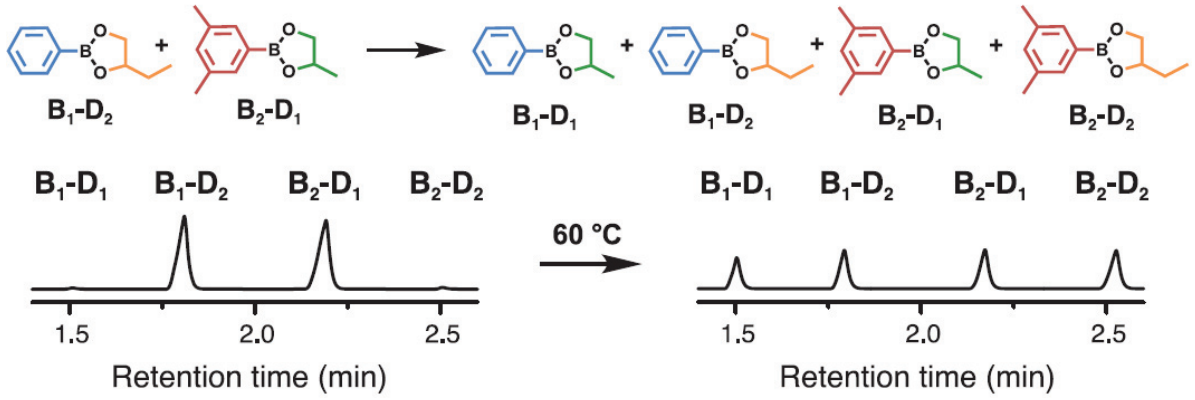

Figure III. 20: Up: Products of exchanges between B1-D2 and B2-D1. Down: Gas chromatography traces of the reaction medium after 2 min (left) and 150 min (right) during exchanges in bulk at 60°C. From [22]. Reprinted with permission from AAAS.

In the 1970's, Gerwarth already mentioned the possibility of metathesis between boronate esters as represented in Figure III. 21. [50] One can reasonably question this metathesis mechanism from evident steric considerations and the very uncomfortable four-atom transition state postulated.

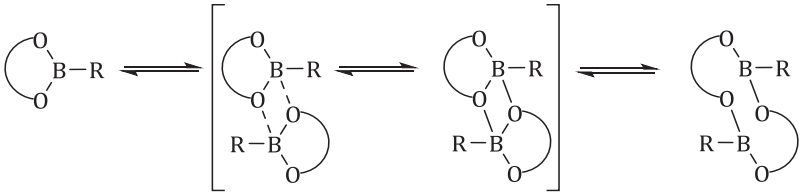

Figure III. 21: Proposed mechanism of reversible cleavage of B-O bonds. [50]

In our work, the exchanges between boronate esters were investigated using fluoro-tagged model molecules, ^{19}F being a nucleus of choice for such studies since reactivity would only be marginally impaired by fluorine substitution. 4-fluoro-phenyl boronate of pinacol was commercially afforded and phenyl boronate of ethylene glycol was synthesized *via* the same procedure as organoboron monomers from phenylboronic acid and ethylene glycol.

The exchange would proceed as follow: a fluoro-tagged phenyl boronate bearing a pinacol (molecule A, Figure III. 22) when mixed with a phenyl boronate bearing an ethylene glycol group (molecule B, Figure III. 22) would inter-convert to yield molecules C and D (Figure III. 22). Both molecules were mixed in a NMR tube at the temperature of 100°C without solvent, but using an insert filled with toluene-d_8 to be able to lock the NMR apparatus.

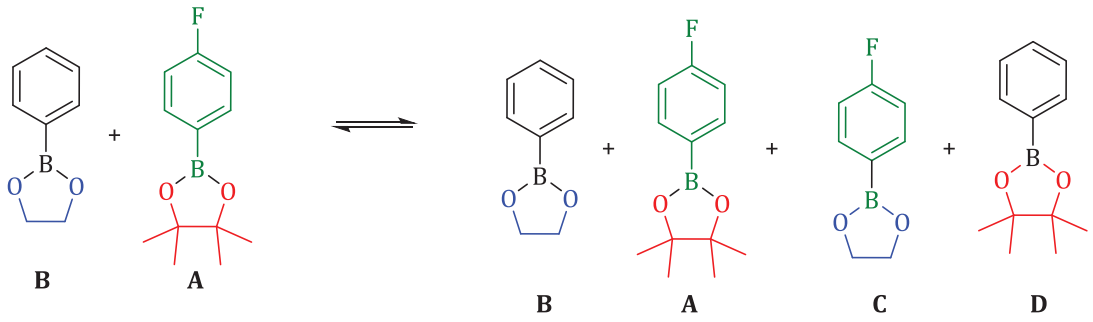

Figure III. 22 : Double-tagging experiments using ^{19}F spectroscopy.

In this experiment, we observed the creation of a second species along time, attributed to fluoro-tagged phenyl boronate bearing an ethylene glycol group (i.e. molecule C on Figure III. 22). This was further asserted by matching the chemical shift on separately synthesized 4-fluoro-phenyl boronate of ethylene glycol. The integrals of the peaks at -107.8 ppm and -108.2 ppm shows that an equilibrium between A and C was almost reached after 50 h. The chemical shifts were referenced to BF_3-OEt_2 (-152.8 ppm). Their evolution are followed in Figure III. 23.

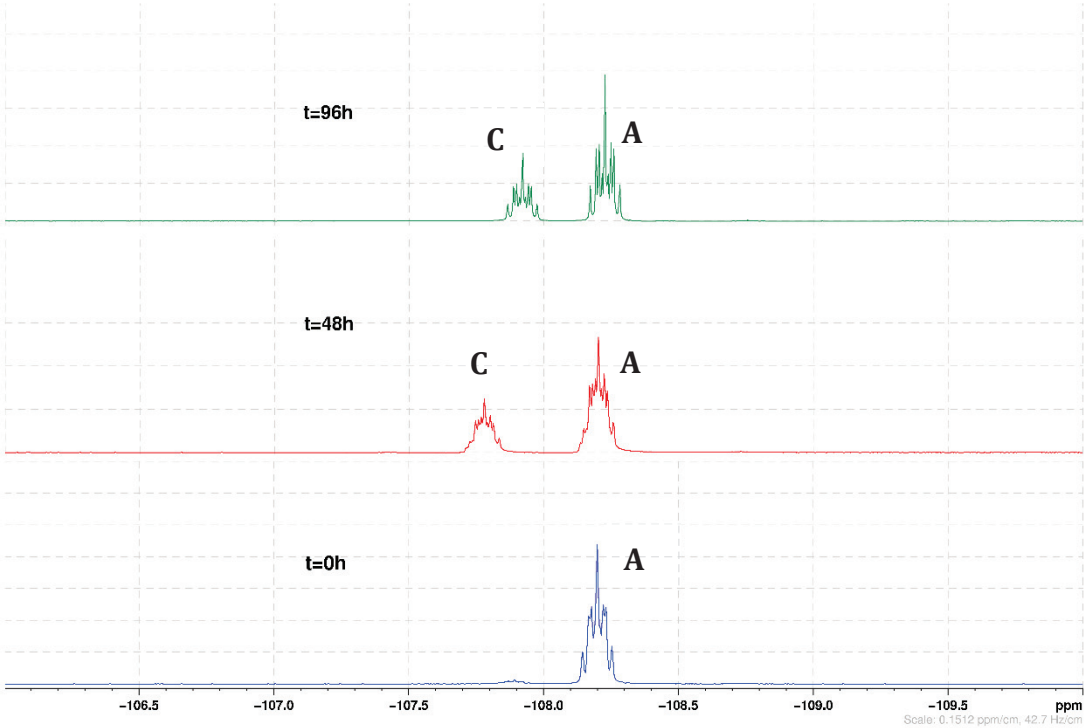

Figure III. 23: Exchanges evidenced by ^{19}F NMR between molecules A and B.

This reaction seemed slow at 100°C consistently with crosslinking experiment and we wondered what could cause it and consequently what might accelerate it. Indeed, we realized that a direct metathesis between boronates might prove difficult from a mechanistic viewpoint based on unfavorable steric repulsions, which would drastically increase the energy level of any putative 4-centered intermediate.

We postulated that, alike many derivatization/deprotection of boronates, the exchange could arise from prior coordination at boron of a nucleophile, effectively pyramidalizing it, and triggering a ring opening of the tetrahedral boronate, revealing a novel oxygen-centered nucleophile, still hanging from the attacked boron, but that could reach another boron atom as illustrated in Figure III. 24.

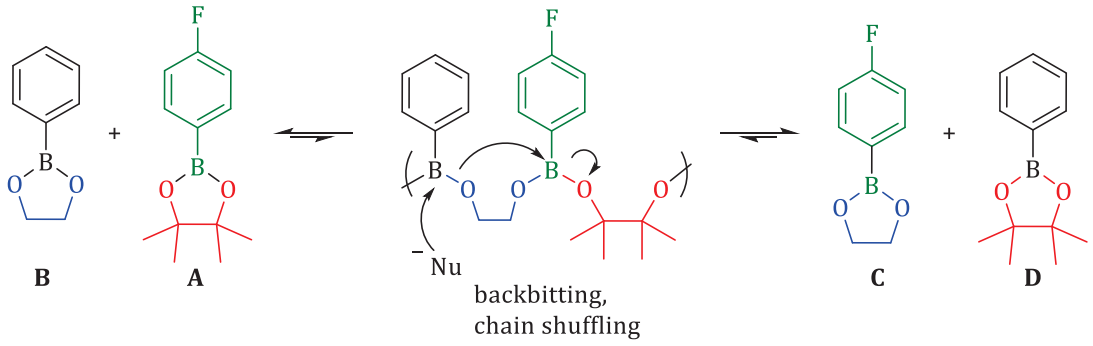

Figure III. 24: Hypothetic exchange path involving a nucleophilic assistance.

Thus, a third component, benzyl alcohol was added in the NMR tube. Benzyl alcohol was chosen for its nucleophilic character and for being non-volatile, easily available and characterizable by NMR spectroscopy. To further underpin the intervention a nucleophilic molecule in the boronate ester exchange, we re-ran an experiment in the presence of A and B and one molar equivalent of benzyl alcohol in the NMR tube at 100°C, monitored by ^{19}F NMR spectroscopy.

^{19}F NMR spectra again show the appearance of the 4-fluoro-phenyl boronate of ethylene glycol, with additional small peaks (Figure III. 27 and Figure III. 28), changing over time and potentially corresponding to intermediate products of reaction. Equilibrium between A and C was this time reached after only 10-12h, consistent with a catalytic effect of benzyl alcohol as shown in Figure III. 25.

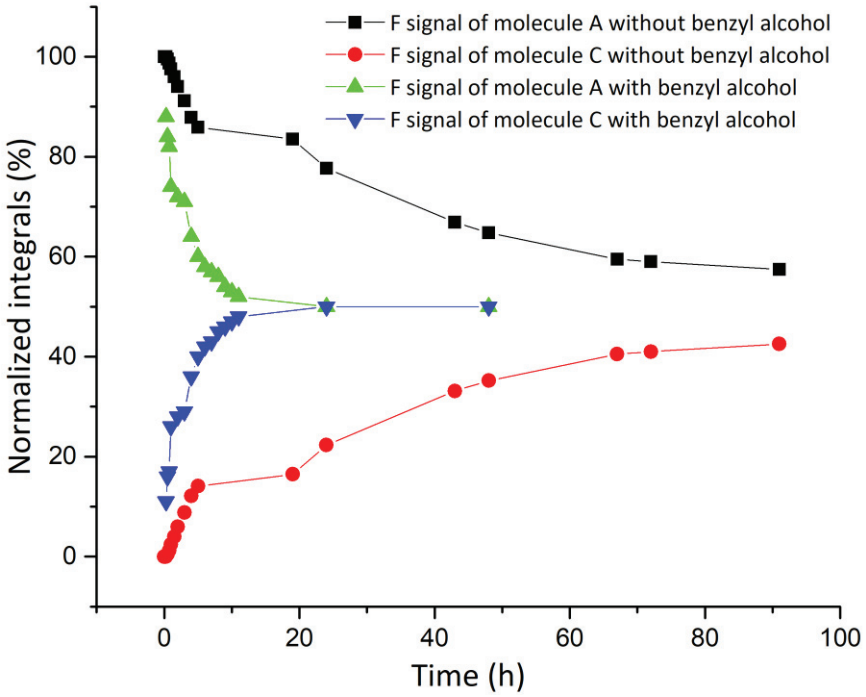

Figure III. 25: Evolution of the integrals corresponding to molecules A and C in double-tagging ^{19}F NMR experiments.

Since, 5-membered boronate rings are favored, it is logical that only minute amounts of phenyl boronate of bis(benzyl alcohol) are seen in the final spectra as depicted in Figure III. 26.

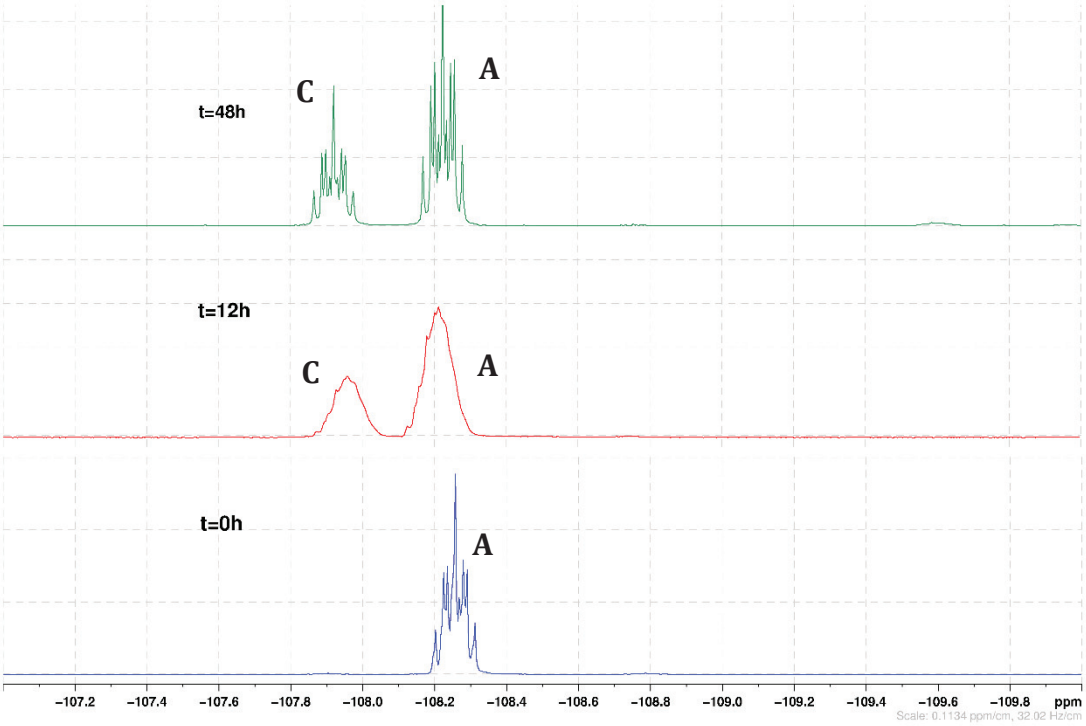

Figure III. 26: Reaction between A and B in the presence of benzyl alcohol monitored by ^{19}F NMR.

Diffusion Ordered spectroscopy (DOSY) experiments were conducted to identify some intermediates and confirmed the presence of a bigger molecule. The diffusion coefficients are obtained by combining radio-frequency pulses as used in classic NMR spectroscopy with magnetic field gradients that encode spatial information. Diffusion spectra are presented as a 2D plot with chemical shift on the horizontal axis and log(diffusion constant) on the vertical axis. The diffusion constant is larger for smaller molecules and less viscous solvents than it is for large molecules and viscous media.

This experiment confirmed the presence of a bigger molecule (with a smaller diffusion coefficient as described in Figure III. 27) and the exchanges between the boronate esters groups. The bigger molecules could correspond to intermediate such as benzyl alcohol on the boron of 4-fluorophenylboronic pinacolate inducing a ring opening of the boronate ester. It suggested that similar reactivity could be possible within the polymer bulk, thanks to the unavoidable presence of nucleophilic contaminants, such as water or residual free pinacol.

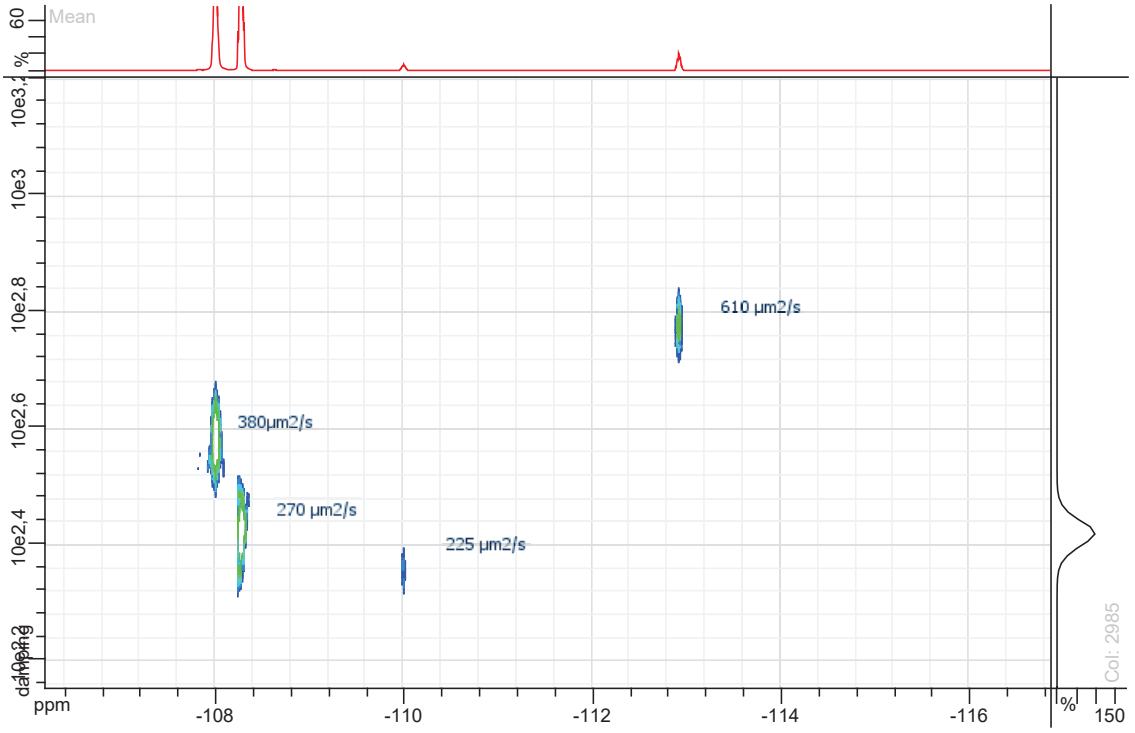

Figure III. 27: ^{19}F DOSY experiment in presence of 4-fluorophenylboronic pinacolate, phenylboronic acid, pinacol ester and benzyl alcohol.

This experiment gave the diffusion coefficients corresponding to each fluorine-containing molecule present in the reaction mixture. In inset of Figure III. 28, we show as an example the fit of attenuation curves of the signal D required to calculate the corresponding diffusion coefficient. Indeed, the diffusion rate can be calculated by a decreasing exponential fit to I versus the gradient field strength: $I(G_i) = I_0 \exp(-D(2\pi\gamma G_i \delta)^2 \left(\Delta - \frac{\delta}{3}\right))$.

Besides, the two main signals of A and C in Figure III. 28, small signals corresponding to intermediates of reaction were detected. The differences between the diffusion coefficients of these species indicate the different nature of each intermediate that involves the intervention of the nucleophile on the boron vacancy yielding the ring opening of the boronate ester groups.

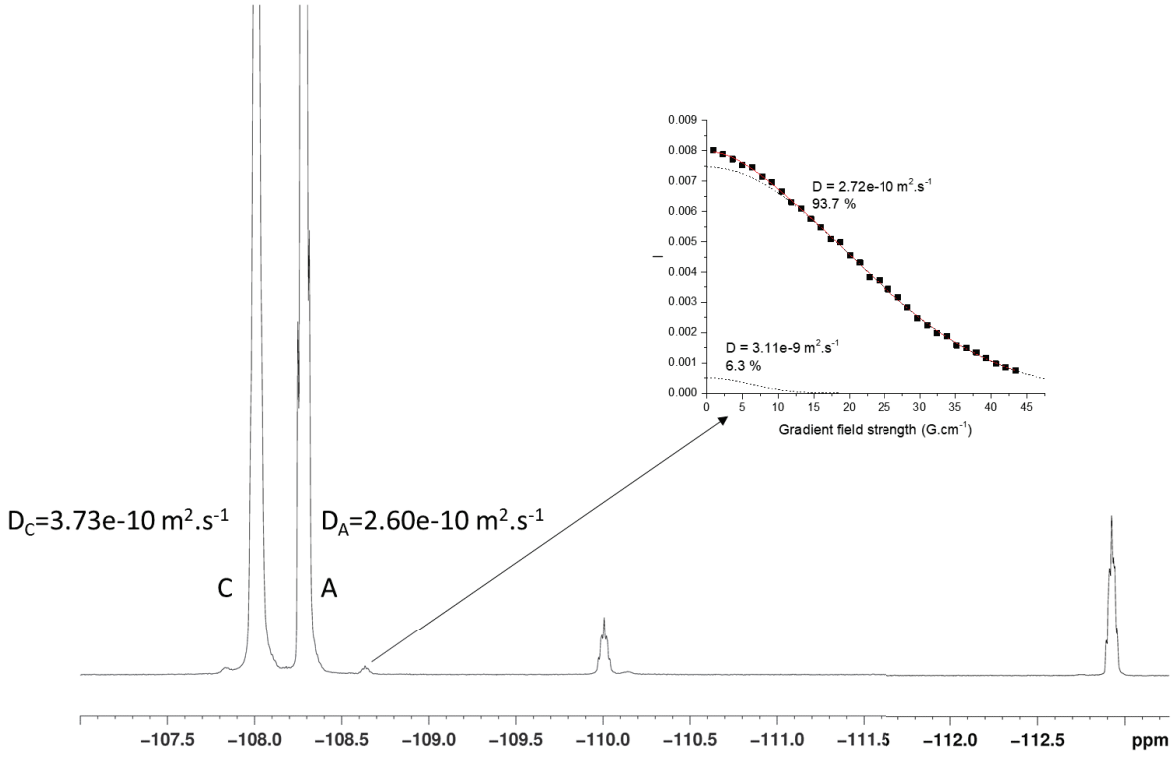

Figure III. 28: Calculation of diffusion coefficient by ^{19}F DOSY experiment via fitting attenuation curves.

B. Additional experimental observations

Dynamic gelation of a 50 wt % concentrated PSBPin solution in toluene in presence of 2 mol % of benzyl alcohol is illustrated in Figure III. 29. After heating the viscous solution for 72 h at 100°C, gelation was observed. Upon cooling to room temperature and further addition of toluene (the final concentration is 25 wt % PSBPin), immediate swelling was visible. After 2 min, the gel was fully broken, and a low-viscosity solution was obtained. This experiment was found to be reproducible above several cycles (Figure III. 29).

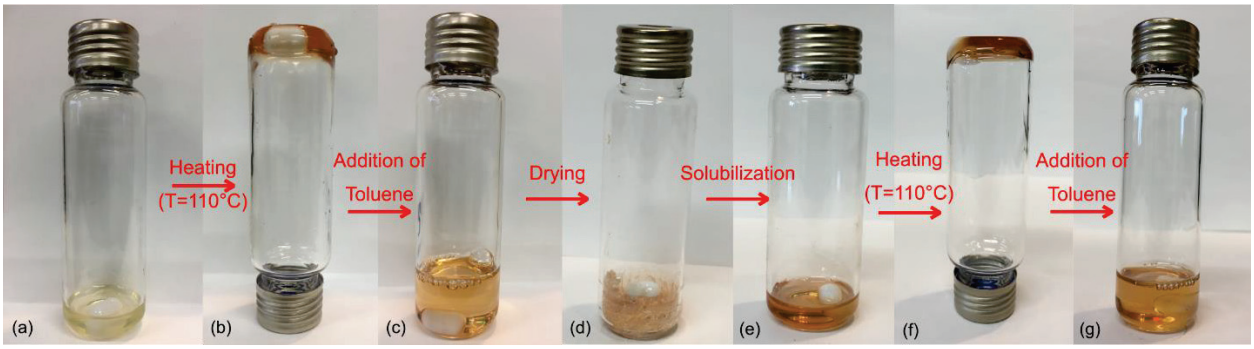

Figure III. 29: Macroscopic aspect of a solution of poly(4-vinylphenylboronic pinacolate), (a) Initial solution of poly(4-vinylphenylboronic pinacolate) at 50 wt% in toluene with 2 % molar equivalent of benzyl alcohol, (b) After 1 night at 110°C, (c) Addition of 2 mL of toluene, (d) Drying of the solution, (e) Second solution of poly(4-vinylphenylboronic pinacolate) at 50 wt% in toluene with 2 % molar equivalent of benzyl alcohol, (f) After 1 night at 110°C, (g) Addition of 2 mL of toluene.

These multiple characterization techniques lead us to conclude that the polymer was crosslinked reversibly by ring opening of the boronate ester linkages.

Indeed, when an apolar solvent is added such as toluene, the inverse path is happening since the intramolecular 5-membered cyclic boronates are entropically favored.

Figure III. 30 displays the chromatograms in toluene of fresh PSBPin and PSBPin after a heating segment at 200°C during 4 h. As no significant change occurred, it appears that the crosslinking reaction is dynamic, and can be fully reversed upon dilution.

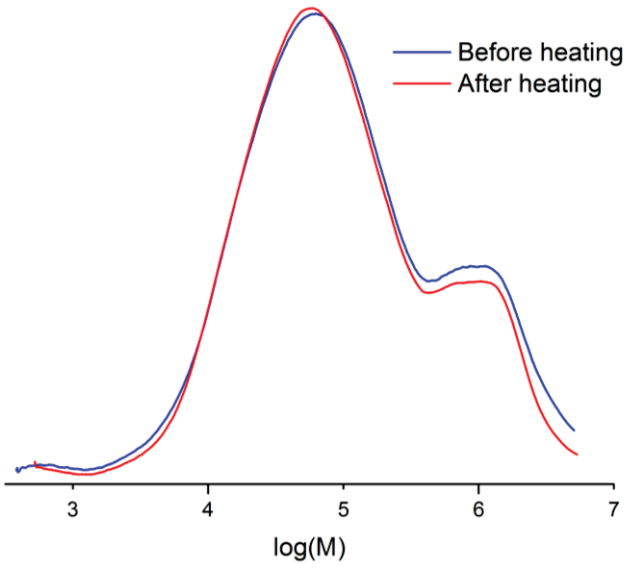

Figure III. 30: Chromatograms of PSBPin before and after a thermic treatment at 200°C during 4 h.

C. Input of DFT calculations in the establishment of the mechanism

Considering the body of evidence obtained so far, we suggest that the ring opening of the boronates releases a free pinacolate moiety that can further reach neighbouring boron atoms thus acting as a rigid crosslink between PSBPin chains as illustrated in Figure III. 31. This leads to a strong decrease in the chain mobility, consistently with the very high T_g observed. DSC and rheology data corroborated this ring opening occurring at high temperatures (130-180°C) and the subsequent dynamic character of the crosslinks formed.

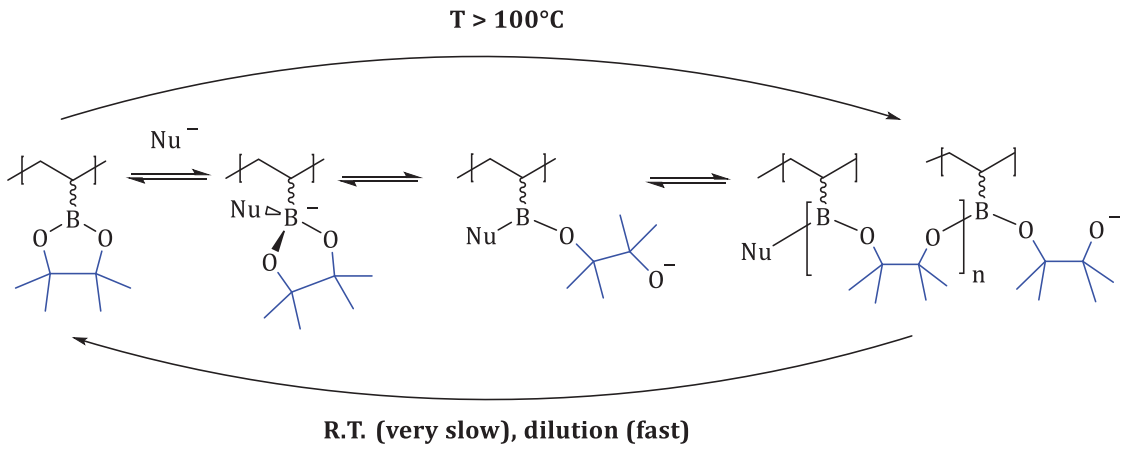

Figure III. 31: Mechanism of ring-opening and subsequent cross-linking induced by a nucleophilic assistance.

Thanks to the intervention of a nucleophilic molecule and the increase of temperature, the opening of the boronate ester group is possible. The boron has a tetrahedral rather than a trigonal environment with the intervention of the nucleophile. This nucleophile can be a water molecule or a pinacol left from the synthesis of the boronate ester. This permits the opening of the pyramidalized boronate group yielding a pendent singly attached diol-derived nucleophile connecting another boron atom, and so forth. The pendent negatively charged group reacts with the electronic vacancy of another boron, which, when borne by another chain results in crosslinking. However, when an apolar solvent is added such as toluene, the inverse path is happening. Indeed, the intramolecular 5-membered cyclic boronates are entropically favored.

Regarding the initiation of the ring opening, the involvement of a nucleophile and the assistance by an acid seem compulsory: adventitious water or the residual pinacol molecules remaining from the synthesis could fill both roles. The nucleophilic attack at boron and the subsequent ring opening would lead to singly attached pinacol group readily available to initiate ring opening of a proximal pinacol boronate, ultimately triggering bridge formation.

We resorted to computational mechanistic investigation performed at the DFT level in order to assess the enthalpy of ring opening of these pinacol boronates. In this investigation, PSBPin units have been represented by phenyl pinacol boronate and a water molecule has been used a

prototype nucleophile. At room temperature, the interaction of H_2O with a pinacol oxygen atom *via* H-bonding is exothermic by 4.4 kcal.mol^{-1} at 293 K. This adduct will be taken as the energy reference hereafter. From this adduct, the subsequent ring opening to yield a singly attached pinacol substituted boronic acid is endothermic by 3 kcal.mol^{-1} (Figure III. 32). In Gibbs energy, the reaction is endergonic by 4.0 kcal.mol^{-1}. Consequently, the ring opening is slightly entropically favoured but requires heating to circumvent the endothermicity of the reaction.

This thermodynamic trend is consistent both with the net endothermic reaction measured in medium pressure capsules by DSC (Figure III. 9) and with crosslinking observed above 100°C. We infer that this system, with a peculiar thermodynamic balance between the enthalpic and entropic contributions, is reminiscent of floor-temperature polymerizations already demonstrated in several low-strained cyclic monomers. [51], [52]

Kinetically, the enthalpy (resp. Gibbs energy) barriers corresponding to ring opening is calculated 27 (resp. 30) kcal.mol^{-1} above the water adduct, with a clear pyramidalisation induced by H_2O nucleophilic attack at B through O. Interestingly, the energy barrier corresponding to a direct metathesis has been estimated to 70 kcal.mol^{-1} relative to free pinacolborane. This mechanism can thus be confidently ruled out. The results are presented in Figure III. 32.

Even though the overall entropy of the system would likely limit the extent of oligomerization, bridging between boron atoms appears sufficient to trigger dense crosslinking at high temperature. Furthermore, the de-crosslinking induced at high dilutions is likely entropically driven by the formation of the more favoured intramolecular 5-membered cycle in the presence of a high concentration of solvent molecules. This de-crosslinking should also be favoured at low temperatures but is most probably kinetically frozen by the glass transition in PSBPin.

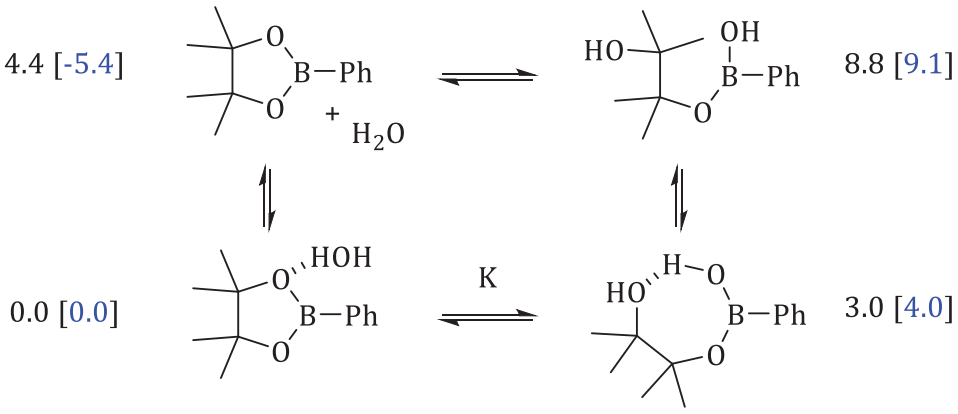

Figure III. 32. Relative enthalpies $\Delta_r H$ and Gibbs energy [$\Delta_r G$] values (kcal.mol^{-1}) for different intermediates calculated at the DFT level (298.15 K, 1 atm, SMD(TolH), M06-def2TZVP).

The Gibbs free energy, also called Gibbs function, is defined as:

$$G = H - TS$$

where S refers to the entropy and H to the enthalpy of the system. The Gibbs free energy of the system is a state function as it is defined in terms of thermodynamic properties that are state functions. Under constant temperature, the relative free energy change becomes:

$$\Delta_r G = \Delta_r H - T\Delta_r S$$

In our case, thanks to DFT data, it is possible to write:

$$\Delta_r G(298.15\ K) = \Delta_r H(298.15\ K) - 298.15\Delta_r S(298.15\ K)$$

As an approximation, the relative enthalpies and entropies are constant over the temperature and the expression becomes:

$$\Delta_r G(T) = \Delta_r H(298.15\ K) - T\Delta_r S(298.15\ K)$$

It is thus possible to calculate the relative Gibbs energy at each defined temperature. Besides, another expression of the relative Gibbs energy implies the equilibrium constant of the reaction such as:

$$\Delta_r G(T) = -RT\ lnK$$

Thanks to these equations and DFT data, we are able to determine the equilibrium constant K of the ring opening reaction at different temperatures. Thus, we obtained the following results:

K(25°C)=0.0018; K(50°C)=0.00174; K(100°C)=0.00326.

By assuming that the increase of temperature constantly increases the number of linkages in the system, it is possible to construct the following graph in Figure III. 33 presenting the evolution of the equilibrium constant with the temperature. The increase of temperature results in the increase of the equilibrium constant and thus favored the ring-opening reaction.

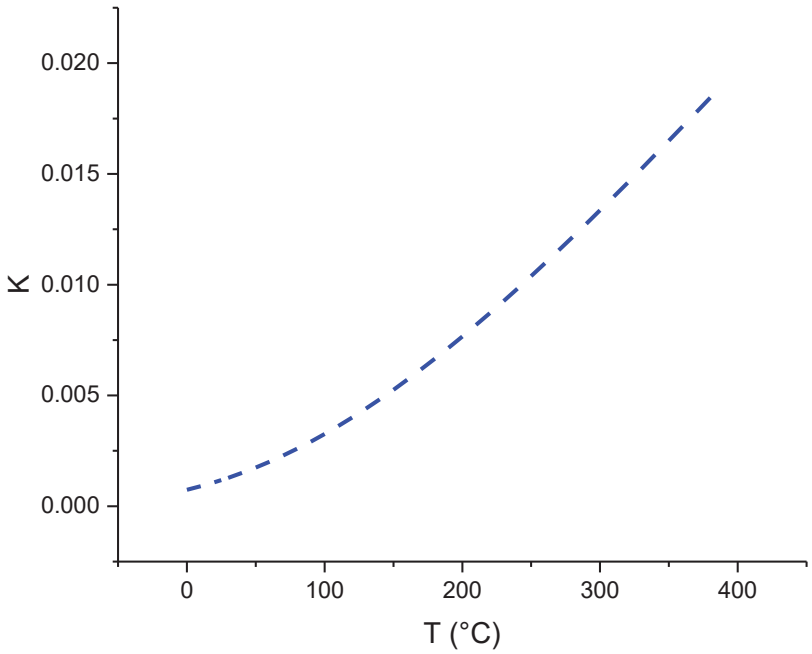

Figure III. 33: Assumed evolution of the equilibrium constant with the temperature.

VII. Conclusion

The synthesis of poly(4-vinylphenylboronic pinacolate) was optimized to reach high molar masses. These polymers were characterized by a wide variety of analytical methods that enabled us to identify interesting dynamic behavior inherent to the polymer that highly caught our attention. Indeed, we obtained polymers with high glass transition temperatures shifted by a reactivity path involving crosslinking between the polymer chains. To deepen our understanding and to evidence the contribution of the 4-vinylphenylboronic pinacolate, it was determined to synthesize copolymers from 4-vinylphenylboronic pinacolate and styrene at different composition. The increase of glass transition temperature obtained after reaction with the increase of the 4-vinylphenylboronic pinacolate molar ratio in the copolymer showed the interest of incorporating such a monomer to reach high glass transition temperatures.

Thanks to differential scanning calorimetry, ss-NMR, DRIFT and rheology, we were able to formulate the mechanism involved in the dynamic crosslinking observed experimentally. We put in evidence a mechanism involving the ring opening of boronates *via* nucleophilic assistance that was highlighted through model compounds and ^{19}F NMR spectroscopy.

This allows for the opening of the pyramidalized boronate group yielding a pendent singly-attached pinacol-derived nucleophile connecting another boron atom, and so forth. The pendent negatively charged group reacts with the electronic vacancy of another boron, which, when borne by another chain results in crosslinking. However, when an apolar solvent is added such as toluene, the inverse path is happening. Indeed, the intramolecular 5-membered cyclic boronates are entropically favored. These specifics guarantee the reversibility of the system.

When comparing our system to vitrimers and CANs, that have either constant crosslinking densities or continuously decreasing crosslinking densities with temperature, it is exciting to note that polymers bearing cyclic boronate esters may constitute the first example of a distinct class of dynamic networks, with a crosslinking density increasing with temperature, at least within a defined temperature range.

We thus reported new reprocessable high-T_g materials advantageously utilizing the reactivity of boron. We demonstrated that the creation of reversible boronate-based bridges between polymeric chains could be exploited to design materials with adjustable glass transitions. We foresee valuable new boron-based materials that could harness this reactivity not only to tune glass transition temperatures and inherent mechanical properties by modifying the backbone of the polymer but also change the dynamic characteristics of the system by appropriately selecting the boronate pendent groups.

VIII. References

[1] F. Jäkle, "Advances in the Synthesis of Organoborane Polymers for Optical, Electronic and Sensory Applications," *Chem. Rev.*, vol. 110, no. 2, pp. 3985–4022, **2010**.

[2] W. L. A. Brooks and B. S. Sumerlin, "Synthesis and Applications of Boronic Acid-Containing Polymers: From Materials to Medicine," *Chem. Rev.*, vol. 116, pp. 1375–1397, **2016**.

[3] G. A. Molander and N. Ellis, "Organotrifluoroborates: Protected Boronic Acids That Expand the Versatility of the Suzuki Coupling Reaction," *Acc. Chem. Res.*, vol. 40, pp. 275–286, **2007**.

[4] E. P. Gillis and M. D. Burke, "Multistep Synthesis of Complex Boronic Acids from Simple MIDA Boronates Multistep Synthesis of Complex Boronic Acids from Simple MIDA Boronates," *J. Am. Chem. Soc.*, vol. 130, pp. 14084–14085, **2008**.

[5] D. M. Knapp, E. P. Gillis, and M. D. Burke, "A general solution for unstable boronic acids: Slow-release cross-coupling from air-stable MIDA boronates," *J. Am. Chem. Soc.*, vol. 131, pp. 6961–6963, **2009**.

[6] D. V. Partyka, "Transmetalation of Unsaturated Carbon Nucleophiles from Boron-Containing Species to the Mid to Late d-Block Metals of Relevance to Catalytic C-X Coupling Reactions (X=C, F, N, O, Pb, S, Se, Te)," *Chem. Mater.*, vol. 111, pp. 1529–1595, **2011**.

[7] A. Biffis, P. Centomo, A. Del Zotto, and M. Zecca, "Pd Metal Catalysts for Cross-Couplings and Related Reactions in the 21st Century: A Critical Review," *Chem. Rev.*, vol. 118, pp. 2249–2295, **2018**.

[8] J. N. Cambre and B. S. Sumerlin, "Biomedical applications of boronic acid polymers," *Polymer (Guildf).*, vol. 52, no. 21, pp. 4631–4643, **2011**.

[9] W. Yang, X. Gao, and B. Wang, "Biological and Medicinal Applications of Boronic Acids," in *Boronic Acids: Preparation and Applications in Organic Synthesis and Medicine*, D. G. Hall, Ed. **2006**, pp. 481–512.

[10] K. Kataoka, H. Miyazaki, and M. Bunya, "Totally Synthetic Polymer Gels Responding to External Glucose Concentration: Their Preparation and Application to On-Off Regulation of Insulin Release," *J. Am. Chem. Soc.*, vol. 120, pp. 12694–12695, **1998**.

[11] O. R. Cromwell, J. Chung, and Z. Guan, "Malleable and Self-Healing Covalent Polymer Networks through Tunable Dynamic Boronic Ester Bonds," *J. Am. Chem. Soc.*, vol. 137, p. 6492–6495, **2015**.

[12] J. J. Cash, T. Kubo, A. P. Bapat, and B. S. Sumerlin, "Room-Temperature Self-Healing Polymers Based on Dynamic-Covalent Boronic Esters," *Macromolecules*, vol. 48, pp. 2098–2106, **2015**.

[13] D. Montarnal, M. Capelot, F. Tournilhac, and L. Leibler, "Silica-Like Malleable Materials from Permanent Organic Networks," *Science (80-.).*, vol. 334, pp. 965–969, **2011**.

[14] W. Denissen, J. M. Winne, and F. E. Du Prez, "Vitrimers: permanent organic networks with glass-like fluidity," *Chem. Sci.*, vol. 7, pp. 30–38, **2016**.

[15] L. Imbernon and S. Norvez, "From landfilling to vitrimer chemistry in rubber life cycle," *Eur. Polym. J.*, vol. 82, pp. 347–376, **2016**.

[16] B. T. Worrell *et al.*, "Bistable and photoswitchable states of matter," *Nat. Commun.*, vol. 9, p.

2804, **2018**.

[17] X. Chen *et al.*, "A Thermally Re-mendable Cross-Linked Polymeric Material," *Science (80-.).*, vol. 295, pp. 1698–1703, **2002**.

[18] C. N. Bowman and C. J. Kloxin, "Covalent Adaptable Networks: Reversible Bond Structures Incorporated in Polymer Networks," *Angew. Chemie - Int. Ed.*, vol. 51, pp. 4272–4274, **2012**.

[19] R. J. Wojtecki, M. A. Meador, and S. J. Rowan, "Using the dynamic bond to access macroscopically responsive structurally dynamic polymers," *Nat. Mater.*, vol. 10, pp. 14–27, **2011**.

[20] W. Zou, J. Dong, Y. Luo, Q. Zhao, and T. Xie, "Dynamic Covalent Polymer Networks: from Old Chemistry to Modern Day Innovations," *Adv. Mater.*, vol. 29, p. 1606100, **2017**.

[21] O. R. Cromwell, J. Chung, and Z. Guan, "Malleable and Self-Healing Covalent Polymer Networks through Tunable Dynamic Boronic Ester Bonds," *J. Am. Chem. Soc.*, vol. 137, no. 20, pp. 6492–6495, **2015**.

[22] M. Röttger, T. Domenech, R. van der Weegen, A. Breuillac, R. Nicolaÿ, and L. Leibler, "High-performance vitrimers from commodity thermoplastics through dioxaborolane metathesis," *Science (80-.).*, vol. 356, no. 6333, pp. 62–65, **2017**.

[23] D. Kyriacos, *High-Temperature Engineering Thermoplastics*. Elsevier Ltd, **2017**.

[24] T. Kaiser, "Highly crosslinked polymers," *Prog. Polym. Sci.*, vol. 14, pp. 373–450, **1989**.

[25] T. Liu *et al.*, "A Self-Healable High Glass Transition Temperature Bioepoxy Material Based on Vitrimer Chemistry," *Macromolecules*, vol. 51, pp. 5577–5585, **2018**.

[26] R. L. Letsinger and S. B. Hamilton, "Organoboron Compounds. X. Popcorn Polymers And Highly Cross-Linked Vinyl Polymers Containing Boron," *J. Am. Chem. Soc.*, vol. 81, no. 12, pp. 3009–3012, **1959**.

[27] Y. Qin, V. Sukul, D. Pagakos, C. Cui, and F. Jäkle, "Preparation of organoboron block copolymers *via* ATRP of silicon and boron-functionalized monomers," *Macromolecules*, vol. 38, pp. 8987–8990, **2005**.

[28] W. Brostow, H. E. Hagg Lobland, and S. Khoja, "Brittleness and toughness of polymers and other materials," *Mater. Lett.*, vol. 159, pp. 478–480, **2015**.

[29] C. B. Baltus *et al.*, "Olefin cross-metathesis/Suzuki-Miyaura reactions on vinylphenylboronic acid pinacol esters," *Tetrahedron Lett.*, vol. 54, no. 10, pp. 1211–1217, **2013**.

[30] J. Pellon, L. H. Schwind, M. J. Guinard, and W. M. Thomas, "Polymerization of vinyl monomers containing boron II. p-vinylphenylboronic acid," *J. Polym. Sci.*, vol. 55, pp. 161–167, **1961**.

[31] A. C. Toohey and K. E. Weale, "Chain transfer to solvent in styrene polymerization," *Trans. Faraday Soc.*, vol. 58, pp. 2439–2445, **1962**.

[32] H. Kamogawa and S. Shiraki, "Effect of Pendant Functional Alcohol Residues of (p-Vinylphenyl)borate Copolymers on Hydrolysis," *Macromolecules*, vol. 24, pp. 4224–4226, **1991**.

[33] M. Hartmann, H. Carlsohn, and J. Pauls, "Über Copolymere der p-Vinylbenzolboronsaure mit Styrol," *Die Makromol. chemie*, vol. 177, pp. 131–144, **1976**.

[34] G. Kahraman, O. Beskares, Z. M. O. Rzaev, and E. Piskin, "Bioengineering polyfunctional copolymers. VII. Synthesis and characterization of copolymers of p-vinylphenyl boronic acid with maleic and citraconic anhydrides and their self-assembled macrobranched supramolecular architectures," *Polymer (Guildf).*, vol. 45, pp. 5813–5828, **2004**.

[35] G. Giffels, J. Beliczey, M. Felder, and U. Kragl, "Polymer enlarged oxazaborolidines in a membrane reactor: Enhancing effectivity by retention of the homogeneous catalyst," *Tetrahedron: Asymmetry*, vol. 9, pp. 691–696, **1998**.

[36] J. M. G. Cowie, *Polymers: Chemistry & Physics of Modern Materials (2nd Edition)*. **1991**.

[37] F. R. Mayo and F. M. Lewis, "Copolymerization. I. A Basis for Comparing the Behavior of Monomers in Copolymerization; The Copolymerization of Styrene and Methyl Methacrylate," *J. Am. Chem. Soc.*, vol. 66, no. 9, pp. 1594–1601, **1944**.

[38] K. F. O'Driscoll, L. T. Kale, L. H. G. Rubio, and P. M. Reilly, "Applicability of the Mayo–Lewis equation to high conversion copolymerization of styrene and methylmethacrylate," *J. Polym. Sci. Polym. Chem. Ed.*, vol. 22, no. 11, pp. 2777–2788, **1984**.

[39] M. Fineman and S. Ross, "Linear Method for Determining Monomer Reactivity Ratios in Copolymerization," *J. Polym. Sci.*, vol. 5, no. 2, pp. 259–265, **1950**.

[40] M. Gordon and J. S. Taylor, "Ideal copolymers and the second-order transitions of synthetic rubbers.," *J. Appl. Chem.*, vol. 2, pp. 493–500, **1952**.

[41] Y. Qin, V. Sukul, D. Pagakos, C. Cui, and F. Jäkle, "Preparation of organoboron block copolymers *via* ATRP of silicon and boron-functionalized monomers," *Macromolecules*, vol. 38, no. 22, pp. 8987–8990, **2005**.

[42] P. Kubelka and F. Munk, "Ein Beitrag zur Optik der Farbanstriche," *Zeitschrift für Tech. Phys.*, vol. 12, pp. 593–601, **1931**.

[43] D. Massiot *et al.*, "Modelling one- and two-dimensional solid-state NMR spectra," *Magn. Reson. Chem.*, vol. 40, pp. 70–76, **2002**.

[44] S. Oh, J. W. E. Weiss, P. A. Kerneghan, I. Korobkov, K. E. Maly, and D. L. Bryce, "Solid-state ^{11}B and ^{13}C NMR, IR, and X-ray crystallographic characterization of selected arylboronic acids and their catechol cyclic esters," *Magn. Reson. Chem.*, vol. 50, pp. 388–401, **2012**.

[45] Y.-T. Angel Wong and D. L. Bryce, *Recent Advances in ^{11}B Solid-State Nuclear Magnetic Resonance Spectroscopy of Crystalline Solids*, vol. 93. Academic Press, **2018**.

[46] M. L. Williams, R. F. Landel, and J. D. Ferry, "The Temperature Dependence of Relaxation Mechanisms in Amorphous Polymers and Other Glass-forming Liquids," *J. Am. Chem. Soc.*, vol. 77, no. 14, pp. 3701–3707, **1955**.

[47] S. Arrhenius, "Über die Reaktionsgeschwindigkeit bei der Inversion von Rohrzucker durch Säuren," *Zeitschrift für Phys. Chemie*, vol. 4U, no. 1, pp. 226–248, **1889**.

[48] M. Capelot, M. M. Unterlass, and L. Leibler, "Catalytic Control of the Vitrimer Glass Transition," *ACS Macro Lett.*, vol. 1, pp. 789–792, **2012**.

[49] M. M. Obadia, A. Jourdain, P. Cassagnau, D. Montarnal, and E. Drockenmuller, "Tuning the Viscosity Profile of Ionic Vitrimers Incorporating 1,2,3-Triazolium Cross-Links," *Adv. Funct. Mater.*, vol. 27, pp. 1703258–17003268, **2017**.

[50] U. Gerwarth, "Rearrangements of medium sized O-B-O heterocycles to cyclic oligomers,"

Naturforsch, vol. 32b, pp. 1408–14145, **1977**.

[51] S. Penczek, A. Duda, K. Kaluzynski, G. Lapienis, A. Nyk, and R. Szymanski, "Thermodynamics and kinetics of ring-opening polymerization of cyclic alkylene phosphates," *Makromol. Chem.*, vol. 73, pp. 91–101, **1993**.

[52] S. Strandman, E. Gautrot, and X. X. Zhu, "Recent advances in entropy-driven ring-opening polymerizations," *Polym. Chem.*, vol. 2, pp. 791–799, **2011**.

Chapter 4:

Extension of pinacol boronates reactivity to a wide variety of polymers

Chapter 4 describes the extension of the concepts established in Chapter 3 to a wide variety of copolymers. Styrenic-based organoboron monomers are copolymerized with acrylates, while vinylic-based organoboron monomers are homopolymerized and copolymerized with vinyl acetate or ethylene. Hydroboration of polybutadiene is also presented for the introduction of boronate ester on pre-synthesized polymers. A breakthrough concept is also investigated with the design of an organic/inorganic hybrid system based a trifunctional boronate ester small molecule that induces the creation of glasses. All (co)polymers are studied through spectroscopic and mechanical analyses.

Table of contents

I. Introduction

In this chapter, we will extend the concepts previously described about the dynamic crosslinking induced by the reactivity of boronate ester moieties between 100°C and 130°C in (co)polymers. We got interested in harnessing this reactivity to afford dynamic crosslinked networks with a variety of polymers and in the ability to finely tune the glass transition temperature of a copolymer by incorporating a controlled amount of reactive monomers.

From a commercial point of view, crosslinking is one of the most important reaction of vinyl polymers and is fundamental to the rubber and elastomer industries. Crosslinked polymers found applications in many uses in the daily life. The most famous example of the utilization of crosslinked polymer for tire productions through process of vulcanization of polybutadiene. They can also be present in coatings, adhesives or electronic parts. Crosslinking bring the entangled material interesting mechanical properties since elastomers and plastics show stronger modulus and no flowing is allowed even at high temperature. At temperatures above the glass transition temperature, tridimensional networks present a rubbery plateau that is theoretically infinite. In addition, the crosslinked networks show a higher stability and heat resistance. When a stress is applied to a crosslinked polymer, it can be deformed several time its length and this deformation can be maintained for a very long time but always resume its original dimensions once released. This behavior contrasts with that of usual solids that can only support reversible deformations of a few percent.

Crosslinking can be induced by a variety of reactions such as:

- Vulcanization, using peroxides, sulfur or sulfur-containing compounds,
- Free radical reactions by ionizing radiation,
- Photolysis *via* photosensitive functional groups,
- Interactions between ionic species,
- Chemical reactions of labile functional groups, which is our method of interest in this part.

Two families of crosslinking exist: chemical crosslinking with the formation of bonds between the polymer chains that induces the creation of a network, and physical crosslinking with the presence of interactions (for instance, ionic interactions) that bring the crosslinked character of the polymer. This distinction can also be made in term of energy of bonds between the crosslinked polymer chains. Indeed, physical crosslinking is based on weak bonds between 1 and 3 kcal/mol whereas chemical crosslinking related on strong bonds between 60 and 100 kcal/mol that can be covalent in some cases. The difference between these two distinct systems is represented in Figure IV. 1.

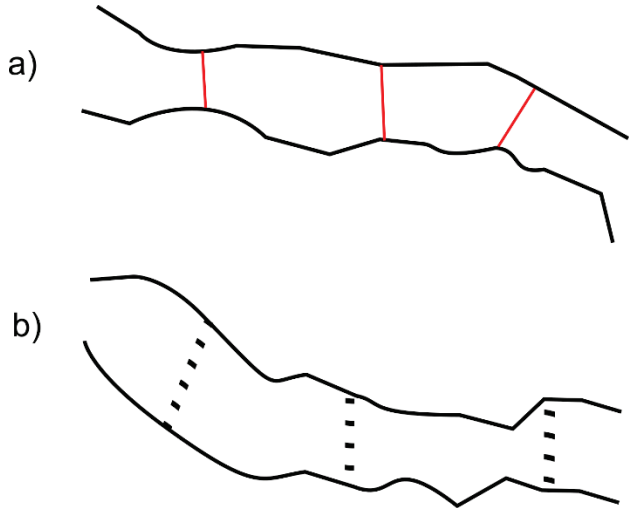

Figure IV. 1: Scheme of chemical (a) and physical (b) crosslinking.

The main drawback of the chemically crosslinked polymers is the difficulty to recycle them. Indeed, as the polymers chains are covalently linked to one another, the crosslinked materials cannot dissolve in solvent but will only swell in solution. Some elastomers exhibit reversible crosslinks that can help recyclability of the materials. In the case of physical crosslinking, the crosslinks are noncovalent or from secondary interactions with less energy between the polymer chains including hydrogen and ionic bonds and thus reversible given the system.

We previously reported the interest of boronate ester cycles in the creation of reversible crosslinking in styrene (co)polymers. This approach was applied to common polymers from acrylate, vinyl or ethylene monomers, representing a wide part of the commercialized polymers worldwide, to probe lower glass transition temperatures. Indeed, we could deepen our understanding of boronate esters reactivity with different polymers by changing the backbone studied and decoupling the crosslinking from the changes of glass transition temperature.

Three main strategies will be used in this part in order to incorporate boronate ester groups in polymer backbone:

- Copolymerization of boron-based monomer with common comonomers such as n-butyl acrylate, vinyl acetate, ethylene.
- Functionalization of existing polymers with the case of high molar masses polybutadiene.
- Use of molecules carrying more than one boronate ester groups (functionality>1) to construct 3D-networks at the frontier between organic and inorganic chemistries. (balance between organic segments and inorganic parts)

We will divide this work in two main parts: firstly, aryl-boron derivatives will be studied and, secondly, vinyl-boron derivatives will be assessed. The structures are schematically presented in Figure IV. 2.

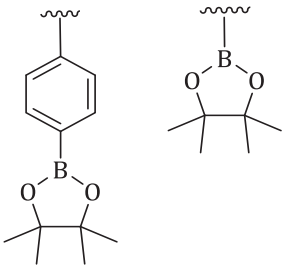

Figure IV. 2: Left: Aryl-boron systems; Right: Vinyl-boron systems.

For each system, the synthesis and characterization of the polymers and copolymers will be fully presented. The influence of the presence of boronate esters will be discussed by the study of the mechanical properties of the synthesized (co)polymers. Several methods of characterization will be used such as spectroscopic, thermal and mechanical methods.

II. Aryl-boron derivatives

This part is dedicated to the extension of the concepts established in the last Chapter to other aryl-boron systems with new copolymers and multifunctional small molecules.

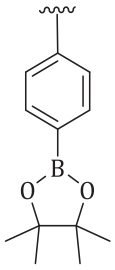

Figure IV. 3: Aryl-boron systems.

A. Copolymers with n-butyl acrylate

a. Synthesis of copolymers from 4-vinylphenylboronic pinacolate and n-butyl acrylate

The strategy of synthesis of copolymers from 4-vinylphenylboronic pinacolate and n-butyl acrylate was the same than for the synthesis of copolymers from 4-vinylphenylboronic pinacolate and styrene studied in Chapter 3. Copolymers involving 4-vinylphenylboronic pinacolate monomer and usual comonomers such as styrene, vinylpyrrolidone, acrylonitrile, maleic anhydride and others have already been reported in the literature. [1]–[5]

We used free radical polymerization between the two co-monomers after the synthesis of the boron-based monomer according to established method involving the transesterification between 4-vinylboronic acid and pinacol. [6] **The conditions of polymerization were the same than in Chapter 3, i.e. the polymerization occurred in toluene with 0.02 molar equivalent of benzoyl peroxide at the temperature of 70°C.**

It was assumed that these optimized conditions could afford higher molar masses (in particular M_w) and thus better mechanical properties as already mentioned in Chapter 2. The ratios of monomers in the reaction were adapted to the ratios targeted within the copolymer. The polymerization is illustrated below in Figure IV. 4:

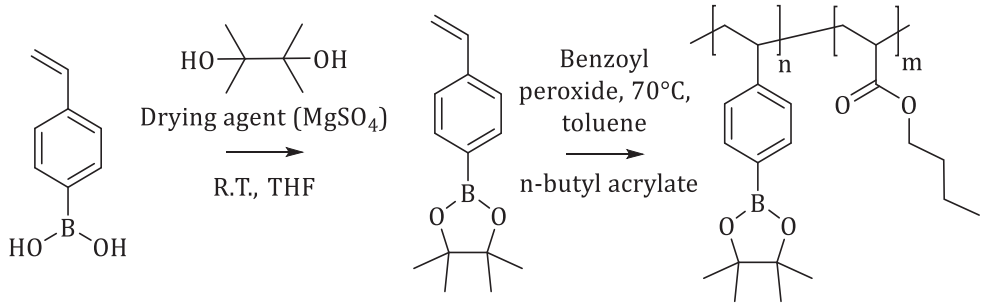

Figure IV. 4: Synthesis of poly(4-vinylphenylboronic pinacolate-co-n-butyl acrylate).

In this study, the copolymer from 4-vinylboronic pinacolate and n-butyl acrylate will be noted as PBA-SBPin – x % with x the molar amount of the boron-based monomer in the final copolymer. This ratio was varied over a large range to screen a variety of copolymers and to finely probe the influence of boronate-ester moities on the mechanical and thermal polymer properties. The molar contents of each co-monomer were calculated based on NMR spectra presented from Figures V. 70 to V. 79 and the chromatograms are depicted in Figure V. 81 in the Experimental Section.

After the syntheses, we obtained copolymers with the properties described in Table IV. 1:

Table IV. 1: Experimental data of the copolymers synthesized from n-butyl acrylate and 4-vinylphenylboronic pinacolate PBA-SBPin – x %. [1]Molar ratio of 4-vinylphenylboronic pinacolate monomer. [2]Values determined by SEC-THF using PS standards and conventional calibration.

Entry	***Theoretical ratio x %[1]***	***Experimental ratio x %[1]***	***M_n (g/mol)[2]***	***M_w (g/mol)[2]***	***Dispersity Đ***	***Yield***
1	10	8	61 000	221 000	3.6	84 %
2	20	18	61 000	217 000	3.5	72 %
3	50	48	44 000	128 000	2.9	65 %
4	80	83	25 000	36 000	1.5	72 %
5	90	90	36 000	495 000	13.6	75 %

The theoretical and experimental ratios of the boronate ester monomer are quite close for each experiment and the yields are close for all the syntheses. The molar masses are quite high which was our goal; however, one of the main drawbacks is the high dispersity measured by size exclusion chromatography, arising from recombination reactions, as aforementioned in Chapter 3.

Thanks to these data, we were able to estimate the reactivity ratios of the two monomers present in the polymerization process. We compared the results obtained by two methods: Mayo-Lewis and Fineman-Ross equations, already detailed in the previous chapter.

Here, we define the reactivity ratios of the two monomers respectively r_1 and r_2 for n-butyl acrylate and 4-vinylphenylboronic pinacolate as:

$$r_1 = {}^{k_{11}}/_{k_{12}} \text{ and } r_2 = {}^{k_{22}}/_{k_{21}}$$

with k_{11} (and k_{22}) the rate constants for addition of n-butyl acrylate (4-vinylboronic pinacolate) to a n-butyl acrylate (respectively 4-vinylboronic pinacolate) chain end and k_{12} (and k_{21}) the rate constants for addition of n-butyl acrylate (4-vinylboronic pinacolate) to a 4-vinylphenylboronic pinacolate (respectively n-butyl acrylate) chain end.

Relying on the Mayo-Lewis equation, plots are generated with arbitrary r_2 values from the experimental data. The intersection of the lines gives the r_1 and r_2 values for the system studied. Following this method, we obtained the graphic in Figure IV. 5 and we found r_1=1.31 and r_2=1.23 for n-butyl acrylate and 4-vinylphenylboronic pinacolate monomers respectively.

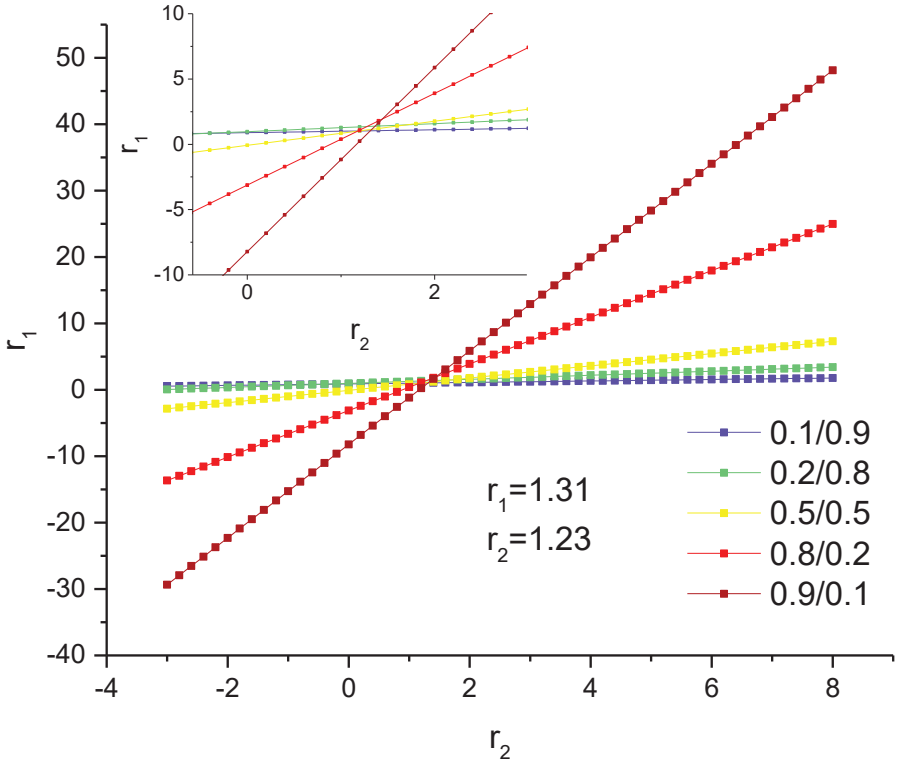

Figure IV. 5: Reactivity ratio determination by Mayo-Lewis equation with the plot of r_1 depending on r_2 for each couple of monomer composition f_1/f_2. Inset: Zoom on the crossing area.

To confirm our determination of the reactivity ratios, we also used the Fineman-Ross method plotting A versus B, parameters related to the theoretical and experimental compositions, that gave us a straight line with slope r_1 and intercept r_2 as showed in Figure IV. 6. This conducted to the following reactivity ratios: r_1=1.32 and r_2=1.23 respectively for the n-butyl acrylate co-monomer and the 4-vinylphenylboronic pinacolate co-monomer in the copolymer synthesized by free radical polymerization.

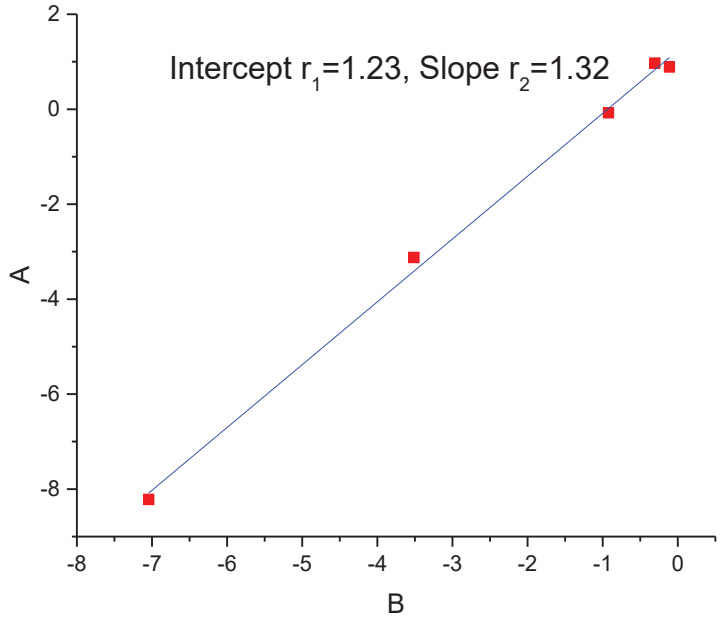

Figure IV. 6: Reactivity ratio determination by Fineman-Ross equation.

The two calculation methods used conducted to very close results validating the final values of the reactivity ratios. They were found to be close to 1, indicating the formation of statistical copolymers. Small blocks of n-butyl acrylate can however be induced *via* the feed composition deviating from a 50/50 mixture of the two monomers. More precise results on the reactivity ratios would have been obtained by stopping the copolymerizations at lower conversions.

After the copolymer syntheses, we focused on the thermal properties of our systems firstly through differential scanning calorimetry investigation.

b. Differential scanning calorimetry investigation

After drying process under vacuum, the synthesized organoboron polymers were characterized by differential scanning calorimetry (DSC) and we recognized the interesting thermal behavior observed in Chapter 3. All DSC thermograms are visible from Figures V. 82 to V. 86 in the Experimental Section.

Firstly, Figure IV. 7 shows DSC analysis of PBA-SBPin – 18 % performed in standard 40 µL aluminum capsules with pierced caps which allow for the evaporation of the still remaining solvent.

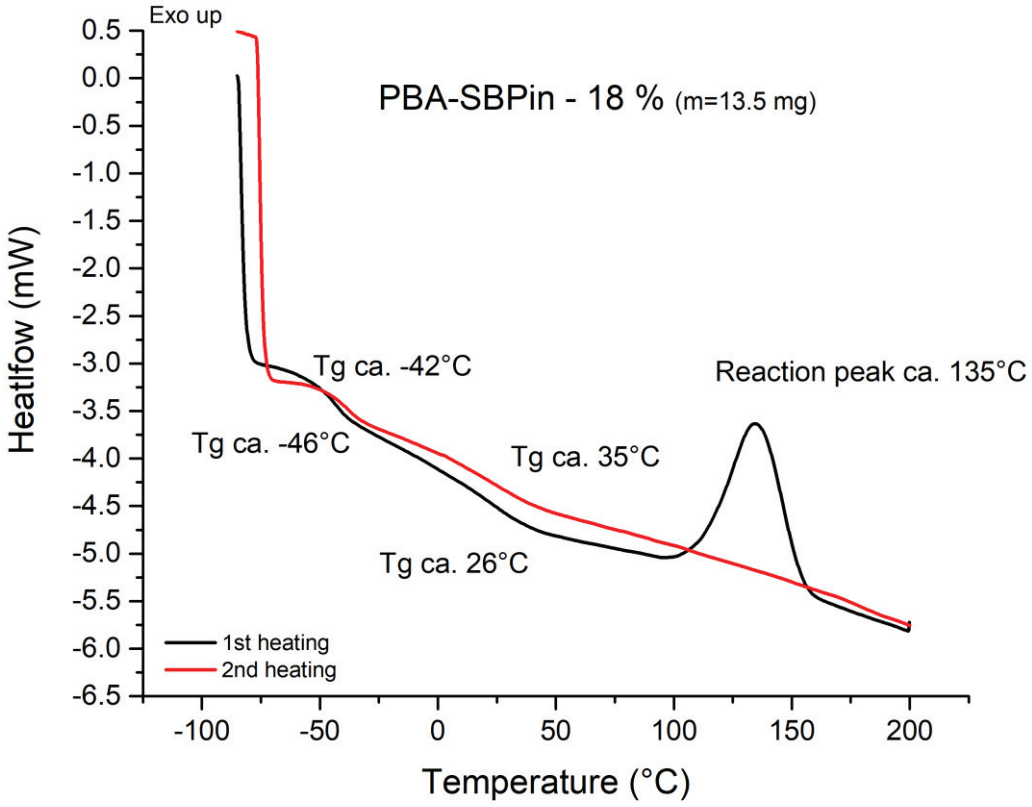

Figure IV. 7: DSC thermograms of copolymer PBA-SBPin - 18 % in 40 µL pierced aluminum pans.

During the first heating, an initial thermal event attributed to a glass transition temperature around -46°C was observed followed by a second glass transition temperature around 26°C. Then, another thermal event around 135°C was evidenced but solely during the first heating segment. In this case, the phenomenon is highly exothermic and is directly related to the reactivity of the boronate ester groups presents in an important proportion in the copolymer.

The second heating segment reveals the same first T_g around -42°C followed by a second T_g around 35°C, higher than in the first heating segment. The second heating segment as well as all other subsequent heating segments revealed the same position for the highest glass transition temperature.

The presence of two glass transition temperatures could correspond to a phase separation between n-butyl acrylate-rich domains with T_g close to -50°C and 4-vinylphenylboronic acid, pinacol ester-rich domains with higher T_g which was found to increase with crosslinking reaction

around 135°C. The reactivity of the boronate esters unveiled in Chapter 1 is once more evidenced with these copolymers.

Contrary to the copolymers with styrene in the latter chapter, the thermic event occurring during the first heating segment is clearly exothermic. This difference could be attributed to the change in the structure of the copolymer.

Differential scanning calorimetry measurements were carried for each copolymer composition. The DSC thermograms of the other copolymers are presented in the Experimental section (from Figures V. 82 to V. 86). The phase separation phenomenon was not obvious for each copolymer and two glass transition temperatures for each heating segment were not readily distinguished. This could arise from the local concentration of 4-vinylphenylboronic acid, pinacol ester that is not as high than in the 18 % mol case, thus only one glass transition temperatures for each heating segment is visible.

However, in accordance with the observations made so far on copolymers from styrene and 4-vinylphenylboronic pinacolate, nearly identical, yet temperature-shifted, thermal behaviors were observed: a first glass transition then an exothermic event and a subsequent second glass transition, again reproducibly observable at all incremental heating cycles. In accordance with the previous chapter, an increase of the second glass transition temperatures with increasing boronate monomer content was observed, which means that the high T_g phenomenon can be finely tuned by adjusting the boronate content.

Likewise, we applied the Gordon-Taylor model to predict the evolution of the glass transition temperature for copolymer from the properties of the pure compounds.

The equation related is expressed as followed:

$$T_g = \frac{[\omega_1 T_{g,1} + K\omega_2 T_{g,2}]}{[\omega_1 + K\omega_2]}$$

with $T_{g,1}$ and $T_{g,2}$ the glass transition temperature of homopolymers from the monomers 1 and 2, ω_1 and ω_2 the mass fraction of each monomer in the copolymer and K an adjustable fitting parameter. [7]

This equation is applicable for fitting the glass transition temperature of many copolymers and it can be used to describe the composition dependence of miscible polymer blends exhibiting negative and position deviation if K is treated as an adjustable parameter. However, the Gordon-Taylor equation should only be applied to blends and mixtures with relative weak specific intermolecular interactions.

We tried to fit the evolution of the glass transition temperature with the Gordon-Taylor equation (Figure IV. 8, blue dashed plot) but a deviation is obvious when the copolymers contain above 20 wt % of the boron-based monomer. This result is consistent with the assumptions of microphase separation within the material, at least in samples with compositions close to 50 wt %.

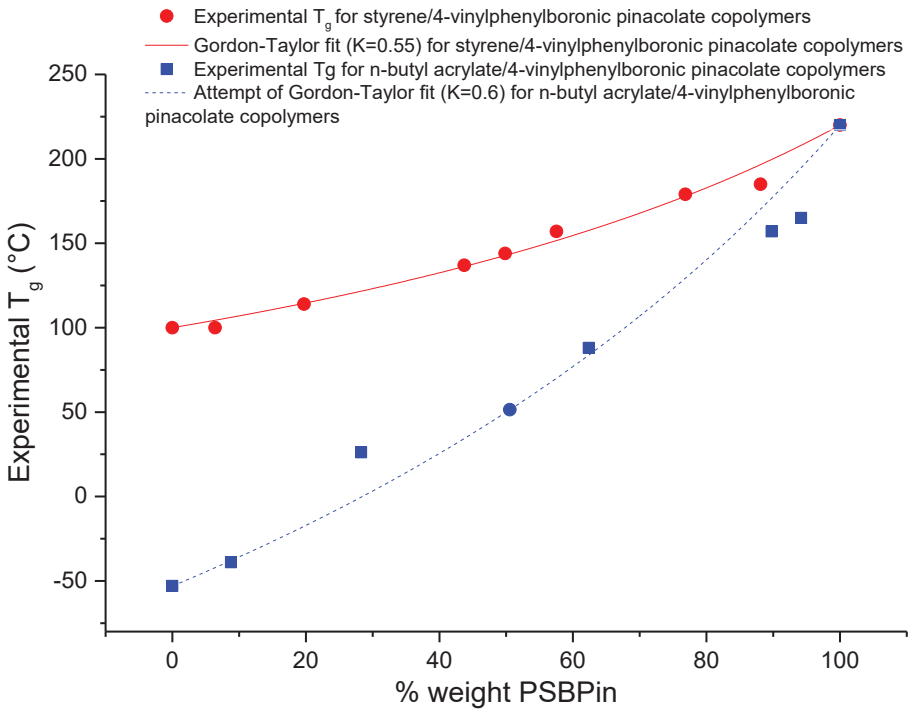

Figure IV. 8: Comparison of the evolution of the second glass transition temperature with the increase of molar proportion of 4-vinylphenylboronic pinacolate monomer and attempts of Gordon-Taylor fits respectively for n-butyl acrylate/4-vinylphenylboronic pinacolate in blue and for styrene/4-vinylphenylboronic pinacolate in red.

c. Contribution of rheology in understanding of dynamic behavior

After characterizing our systems using thermic techniques, we decided to assess the macroscopic behavior of poly(4-vinylphenylboronic pinacolate-*co*-n-butyl acrylate) containing 18 % molar of the boron-based monomer. We probed the behavior of the copolymer in bulk before and after a heating segment at 110°C during several hours as represented in Figure IV. 9.

In this case, we observed the intersection of G' and G'' moduli confirming the effective crosslinking within the copolymer and the increase of G' and G'' until the establishment of a plateau where we assumed that the crosslinking reaction is complete. The intersection of G' and G'' moduli was possible for this specific copolymer as the local concentration of 4-vinylphenylboronic pinacolate was high enough to detect effective crosslinking.

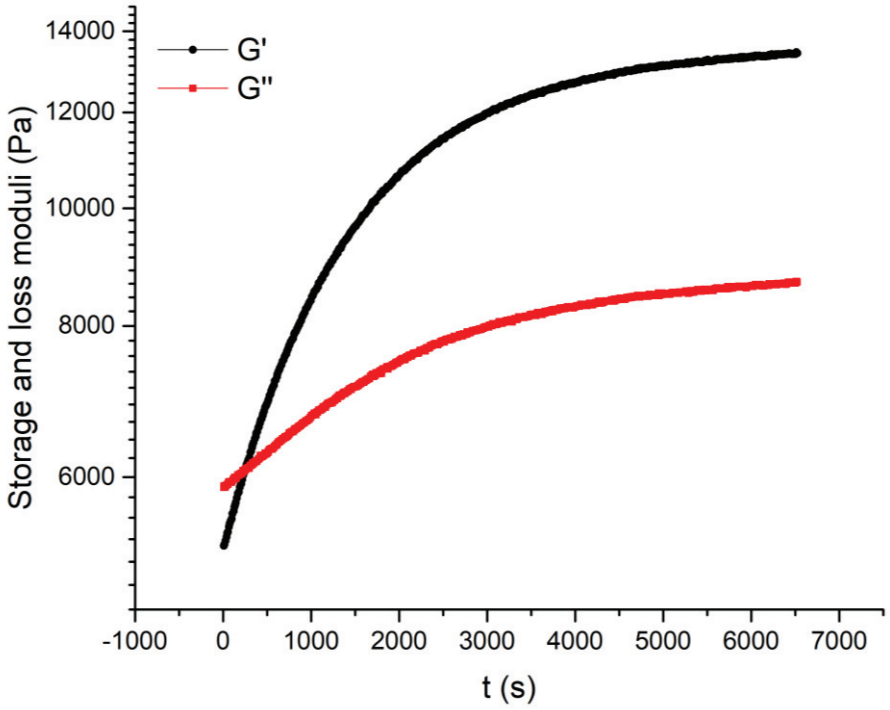

Figure IV. 9: Monitoring of the storage and loss moduli at 110°C on PBA-SBPin – 18 % in bulk.

In order to better characterize the polymer after heating step, we investigated its viscoelastic properties from 50 to 110°C by shear rheology, using small amplitude oscillations. Frequency-dependent storage and loss moduli at different temperatures were shifted by conventional time-temperature superposition in order to build a master curve using 50°C as reference temperature (Figure IV. 10).

The parallel behavior of G' and G'' at high frequencies can be attributed to the phase separation between the two domains: n-butyl acrylate-rich and 4-vinylphenylboronic pinacolate-rich, that induces a microstructure of the material. Besides, the similar behavior of G' and G'' following a same law G', G''$\approx\omega^n$ with n close to 0.5 is characteristic of phase separation. [8], [9] This is consistent with the assumptions made from DSC experiments. The curing at 110°C has two main effects: the increase of T_g and a crosslinking visible with the starting of G' plateau at lower frequencies.

The phase separation phenomenon observed is also consistent with the tendency to form small blocks of n-butyl acrylate due to the feed composition as aforementioned.

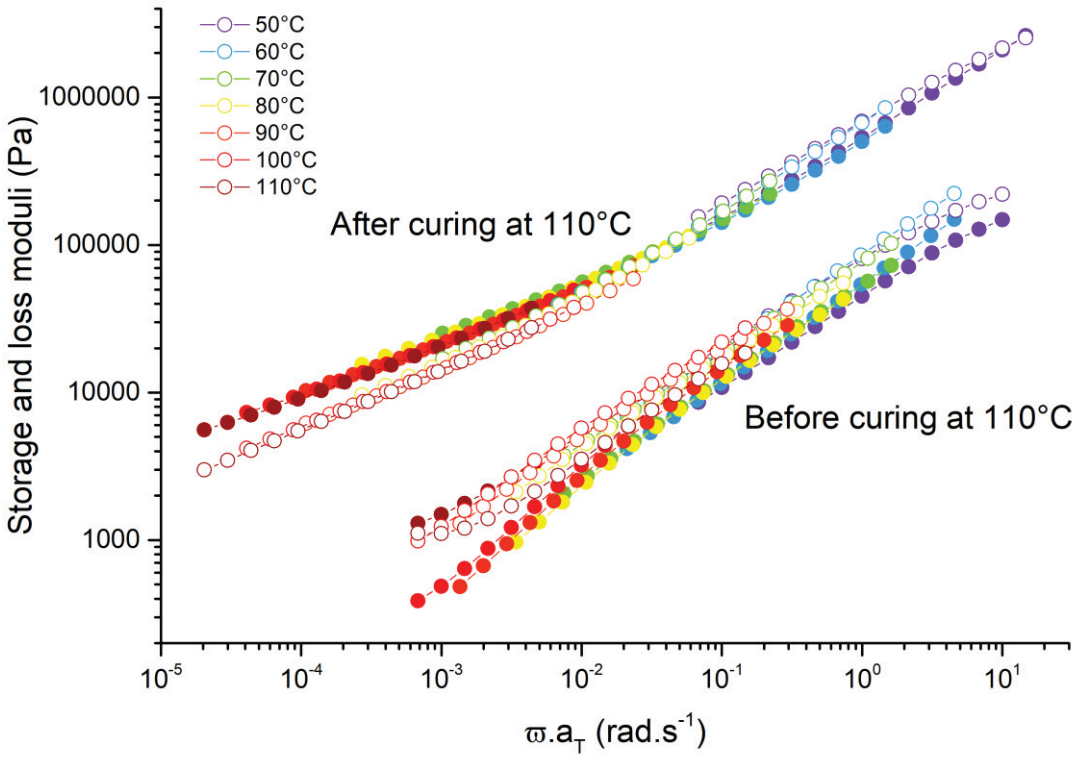

Figure IV. 10: Master curves of dynamic storage and loss moduli of PBA-SBPin – 18 % in bulk, referenced at 50°C before and after the curing at 110°C. G' in closed circles and G'' in opened circles.

The temperature dependency of the shift factors determined from the time-temperature superposition (TTS) of frequency sweeps and referenced at T_0=50°C is plotted in Figure IV. 10. The strong left shift indicates a significant increase of the glass transition temperature after the crosslinking event.

The WLF equation is an empirical equation associated with the time-temperature superposition. [10] The equation is used to fit the shift factors a_T to the temperature. The superposition parameters a_T follow the equation:

$$\log(a_T) = \frac{-C_1(T - T_0)}{C_2 + (T - T_0)}$$

where T is the temperature, T_0 the reference temperature used for the determination of the superposition parameters and, C_1 and C_2 empirical constants to fit the values of a_T.

We plotted in Figure IV. 11 the Williams-Landel-Ferry (WLF) law using the so-called "universal constants" that are C_1=15 and C_2=50 K. [10]

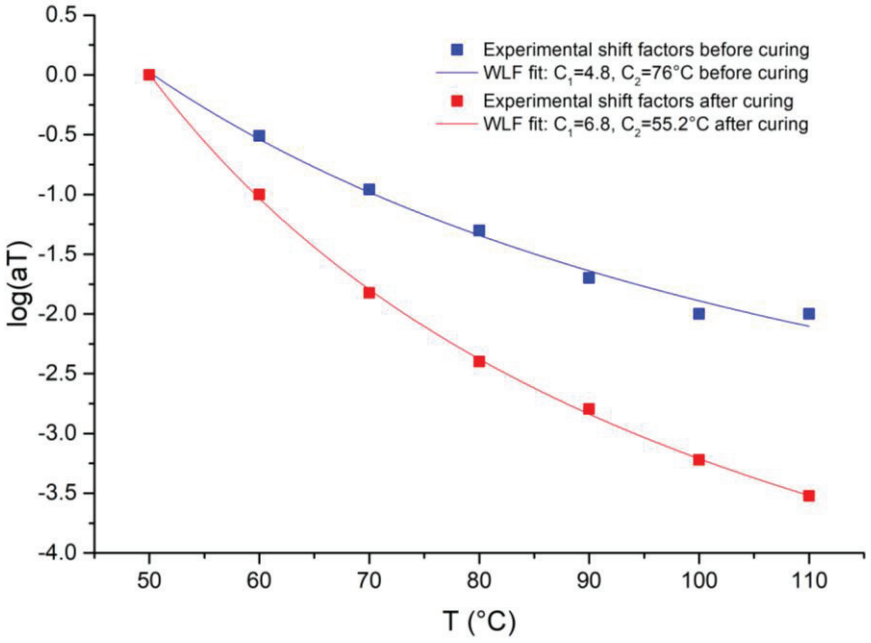

Figure IV. 11: WLF profiles of shift factors before and after curing.

The dependency of the shifts factors with the temperature was successfully fitted with the classical Williams-Landel-Ferry model before and after curing using realistic parameters from a physical standpoint, which is a quiet surprising result regarding the last Chapter. However, this can be explained by the fact that the copolymer have a phase separation microstructure.

From the parameters obtained with WLF fit, we are able to recalculate the T_g before and after curing at 110°C *via* $T_g=T_0+50-C_2$. Thus, we obtained T_gs around 24°C before curing and around 45°C after curing which is consistent with the DSC thermograms.

To conclude, in the case of n-butyl acrylate/4-vinylphenylboronic pinacolate, phase separation between SBPin-rich and SBPin-poor domains is evidenced by DSC and rheology, at least on sample with 18 mol % PSBPin. In this sample, reactivity of boronate esters at 110°C induced an increase of the glass transition temperature of the SBPin-rich domain, as well as low-density crosslinking.

B. Extension to organic dynamic glasses

a. Synthesis of glasses and macroscopic observations

In this section, we diametrically changed our strategy by studying small molecules carrying boronate ester groups and their ability to form 3D-network. We focused on the use of 1,3,5-phenyltriboronic acid, tris(pinacol) ester interacting with controlled amounts of a nucleophilic molecule, in this peculiar case, pentaerythritol. The structures of the molecules are illustrated in Figure IV. 12 and their physical properties are listed in Table IV. 2. NMR spectra of the two compounds are available from Figures V. 91 to V. 95 in the Experimental Section.

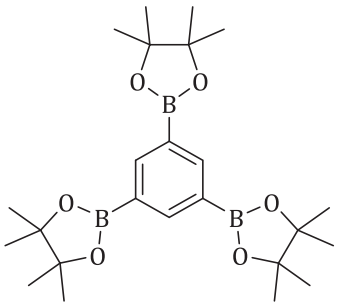

1,3,5-Phenyltriboronic acid, tris(pinacol) ester

Pentaerythritol

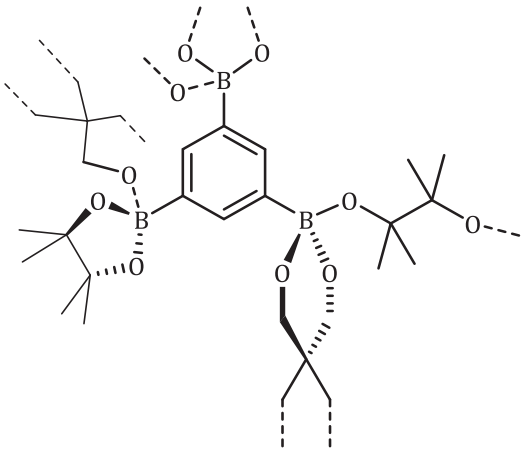

Expected network

Figure IV. 12: Structures of the molecules involved in this study and expected network.

Table IV. 2: Properties of the molecules involved in this study.

Properties	***1,3,5-Phenyltriboronic acid, tris(pinacol) ester***	***Pentaerythritol***
Molecular weight (g/mol)	456.3	136.15
Melting point (°C)	286-287	253-258
Boiling point (°C)	555.6	276/30 mmHg

The main goal targeted was to form hybrid organic/inorganic networks simply by taking advantage of the evidenced reactivity of the boronate ester groups. The functionality of the 1,3,5-phenyltriboronic acid, tris(pinacol)ester (TPBPin) is 3 considering its 3 functions that are able to induce crosslinking. Pentaerythritol could have two possible roles on the reactivity of the trifunctional molecule. On the one hand, it could assist the ring opening of the boronate ester moieties by its nucleophilic character. On the other hand, it can react with the boronate esters *via* transesterification reactions. In each case, bridging between boron atoms could be created

affording network as represented in Figure IV. 12. Besides, pentaerythritol is a good candidate as its boiling point is high (276°C/30 mmHg) allowing for the reaction in molten state of the trifunctional molecule having a melting point at 280°C. It has to be notice that the concomitant reactions on the three boronate ester moieties are not that obvious and one or two boronate esters could only react through the mechanisms mentioned.

The reaction was firstly investigated simply through macroscopic observations. The two solid compounds were crushed in a mortar in controlled amounts and, after being dried under vacuum, the powder mixture was heated in a Schlenk vessel at 300°C in an oven during 15 minutes to allow the reaction in the molten state. Starting from a low viscosity liquid at 300°C, the medium progressively thickens when cooled down, yielding a transparent, amorphous glass at room temperature as shown in Figure IV. 13.

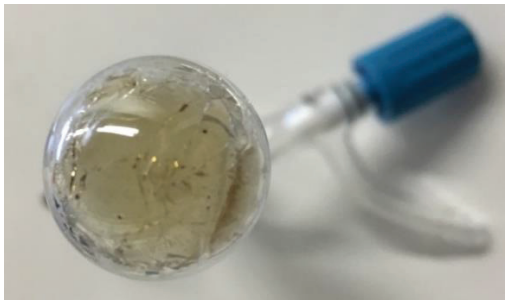

Figure IV. 13: Visual result of the reaction between 1,3,5-phenyltriboronic acid, tris(pinacol)ester and pentaerythritol.

The transparency was found to be highly dependent on the quantity of pentaerythritol added to the trifunctional molecule. Indeed, if not enough pentaerythritol is added, a part of TPBPin do not react and can thus recrystallize at lower temperatures. Pentaerythritol plays a major role in this reactivity as it assists each reactive sites to induce the ring opening. The comparative reaction without pentaerythritol was also performed in the oven without any effect as the trifunctional compounds fully recovered its crystallinity. The macroscopic aspects of the synthesized glasses are illustrated in Table V. 1 in the Experimental section.

Experimentally, we faced problems of brittleness during the shaping of the material at low temperatures. It can be explained at the molecular level by the shortness of the B-C bond in 1,3,5-phenyltriboronic, tris(pinacol) ester that can induce fragility in the material. Indeed, the strong rigidity of the short bond B-C as well as no possible rotation around the bonds thus prompt the difficulty to dissipate constraints.

Besides, it was witnessed that the newly formed glass could be solubilized in a polar solvent such as tetrahydrofuran (THF) as showed Figure IV. 14. Indeed, it is entropically favored to return to monomers (depolymerization process).

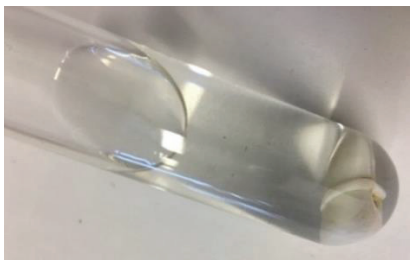

Figure IV. 14: Solubilization in THF of a glass formed from the reaction of TPBPin with 30 % molar of pentaerythritol compared to BPin groups.

Hence, we can conclude that the network formed by the ring-opening reaction of the boronate esters of the trifunctional molecule seems to be once more reversible. We created an inorganic/organic hybrid soluble glass harnessing the reactivity of boronate esters.

b. Differential scanning calorimetry

Prior to the study of the glass by differential scanning calorimetry, the two compounds were analyzed separately to obtain their thermal profiles. The thermograms of 1,3,5-phenyltriboronic acid, tris(pinacol)ester and pentaerythritol are respectively represented in Figure IV. 15 and Figure IV. 16. The trifunctional molecule exhibits a classical thermal behavior with a melting around 280 °C and a recrystallization at considerably lower temperatures, around 170°C.

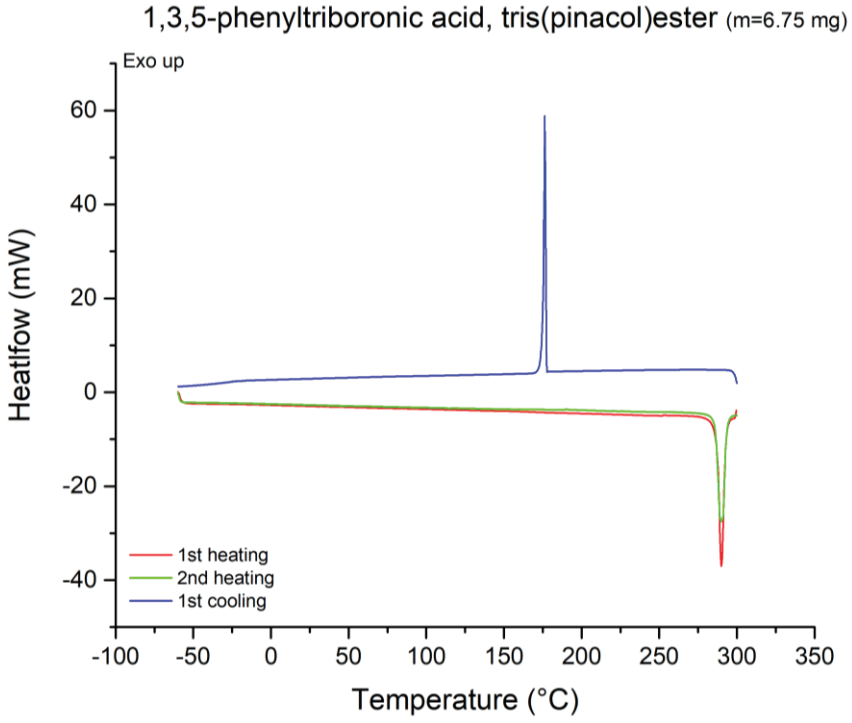

Figure IV. 15: DSC thermograms of 1,3,5-phenyltriboronic acid, tris(pinacol)ester in 40 µL opened aluminum pans.

On the other hand, pentaerythritol shows a complex profile, already assigned in the literature to a phase transition from a low symmetry layered crystal structure to a highly symmetric face centered cubic structure around 190°C followed by the melting point at 255°C. [11] Further cycling shows considerable differences that could be related to the oligomerization by condensation reaction *via* the creation of ether linkages. [12]

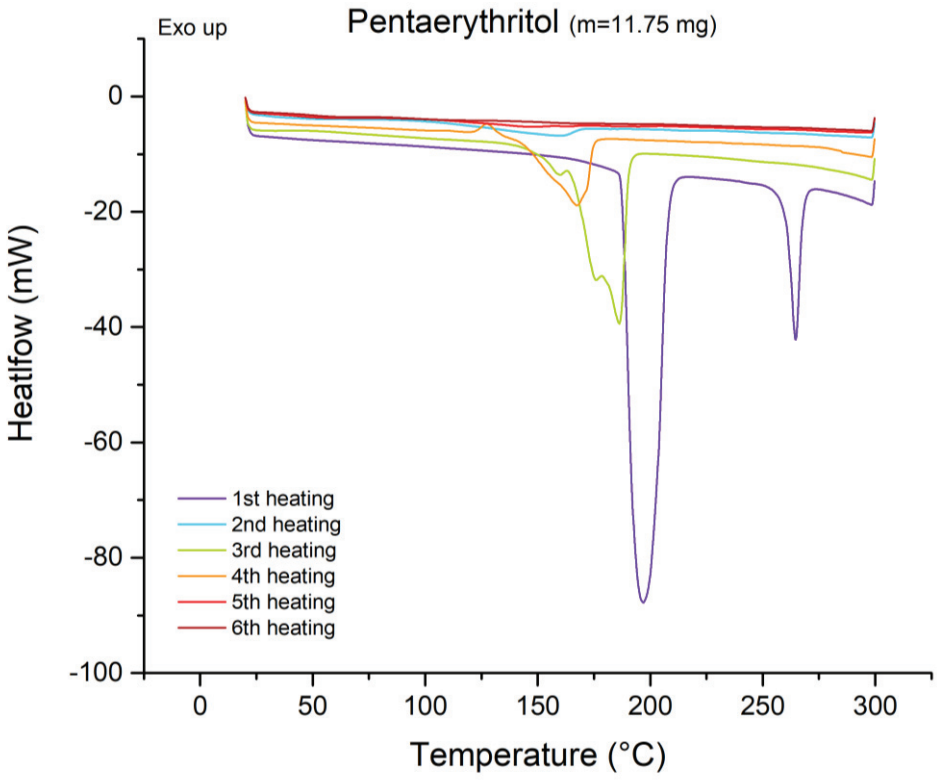

Figure IV. 16: DSC thermograms of pentaerythritol in 40 µL opened aluminum pans.

The mixture system was then studied by differential scanning calorimetry to understand the phenomenon occurring at high temperatures within the material. The amount of pentaerythritol was varied from 2 to 50 mol % of pentaerythritol compared to the boronate ester groups corresponding to 0.5 to 12.5 mol % of –OH to boronate ester groups. The reaction was followed in the DSC capsules through successive heating cycles. The DSC thermograms are detailed from Figures V. 98 to V. 106 in the Experimental Section.

At first sight, no glass transition was observed for low percent of pentaerythritol (2 % mol pentaerythritol / boronate esters), only a decrease of the importance of the melting phenomenon over the heating/isotherm cycles. This is represented in Figure IV. 17.

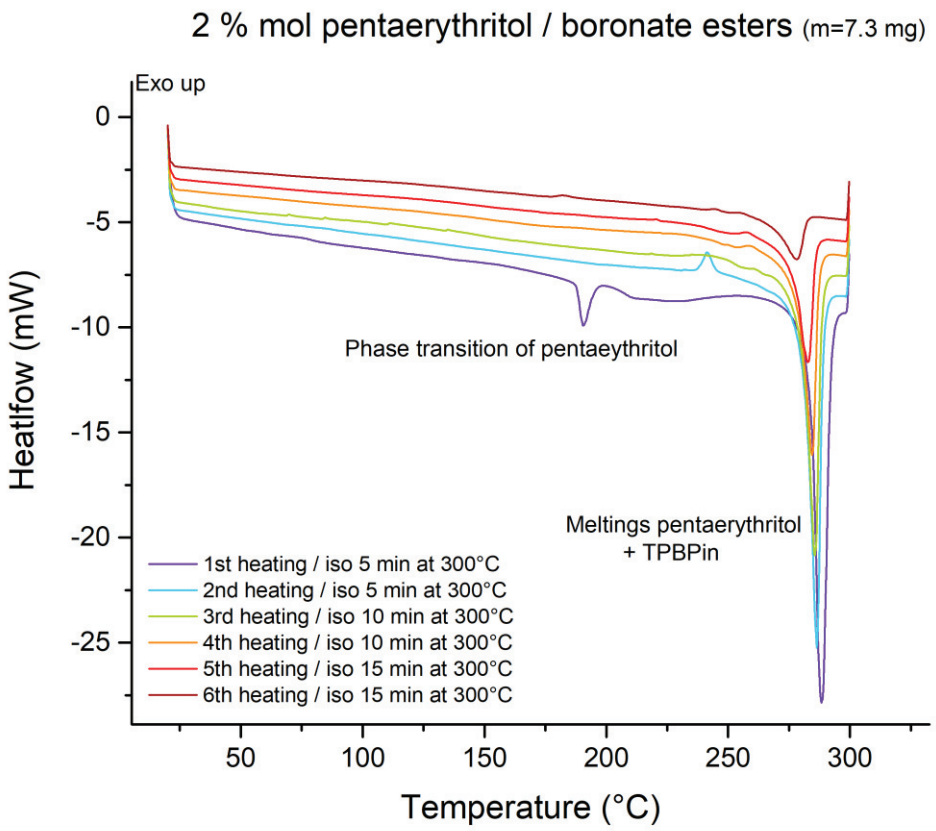

Figure IV. 17: DSC thermograms of the reaction of 1,3,5-phenyltriboronic acid, tris(pinacol)ester with 2 % molar of pentaerythritol compared to boronate ester groups in 40 µL opened aluminum pans.

However, from 5 mol % of pentaerythritol compared to boronate ester groups, we detected the appearance of glass transition temperature after the first heating segment and the first isotherm at 300°C during 5 minutes. Indeed, during the first heating segment, we observed endothermic phenomenon corresponding to the phase transition of pentaerythritol followed by the meltings of pentaerythritol and TPBPin lowered by the presence of pentaerythritol. After this segment and the isotherm at 300°C, a first T_g was noticed around 116°C. Over the cycles, the measured glass transition temperature was found to increase up to 131°C. The DSC thermograms are illustrated in Figure IV. 18.

This growth indicates that the reaction kept on going over the cycles and that linkages are created over the time through the ring opening of the boronate ester groups. In the same time, the cold crystallization was found to decrease, as a result of the reaction between 1,3,5-phenyltriboronic, tris(pinacol)ester and pentaerythritol.

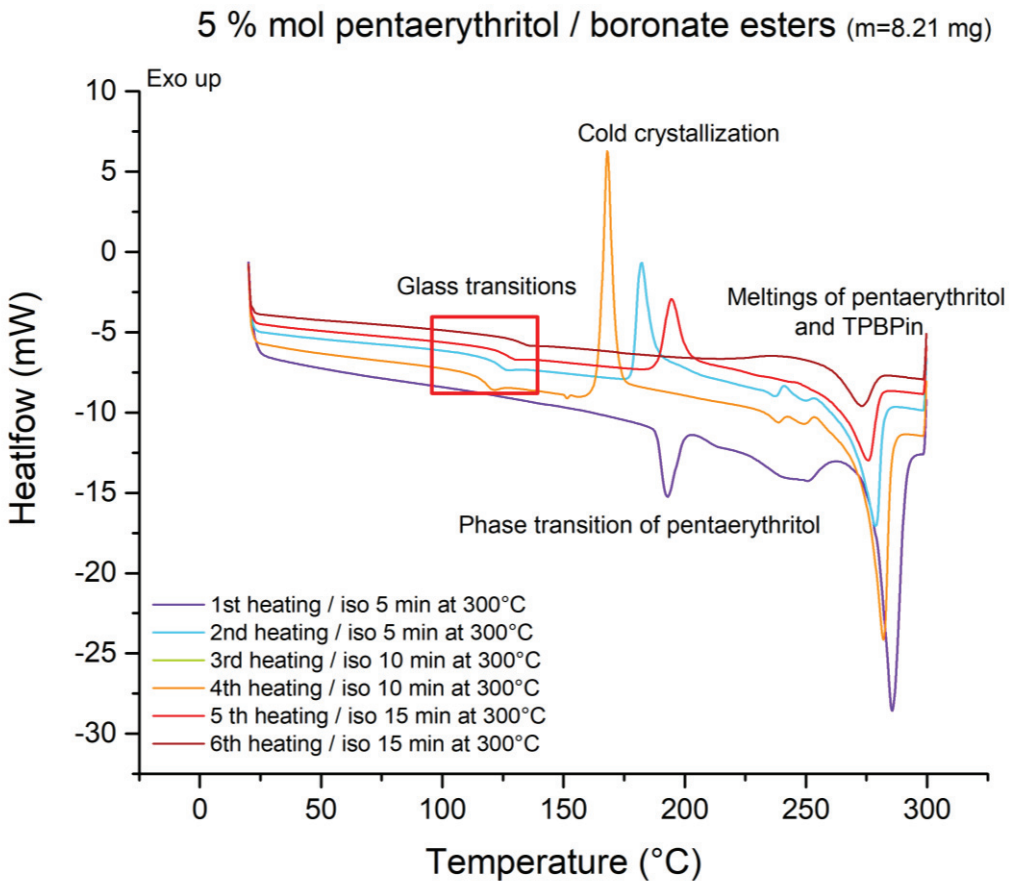

Figure IV. 18: DSC thermograms of the reaction of 1,3,5-phenyltriboronic acid, tris(pinacol)ester with 5 % molar of pentaerythritol compared to boronate ester groups in 40 µL opened aluminum pans.

The addition of pentaerythritol in the reaction has the effect to increase the T_g measured by DSC. By increasing the quantity of pentaerythritol, the sites of ring opening of the boronate esters moieties of TPBPin and the linkages created were more numerous. In this optic, we were able to reach glass transition temperatures up to 250°C only with trifunctional molecules harnessing the boronate esters reactivity. The evolution of the glass transition temperatures depending on the time at 300°C and the amount of pentaerythritol is monitored in Figure IV. 19.

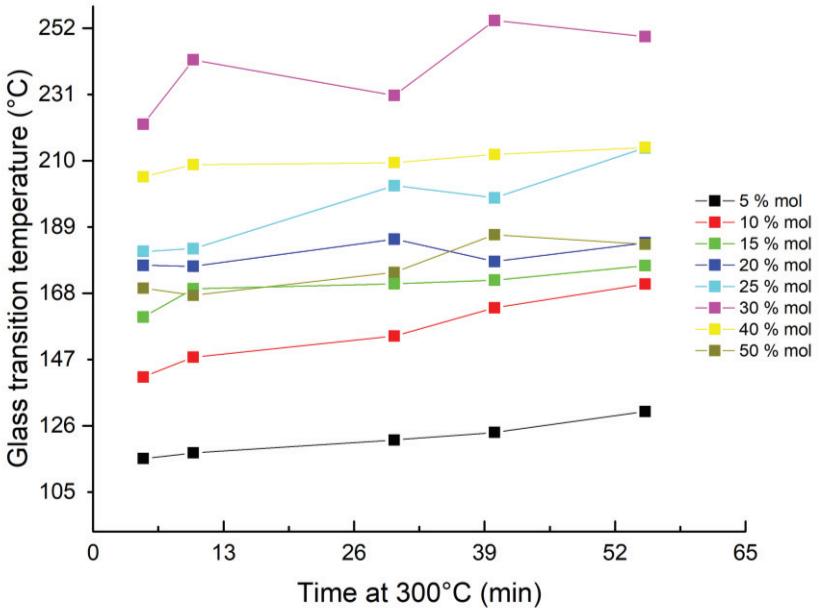

Figure IV. 19: Monitoring of the glass transition temperatures as a function of time at 300°C.

These observations were made for several experiments from 5 to 30 mol % of pentaerythritol compared to the boronate ester moieties. Above these quantities of pentaerythritol, it was remarked that the glass transition temperatures reached were lower. In this fashion, we were able to determine an ideal O/B ratio at 3.2 for maximizing the boronate esters reactivity as indicated in Figure IV. 20. This specific value is related to the pyramidalized environment of boron atoms that can be surrounded by three oxygen atoms.

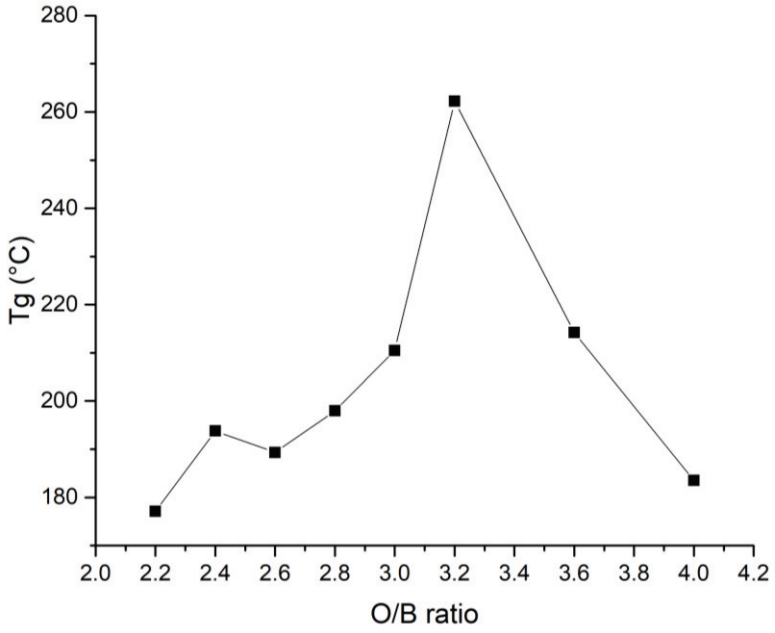

Figure IV. 20: Evolution of the glass transition temperature according to O/B ratio after 60 min at 300°C.

c. Rheology measurements

Usually glasses are described as liquids that have lost their ability to flow. Open networks liquids such as SiO_2 and GeO_2 show an Arrhenius variation of viscosity (or structural relaxation time) over temperature and they provide "strong" liquid. Conversely, other systems that can be characterized by simple non-directional Coulomb attractions or by van der Waals interactions in aromatic groups provide "fragile" liquids where the viscosities vary in a strongly non-Arrhenius way over temperature. [13]

These two extremes of strong and fragile liquids have been used to classify the glasses to represent their sensitivity to temperature variations. [14] The first "strong" class of liquids offer resistance to structural change and their vibrational spectra and radial distribution functions exhibit little reorganization over temperature changes. On the other hand, the second category of "fragile" liquids has glassy state structures that are close to collapse at their T_gs and that reorganize to structures that fluctuate over a wide variety of different particles orientation and coordination states. In the case of boron, it can be tricoordinated (III) or tetracoordinated (IV) adding rotational flexibility to the system. Besides, strong liquids show small jumps in ΔC_p at T_g, whereas fragile liquids have large jumps. [13]

This dual pattern has been fitted in a modified version of the Vogel-Fulcher [15], [16] or Vogel-Tammann-Fulcher [17] equation originally written as:

$$\eta = \eta_0 \exp\left[\frac{B}{T - T_0}\right]$$

with η_0, B and T_0 are positive constants. From this equation, a measure of the fragility can be defined in terms of the effective activation enthalpy at T_g:

$$m \equiv \left|\frac{d\log\eta}{d(\frac{T_g}{T})}\right|_{T=T_g} = \frac{BT_g}{(T_g - T_0)^2 \ln(10)}$$

The index m represents the dynamic fragility of the material. When m is high, the material is classified as fragile whereas when m is low, it is a strong liquid. [18]

In this part, rheology measurements were used to determine the viscosity of the material at different temperatures and thus to plot the temperature-dependency of the viscosity of the material in Figure IV. 21 for a mixture of trifunctional molecule with 10 mol % of pentaerythritol compared to pinacol functions. It should be noted that lower temperatures (and consequently higher viscosities) were very difficult to probe due to the partial recrystallization of unreacted trifunctional boronic pinacolate that greatly increases the viscosity. The measured viscosities

were fitted with the Vogel-Tammann-Fulcher equation to afford the η_0, B and T_0 parameters. Empirically, T_0 and T_g are often found to be strongly related, in the form $T_0=T_g-A$ with A=[30-70 K]. In our case, we found, T_0=403 K and T_g=443 K and thus A=40 K.

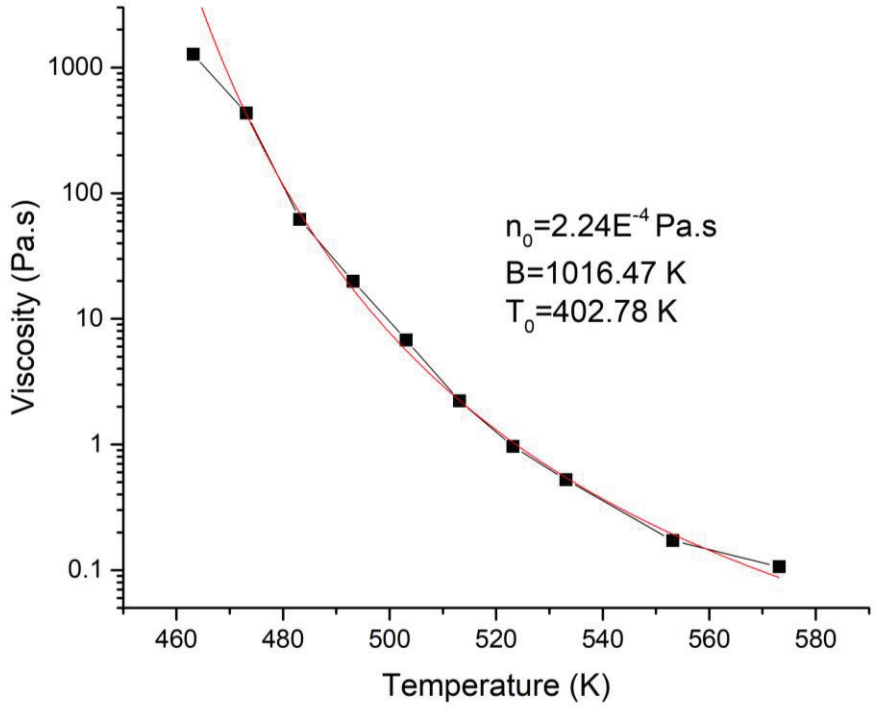

Figure IV. 21: Temperature-dependency of the viscosity of a 10 % mol mixture fitted by Vogel-Tammann-Fulcher equation.

Thanks to the equations reported above, we were also able to estimate the m index representing the dynamic fragility of the material. In our case, m≈122 that is a high value, thus classifying our material as fragile. For comparison, SiO_2, classified as a strong glass-forming liquid, exhibits an m index close to 18. [18]

d. Input of IR and ^{11}B solid-state NMR spectroscopies

i. IR spectroscopy

To provide information on the structure of the new boron compounds formed at high temperature, we probed the infrared spectra of the mix containing 10 mol % of pentaerythritol compared to the boronate ester groups after 15 min at 300°C and the initial product 1,3,5-phenyltriboronic, tris(pinacol)ester. The two spectra are compared in Figure IV. 22.

The infrared spectra of a number of organoboron compounds have been reviewed by Bellamy *et al.* and a number of characteristic group frequencies have been assigned. [19]

We focused on changes in the 1000-1500 cm^{-1} and the 600-900 cm^{-1} regions. It was observed a growth of the signal at 1260 cm^{-1} that matches to the O-B-O stretching mode in equilibrium with

the 1318 cm^{-1} signal due to the B-O stretching mode. Besides, a new signal was detected at 760 cm^{-1} as well as a shouldering around 861 cm^{-1} that could correspond to the out-of-plane vibrations of the O-B-O skeletons. This could correspond to the change from boron in a planar form to pyramidalized form after reaction.

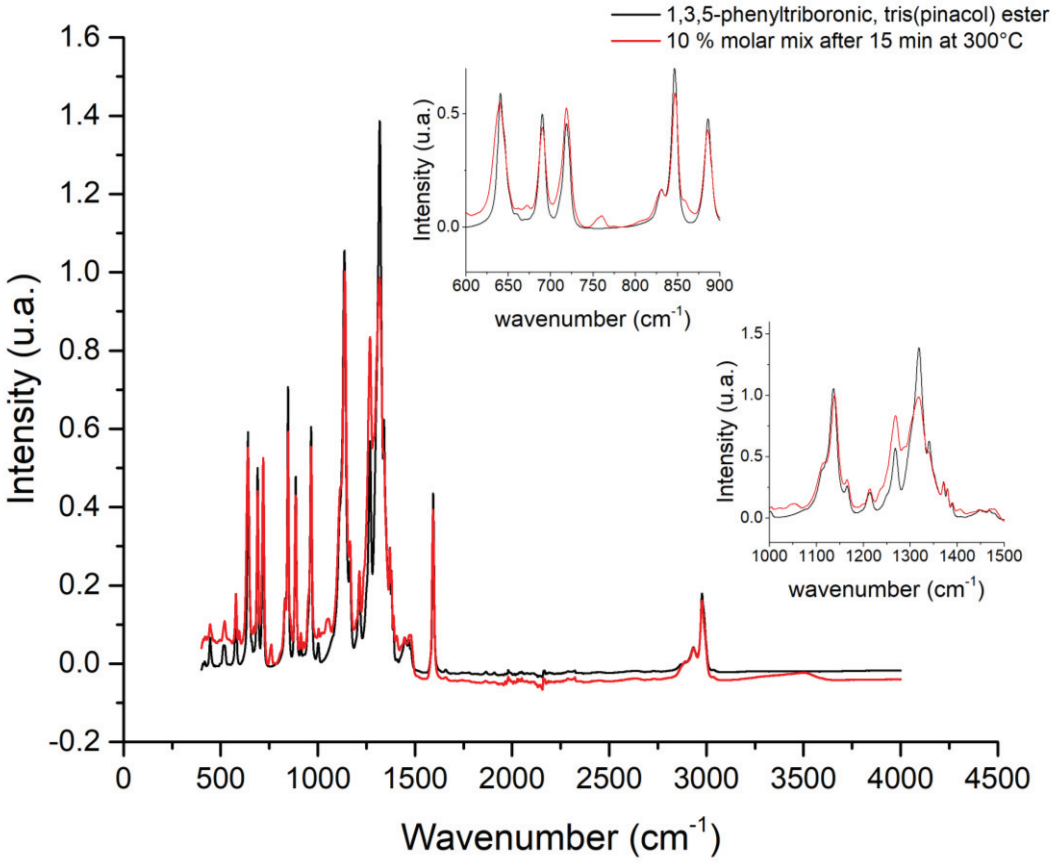

Figure IV. 22: Comparison of IR spectra of 1,3,5-phenylboronic acid, tris(pinacol) ester and a mix with 10 mol % of pentaerythritol compared to the boronate esters after 15 minutes at 300°C. Insets on the wavenumber regions of interest.

These aforementioned changes of infrared spectra could indicate changes around the boron atom after 15 min at high temperature in the presence of a controlled amount of nucleophilic molecule such as pentaerythritol. This evidenced once again a reactivity around the boronate ester moieties.

ii. Solid-state NMR spectroscopy

Solid-state NMR spectroscopy was used to detect differences in the environment of the boron and carbon atoms before and after heating treatment of the synthesized glasses to set hypothesis concerning the mechanisms occurring between 1,3,5-phenyltriboronic acid, tris(pinacol) ester and pentaerythritol. This non-destructive method is the best choice for probing the nature of the molecules formed in our sample. Concerning ^{11}B ss-NMR of boron, it is not an obvious method at

first sight due to the difficulty of interpretation from the quadrupolar nature of the nucleus (spin 3/2). Besides, the solid state hindered the mobility inside the material and the observed large signals are due to the anisotropic (directionally dependent) interactions.

We will focus mainly on two samples: a mix of 1,3,5-triboronic acid, tris(pinacol) ester with 10 mol % of pentaerythritol compared to the boronate esters and a mix of 1,3,5-triboronic acid, tris(pinacol) ester with 30 mol % of pentaerythritol compared to the boronate esters.

First the ^{11}B ss-NMR spectrum of the native trifunctional molecule was acquired in Figure IV. 23 confirming that only one boron specie is present *via* 1D ^{11}B NMR spectroscopy and Multiple-Quantum Magic-Angle Spinning (MQMAS) NMR that shows the ^{11}B-^{11}B correlation spectrum evidencing the presence of only one boron species.

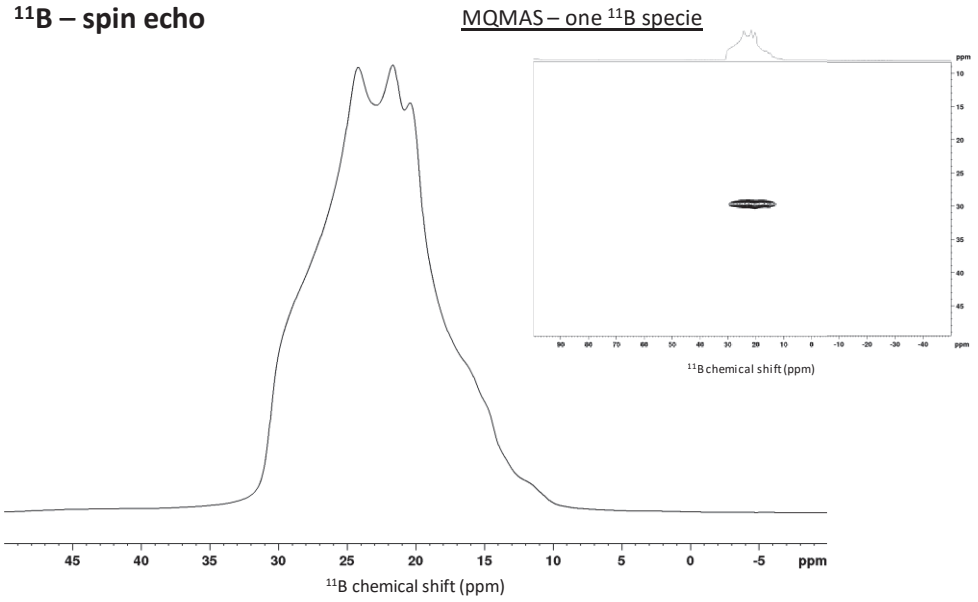

Figure IV. 23: ^{11}B ss-NMR spectrum of 1,3,5-triboronic acid, tris(pinacol) ester. Inset: Multiple-Quantum Magic-Angle Spinning (MQMAS) ss-NMR spectrum ^{11}B-^{11}B.

Besides, simulations are mandatory to evaluate the presence of only one or several types of boron chemical environments on the 1D ^{11}B NMR spectrum. The "dmfit" program was developed to account for quadrupolar couplings and render easy such simulations of spectra obtained from combination of discrete species. [20] When fitting the signal, two types of boron are found to achieve match between the simulation and the experimental spectrum as illustrated in Figure IV. 24. Simulations using the "dmfit" program allows for the calculations of two parameters: δ_{iso} and ηQ. This last feature is related to the constraints applied around the boron atom and will be a useful parameter in this following of this study. In the case of the trifunctional molecule, we found out two species with very close δ_{iso} (30.9 and 31.1 ppm) and ηQ (0.60 and 0.64) parameters. This can be due to the presence of the hydrated form of the trifunctional molecule.

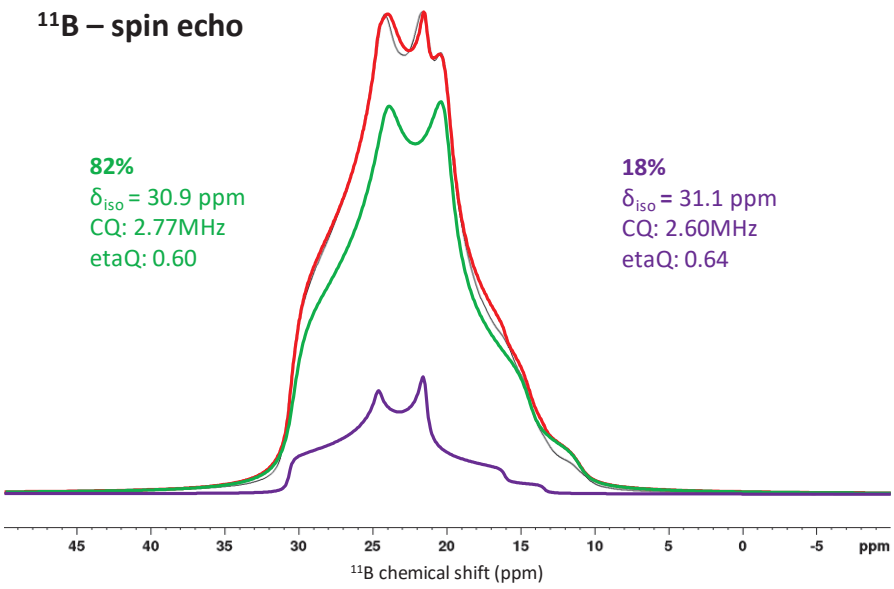

Figure IV. 24: ^{11}B ss-NMR spectrum of 1,3,5-triboronic acid, tris(pinacol) ester and fits performed with « dmfit » software.

Trifunctional boron-based molecule/pentaerythritol mixtures were then prepared by crushing the two compounds in controlled amounts in a mortar. The reactive blends were firstly analyzed in their native forms (before any heating) and the spectra obtained in ^{11}B (Figure IV. 25) and ^{13}C (Figure IV. 26) ss-NMR spectroscopies showed no difference between the mixtures and 1,3,5-phenyltriboronic, tris(pinacol) ester. One can notice that pentaerythritol is in two low concentrations to be detected by ^{13}C ss-NMR spectroscopy. Besides, the signal corresponding to the CH_3 of pinacol groups is double, due to the different conformations of the CH_3 groups.

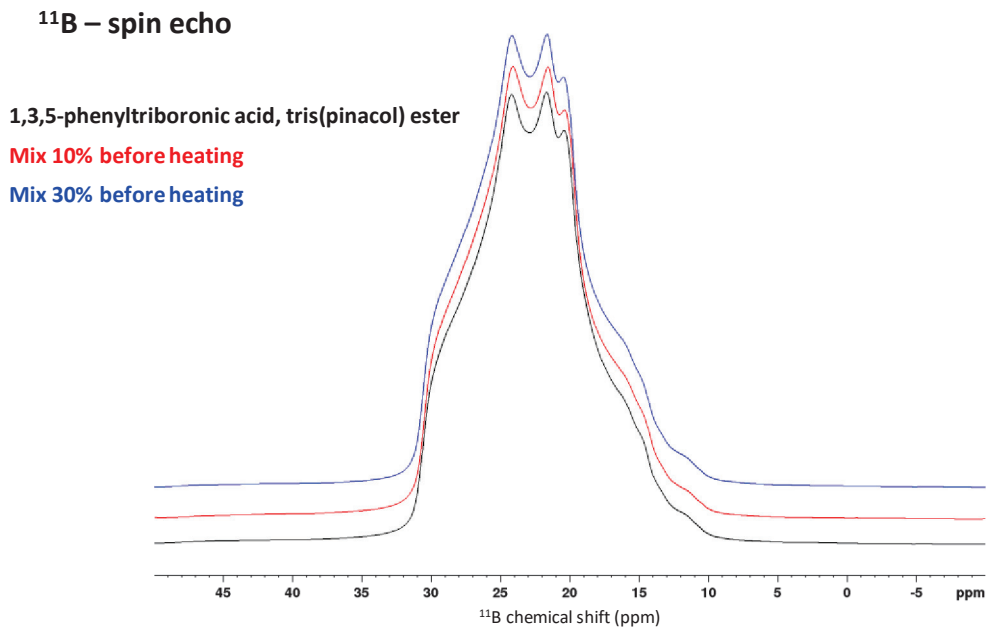

Figure IV. 25: Superposition of the ^{11}B ss-NMR spectra of 1,3,5-phenyltriboronic acid, tris(pinacol) ester in black, the native 10 % mix in red and the native 30 % mix in blue.

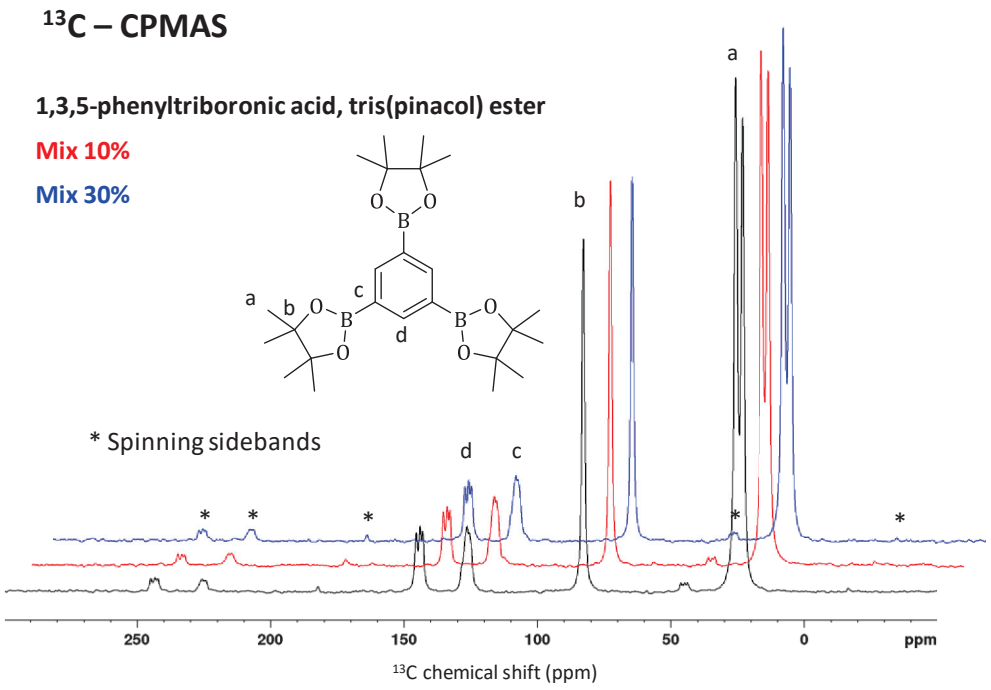

Figure IV. 26: Superposition of the ^{13}C ss-NMR spectra of 1,3,5-phenyltriboronic acid, tris(pinacol) ester in black, the native 10 % mix in red and the native 30 % mix in blue. Attributions of the signals are only made on one side of the molecule for clarity.

The mixtures were then dried under vacuum in a vial for 30 minutes and sealed to keep the sample under vacuum. The vials were placed in a furnace at 300°C during 2 h and then cooled down to room temperature. The samples were recovered by breaking the vials and crushed to be analyzed in a 4 mm rotor.

Concerning the 10 % mixture after the heating treatment, only very weak differences can be seen in the ^{11}B ss-NMR spectrum comparing to 1,3,5-phenyltriboronic acid, tris(pinacol) ester as mentioned in Figure IV. 27. Nonetheless, we observed some changes in the ^{13}C ss-NMR spectrum compared to the one of 1,3,5-phenyltriboronic acid, tris(pinacol) ester with the apparition of signals around 40 ppm, 55-68 ppm and 135-140 ppm. These changes are indicated by the black circles in Figure IV. 28 and could be the results of reactivity at a small extent of boronate ester groups.

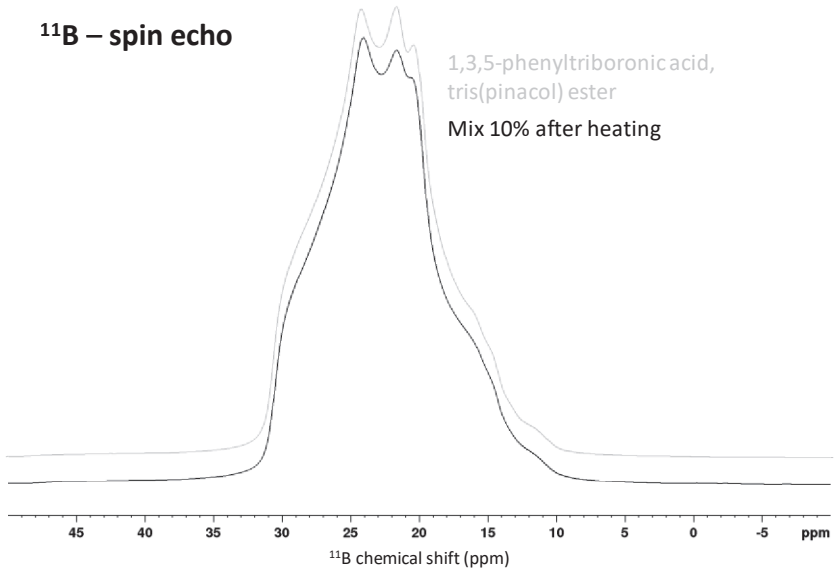

Figure IV. 27: Superposition of the ^{11}B ss-NMR spectra of 1,3,5-phenyltriboronic acid, tris(pinacol) ester in grey and the 10 % mix after 2 h at 300°C in black.

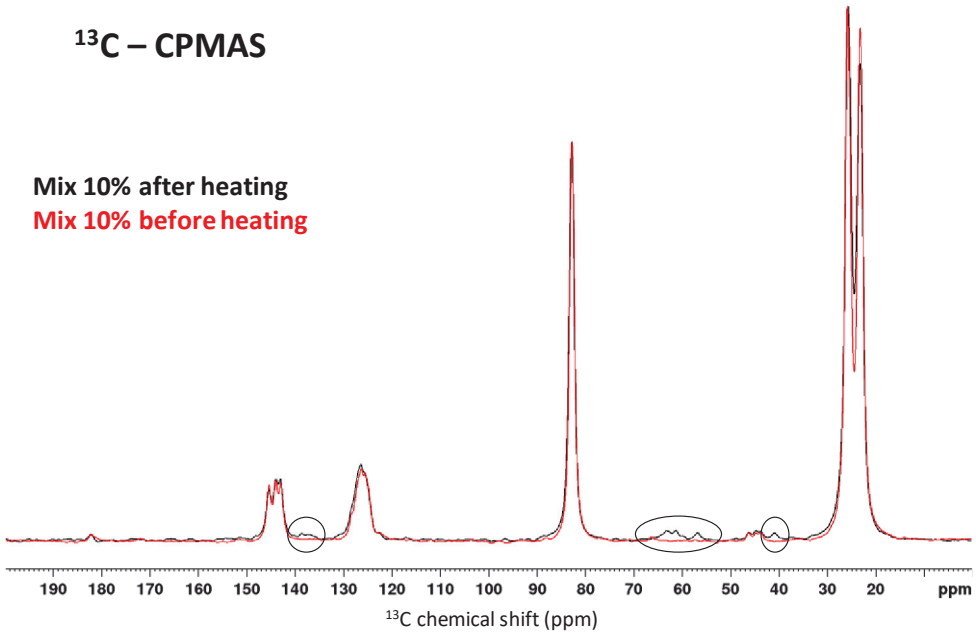

Figure IV. 28: Superposition of the ^{13}C ss-NMR spectra of native 10 % mix in black and the 10 % mix after 2 h at 300°C in red. Black circles indicate the differences between the two spectra.

Regarding the ^{11}B ss-NMR spectra obtained for the 30 % mix after heating treatment, the shape of the signal is considerably different from the boron signal of the 1,3,5-phenyltriboronic acid, tris(pinacol) ester as observed in Figure IV. 29.

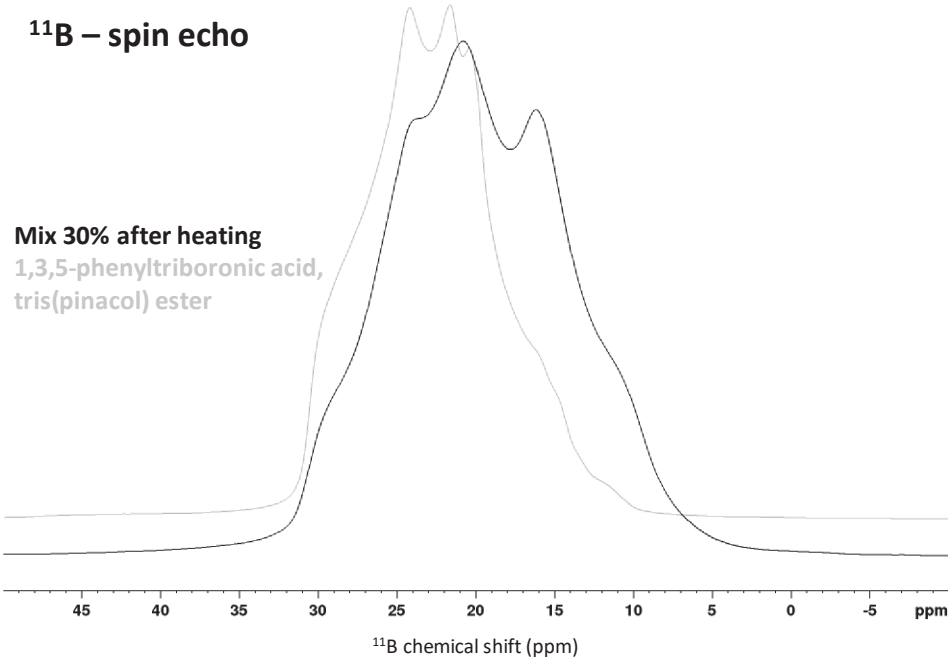

Figure IV. 29: Superposition of the ^{11}B ss-NMR spectra of 1,3,5-phenyltriboronic acid, tris(pinacol) ester in grey and the 30 % mix after 2 h at 300°C in black.

When fitting the signal with "dmfit" sofware after heating treatment, four types of boron are necessary to achieve perfect match between the simulation and the experimental spectrum as illustrated in Figure IV. 30. The green fit exhibits close δ_{iso} (31.1 ppm) and ηQ (0.58) parameters compared to the simulation made before any heating in Figure IV. 24 (30.9 ppm and 0.60) and thus corresponds to the native species. Simulations using the "dmfit" program therefore allowed us to unveil new boron environments after heating, displaying different features in terms of ηQ related to the constraints applied around the boron atom. The new species formed are more (orange) or less constrained (purple and blue) that the native one in green depending on the linkages formed between the boronate ester moieties. Indeed, numerous possibilities of geometries exist for the new species formed and some of them will be presented in the next part concerning the mechanism of formation of the network. Moreover, the presence of less constrained boron species is consistent with the assumption of pyramidalization at boron in agreement with was foreseen.

However, we were quite surprised of the high quantity of native boronate esters that did not react (43 %) which means that the quantity of pentaerythritol added is not sufficient to create linkages between all the boronate ester groups. This value has to be taken carefully as the analysis is only qualitative. This is also consistent with the recrystallization of 1,3,5-phenyltriboronic acid,

tris(pinacol) ester at low temperatures evidencing the presence of unreacted trifunctional molecules.

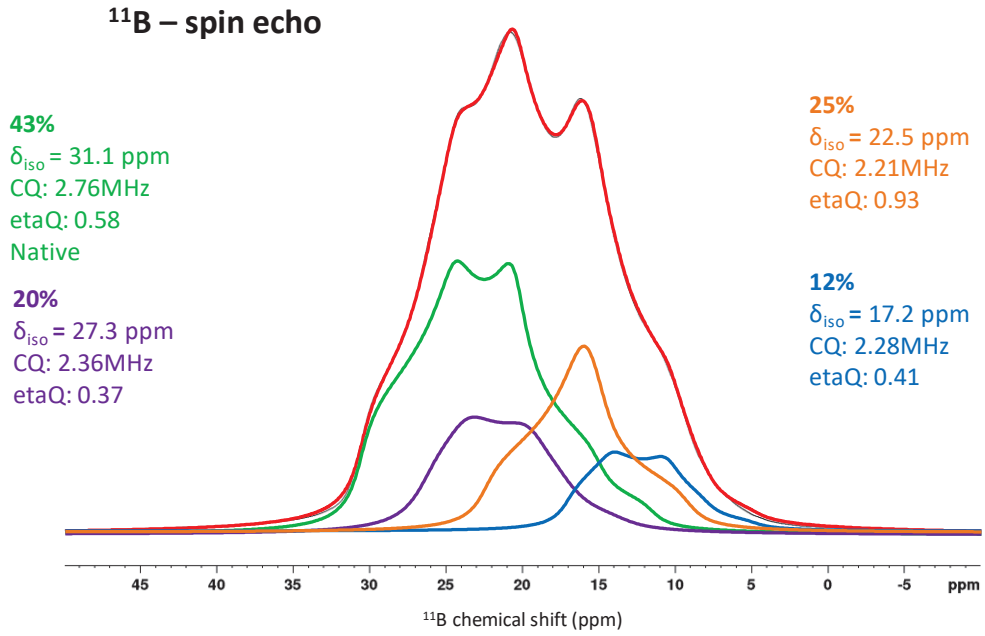

Figure IV. 30: ^{11}B ss-NMR spectrum of the 30 % mix after 2 h at 300°C in red and fits of four species in green, purple, orange and blue performed with « dmfit » software.

Thanks to 2D ^{11}B-^{11}B ss-NMR spectrum in Figure IV. 31, it was confirmed that four different boron species can be differentiate after the thermic treatment in the 30 % mix. The signal at 31 ppm corresponds to the native boron specie of the 1,3,5-phenyltriboronic acid, tris(pinacol) ester.

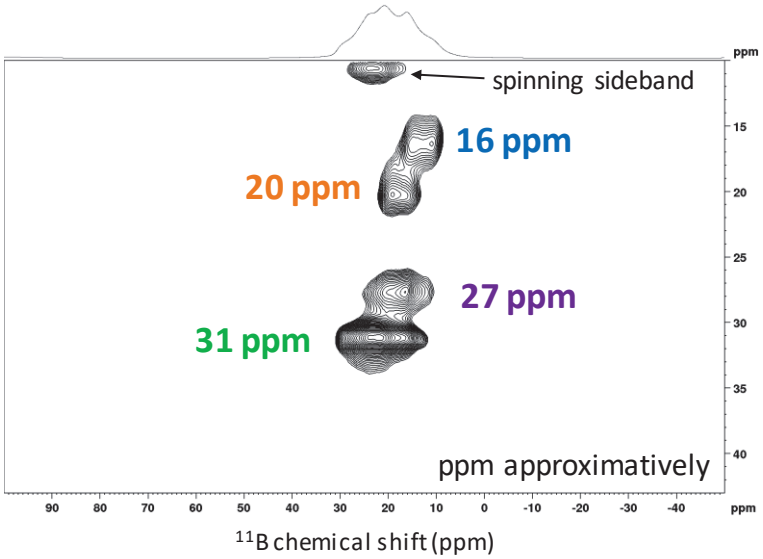

Figure IV. 31: Multiple-Quantum Magic-Angle Spinning (MQMAS) ss-NMR spectrum ^{11}B-^{11}B of the 30 % mix after 2 h at 300°C.

It was also possible to compare by ^{13}C ss-NMR spectroscopy the signals of the 30 mol % mixture before and after the thermic treatment as depicted in Figure IV. 32 and there are some obvious

new signals indicating the creation of new species, especially an important signal around 62 ppm that could correspond to **C**H_2-O-B, in accordance with the assumptions made so far.

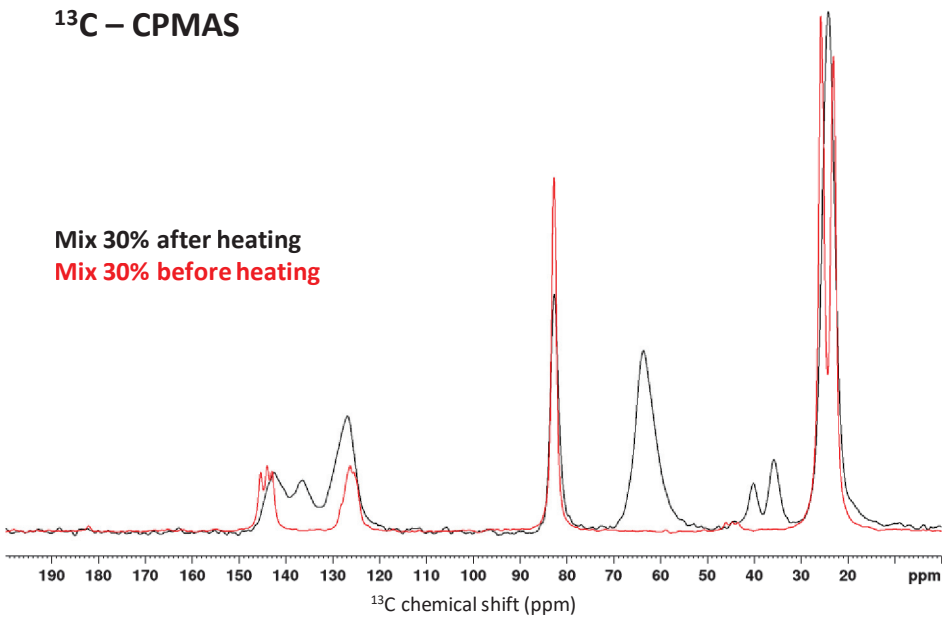

Figure IV. 32: Superposition of the ^{13}C ss-NMR spectra of the 30 % mix before 2 h at 300°C in red and after 2 h at 300°C in black.

When comparing the two mixtures at 10 mol % and 30 mol % after heating at 300°C in Figure IV. 33, we noted that the small signals aforementioned appearing for the 10 mol % mix are in the same position that the new signals observed in the case of the 30 mol % mixture. We assumed that the new signals are the results of the reactivity of the boronate esters and the more we added pentaerythritol, the more we allowed for the reactivity of the boronate ester groups.

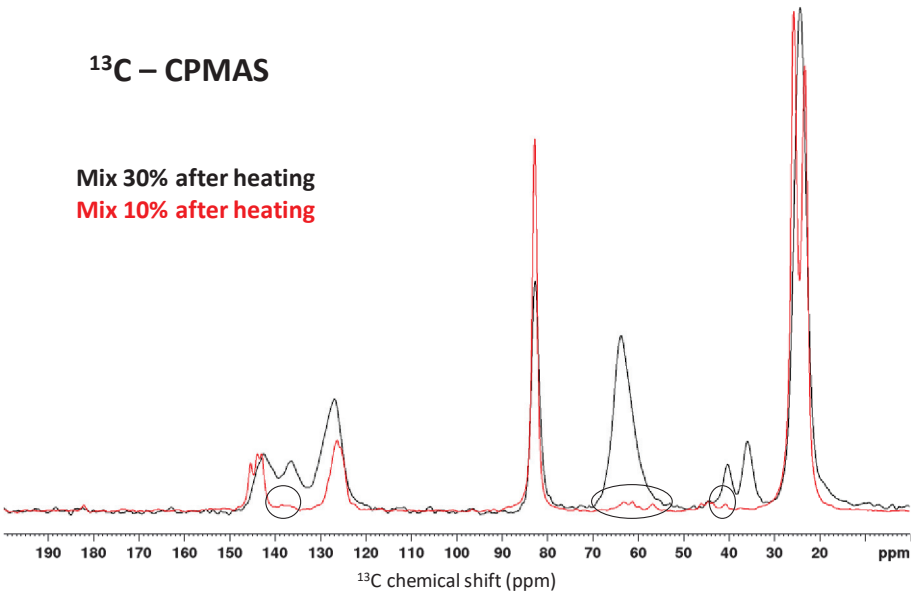

Figure IV. 33: Superposition of the ^{13}C ss-NMR spectra of the 10 % mix after 2 h at 300°C in red and of the 30 % mix after 2 h at 300°C in black.

e. Mechanism hypothesis for the formation of hybrid glasses

After the reaction, we assumed that several types of rearrangements could induce the glass formation observed in molten state. (Figure IV. 34) Mainly, we assumed that the boronate esters exhibit the same reactivity described so long. In this case, pentaerythritol, willingly added to the reaction media, could induce the ring opening of the cyclic boronate esters creating linkages between the trifunctional molecules.

In another hypothesis, the linkages could be formed through pentaerythritol molecules, which have a functionality of four *via* transesterification reactions. Hence, they could react on several boron atoms at the same time inducing the crosslinking.

Besides, ss-NMR spectroscopy indicates the creation of three new species by reaction of 1,3,5-phenyltriboronic acid, tris(pinacol) ester which is consistent with the hypothesis of mechanism described in Figure IV. 34 as many structures are possible depending on the ability of pentaerythritol to react with each of the alcohol groups.

Moreover, the optimized ratio O/B found to reach the maximum of glass transition temperature is 3.2 suggesting the pyramidalization at the boron atom that might be surrounded by three oxygen atoms. An excess is needed as we supposed that, due to geometric issues, the four oxygen atoms of pentaerythritol could not be linked to boron atoms at the same time.

This was also confirmed by ss-NMR spectroscopy as in the mixture at 30 mol % where we reach 3.2 ratio O/B, the reactivity of the boronate esters was not quantitative and an important of boronate esters might not be impacted by the ring-opening or transesterification reactions.

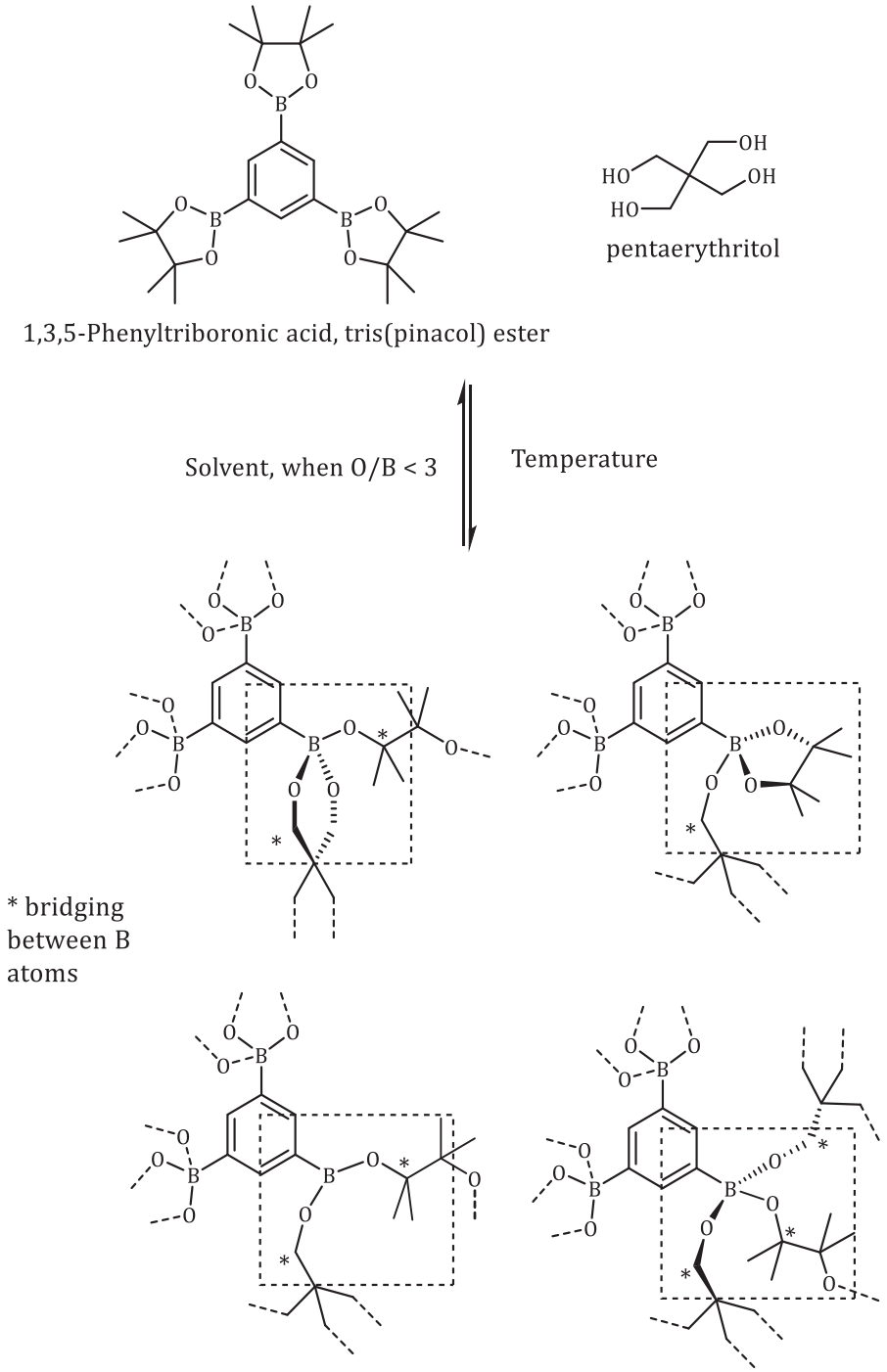

Figure IV. 34: Types of boronate arrangements in the boronate hybrid glass. Hydrogen atoms are omitted for clarity.

Through this example, we showed that the reactivity of boronate esters can be extended to small molecule systems proving that we are able to form hybrid organic/inorganic glasses.

III. Vinyl-boron derivatives

So far, we investigated systems with boronate esters installed on an aryl group such as styrenic functionalized monomer. In this part, we wanted to push the understanding further with the study of vinyl-boronate esters groups.

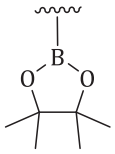

Figure IV. 35: Vinyl-boron systems.

A. Dynamic cross-linked polymers with boronate esters on ethylenic backbone

a. Strategy of synthesis of poly(vinylboronic pinacolate)

In this optic, we synthesized a vinylic polymer bearing boronate esters based on the vinylboronic pinacolate as represented in Figure IV. 36. However, as far as we know, we did not find any attempt of polymerizing this compound in the literature until 2017, when we performed the polymerization for the first time. Indeed, similar compounds are supposed not to polymerize due to the proximity of the double bond to the electronic vacancy of the boron atom trapping radicals.

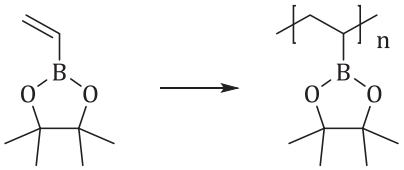

Figure IV. 36: Vinyl polymer carrying boronic pinacolates.

Indeed, it is a reagent mainly used for reactions such as

- Suzuki-Miyaura couplings [21]
- Mizoroki-Heck reactions [21]
- Intramolecular Nozaki-Hiyama-Kishi reactions [22]
- Stereoselective copper-catalyzed selective couplings [23]
- Cycloaddition of dialkoxycarbenes [24]
- Regio- and stereoselective synthesis of trisubstituted alkenes *via* gold-catalyzed hydrophosphoryloxylation of haloalkynes followed by palladium-catalyzed consecutive cross-coupling [25]
- Asymmetric Birch reaction alkylation [26]
- Preparation of molecular tubes for lipid sensing or enzymatic inhibitors, antibiotics and other biologically compounds. [27]–[30]

At that time, we considered the free radical polymerization of the boron-based monomer in the same conditions as usual i.e. the use of 0.02 molar equivalents of benzoyl peroxide, toluene as the solvent of polymerization and 70°C as the temperature. Nevertheless, the polymerization was not effective in these conditions.

We assumed that the proximity of the double C=C bond and the boron atom bearing an electron vacancy is the main issue. Indeed, instead of reacting on the double C=C bond of the monomer, the benzoyl peroxide radical formed by thermal decomposition is directly attacking the vacancy of the boron atom of the monomer. Consequently, it stops the polymerization process directly.

Therefore, we decided to adopt a capping strategy on the electron vacancy of the boron atom. THF was intentionally added to the reaction media during the polymerization process and formed a complex with the boron-based monomer thus preventing the boron atom from any radical attack and allowing the double bond to be the active site for the polymerization.

According to this strategy, **the polymerization was conducted with one molar equivalent of THF compared to the monomer, 0.02 molar equivalents of benzoyl peroxide in toluene and at the temperature of 70°C.** The ^{1}H, ^{13}C and ^{11}B are respectively illustrated from Figures V. 107 to V. 109 in the Experimental Section as well as the chromatograms in Figure V. 111.

Table IV. 3: Synthesis results of poly(4-vinylphenylboronic pinacolate). [1]Values determined by SEC-THF using PS standards and conventional calibration.

Entry	*Solvent*	*T (°C)*	*M_n[1]*	*M_w[1]*	*Dispersity Đ*	*Yield*
1	Toluene	70	1 500	2 900	1.9	50 %
2	Toluene	70	1 600	3 100	1.9	30 %
3	Toluene	70	1 700	3 100	1.9	100 %
4	Toluene	80	1 600	2 600	1.6	35 %
5	Toluene	80	1 400	2 000	1.5	78 %
6	Toluene	90	1 300	2 500	1.9	56 %
7	Toluene	90	1 700	2 500	1.5	85 %
8	Bulk	70	2 600	4 300	1.6	55 %

The main drawback of this polymerization is the low molar masses obtained from the entries 1 to 7 in Table IV. 3 that can have an impact on the mechanical properties of the material, as

entanglement seems unlikely. To allow for the formation of high molar masses, we tried to work in bulk but the result was moderately successful. (Entry 8, Table IV. 3)

After our study on this polymer and its properties, Whang *et al.* reported, at the beginning of 2019, the polymerization of vinylboronic pinacolate for the synthesis of electrolytes. In their work, they introduced poly(vinylboronic pinacolate) segments into an hyperbranched polymer *via* RAFT polymerization using a macromolecular chain transfer agent, AIBN as initiator and DMF as polymerization solvent. [31] Concerning the molar masses, no information was mentioned so we were not able to compare. We can also raise some doubts on the use of AIBN as initiator in this polymerization, since the nitrile groups can react on the boron vacancy of the monomer.

b. Differential scanning calorimetry study

After a drying process under high vacuum during several hours, the freshly synthesized polymer was analyzed by differential scanning calorimetry.

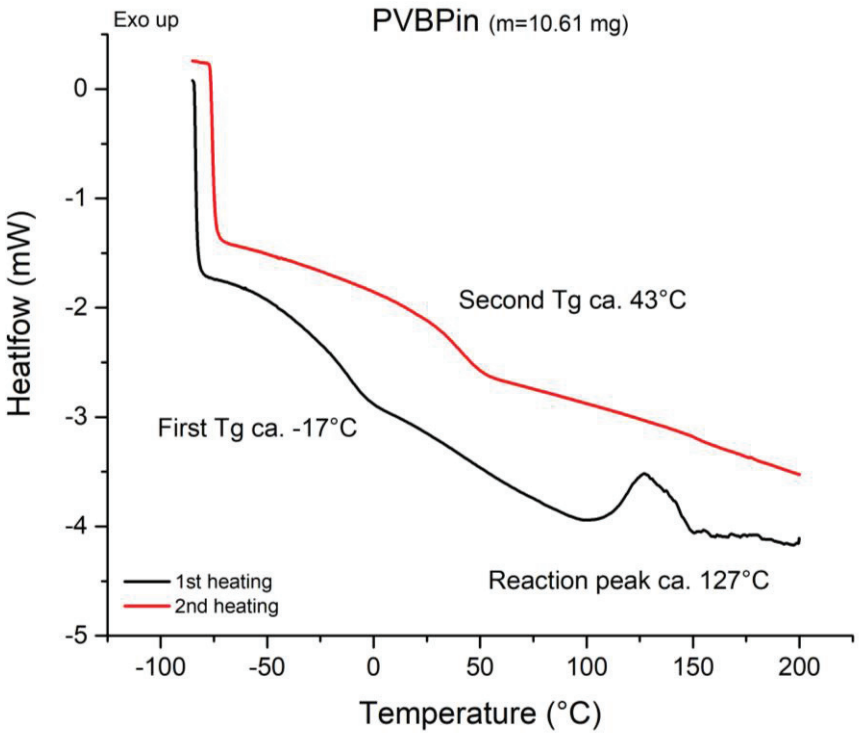

Figure IV. 37: DSC thermograms of poly(vinylboronic pinacolate) in 40 µL opened aluminum pans.

Unsurprisingly, we observed the same behavior as we can see in Figure IV. 37. In this manner, during the first heating segment, a first glass transition temperature is detected around -17°C which is a normal T_g for a polymer with a vinylic backbone thus exhibiting higher flexibility and ability to flow under temperature. Starting around 100°C, a clearly exothermic event happened corresponding to the crosslinking within the polymer due to the ring opening of boronate ester

moieties. It is also interesting to note that the increase of T_g after the first heating ($\Delta T_g \approx 60°C$) is much lower than for PSBPin studied in the previous chapter ($\Delta T_g \approx 140°C$).

This variety of polymer structures enables to reach very different glass transition temperatures as well as many different mechanical properties. Still, all the polymer networks are constructed on the same basis namely harnessing the boronate esters reactivity. From this finding, we can reach a large range of crosslinked structures with all the commercial common monomers used in industry.

c. Rheology investigation

After the DSC analyses of the newly synthesized polymer, we assessed its macroscopic behavior in order to distinguish the effect of type of boronate ester groups on the mechanical properties of the polymer in bulk.

For comparison to PSBPin from the previous chapter, the low glass transition temperature of the initial state enables to process the polymer at room temperature, e.g. without triggering any reaction, and to study the crosslinking phenomenon in-situ.

Firstly, we probed the storage and loss moduli of the polymer in bulk with the temperature ramping up from 50°C to 150°C at 0.02°C/min as represented in Figure IV. 38.

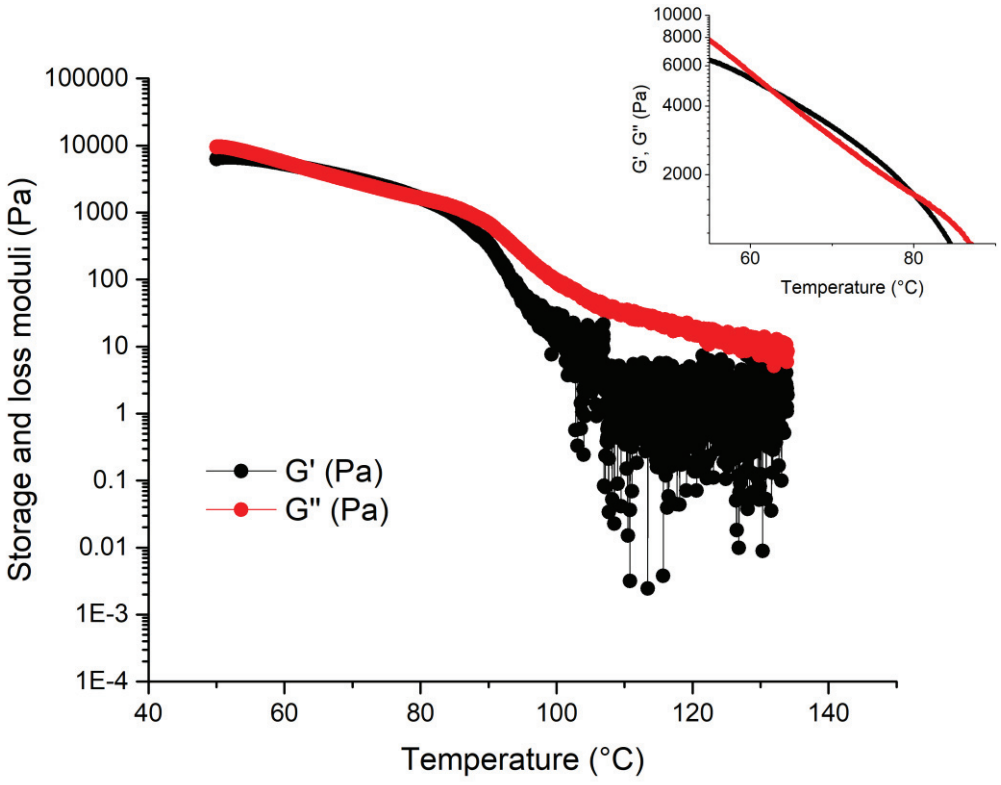

Figure IV. 38: Monitoring of the storage and loss moduli from 50°C to 150°C at 1 Hz. Inset: Zoom between 55 °C and 90°C.

We would have expect a transition to an elastic behavior (G'>G'') at high temperatures if the behavior were the same as in the case of the styrenic boron-based polymers.

Surprisingly, in this peculiar case, the material only shows an elastic behavior (G'>G'') over a very short temperature range between 60°C and 80°C as it can be seen in the inset of Figure IV. 38. This is the signature of a dynamic crosslinking only effective in a specific range of temperature.

This could indicate that the ring opening and the induced crosslinking is occurring in the 60-80°C temperature range. Beyond these temperatures, the reverse reaction could be favored with the closed cycle of the boronate esters favored. Besides, in the specific case of the vinylic boron-based polymers, the C-B bond is a lot less stable than in the case of sytrenic boron-based polymers and could be oxidized with the increase of temperatures. To guarantee the integrity of the C-B bond over temperature range, it could be interesting to perform some ss-NMR analyses.

The investigation was pursued by the measurements of the storage and loss moduli during frequency sweeps at different temperatures after the heating segment up to 150°C as depicted in Figure IV. 39.

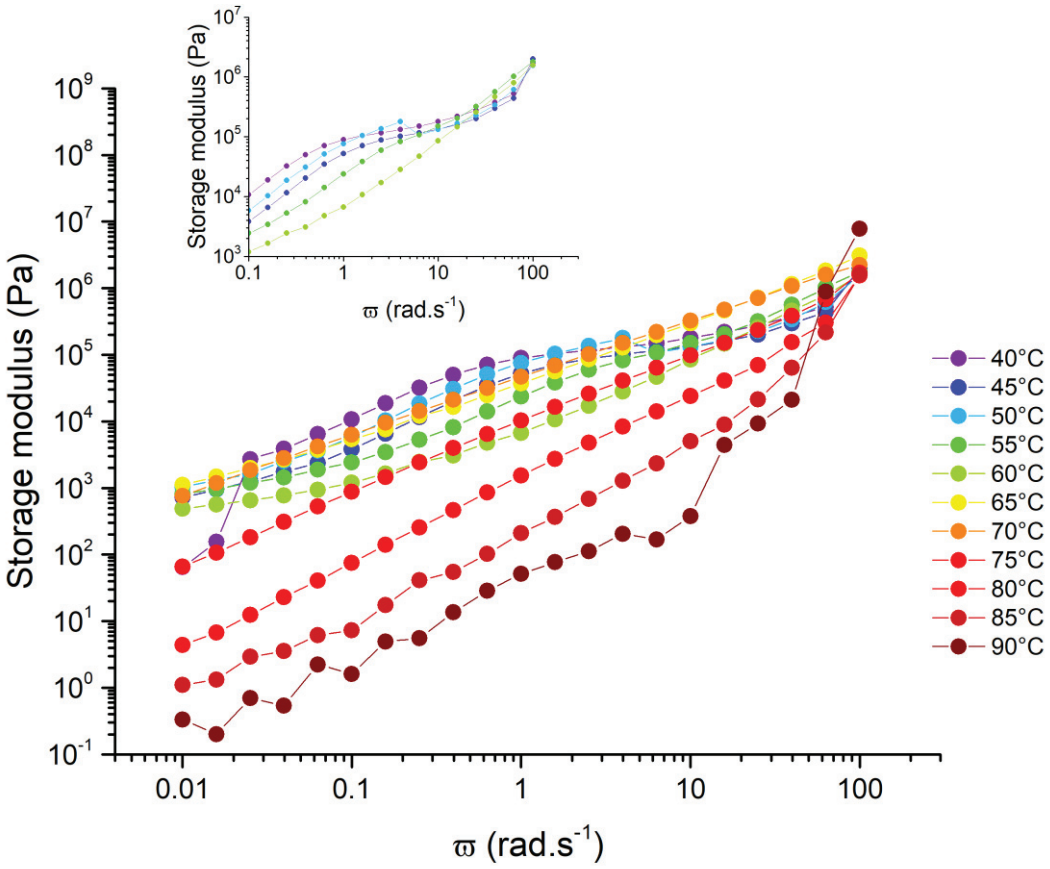

Figure IV. 39: Monitoring of the storage modulus during frequency sweeps on poly(vinylboronic pinacolate) from 90°C to 40°C. The loss modulus is not represented for easier reading of the curves.

From 90°C to 70°C, the storage modulus and thus the viscosity was found to increase which is a normal effect of the decrease of temperature. The polymer exhibits a viscoelastic behavior in this range of temperatures. However, unexpectedly, the modulus roughly decreased from 70°C to 60°C. This tendency was reversed decreasing under 60°C where the modulus was found to increase again. Besides, from 50°C to 40°C a clear rubber plateau is detected.

These data confirmed the presence of a crosslinking in a certain temperature range and also evidenced the presence of an elastomer behavior in a range of frequencies that varies with the temperature. We hypothesized that probing the material at higher frequencies for the higher temperatures would have put into light a rubber plateau at high frequencies.

This confirms the dynamic character of the crosslinking induced by the ring opening of the boronate esters moieties in the polymer. Indeed, it was determined that the crosslinking is favored on a precise temperature range and that the de-crosslinking is possible at high temperatures. However, to confirm these assumptions, further studies are required, especially by spectroscopies.

B. Attempt of copolymerization of vinylboronic pinacolate with a common monomer: ethylene

a. Attempt of copolymerization with vinyl acetate and thermal results

Before running the copolymerization of vinylboronic pinacolate with ethylene, we first tested the copolymerization of this boron-based monomer with vinyl acetate, which is often involved in copolymerization with ethylene. Ethylene and vinyl acetate exhibit some close properties in terms of polymerization and we assumed that if the copolymerization of vinylboronic pinacolate with vinyl acetate is effective, the copolymerization with ethylene could be accessible. Indeed, vinyl acetate and ethylene are two monomers that are co-polymerizable.

The copolymerization of vinylboronic pinacolate and vinyl acetate is conducted in the optimized conditions determined in the last part about the homopolymerization of vinylboronic pinacolate. In these conditions, the copolymerization is performed at 70°C in toluene with one molar equivalent of dried THF compared to the boron-based monomer and 0.02 molar equivalent of benzoyl peroxide compared to the total amount of co-monomers. The copolymers from vinyl acetate and vinylboronic pinacolate will be further noted as PVac-VBPin – x % with x % the molar ratio of vinylboronic pinacolate in the final copolymer (Figure IV. 40).

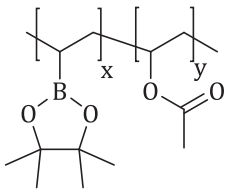

Figure IV. 40: Copolymer from vinylboronic pinacolate and vinyl acetate PVac-VBPin - x % with x % the ratio of vinylboronic pinacolate.

From these conditions, we were able to copolymerize the two monomers in controlled ratios. The results are set in Table IV. 4 and the NMR spectra and chromatograms are respectively available from Figures V. 112 to V. 115 and Figure V. 119 in the Experimental Section.

Table IV. 4 : Results of copolymers syntheses from vinyl acetate and vinylboronic pinacolate [1]Determination by NMR spectroscopy. [2]Values determined by SEC-THF using PS standards and conventional calibration.

Entry	***Experimental ratio of VBPin %[1]***	***M_n[2]***	***M_w[2]***	***Dispersity Đ***	***Yield***
1	0	6 700	11 900	1.8	27%
2	15	2 700	5 800	2.1	70 %
3	52	5 100	11 000	2.1	56 %

As usual, the copolymers were firstly characterized by differential scanning calorimetry.

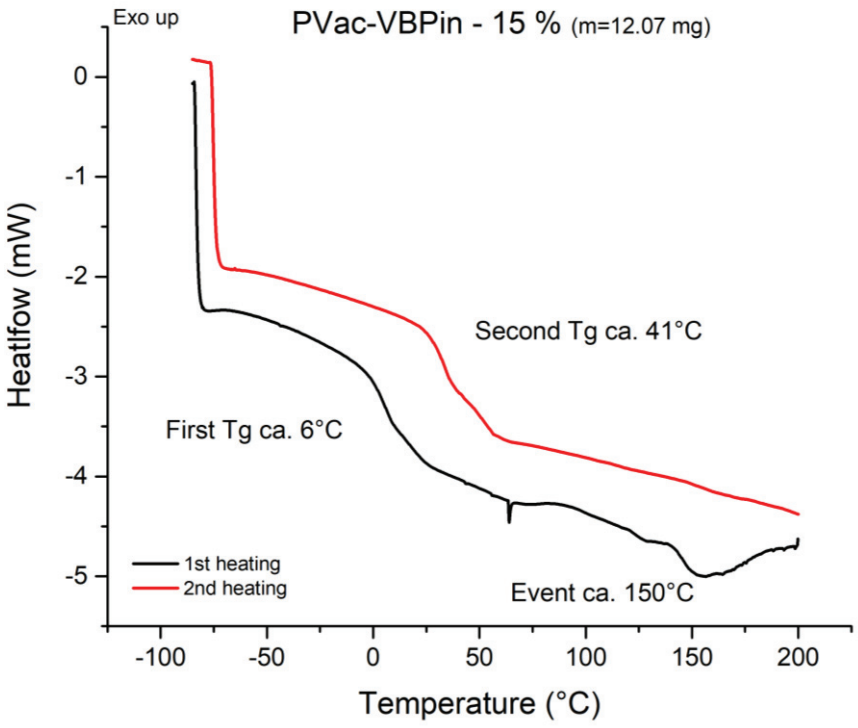

Figure IV. 41: DSC thermograms of poly(vinylboronic pinacolate-co-vinyl acetate) with 15 % of VBPin in 40 µL opened aluminum pans.

Unsurprisingly, we found again the same behavior as we can see in Figure IV. 41. In this manner, during the first heating segment, a first glass transition temperature is detected around 6°C. A thermal event is happening from 90 to 180°C corresponding to the crosslinking within the polymer due to the ring opening of boronate ester moieties. However, in this case, it seems to be harder to determine if the event is endothermic or exothermic. A superposition of the reactive and evaporation events could hinder the outlook of the phenomena.

The effective copolymerization of vinyl acetate and vinylboronic pinacolate gave us hope concerning the possibility of copolymerization of ethylene and vinylboronic pinacolate. Only used as a synthetic attempt, it could still be interesting to study this copolymer by rheology to probe the mechanical properties of the material.

b. Strategy used for the copolymerization of vinylboronic pinacolate and ethylene

Ethylene is at the origin of numerous polymers and plastic materials in the chemical industry. Indeed, polyethylene (PE) is one of the simplest and less expensive polymer, part of the polyolefin family. The world production of polyethylene was estimated at 100 million tons in 2018 and represents a third of the plastics' production. [32] It is mainly synthesized by radical polymerization or *via* Ziegler-Natta catalysis. [33] Polyethylene is a thermoplastic chemically inert and is mainly used in packaging applications. Depending on the branching present in the polymer, polyethylene can be classified as low-density polyethylene (LDPE) containing a lot of branching, or high-density polyethylene (HDPE) exhibiting more linear chains. Related to their structure, they are thus used in different applications: plastic bottles, plastic bags and packaging for LDPE, and chemical containers and insulation of electric cables for HDPE. [32] Besides, polyethylene can also be crosslinked and used in pipework systems, hydronic radiant heating and cooling systems. Various methods can be used to obtain crosslinked polyethylene such as:

- Peroxide crosslinking using, for instance, dicumyl peroxide or di-tert-butyl peroxide in an extruder at high temperatures to initiate the reaction of crosslinking. [34]
- Silane crosslinking *via* Si-functionalized polyethylene, the crosslinking can be initiated by radiation or by a small addition of peroxide or still by condensation of Si-OH groups to form Si-O-Si bridges. [34]
- Irradiation crosslinking through splitting of hydrogen atoms by a radiation source (usually an electron accelerator, occasionally an isotopic radiator). [34]
- Azo crosslinking by extrusion at high temperatures with pre-added azo compounds (for instance, 2,2'-azo-bis(2-acetoxy-propane). [34], [35]

In this part, the goal is to create a new way for the crosslinking of polyethylene *via* the copolymerization with vinylboronic pinacolate. Indeed, by harnessing the reactivity of boronate esters, it is possible to afford a crosslinked polymer as described in the previous parts and in the previous chapter.

The main challenge is the ability to copolymerize the ethylenic monomer with the boron-based monomer as targeted in Figure IV. 42. Besides, we were attracted by the possibility to run this polymerization without solvent in supercritical CO_2 making the process greener.

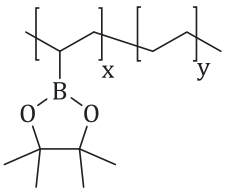

Figure IV. 42: Copolymer from ethylene and vinylboronic pinacolate.

To perform the attempt of copolymerization, we worked in a high-pressure reactor, necessary for the ethylene gas monomer. The reactor used is represented in Figure IV. 43.

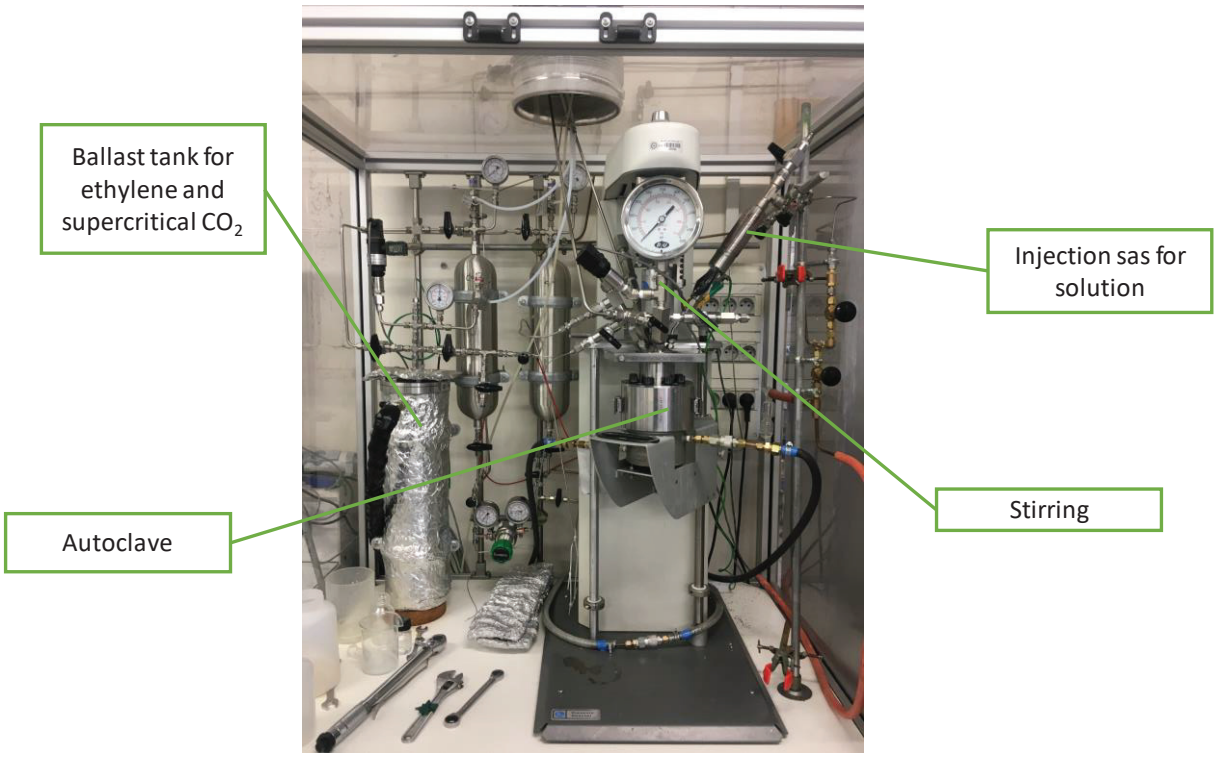

Figure IV. 43: High-pressure reactor used for the copolymerization with ethylene.

An intermediate 1.5 L tank filled with ethylene was used to fill up the reactor. The tank was cooled down to -20°C to transfer ethylene as a liquid at 35 bars. Then, when thermodynamic equilibrium was reached, the intermediate tank was isolated and heated to reach up to 300 bars of ethylene pressure. In a Schlenk tube was introduced the desired quantity of benzoyl peroxide, vinylboronic pinacolate protected by THF and dimethyl carbonate as solvent in the case of polymerization in solution. We chose dimethyl carbonate as it is often used in the polymerization of ethylene and that has the advantage of being low-transferring thus avoiding transfer reactions. Then the solution was introduced into the reactor through the injection sas. Afterward, ethylene was added until the desire pressure (200 bars). For polymerization in supercritical CO_2, the tank was once again cooled down to -20°C to liquefy CO_2 at 35 bars and, when thermodynamic equilibrium was reached, it was isolated and pressurized up to 300 bar to have CO_2 in supercritical state. The CO_2 is added after ethylene in the reactor autoclave. After 4 hours of polymerization under stirring at 70°C, the reactor was slowly cooled down and degassed. After opening the reactor, we could take back the polymer that is studied without further purification.

c. Problems during synthesis and hypothesis

After the synthesis process, the yields of the copolymerization remained very low whether the reaction took place in dimethyl carbonate or in supercritical CO_2.

We assumed that, in this case, the THF protection on the electronic vacancy of the boron atom of the monomer is not enough to allow for radical polymerization under pressure. The radical formed from ethylene is extremely reactive and might better react on the boron to form another radical than on the double C=C bond of the boron-based monomer. This has the effect to immediately stop the propagation process as the growing chains are ended by the transfer to the boron atom. The molar masses obtained should thus be very low as well, mostly forming some oligomers. It could be interesting to find better protecting agents than THF with a stronger Lewis basicity (for example, triethylamine).

However, the small amounts of powder obtained were characterized by molecular and thermal methods without further purification. Firstly, NMR spectroscopy showed that the copolymer synthesis was evidenced by the presence of signals corresponding to ethylene and vinylboronic pinacolate monomer units in the copolymer whether the synthesis was run in dimethyl carbonate or in supercritical CO_2. The NMR spectra and attributions are detailed in Experimental section from Figures V. 121 to V. 124.

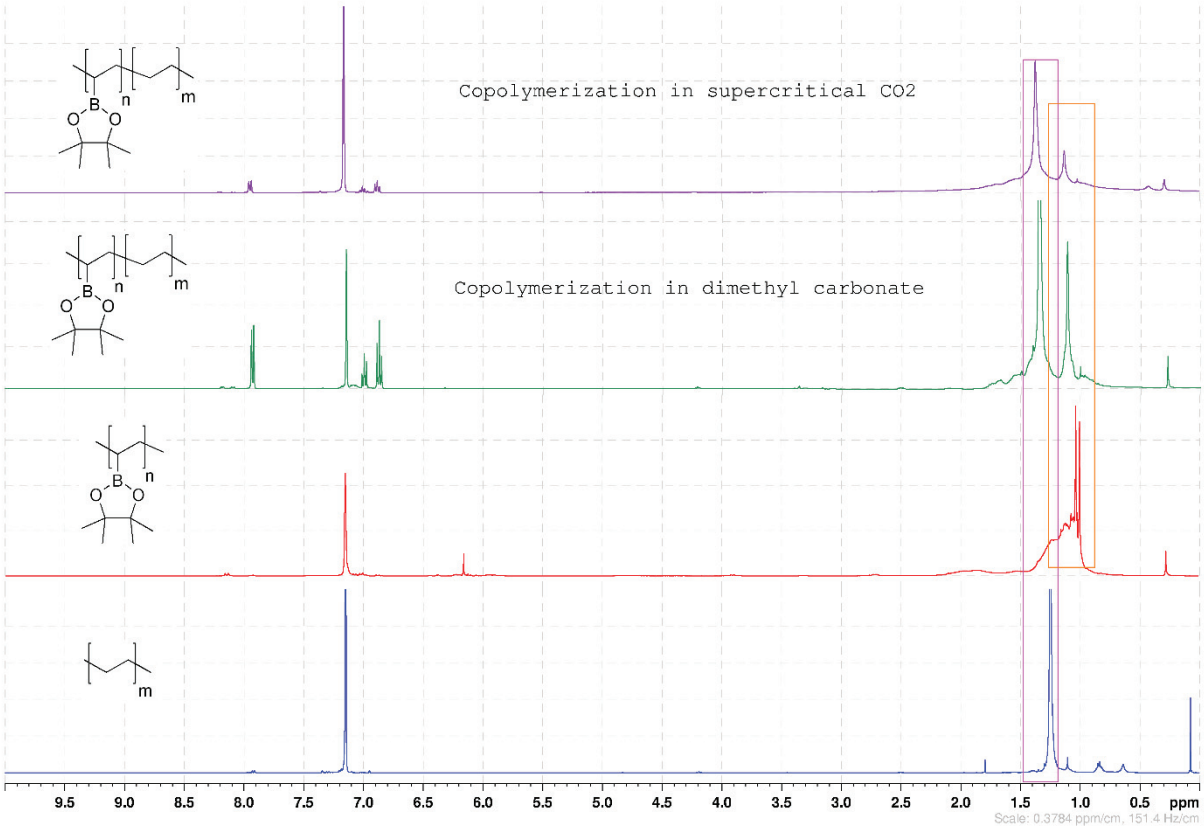

Figure IV. 44: ^{1}H NMR spetra of polyethylene (blue), poly(vinylboronic pinacolate) (red), poly(vinylboronic pinacolate-co-ethylene) synthesized in dimethyl carbonate (green) and in supercritical CO_2 (purple).

As we can notice on Figure IV. 44, the copolymers synthesized in dimethyl carbonate or in supercritical CO_2 contain polyethylene segments (pink box) and also poly(vinylboronic pinacolate) ones (orange box). The copolymerizations were found to be effective even if the yields and supposedly the molar masses remain very low. Chain-ends from initiation and from transfer to benzoyl peroxide can even be observed on NMR spectra. Size-exclusion chromatography at high temperature should be performed to confirm our hypothesis.

The incorporation of vinylboronic pinacolate monomer in the copolymer was estimated between 10 and 20 mol % depending on the batch studied.

d. DSC data

The main goal of these syntheses was to determine the influence of the presence of boronate ester moieties in a copolymer from ethylene. To access the thermal properties of the copolymers synthesized, differential scanning calorimetry measurements were conducted on the materials after drying under high vacuum.

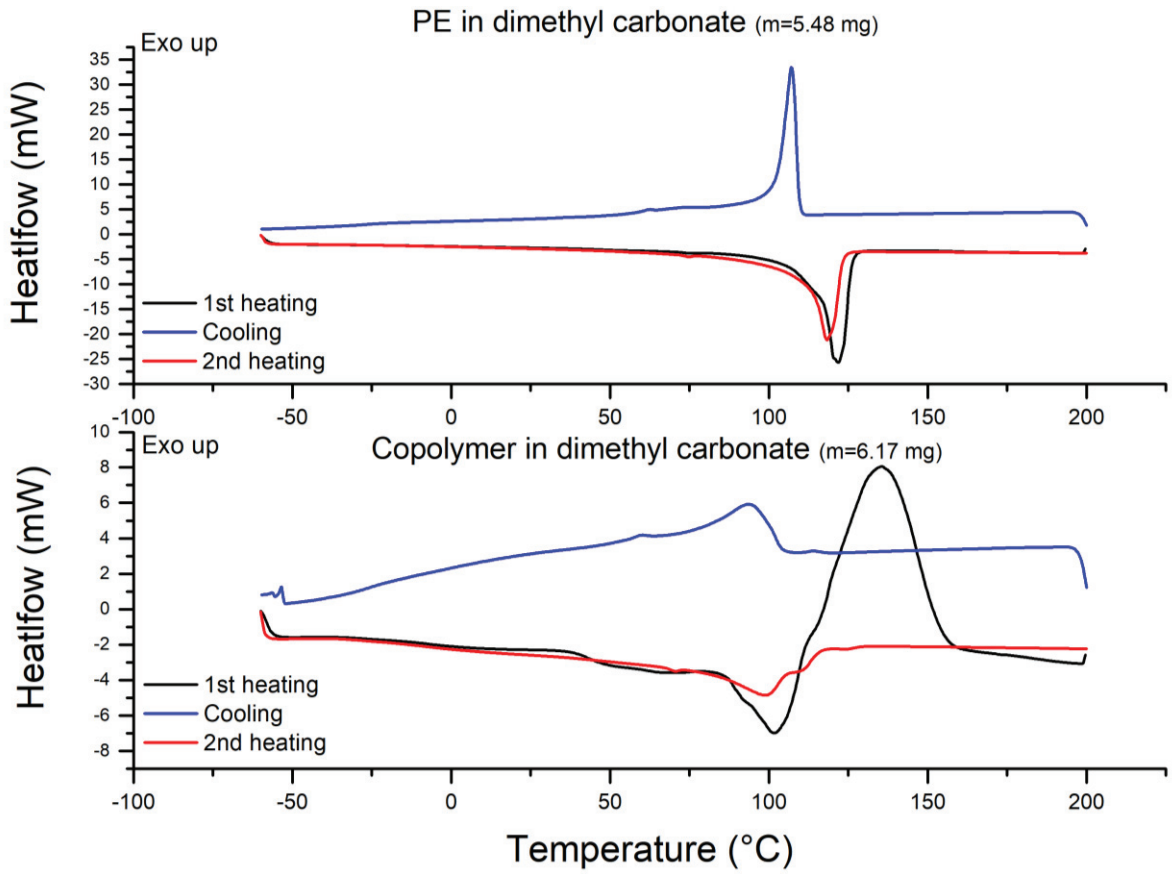

Figure IV. 45: DSC thermograms of polyethylene (up) and poly(vinylboronic pinacolate-co-ethylene) (down) synthesized in dimethyl carbonate in 40 µL opened aluminum pans.

In Figure IV. 45, the DSC thermograms of polyethylene and poly(vinylboronic pinacolate-*co*-ethylene) both synthesized in dimethyl carbonate are compared. An important perturbation of the melting and crystallization events was identified. This is quite obvious when comparing the first heating segment. In the polyethylene homopolymer, narrow melting endotherm is detected around 120°C. However, when focusing on the copolymer, several events are happening within the polymer. Firstly, an endothermic event is starting around 50°C followed by the melting identified around 110°C. Then, a clearly exothermic event is recognized starting after the melting from 115°C to 155°C. This exotherm is only noticeable on the first heating segment. On the cooling event, the crystallization seems to be perturbed as the signal is large compared to the crystallization of the homopolymers.

The same findings were made on the DSC thermograms of polyethylene and poly(vinylboronic pinacolate-*co*-ethylene) synthesized in supercritical CO_2. The only difference is the decrease of the exothermic event that might be related to the lower amount of boron-based monomer in the final copolymer. (Figure IV. 46)

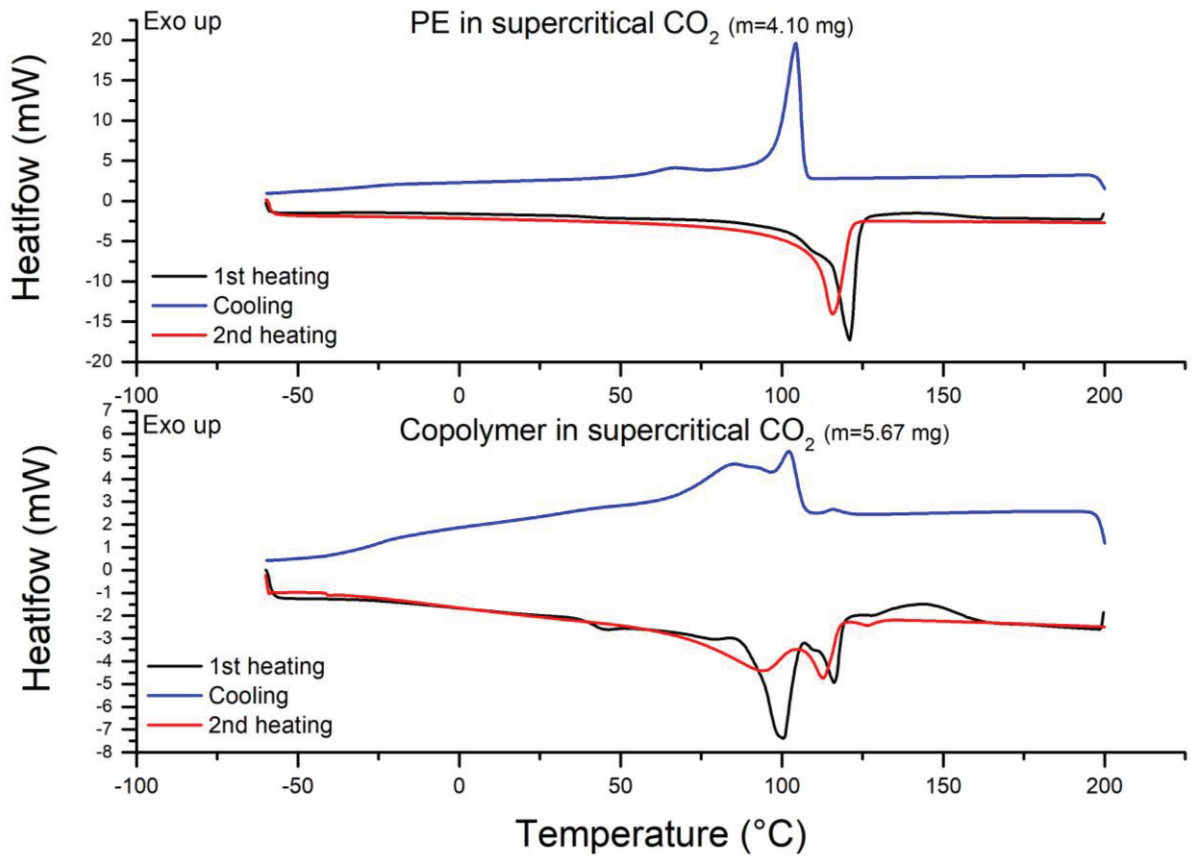

Figure IV. 46: DSC thermograms of polyethylene (up) and poly(vinylboronic pinacolate-co-ethylene) (down) synthesized in supercritical CO_2 in 40 µL opened aluminum pans.

From these outcomes, we hypothesized that the reactivity induced by the boronate ester ring-opening may hinder the rearrangements of the polyethylene segments and thus disturbe the melting and crystallization of the polymer as observed by DSC. Unfortunately, the lack of polymers due to the low yields impeded further investigation on these copolymers. Besides, due to the low T_g of the polymer, it is hard to evidence an effect of the boronate esters' reactivity on the amorphous phase.

C. Strategy used for the incorporation of boronate ester groups: functionalization of existing polymers by hydroboration

a. Objective of the hydroboration of polybutadiene

In this present work, another strategy was used for the incorporation of boronate esters in existing polymers. Indeed, we focused on the post-functionalization of polymers with boronate ester moieties working with high molar masses polybutadiene. The functionalization was conducted *via* hydroboration with pinacolborane (HBPin) on the double C=C bonds of the diene polymer.

Polybutadiene is a general-purpose rubber, often abbreviated as BR that has a high output and high consumption. The production of polybutadiene has increased in the world to reach 4.6 million tons in 2013, representing 22 % of synthetic elastomer production. It is an addition polymer of the conjugated diene monomer 1,3-butadiene and thus, depending on the monomers combination, three different microstructures can be formed in the polymer chain: cis-1,4, trans-1,4 and 1,2-linked (vinyl) chains (Figure IV. 47). The structure of the polymer can be defined by the mode of polymerization. Indeed, BR synthesized by coordination/insertion polymerization with Ziegler-Natta catalysts contains 90 % or above cis structures while anionic polymerization gives BR with less than 40 % of the cis monomer unit. These polymerization processes are the main used in industry. Emulsion polymerization can also be a method for BR synthesis, generally supplied as latex. [36]

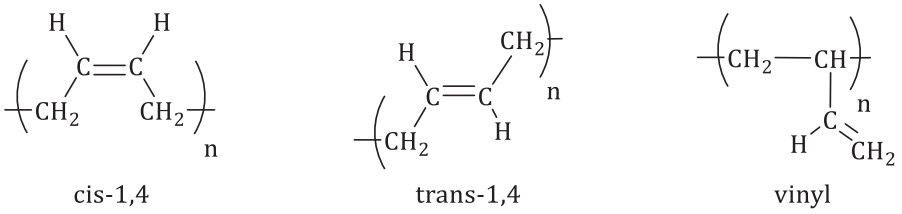

Figure IV. 47: Structures present in polybutadiene.

Polybutadiene has a low glass transition temperature between -105°C and -85°C depending on the microstructure present in the polymer after crosslinking and has characteristics of high resilience, low hysteresis loss and excellent wear resistance making it a polymer of high interests for many applications, such as in automotive tires, footwear, golf ball core... [36] In the case of automotive tires, polybutadiene is used in blends and crosslinked *via* sulfur vulcanization that enables the formation of bridges between polymers chains resulting in an increase of the mechanical properties (increased rigidity and durability). [37] It can be crosslinked by other methods such as peroxide crosslinking or still radiation-induced crosslinking. [38]

Hydroboration allows for the formation of organoborane compounds by addition of a hydrogen-boron bond across a carbon-carbon, carbon-nitrogen, carbon-oxygen double bonds as well as carbon-carbon triple bonds. As described in Chapter 1, the hydroboration of polybutadiene was reported with hydroboration agent such as bis-boracyclanes in the work of Pinazzi and Chung. [39]–[41]

However, the hydrobration involving pinacolborane (HBPin) was mainly used for the functionalization of alkenes and, as far as we know, there is no example of functionalization of dienic polymers in the literature with this precise hydroboration agent.

For the functionalization of double C=C bonds with pinacolborane as the hydroboration agent, we identified two interesting catalysts used in hydroboration: copper-based and iron-based catalysts. We relied on the work of Chirik for the iron catalysis [42] and on the work of Hartwig for the copper catalysis that are specifics to the alkenes tested. [43] We transposed some key points of their synthetically path to reach our goal on polybutadiene. Another path relying on copper catalysis was reported by Montgomery and Kerchner, but the main drawback was the use of B_2Pin_2 instead of HBPin that conducts to undesirable boron side products and that is not atom economical with ½ B_2Pin_2 consumed for the hydroboration. [44]

To set the best conditions to obtain interesting mechanical properties, we performed the functionalization on high molecular weight commercial polybutadiene from Sigma Aldrich with M_w up to 200,000 g/mol containing 11% of 1,2-vinyl, 37% 1,4-cis and 52% of 1,4-trans of conformations of double bonds. We also estimated by NMR spectroscopy the proportions of the different carbons present in the commercial polymer: -CH_2- 63.8 %, =CH_2- 3.7 %, =CH- 32.42 % by comparing the integrals. The molar masses of the commercial polybutadiene were verified by size exclusion chromatography in THF. The resulting chromatogram is disclosed in Figure IV. 48 and it is important to note that the dispersity is quite high. Analyses concerning the commercial polybutadiene are disclosed from Figures V. 125 to V. 130 in the Experimental Section.

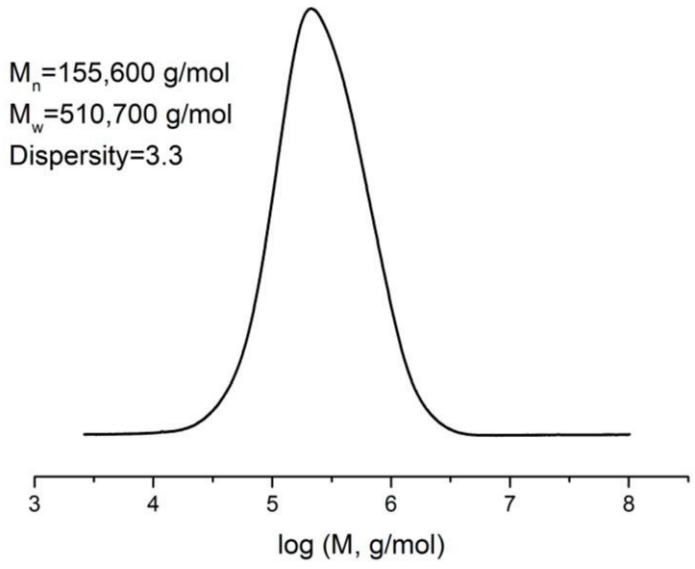

Figure IV. 48: Chromatogram of the native polybutadiene in THF.

Indeed, thanks to the ring opening of the boronate esters due to a nucleophilic intervention, the created alkoxide on the polybutadiene backbone could intermolecularly connect one boron to another through a reversible bond and thus link the polymer chains reversibly. In this optic, we could obtain a new way to reversibly crosslink a dienic polymer harnessing the reactivity of boronate esters.

b. Hydroboration by copper catalysis

i. Synthesis of the functionalized polybutadiene

For this copper catalysis, we relied on the work of Hartwig that reported a two-step strategy for diverse hydrofunctionalizations of internal alkenes. The first step is the copper-catalysis asymmetric hydroboration of internal alkenes and is the object of our interest. To reach this asymmetric functionalization, they investigated the reaction of pinacolborane (HBPin) and an alkene in the presence of a copper catalyst generated from CuCl(I) and (S)-(+)-5,5′-bis[di(3,5-di-tert-butyl-4-methoxyphenyl)phosphino]-4,4′-bi-1,3-benzodioxole ((S)-DTBM-SEGPHOS) and a base additive. (S)-DTBM-SEGPHOS was chosen for its ability to perform regioselective hydroboration with CuCl, due to its inherent chirality. [43]

However, the stereoselectivity of the hydroboration is not a necessity in our case; hence, we used another phosphine, less costly, to generate the copper catalyst with CuCl.

The functionalization *via* copper catalysis was performed with CuCl and 1,2-bis(dicyclohexylphoshino)ethane playing the role of ligand instead of (S)-DTBM-SEGPHOS. The reaction was conducted in toluene and we targeted the functionalization of 30 % molar of double C=C bonds. The experimental conditions are detailed in the Experimental section.

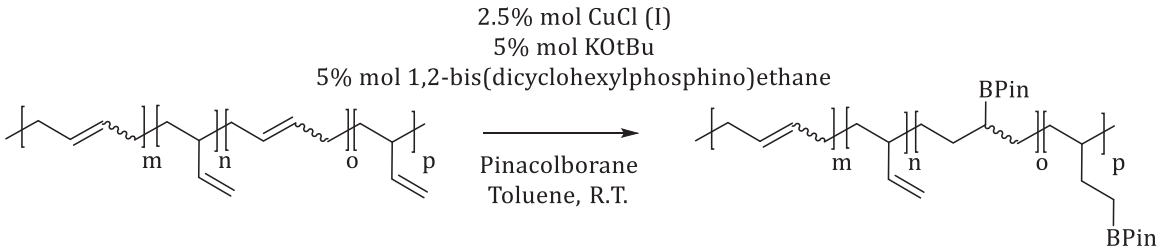

Figure IV. 49: Use of copper catalysis for hydroboration of polybutadiene.

During the reaction, some issues were faced as the rapid and important increase of the viscosity (gelation) upon addition of the catalyst. The copper catalyst might create some radicals on the double bonds that could perform coupling reactions between the chains. This is an hypothesis for the creation of a covalent network in our system. In another fashion, Guan and co-workers reported the crosslinking of polybutadiene by introducing a very low level of a Grubb's second-generation ruthenium catalyst that induces a metathesis between the C=C bonds of the polymer. [45], [46] This is unlikely to be the explanation in our case due to the absence of ruthenium in the system.

After the functionalization, the polymer obtained was characterized through several techniques without further purification. Firstly, by NMR spectroscopy, we attempted to control the efficiency of the functionalization. In this optic, the NMR spectra of the native polybutadiene and of the result of the reaction were compared as illustrated in Figure IV. 50.

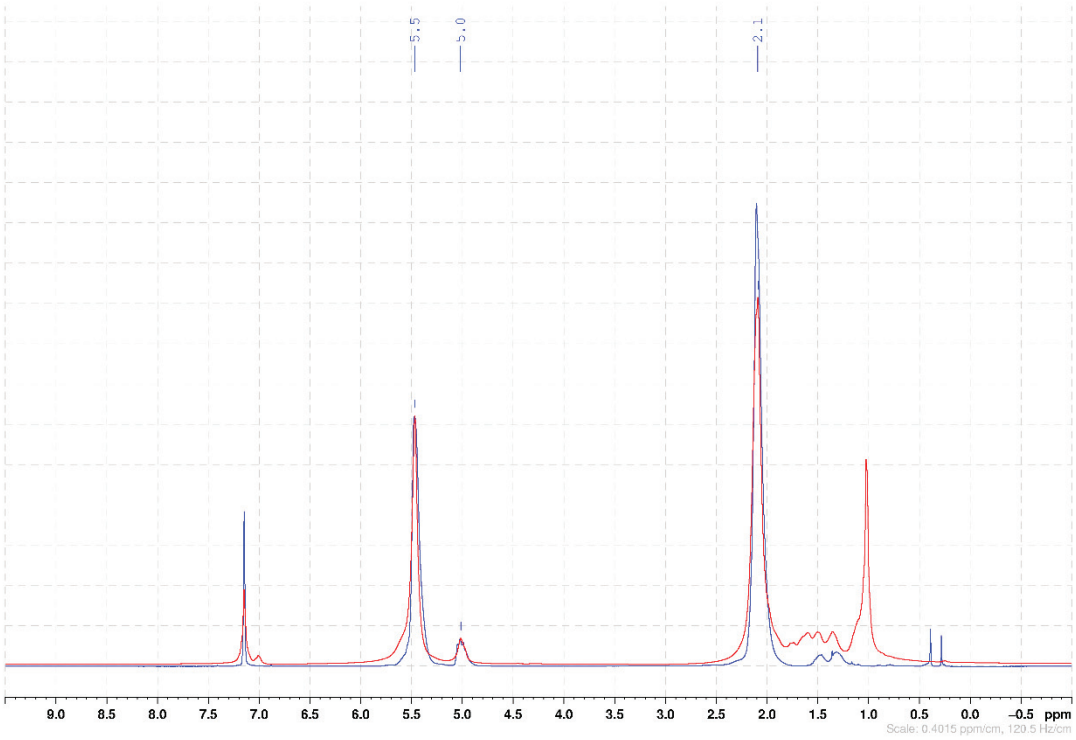

Figure IV. 50: Superposition of the native polybutadiene (blue) and polybutadiene after the functionalization via *copper catalysis (red).*

By assignments of the shifts for each structure on ^{1}H and ^{13}C NMR spectra (Figure IV. 51, Figure IV. 52), we were able to calculate the percentage of each structure present in the modified polybutadiene. The sample used for ^{13}C was more dried than the one for ^{1}H, explaining the difference of signals corresponding to the residual free HBPin. The NMR spectra are presented from Figures V. 131 to V. 133 in the Experimental Section. The assignments for the shifts are detailed in Table IV. 5.

Table IV. 5: Assignments of the shifts for microstructures in polybutadiene for ^{1}H and ^{13}C NMR spectroscopies in literature. [47]

^{1}H NMR

Shifts (ppm)	Assignments
4.9	1,2-vinyl $=CH_2$-
5.4	cis-1,4 + trans-1,4 =CH-
5.6	1,2-vinyl $=CH_2$

^{13}C NMR

Shifts (ppm)	Assignments
27.4	cis-1,4
32.7	trans-1,4

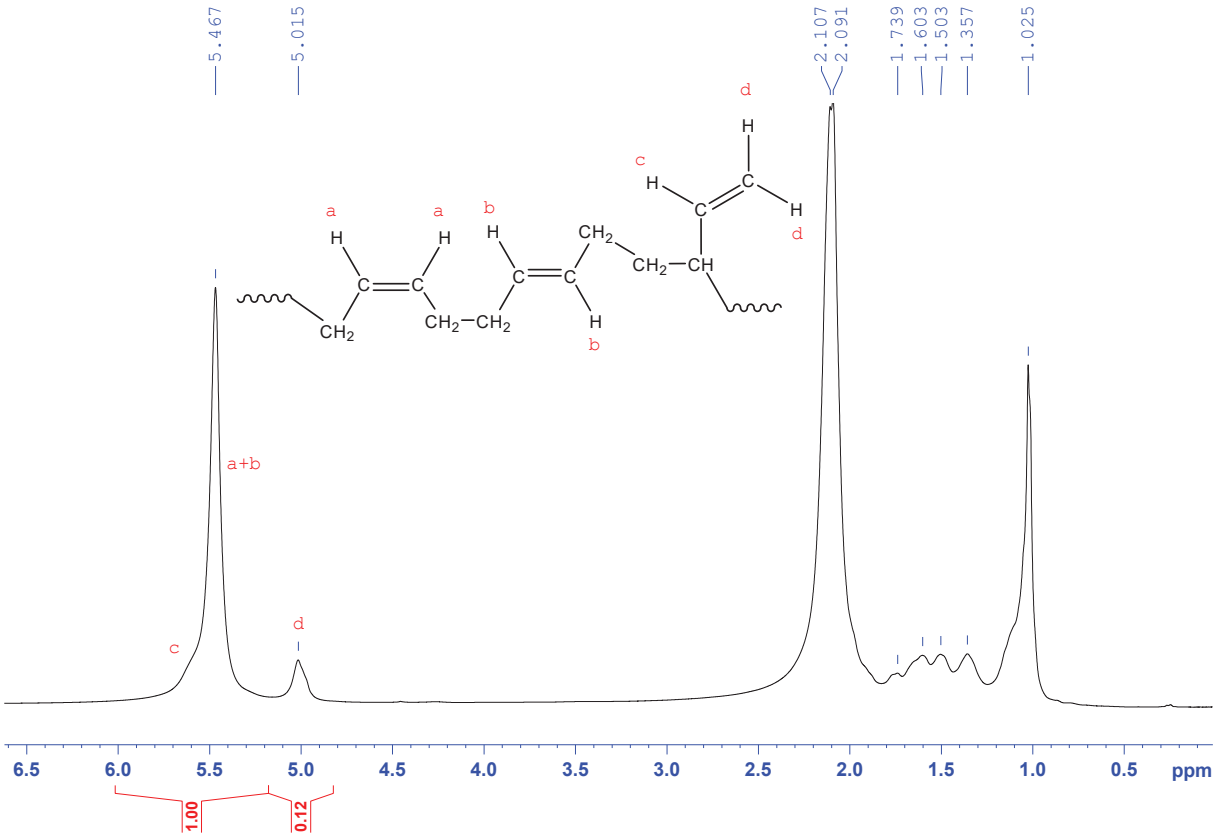

Figure IV. 51:¹H NMR spectrum of modified polybutadiene via *copper catalysis in C_6D_6. (Figure V. 131)*

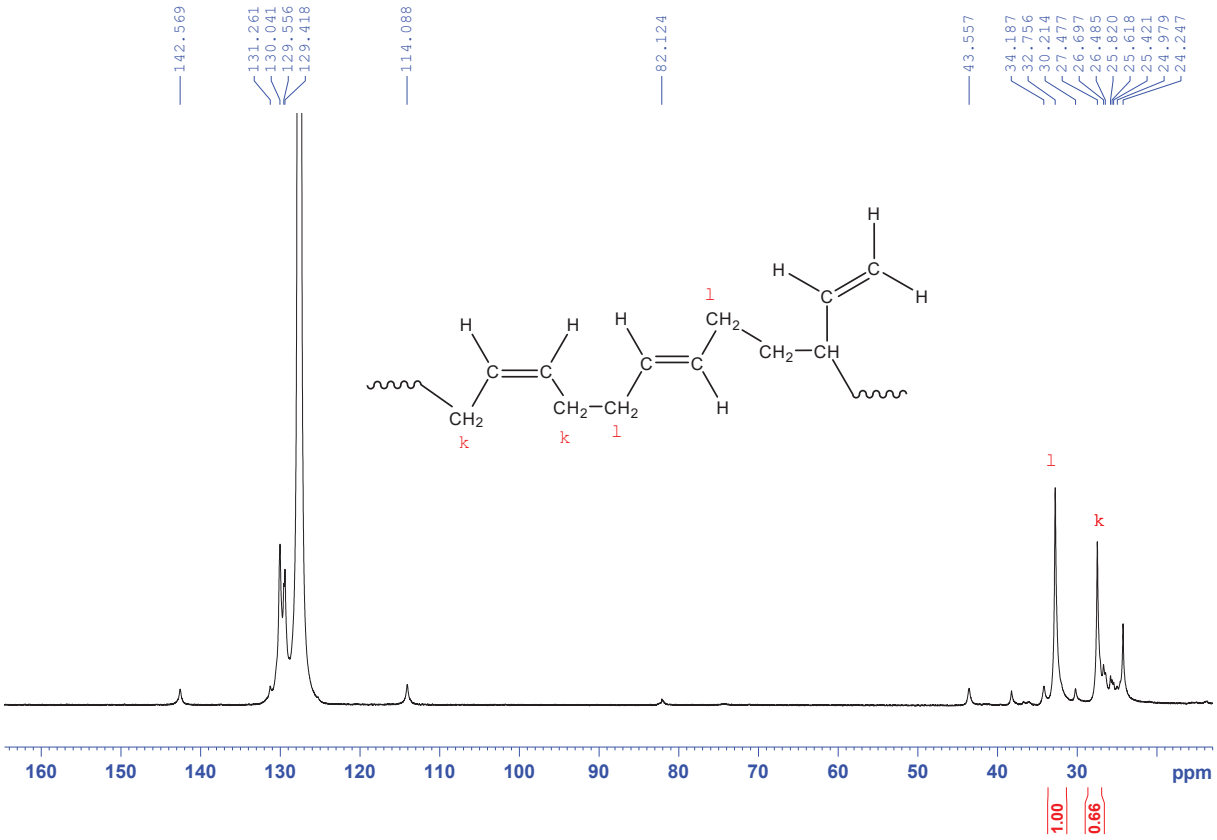

Figure IV. 52: ¹³C NMR spectrum of modified polybutadiene via *copper catalysis in C_6D_6. (Figure V. 132)*

The total molar content of 1,2 and 1,4 structures can be easily estimated by ^{1}H NMR spectrum while ^{13}C NMR spectrum allows for the calculation of cis-1,4 and trans-1,4 contents.

For ^{1}H spectrum, the molar contents are calculated as below:

$$C_{1,2-structure} = \frac{A_d/_2}{\frac{A_{a+b} + A_c - A_d/_2}{2} + A_d/_2} \times 100\ \%$$

$$C_{1,4-structure} = 100 - C_{1,2-structure}$$

For ^{13}C spectrum, the relative molar contents are expressed as below:

$$R_{cis-1,4} = \frac{A_k/_2}{A_k/_2 + A_l/_2} \times 100\ \%$$

$$R_{trans-1,4} = 100 - R_{cis-1,4}$$

The molar contents can thus be deduced as:

$$C_{cis-1,4} = R_{cis-1,4} \times C_{1,4-structure}$$

$$C_{trans-1,4} = R_{trans-1,4} \times C_{1,4-structure}$$

The percentages of each structure were calculated, and the results gave the following relative molar contents:

$C_{1,2\text{-structure}}$=12.2 %,

$C_{cis\text{-}1,4}$=36.2 %,

$C_{trans\text{-}1,4}$ =51.6 %.

This distribution is very close to the one of the native polybutadiene meaning that the catalysis is not selective toward one sort of double bonds for the functionalization and thus, it affected indifferently the internal and vinylic structures in the polymer.

To control the efficiency of the functionalization, it is interesting to evaluate the differences in the proportions of double C=C bonds compared to simple C-C bonds. We estimated by NMR spectroscopy the proportions of the different carbons present in the commercial polymer: -CH_2- 65.42 %, =CH_2 3.65 %, =CH- 30.82 % by comparing the integrals corresponding to each sort of carbon respectively at 2.1, 4.9 and 5.6 ppm (Figure IV. 53). This is relatively different from the native polybutadiene and we can estimate that 2 % molar of the C=C bonds were functionalized by boronate esters.

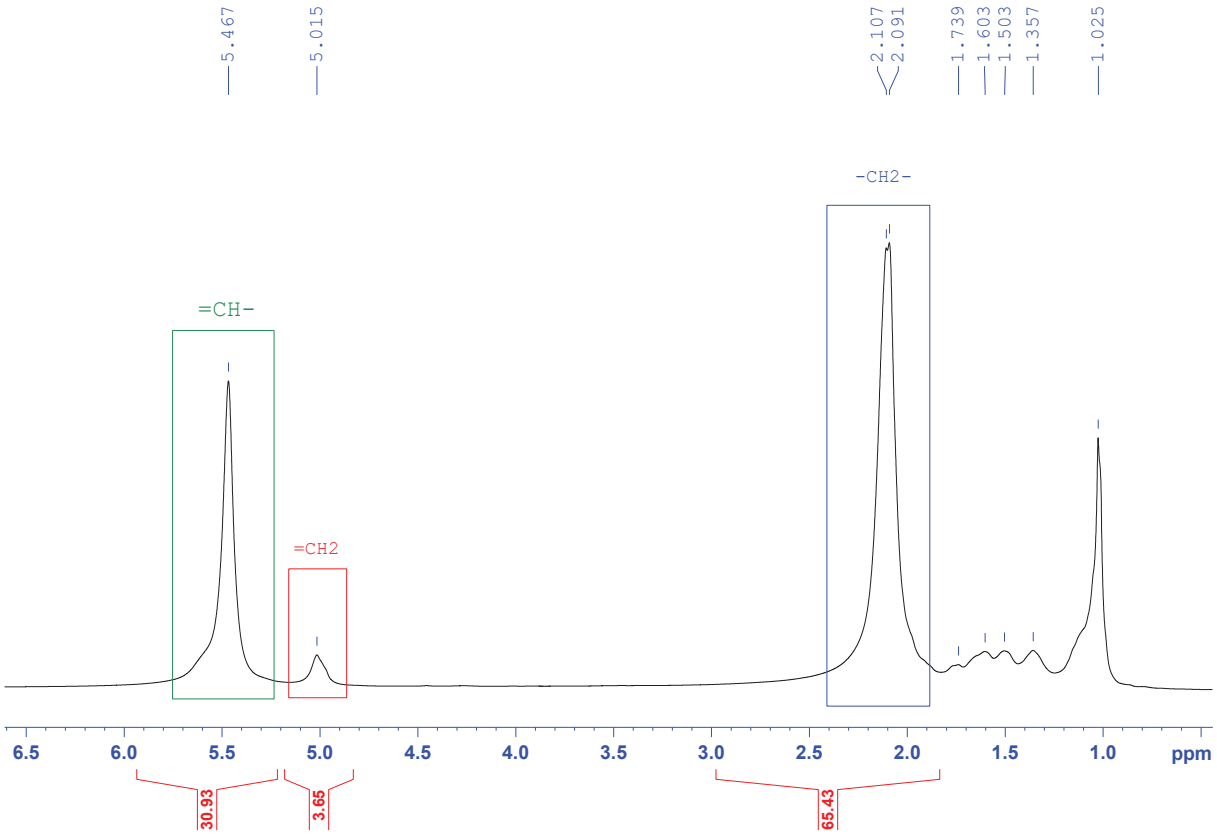

Figure IV. 53: Determination of the proportions of –CH_2-, =CH_2 and =CH- in the modified polybutadiene by copper catalysis.

ii. DSC investigation on the functionalized polybutadiene

The polybutadiene after the functionalization *via* copper catalysis was analyzed by differential scanning calorimetry. The main goal was to find differences in glass transition temperatures and to distinguish any reactivity event during heating segments.

The DSC thermograms are presented in Figure IV. 54. The first ascertainment made is that the glass transition temperature during the first heating segment is close (-84°C) to the one of the commercial polybutadiene. Secondly, thermal events are occurring between 80°C and 140°C that are both endothermic and exothermic. During the second heating segments, the new glass transition assessed is around -77°C making a slight difference that we assumed to attribute to the boronate esters reactivity.

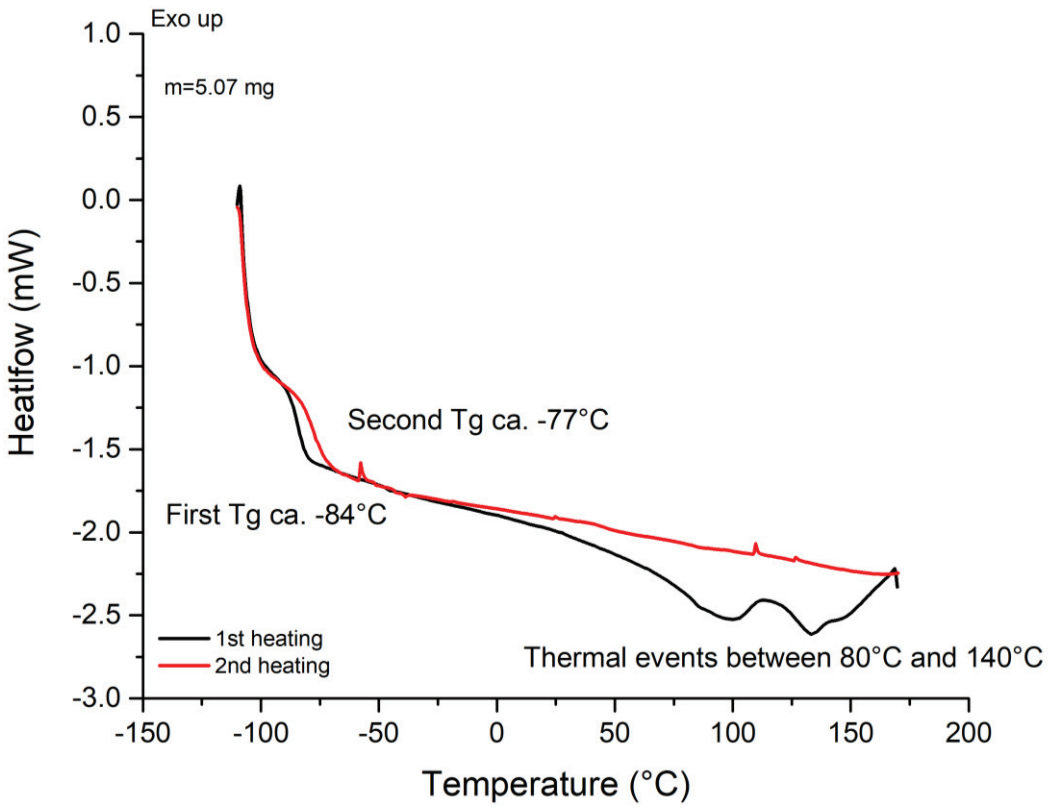

Figure IV. 54: DSC thermograms of modified polybutadiene via *copper catalysis in 40 µL opened aluminum pans.*

iii. Rheology experiments on the functionalized polybutadiene

In the same manner as for the previous system, the material was further investigated by rheology to assess its macroscopic properties that could be then related to the structure and the chemical behavior of the functionalized polymer.

At the beginning, the polymer was probed without further purification by frequency sweeps at different temperatures and the storage and loss moduli obtained were compared to the values acquired for the native polybutadiene. The results are set forth in Figure IV. 55 and the two mechanical behaviors are divergent.

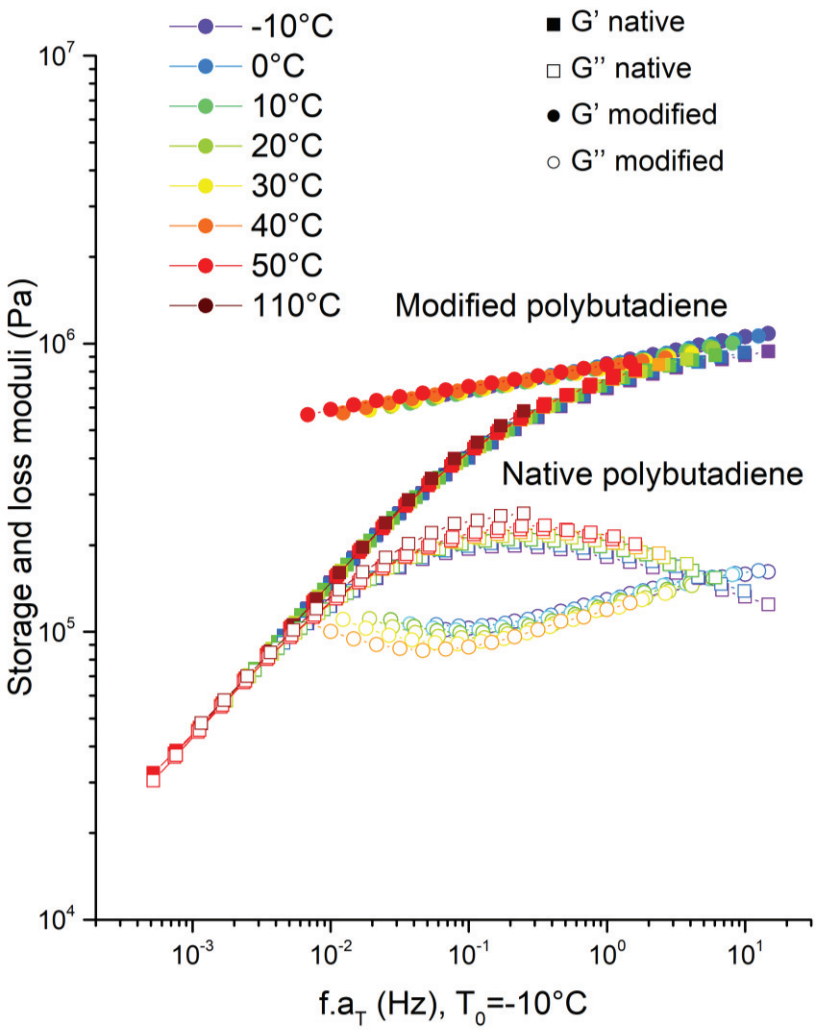

Figure IV. 55: Superposition of master curves of the native (squares) and modified polybutadienes (circles), referenced at -10°C. G' in closed forms and G'' in opened forms.

Firstly, it is noteworthy that the unmodified commercial polybutadiene shows a rubbery plateau at high frequencies characteristic of entangled regime whereas, at low frequencies, the absence of clear terminal relaxation could be due to the large dispersity of the polybutadiene, confirmed by SEC in Figure IV. 48.

Surprisingly, the modified polymer does not show any relaxation at low frequencies contrary to the native polybutadiene. This behavior might be the results of the supposed radical couplings occurring during the reaction path as the master curves is characteristic for a permanently crosslinked polymer.

The storage and loss moduli were monitored during several hours at 110°C in order to explore the influence of the boronate esters in the polymer behavior at high temperatures. Indeed, we previously assumed that the boronate esters reactivity occured at temperatures above 100°C.

In Figure IV. 56, the storage and loss did not undergo any modification from the supposed boronate ester reactivity at 110°C. In this case, we may not have many functional groups installed on the polymer backbone to be able to probe any change in the mechanical properties. Furthermore, as explaining during the synthesis part, the polymer suffered from unwanted covalent crosslinking resulting from the radical couplings between the double C=C bonds. As a result, the lesser contribution of the reactivity between boronate esters might be difficult to distinguish due to the dynamic character of this crosslinking.

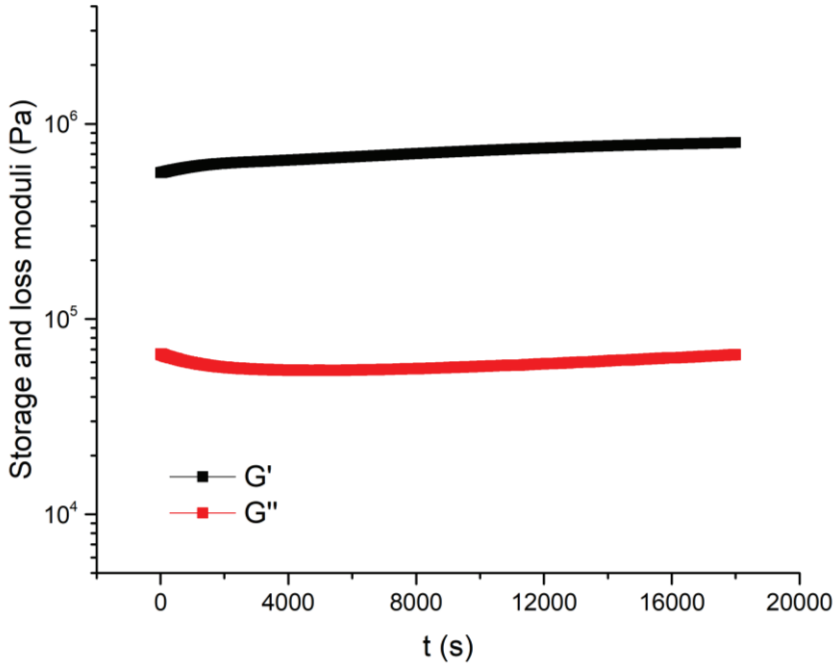

Figure IV. 56: Monitoring of the storage and loss moduli during oscillation time at 110°C for the modified polybutadiene via *copper catalysis.*

Moreover, the time-temperature superposition master curves before and after curing for the modified polymer as illustrated in Figure IV. 57 do not show any differences in the storage and moduli values.

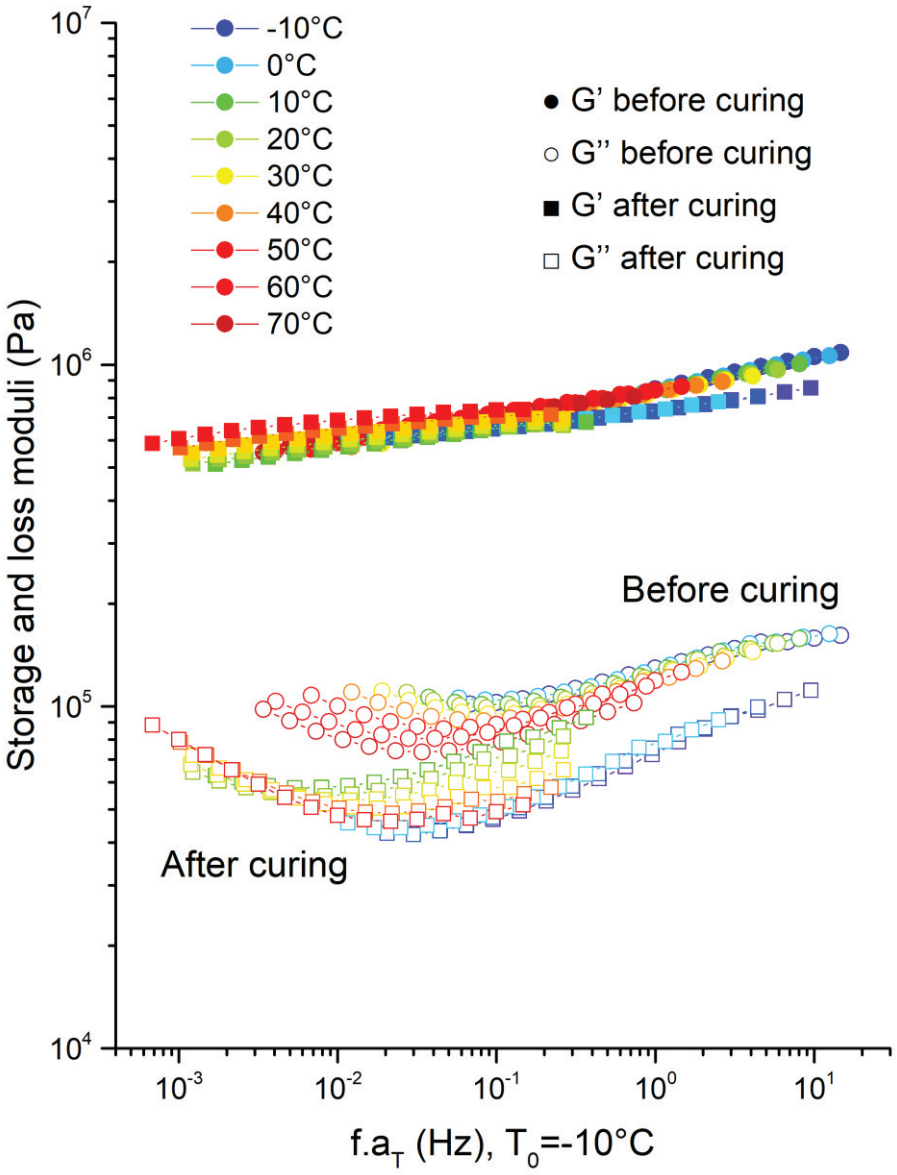

Figure IV. 57: Superposition of master curves of the modified polybutadiene before (circles) and after (squares) curing at 110°C, referenced at -10°C. G' in closed forms and G'' in opened forms.

We assumed that, for this functionalization *via* copper catalysis, the contribution of the boronate esters in the establishment of a dynamic crosslinking within the polymer is hindered by the issues encountered during the reaction path. Undoubtedly, a covalent crosslinking is prevailing on the mechanical properties of the final materials. This modified polybutadiene will not be further investigated.

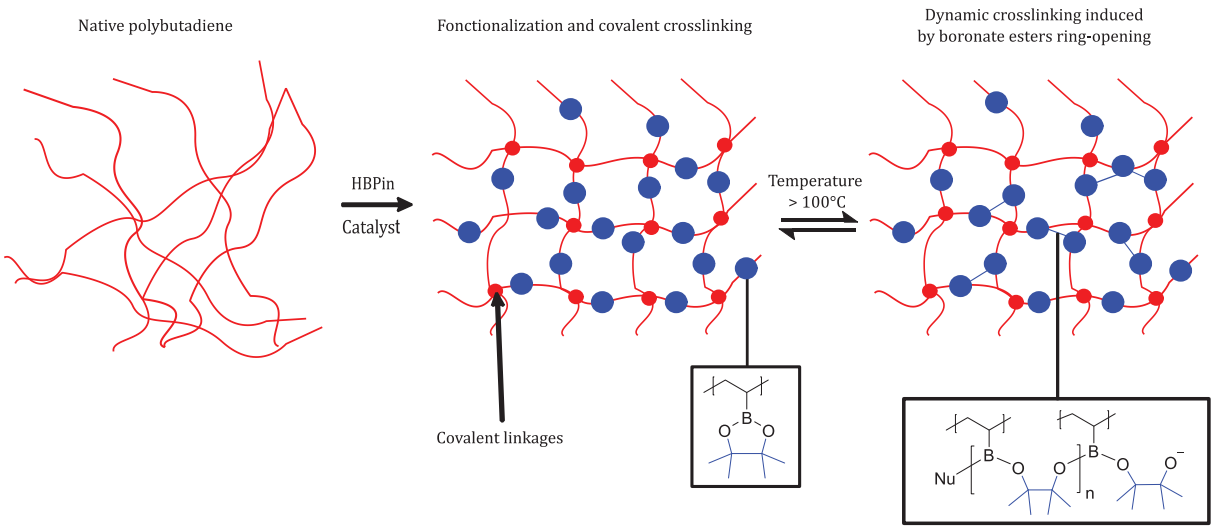

Figure IV. 58: Structures and reactivity of the modified polybutadiene by copper catalysis.

As described in Figure IV. 58, the reaction *via* the copper catalysis induced the functionalization of the polybutadiene chains as well as the creation of a covalent network due to radical coupling reactions between C=C bonds. At high temperature, we assumed that the boronate ester moieties could exhibit the same reactivity i.e. ring opening and thus create a dynamic network. To sum it up, after the reaction, we hypothesized that the system presents a double network (DN) with one covalently crosslinked and to a lesser extent, one dynamically crosslinked.

c. Hydroboration by iron catalysis

i. Synthesis of the functionalized polybutadiene

For this second strategy *via* iron catalysis, we relied on the work of Chirik of 2013 where they reported the hydroboration of alkene by a highly selective bis(imino)pyridine iron-catalyst. They had previously demonstrated that the bis(imino)pyridine iron (Fe(0)) dinitrogen complexes are highly active catalysts for hydrofunctionalizations and that the more sterically protected the iron precursor is, the more selective and less active it is. [42] Besides, an iron-based catalyst is a good alternative to a copper one as iron is a less expensive and readily available metal.

We used an iso-propyl bis(imino)pyridine iron dinitrogen compound noted (^{iPr}PDI)Fe(Cl_2)$_2$ with Fe(II) reduced in-situ with a Grignard agent (MeMgBr) to activate the catalyst (Figure IV. 59). Pinacolborane was preferred to install boronate ester groups and the functionalization was performed in tetrahydrofuran. The same functionalization of 30 % molar of double bonds was targeted.

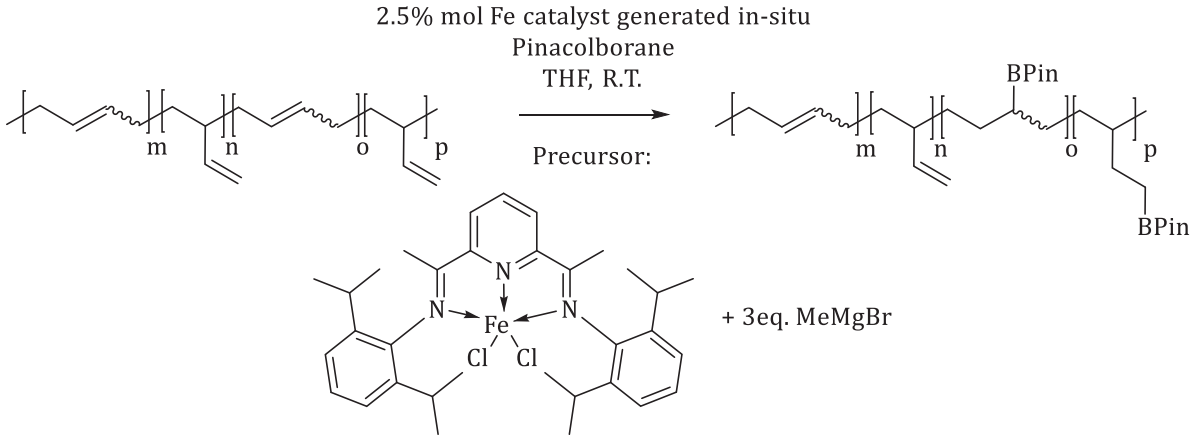

Figure IV. 59: Use of iron catalysis for hydroboration of polybutadiene with representation of the iron catalyst used.

After the functionalization, the polymer obtained was characterized through several techniques without further purification. Firstly, by NMR spectroscopy, we attempted to control the efficiency of the functionalization. In this fashion, the NMR spectra of the native polybutadiene and of the result of the reaction were compared as illustrated in Figure IV. 60.

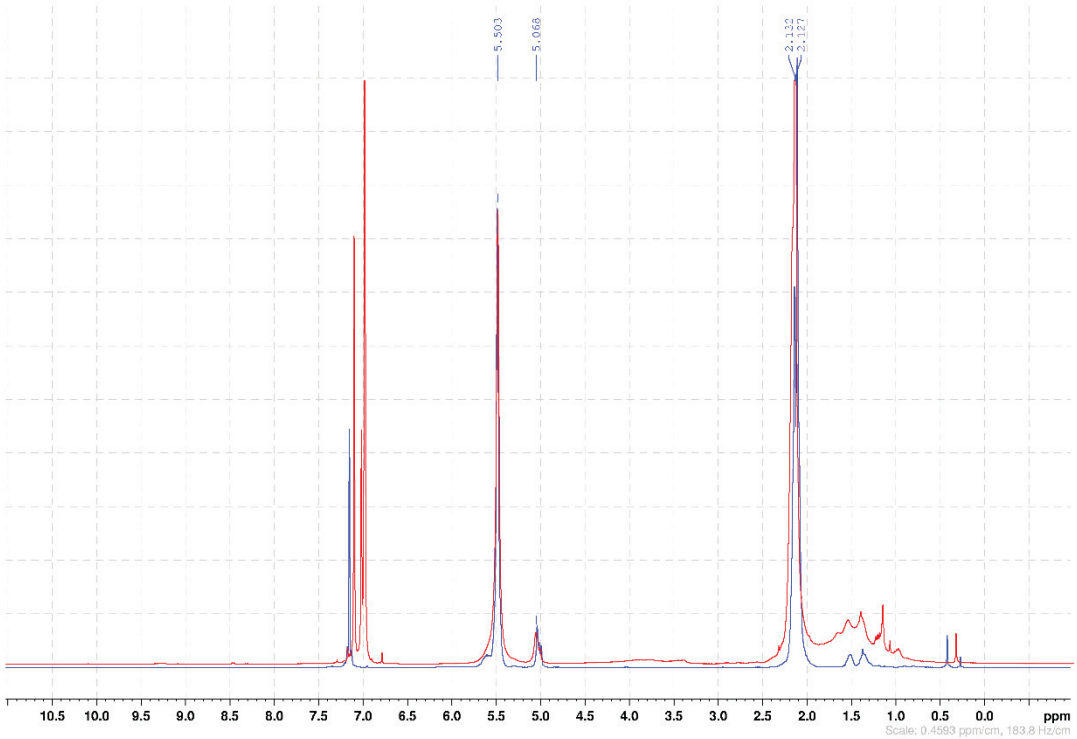

Figure IV. 60: Superposition of the native polybutadiene (blue) and polybutadiene after the functionalization via *iron catalysis (red).*

Relying on the same equations than in the previous part and on the NMR spectra from Figures V. 135 to V. 137 in the Experimental Section, the percentage of each structure was then calculated and the results gave the following relative molar contents:

$C_{1,2\text{-structure}}$=8.8 %,

$C_{cis\text{-}1,4}$=39.6 %,

$C_{trans\text{-}1,4}$ =51.5 %.

This distribution is slightly different to the one of the native polybutadiene meaning that the iron catalysis used is somewhat selective for vinylic structures.

To control the efficiency of the functionalization, it is interesting to evaluate the differences in the proportions of double C=C bonds compared to simple C-C bonds. We estimated by NMR spectroscopy the proportions of the different carbons present in the commercial polymer: -CH_2- 69.82 %, =CH_2 2.06 %, =CH- 30.92 % by comparing the integrals (Figure IV. 61). This is relatively different from the native polybutadiene and we can estimate that 6 % molar of the C=C bonds were functionalized by boronate esters, which is slightly better than by copper catalysis used in the previous part.

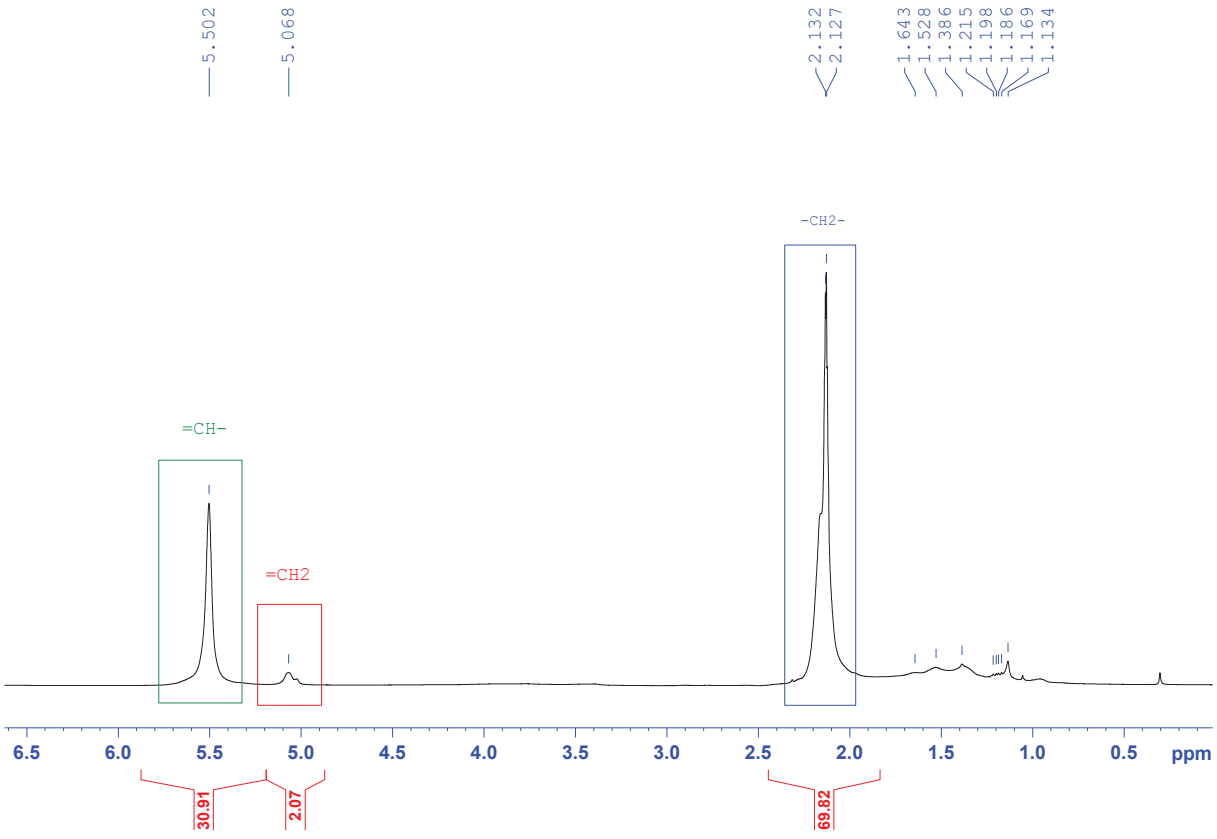

Figure IV. 61: Determination of the proportions of –CH_2-, =CH_2 and =CH- in the modified polybutadiene by iron catalysis.

ii. DSC investigation on the functionalized polybutadiene

After the reaction with iron catalyst, the polybutadiene was analyzed by differential scanning calorimetry. The main goal was to find differences in glass transition temperatures and to distinguish any reactivity event during heating segments.

The first remark that can be pronounced on the DSC thermograms presented in Figure IV. 62 is the shift of + 10°C of the measured glass transition temperature during the first heating segment compared to the glass transition temperature of the commercial polybutadiene due to the partial functionalization of the C=C bonds. This difference will be further discussed in the next part.

The first heating segment then exhibits some thermal events between 100°C and 160°C that might be related to the boronate esters reactivity. Nonetheless, the second glass transition temperature remains about the same around -72°C.

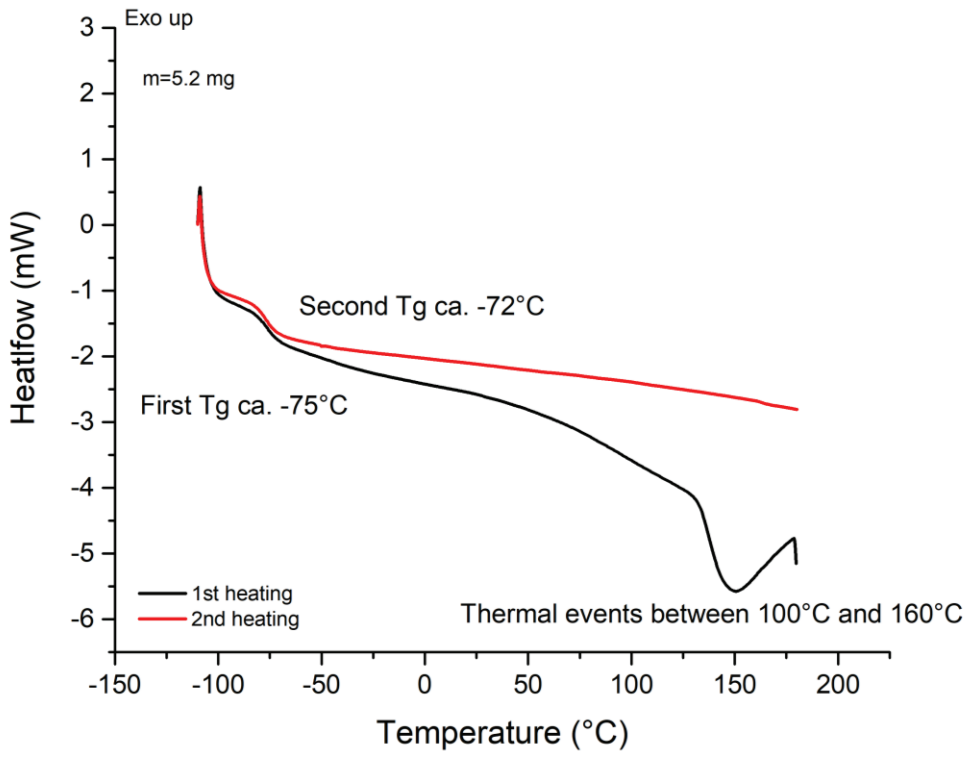

Figure IV. 62: DSC thermograms of modified polybutadiene via *iron catalysis in 40 µL opened aluminum pans.*

iii. Rheology experiments on the functionalized polybutadiene

As usual, we used rheology on the modified polymer without further purification to be able to probe the role of the boronate esters on the mechanical properties of polybutadiene.

First, through frequency sweeps and time-temperature superposition principle, we compared the master curves of the commercial and native polybutadiene on Figure IV. 63. The master curves are completely different before and after functionalization. Indeed, the modified polybutadiene does not show the rubbery plateau around G_N=1 MPa corresponding to entanglements at high frequencies contrary to the native one. However, a short rubber plateau can be distinguished on the storage and loss moduli curves between 10^{-1} and 10^{-2} Hz.

More importantly, the parallel behavior of G' and G'' at high frequencies can be attributed to a phase separation occurring after the functionalization between boronic pinacolate moieties and polybutadiene chain segments. Indeed, the chemical nature of the two phases are incompatible with one polar phase composed of the boronic pinacolates and one apolar phase with the polybutadiene segments. This separation phase phenomenon was already observed by Leibler in systems composed of polyethylene and dioxaborolane maleimide groups where a coexistence of dioxaborolane-rich and –poor regions was evidenced. [48]

The boronate esters behave as nodules in the polymer matrix and hindered the relaxation of the polymer segments. This microphase separation might severely shorte the times of the relaxation processes in this system. Nevertheless, we can also see around 0.1 Hz the presence of an elastic plateau that could correspond to an entangled regime. The contribution of entanglements is much smaller than for the native polybutadiene, which could point to a strong decrease of the molar masses in the sample after reaction.

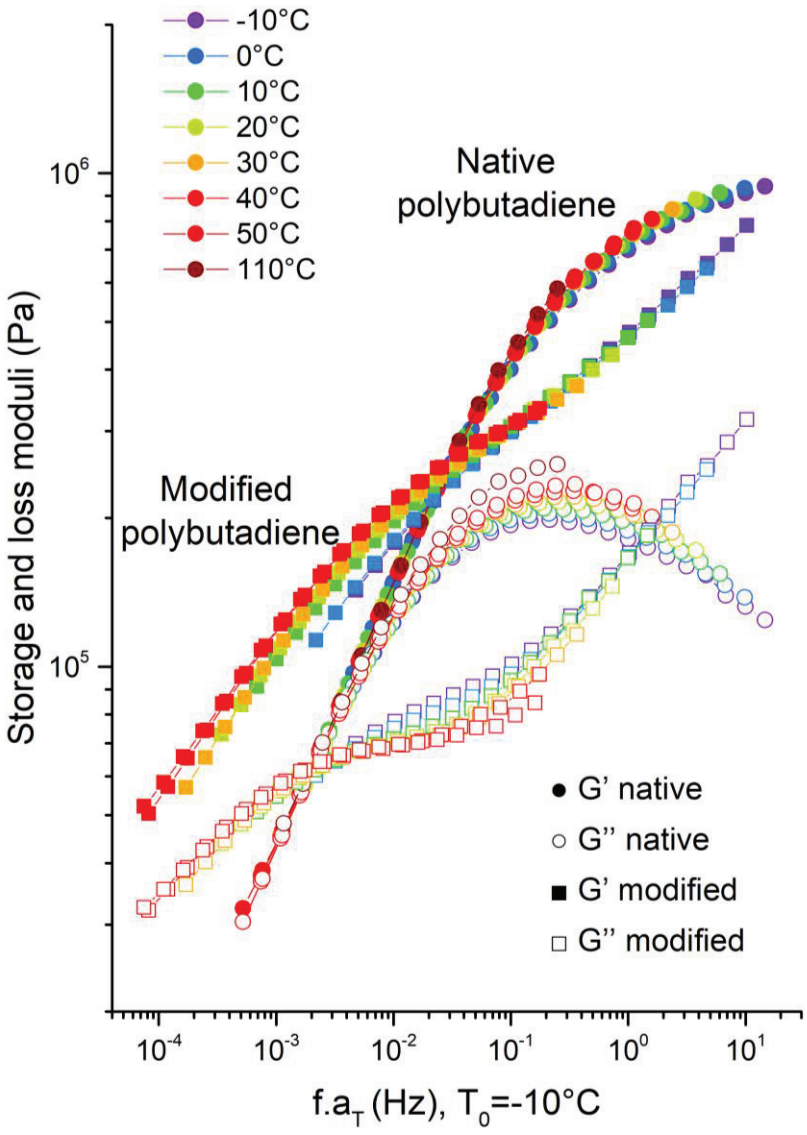

Figure IV. 63: Superposition of master curves of the native (circles) and modified (squares) polybutadiene, referenced at -10°C. G' in closed forms and G'' in opened forms.

This change of molar masses was confirmed by size exclusion chromatography and the results obtained were compared to the native polybutadiene as represented in Figure IV. 64. The molar masses were thus drastically lowered by the reaction performed with an increase of the dispersity. Some ruthenium-based catalysts can induce chain cuttings *via* acyclic diene metathesis (ADMET) [49]–[51] but this should not be our case in this study. However, different possibilities could be considered such as mechanical cuttings of the chains during the processes of solubilization and drying of the polymer where the polymer is highly stirred or sigmatropic rearrangements with iron (Fe-H catalyzed chain-scission).

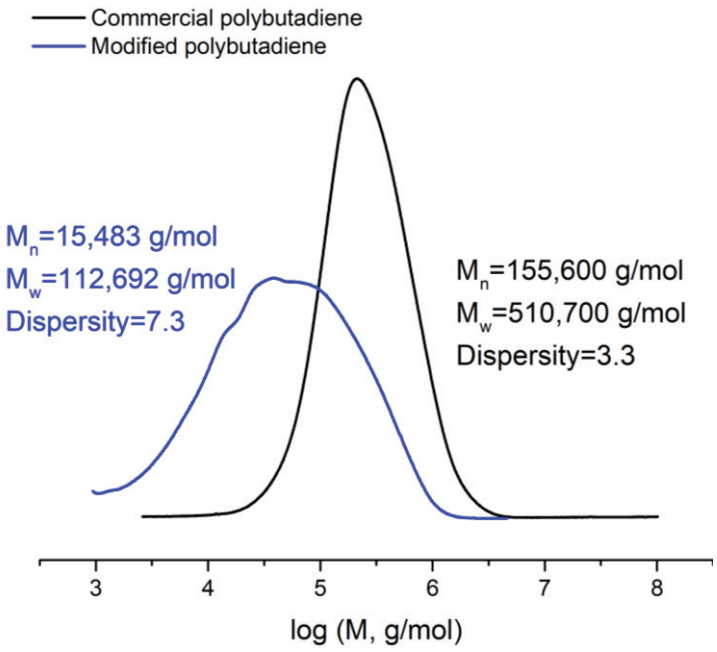

Figure IV. 64: Comparison of the chromatograms of the native (black) and modified (blue) polybutadiene.

In a second part, we monitored the storage and loss moduli over time at the temperature of 110°C as we evidenced the ring opening and subsequent cross-linking of the boronate esters moieties above this temperature in Chapter 3.

Unsurprisingly, we witnessed an increase of the viscosity as well as the storage and loss moduli over time. We attributed this increase to the boronate esters reactivity and to the creation of linkages between the polymer chains of the material and in the polar nodules. This result also testifies to the efficiency of the functionalization by iron catalysis. The experiment is illustrated in Figure IV. 65.

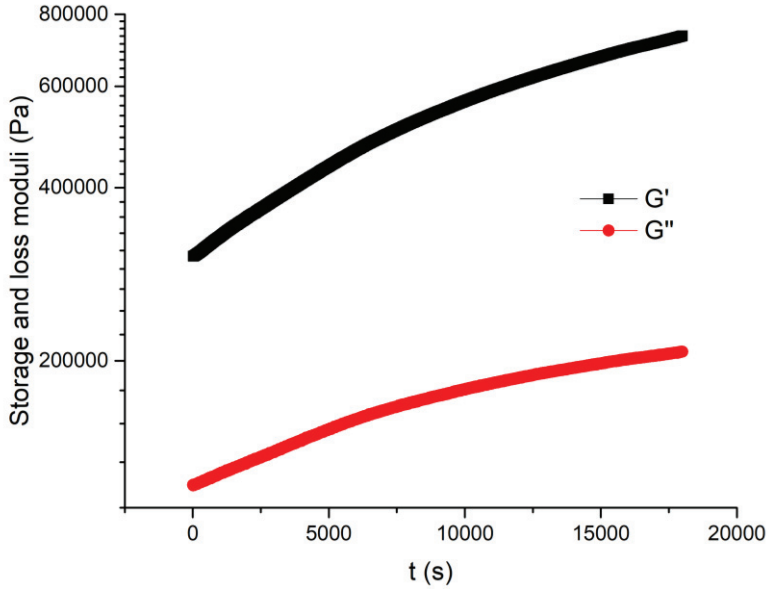

Figure IV. 65: Monitoring of storage and loss moduli during oscillation time at 110°C for the modified polybutadiene via *iron catalysis.*

After the heating segment at 110°C during several hours, the master curve of the modified polybutadiene was constructed by time-temperature superposition and compared to the master curves of the modified polymer before the heating segment as shown in Figure IV. 66.

The first observation that can be made is the strong increase in the measured moduli after the heating segment. This confirms our hypothesis about the ring opening of the boronate ester groups followed by the crosslinking between the polymer chains.

Moreover, the rubber plateau is larger after the heating segment and relaxation occurred later in this case. This could indicate that the crosslinking induced by the reactivity is dynamic in the boronate esters phase.

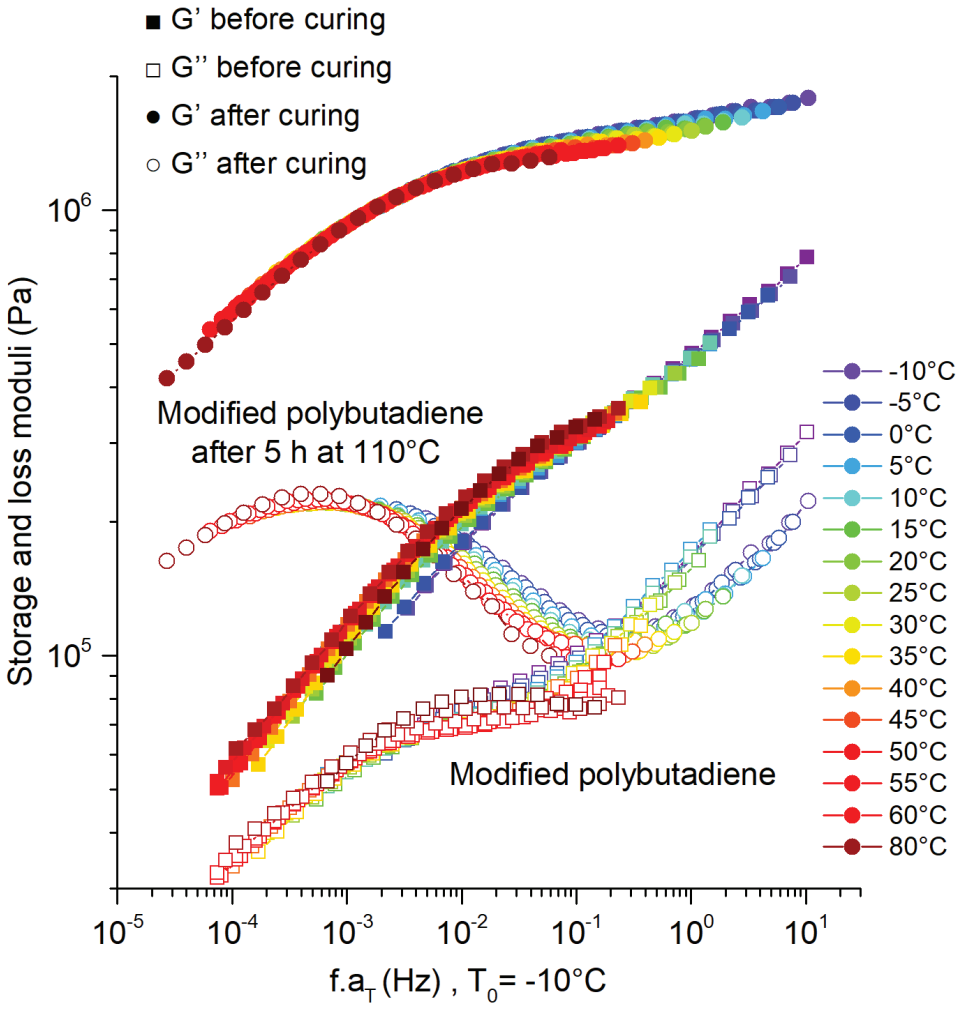

Figure IV. 66: Superposition of master curves of the modified polybutadiene before (squares) and after (circles) curing at 110°C, referenced at -10°C. G' in closed forms and G'' in opened forms.

The ultimate comparison can be conducted between the cured modified and native polymer after heating segments as depicted in Figure IV. 67. The main feature is the presence of a rubber plateau for the modified polybutadiene demonstrating effective crosslinking with the relaxation at low frequencies testifying of the dynamic character of the crosslinking brought in the polymer.

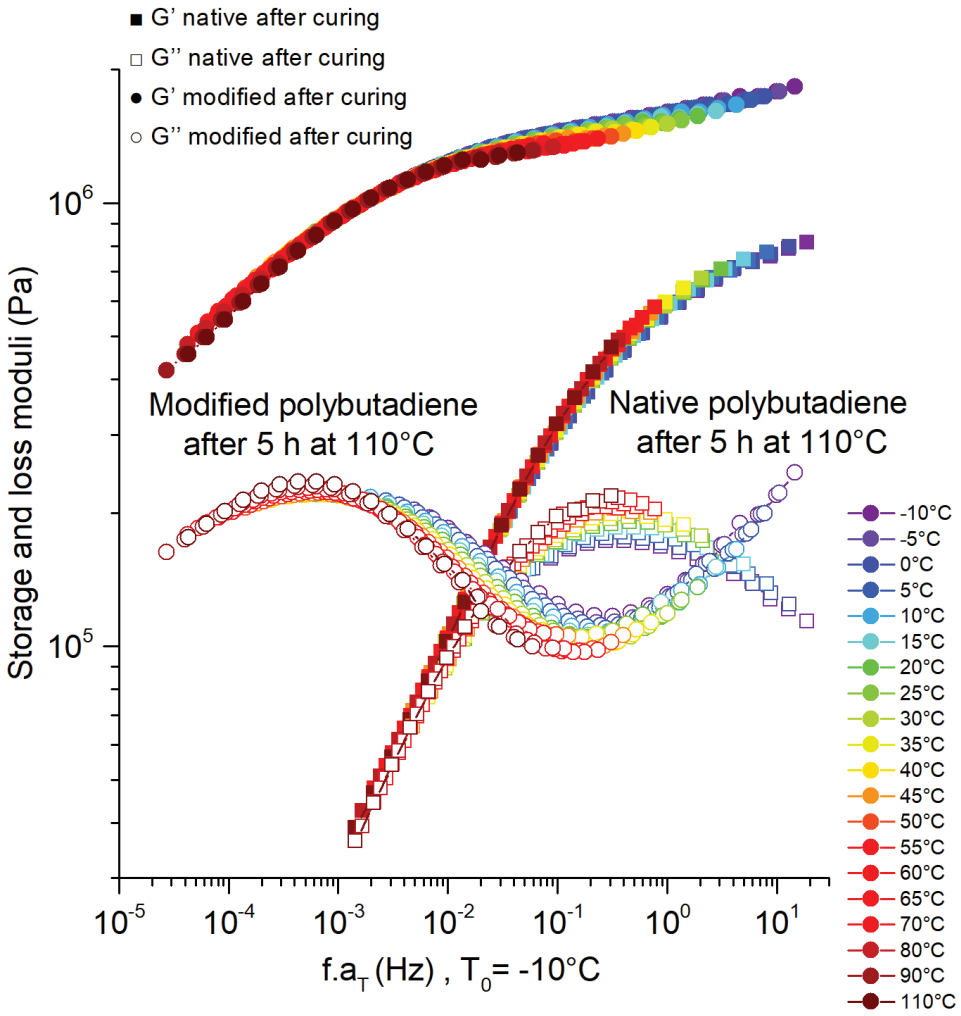

Figure IV. 67: Master curves of the native (squares) and modified (circles) polybutadienes after heating at 110°C during 5 h, referenced at -10°C. G' in closed forms and G'' in opened forms.

In order to understand the mechanism of this dynamic crosslinking, the shift factors of the cured polybutadiene were fitted with the Williams-Landel-Ferry equation (Figure IV. 68), but the fitting parameters found were not realistic from a physical standpoint. (C_2>>T_g) WLF equation is deeply explained in Chapter 3.

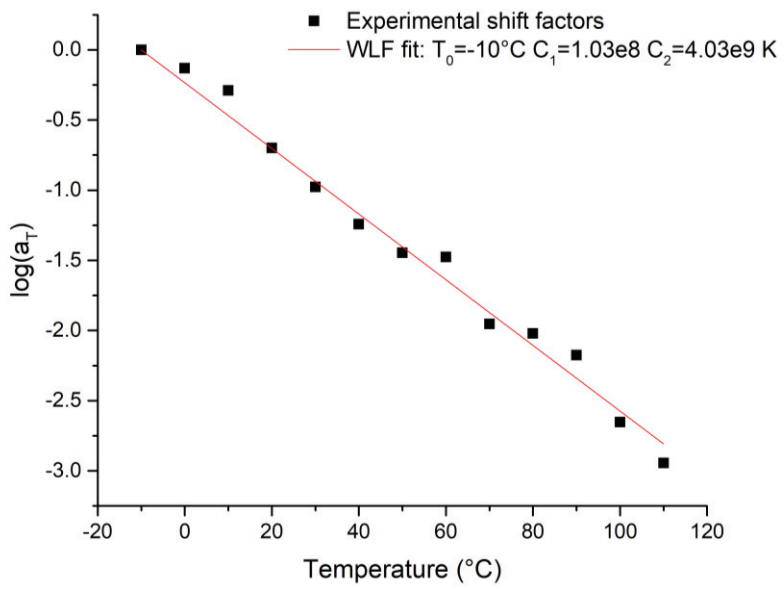

Figure IV. 68: Fit of the shift factors with WLF equation.

In this case, the experimental shift factors showed an Arrhenius-like dependency that is consistent with the presence of a chemical reaction responsible for the dynamic crosslinking. The plot in Figure IV. 69 allowed us to determine that the energy activation of the crosslinking reaction is about 20.3 kJ.mol^{-1}.

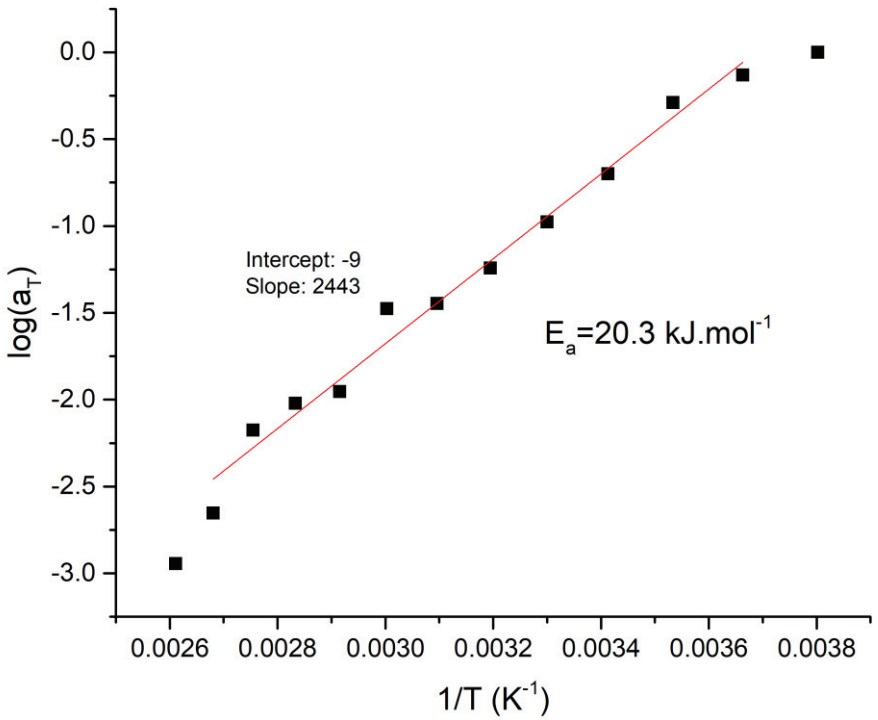

Figure IV. 69: Arrhenius-like dependency of the shift factors.

The stress-relaxation of the modified polymer after heating was also probed by rheology. We obtained the response in Figure IV. 70 (a) and then we applied the already determined shift factors by oscillation experiments to the raw data in Figure IV. 70 (b).

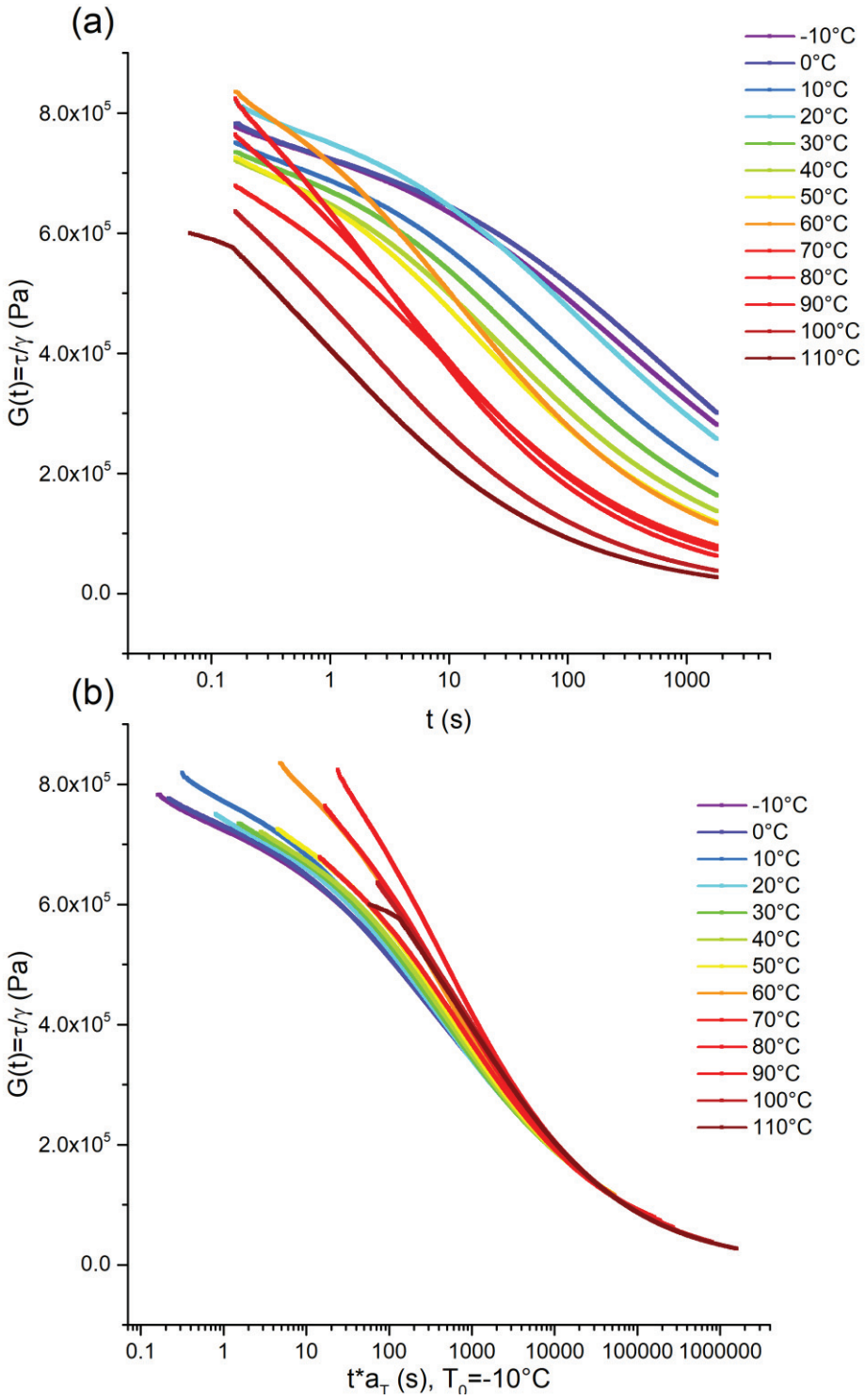

Figure IV. 70: Stress-relaxation response probed for the modified polymer after heating. (a) Raw data, (b) Data shifted with the already determined a_T factors.

First, it is interesting to see that the shift factors determined by oscillation experiments successfully fitted the data obtained by stress-relaxation experiments.

At short relaxation times, the plateau region is associated with the elasticity due to the entanglement at G_N. At longer relaxation times, the chain motion is slowed down evidencing the interactions between polymer chains.

After all the rheology experiments, we were able to reconstruct what is occurring in the polymer material. Indeed, a phase separation between the polar (boronic pinacolates rich) and apolar (boronic pinacolates poor) segments was evidenced as well as the contribution of the boronate esters reactivity to allow the creation of a dynamically crosslinked network. This pathway is represented in Figure IV. 71.

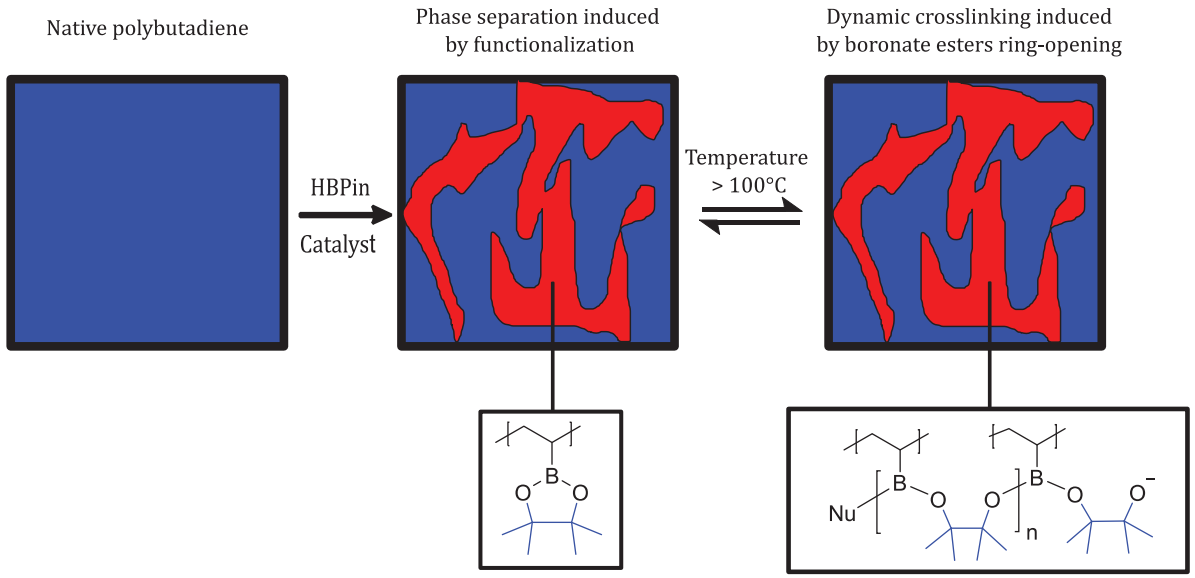

Figure IV. 71: Microstructure and reactivity of the modified polybutadiene by iron catalysis.

iv. Dynamic mechanical analysis

Dynamic mechanical analysis (DMA) applies an oscillatory force at a specified frequency to the sample and reports changes in terms of stiffness and damping. This allows to determine the materials response to stress, temperature and other values studied. It measures the storage modulus E' which is the sample's elastic behavior. The ratio of the loss of the storage is tan δ and is called damping representing the measure of the energy dissipation of the material.

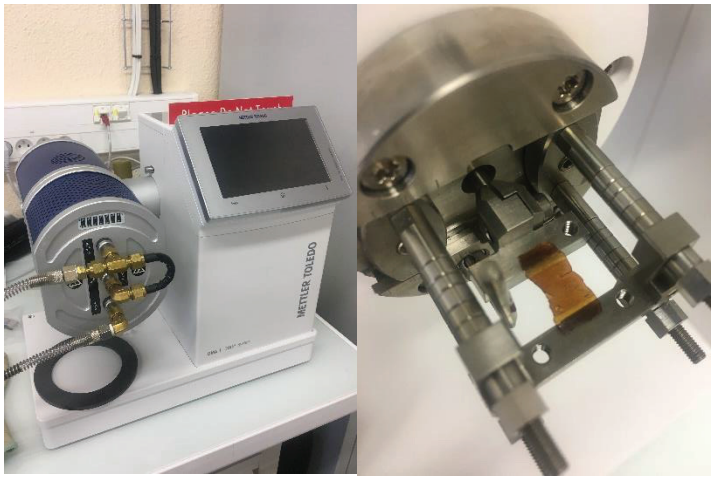

Figure IV. 72: Left: DMA device; Right: Experimental set up of the sample.

The samples were probed in a tensile mode to evaluate E' and tan δ represented in Figure IV. 73. The drop of storage modulus E' occurs at the same temperature, which confirms that the glass transition temperature was barely modified and is consistent with the DSC measurements above. It is also indicated at the same temperature by the maximum of tan δ (or T_α at maximum E").

The tan δ value remains very high even above the glass transition temperature, thus demonstrating a highly dampening behavior, compatible with the hypothesized microphase separation. Above 80°C, as the polymer continues to decrease in modulus, the DMA apparatus cannot reliably measure the viscoelastic properties. After curing, the sample demonstrates an elastic plateau with low tan δ values from -60 to 80°C. At higher temperatures, the increase of tan δ also indicates the relaxation that we attributed to chemical exchanges and subsequent dynamic crosslinking.

The results of the DMA experiments are consistent with the assumptions made so far.

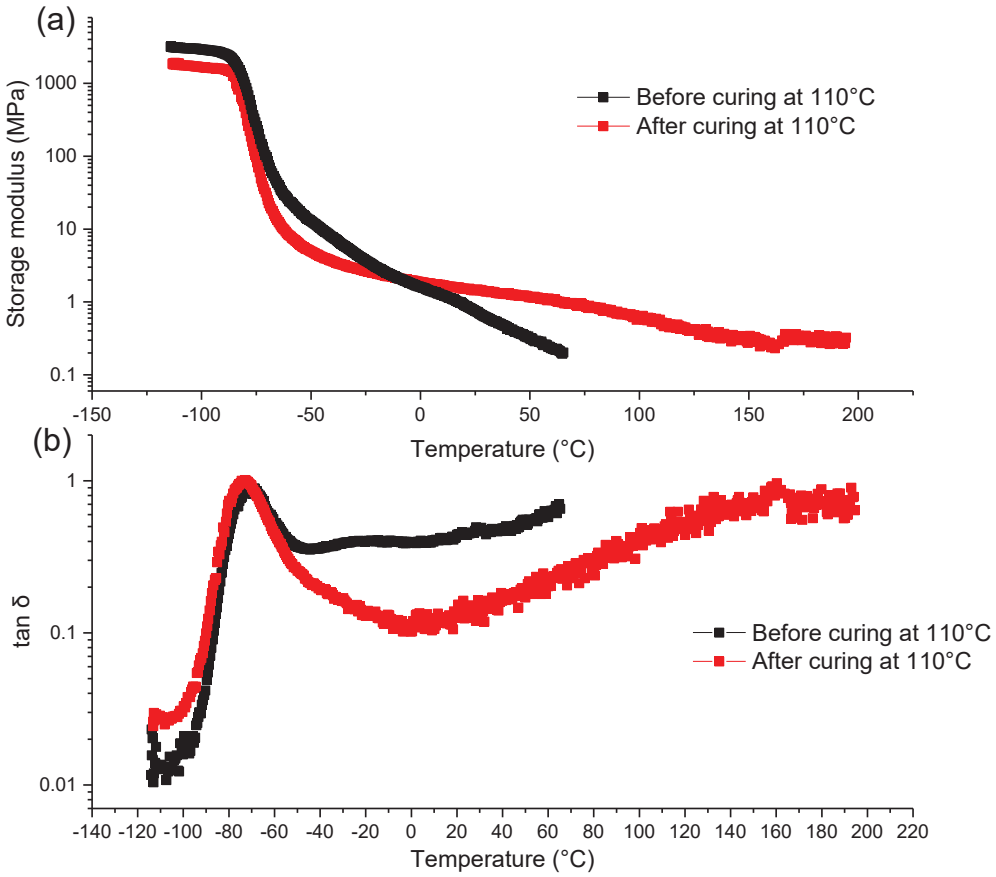

Figure IV. 73: (a) Monitoring of storage modulus for sample before and after curing at 110°C. (b) Monitoring of tan δ before and after curing at 110°C.

v. Tensile tests

Tensile tests are widely used in polymer industry to probe the mechanical properties of materials and predict how a material will behave under normal and extreme forces. This test consists in applying an uniaxial deformation at constant speed until failure. The sample is placed in the testing machine and extended with a controlled speed until failure. Large deformation occurring in elastomers ideally require the measurement of true strain by (video) extensometers. In the current case, we will only refer the nominal strain as $\varepsilon=(L-L_0)/L_0$.

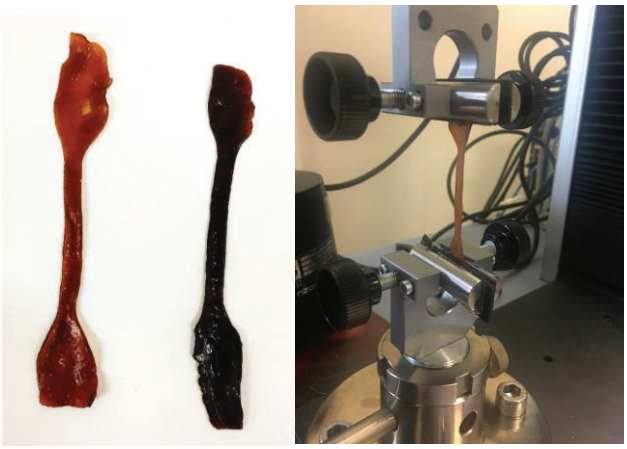

Figure IV. 74: Left: Tensile test samples before (brown) and after curing at 110°C (dark) for several hours. Right: Experimental tensile test set up.

The properties probed are the elongation of the sample used to determine the strain using the following equation:

$$\varepsilon = \frac{\Delta L}{L_0} = \frac{L - L_0}{L_0}$$

with ΔL the change of length, L_0 the initial length of the sample and L its final length.

The force measured by the apparatus allows the calculation of the stress: $\sigma = \frac{F}{S}$

with F the tensile force and S the section of the sample probed. Thus, the strain-strain curve can be graphed as represented in Figure IV. 75.

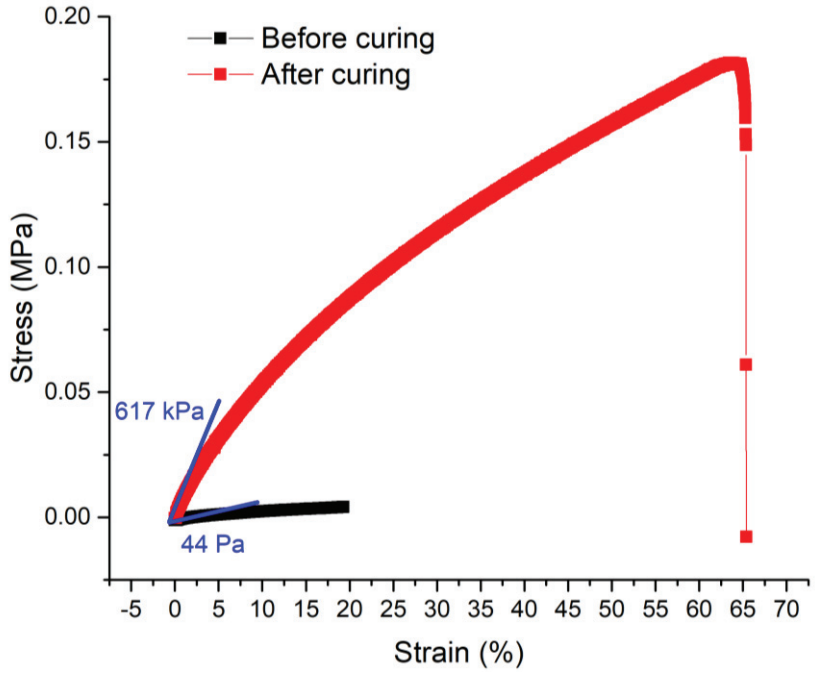

Figure IV. 75: Strain-stress curve from tensile experiments for the modified polybutadiene before (black) and after (red) curing at 110°C for several hours.

The slope at the origin should give the value of the Young modulus that should be the same than E' at ambient temperature. For the modified polybutadiene before curing, the slope is 44 kPa and for the modified polybutadiene after curing, the slope is 617 kPa, while the maxima of E' at 25°C are respectively 67 kPa and 168 kPa for the same systems. The values are close for the modified polybutadiene before curing whereas the values are less concordant after curing. The main result is the increase of the modulus of the modified polybutadiene after curing thanks to the reactivity of the boronate esters inducing crosslinking.

Besides, the elongation at break of the polybutadiene after curing is not that high for a crosslinked polybutadiene. This could be the result of the strong decrease of the molar masses that reduces the entanglements between the polymer chains and that affects the mechanical properties of the material studied. One can suggest that leftover catalyst could also favor oxidative chain-scission.

IV. Conclusion

In this chapter, two main boronate esters-based polymer families (aryl-pinacolboronate and vinyl-pinacolboronate) were studied and were found to present different thermoresponsive behaviors.

On the one hand, systems featuring aryl-boron bonds were assessed in order to extend the results observed in Chapter 3, i.e. the ring opening of the boronate ester moieties inducing a dynamic crosslinking. The styrenic boronic pinacolate was successfully copolymerized with n-butyl acrylate at different ratios. The rheology investigation of this polymer proved once more the interesting ability of boronate esters to perform ring-opening and subsequent crosslinking at high temperatures through nucleophilic assistance. This new argument prompted us to confirm the hypothesis aforementioned. In addition, through the copolymerization of 4-vinylphenylboronic acid, pinacol ester with n-butyl acrylate, we were able to reach different glass transition temperature range from -50°C to 220°C. Hence, we could be able to tune the glass transition temperature of commodity polymers widely used in industry. However, we noted in this case that phase separation occurred between boronate ester rich- and poor-domains due to the different nature of the co-monomers used affecting the mechanical properties of the copolymers studied.

From these findings, we committed ourselves to a conceptual extension with the design of the new hybrid glasses harnessing the same reactivity. In this part, we were able to create incoming tridimensional networks from trifunctional molecules bearing boronic pinacolates moieties. This work seems to be very promising and lot of applications could be found to put forward this reactivity. Besides, it covers a hot topic on hybrid organic/inorganic glasses presenting a reversibility. Unfortunately, the brittleness of the material hindered material shaping and further mechanical investigation. One can suggest the use of more flexible trifunctional boronate esters, for example with an alkyl linker contrary to an aryl linker.

On the other hand, polymers arising from vinyl-boron systems were exemplified through (co)polymerization and functionalization of existing polymers. The first noticeable result was the novel polymerization of the vinylic version of boronic pinacolate usually used as a simple Suzuki coupling partner with a protecting strategy involving complexation of the boron electronic vacancy. This polymer exhibits a disconcerting thermal behavior with a crosslinking only in a certain temperature range. We reported here a complete thermoresponsive polymer whose glass transition temperature is varying depending on the probing temperature. This puzzling behavior was quite surprising in our research path, but we assumed that the vinylic and styrenic versions of boronic pinacolate should not be acting the exact same way, as the boronate esters do not exhibit the same ring-opening behaviors from sp^2 C-B to sp^3 C-B bonds.

To go further, we got interested in the ability to copolymerize this vinylic monomer with commonly used monomers such as vinyl acetate and ethylene. The copolymerizations were successful even if we obtained short chain lengths, especially in case of the copolymerization with ethylene where we suspected the trapping of the propagating radical by the boron atom stopping the propagation and the chain growth. For copolymers from vinyl acetate, we recovered the same mechanical and thermal behavior as previously observed with the ring opening of the boronate ester cycles inducing the dynamical crosslinking. Concerning the copolymers from ethylene, the low yields obtained hindered further investigation concerning the thermal properties. However, the differential scanning calorimetry experiments showed that the incorporation of boronic pinacolates on the ethylenic backbone highly disrupted the melting and crystallization events. The copolymerization of vinylboronic pinacolate and ethylene is a prowess by itself. This work opens perspectives in optimizing the synthesis and understanding the boronate esters contribution in this specific case.

In the last part, we reported the functionalization of polybutadiene by hydroboration that allowed the installation on boronic pinacolate on the rubber backbone. Two synthetic paths were here presented and the most promising remains the hydroboration by iron catalysis. The rheology experiments brought many information about the microstructure in the modified polybutadiene. Actually, the modified polymer presents a phase separation between incompatible polar and apolar phases, respectively rich in boronic pinacolate and poor in boronic pinacolate groups. Above 100°C, the boronic pinacolate moieties were found to react and induced a dynamic crosslinking.

To generally conclude on this chapter work, we demonstrated the ability to copolymerize both styrenic and vinylic monomers carrying boronic pinacolate moieties with monomers of interests highly used in industry. From these syntheses, all the copolymers were characterized by a variety of methods and the boronate esters reactivity was once more evidenced as aforementioned in the previous chapter. Innovative approach was adopted for the design of hybrid organic/inorganic glasses from trifunctional boronate ester small molecules. Besides, hydroboration to install boronate ester groups, using an atom-economical strategy with HBPin as reagent, opened the path for numerous functionalizations of diene polymers to afford dynamic crosslinking. All these results show that the ubiquitous pinacol boronate moieties are very promising for the synthesis of thermoresponsive polymers and dynamically crosslinked networks. It allows for the creation of reprocessable crosslinked common materials such as elastomers or glasses.

V. References

[1] R. L. Letsinger and S. B. Hamilton, "Organoboron Compounds. X. Popcorn Polymers And Highly Cross-Linked Vinyl Polymers Containing Boron," *J. Am. Chem. Soc.*, vol. 81, no. 12, pp. 3009–3012, **1959**.

[2] M. Hartmann, H. Carlsohn, and J. Pauls, "Über Copolymere der p-Vinylbenzolboronsaure mit Styrol," *Die Makromol. chemie*, vol. 177, pp. 131–144, **1976**.

[3] G. Kahraman, O. Beskares, Z. M. O. Rzaev, and E. Piskin, "Bioengineering polyfunctional copolymers. VII. Synthesis and characterization of copolymers of p-vinylphenyl boronic acid with maleic and citraconic anhydrides and their self-assembled macrobranched supramolecular architectures," *Polymer (Guildf).*, vol. 45, pp. 5813–5828, **2004**.

[4] G. Giffels, J. Beliczey, M. Felder, and U. Kragl, "Polymer enlarged oxazaborolidines in a membrane reactor: Enhancing effectivity by retention of the homogeneous catalyst," *Tetrahedron: Asymmetry*, vol. 9, pp. 691–696, **1998**.

[5] J. M. G. Cowie, *Polymers: Chemistry & Physics of Modern Materials (2nd Edition)*. **1991**.

[6] J. Pellon, L. H. Schwind, M. J. Guinard, and W. M. Thomas, "Polymerization of vinyl monomers containing boron II. p-vinylphenylboronic acid," *J. Polym. Sci.*, vol. 55, pp. 161–167, **1961**.

[7] M. Gordon and J. S. Taylor, "Ideal copolymers and the second-order transitions of synthetic rubbers," *J. Appl. Chem.*, vol. 2, pp. 493–500, **1952**.

[8] R. H. Colby, "Block Copolymers, Melt Rheology of," in *Encyclopedia of Materials: Science and Technology*, **2004**, pp. 727–730.

[9] J. H. Rosedale and F. S. Bates, "Rheology of Ordered and Disordered Symmetric Poly(ethylenepropylene)-Poly(ethylethylene) Diblock Copolymers," *Macromolecules*, vol. 23, no. 8, pp. 2329–2338, **1990**.

[10] M. L. Williams, R. F. Landel, and J. D. Ferry, "The Temperature Dependence of Relaxation Mechanisms in Amorphous Polymers and Other Glass-forming Liquids," *J. Am. Chem. Soc.*, vol. 77, no. 14, pp. 3701–3707, **1955**.

[11] D. K. Benson, R. W. Burrows, and J. D. Webb, "Solid-state phase transitions in pentaerythritol and related polyhydric alcohols," *Sol. Energy Mater.*, vol. 13, pp. 133–152, **1986**.

[12] J. A. Wyler, "Pentaerythritol condensation products," 2,462,047, **1949**.

[13] C. A. Angell, "Formation of Glasses from Liquids and Biopolymers," *Science (80-.).*, vol. 267, pp. 1924–1935, **1995**.

[14] C. A. Angell, "Relaxation in liquids, polymers and plastic crystals-strong/fragile patterns and problems," *J. Non. Cryst. Solids*, vol. 131–133, pp. 13–31, **1991**.

[15] D. H. Vogel, "Das Temperaturabhaengigkeitsgesetz der Viskositaet von Fluessigkeiten," *Phys. Zeitschrift*, vol. 22, p. 645, **1921**.

[16] G. S. Fulcher, "Analysis of recent measurements of the viscosity," *J. Am. Ceram. Soc.*, vol. 8, pp. 339–353, **1925**.

[17] V. G. Tammann and W. Hesse, "Die Abhangigkeit der Viscositat von der Temperatur bei unterkuhlten Fltissigkeiten," *Anorg. Allgem. Chem.*, vol. 156, pp. 245–256, **1924**.

[18] M. Luis Ferreira Nascimento and C. Aparicio, "Viscosity of strong and fragile glass-forming

liquids investigated by means of principal component analysis," *J. Phys. Chem. Solids*, vol. 68, no. 1, pp. 104–110, **2007**.

[19] L. J. Bellamy, W. Gerrard, M. F. Lappert, and L. R. Williams, "Infrared spectra of boron compounds," *J. Am. Chem. Soc.*, pp. 2412–2415, **1958**.

[20] D. Massiot *et al.*, "Modelling one- and two-dimensional solid-state NMR spectra," *Magn. Reson. Chem.*, vol. 40, pp. 70–76, **2002**.

[21] K. Yamashita, K. Kimura, S. Tazawa, M. S. Asano, and K. Suguira, "A Forgotten Olefin: A Convenient One-pot Cascade Reaction Involving Suzuki-Miyaura and Mizoroki-Heck Couplings to Form (E)-1,2-Di(pyren-1-yl)ethylene," *Chem. Lett.*, vol. 40, pp. 1459–1461, **2011**.

[22] C. A. Leclair, M. B. Bower, C. J. Thomas, and D. J. Maloney, "Total synthesis of LL-Z1640-2 utilizing a late-stage intramolecular Nozaki-Hiyama-Kishi reaction," *Tetrahedron Lett.*, vol. 51, no. 52, pp. 6852–6855, **2011**.

[23] M. Yang, N. Yokokawa, H. Ohmiya, and M. Sawamura, "Synthesis of Conjugated Allenes through Copper-Catalyzed γ-Selective and Stereospecific Coupling between Propargylic Phosphates and Aryl- or Alkenylboronates," *Org. Lett.*, vol. 14, no. 3, pp. 816–819, **2012**.

[24] F. Beaumier, M. Dupuis, C. Spino, and C. Y. Legault, "Formal Intramolecular (4+1)-Cycloaddition of Dialkoxycarbenes: Control of the Stereoselectivity and a Mechanistic Portrait," *J. Am. Chem. Soc.*, vol. 134, pp. 5938–5953, **2012**.

[25] B. C. Chary, S. Kim, D. Shin, and P. H. Lee, "A regio- and stereoselective synthesis of trisubstituted alkenes *via* gold (I)-catalyzed hydrophosphoryloxylation of haloalkynes," *Chem. Commun.*, vol. 47, pp. 7851–7853, **2011**.

[26] T. Jousseaume, P. Retailleau, L. Chabaud, and C. Guillou, "Studies on the asymmetric Birch reductive alkylation to access spiroimines," *Tetrahedron Lett.*, vol. 53, pp. 1370–1372, **2012**.

[27] C. T. Avetta, B. J. Shorthill, C. Ren, and T. E. Glass, "Molecular Tubes for Lipid Sensing: Tube Conformations Control Analyte Selectivity and Fluorescent Response," *J. Org. Chem.*, vol. 77, pp. 851–857, **2012**.

[28] B. Blanco *et al.*, "Synthesis of 3-alkyl enol mimics inhibitors of type II dehydroquinase: factors influencing their inhibition potency," *Org. Biomol. Chem.*, vol. 10, pp. 3662–3676, **2012**.

[29] L. Duroure *et al.*, "6,6-spiroimine analogs of (-)-gymnodimine A: synthesis and biological evaluation on nicotinic acetylcholine receptors," *Org. Biomol. Chem.*, vol. 9, pp. 8112–8118, **2011**.

[30] G. Y. C. Leung *et al.*, "Total Synthesis and Biological Evaluation of the Fab-Inhibitory Antibiotic Platencin and Analogues Thereof," *European J. Org. Chem.*, pp. 183–196, **2011**.

[31] S. Wang *et al.*, "Topological polymer electrolyte containing poly(pinacol vinylboronate) segments composited with ceramic nanowires towards ambient-temperature superior performance all-solid-state lithium batteries," *J. Power Sources*, vol. 413, pp. 318–326, **2019**.

[32] O. G. Piringer and A. L. Baner, *Plastic Packaging: Interactions with Food and Pharmaceuticals*. Wiley-VCH Verlag GmbH & Co. KGaA, **2008**.

[33] M. Carrega, *Aide-mémoire Matières plastiques*. **2009**.

[34] E. Baur and T. A. Osswald, *Saechtling Kunststoff Taschenbuch*. **2013**.

[35] K. Rauer, H. Hofmann, H. Schiller, and C. S. Sheppard, "Crosslinking of polymers with azo-esters," 4,129,531, **1978**.

[36] T. Sone, "Industrial Synthetic Method of the Rubbers. 1. Butadiene rubber," *Nippon Gomu Kyokaishi*, no. 5, pp. 178–183, **2016**.

[37] J. Mark and B. Erman, *Science and Technology of Rubber*. Elsevier, **2005**.

[38] M. Akiba and A. S. Hashim, "Vulcanization and crosslinking of elastomers," *Prog. Polym. Sci.*, vol. 22, pp. 475–521, **1997**.

[39] C. P. Pinazzi, P. Guillaume, and D. Reyx, "Fixation de microchaînons carbonyles sur des polyisoprènes et polybutadiènes par hydroboration. Réaction sur modèles macromoléculaires.," *J. Polym. Sci. Symp.*, vol. 47, no. 1, pp. 167–178, **1974**.

[40] C. P. Pinazzi, P. Guillaume, and D. Reyx, "Gamma-oxoalkylation de polyalcadiènes à structures-1,4 predominantes par réaction couplée à l'hydroboration," *Eur. Polym. J.*, vol. 13, no. 9, pp. 707–711, **1977**.

[41] T. C. Chung, M. Raate, E. Berluche, and D. N. Schulz, "Synthesis of functional hydrocarbon polymers with well-defined molecular structures," *Macromolecules*, vol. 21, no. 7, pp. 1903–1907, **1988**.

[42] J. V. Obligacion and P. J. Chirik, "Highly selective bis(imino)pyridine iron-catalyzed alkene hydroboration," *Org. Lett.*, vol. 15, no. 11, pp. 2680–2683, **2013**.

[43] Y. Xi and J. F. Hartwig, "Diverse asymmetric hydrofunctionalization of aliphatic internal alkenes through catalytic regioselective hydroboration," *J. Am. Chem. Soc.*, vol. 138, no. 21, pp. 6703–6706, **2016**.

[44] H. A. Kerchner and J. Montgomery, "Synthesis of Secondary and Tertiary Alkylboranes *via* Formal Hydroboration of Terminal and 1,1-Disubstituted Alkenes," *Org. Lett.*, vol. 18, no. 21, pp. 5760–5763, **2016**.

[45] Y. X. Lu, F. Tournilhac, L. Leibler, and Z. Guan, "Making insoluble polymer networks malleable *via* olefin metathesis," *J. Am. Chem. Soc.*, vol. 134, no. 20, pp. 8424–8427, **2012**.

[46] Y. X. Lu and Z. Guan, "Olefin metathesis for effective polymer healing *via* dynamic exchange of strong carbon-carbon double bonds," *J. Am. Chem. Soc.*, vol. 134, no. 34, pp. 14226–14231, **2012**.

[47] K. Voigtritter, S. Ghorai, and B. H. Lipshutz, "Rate Enhanced Olefin Cross-Metathesis Reactions," *J. Orga*, vol. 76, pp. 4697–4702, **2011**.

[48] R. G. Ricarte, F. Tournilhac, and L. Leibler, "Phase Separation and Self-Assembly in Vitrimers: Hierarchical Morphology of Molten and Semicrystalline Polyethylene/ Dioxaborolane Maleimide Systems," *Macromolecules*, vol. 52, pp. 432–443, **2019**.

[49] S. W. Craig, J. A. Manzer, and E. B. Coughlin, "Highly efficient acyclic diene metathesis depolymerization using a Ruthenium catalyst containing a N-heterocyclic carbene ligand," *Macromolecules*, vol. 34, no. 23, pp. 7929–7931, **2001**.

[50] A. Dewaele, T. Renders, B. Yu, F. Verpoort, and B. F. Sels, "Depolymerization of 1,4-polybutadiene by metathesis: High yield of large macrocyclic oligo(butadiene)s by ligand selectivity control," *Catal. Sci. Technol.*, vol. 6, no. 21, pp. 7708–7717, **2016**.

[51] M. D. Watson and K. B. Wagener, "Solvent-free olefin metathesis depolymerization of 1,4-polybutadiene," *Macromolecules*, vol. 33, no. 5, pp. 1494–1496, **2000**.

General conclusion and perspectives

During our research assessing new reactivity at boron, we evidenced innovative uses of organoboron polymers to provide dynamic networks harnessing the tunable Lewis acidic character of boron groups and boronate esters' reactivity. In this fashion, two principal families of networks have been designed. The first family was constituted B-P and B-N Lewis pairs equipped with difunctional molecules or polymers. On the other hand, organoboron polymers with B-O linkages bearing side-chain boronate esters displayed fascinating dynamic thermomechanical properties.

By conveniently adjusting the electronic and steric constraints of a boron-based moiety, we were able to finely tune the Lewis acidity of a molecule. In this optic, one of our goal was to harness the exciting reactivity of Frustrated Lewis Pairs to be able to form supramolecular networks. Previous works showed the ability of these pairs to reversibly capture CO_2. Different networks were designed such as difunctional molecules bearing two Lewis acidic groups or two Lewis basic groups, or polymers comprising pendent Lewis bases able to interact with a difunctional Lewis acid.

The synthesis of the difunctional Lewis-acid molecule bearing two pentafluoroaryl boranes in para positions on a phenylene linker was particularly challenging due to an enhanced reactivity at boron and requested many optimizations to reach the desired product with good purity. This explained why this difunctional molecule was at the center of our study, in interaction with difunctional Lewis base molecules or Lewis base-functionalized (co)polymers.

The selected Lewis bases were nitrogen or phosphorus-based whose syntheses were already reported in literature. For the nitrogen-based copolymers, we synthesized copolymers from styrene and 4-vinylpyridine. Unfortunately, the Lewis basicity of pyridine groups does not display a frustrated character due to the lack of steric hindrance. Thus, this functionalized polymer could not be used in the capture of CO_2 as it does not present FLP properties. In a same manner, copolymers from styrene and 4-styryldiphenylphosphine were synthesized with controlled amounts of phosphine groups. Even though not frustrated, the pair with pentafluoroaryl borane moieties retains its reactivity towards CO_2.

Thus, we focused on the system with the difunctionalized pentafluoroaryl borane with a phenylene linker interacting with poly(styrene-*co*-4-styryldiphenylphosphine). We put in evidence the capture of CO_2 by our supramolecular network by NMR spectroscopy as well as

rheology. The reversible character of this capture is practically of very high importance in order to create actuators or reusable detectors and was probed by rheology and UV spectroscopy by heating up to 70°C. We demonstrated a partial reversibility of CO_2 from the Lewis pair system.

Synthesis of poly(Lewis acid)s would be interesting to go further than the syntheses offered in this thesis work, with the design of two functionalized copolymers able to interact with gas molecules. The mechanical properties, e.g. storage moduli of the gels, achieved would be more interesting if no small molecule was used in this system. Besides, the Lewis groups could be finely tuned to reach the desired properties in terms of frustration. This last route could be a perspective for this work combined with the use of rheology. Some examples have been already reported on this topic but some innovations could still be done in future works, especially concerning the study of the mechanical properties.

The second research axis of this thesis work focused on the synthesis of organoboron polymers comprising boron-oxygen bonds, especially boronic pinacolates. By firstly working on poly(4-vinylphenylboronic pinacolate), we reported a reactivity of these boronate esters up-to-now disregarded to afford dynamic polymers. Through a variety of analytical methods, we were able to identify an interesting dynamic behavior inherent to the polymer that highly caught our attention.

A crosslinking between the polymer chains triggered by a nucleophilic assistance (water or pinacol molecules) was put in evidence at high temperature or at least in a certain temperature range. Thus, we reported the opening of the pyramidalized boronate group yielding a pendent singly-attached pinacol-derived nucleophile connecting another boron atom, and so forth. The pendent negatively charged group reacts with the electronic vacancy of another boron, which, when borne by another chain results in crosslinking. Indeed, we obtained polymers with high glass-transition temperatures up to 220°C. The dynamic character of the crosslinking was observed when solvents such as toluene were added, as the inverse path heading to dissolution happened. Indeed, the intramolecular 5-membered cyclic boronates are entropically favored under high dilution. These specifics are critical for the reversibility of the system.

When comparing our system to vitrimers and covalent adaptable networks, that have either constant crosslinking densities or continuously decreasing crosslinking densities with temperature, it is exciting to note that polymers bearing cyclic boronate esters may constitute the first example of a distinct class of dynamic networks, with a crosslinking density increasing with temperature, at least within a defined temperature range.

After the establishment of this reaction path and to deepen our understanding of the contribution of the boronic pinacolate, it was decided to extend the concept reported to a wide range of polymers, separating the boronate esters on styrenic-born and vinylic-born backbones.

In a first extension example, copolymers from 4-vinylphenylboronic pinacolate and styrene were afforded at different composition. The glass transition temperature strongly increased obtained after incorporating 4-vinylphenylboronic pinacolate enabling to finely tune the glass transition temperature of PS in the 100-200°C range. Copolymers from 4-vinylphenylboronic pinacolate and n-butyl acrylate also showed the same proprieties that allowed to extent the boronate esters reactivity to low glass transition temperature polymers. However, it was interesting to note in this case a phase separation may occur between boronate ester rich- and poor-domains due to the strong incompatibility between the co-monomers used. It could be interesting to perform in future works SAXS or microscopies (TEM, AFM) experiments to analyze the phase separation and understand its role in the dynamics of these materials.

On the other hand, polymers arising from vinyl-boron systems were exemplified through (co)polymerization and functionalization of existing polymers. The first noticeable result was the novel polymerization of the vinylic version of boronic pinacolate used so far with a smart strategy involving complexation of the boron electronic vacancy. This polymer exhibits a disconcerting thermal behavior with a crosslinking only in a certain temperature range. We reported here a complete thermoresponsive polymer whose glass transition temperature is varying depending on the probing temperature. This puzzling behavior was quite surprising in our research path, but we assumed that the vinylic and styrenic versions of boronic pinacolate should not be acting the exact same way for evident geometric reasons. (sp^3 vs. sp^2 carbon connected to boron induces less rigidity).

We also went further by successfully copolymerizing vinylboronic pinacolate with vinyl acetate and ethylene. For copolymers from vinyl acetate, we recovered the same mechanical and thermal behavior as previously with the ring opening of the boronate ester cycles inducing the dynamical crosslinking. Concerning the copolymers from ethylene, the differential scanning calorimetry experiments showed that the incorporation of boronic pinacolates on the ethylenic backbone highly disrupted the melting and crystallization events. The copolymerization of vinylboronic pinacolate and ethylene is a prowess by itself and opens perspectives for the incorporation of boronate esters in industrially relevant (co)polymers.

Beyond copolymerization, another strategy was used for the incorporation of boronic pinacolates on polymer backbones. Thus, we reported the functionalization of polybutadiene by hydroboration that allowed for the installation of boronic pinacolate moieties on the rubber

backbone. Two synthetic paths were here presented and the most promising remains the hydroboration by iron catalysis. The rheology experiments brought some information about the microstructure in the modified polybutadiene. Actually, the modified polymer presents a phase separation between incompatible polar and apolar phases, respectively rich in boronic pinacolate and poor in boronic pinacolate groups. Above 100°C, the boronic pinacolate moieties were found to react and induced a dynamic crosslinking. However, a strong decrease of the molar masses was evidenced, which requires further improvement in the future.

In an original approach, we committed ourselves to a conceptual extension with the design of new hybrid glasses harnessing the same reactivity. We were able to create new tridimensional networks from trifunctional molecules bearing boronic pinacolates moieties, soluble in solvents such as THF. This work seems to be very promising as it covers a hot topic on hydrid organic/inorganic glasses presenting reversibility. However, improvements need to be done, especially on the fragility of the material that hinders the use of this hybrid glass and the study of its mechanical properties. It is possible to imagine the use of other more flexible trifunctional molecules carrying boronic pinacolates or the incorporation of flexible molecules in the mixtures.

Supramolecular networks able to capture reversibly CO_2 and new reprocessable high-T_g materials reported were all based on boron chemistry. For the latter, we demonstrated that the creation of reversible boronate-based bridges between polymeric chains could be exploited to design materials with adjustable glass transitions. We foresee valuable new boron-based materials that could harness this reactivity to not only tune glass transition temperatures and inherent mechanical properties by modifying the backbone of the polymer but also change the dynamic characteristics of the system by appropriately selecting the boronate pendent groups.

In future works, it would be very interesting to work on poly(Lewis acid)s and poly(Lewis base)s with different designs to reach better mechanical properties and also to tune the reversibility of CO_2 capture. We could also work on the capture of other small molecules such as SO_2 or N_2O, but also study the use of the Lewis Pairs in catalysis. These systems could be used in membranes or actuators with changing mechanical properties depending on the capture and the release of CO_2.

Hydroboration brought very attractive perspectives concerning the synthesis of functionalized polymers carrying boronate esters and harnessing the dynamic crosslinking *via* the ring-opening path. A better selectivity of the functionalization could be targeted as well as process solutions to guarantee the integrity of the molar masses of the polymers.

In addition, the innovative use of the boronate esters' reactivity for the synthesis of glasses requires further investigation. Many different designs of the starting molecules could be tested, especially to improve the mechanical resistance of the final material. The incorporation of other molecules bearing flexible groups could also be considered.

The perspectives of this thesis work could be summarized as below:

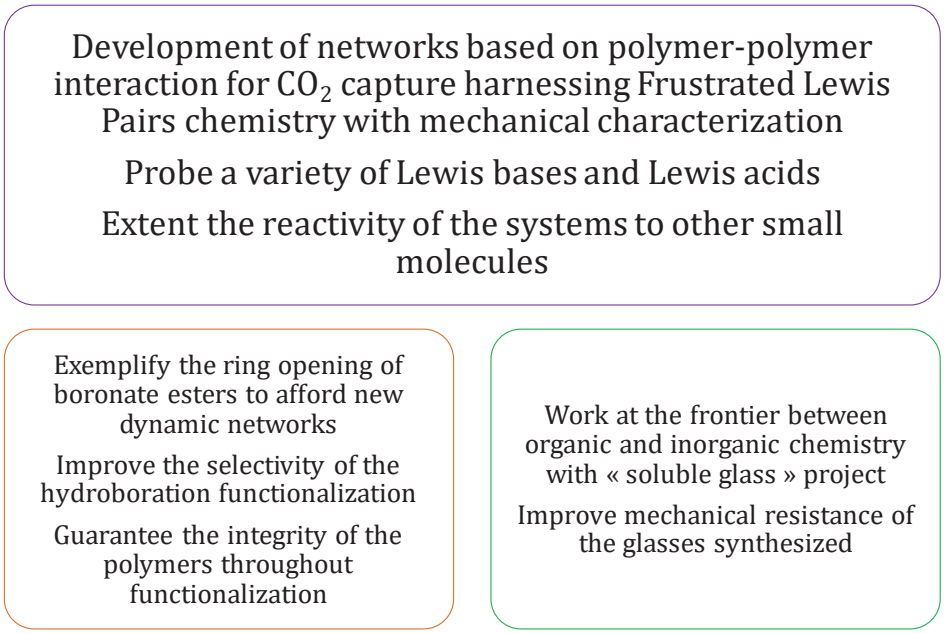

Figure 1: Perspectives of this PhD work.

Experimental section

Table of contents

I. Materials and methods

Unless otherwise stated, all reactions were conducted under inert atmosphere (argon) using standard techniques for manipulating air-sensitive compounds. All glassware was stored in an oven or was flame-dried prior to establishing an argon atmosphere. Yields refer to spectroscopically pure compounds. The reagents were purchased from Combi Blocks, Sigma Aldrich, Alfa Aesar and TCI, and used without any further purification. The solvents were purified by freeze-pump-thaw technique and stored on 4 Å molecular sieves.

Nuclear Magnetic Resonance (NMR) spectra (^{1}H, ^{13}C, ^{11}B, ^{19}F, ^{31}P) were recorded on a Bruker AC 300 spectrometer operating at 300 MHz or on a Avance III 400 (US+) spectrometer operating at 400 MHz equipped with a BBFO+ probe for 5 mm NMR tube. For 10 mm NMR tube, NMR spectra were recorded on a Bruker Avance II 400 (Ascend) spectrometer operating at 400 MHz and equipped with a SEX ^{13}C 10 mm probe. Prior to use, C_6D_6 (Eurisotop) was dried on 4 Å molecular sieves. All chemical shifts were measured relative to residual ^{1}H or ^{13}C resonance in the deuterated solvent: C_6D_6, δ 7.16 ppm for ^{1}H, 128.0 ppm for ^{13}C, THF-d_8, δ 1.72 ppm, 2.58 ppm for ^{1}H, 25.31 ppm, 67.21 ppm for ^{13}C, $CDCl_3$, δ 7.26 for ^{1}H, 77.16 ppm for ^{13}C, DMSO-d_6, δ 2.5 ppm for ^{1}H and 39.52 ppm for ^{13}C, D_2O, δ 4.79 ppm for ^{1}H, toluene-d_8, δ 2.08 ppm, 6.97 ppm, 7.01 ppm, 7.09 ppm for ^{1}H, 20.43 ppm, 125.13 ppm, 127.96 ppm, 128.87 ppm, 137.48 ppm for ^{13}C .^{11}B NMR spectra were calibrated using BF_3 Et_2O (0.0 ppm) as external reference. ^{19}F NMR chemical shifts were referenced with $CFCl_3$ (0.0 ppm). ^{31}P NMR spectra were calibrated with triphenylphosphate at -17.6 ppm in 0.0485 M in acetone-d_6. The monitorings of exchange reactions in Chapter 3 were run on single NMR tubes containing the 1:1 molar mixture of boronic esters (with and without 1 equivalents of benzyl alcohol) heated in an oil bath at 100°C. No additional solvent was added in the tube. At different times, the tubes were taken out from the oil bath, equipped with an insert containing toluene-d_8 was added during the NMR measurement to lock the signal and analyzed by ^{19}F NMR at 25°C. Chapters 2, 3 and 4 are concerned by NMR measurements.

Solid-state NMR spectra in Chapters 3 and 4 were recorded on a Bruker advanced 500 and 700 MHz spectrometers with a conventional double resonance 1.3 mm and 2.5 mm CP-MAS probes at the "Institute of Analytical Sciences" (Centre de RMN à Très Hauts Champs) at University of Lyon. Chemical shifts were given in ppm with respect to $B(OH)_3$ as reference. The spinning frequency were set at 4200 Hz and the NMR data were processed with TopSpin 3.2 and fitted with DMfit.

Diffusion ordered spectroscopy (DOSY) ^{19}F experiments in Chapter 3 were performed on Bruker AV500 spectrometer equipped with Multinuclear Broadband Fluorine Observe (BBFO) probe with z-axis gradient coil. The experiment duration was 1 h at the temperature of 25°C controlled by BCU-X of Bruker. The standard Bruker pulse sequence (ledbpgp2s) using stimulated

echo was used for ^{19}F DOSY experiments with bipolar gradient pulses for diffusion. [1] For ^{19}F diffusion measurements, the delays δ and Δ were set to 750 µs and 80 ms, respectively. The relaxation time D_1 was 5 sec and the number of scans was 16 by spectrum. Diffusion coefficients D were obtained by fitting the attenuation curves of individual signals of the ^{19}F spectra $I(G_i)$ by mono-exponential decays: $I(G_i) = I_0 \exp(-D(2\pi\gamma G_i \delta)^2 \left(\Delta - \frac{\delta}{3}\right))$, with γ=4006 Hz/Gauss the gyromagnetic ratio for the Fluor nucleus.

Differential scanning calorimetry (DSC) experiments in Chapters 3 and 4 were performed on a Mettler DSC 2 StarSyst apparatus. After initial equilibration at a low temperature, heating/cooling cycles between specified temperatures were run at 10 or 20 K/min. 40 µL aluminum crucibles (containing between 5 and 20 mg of polymers)or 100 µL medium pressure aluminum crucibles (containing between 10 and 30 mg of polymers) were used depending on the measurement.

Thermogravimetric analyses (TGA) were performed in 100 µL alumina crucibles using 10 K/min heating ramps on a Mettler TGA/DSC StarSyst. Between 10 and 20 mg of polymers were weighed depending on the batch and analyzed by TGA technique. Chapters 3 and 4 contain information from TGA experiments.

Size-exclusion chromatography (SEC) analyses was performed on Viscotek GPCmax instrument from Malvern Instruments with tetrahydrofuran (THF) as eluent was used for evaluating the molar masses of the synthesized polymers. The system is equipped with an online Triple Detector Array including a right and low angle light scattering detector (RALS and LALS), a four-capillary differential viscometer, and a differential refractive index detector (RI). THF was used as an eluent at a constant flow rate of 1 mL/min. The measurement was carried at the temperature of 35°C. All polymers were prepared at a concentration of 5 mg/mL. They were filtrated through a 0.22 µm PTFE filter. The sample injection is set at 100 µL. The separation was carried out on three serial columns (PLgel Olexis, 300 × 7.5 mm) and a guard column (PLgel Olexis Guard, 300 × 7.5 mm). The OmniSEC 4.7 software was used for data acquisition and data analysis. The size distribution was obtained from the RI signal using conventional calibration with PS standards. Chapters 3 and 4 are concerned.

Infra-red-Attenuated Total Reflectance (IR-ATR) measurements were performed at room temperature on a Nicolet i550 FT-IR apparatus, in Chapters 3 and 4.

In-situ IR experiments in Chapters 3 and 4 were done on a Thermo Fisher Nicolet 6700 apparatus equipped with a DRIFT cell equipped with CaF_2 windows (diffuse reflectance FTIR spectroscopy) operating under argon atmosphere. The spectra were taken at different temperatures starting from 25°C to 250°C with 10 min of temperature equilibration steps.

High temperature, Melt Rheology experiments in Chapter 3 were carried out on an ARES G2 from TA Instruments, using an electric oven and an N_2 atmosphere. The polymer sample was pressed into an 8 mm x 1.5 mm disk and analyzed using 8 mm plate-plate geometries. After each equilibration step at temperatures ranging from 230 to 260°C, strain-controlled oscillatory shears (1 %) were applied at angular frequencies varying from 200 to 0.2 rad.s^{-1}.

Rheology experiments presented in Chapters 2, 3 and 4 were carried out on a MARS 60 apparatus from Thermo Scientific equipped with a Peltier cell, using a 16mm concentric cylinder geometry or an 8 mm plate-plate geometry.

Computational Details of Thermodynamics of Ring Opening and FTIR Spectra. Geometry optimization were carried out at a DFT level of theory using the hybrid meta-GGA functional M06 [2] without any symmetry restrictions. Carbon, oxygen, boron and hydrogen atoms were represented by polarized all electron def2-TZVP basis sets. [3] In order to mimic polymer bulk, solvation by toluene was implicitly represented during optimization using the SMD method. [4] Analytical frequency calculations were carried out to verify the nature of the extrema. Enthalpies and Gibbs energy have been computed within the harmonic approximation and estimated at 298.15 K, 1 atm. Criteria for SCF convergence and geometry optimization, and integration grids are set to default values. All these computations have been performed with the gaussian09 suite of programs. [5] This is related to Chapter 3.

Cartesian coordinates of optimized structures and associated energies. The Cartesian coordinates of optimized structures and associated energies are in ESI.xyz. These data are readable with Mercury, CCDC. Each structure contains associated energies in a.u., visible in its title. This is related to Chapter 3.

Dynamic mechanical analyses (DMA) in Chapter 4 were performed on DMA 1 StarSyst using Tension clap deformation mode at 1 Hz with temperature ramp for -110°C to 200°C at 3 K/min.

Tensile tests on polybutadiene in Chapter 4 were done on SHIMADZU Autograph AG-X plus apparatus equipped with a 100 N cell. The experiments were performed at room temperature at 10 mm/min.

II. Reactive networks based on Lewis pairs

A. Syntheses of difunctionalized molecules

a. Synthesis of difunctional Lewis acid A2

This synthesis relies on the work of Lennox and Jones that they applied to the monofunctionalization of a boronic acid molecule. [6] This synthesis was pursued with the addition of Grignard on BF_3K groups.

Experimental protocol:

1) First step

To a suspension of benzene-1,4-diboronic acid (2 g, 12 mmol) in acetonitrile (200 mL) was added potassium fluoride (8 eq, 96 mmol, 5.56 g) in H_2O (80 mL) at room temperature. The mixture was stirred until complete dissolution of the boronic acid (usually 0.5-5 min). L-(+)-tartaric acid (4.1 eq, 49.2 mmol, 7.38 g) was dissolved into THF (40 mL) at 50°C for easier dissolution and added dropwise to the rapidly stirring biphasic mixture over a period of one minute. A white precipitate formed instantly, which flocculated over a period of 1–5 min. The reaction mixture was then diluted with acetonitrile (50 mL) and filtered. The flask and filter cake were rinsed with further portions of acetonitrile (3 x 100 mL) and then the combined filtrates were concentrated in vacuum to give the corresponding potassium 1,4-phenylenebis(trifluoroborate) as a white solid that was further dried under high vacuum. Yield: 3.81 g, 100 %

^{1}H NMR (300 MHz, DMSO-d_6, 25°C, δ): 7.04 (4H).

^{11}B NMR (300 MHz, DMSO-d_6, 25°C, δ): -1.29.

^{19}F NMR (300 MHz, DMSO-d_6, 25°C, δ): -137.97.

^{13}C NMR (300 MHz, DMSO-d_6, 25°C, δ): 129.4.

2) Second step

Potassium 1,4-phenylenebis(trifluoroborate) (0.36 g, 1.24 mmol) is put in suspension with 5 mL of dried THF. C_6F_5MgBr solution in 0.5 M Et_2O (4.5 eq, 12 mL) is added to the suspension at 0°C dropwise. The reaction warms up to room temperature and is stirred for 24 h. Filtration, washings with THF are done, and the product is dried under vacuum to obtain a sand color solid.

^{11}B NMR (300 MHz, DMSO-d_6, 25°C, δ): -4.79 (B), -14.67 (B---THF).

^{19}F NMR (300 MHz, DMSO-d_6, 25°C, δ): -133.4 (2F, ortho), -167.5 (1F, para), -169.9 (2F, meta).

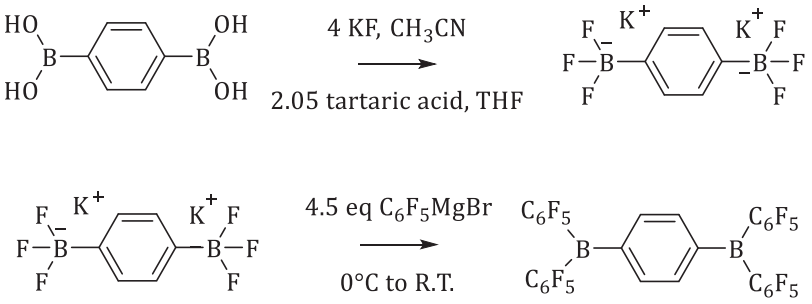

Figure V. 1: Two-step reaction path for the synthesis of A2.

NMR spectroscopies:

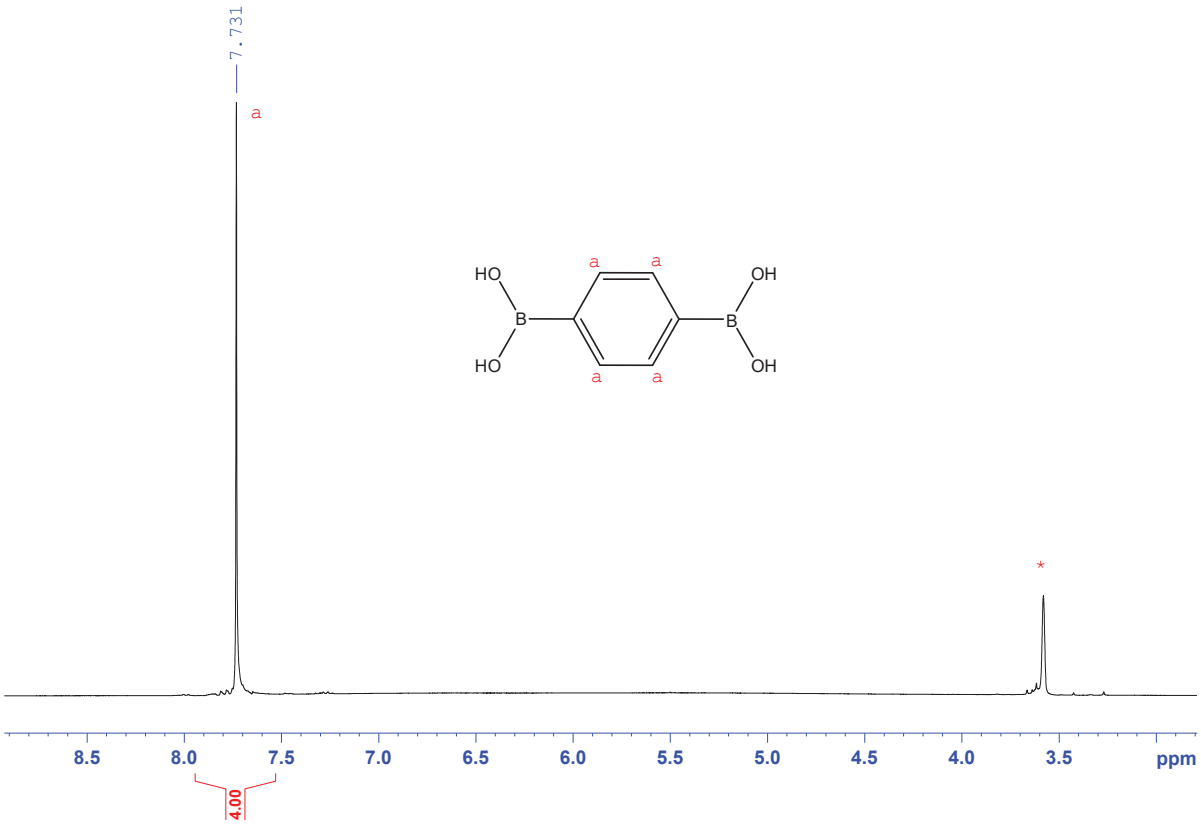

*Figure V. 2: ^{1}H NMR spectrum of commercial benzene-1,4-diboronic acid in THF-d_8. * THF-d_8*

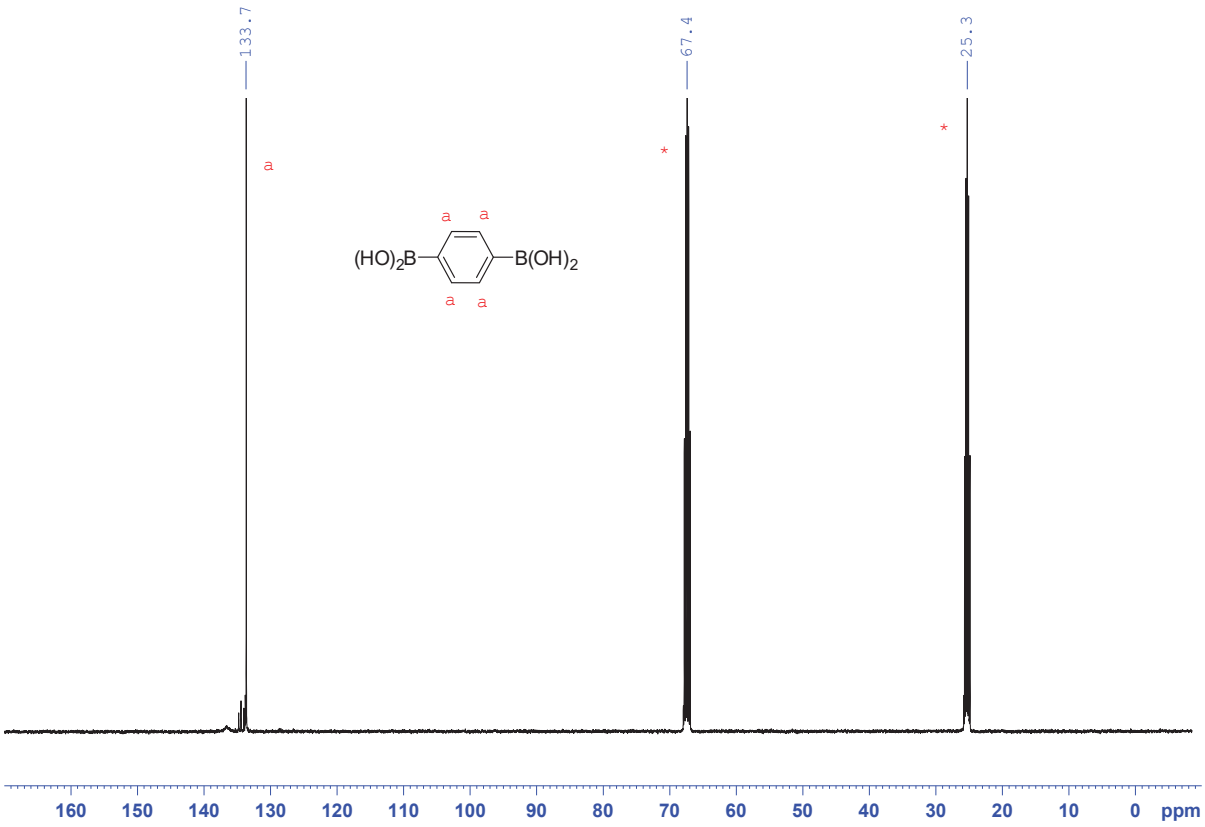

*Figure V. 3: ^{13}C NMR spectrum of commercial benzene-1,4-diboronic acid in THF-d_8. * THF-d_8*

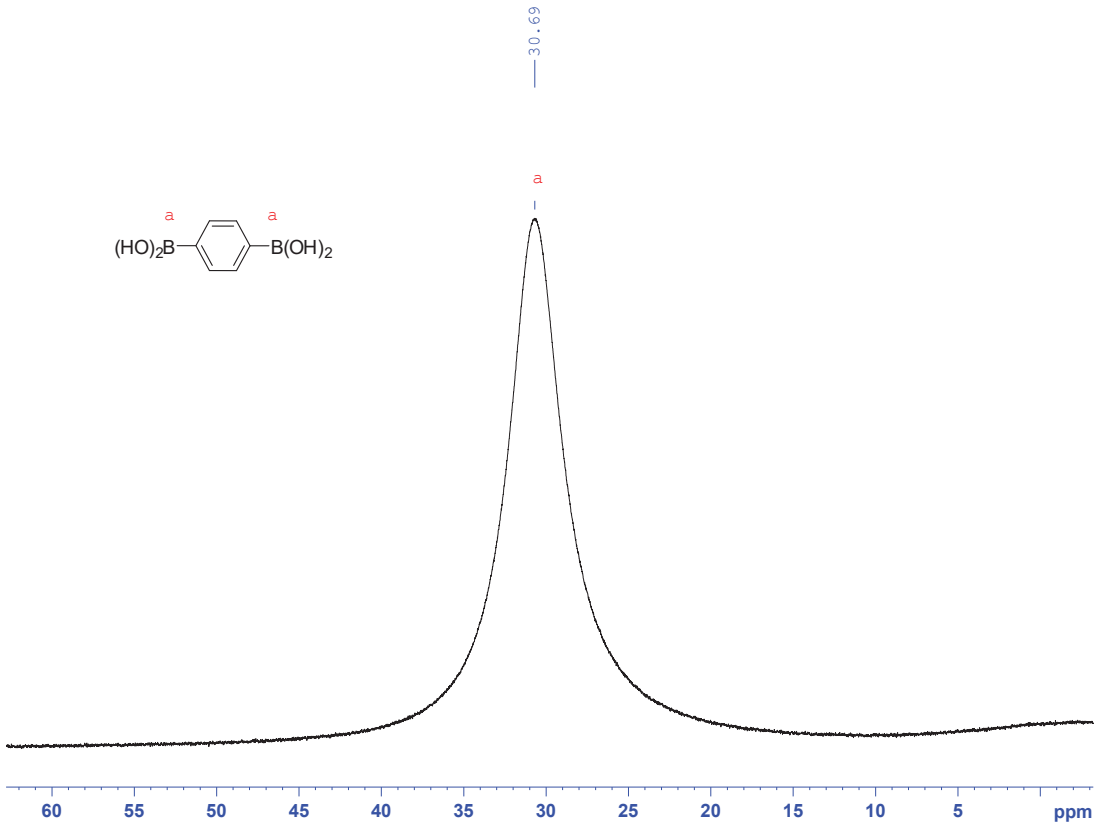

Figure V. 4: ^{11}B NMR spectrum of commercial benzene-1,4-diboronic acid in THF-d_8.

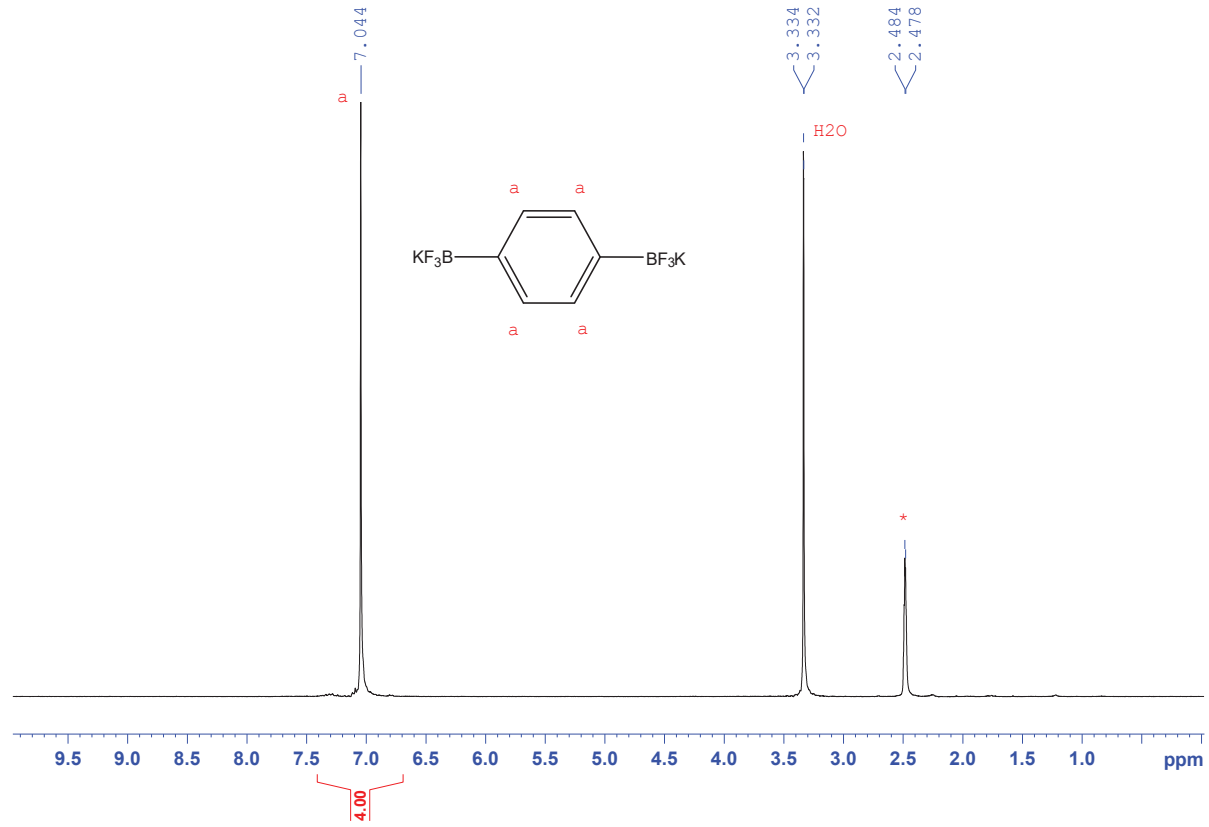

*Figure V. 5: ^{1}H NMR spectrum of potassium 1,4-phenylenebis(trifluoroborate) in DMSO-d_6. * DMSO-d_6*

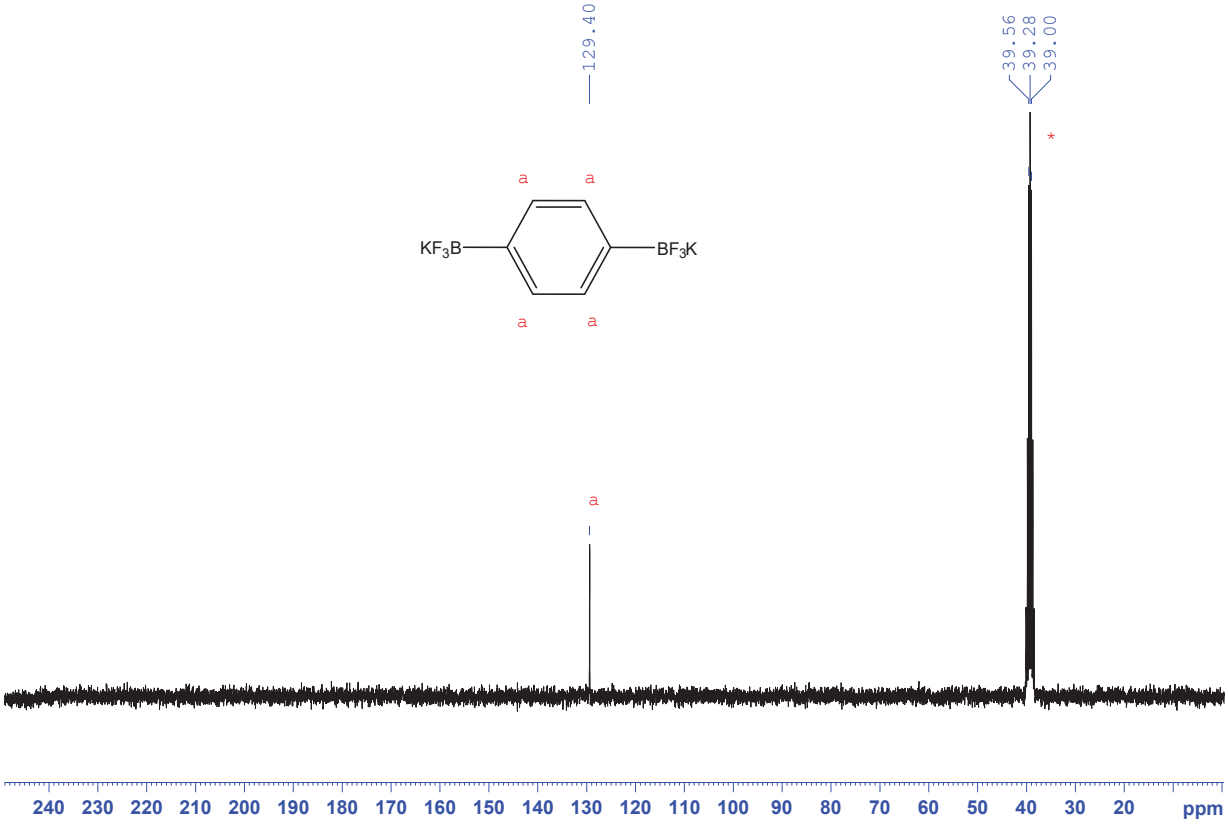

*Figure V. 6: ^{13}C NMR spectrum of potassium 1,4-phenylenebis(trifluoroborate) in DMSO-d_6. * DMSO-d_6*

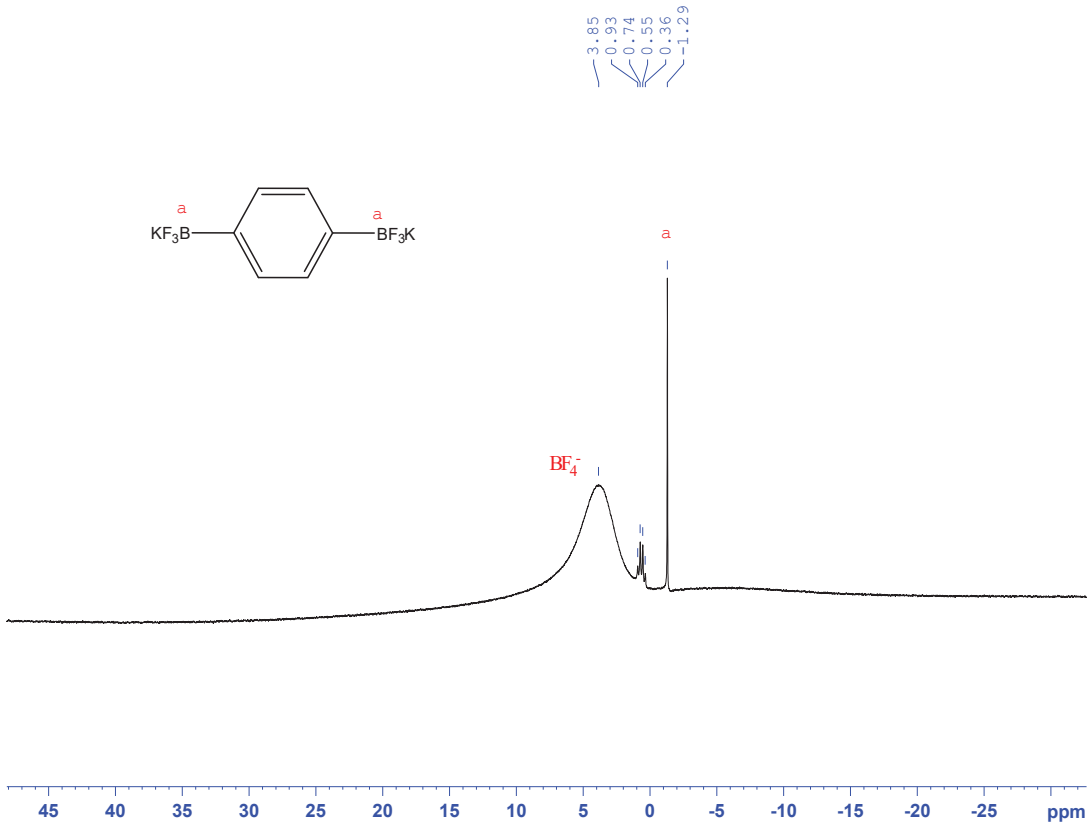

*Figure V. 7: ^{11}B NMR spectrum of potassium 1,4-phenylenebis(trifluoroborate) in DMSO-d_6. * DMSO-d_6*

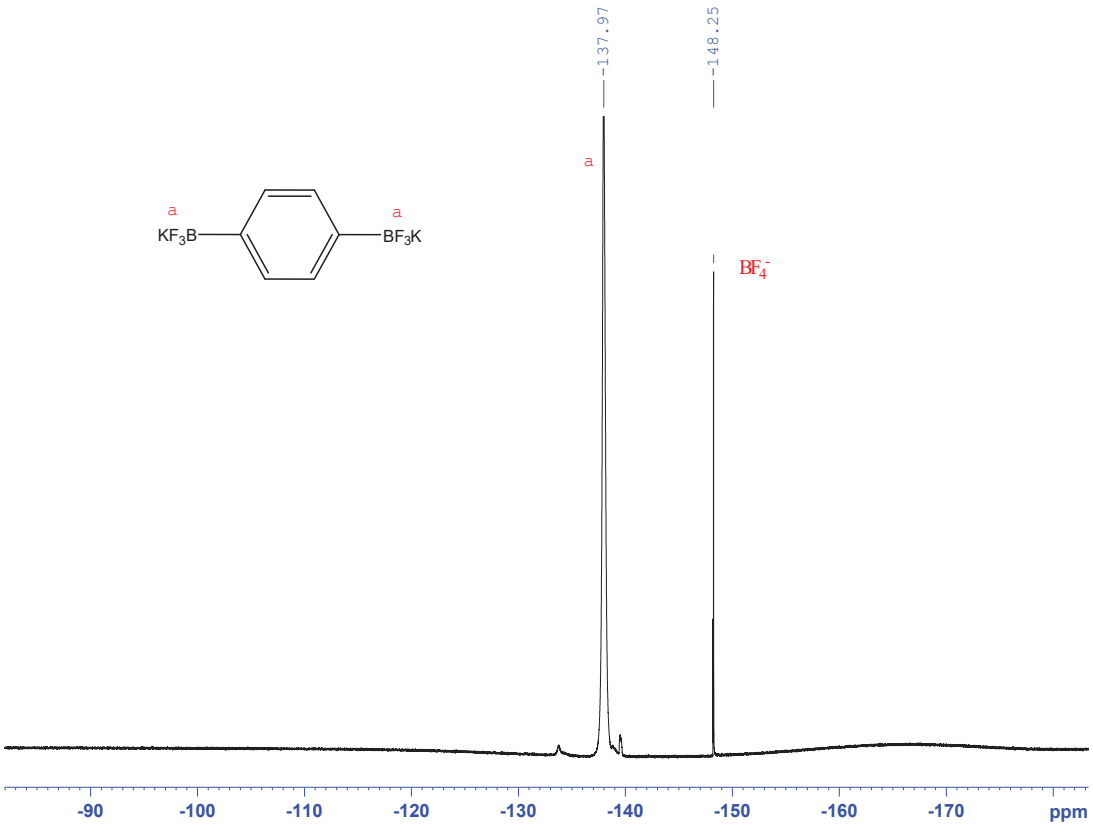

*Figure V. 8: ^{19}F NMR spectrum of potassium 1,4-phenylenebis(trifluoroborate) in DMSO-d_6. * DMSO-d_6*

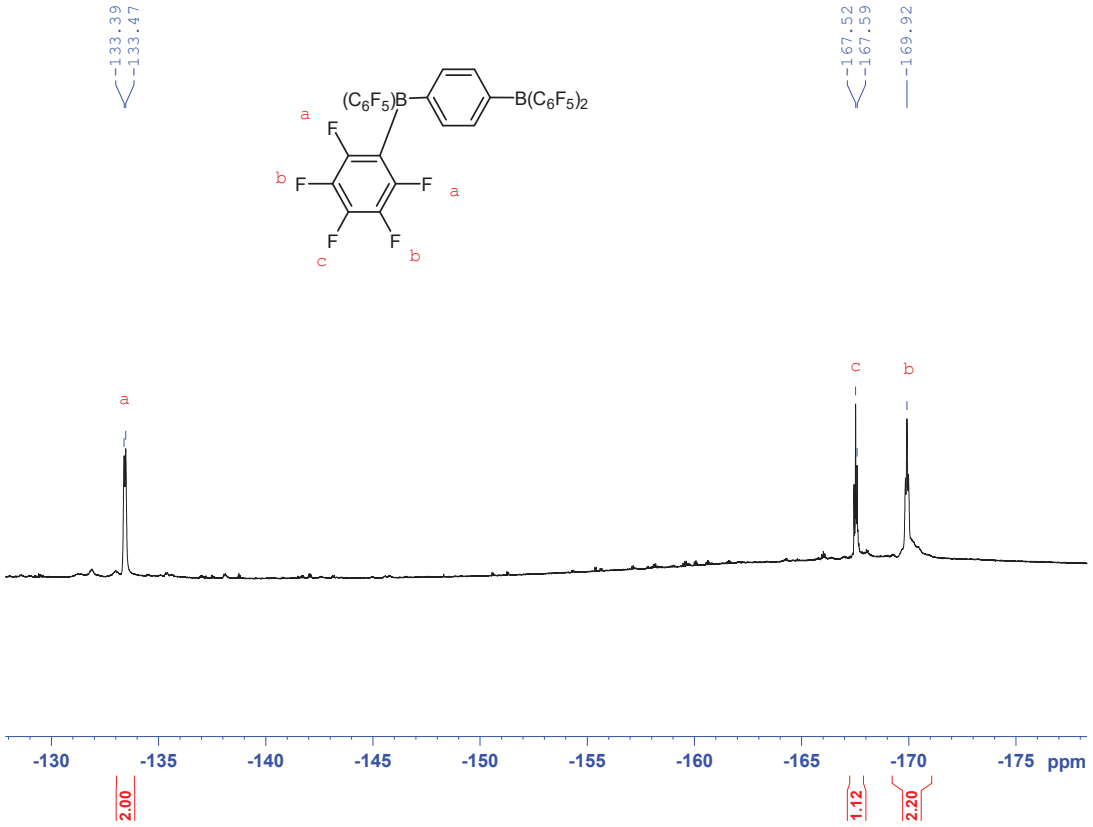

Figure V. 9: ^{19}F NMR spectrum of $B(C_6F_5)_2$-Ph-$B(C_6F_5)_2$ in THF-d_8.

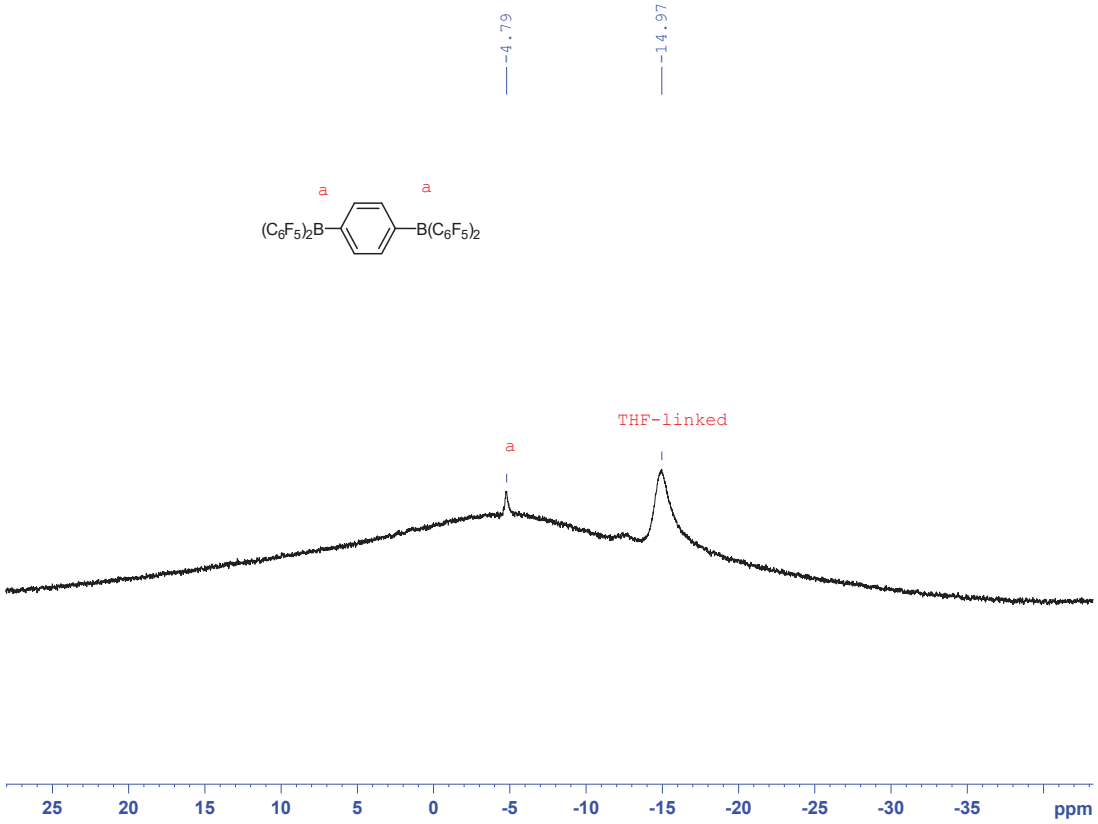

Figure V. 10: ^{11}B NMR spectrum of $B(C_6F_5)_2$-Ph-$B(C_6F_5)_2$ in THF-d_8.

b. Synthesis of difunctional Lewis base B2

For the synthesis of the difunctional molecule carrying two lutidine groups on a central phenylene linking group in para positions, we relied on the work of Hayashi. [7]

Experimental protocol:

1) First step

In a 500-mL round-bottomed flask, terephtaldehyde (2.68 g, 20 mmol), ethyl acetoacetate (10.42 g, 80 mmol), 25 wt % ammonia solution (4 g), and ethanol (40 mL) were charged and the mixture was heated to reflux at 80°C. After confirmation of the completion of the reaction by TLC, the mixture was cooled to room temperature. A solid product was obtained by filtration, then washed with ethanol and dried in vacuum to give as a pale yellow solid (5.64 g, 97 %).

^{1}H NMR (300 MHz, DMSO-d_6, 25°C, δ): 8.76 (2H, s), 6.96 (4H, s), 4.78 (2H, s), 3.89-4.03 (8H, m), 2.28 (8H, s), 1.09 (12H, t).

^{13}C NMR (300 MHz, DMSO-d_6, 25°C, δ): 166.65, 145.22, 144.88, 126.44, 101.48, 58.57, 37.92, 17.85, 13.76.

2) Second step

The freshly synthesized 1,4-dihydropridine (5.48 g, 9.44 mmol) and activated carbon (from TCI) (5 g) in xylene (20 mL) was placed in a 500-mL three-necked flask under an oxygen atmosphere and stirred at 120°C. After confirmation of the completion of the reaction by TLC, the mixture was filtered using Celite. The filtrate was then dried under vacuum to give the corresponding pyridine as a pale yellow solid (3.37 g, 62 %).

^{1}H NMR (300 MHz, $CDCl_3$, 25°C, δ): 8.76 (2H, s), 6.96 (4H, s), 4.78 (2H, s), 3.89-4.03 (8H, m), 2.28 (8H, s), 1.09 (12H, t).

^{13}C NMR (300 MHz, $CDCl_3$, 25°C, δ): 166.65, 145.22, 144.88, 126.44, 101.48, 58.57, 37.92, 17.85, 13.76.

3) Third step

A suspension of the latter step pyridine ester (3.37 g, 5.8 mmol) in KOH solution (98 mL, 1 M solution) and ethanol (100 mL) was heated to reflux at 80°C until a clear liquid was formed. After solvent was removed under vacuum, the dried residue was mixed with CaO (2 g). After heating in an oven at 340°C for 4 h, the mixture was cooled to room temperature. After extraction using $CHCl_3$, the precipitates were removed by filtration. The filtrate was concentrated and dried. The NMR spectra revealed that this last step was not successful.

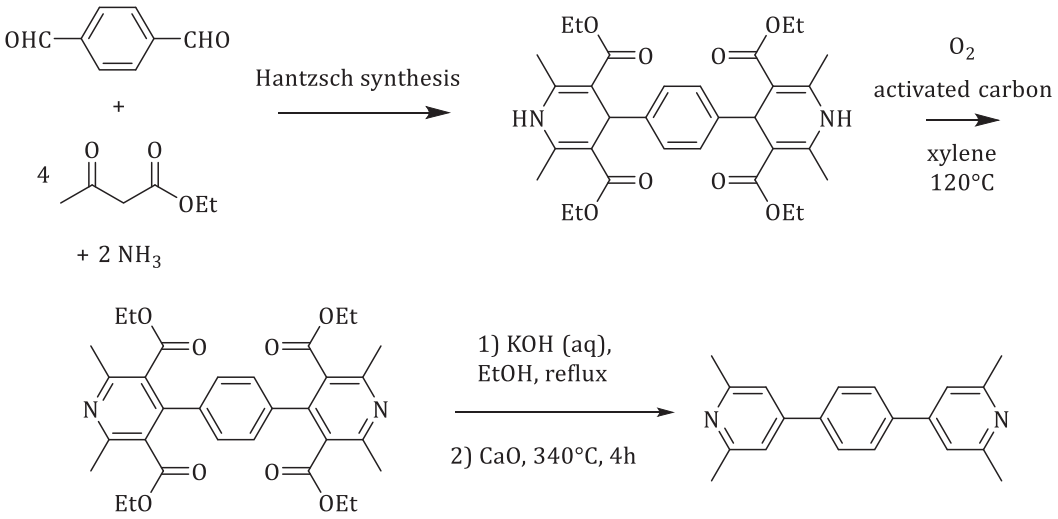

Figure V. 11: Three-step synthesis of the difunctional molecule B2. [7]

NMR spectroscopies:

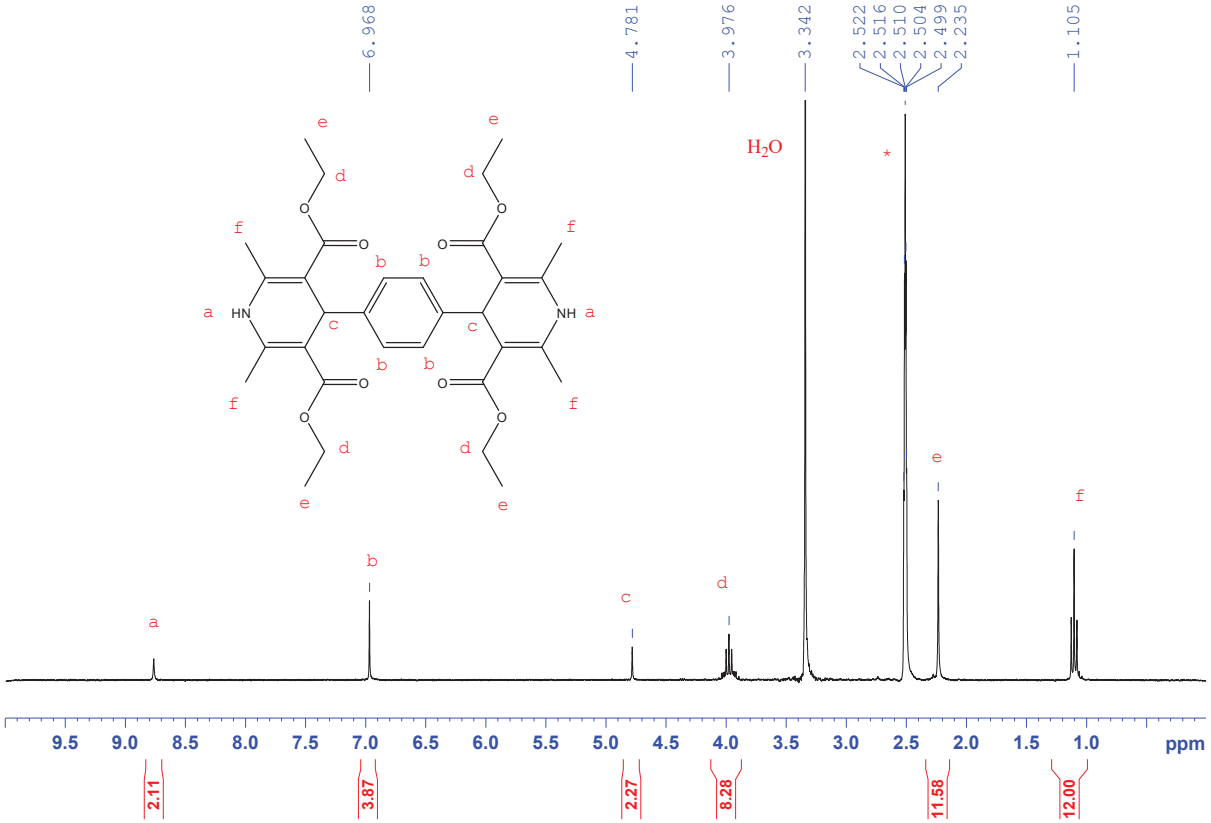

*Figure V. 12: ^{1}H NMR spectrum of the first step product 1,4-dihydropridine in DMSO-d_6. * DMSO-d_6*

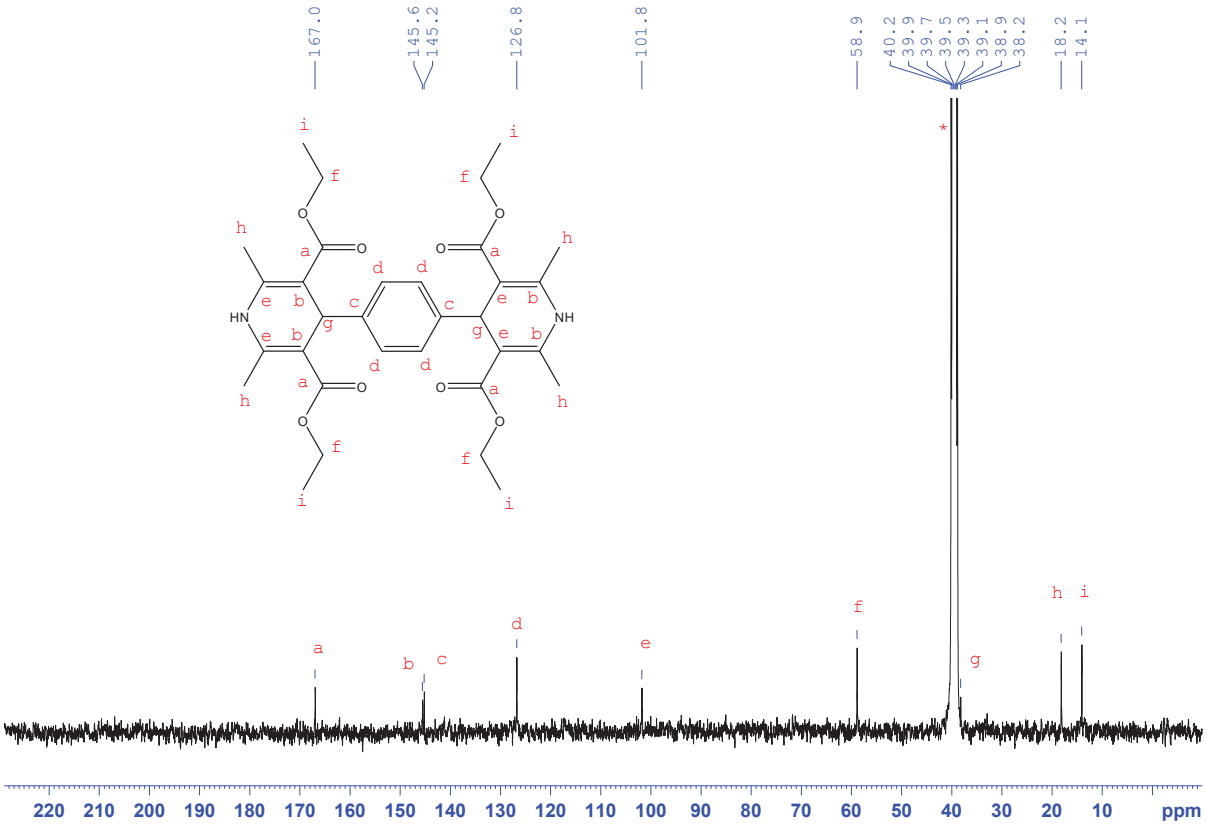

*Figure V. 13: ^{13}C NMR spectrum of the first step product 1,4-dihydropridine in DMSO-d_6. * DMSO-d_6*

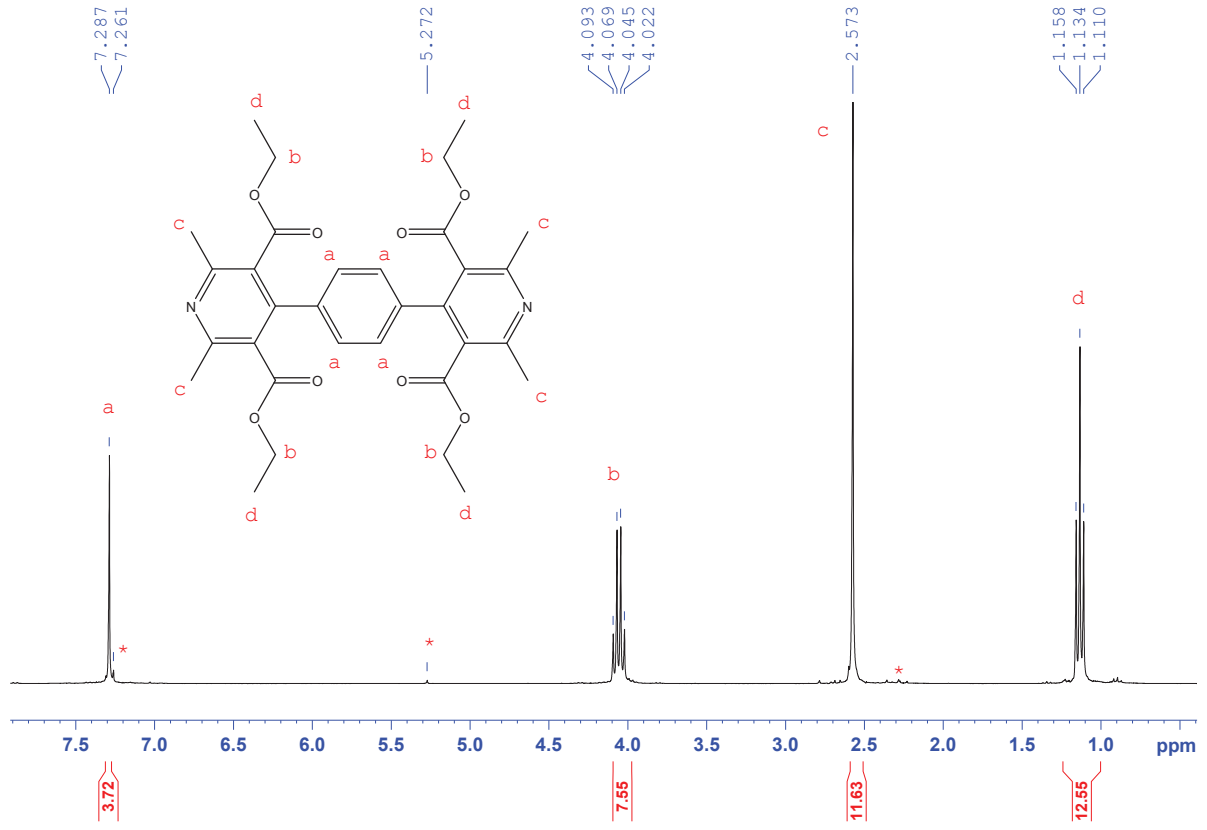

*Figure V. 14: ^{1}H NMR spectrum of the second step product pyridine ester in $CDCl_3$. * $CDCl_3$ and residual solvents*

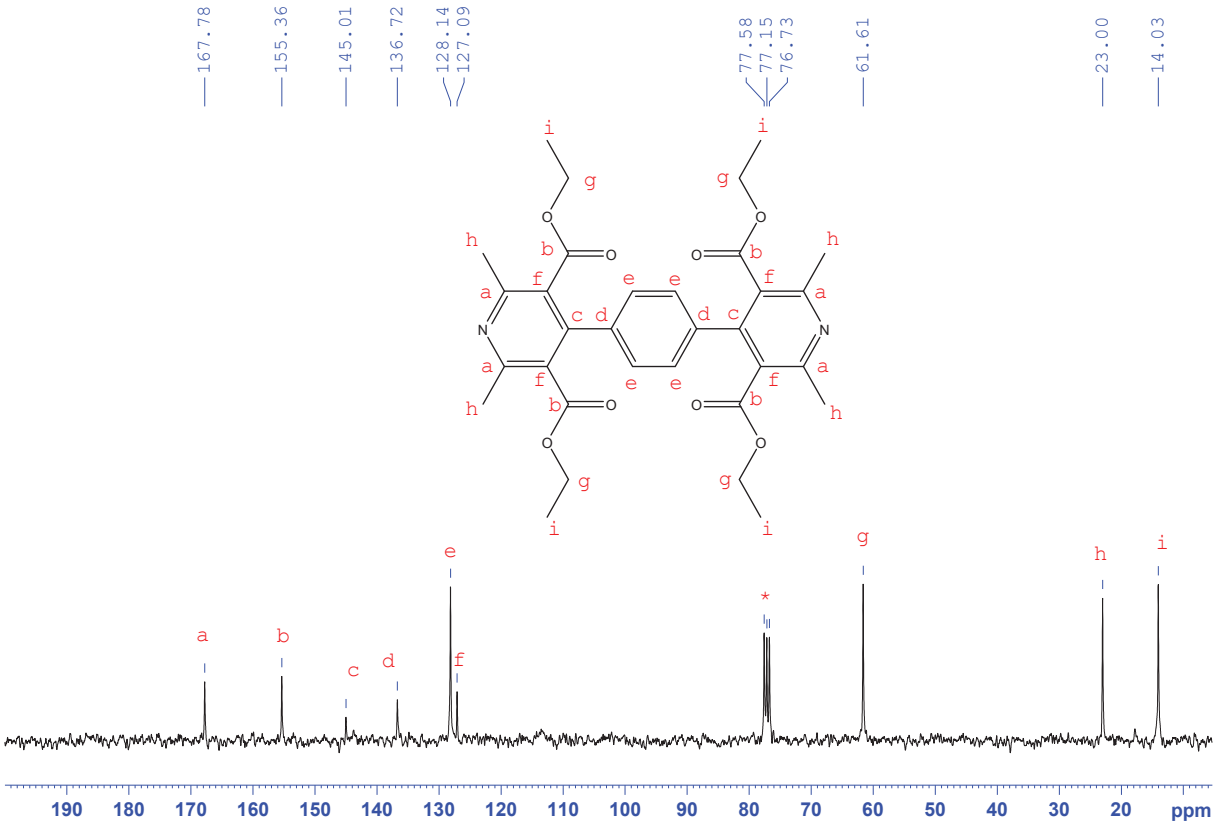

*Figure V. 15: ^{13}C NMR spectrum of the second step product pyridine ester in $CDCl_3$. * $CDCl_3$ and residual solvents*

B. Syntheses of functionalized polymers

a. Synthesis of Lewis acid functionalized polymer (polyA)

Experimental protocol:

1) Synthesis of poly(styrene-*co*-4-vinylboronic acid)

These copolymers will be noted PS-$B(OH)_2$ – x % with x % the molar content of 4-vinylphenylboronic acid.

Representative procedure for PS-$B(OH)_2$ – 40 %

4-vinylphenylboronic acid (2 g, 13.53 mmol) and styrene (1.51 mL, 10.26 mmmol) were dissolved in THF (10 mL) in a Schlenk vessel. The mixture was degassed and benzoyl peroxide (115.29 mg, 0.48 mmol, 2 mol %) was added. The system was closed and the reaction mixture was heated at 70°C for 12 h. The mixture was precipitate into pentane and filtrate to recover a white solid dried under vacuum. Yield: 89 %.

^1H NMR (300 MHz, benzene-d_6, 25°C, δ): 8.01 (2H), 7.02 (2H), 6.74 (2H), 2.09 (1H), 1.21 (12H).

2) Post-functionalization

The same procedure was used than for the post-functionalization of the difunctional molecule.

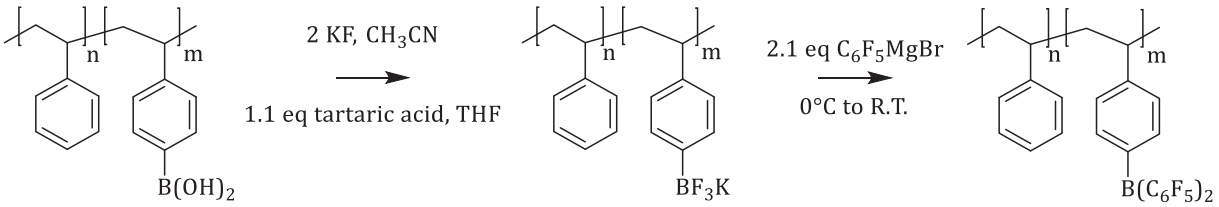

Figure V. 16: Reaction path for the synthesis of poly(A).

a) First step

Yield: 100 %.

^{11}B NMR (300 MHz, DMSO-d6, 25°C, δ): 0.51.

^{19}F NMR (300 MHz, DMSO-d6, 25°C, δ): -138.39.

b) Second step

This step was not successful and we were not able to correctly isolate the final product.

NMR spectroscopies:

PS-B(OH)$_2$ – x % were transformed in PS-BPin – x % to improve solubility in usual solvents.

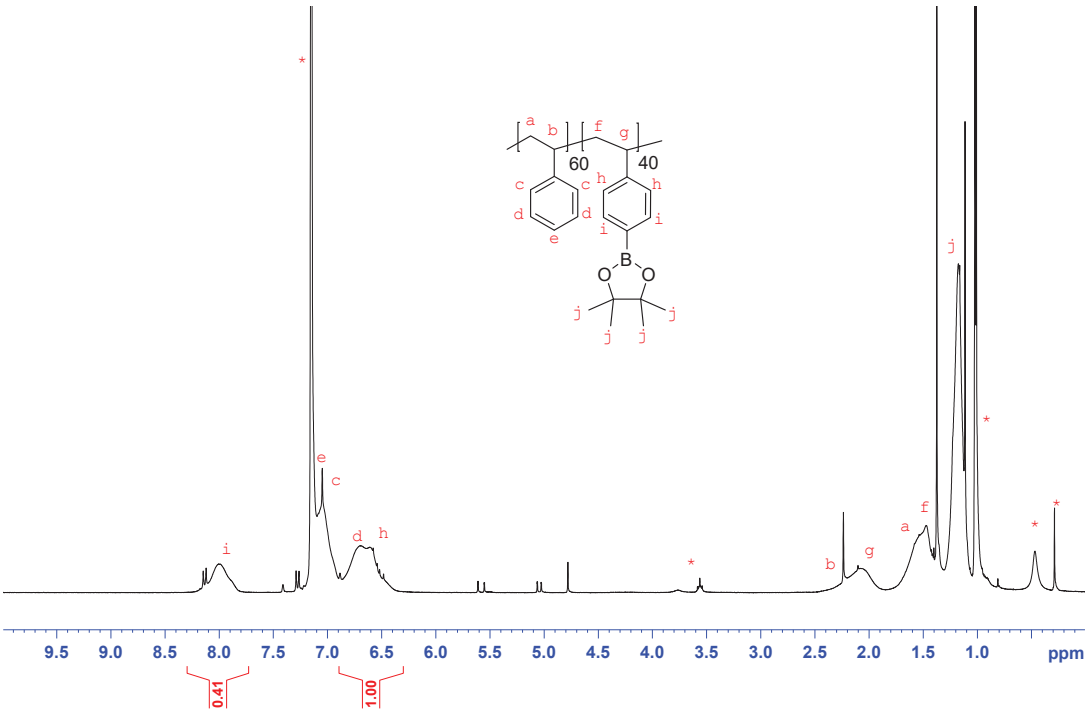

*Figure V. 17: ^{1}H NMR spectrum of poly(4-vinylphenylboronic acid-co-styrene) transformed in poly(4-vinylphenylboronic pinacolate-co-styrene) with 40 % mol of 4-vinylphenylboronic pinacolate in the copolymer in C_6D_6. *C_6D_6 and residual solvents.*

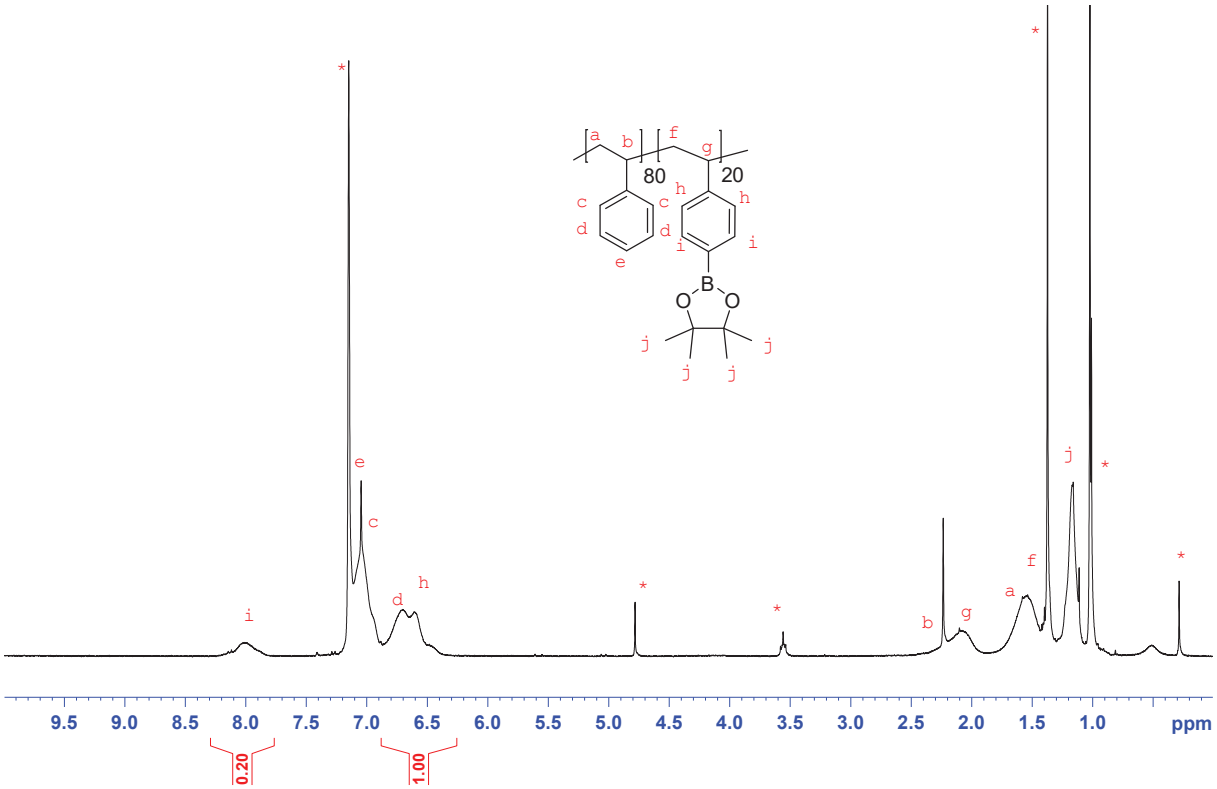

*Figure V. 18: ^{1}H NMR spectrum of poly(4-vinylphenylboronic acid-co-styrene) transformed in poly(4-vinylphenylboronic pinacolate-co-styrene) with 20 % mol of 4-vinylphenylboronic pinacolate in the copolymer in C_6D_6. *C_6D_6 and residual solvents.*

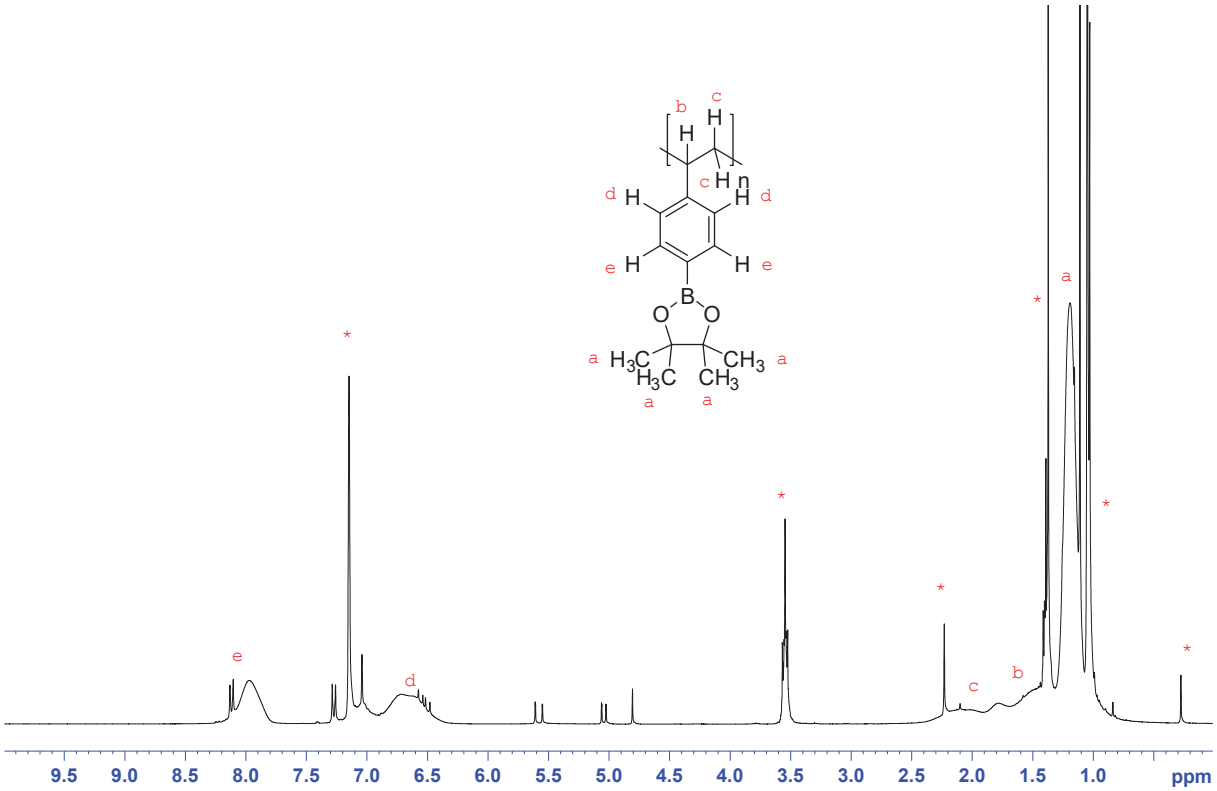

*Figure V. 19: ^{1}H NMR spectrum of poly(4-vinylphenylboronic acid) transformed in poly(4-vinylphenylboronic) in C_6D_6. *C_6D_6 and residual solvents.*

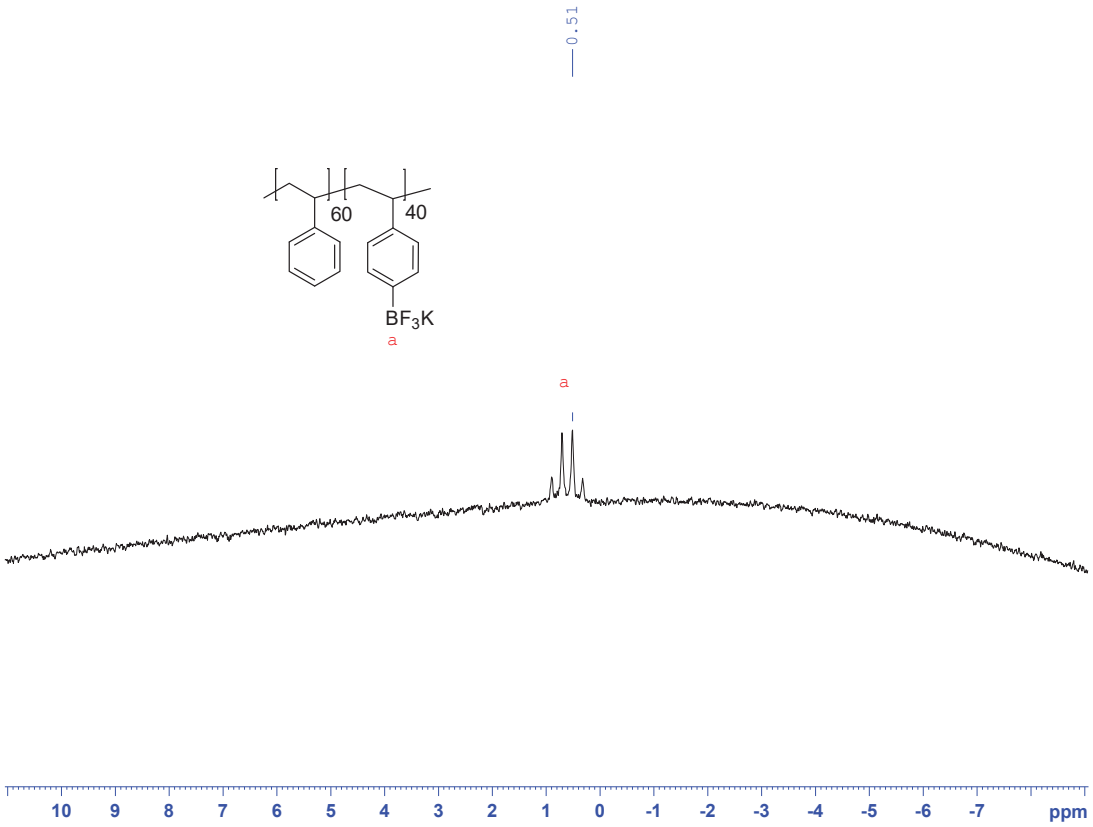

Figure V. 20: ^{11}B NMR spectrum of poly(potassium 4-vinylphenyltrifluoroborate-co-styrene) with 40 % mol of potassium 4-vinylphenyltrifluoroborate in the copolymer in DMSO-d_6.

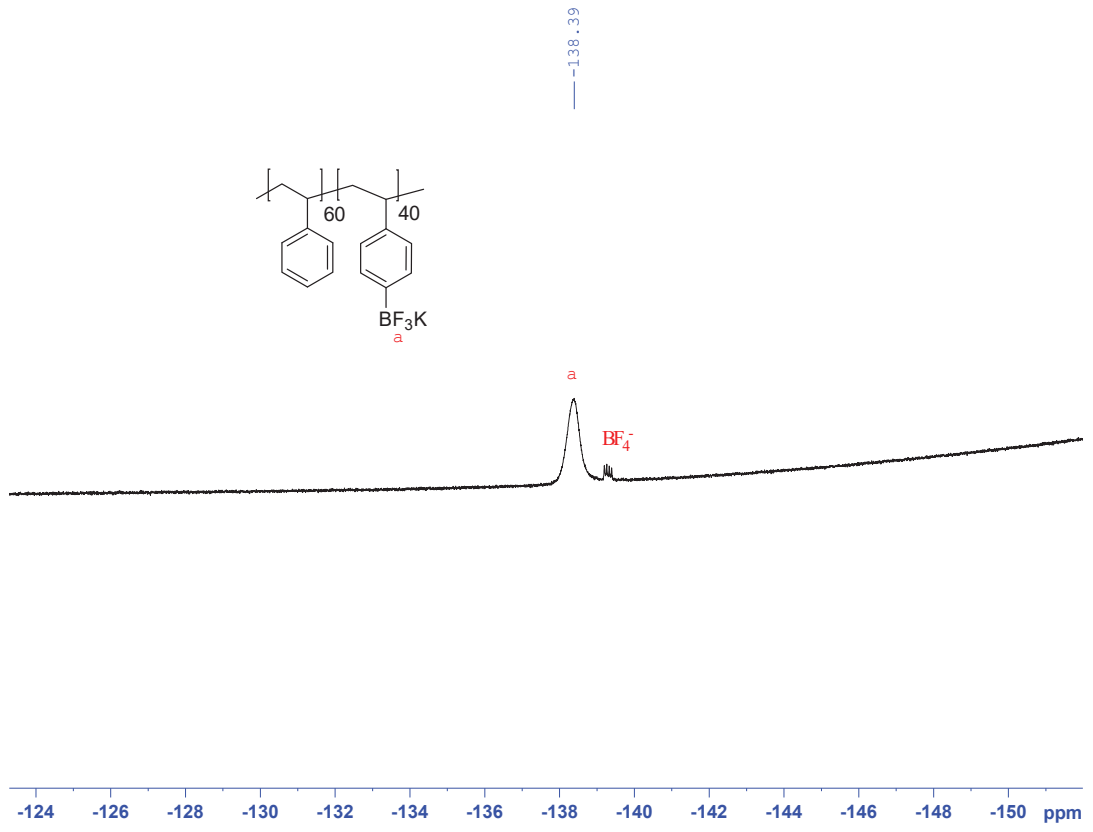

Figure V. 21: ^{19}F NMR spectrum of poly(potassium 4-vinylphenyltrifluoroborate-co-styrene) with 40 % mol of potassium 4-vinylphenyltrifluoroborate in the copolymer in DMSO-d_6.

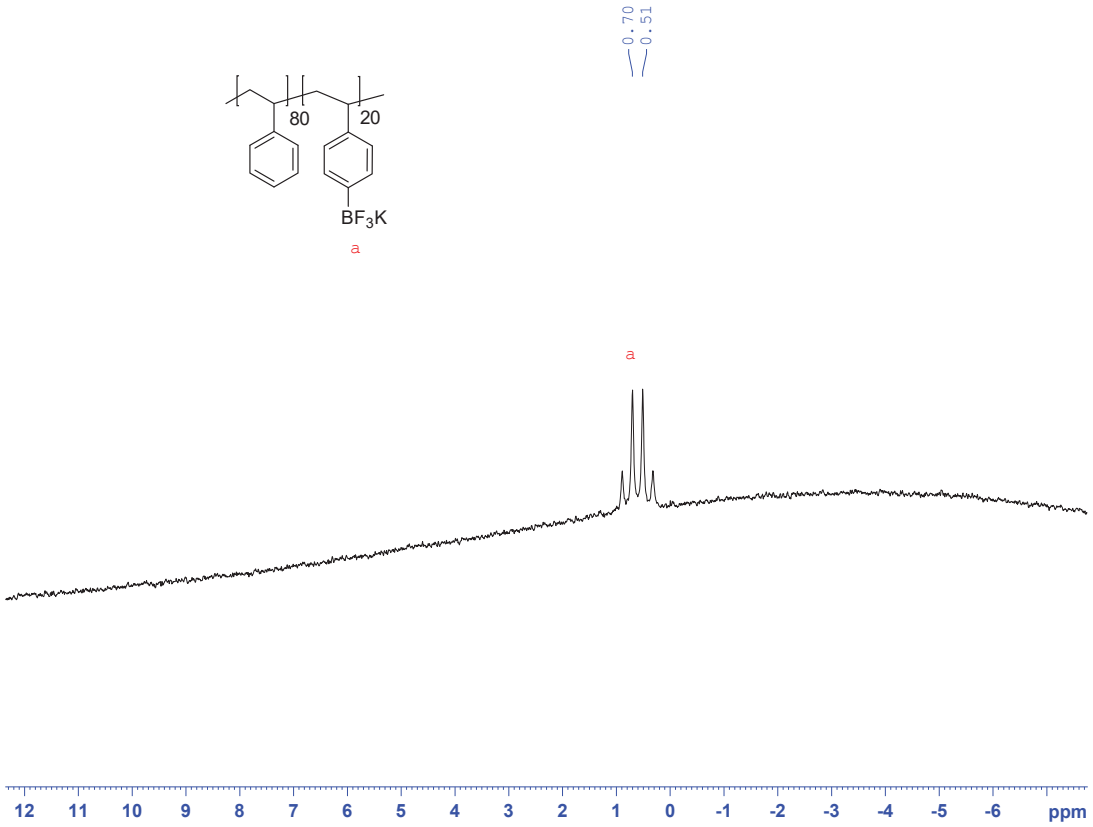

Figure V. 22: ^{11}B NMR spectrum of poly(potassium 4-vinylphenyltrifluoroborate-co-styrene) with 20 % mol of potassium 4-vinylphenyltrifluoroborate in the copolymer in DMSO-d_6.

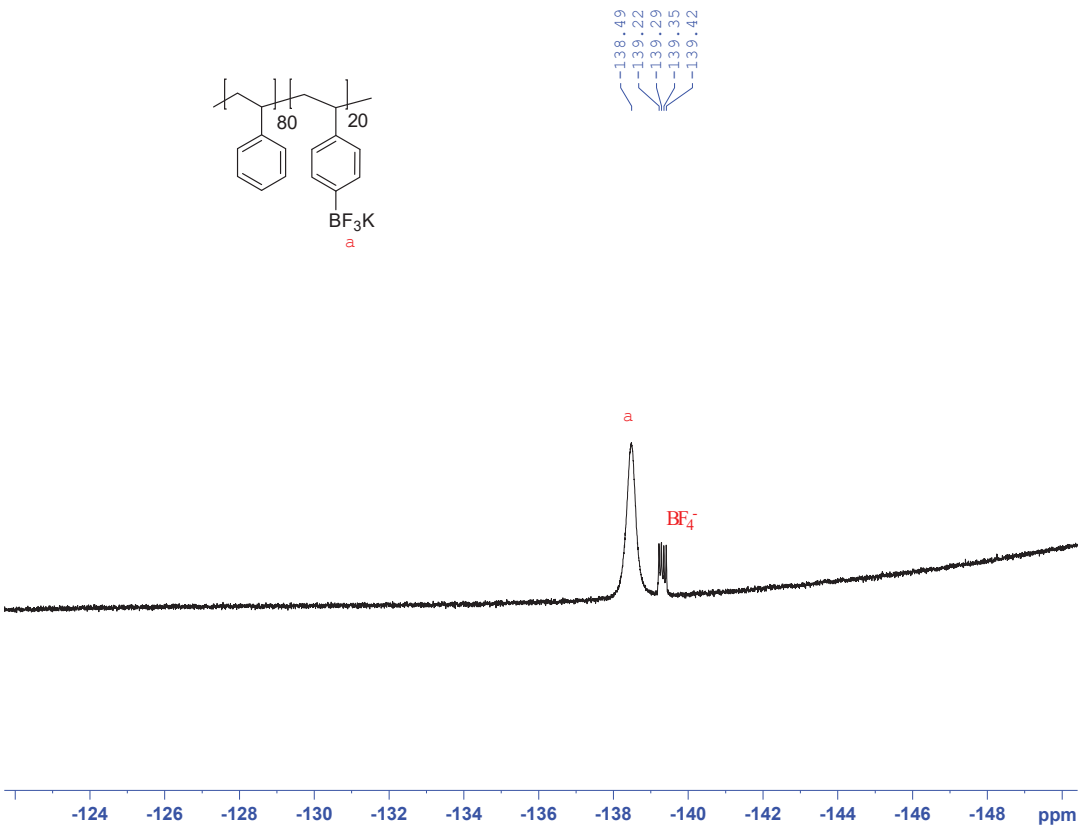

Figure V. 23: ^{19}F NMR spectrum of poly(potassium 4-vinylphenyltrifluoroborate-co-styrene) with 20 % mol of potassium 4-vinylphenyltrifluoroborate in the copolymer in DMSO-d_6.

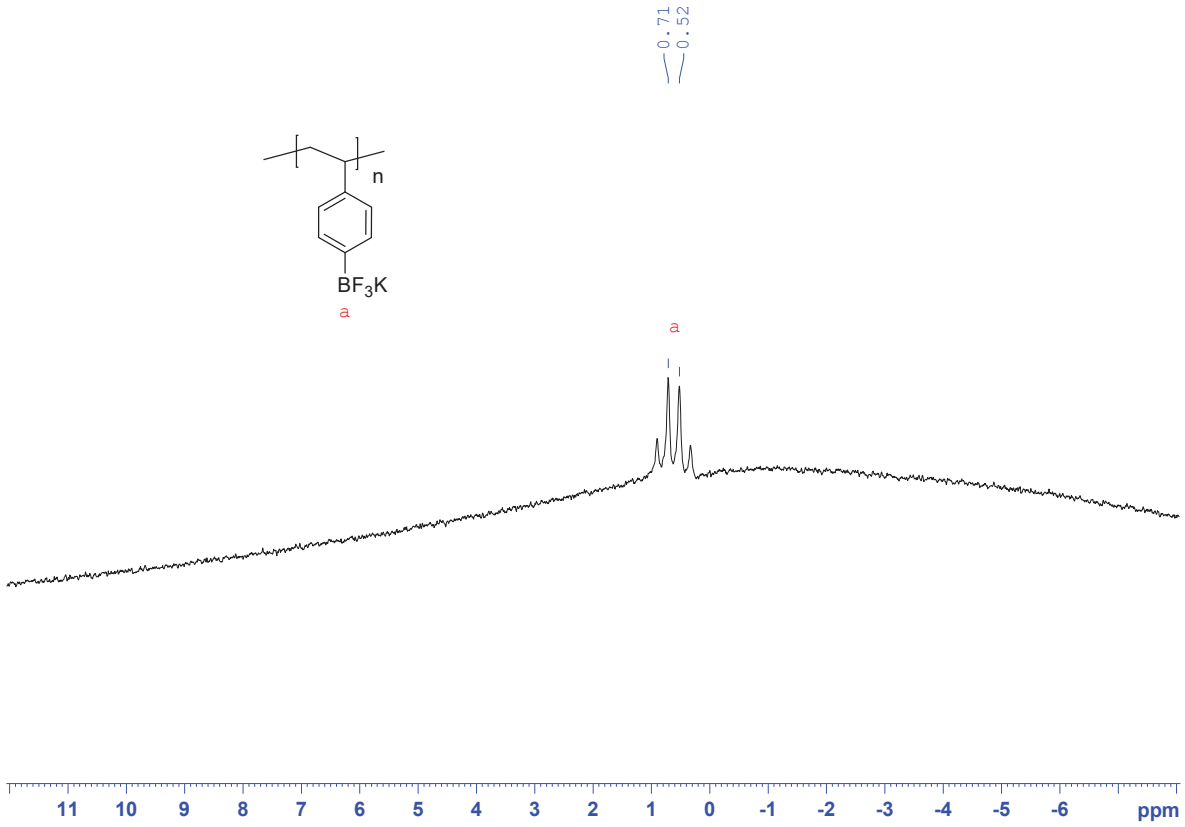

Figure V. 24: ^{11}B NMR spectrum of poly(potassium 4-vinylphenyltrifluoroborate) in DMSO-d_6.

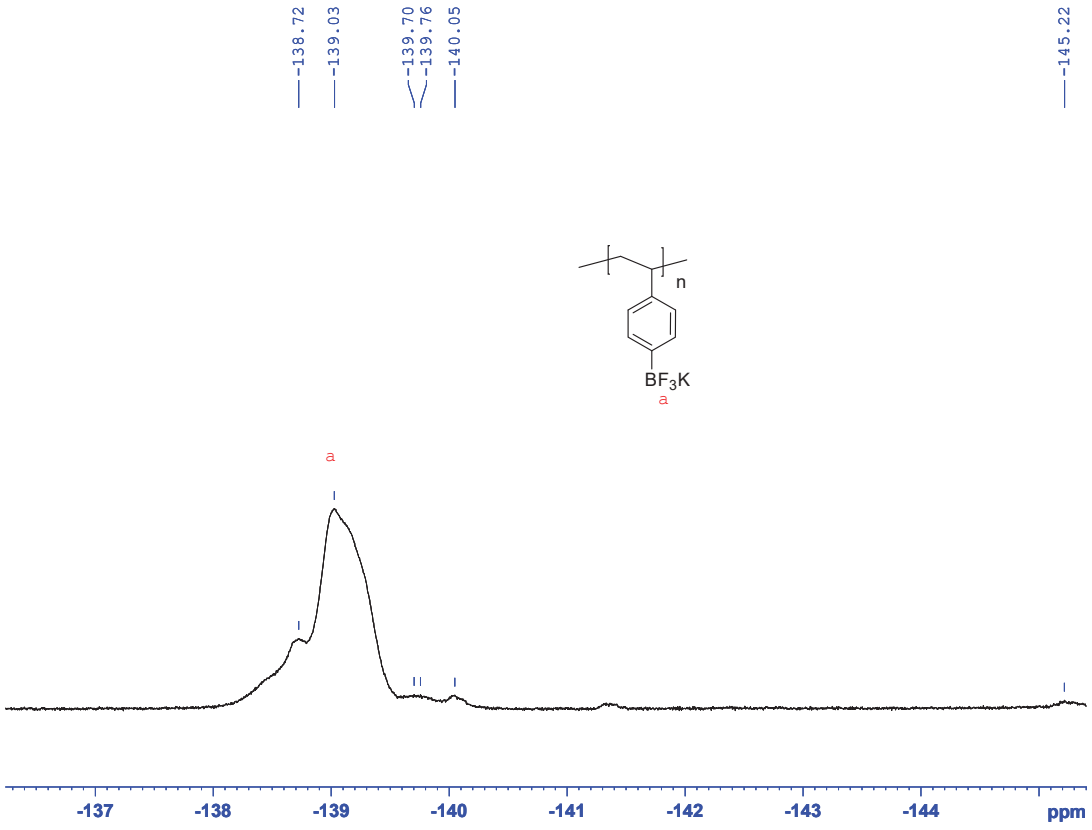

Figure V. 25: ^{19}F NMR spectrum of poly(potassium 4-vinylphenyltrifluoroborate) in DMSO-d_6.

Size-exclusion chromatography in THF:

PS-$B(OH)_2$ – x % were transformed in PS-BPin – x % to improve solubility in usual solvents.

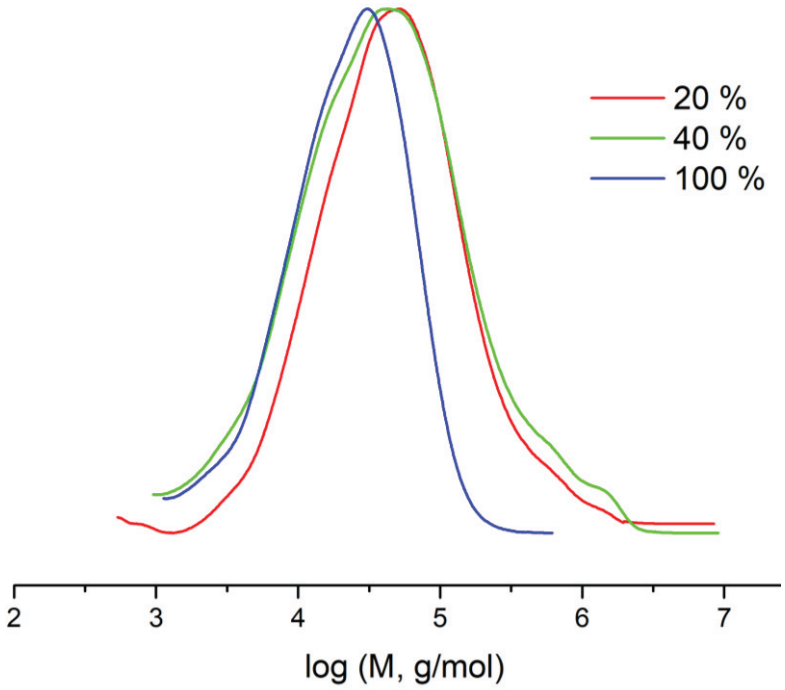

Figure V. 26: Chromatograms of poly(4-vinylphenylboronic acid-co-styrene) for different molar contents of 4-vinylphenylboronic acid.

b. Syntheses of Lewis base functionalized polymers (polyB)

i. Polymers functionalized by phosphine groups

Firstly, we got interested in the copolymerization of styrene with 4-styryldiphenylphosphine relying on the work of Choi *et al.* [8] The copolymer synthesized will be noted PS-PPh_2 – x % with x % the molar content of 4-styryldiphenylphosphine.

Experimental protocol:

Representative procedure for PS-PPh_2 – 50 %:

To a solution of styrene (0.55 mL, 5 mmol) and 4-styryldiphenylphosphine (1.44 g, 5 mmol) in toluene (5 mL) was added AIBN (32.84 mg, 0.2 mmol, 2 mol %). The mixture was purged with N2 for 30 min, and the solution was stirred at 70-90 °C for 24 h. The solution was concentrated in vacuo, and the residue was taken up in 10 mL of THF. This solution was added dropwise to a vigorously stirred cold methanol (0 °C, 200 mL). The white precipitate was filtered and dried to afford a white powder. Yield: 1.57 g, 81 %.

^{1}H NMR (300 MHz, benzene-d_6, 25°C, δ): 7.43 (2H), 7.28-7.09 (8H), 6.84-6.14 (9H), 2.50-1.82 (2H), 1.82-1.17 (2H).

^{31}P NMR (400 MHz, benzene-d_6, 25°C, δ): -6.13.

^{13}C NMR (400 MHz, benzene-d_6, 25°C, δ): 138.13, 134.73, 133.92, 133.74, 132.18, 132.09, 131.29, 128.52, 128.19, 125.87, 46.46, 44.42, 42.78, 40.68.

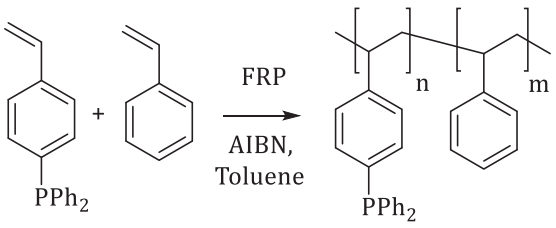

Figure V. 27: Copolymerization of styrene and 4-styryldiphenylphosphine.

NMR spectroscopies:

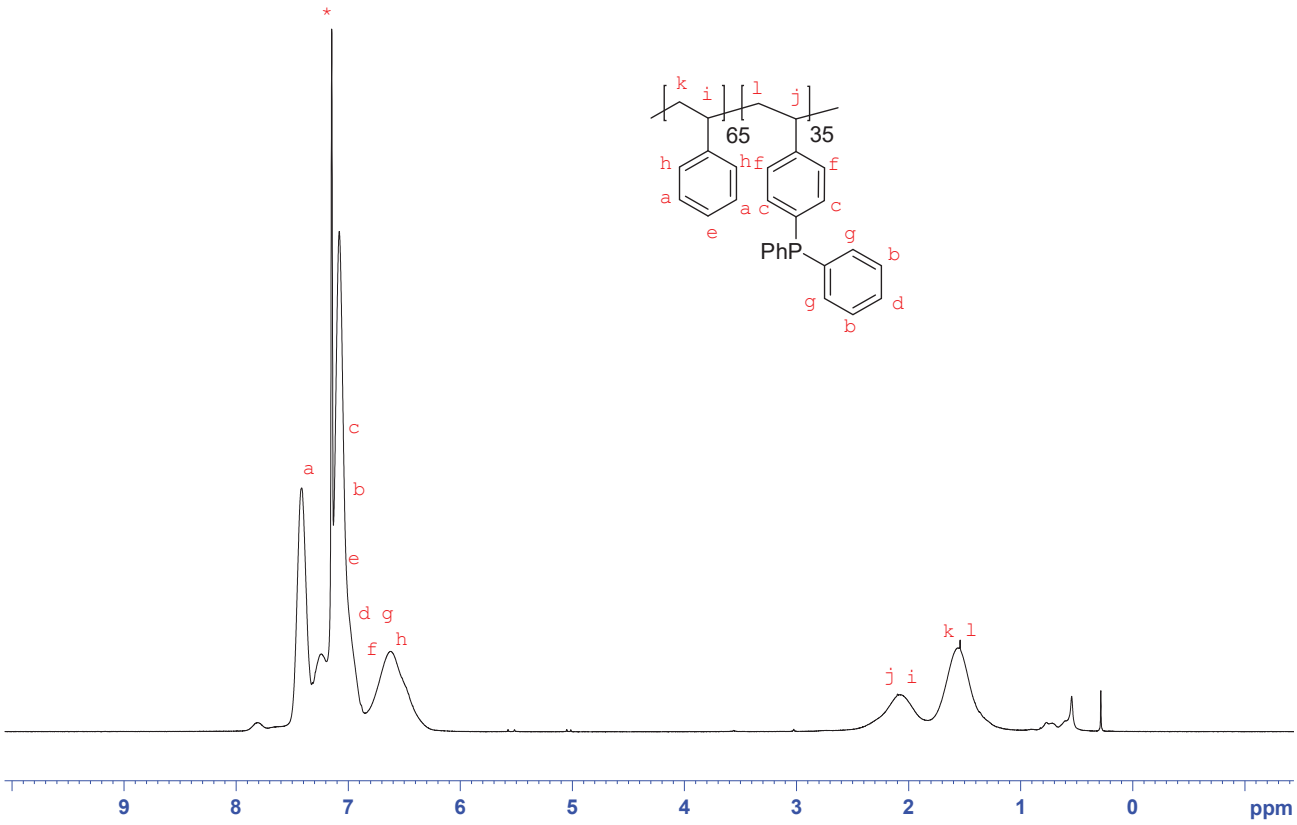

Figure V. 28: ^{1}H NMR spectrum of poly(4-styryldiphenylphosphine-co-styrene) with 35 % mol of potassium 4-styryldiphenylphosphine in the copolymer in C_6D_6.C_6D_6*

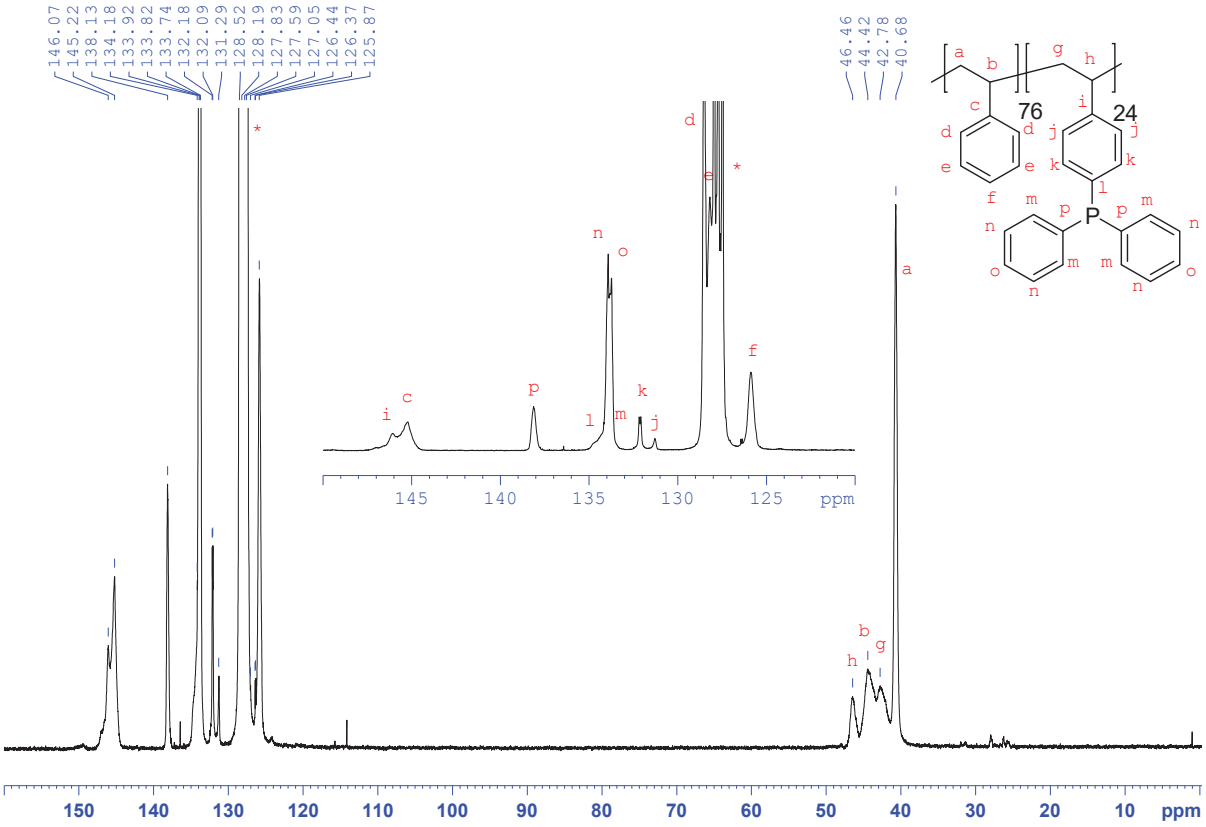

Figure V. 29: ^{13}C NMR spectrum of poly(4-styryldiphenylphosphine-co-styrene) with 24 % mol of potassium 4-styryldiphenylphosphine in the copolymer in C_6D_6.C_6D_6*

Figure V. 30: ^{31}P NMR spectrum of poly(4-styryldiphenylphosphine-co-styrene) with 35 % mol of 4-styryldiphenylphosphine in the copolymer in C_6D_6.

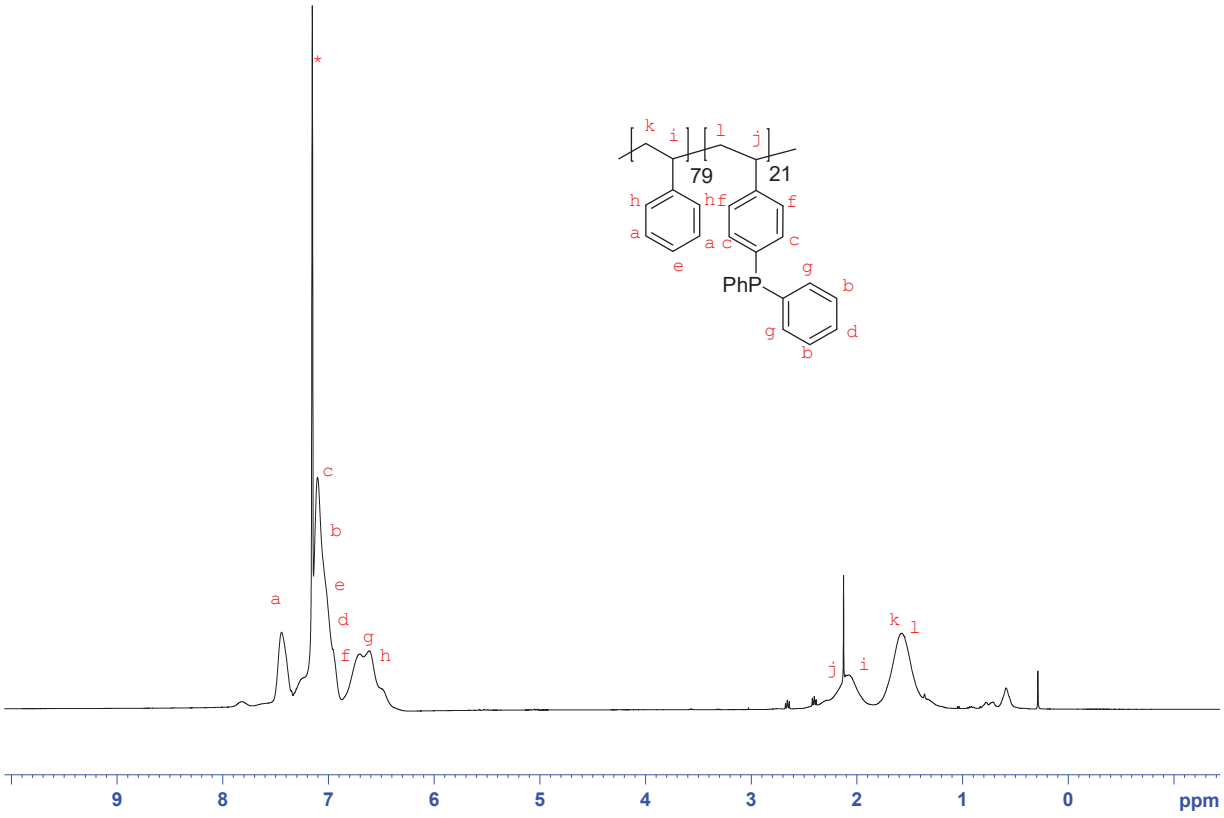

Figure V. 31: ^{1}H NMR spectrum of poly(4-styryldiphenylphosphine-co-styrene) with 21 % mol of 4-styryldiphenylphosphine in the copolymer in C_6D_6.C_6D_6*

Figure V. 32: ^{31}P NMR spectrum of poly(4-styryldiphenylphosphine-co-styrene) with 21 % mol of 4-styryldiphenylphosphine in the copolymer in C_6D_6.C_6D_6*

Size-exclusion chromatography in THF:

To avoid affinity with the chromatography columns, drops of BH_3-THF were added before analysis.

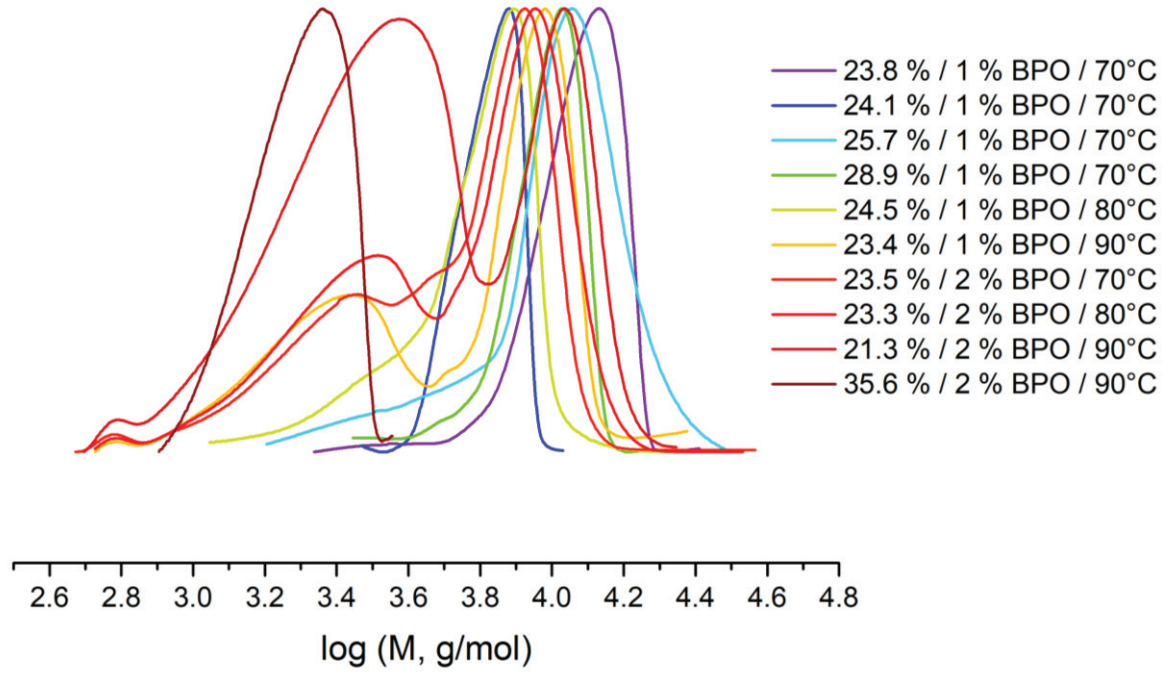

Figure V. 33: Chromatograms of series of poly(4-styryldiphenylphosphine-co-styrene)s with different composition and different polymerization parameters. For each chromatogram, the molar content of 4-styryldiphenylphosphine, the amount of benzoyl peroxide added (BPO) and the polymerization temperature are indicated.

ii. Polymer functionalized by pyridine groups

Experimental protocol:

4-vinylpyridine (2 g, 19 mmol) and styrene (8.83 mL, 80 mmmol) were dissolved in toluene (12 mL) in a Schlenk vessel. The mixture was degassed and benzoyl peroxide (232 mg, 1 mmol, 1 mol %) was added. The system was closed and the reaction mixture was heated at 70°C for 12 h. The mixture was precipitate into pentane and filtrate to recover a white solid dried under vacuum. Yield: 9.5 g, 95 %.

^{1}H NMR (300 MHz, benzene-d_6, 25°C, δ): 8.43 (2H), 6.7 (2H), 6.61 (1H), 6.36 (2H), 6.29 (2H), 1.9 (1H), 1.88 (1H), 1.54 (1H), 1.45 (1H).

^{13}C NMR (400 MHz, $CDCl_3$, 25°C, δ): 153.99, 148.56, 145.15, 128.29, 127.64, 125.96, 123.12, 45.84-43.18, 40.48, 29.85.

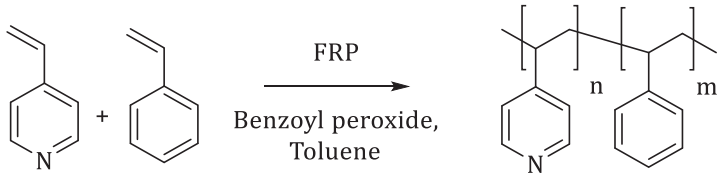

Figure V. 34: Copolymerization of styrene and 4-vinylpyridine.

NMR spectroscopies:

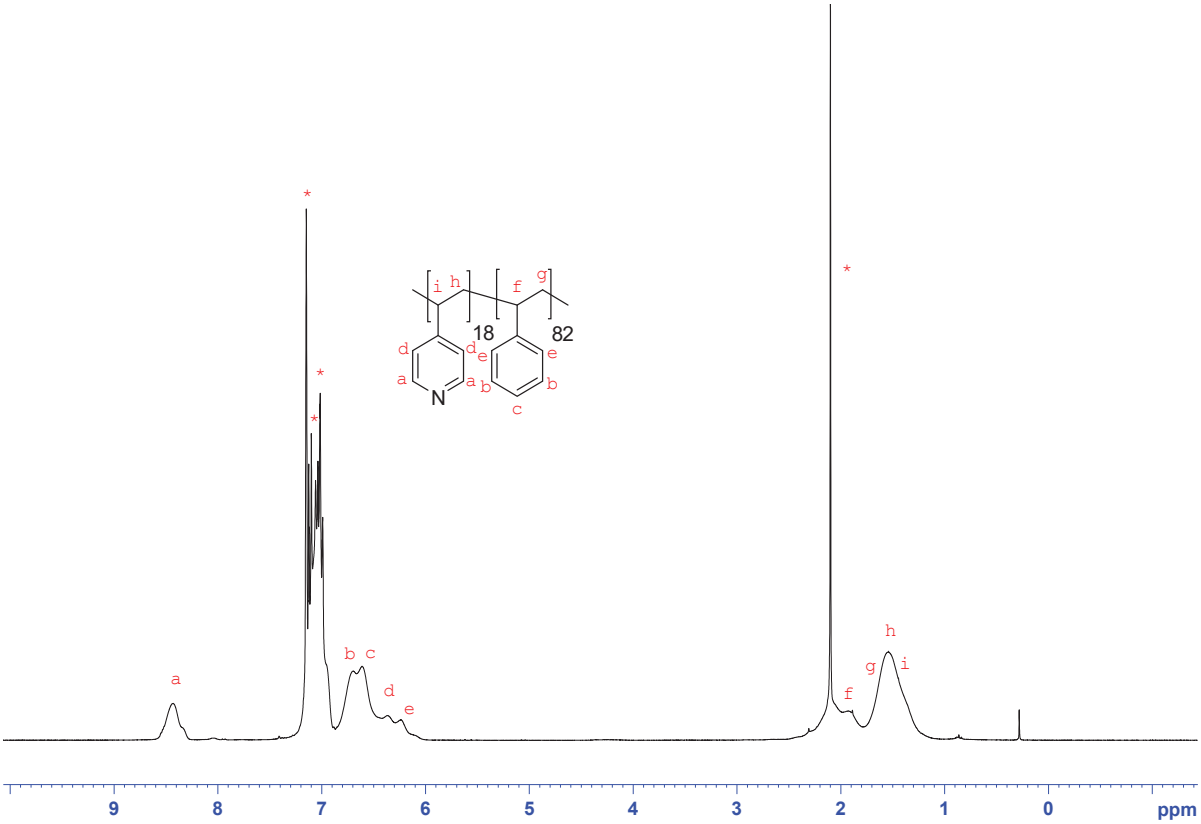

Figure V. 35: ^1H NMR spectrum of poly(4-vinylpyridine-co-styrene) with 18 % mol of 4-vinylpyridine in the copolymer in in C_6D_6.C_6D_6 and residual solvents.*

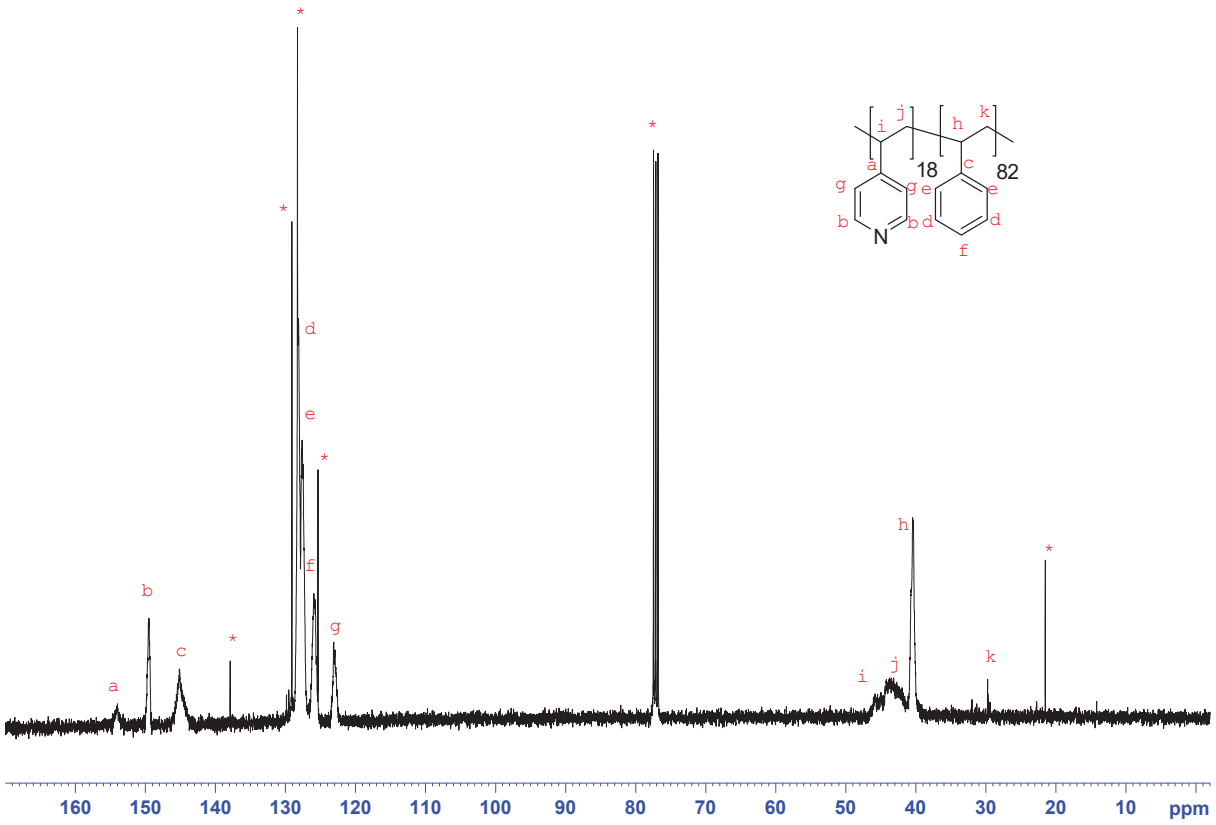

Figure V. 36: ^{13}C NMR spectrum of poly(4-vinylpyridine-co-styrene) with 18 % mol of 4-vinylpyridine in the copolymer in in $CDCl_3$.$CDCl_3$ and residual solvents.*

Size-exclusion chromatography in THF:

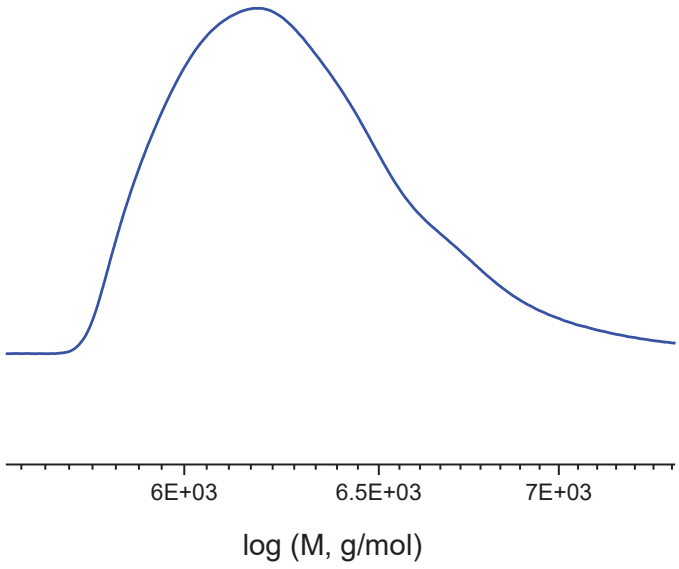

Figure V. 37: Chromatogram of poly(4-vinylpyridine-co-styrene) with 18 % mol of 4-vinylpyridine. (M_n=22 500 g/mol, M_w=39 400 g/mol), Đ=1.8)

III. Dynamic organoboron polymers harnessing the reactivity of boronate esters

A. Synthesis and characterization of monomer 4-vinylphenylboronic pinacolate

Experimental protocol:

4-vinylphenylboronic acid (10 g, 67.6 mmol) and pinacol (8.03 g, 68.0 mmol) as well as 0.05 mL distilled water were stirred in THF (100 mL) at room temperature for 30 min. Then 2 g of anhydrous magnesium sulfate were added to the solution and stirred at room temperature for 2 h. The mixture was filtered and volatiles were removed under vacuum to yield a clear yellow oil. Yield: 14.7 g, 95%.

^{1}H NMR (300 MHz, benzene-d_6, 25°C, δ) : 8.07 (d, J=15.6 Hz, 2H), 7.27 (d, J=8,0 Hz, 2H), 6.32 (dd, J=17.6 Hz, 1H), 5.60 (d, J=17,5 Hz, 1H), 5.04 (d, J=10,8 Hz, 1H), 1.11 (s, 12H, 3H).

^{13}C NMR (300 MHz, benzene-d_6, 25°C, δ): 140.5, 137.1, 135.6, 125.5, 83.61, 24.8.

^{11}B NMR (300 MHz, benzene-d_6, 25°C, δ): 31.3.

NMR spectroscopies:

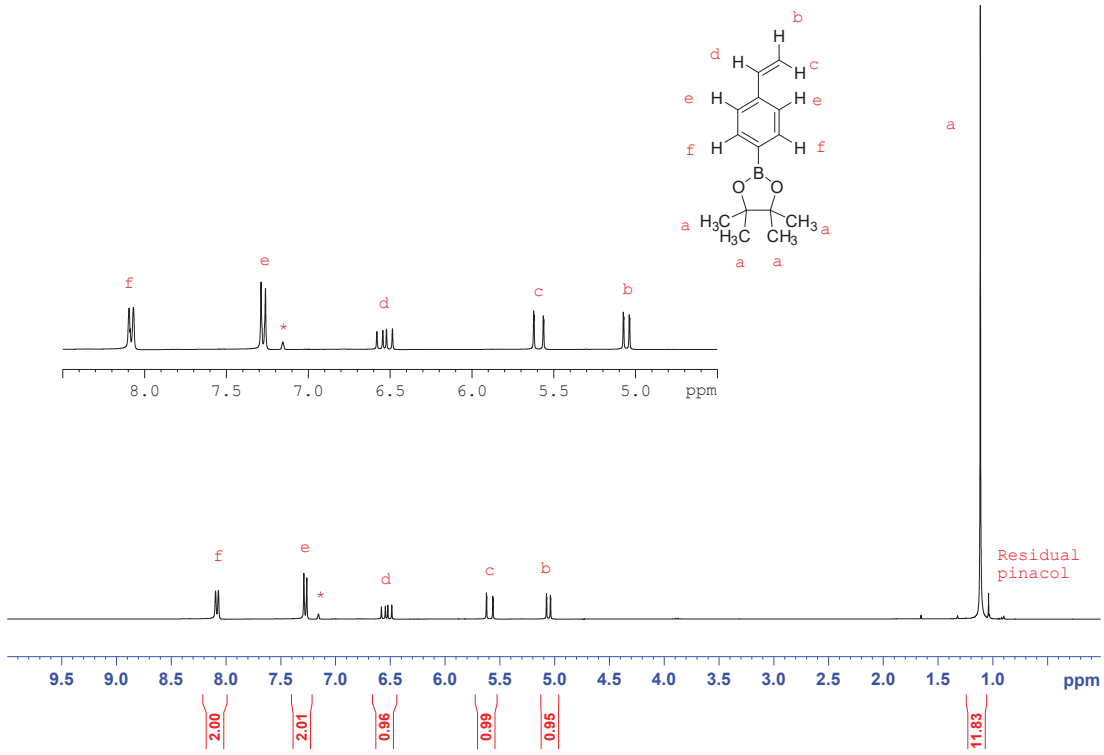

*Figure V. 38: ^{1}H NMR spectrum of the monomer 4-vinylphenylboronic pinacolate in C_6D_6. *C_6D_6*

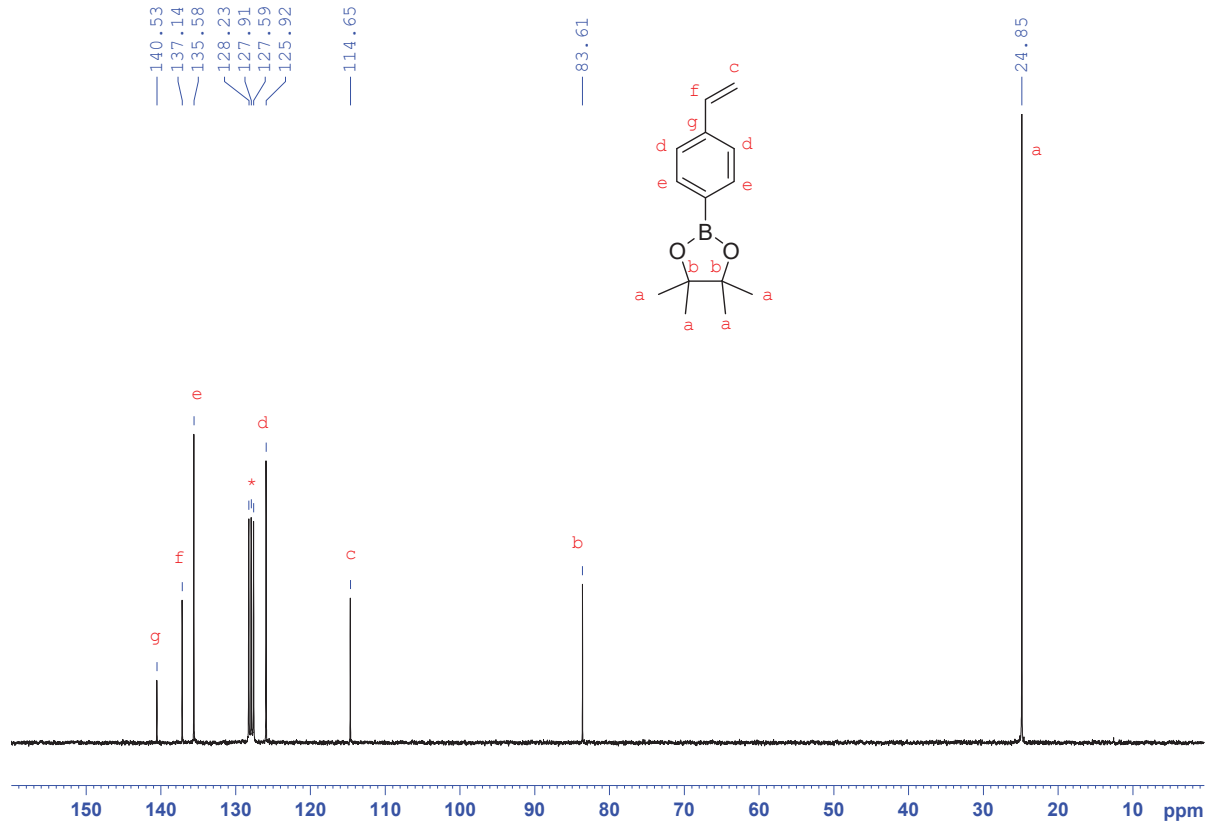

*Figure V. 39: ^{13}C NMR spectrum of the monomer 4-vinylphenylboronic pinacolate in C_6D_6. *C_6D_6*

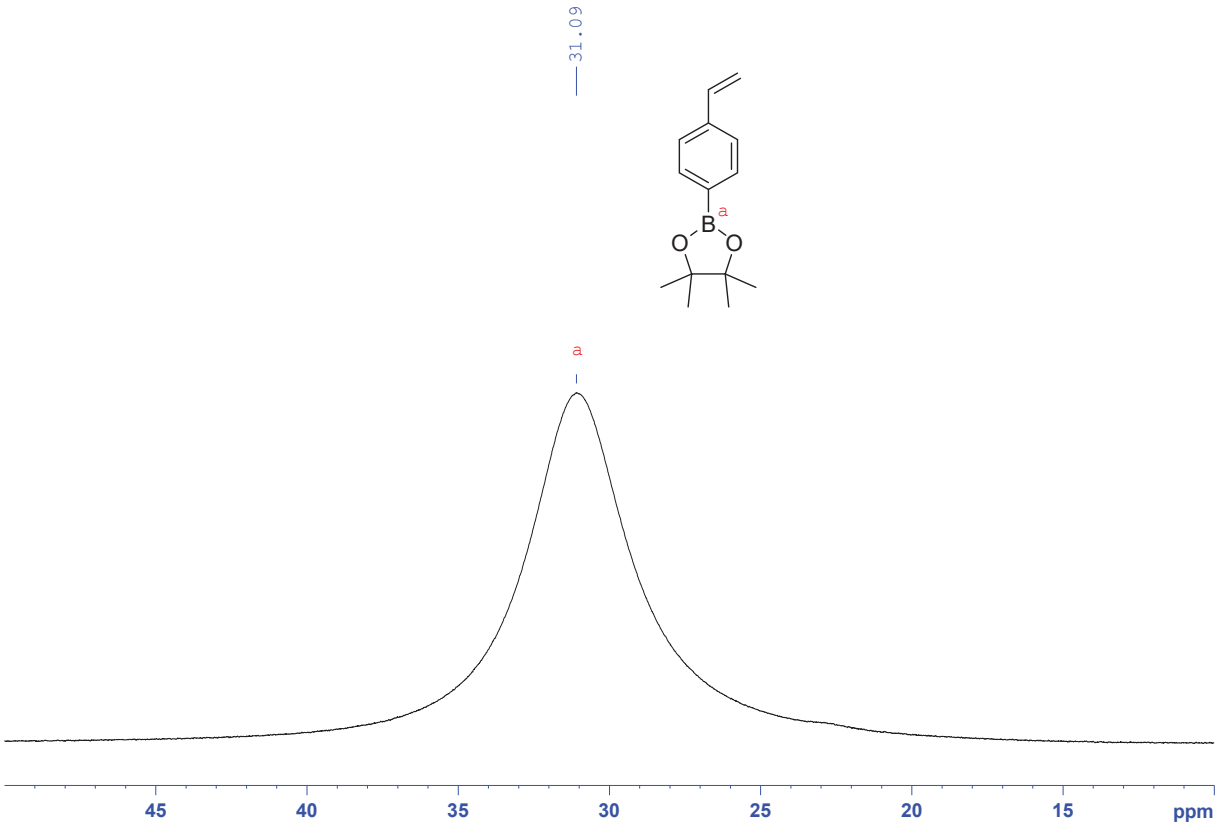

Figure V. 40: ^{11}B NMR spectrum of 4-vinylphenylboronic pinacolate in C_6D_6.

B. Synthesis and characterization of poly(4-vinylphenylboronic pinacolate) PSBPin

Experimental protocol:

4-vinylphenylboronic pinacolate (3.8 g, 16 mmol) and benzoyl peroxide (0.02 eq, 0.33 mmol, 80 mg) were introduced in a Schlenk vessel with 3.8 mL toluene (degassed by three freeze-pump-thawing cycles). The polymerization was conducted at 70°C during 72 h. Then, the reaction media was precipitated in pentane and the solid was obtained by filtration and dried under vacuum for one night. The polymer was obtained as a white powder. Yield: 87%.

^{1}H NMR (300 MHz, benzene-d_6, 25°C, δ): 8.01 (2H), 7.02 (2H), 6.74 (2H), 2.09 (1H), 1.21 (12H).

^{13}C NMR (400 MHz, benzene-d_6, 25°C, δ): 149, 135.3, 126.5, 83.0, 46.1, 41.2, 24.7.

^{11}B NMR (300 MHz, benzene-d_6, 25°C, δ): 31.3.

NMR spectroscopies:

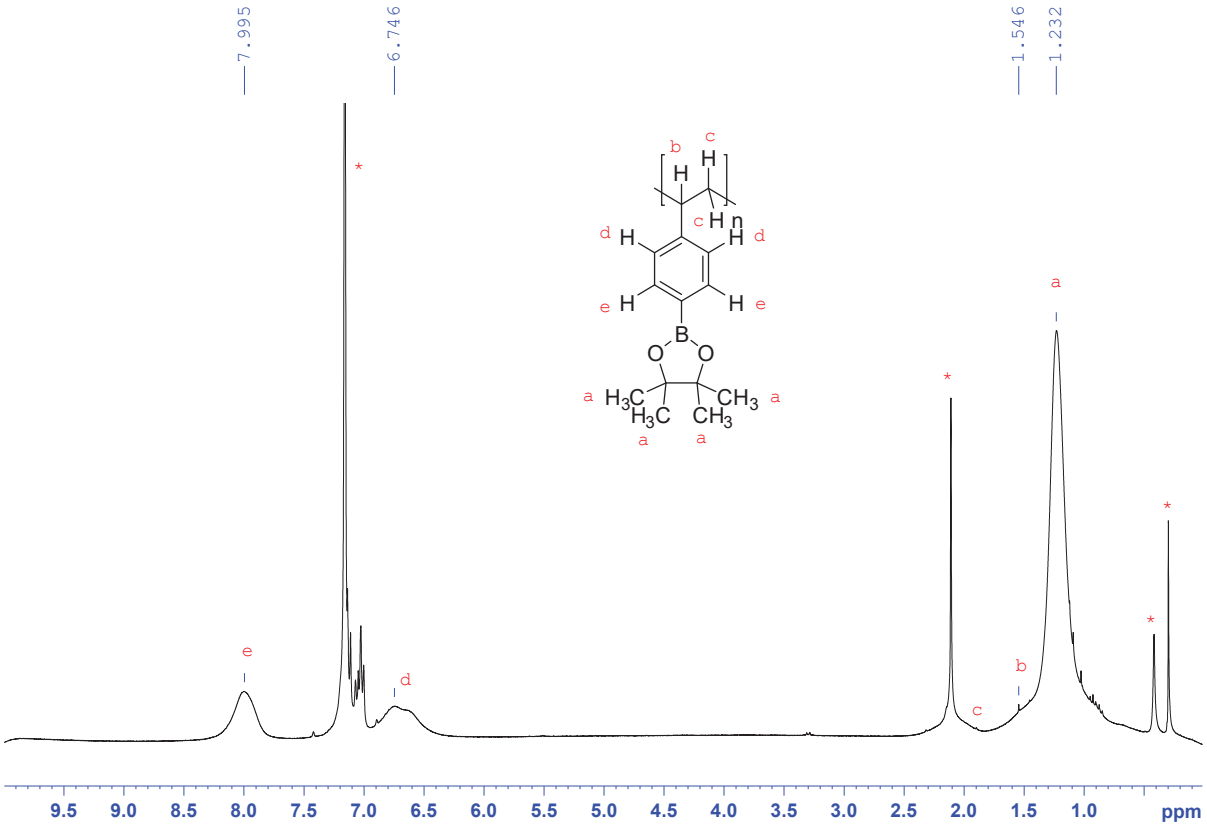

*Figure V. 41: ^{1}H NMR spectrum of poly(4-vinylphenylboronic pinacolate) in C_6D_6. *C_6D_6 and residual solvents.*

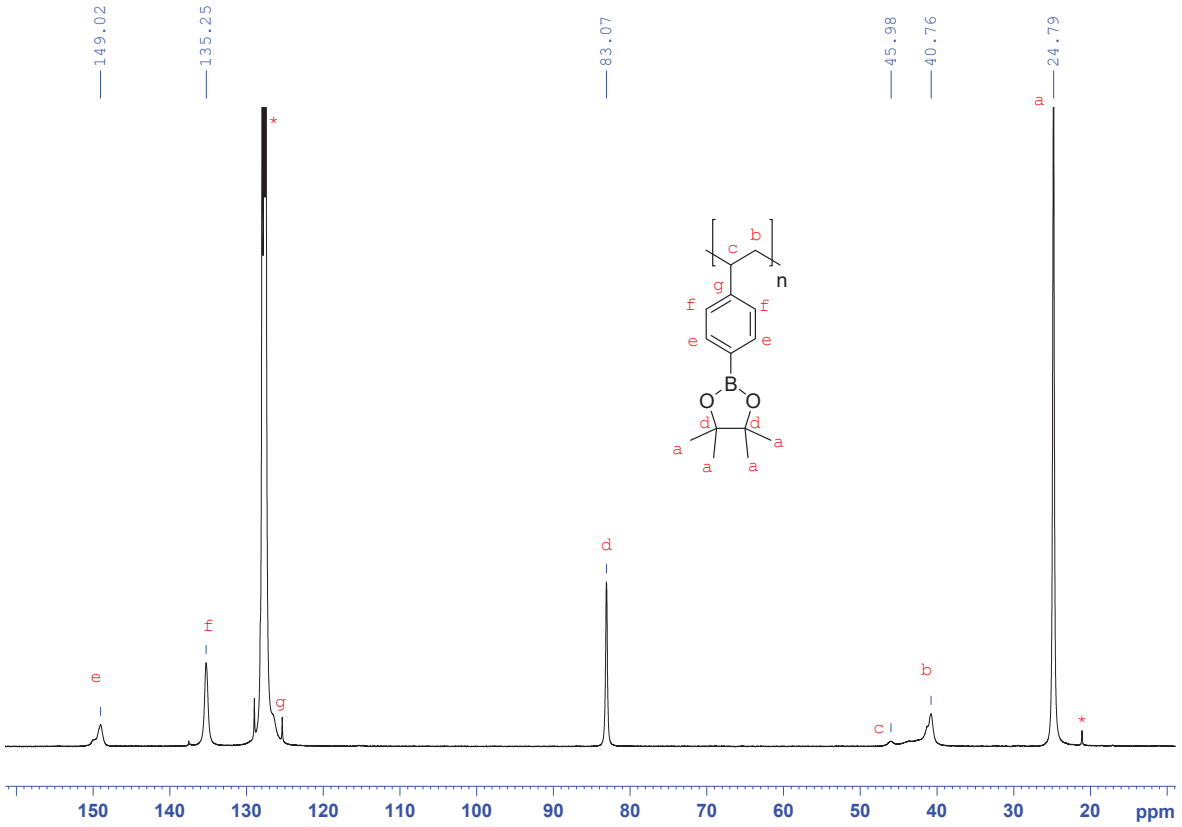

*Figure V. 42: ^{13}C NMR of poly(4-vinylphenylboronic pinacolate) in C_6D_6. *C_6D_6 and residual solvents.*

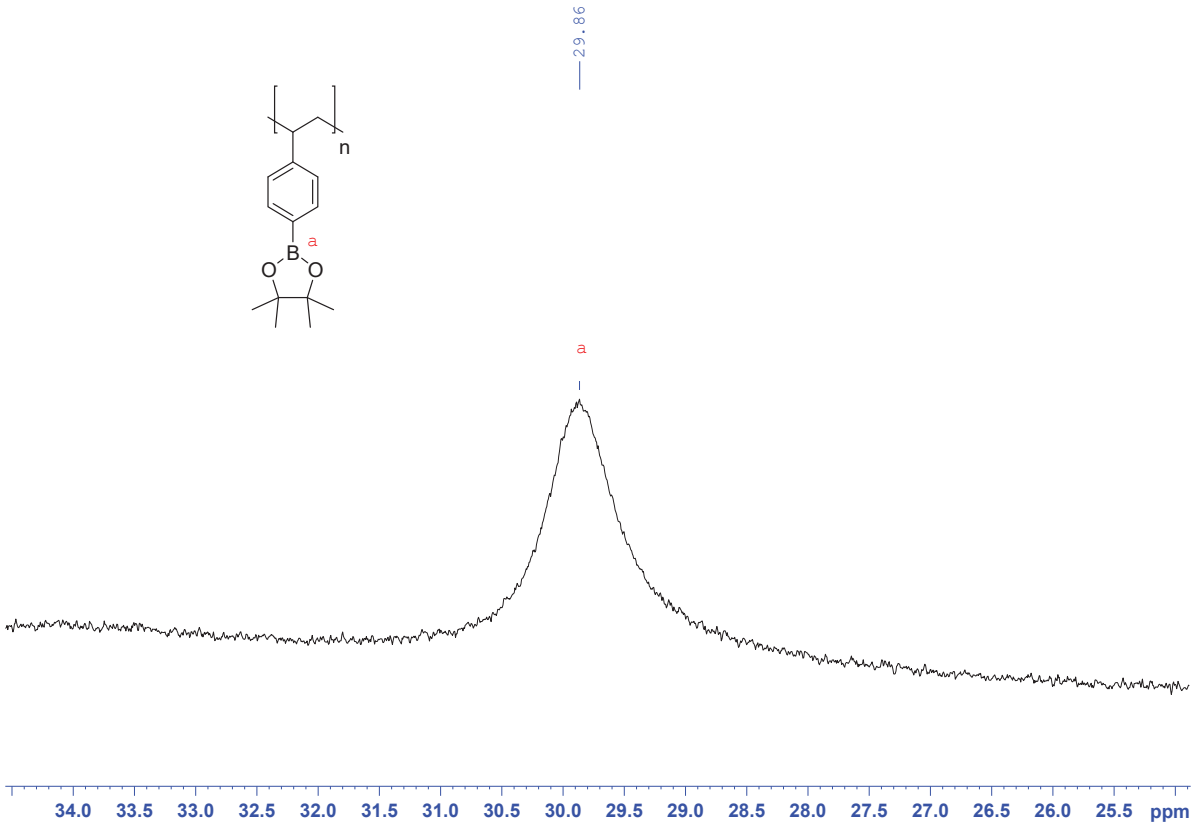

Figure V. 43: ^{11}B NMR spectrum of poly(4-vinylphenylboronic pinacolate) in C_6D_6.

Monitoring of polymerization by ^{1}H NMR spectroscopy and SEC-THF:

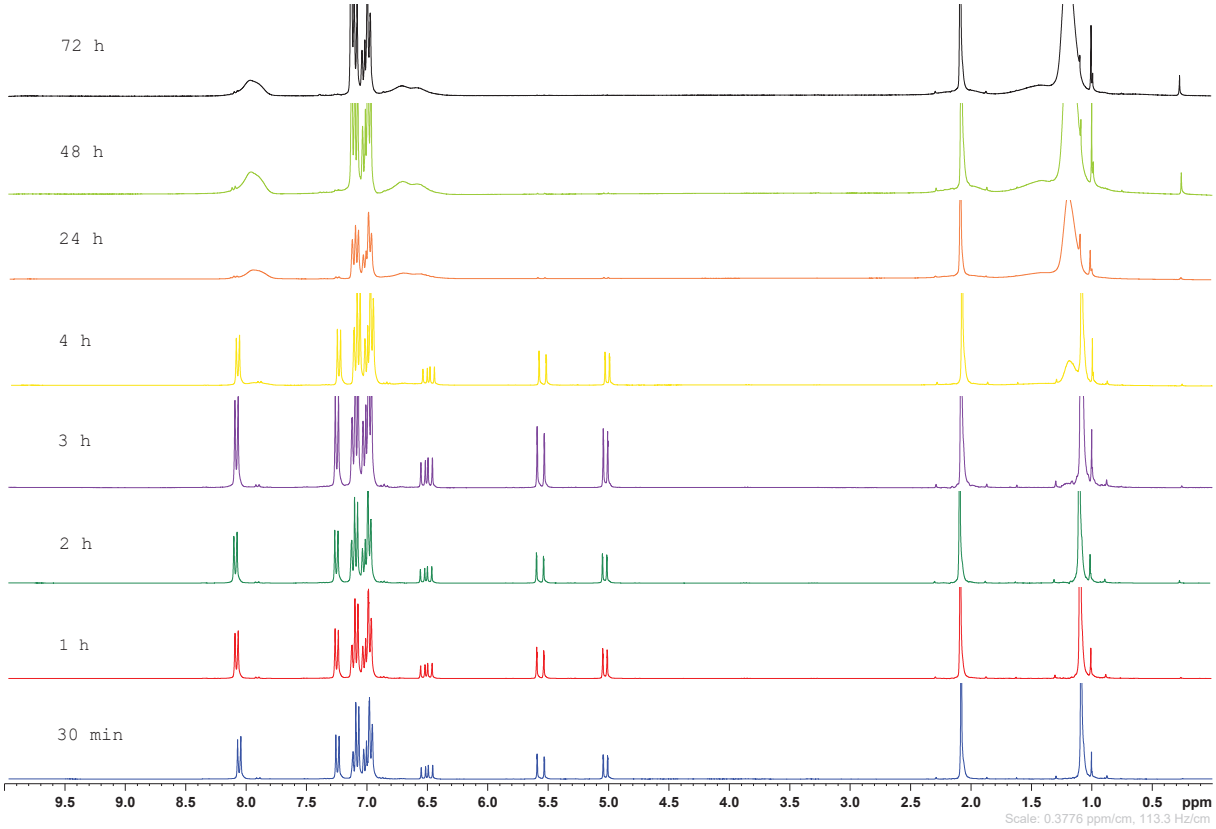

Figure V. 44: NMR monitoring of the homopolymerization of 4-vinylphenylboronic pinacolate.

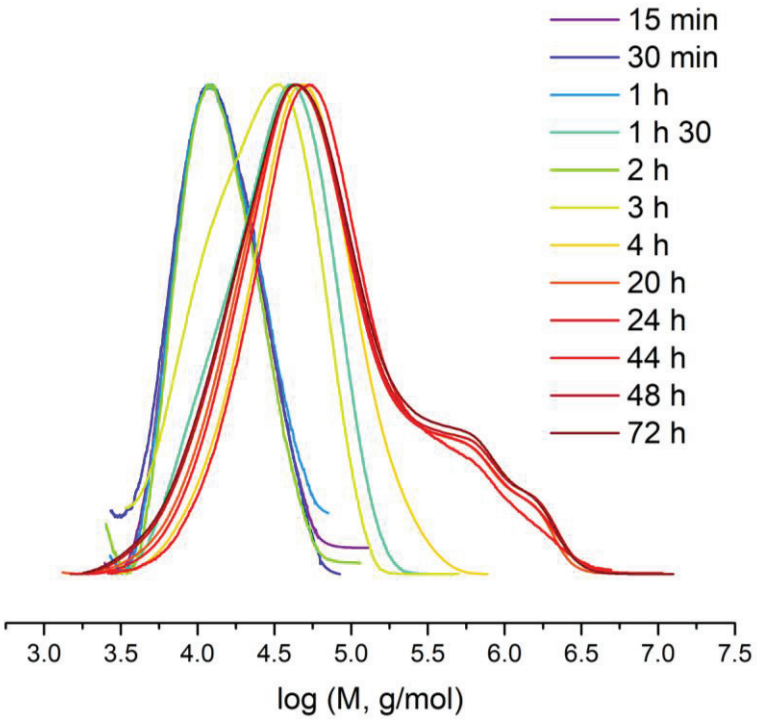

Figure V. 45: Monitoring of the homopolymerization of 4-vinylphenylboronic pinacolate by size-exclusion chromatography in THF.

Thermogravimetric analysis:

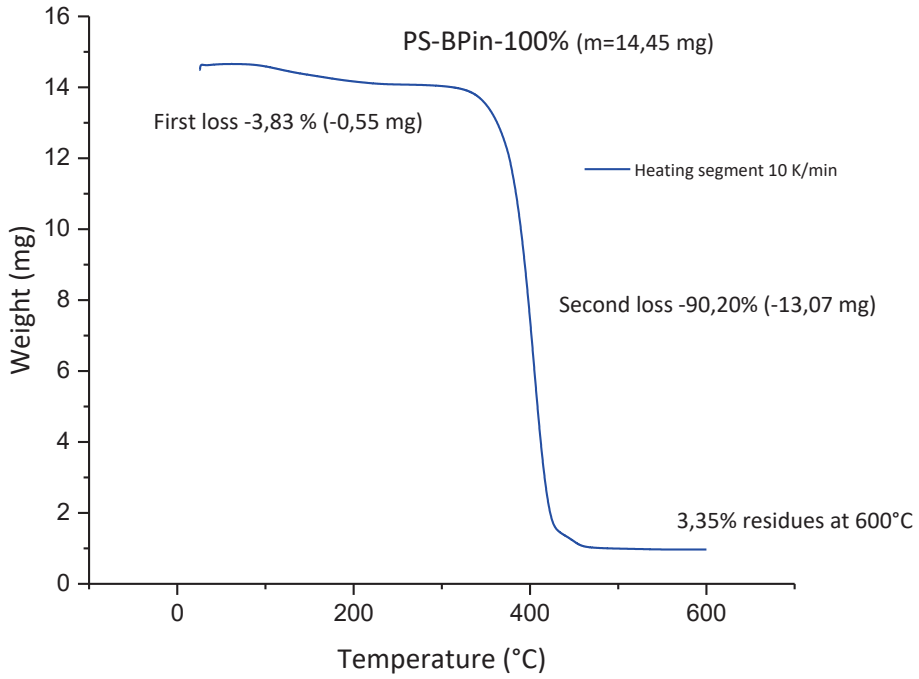

Figure V. 46: TGA thermal curve of poly(4-vinylphenylboronic pinacolate) in 100 µL alumina crucible.

The first loss observed corresponds to the remaining solvent present in the polymer after the synthesis and the second loss is the degradation of the polymer.

Gel observation:

The macroscopic of the polymer in solution was observed during different steps. A solution of poly(4-vinylphenylboronic pinacolate) (0.5 g) at 50 wt % in toluene was prepared with 2 mol % equivalent of benzyl alcohol (0.04 mmol, 4.69 mg, 4.5 µL).

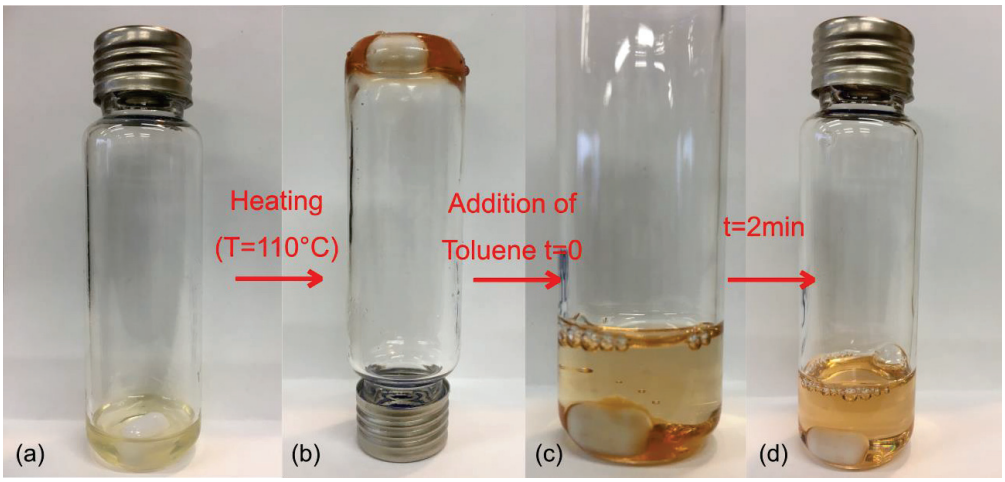

Figure V. 47: Macroscopic aspect of a solution of poly(4-vinylphenylboronic pinacolate), (a) Initial solution of poly(4-vinylphenylboronic pinacolate) at 50 wt% in toluene with 2 % molar equivalent of benzyl alcohol, (b) After 1 night at 110°C, (c) Addition of 2 mL of toluene at t=0, (d) t=2 min after the addition of 2 mL of toluene.

After heating the sample at 110°C, the polymer formed a gel. At the addition of toluene, the gel starts to dissociate to afford a clear solution after a few minutes.

Gel Rheology experiments presented in Chapter 3 were carried out on a MARS 60 apparatus from Thermo Scientific equipped with a Peltier cell, using a 16mm concentric cylinder geometry. The polymer solution at 50 wt % in xylene was introduced at 100°C, and the gelation was monitored by stress-controlled oscillatory shear (the shear stresses start at 1 Pa and are adjusted to 50 and 1000 Pa during the gelation process to maintain the corresponding strains within measuring coge and within the linear viscoelastic regime). A passive thermal insulated hood comprising solvent traps sealed with low viscosity oil ensured negligible evaporation of xylene throughout the study.

C. Synthesis and characterization of poly(4-vinylphenylboronic pinacolate-*co*-styrene) (PS-BPin – x %)

Experimental protocol:

The procedure used was the same than the one for the synthesis of the homopolymers. The monomer quantities were simply adapted depending on the ratio targeted.

^{1}H NMR (300 MHz, benzene-d_6, 25°C, δ): 8.01 (2H), 7.02 (2H + 3H), 6.74 (2H), 2.09 (1H), 1.21 (2H), 1.55 (1H).

^{13}C NMR (400 MHz, benzene-d_6, 25°C, δ): 149.2, 145.3, 135.3, 128.1, 127.9, 126.5, 125.6, 83.0, 46.1, 41.2, 24.7.

^{11}B NMR (300 MHz, benzene-d_6, 25°C, δ): 31.3.

Chemical shifts are identical for all copolymers PS-BPin – x %. Proton attributions corresponds to isolated units. Integration of chemical shifts is proportional to the value of x (see NMR spectra).

NMR spectroscopies:

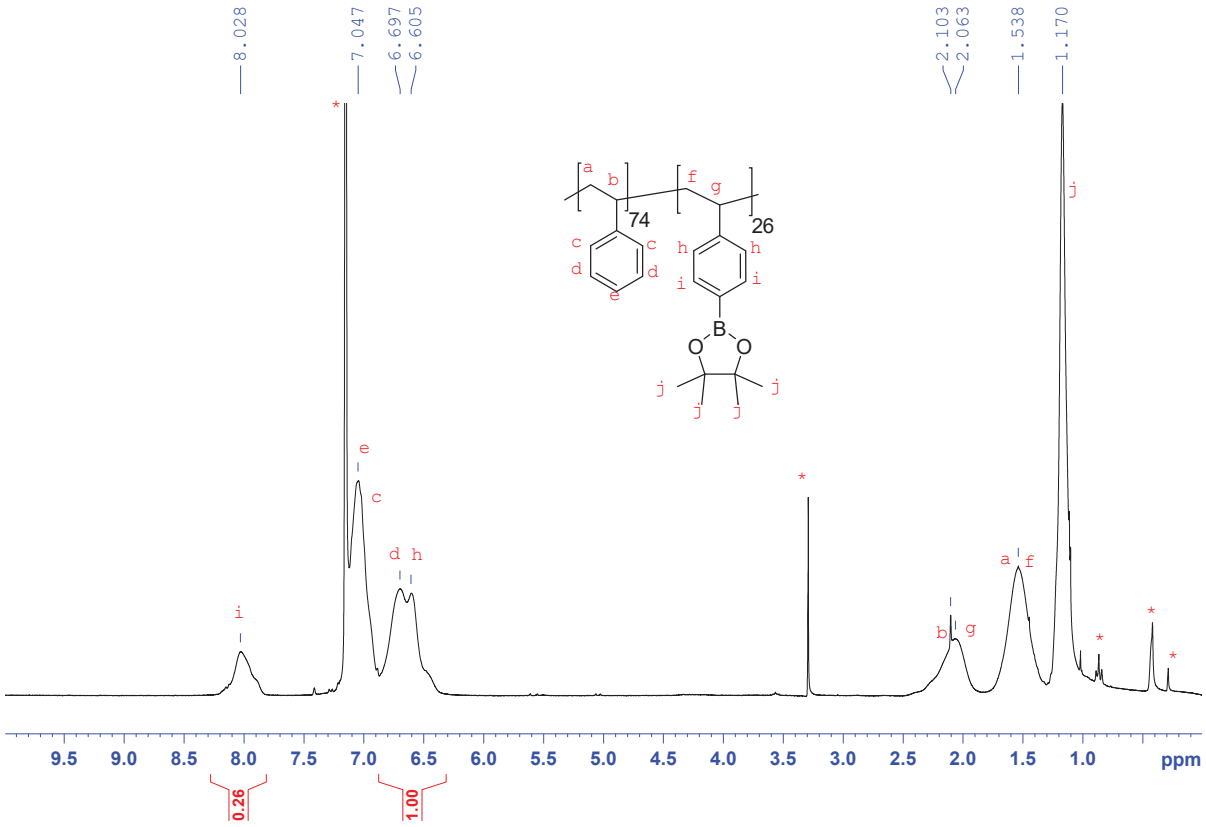

*Figure V. 48: ^{1}H NMR spectrum of poly(4-vinylphenylboronic pinacolate-co-styrene) with 26 mol % of 4-vinylphenylboronic pinacolate in the copolymer in C_6D_6. *C_6D_6 and residual solvents.*

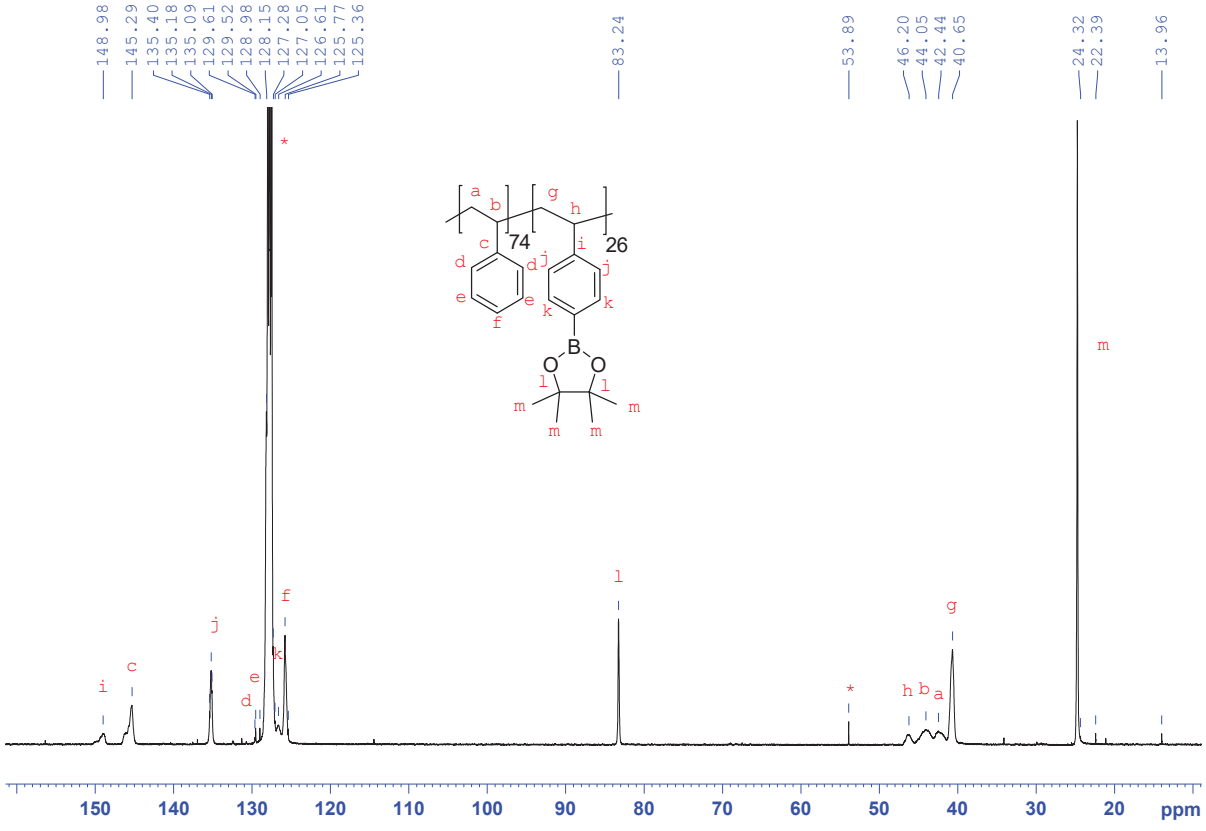

*Figure V. 49: ^{13}C NMR spectrum of poly(4-vinylphenylboronic pinacolate-co-styrene) with 26 mol % of 4-vinylphenylboronic pinacolate in the copolymer in C_6D_6. *C_6D_6 and residual solvents.*

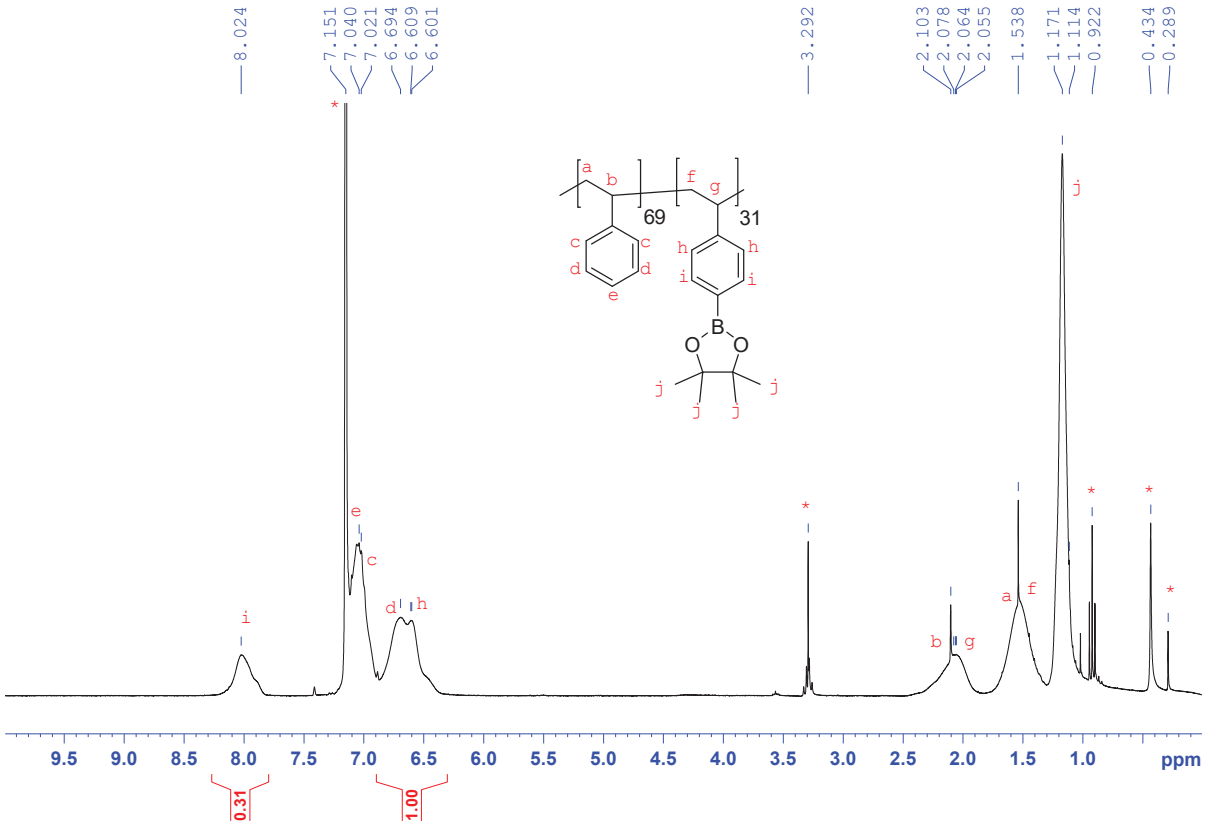

*Figure V. 50: ^{1}H NMR spectrum of poly(4-vinylphenylboronic pinacolate-co-styrene) with 31 mol % of 4-vinylphenylboronic pinacolate in the copolymer in C_6D_6. *C_6D_6 and residual solvents.*

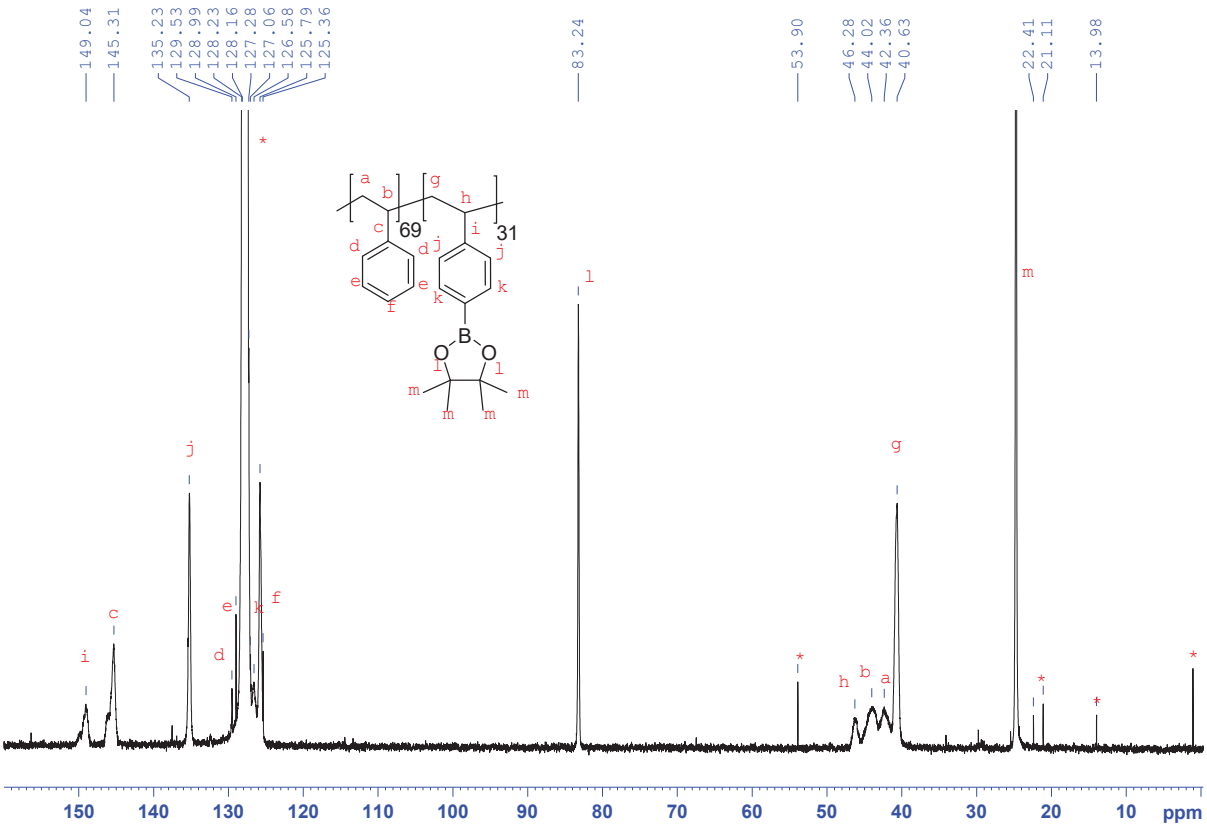

*Figure V. 51: ^{13}CNMR spectrum of poly(4-vinylphenylboronic pinacolate-co-styrene) with 31 mol % of 4-vinylphenylboronic pinacolate in the copolymer in C_6D_6. *C_6D_6 and residual solvents.*

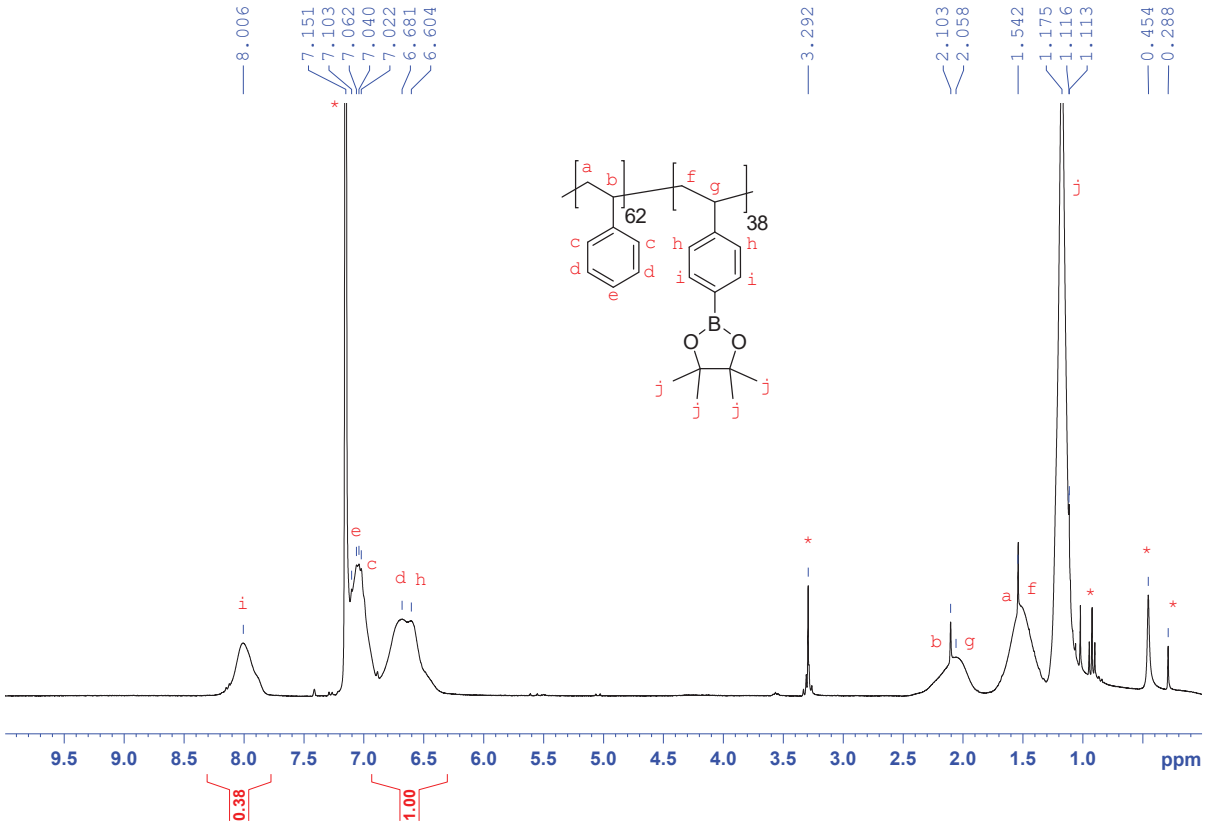

*Figure V. 52: ^{1}H NMR spectrum of poly(4-vinylphenylboronic pinacolate-co-styrene) with 38 mol % of 4-vinylphenylboronic pinacolate in the copolymer in C_6D_6. *C_6D_6 and residual solvents.*

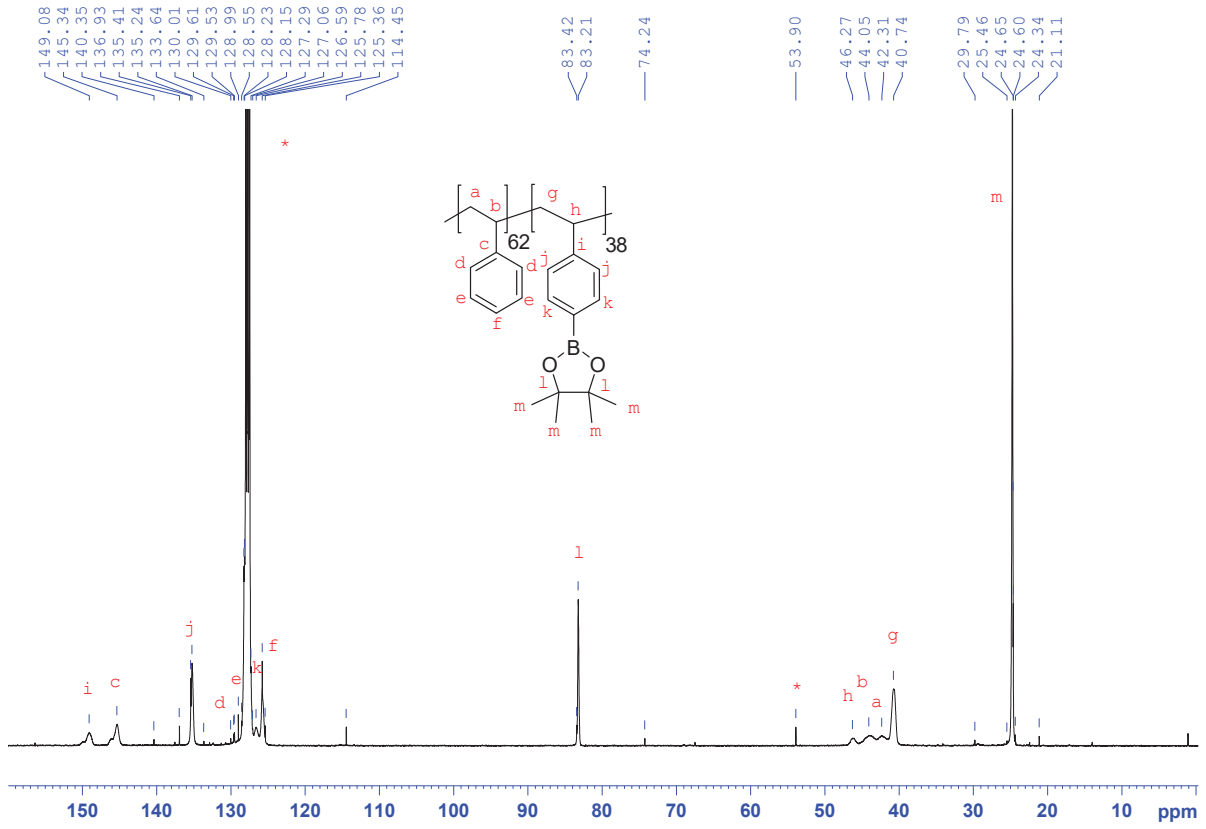

*Figure V. 53: ^{31}C NMR spectrum of poly(4-vinylphenylboronic pinacolate-co-styrene) with 38 mol % of 4-vinylphenylboronic pinacolate in the copolymer in C_6D_6. *C_6D_6 and residual solvents.*

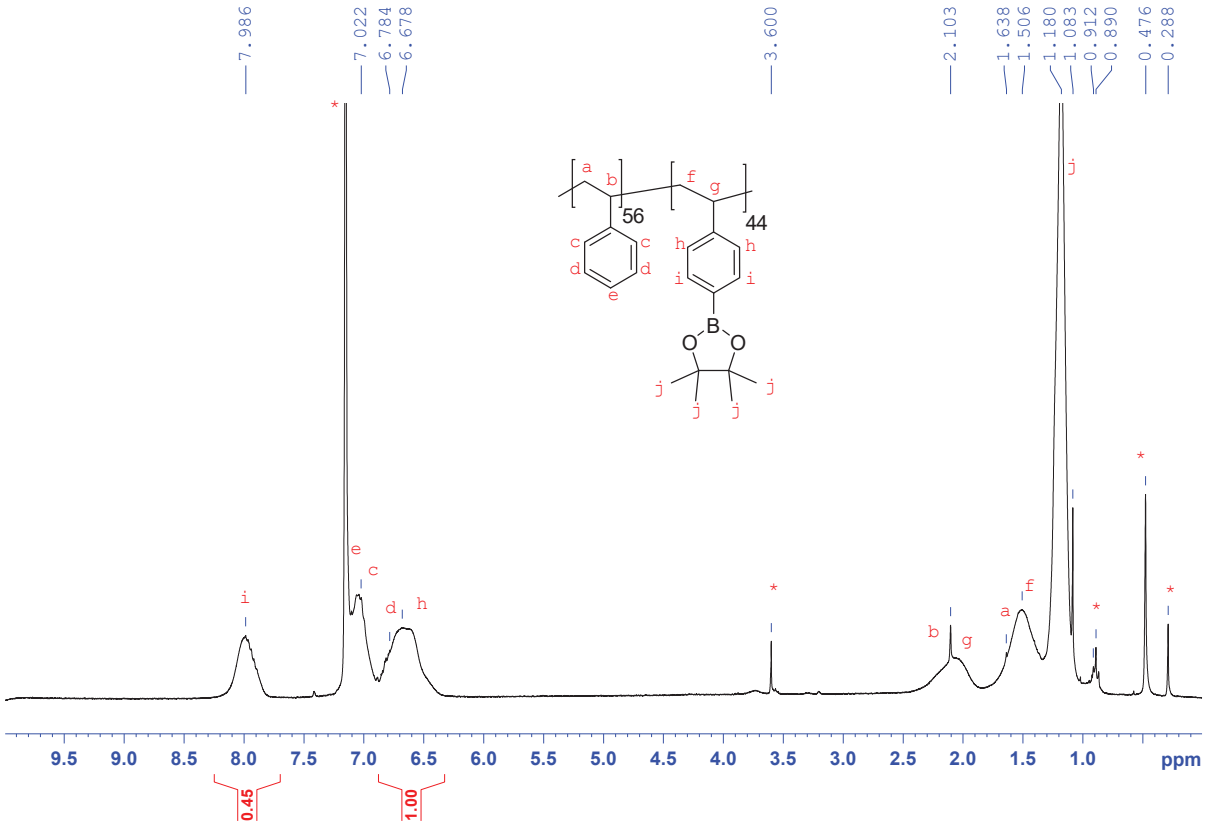

*Figure V. 54: ^{1}H NMR spectrum of poly(4-vinylphenylboronic pinacolate-co-styrene) with 44 mol % of 4-vinylphenylboronic pinacolate in the copolymer in C_6D_6. *C_6D_6 and residual solvents.*

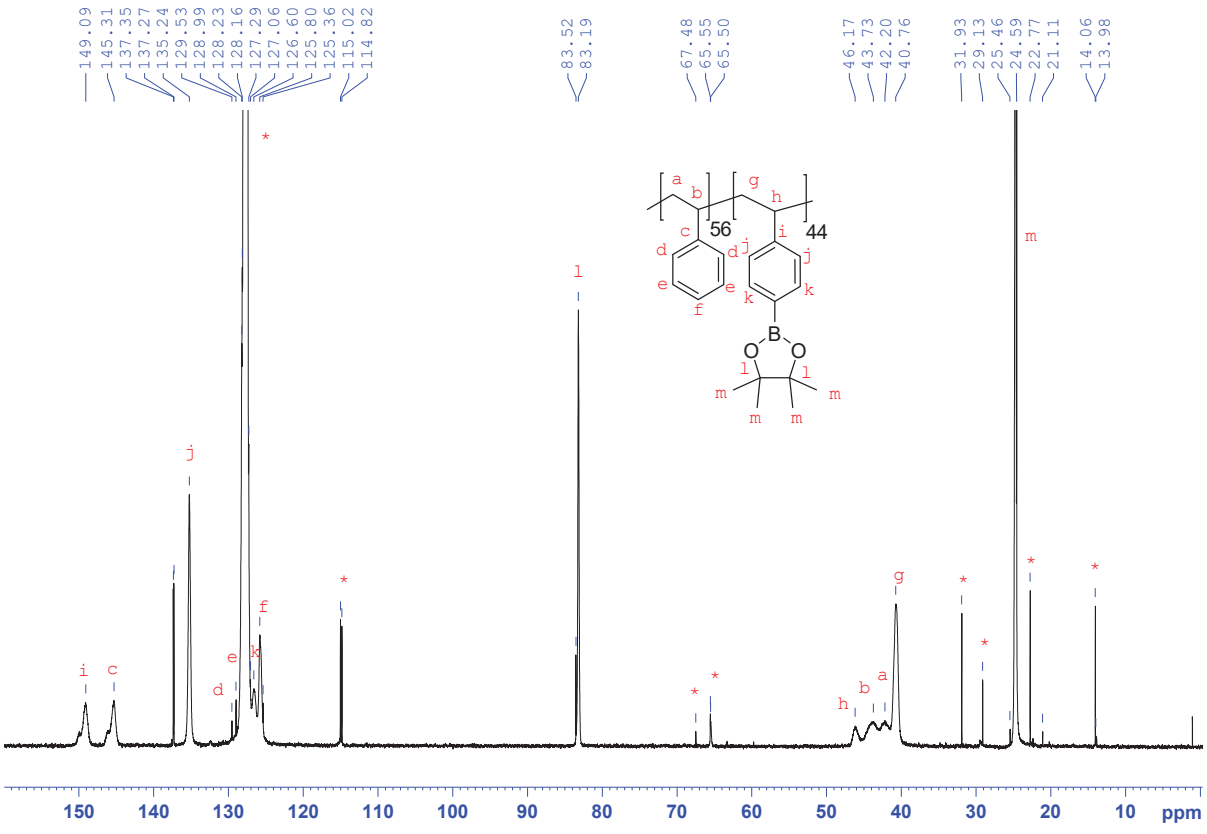

*Figure V. 55: ^{13}C NMR spectrum of poly(4-vinylphenylboronic pinacolate-co-styrene) with 44 mol % of 4-vinylphenylboronic pinacolate in the copolymer in C_6D_6. *C_6D_6 and residual solvents.*

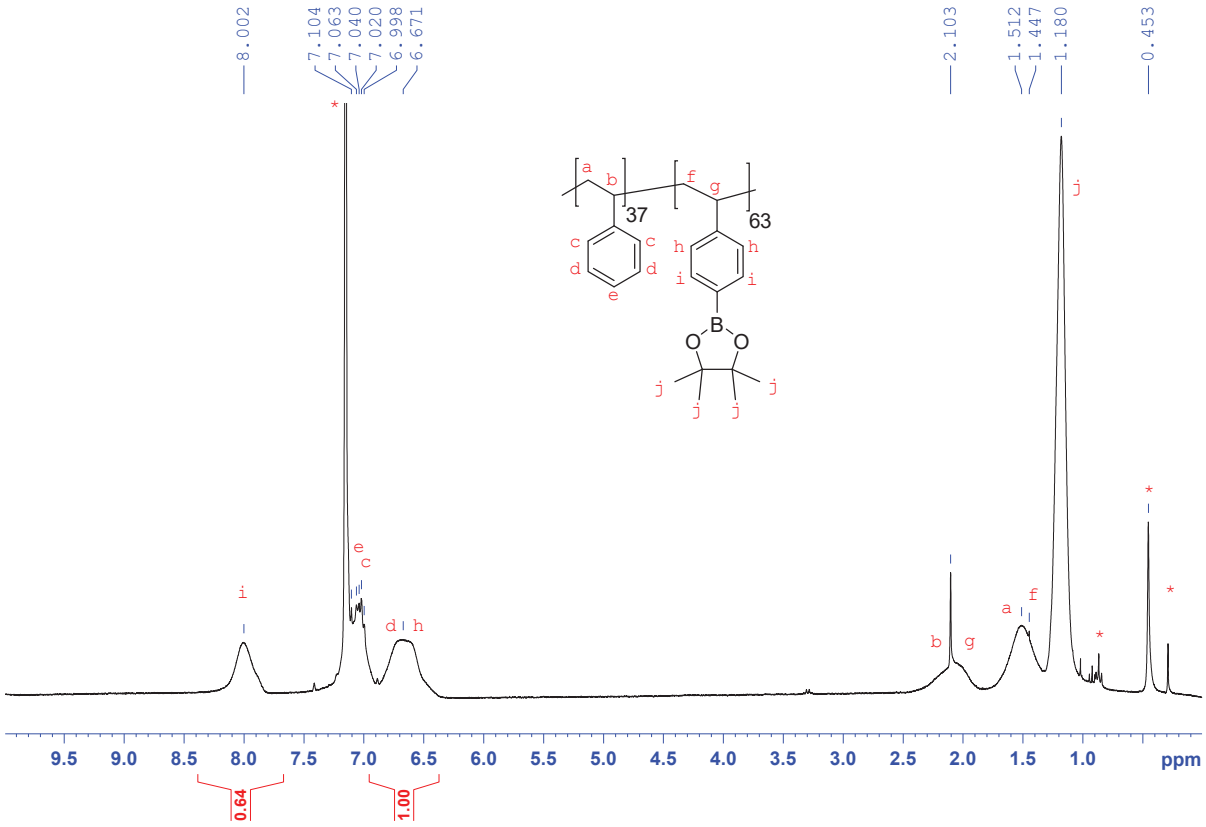

*Figure V. 56: ^{1}H NMR spectrum of poly(4-vinylphenylboronic pinacolate-co-styrene) with 63 mol % of 4-vinylphenylboronic pinacolate in the copolymer in C_6D_6. *C_6D_6 and residual solvents.*

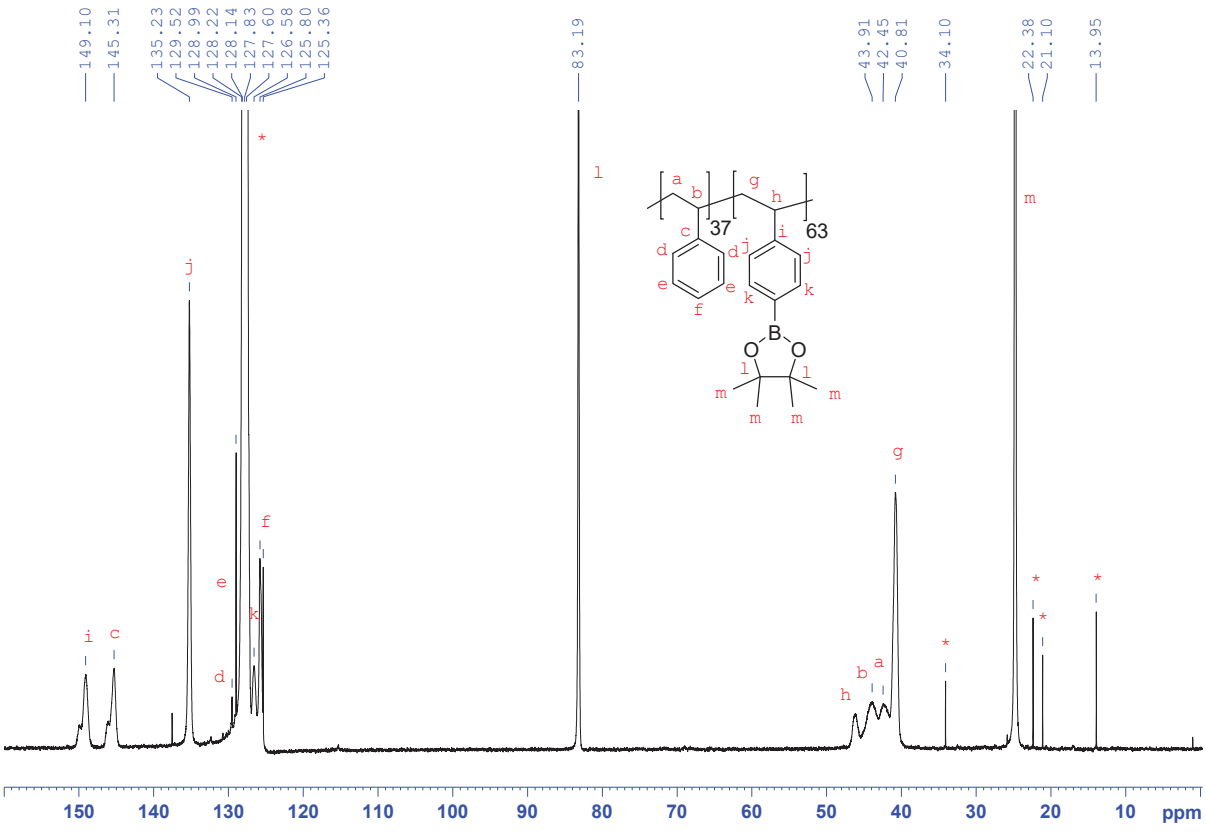

*Figure V. 57: ^{13}C NMR spectrum of poly(4-vinylphenylboronic pinacolate-co-styrene) with 63 mol % of 4-vinylphenylboronic pinacolate in the copolymer in C_6D_6. *C_6D_6 and residual solvents.*

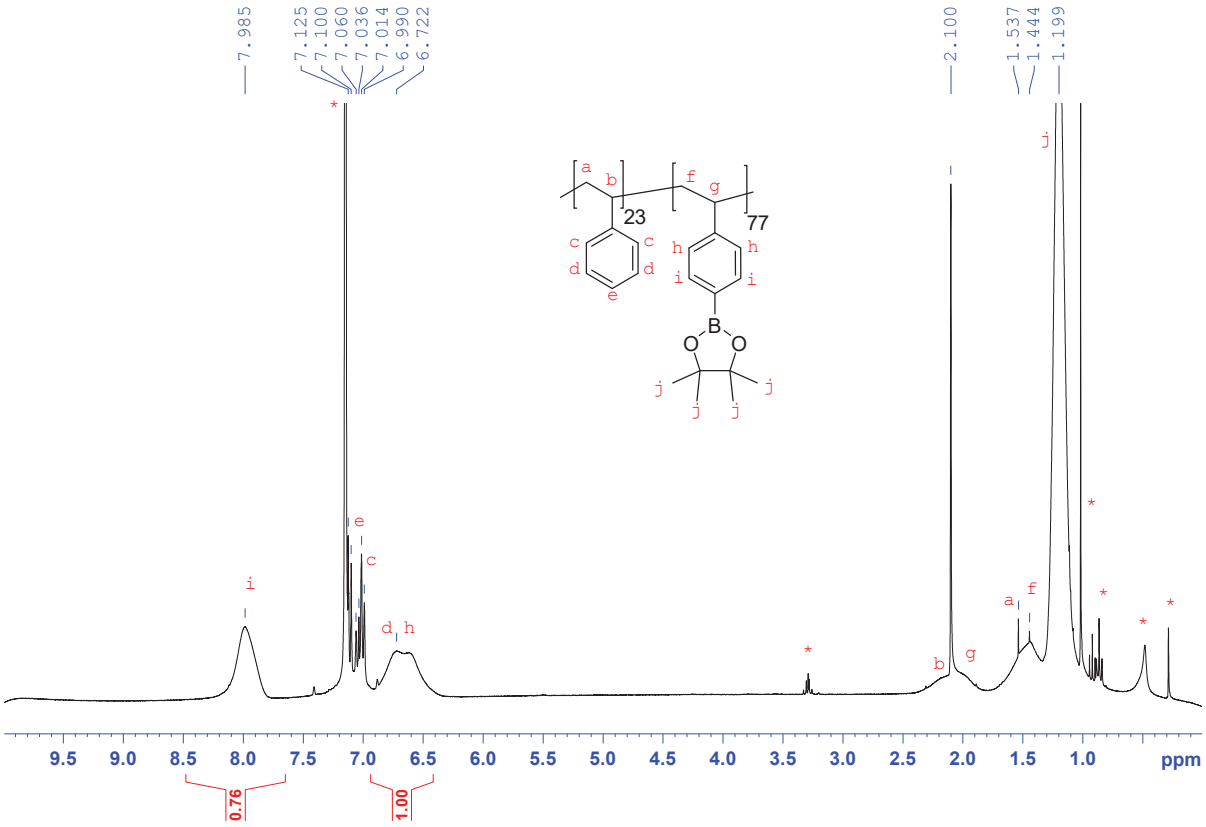

*Figure V. 58: ^{1}H NMR spectrum of poly(4-vinylphenylboronic pinacolate-co-styrene) with 77 mol % of 4-vinylphenylboronic pinacolate in the copolymer in C_6D_6. *C_6D_6 and residual solvents.*

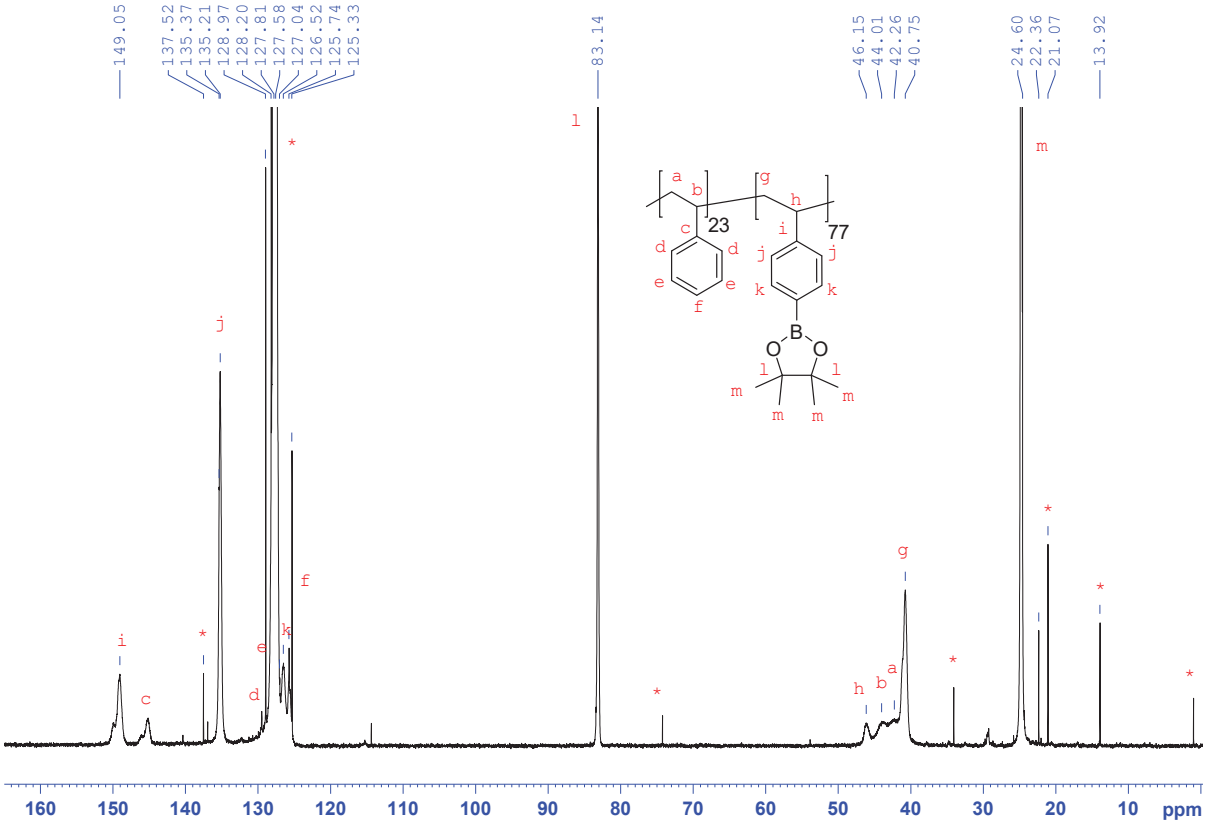

*Figure V. 59: ^{13}C NMR spectrum of poly(4-vinylphenylboronic pinacolate-co-styrene) with 77 mol % of 4-vinylphenylboronic pinacolate in the copolymer in C_6D_6. *C_6D_6 and residual solvents.*

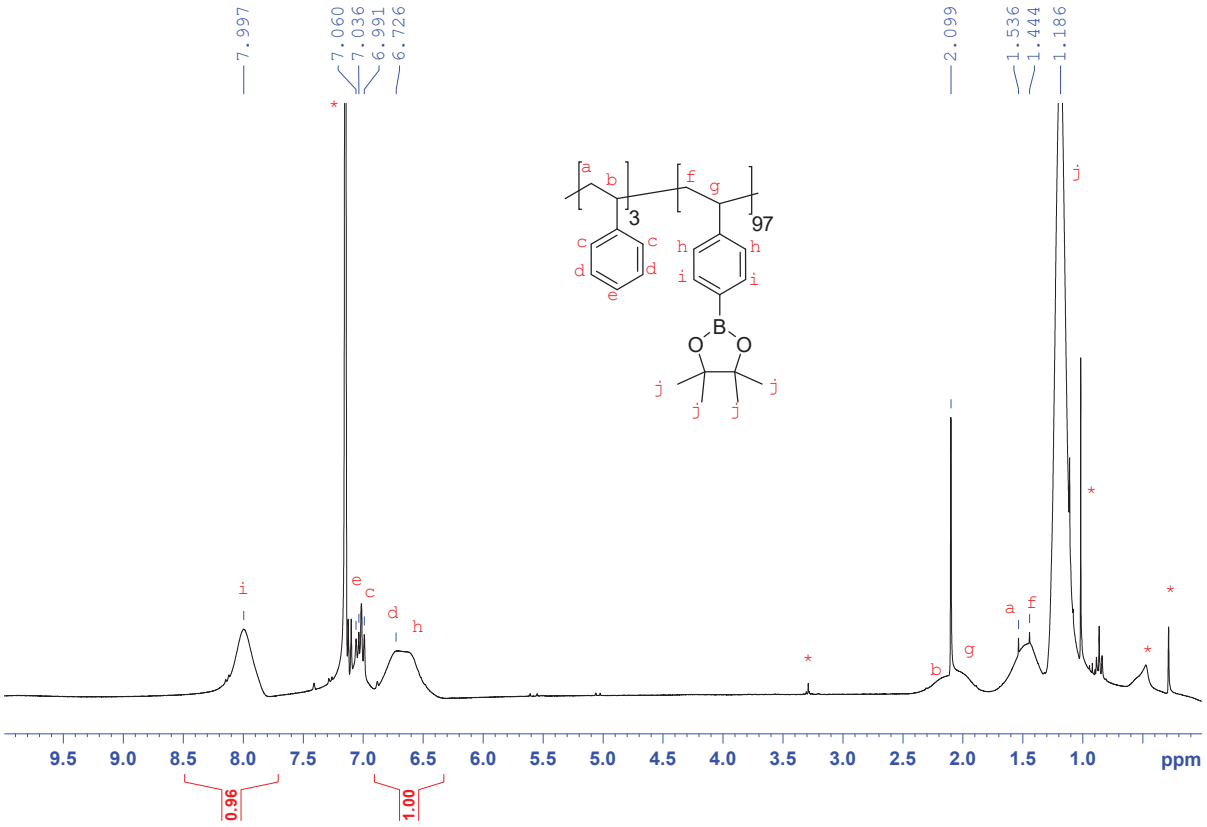

*Figure V. 60: ^{1}H NMR spectrum of poly(4-vinylphenylboronic pinacolate-co-styrene) with 97 mol % of 4-vinylphenylboronic pinacolate in the copolymer in C_6D_6. *C_6D_6 and residual solvents.*

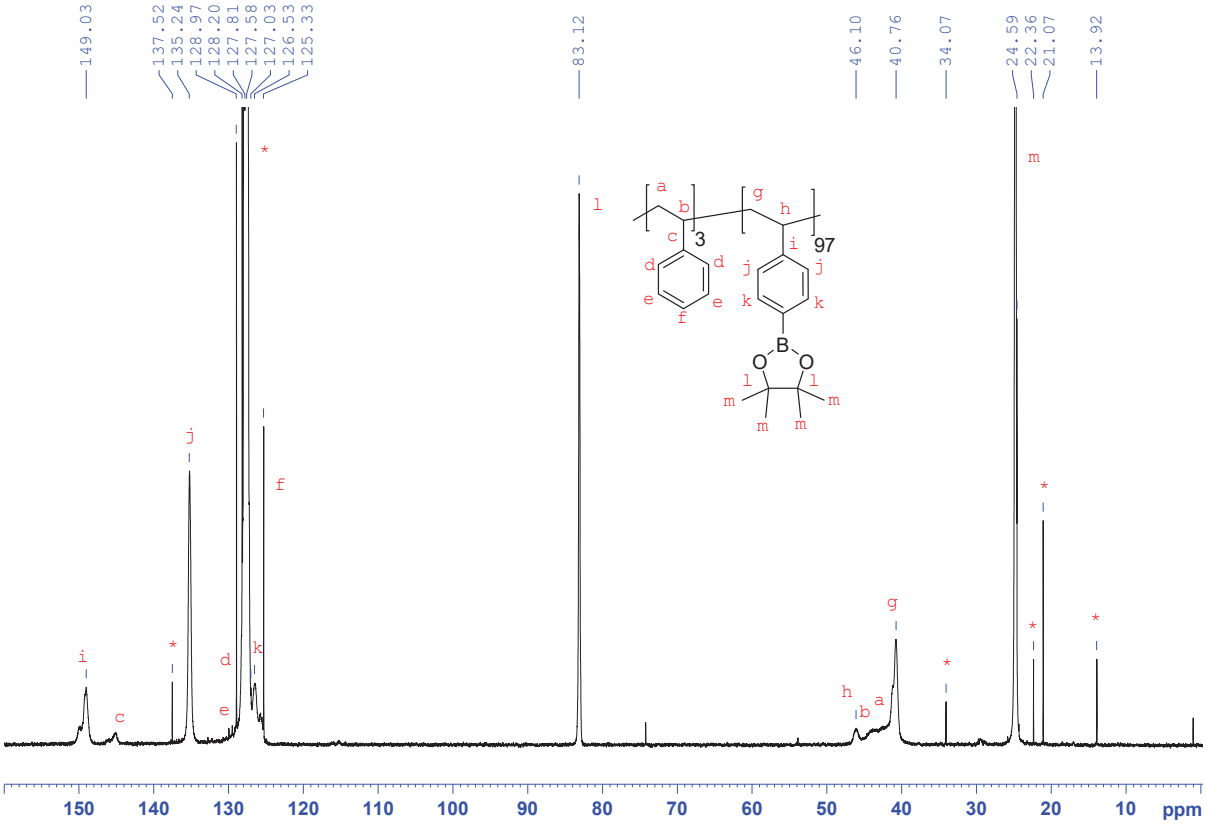

*Figure V. 61: ^{13}C NMR spectrum of poly(4-vinylphenylboronic pinacolate-co-styrene) with 97 mol % of 4-vinylphenylboronic pinacolate in the copolymer in C_6D_6. *C_6D_6 and residual solvents.*

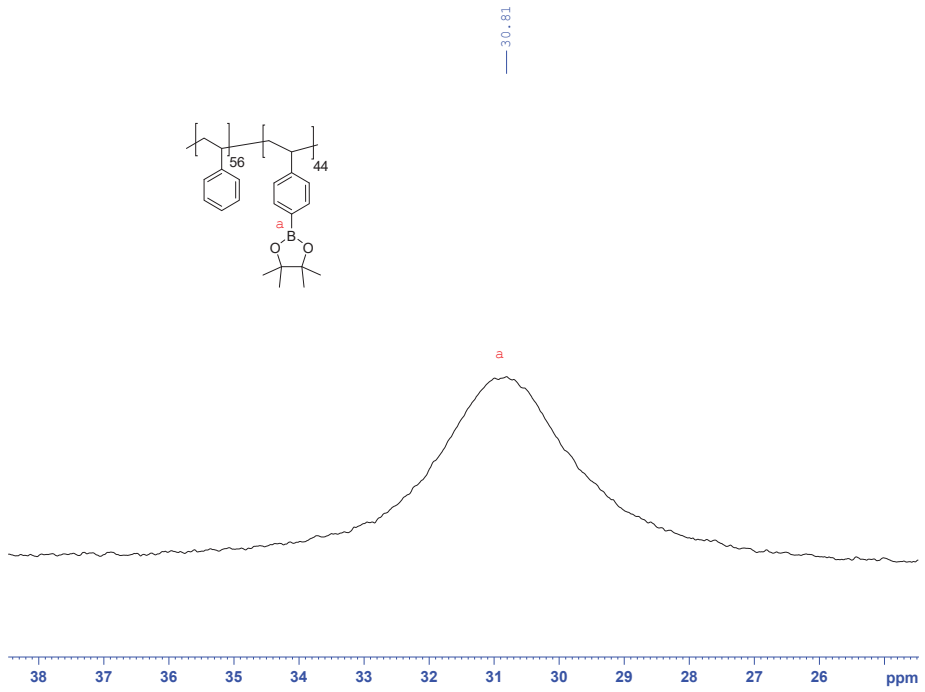

*Figure V. 62: ^{11}B NMR spectrum of poly(4-vinylphenylboronic pinacolate-co-styrene) with 44 mol % of 4-vinylphenylboronic pinacolate in the copolymer in C_6D_6. *C_6D_6 and residual solvents.*

Differential scanning calorimetry measurements:

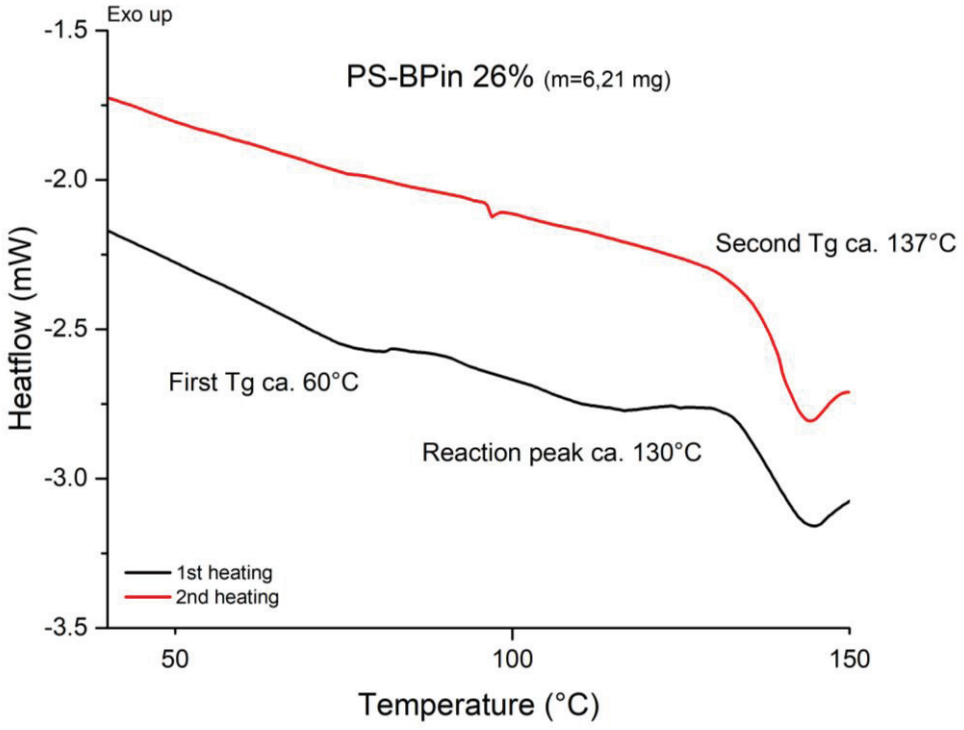

Figure V. 63: DSC thermograms of PS-BPin 26 mol % in 40 µL opened aluminum pans.

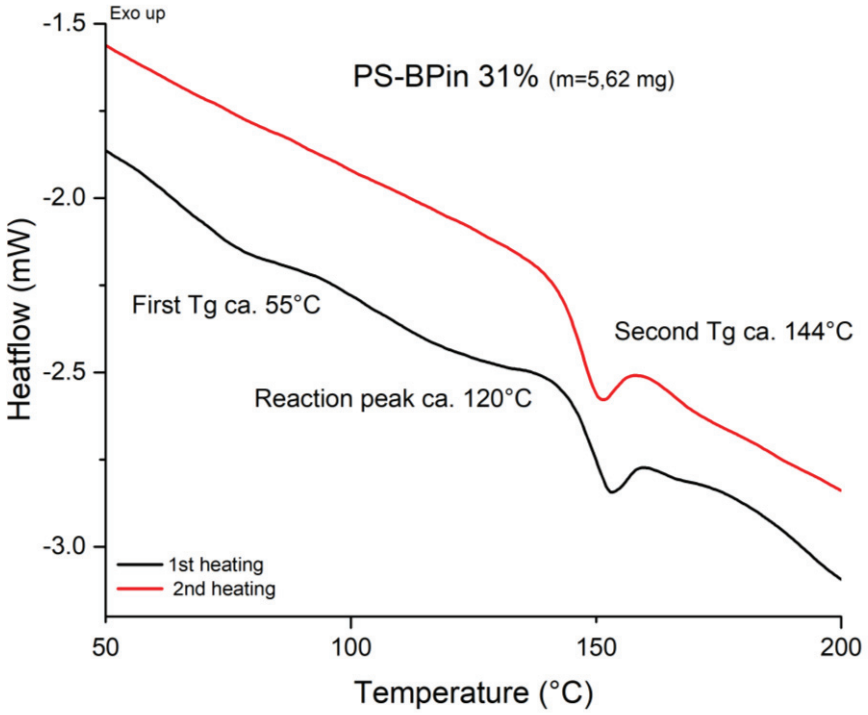

Figure V. 64: DSC thermograms of PS-BPin 31 mol % in 40 µL opened aluminum pans.

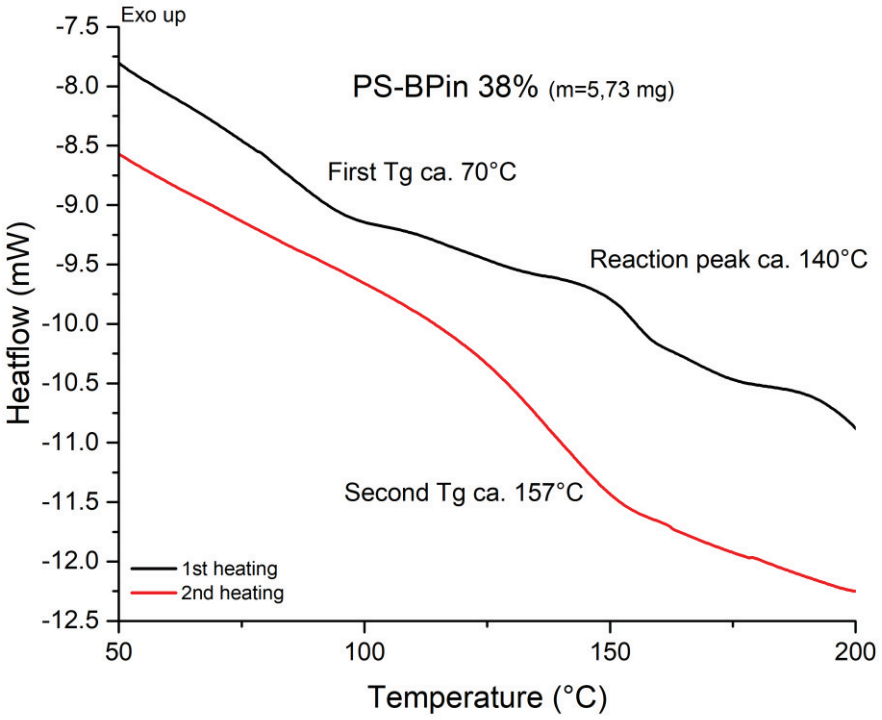

Figure V. 65: DSC thermograms of PS-BPin 38 mol % in 40 µL opened aluminum pans.

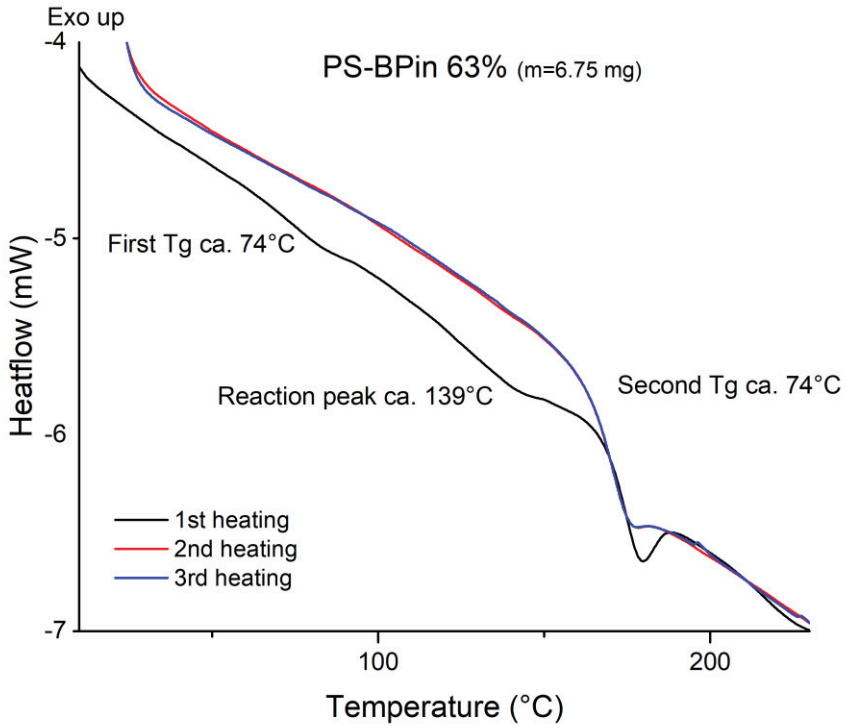

Figure V. 66: DSC thermograms of PS-BPin 63 mol % in 40 µL opened aluminum pans.

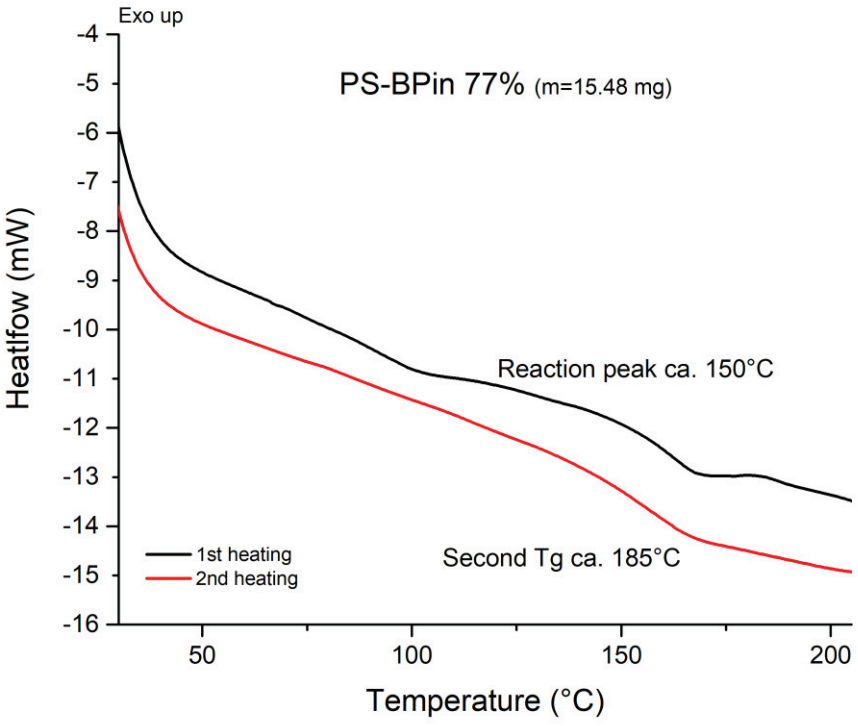

Figure V. 67: DSC thermograms of PS-BPin 77 mol % in 40 µL opened aluminum pans.

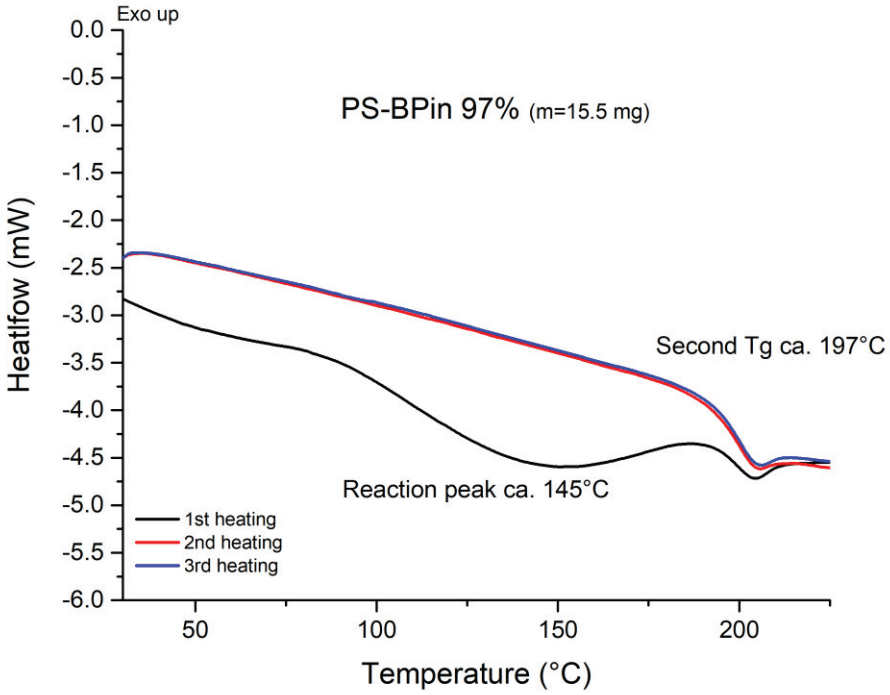

Figure V. 68: DSC thermograms of PS-BPin 97 mol % in 40 µL opened aluminum pans.

Size-exclusion chromatography in THF:

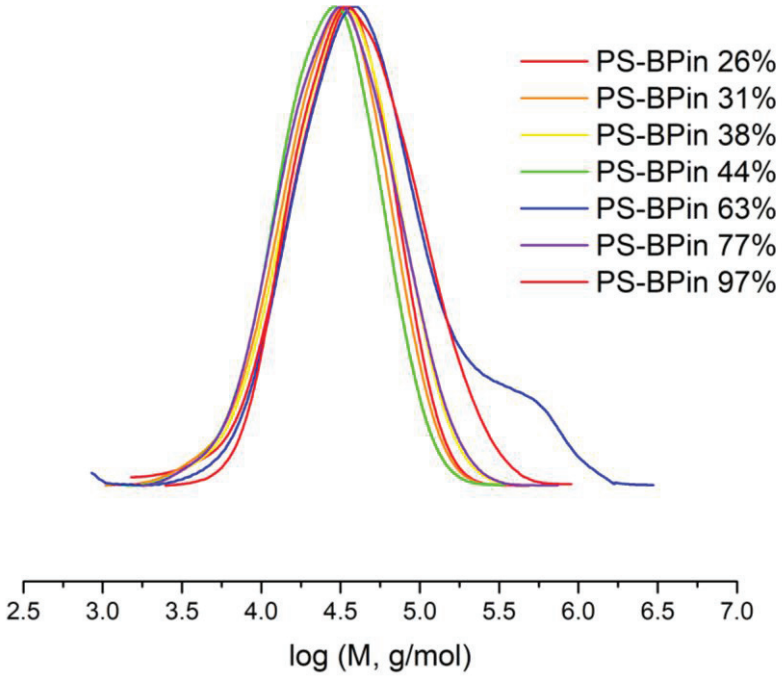

Figure V. 69: Chromatograms of copolymers with different ratios of 4-vinylphenylboronic pinacolate. (Calculations done with PS standards calibrations)

IV. Extension of pinacol boronates reactivity to a wide variety of polymers

A. Synthesis and characterization of copolymers from n-butyl acrylate and 4-vinylphenylboronic pinacolate (PBA-SBPin – x %)

Experimental protocol:

The procedure used was the same than the one for the synthesis of the styrenic homopolymers in the previous chapter. The monomer quantities were adapted depending on the ratio targeted.

^{1}H NMR (300 MHz, benzene-d_6, 25°C, δ): 8.07 (2H), 7.25 (2H), 4.13 (2H), 2.71 (1H), 2.24 (1H), 1.89 (2H), 1.51 (2H), 1.33 (2H), 1.31 (2H), 1.15 (12H), 0.88 (3H).

^{13}C NMR (400 MHz, benzene-d_6, 25°C, δ): 174.69, 147.59, 133.61, 130.29, 83.17, 63.63, 43.2, 41.39, 39.51, 30.58, 24.41, 21.07, 13.71.

^{11}B NMR (300 MHz, benzene-d_6, 25°C, δ): 30.91.

Chemical shifts are identical for all copolymers PBA-SBPin – x %. Proton attributions corresponds to isolated units. Integration of chemical shifts is proportional to the value of x (see NMR spectra).

NMR spectroscopies:

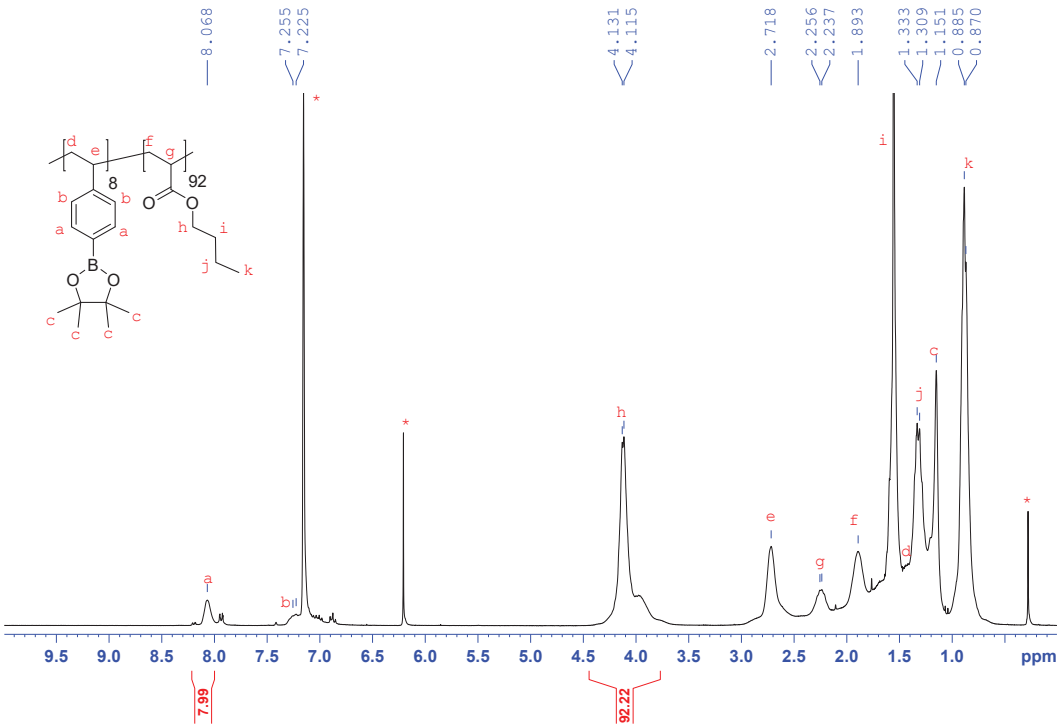

*Figure V. 70: ^{1}H NMR spectrum of poly(4-vinylphenylboronic pinacolate-co-n-butyl acrylate) with 8 mol % of 4-vinylphenylboronic pinacolate in the copolymer in C_6D_6. *C_6D_6 and residual solvents.*

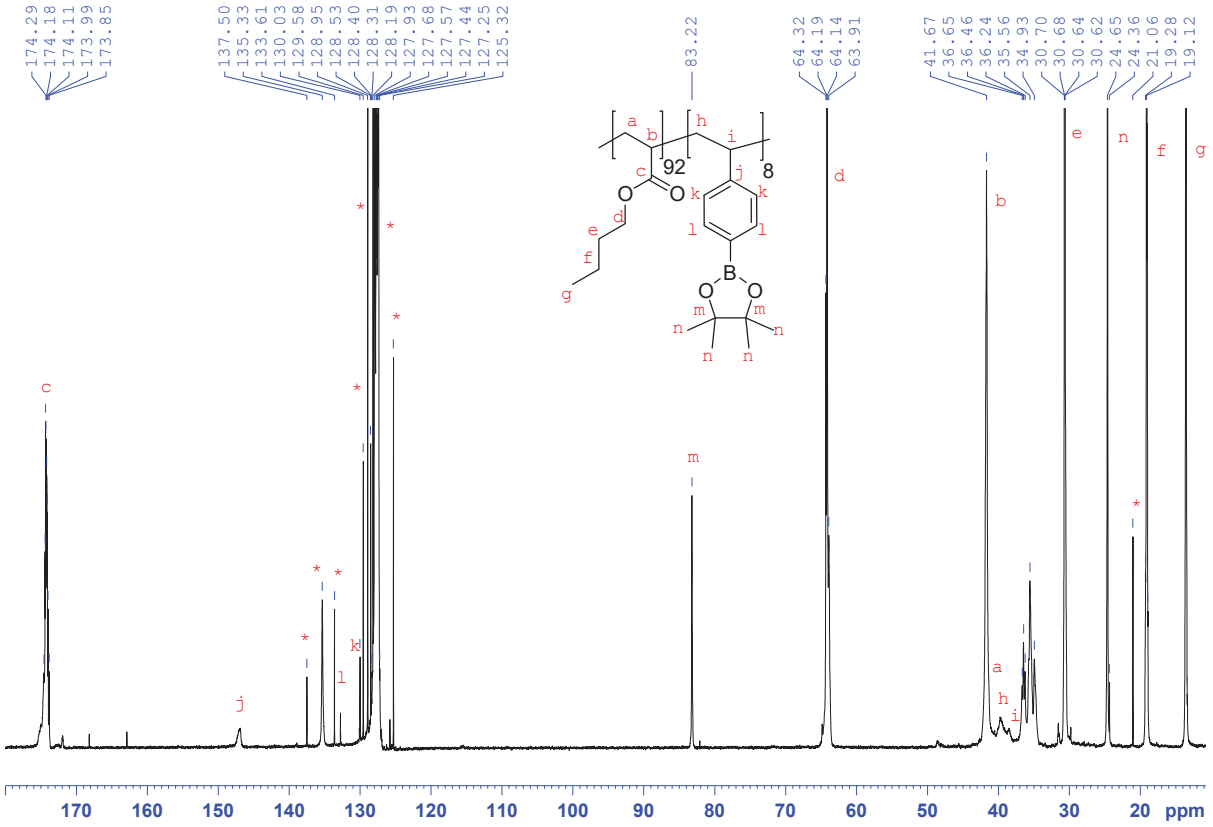

*Figure V. 71: ^{13}C NMR spectrum of poly(4-vinylphenylboronic pinacolate-co-n-butyl acrylate) with 8 mol % of 4-vinylphenylboronic pinacolate in the copolymer in C_6D_6. *C_6D_6 and residual solvents.*

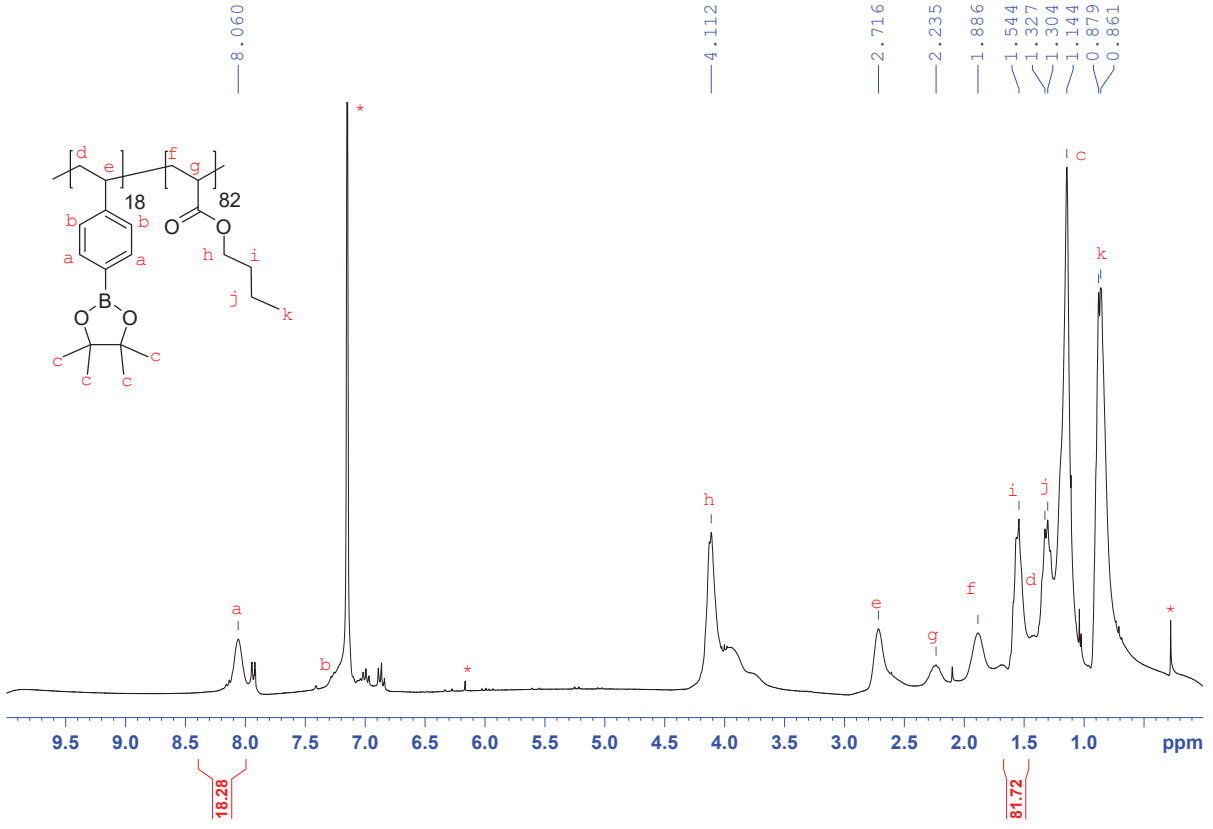

*Figure V. 72: ^{1}H NMR spectrum of poly(4-vinylphenylboronic pinacolate-co-n-butyl acrylate) with 18 mol % of 4-vinylphenylboronic pinacolate in the copolymer in C_6D_6. *C_6D_6 and residual solvents.*

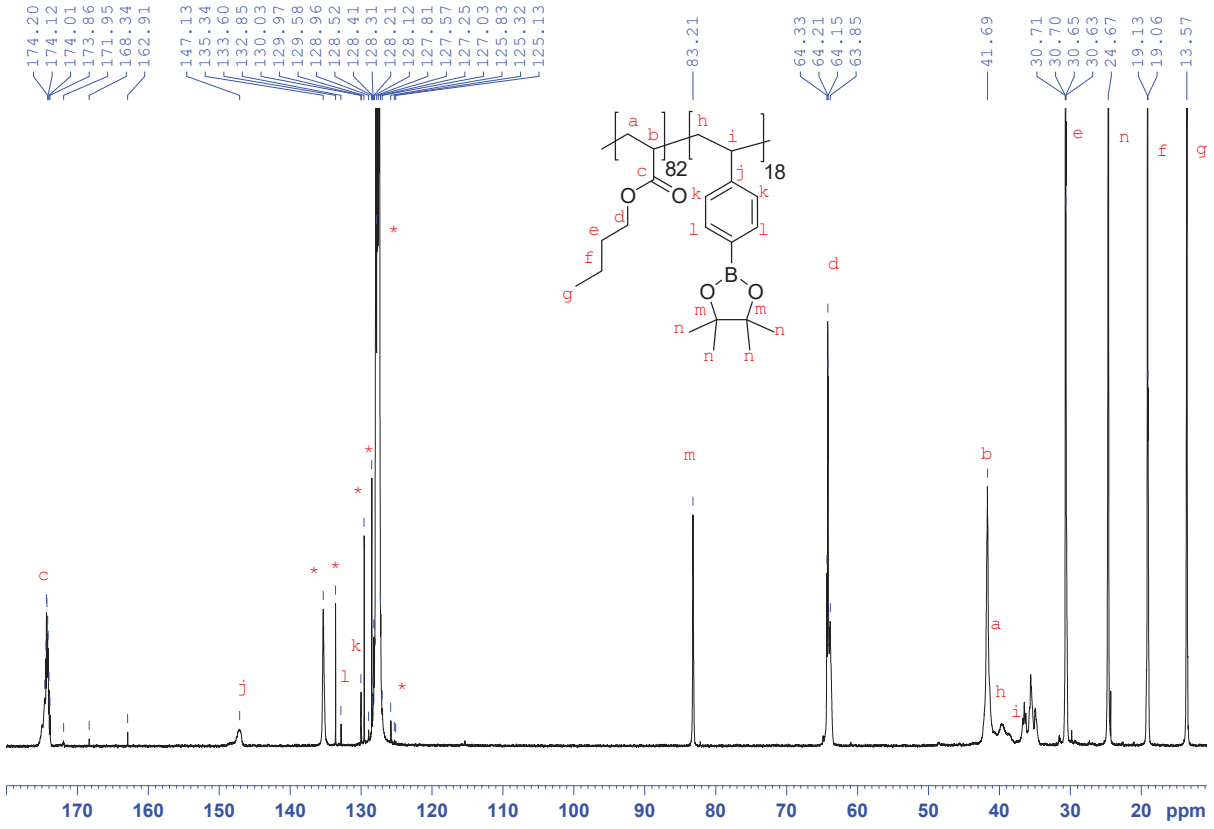

*Figure V. 73: ^{13}C NMR spectrum of poly(4-vinylphenylboronic pinacolate-co-n-butyl acrylate) with 18 mol % of 4-vinylphenylboronic pinacolate in the copolymer in C_6D_6. *C_6D_6 and residual solvents.*

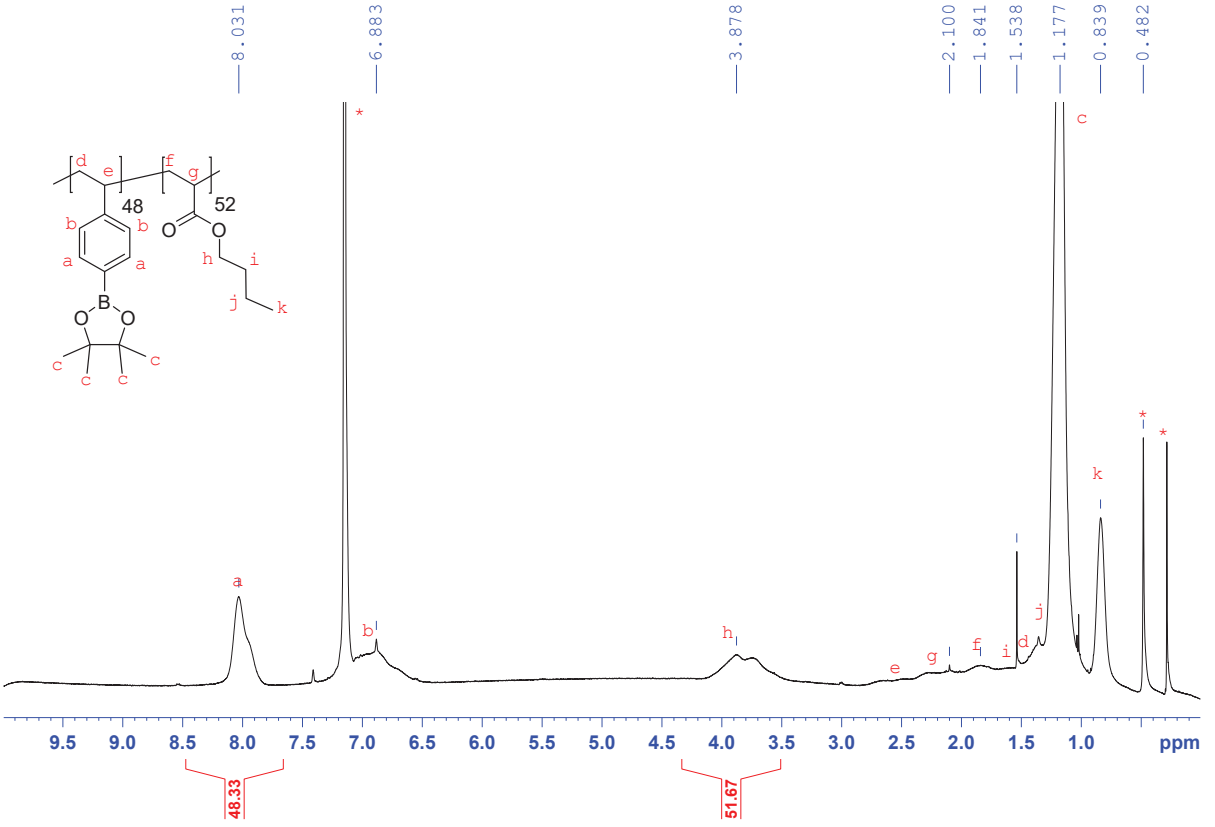

*Figure V. 74: ^{1}H NMR spectrum of poly(4-vinylphenylboronic pinacolate-co-n-butyl acrylate) with 48 mol % of 4-vinylphenylboronic pinacolate in the copolymer in C_6D_6. *C_6D_6 and residual solvents.*

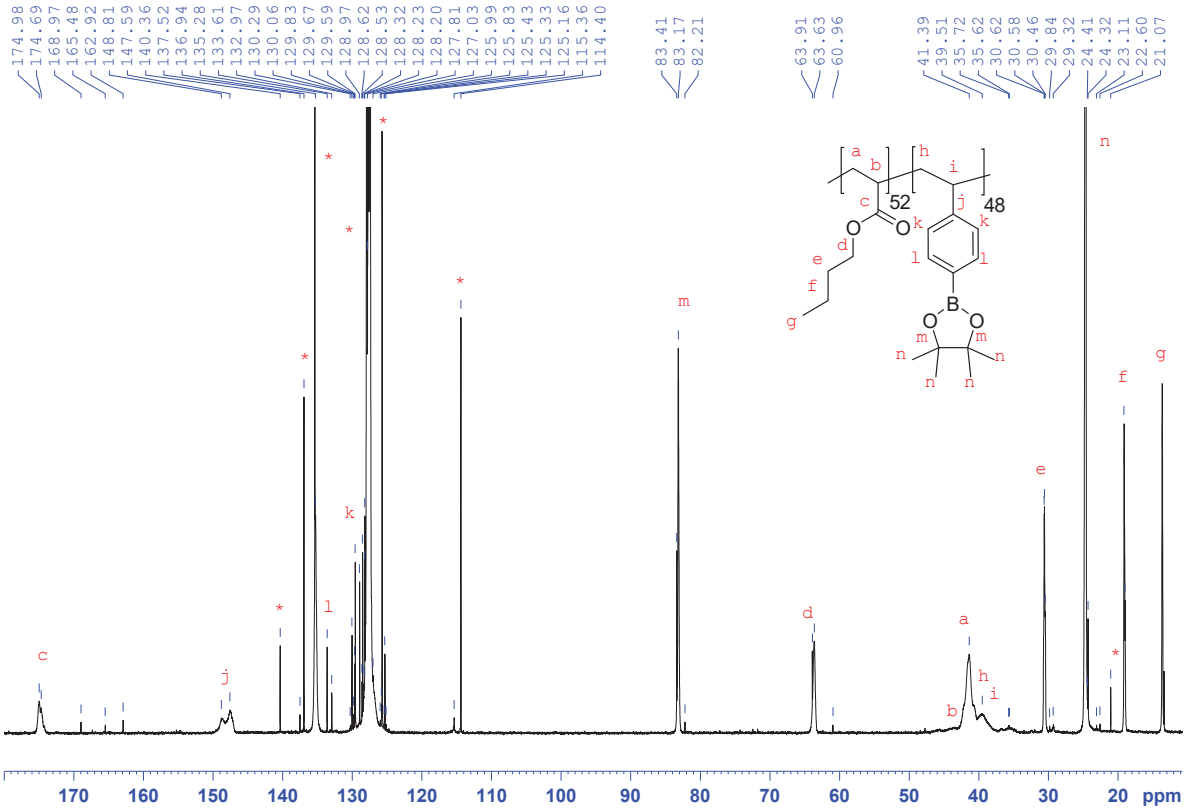

*Figure V. 75: ^{13}C NMR spectrum of poly(4-vinylphenylboronic pinacolate-co-n-butyl acrylate) with 48 mol % of 4-vinylphenylboronic pinacolate in the copolymer in C_6D_6. *C_6D_6 and residual solvents.*

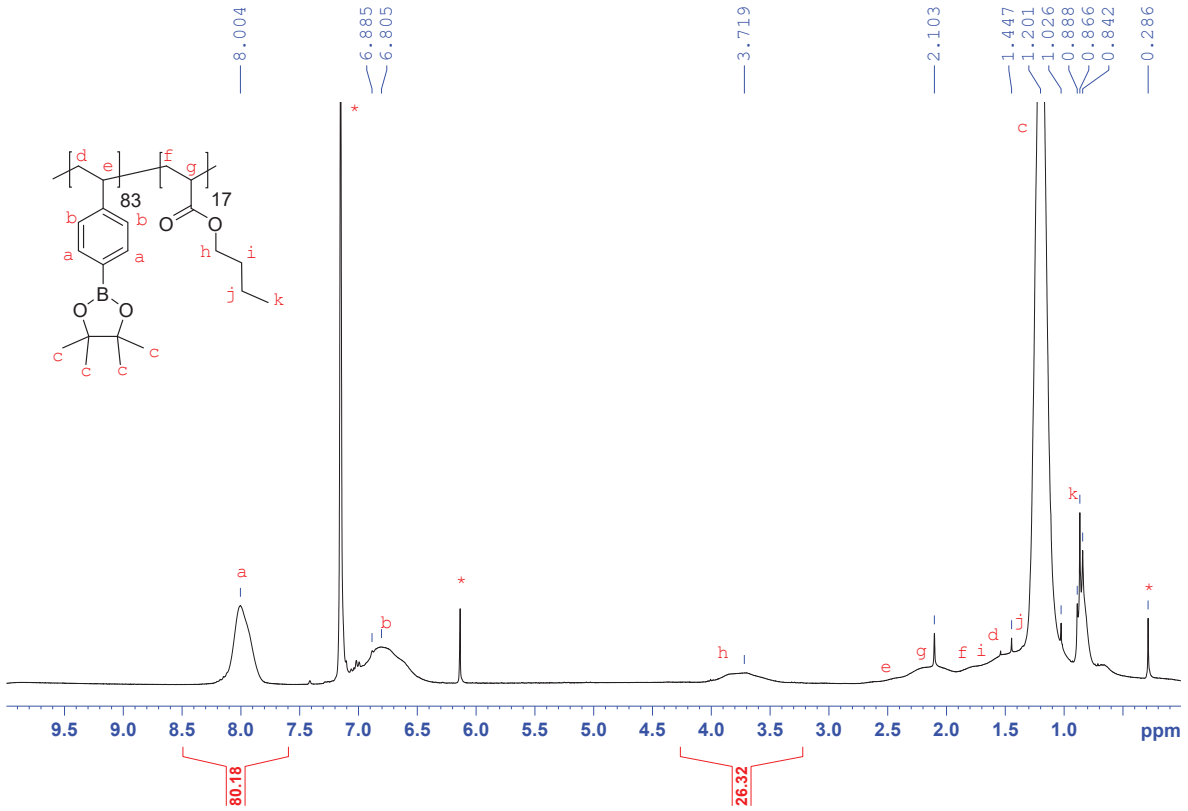

*Figure V. 76: ^{1}H NMR spectrum of poly(4-vinylphenylboronic pinacolate-co-n-butyl acrylate) with 83 mol % of 4-vinylphenylboronic pinacolate in the copolymer in C_6D_6. *C_6D_6 and residual solvents.*

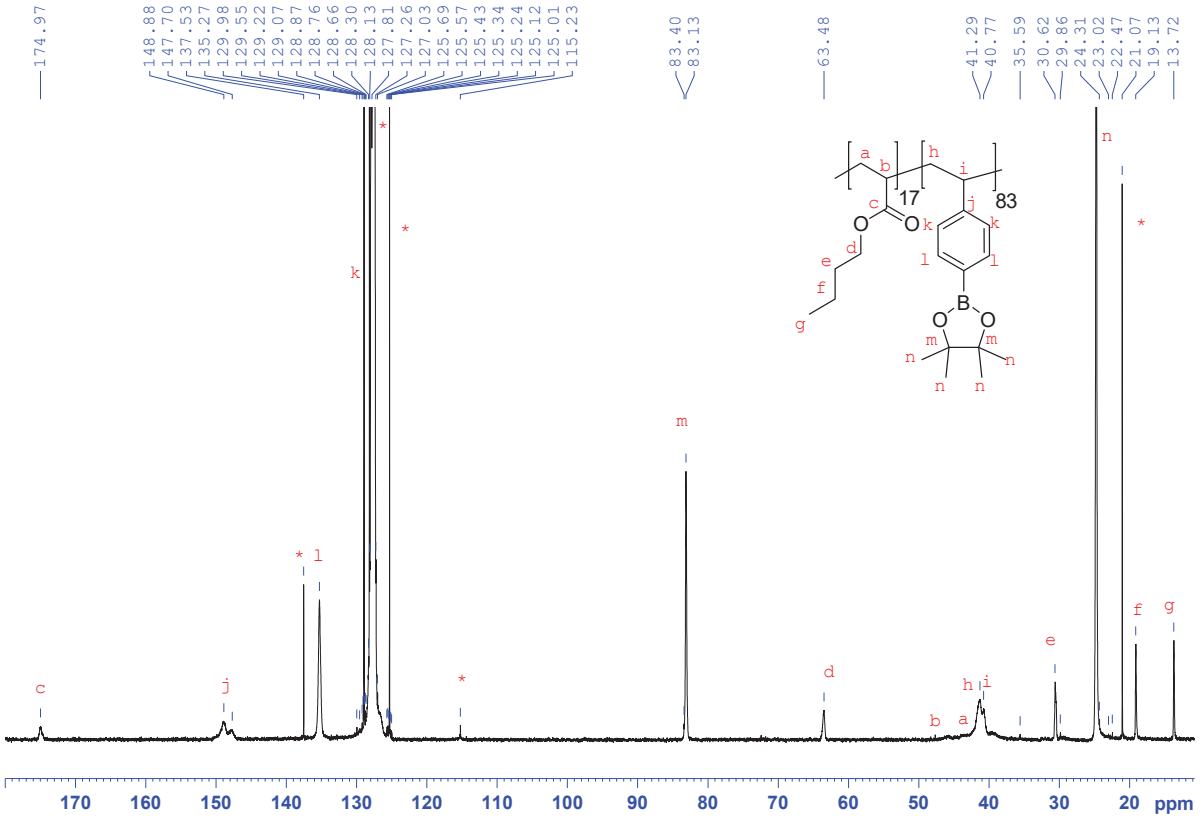

*Figure V. 77: ^{13}C NMR spectrum of poly(4-vinylphenylboronic pinacolate-co-n-butyl acrylate) with 83 mol % of 4-vinylphenylboronic pinacolate in the copolymer in C_6D_6. *C_6D_6 and residual solvents.*

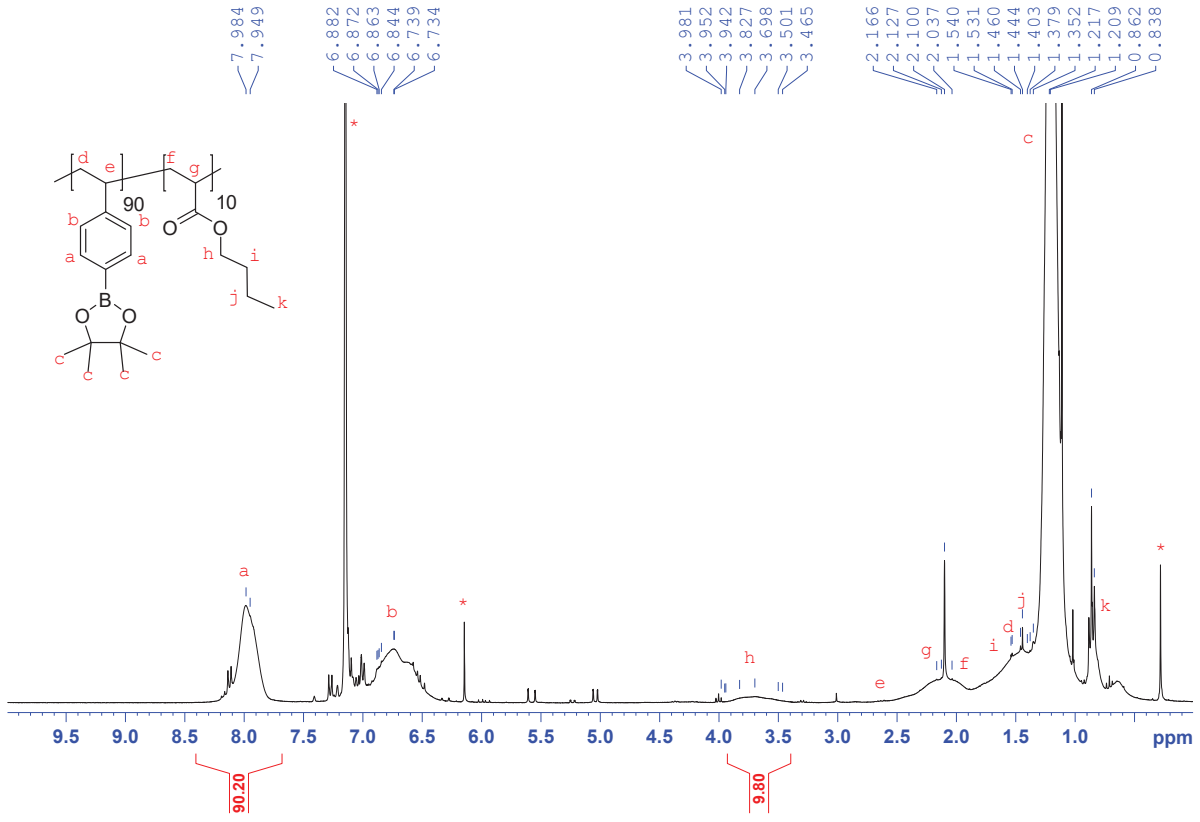

*Figure V. 78: ^{1}H NMR spectrum of poly(4-vinylphenylboronic pinacolate-co-n-butyl acrylate) with 90 mol % of 4-vinylphenylboronic pinacolate in the copolymer in C_6D_6. *C_6D_6 and residual solvents.*

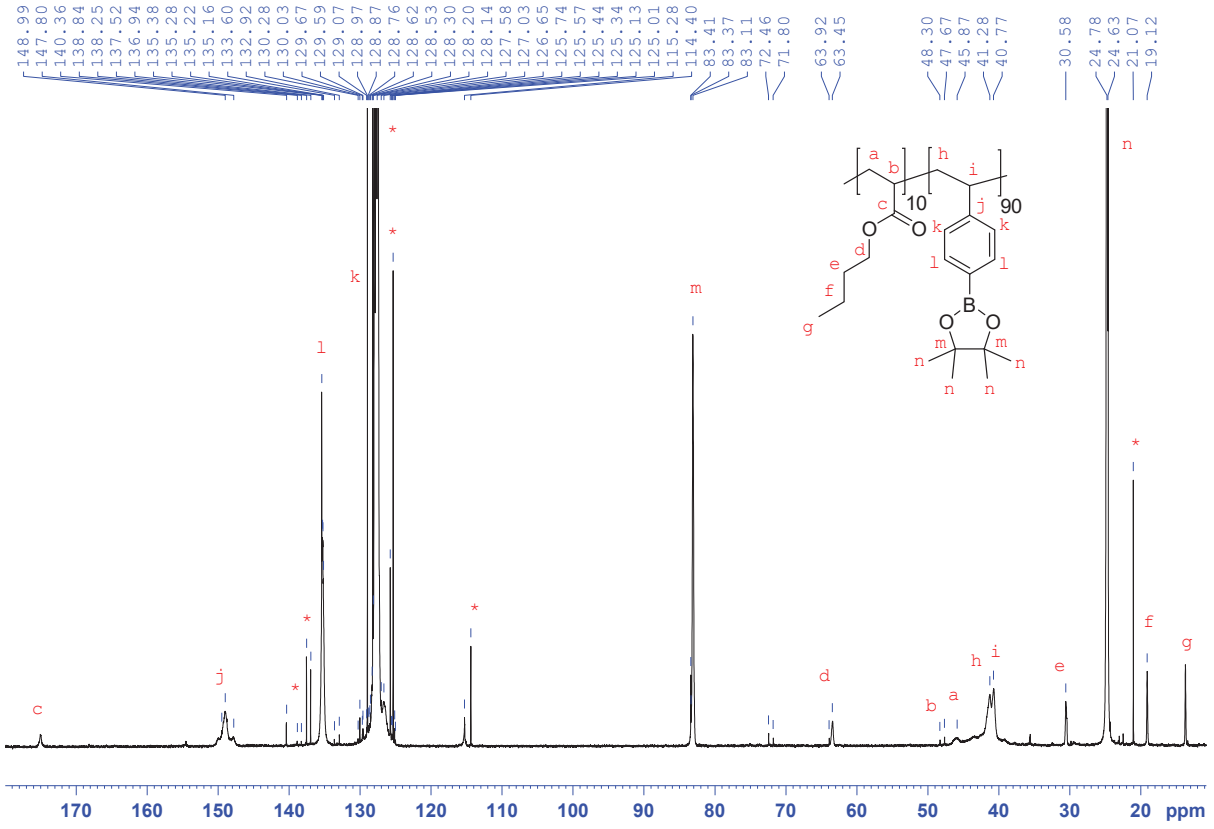

*Figure V. 79: ^{13}C NMR spectrum of poly(4-vinylphenylboronic pinacolate-co-n-butyl acrylate) with 90 mol % of 4-vinylphenylboronic pinacolate in the copolymer in C_6D_6. *C_6D_6 and residual solvents.*

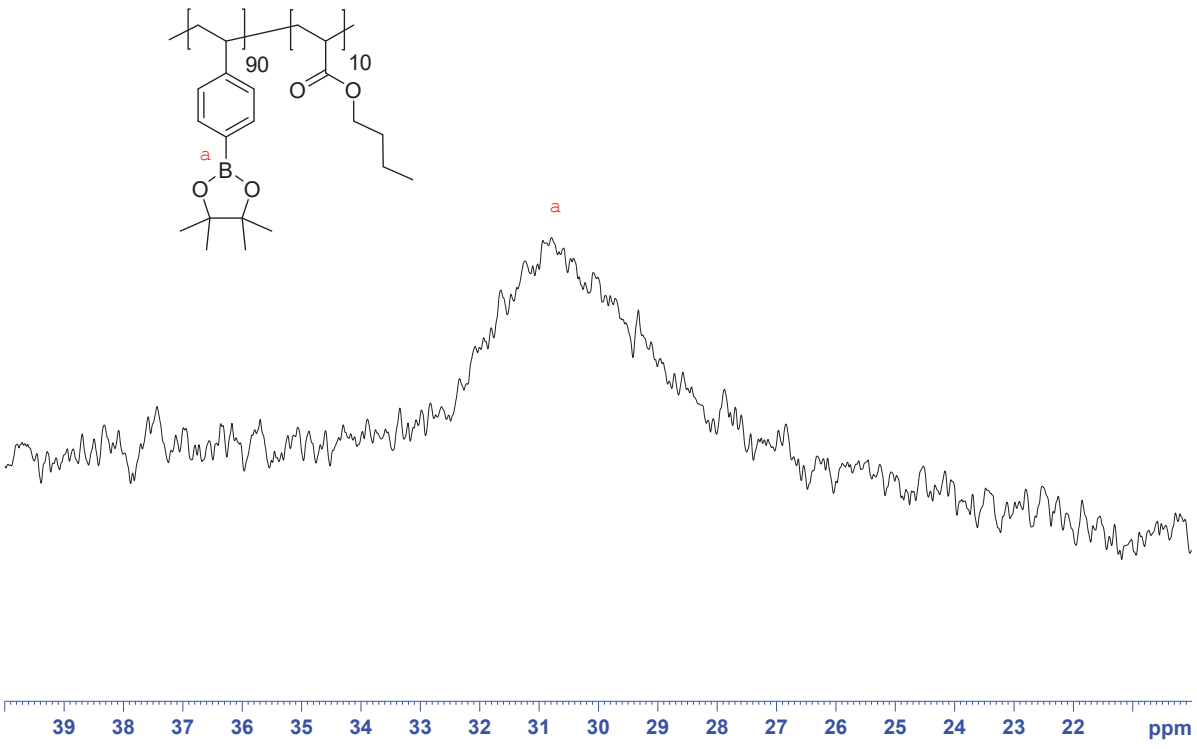

Figure V. 80: ^{11}B NMR spectrum of poly(4-vinylphenylboronic pinacolate-co-n-butyl acrylate) with 90 mol % of 4-vinylphenylboronic pinacolate in the copolymer in C_6D_6.

Size-exclusion chromatography in THF:

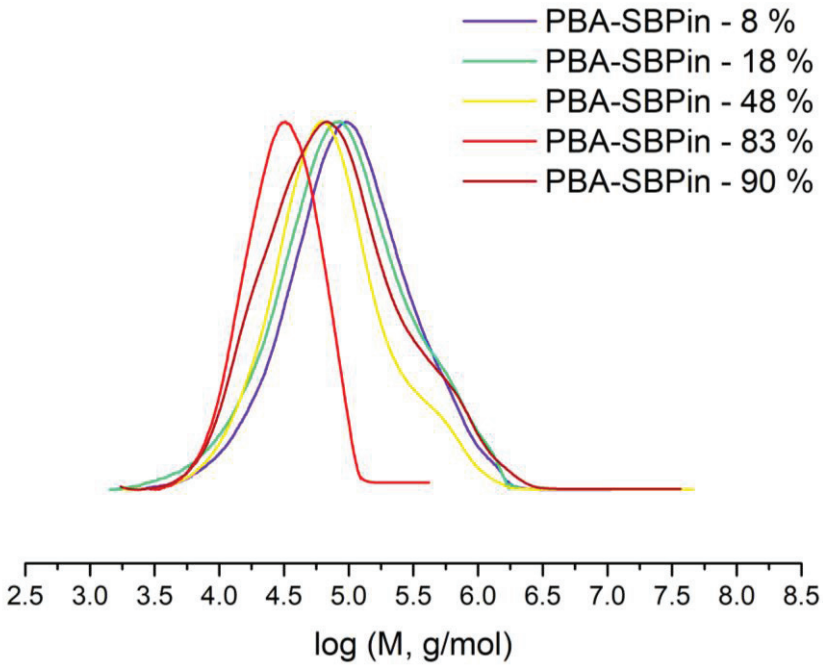

Figure V. 81: Comparison of SEC-THF results for the poly(4-vinylphenylboronic pinacolate-co-n-butyl acrylate).

Differential scanning calorimetry measurements:

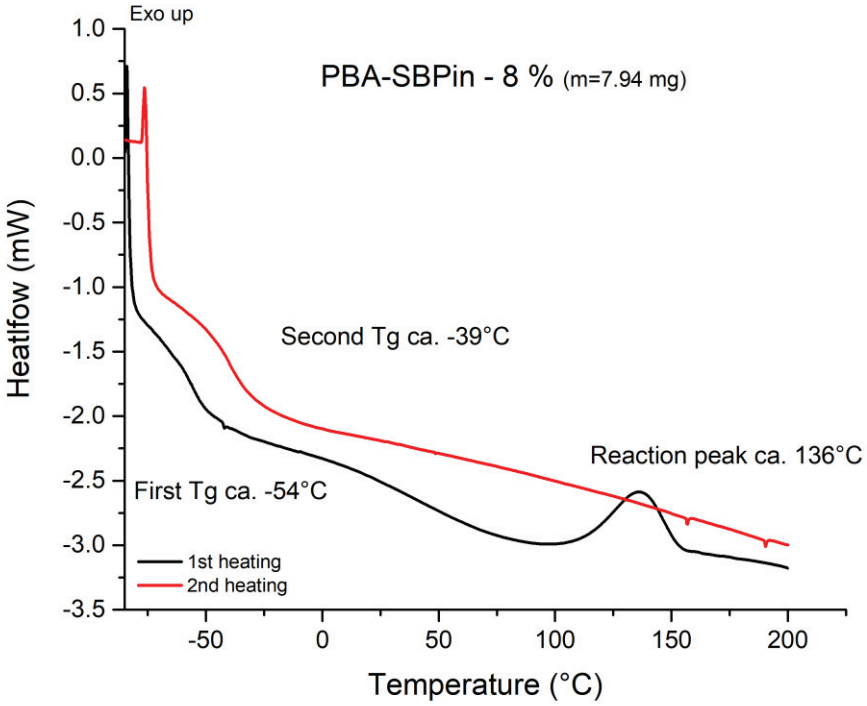

Figure V. 82: DSC thermograms of poly(4-vinylphenylboronic pinacolate-co-n-butyl acrylate) containing 8 mol % of SBPin in 40 µL opened aluminum pans.

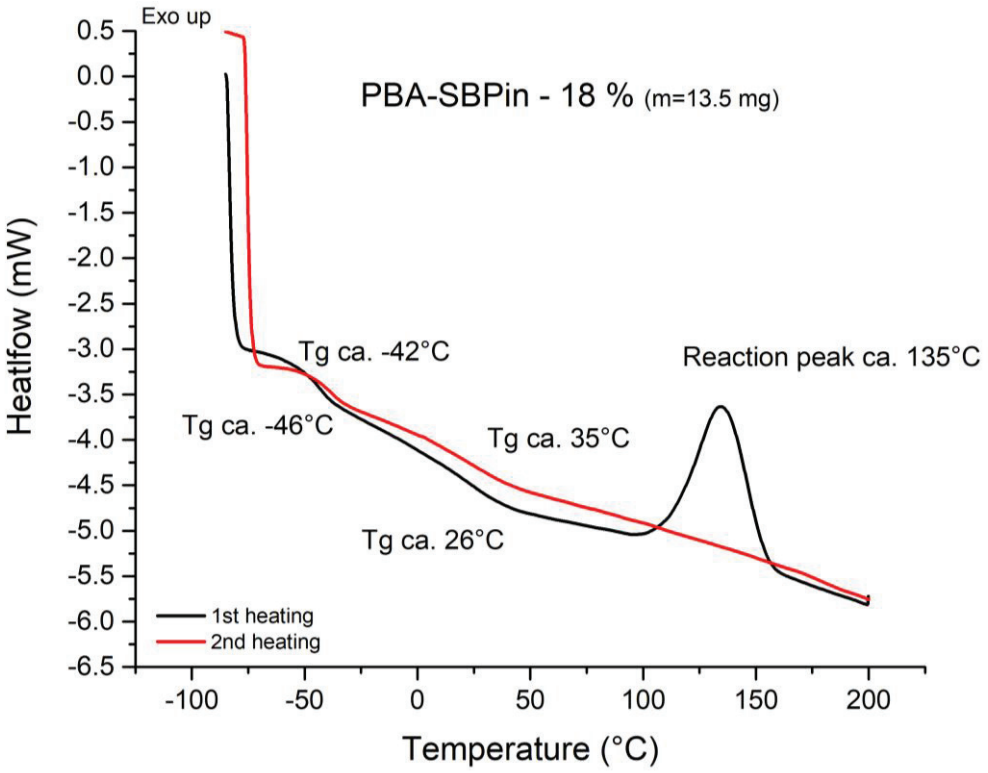

Figure V. 83: DSC thermograms of poly(4-vinylphenylboronic pinacolate-co-n-butyl acrylate) containing 18 mol % of SBPin in 40 µL opened aluminum pans.

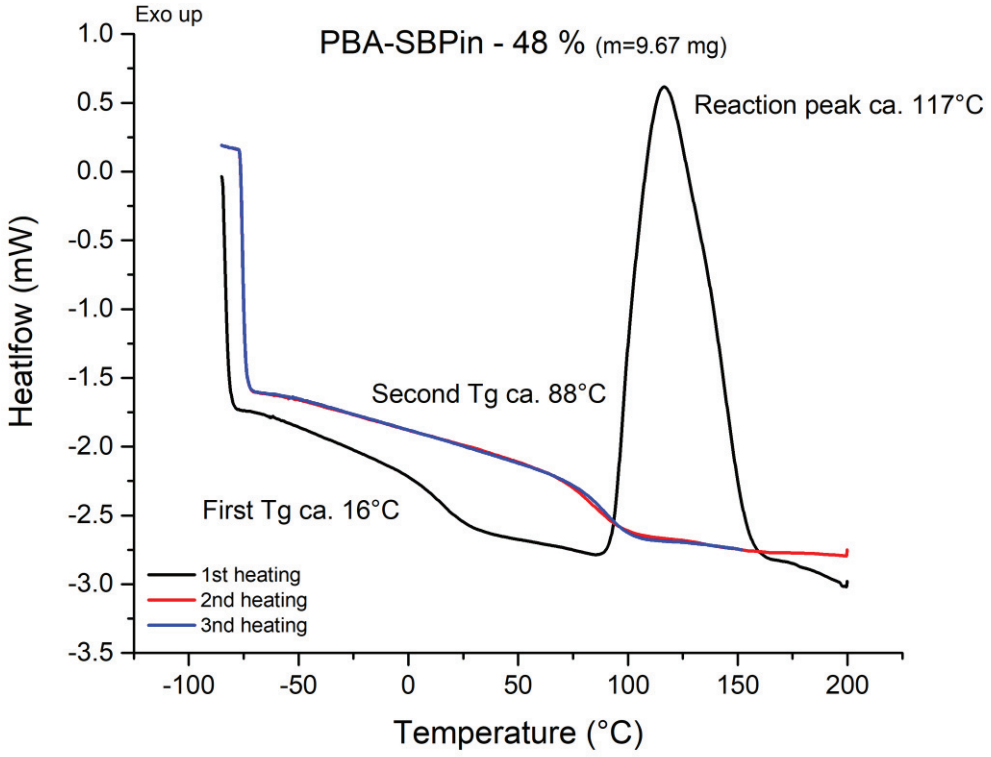

Figure V. 84: DSC thermograms of poly(4-vinylphenylboronic pinacolate-co-n-butyl acrylate) containing 48 mol % of SBPin in 40 µL opened aluminum pans.

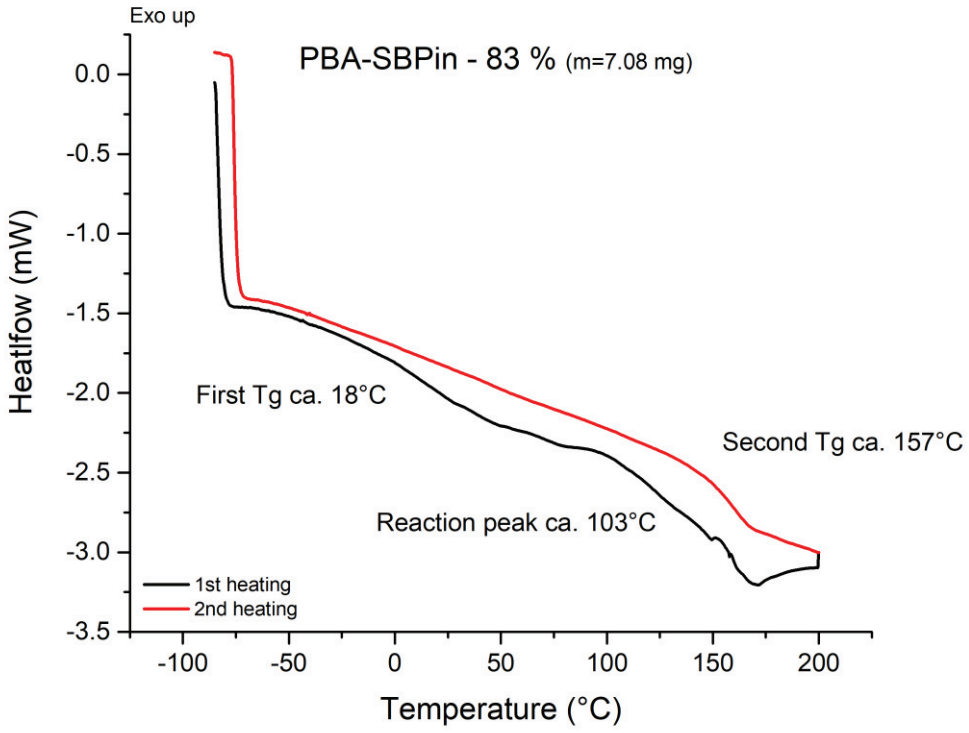

Figure V. 85: DSC thermograms of poly(4-vinylphenylboronic pinacolate-co-n-butyl acrylate) containing 83 mol % of SBPin in 40 µL opened aluminum pans.

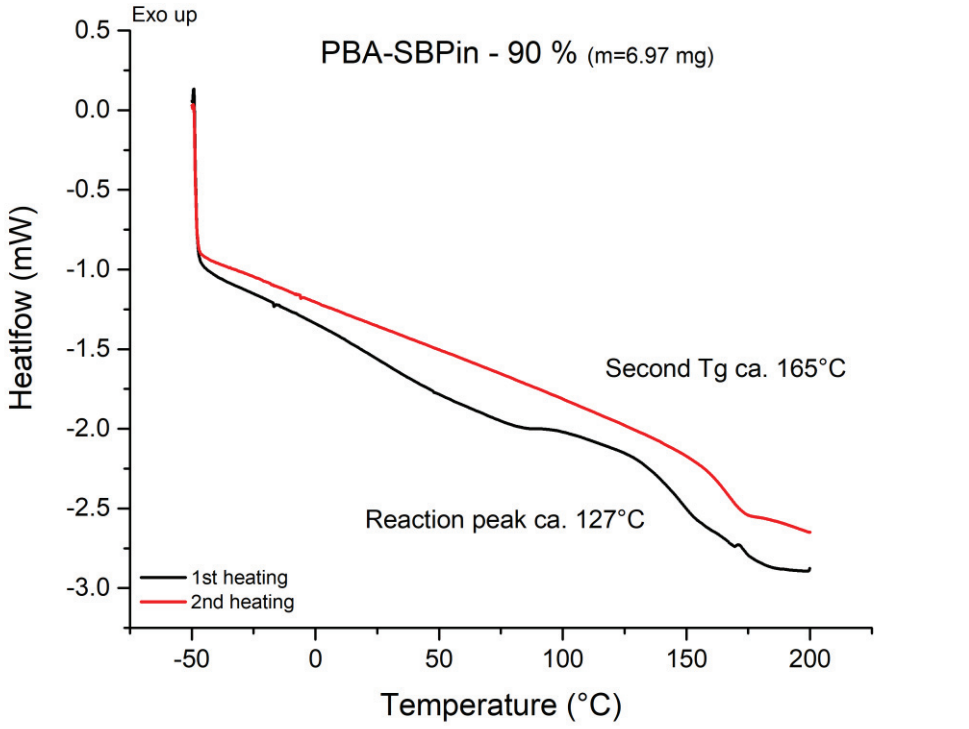

Figure V. 86: DSC thermograms of poly(4-vinylphenylboronic pinacolate-co-n-butyl acrylate) containing 90 mol % of SBPin in 40 µL opened aluminum pans.

Thermogravimetric analysis:

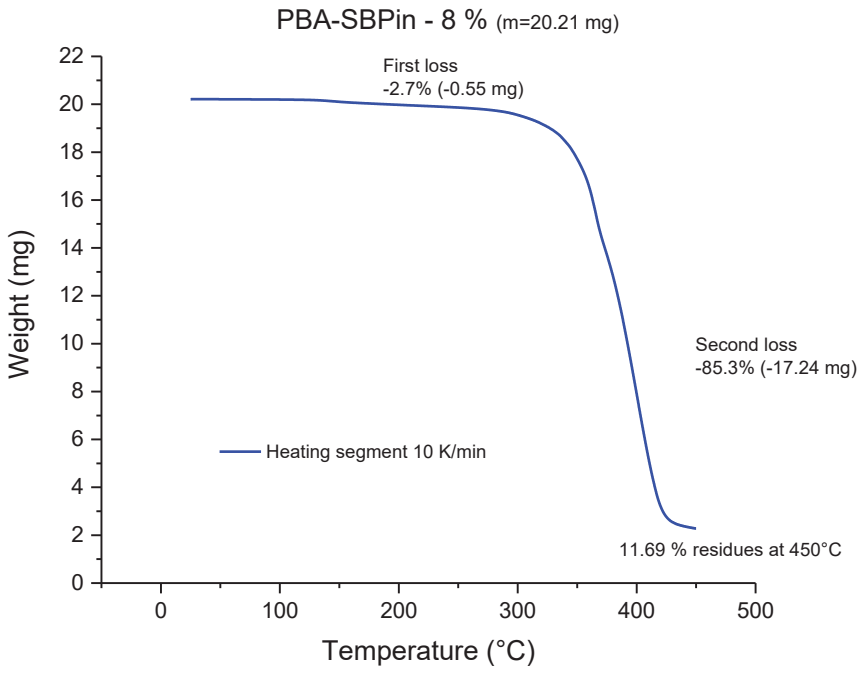

Figure V. 87: TGA thermal curve of poly(n-butyl acrylate-co-4-vinylphenylboronic pinacolate) containing 8 mol % of 4-vinylphenylboronic pinacolate in 100 µL alumina crucible.

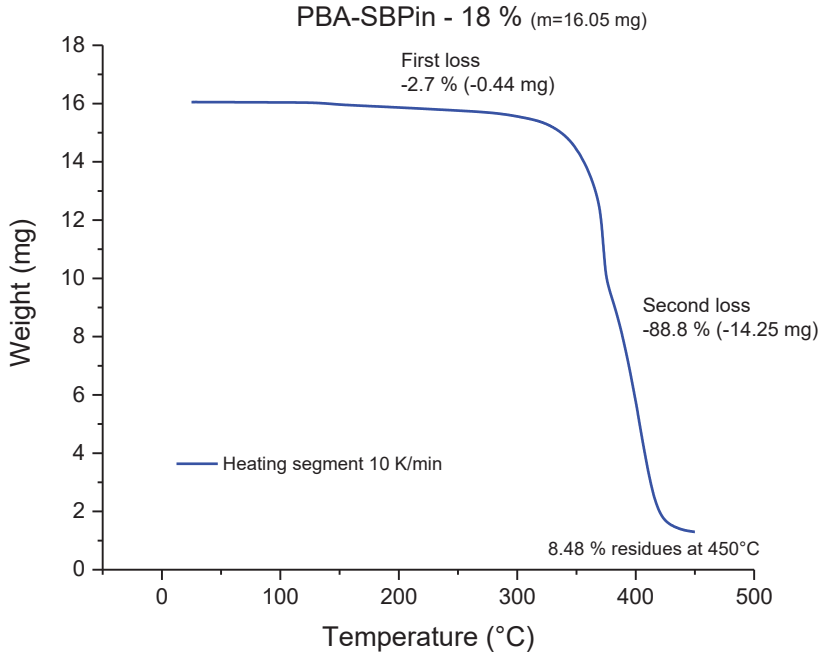

Figure V. 88: TGA thermal curve of poly(n-butyl acrylate-co-4-vinylphenylboronic pinacolate) containing 18 mol % of 4-vinylphenylboronic pinacolate in 100 µL alumina crucible.

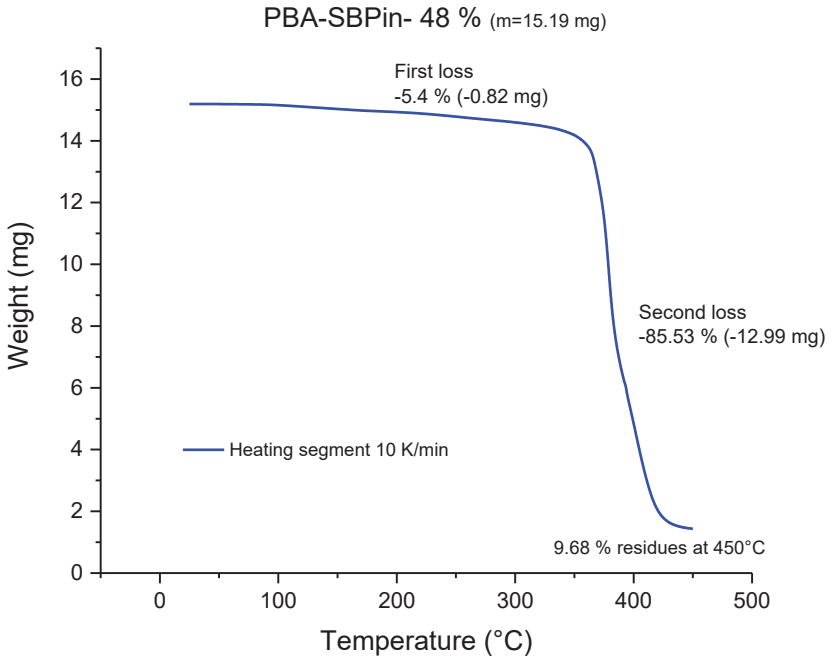

Figure V. 89: TGA thermal curve of poly(n-butyl acrylate-co-4-vinylphenylboronic pinacolate) containing 48 mol % of 4-vinylphenylboronic pinacolate in 100 µL alumina crucible.

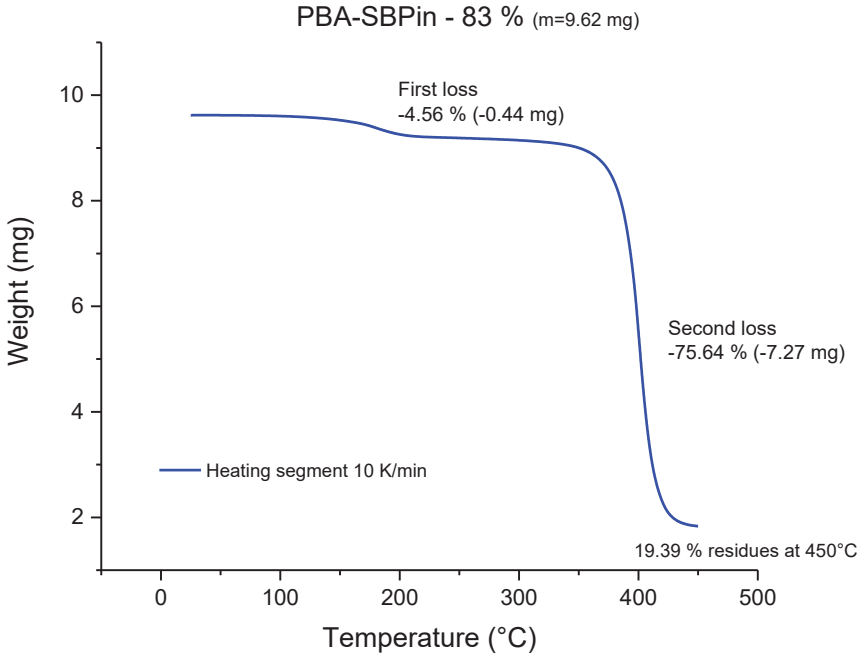

Figure V. 90: TGA thermal curve of poly(n-butyl acrylate-co-4-vinylphenylboronic pinacolate) containing 83 mol % of 4-vinylphenylboronic pinacolate in 100 µL alumina crucible.

B. Synthesis and characterization of hybrid glasses

Experimental protocol:

1,3,5-phenyltriboronic, tris(pinacol) ester and pentaerythritol were crushed in solid state in a mortar in controlled amounts. The solid mix obtained was then dried under vacuum during 20 minutes. The powder mix was heated in a Schlenk vessel under argon at 300°C in an oven to allow the reaction in the molten state. The reaction was then tempered at ambient temperature and the viscosity of the mix increased until the complete curing.

NMR spectroscopies:

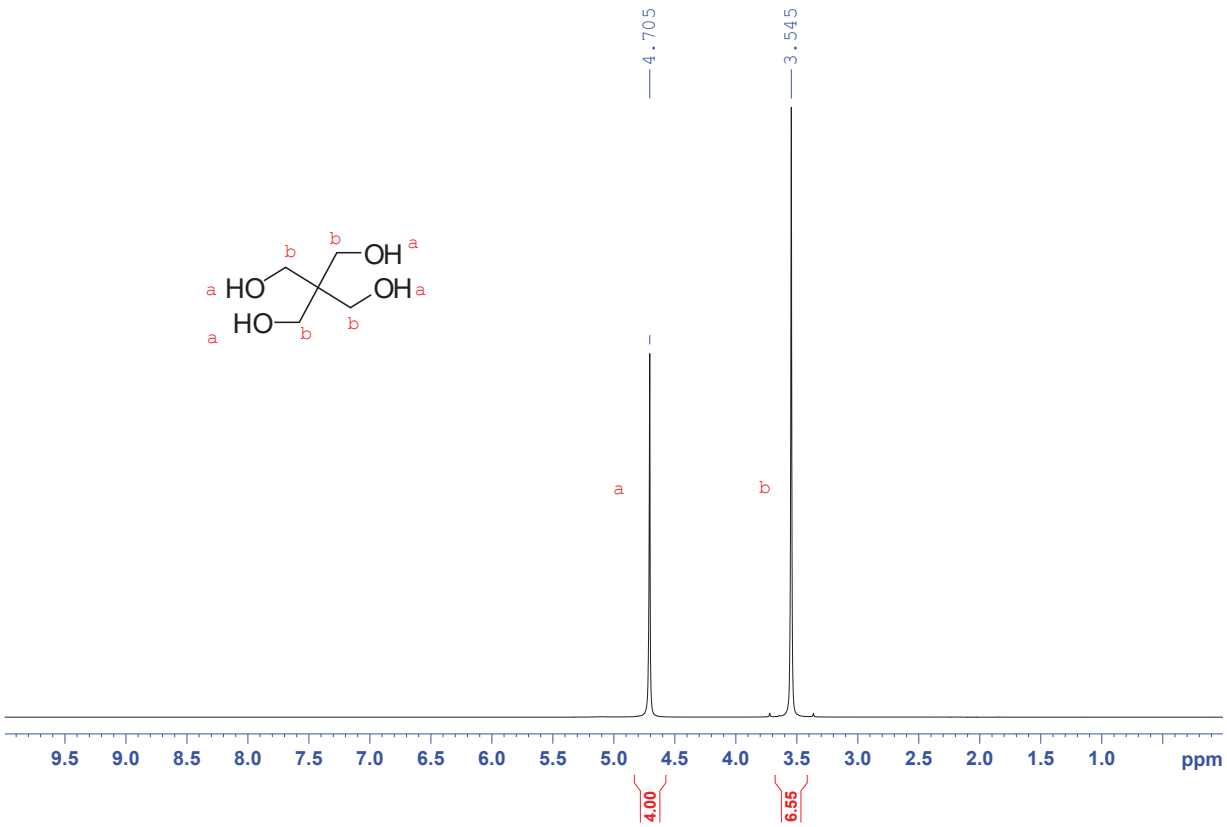

Figure V. 91: ^{1}H NMR spectrum of pentaerythritol in D_2O.

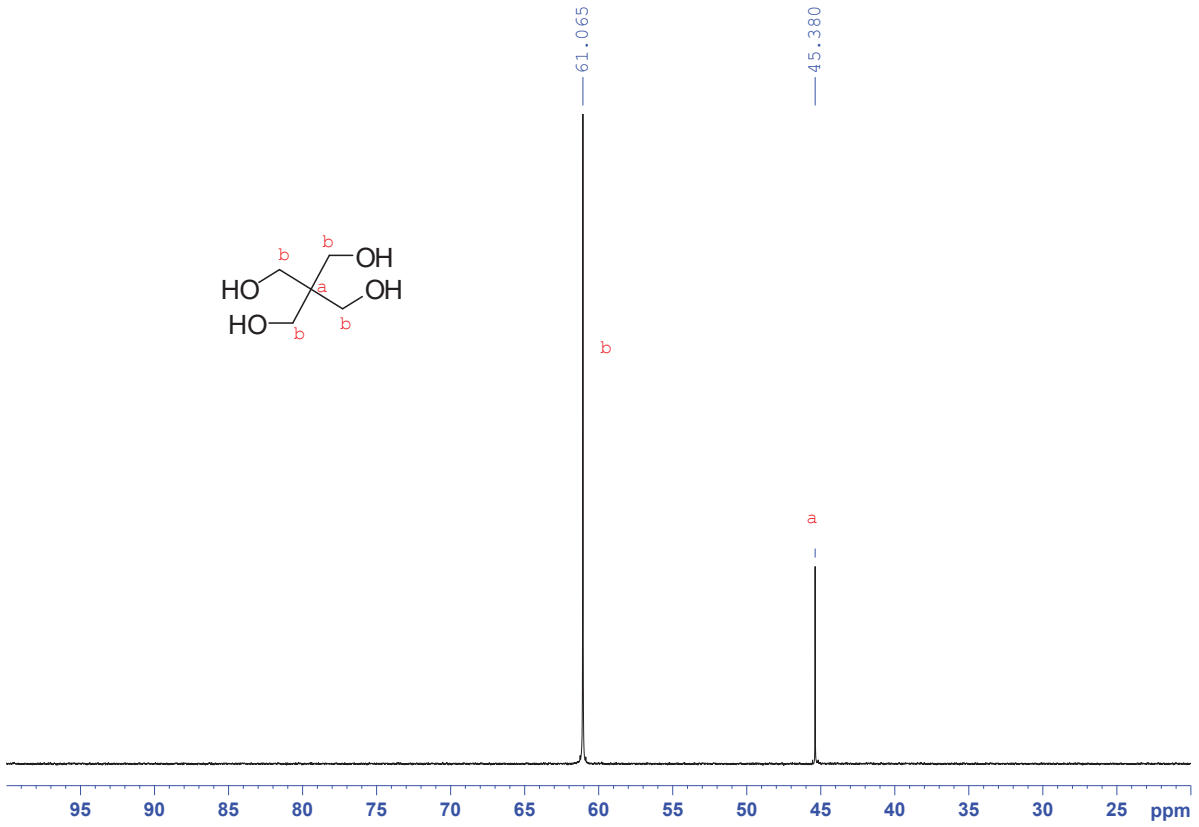

Figure V. 92: ^{13}C NMR spectrum of pentaerythritol in D_2O.

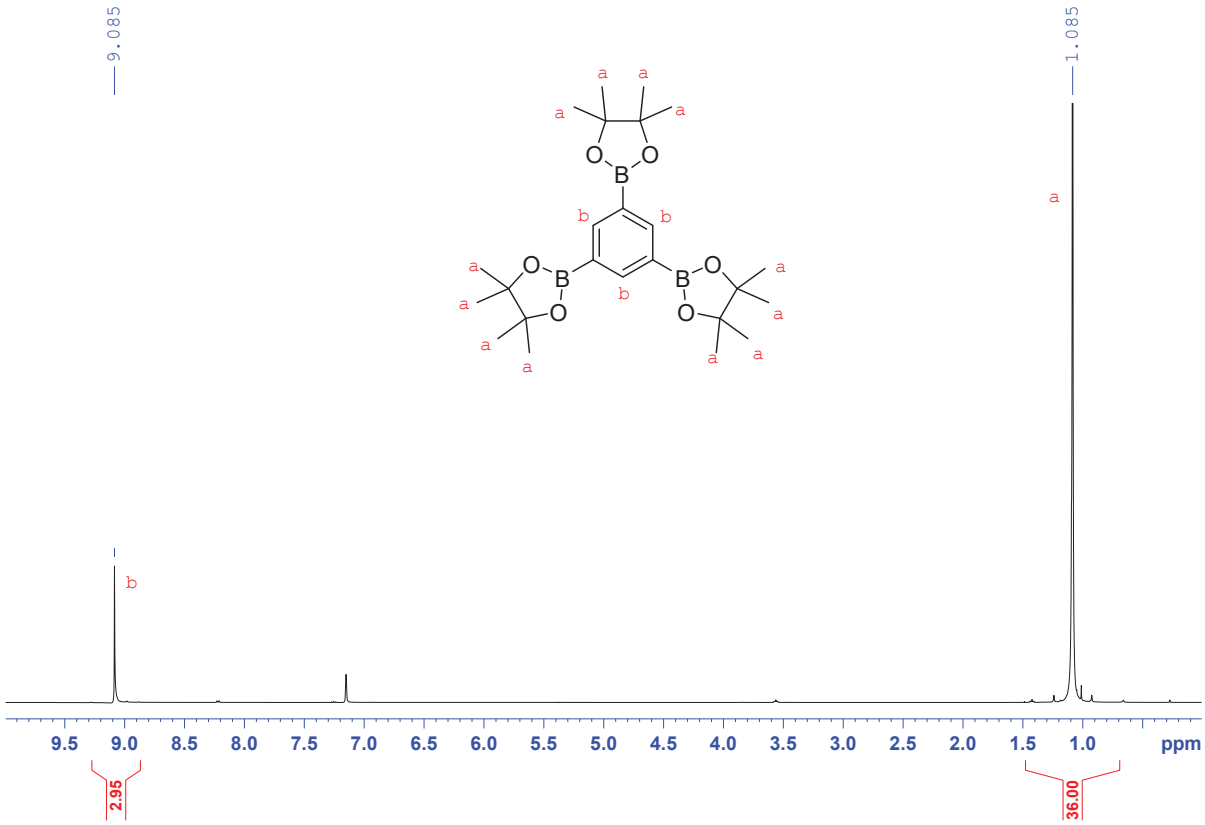

Figure V. 93: ^1H NMR spectrum of 1,3,5-phenyltriboronic acid, tris(pinacol)ester in C_6D_6.

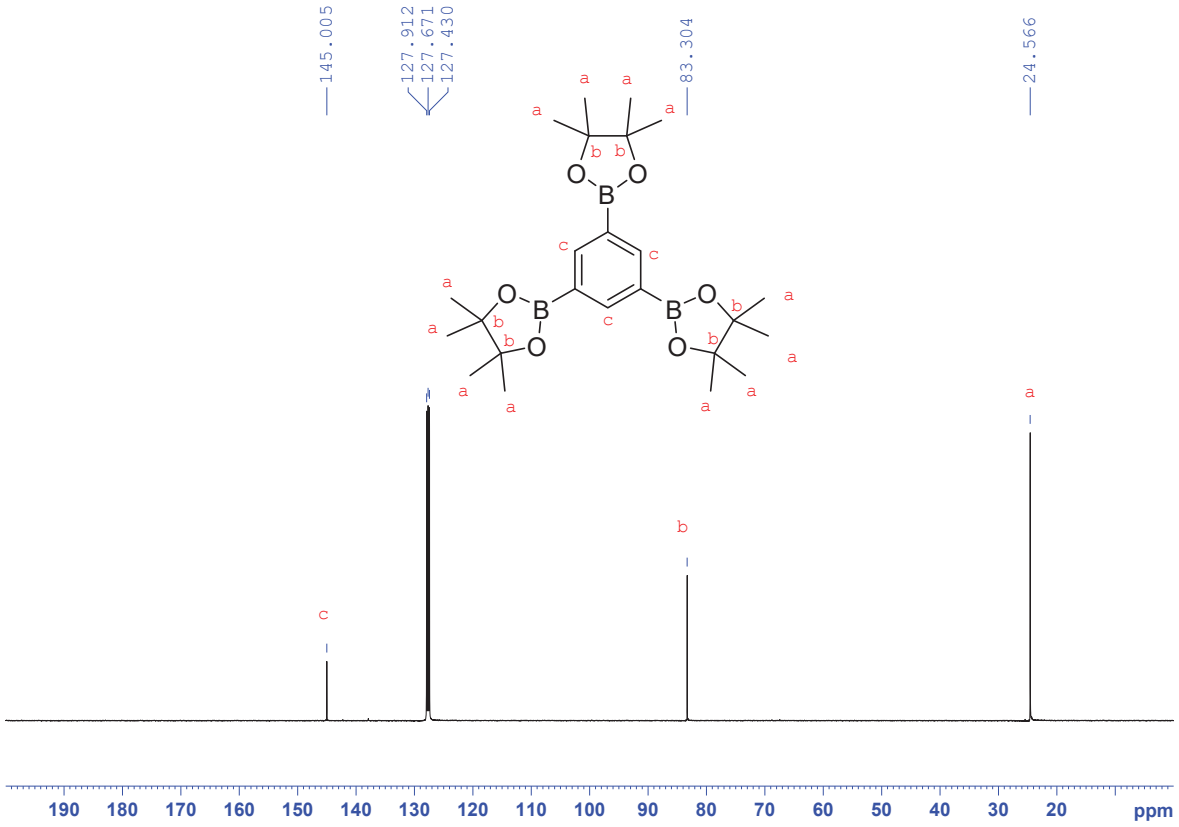

Figure V. 94: ^{13}C NMR spectrum of 1,3,5-phenyltriboronic acid, tris(pinacol)ester in C_6D_6.

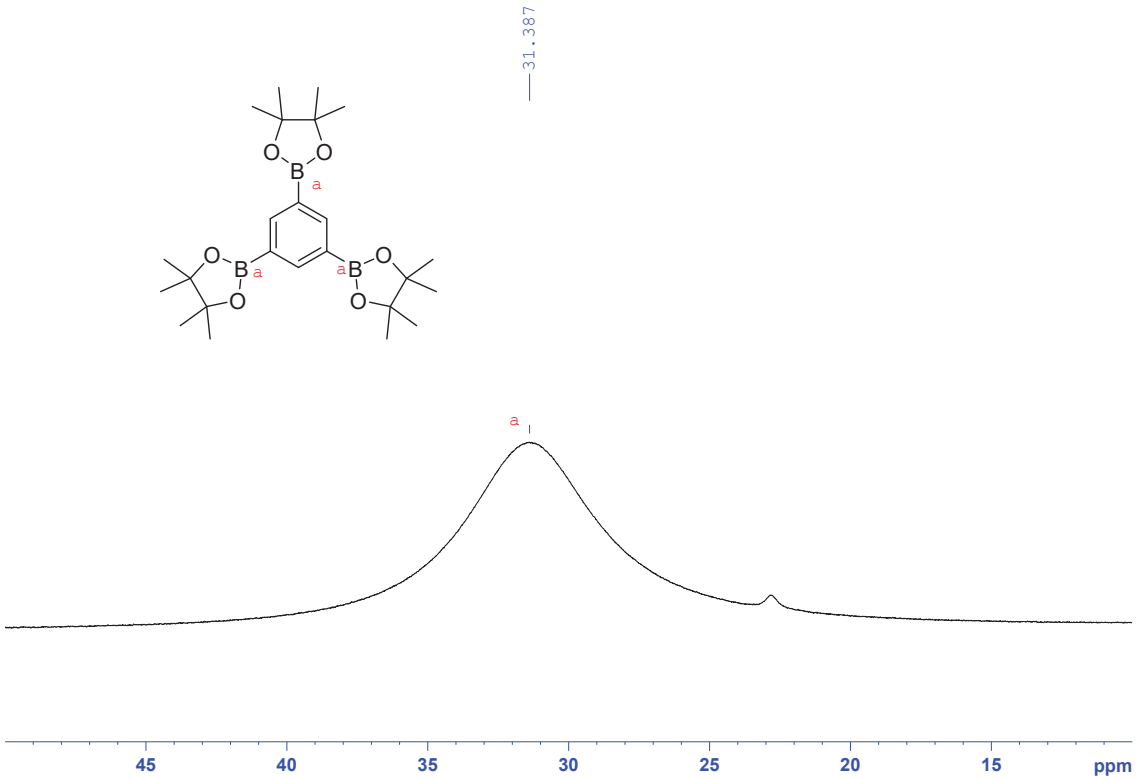

Figure V. 95: ^{11}B NMR spectrum of 1,3,5-phenyltriboronic acid, tris(pinacol)ester in C_6D_6. Small signal at 22.5 ppm could be due to hydration of the product.

Table V. 1: Macroscopic observations of the formation of hybrid glasses from the reaction of 1,3,5-phenyltriboronic acid, tris(pinacol)ester with different ratios of pentaerythritol.

0 % mol of pentaerythritol / BPin 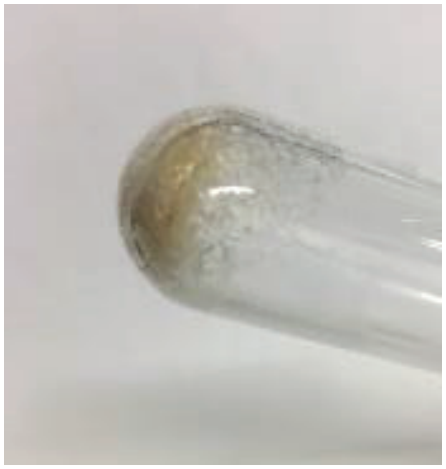	**2 % mol of pentaerythritol / BPin** 
5 % mol of pentaerythritol / BPin 	**10 % mol of pentaerythritol / BPin** 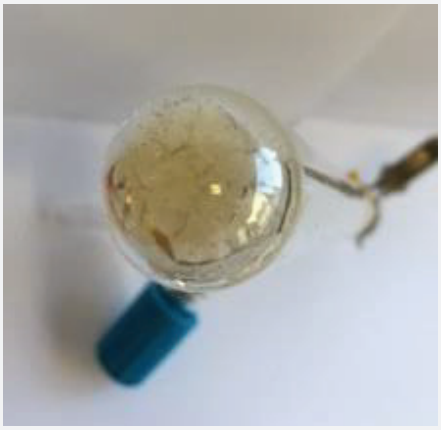
20 % mol of pentaerythritol / BPin 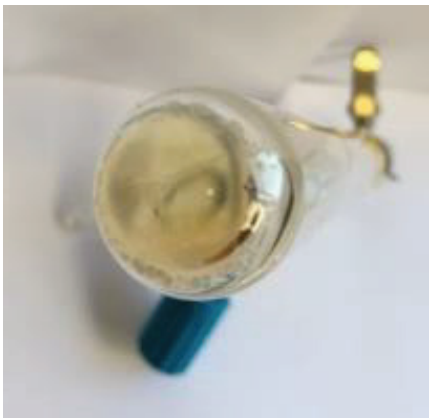	

Differential scanning calorimetry measurements:

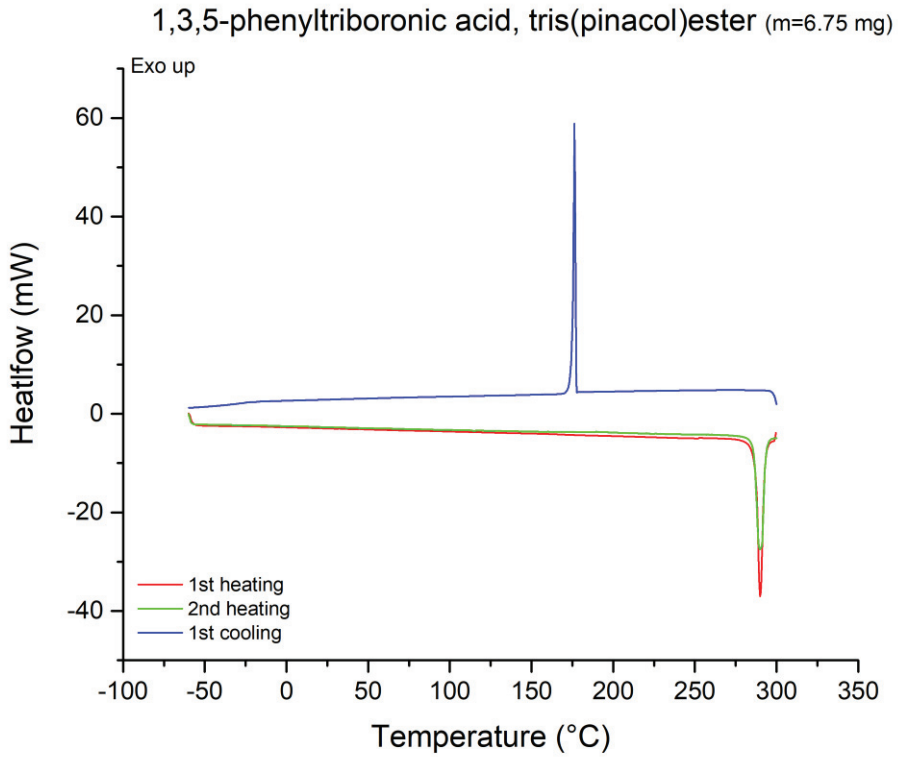

Figure V. 96: DSC thermograms of 1,3,5-phenyltriboronic acid, tris(pinacol)ester in 40 µL opened aluminum pans.

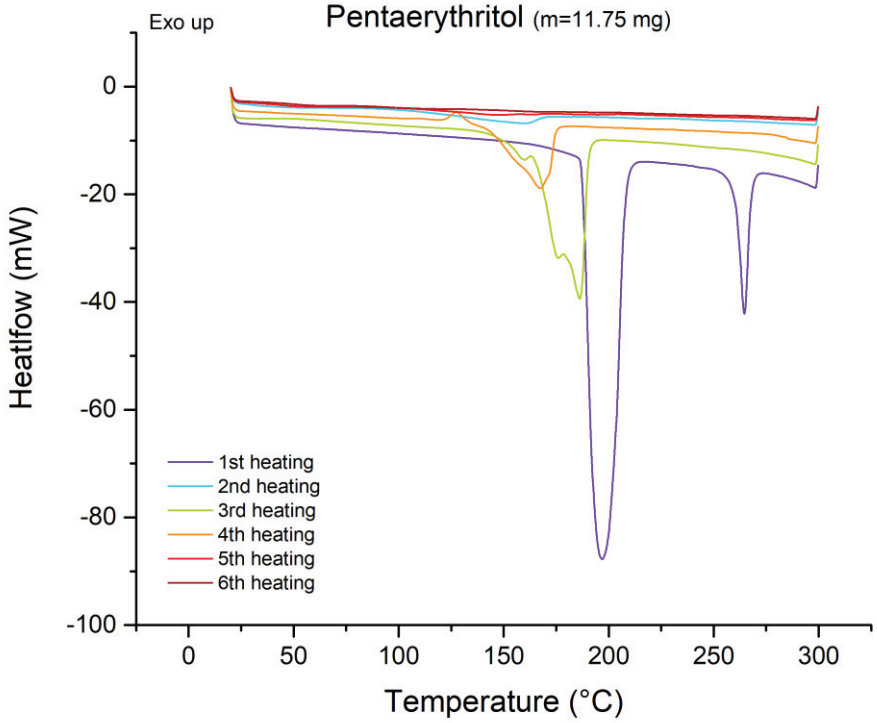

Figure V. 97: DSC thermograms of pentaerythritol in 40 µL opened aluminum pans.

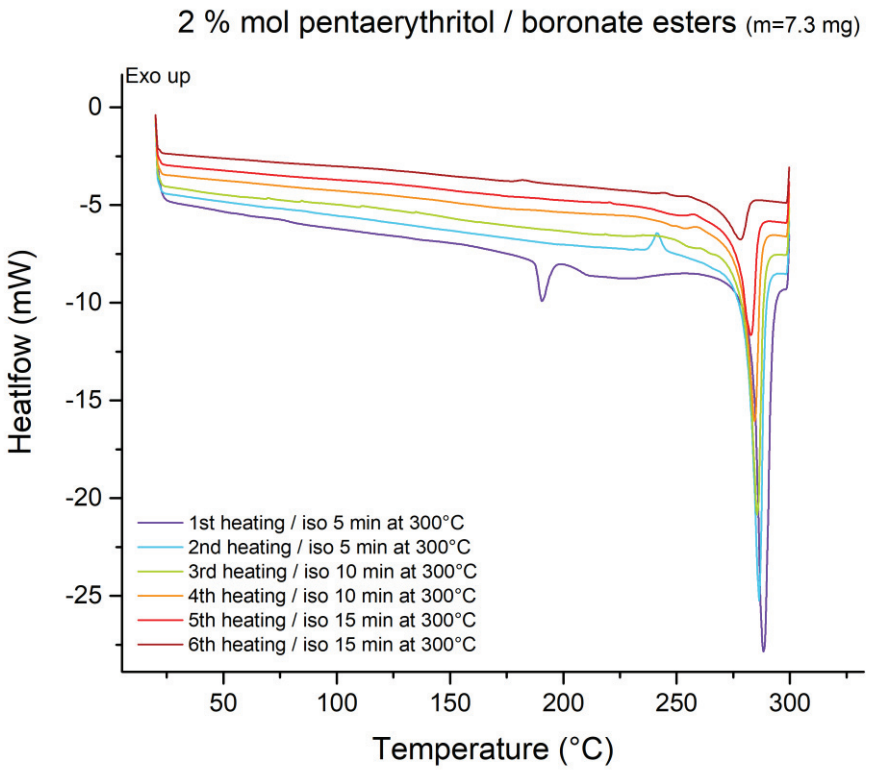

Figure V. 98: DSC thermograms of the reaction of 1,3,5-phenyltriboronic acid, tris(pinacol)ester with 2 mol % of pentaerythritol compared to boronate ester groups in 40 µL opened aluminum pans.

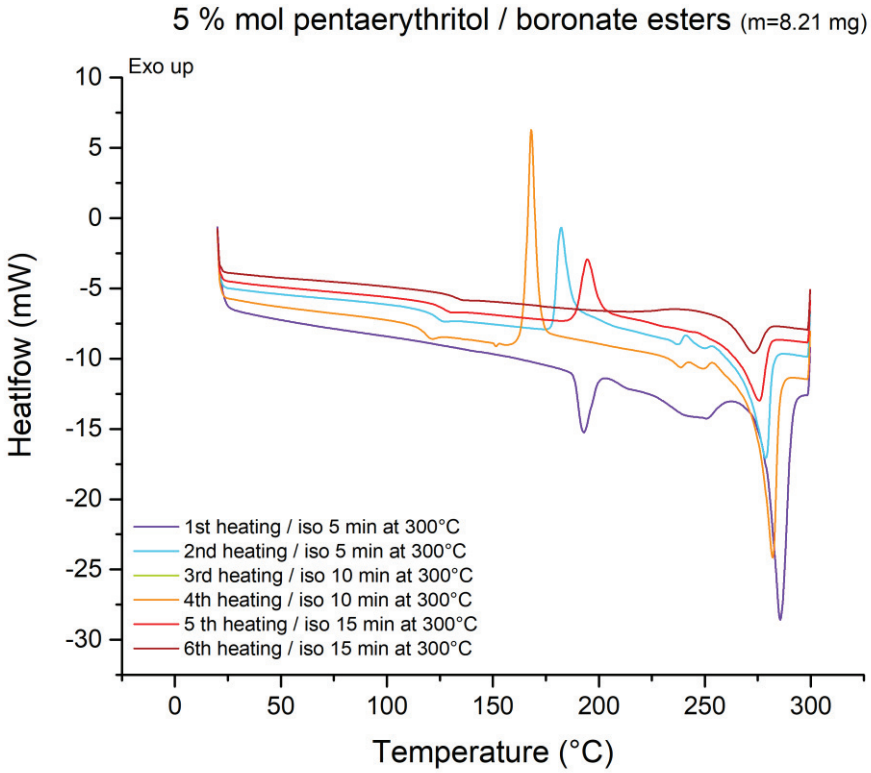

Figure V. 99: DSC thermograms of the reaction of 1,3,5-phenyltriboronic acid, tris(pinacol)ester with 5 mol % of pentaerythritol compared to boronate ester groups in 40 µL opened aluminum pans.

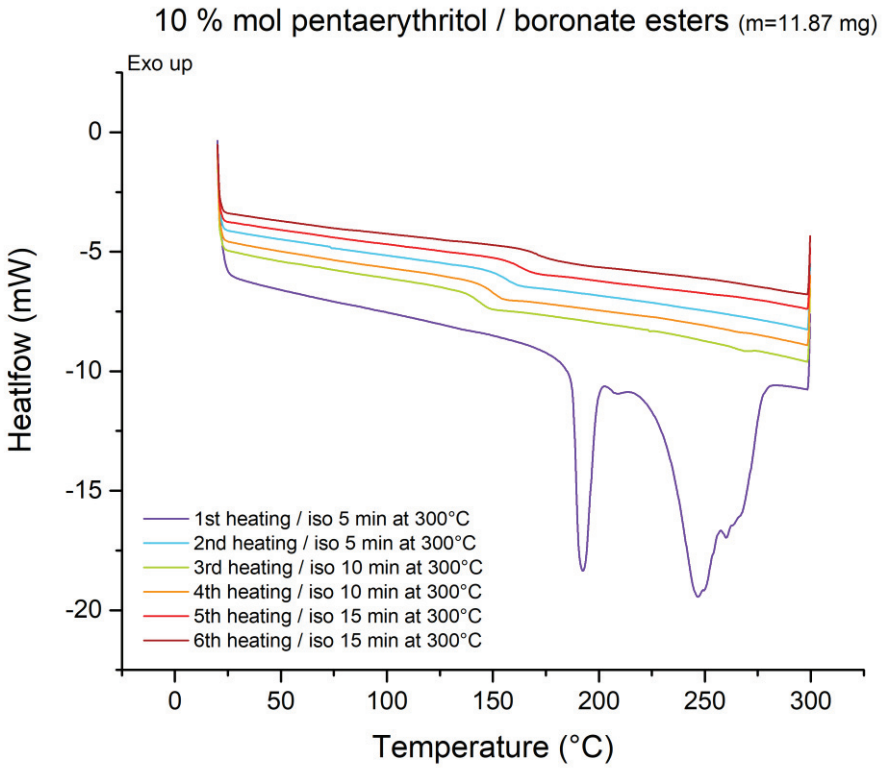

Figure V. 100: DSC thermograms of the reaction of 1,3,5-phenyltriboronic acid, tris(pinacol)ester with 10 mol % of pentaerythritol compared to boronate ester groups in 40 µL opened aluminum pans.

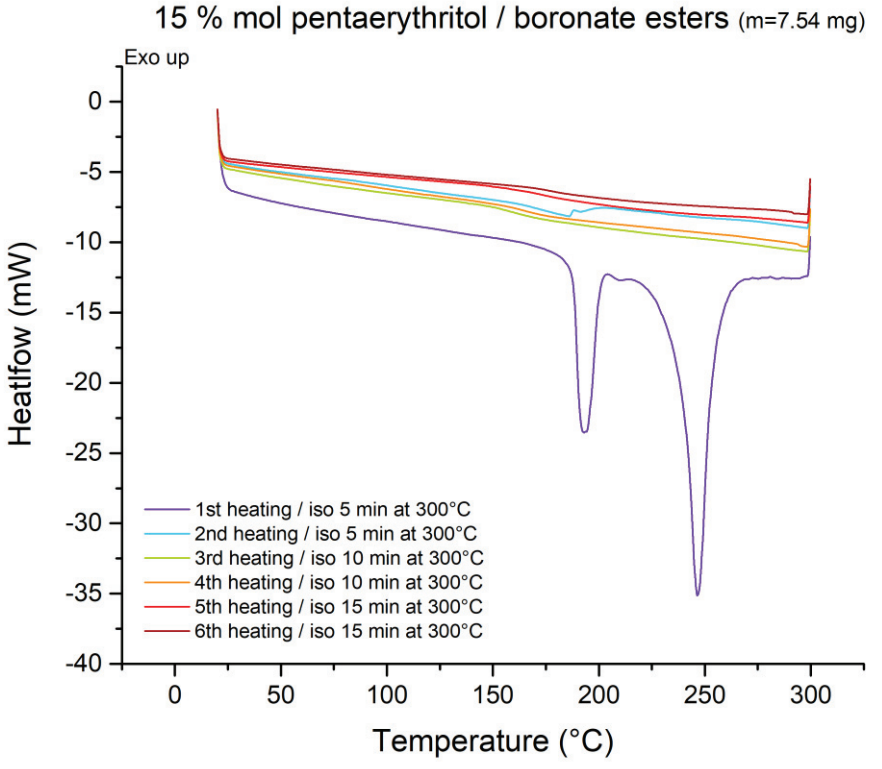

Figure V. 101: DSC thermograms of the reaction of 1,3,5-phenyltriboronic acid, tris(pinacol)ester with 15 mol % of pentaerythritol compared to boronate ester groups in 40 µL opened aluminum pans.

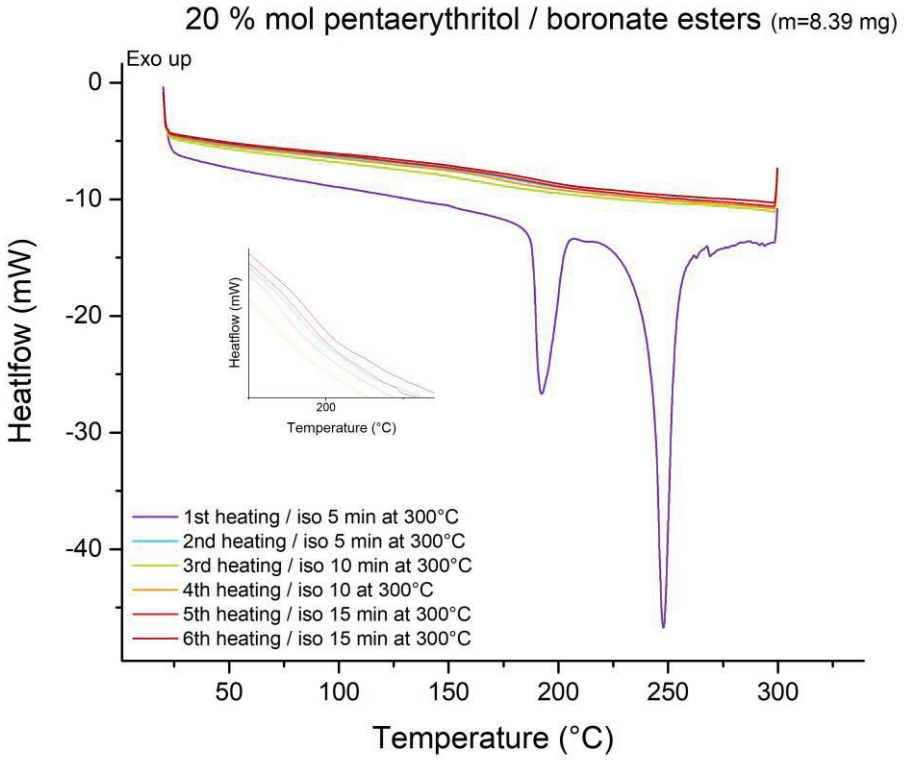

Figure V. 102: DSC thermograms of the reaction of 1,3,5-phenyltriboronic acid, tris(pinacol)ester with 20 mol % of pentaerythritol compared to boronate ester groups in 40 µL opened aluminum pans.

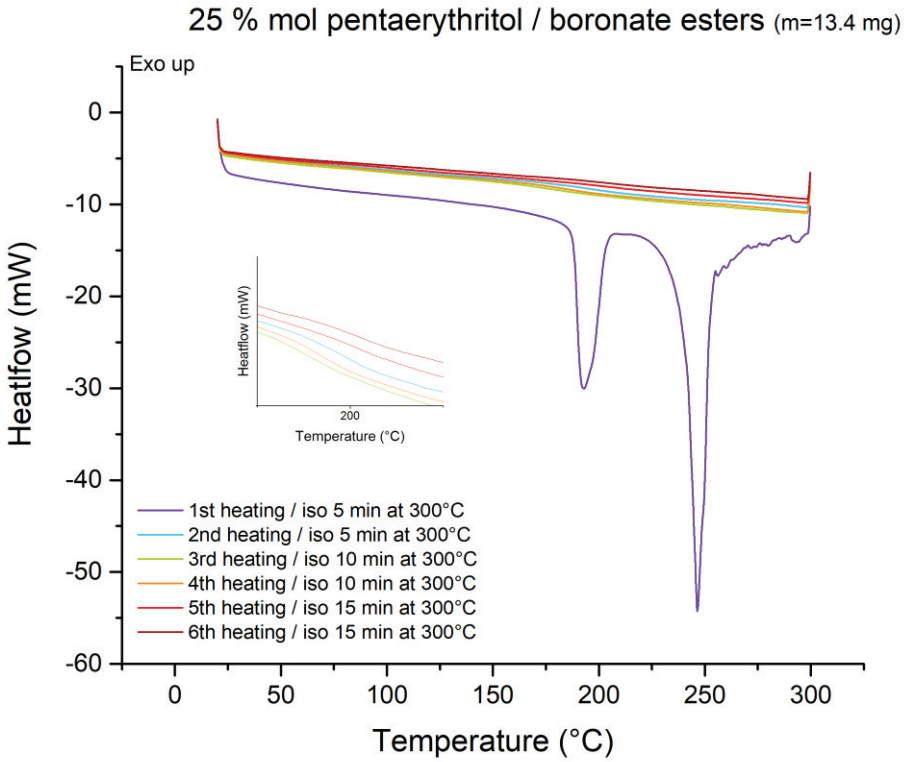

Figure V. 103: DSC thermograms of the reaction of 1,3,5-phenyltriboronic acid, tris(pinacol)ester with 25 mol % of pentaerythritol compared to boronate ester groups in 40 µL opened aluminum pans.

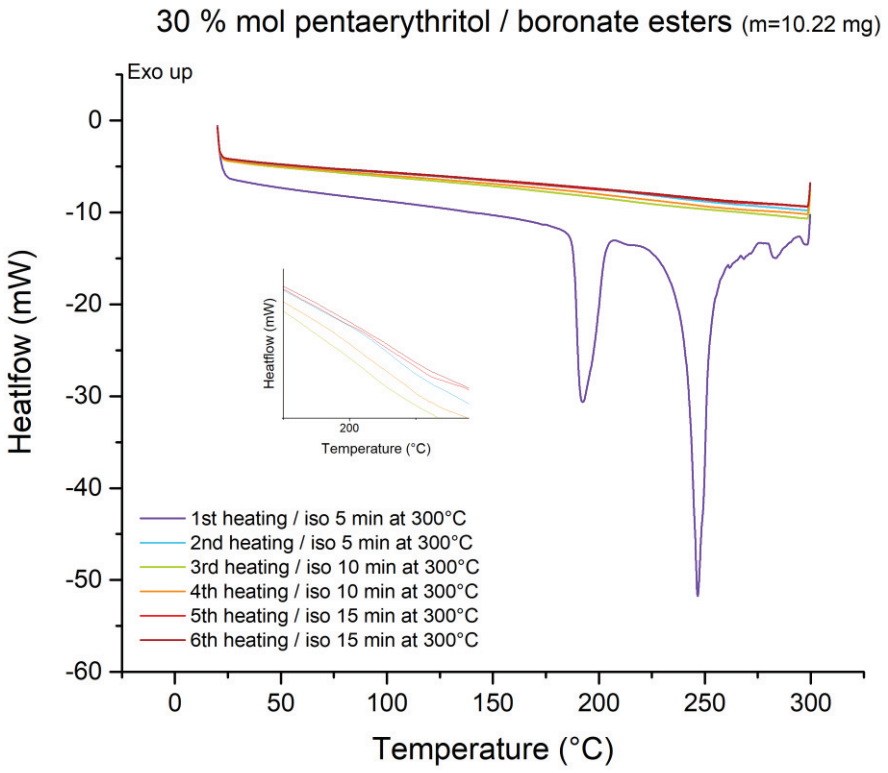

Figure V. 104: DSC thermograms of the reaction of 1,3,5-phenyltriboronic acid, tris(pinacol)ester with 30 mol % of pentaerythritol compared to boronate ester groups in 40 µL opened aluminum pans.

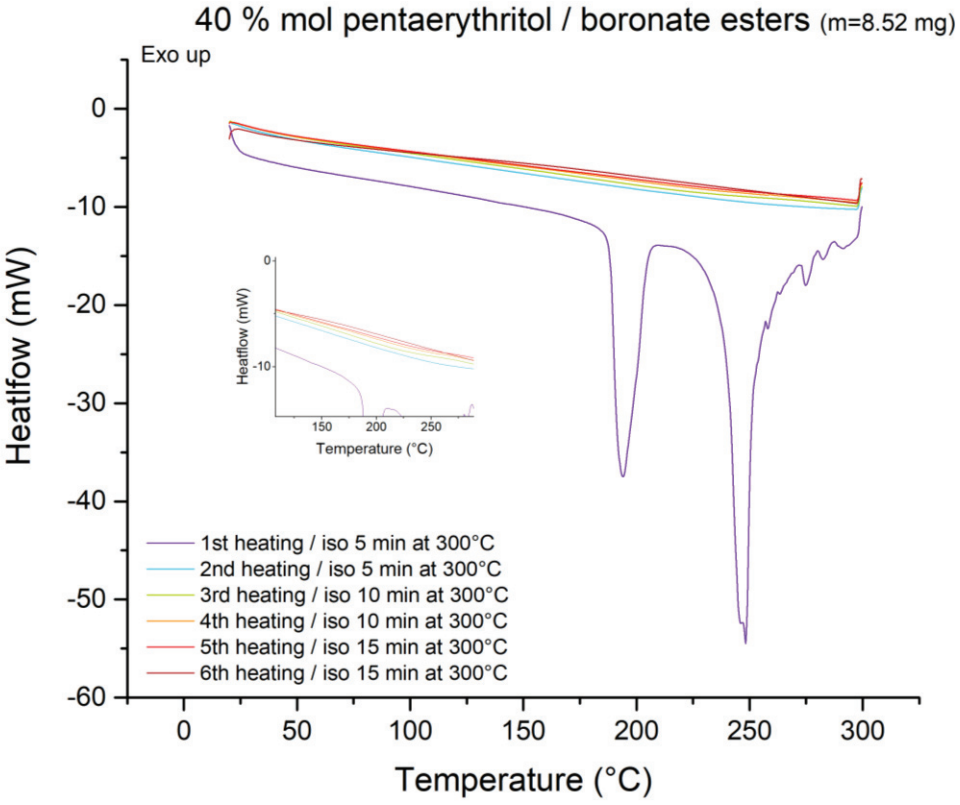

Figure V. 105: DSC thermograms of the reaction of 1,3,5-phenyltriboronic acid, tris(pinacol)ester with 40 mol % of pentaerythritol compared to boronate ester groups in 40 µL opened aluminum pans.

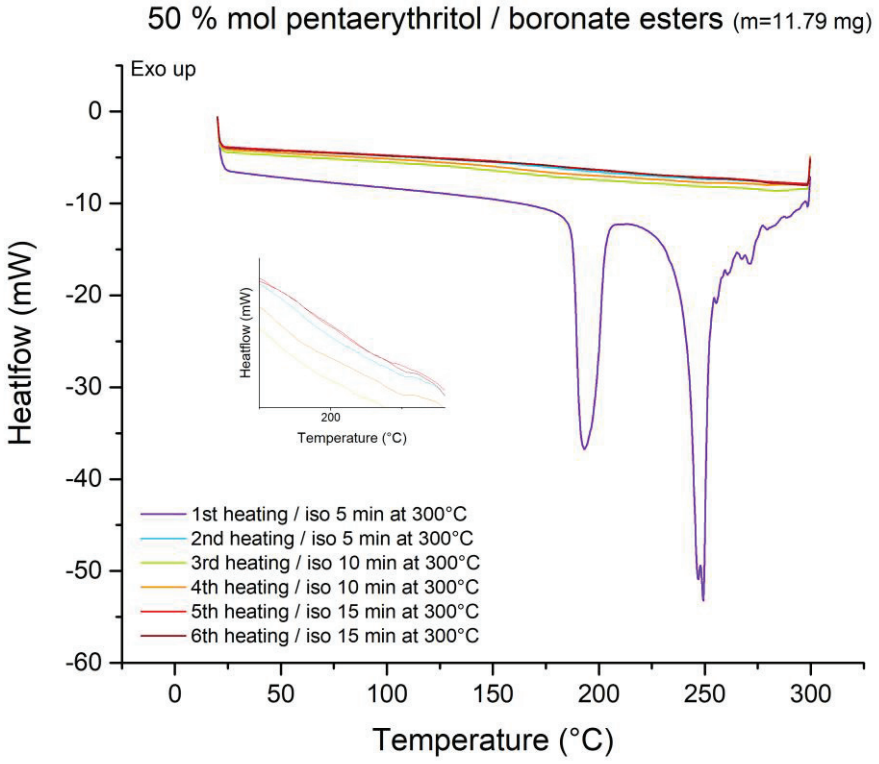

Figure V. 106: DSC thermograms of the reaction of 1,3,5-phenyltriboronic acid, tris(pinacol)ester with 50 mol % of pentaerythritol compared to boronate ester groups in 40 µL opened aluminum pans.

C. Synthesis and characterization of poly(vinylboronic pinacolate)

Experimental protocol:

Vinylboronic acid, pinacol ester (3.8 g, 16 mmol) and benzoyl peroxide (0.02 eq, 0.33 mmol, 80 mg) were introduced in a Schlenk vessel with 3.8 mL toluene (degassed by three freeze-pump-thawing cycles). Prior to the polymerization reaction, one molar equivalent of THF was added to the media compared to the monomer amount. Then, the media was heated to 70°C. The polymerization was conducted during 72h. Then, the reaction media was concentrated under vacuum and dissolved in chloroform then dried under high vacuum. The polymer was obtained as a white powder. Yield: 61%.

^{1}H NMR (300 MHz, benzene-d_6, 25°C, δ): 2.27-1.70 (1H), 1.69-1.40 (2H), 1.40-0.66 (12H).

^{13}C NMR (400 MHz, benzene-d_6, 25°C, δ): 82.2, 35.1, 24.6, 23.2.

^{11}B NMR (300 MHz, benzene-d_6, 25°C, δ): 29.5.

NMR spectroscopies:

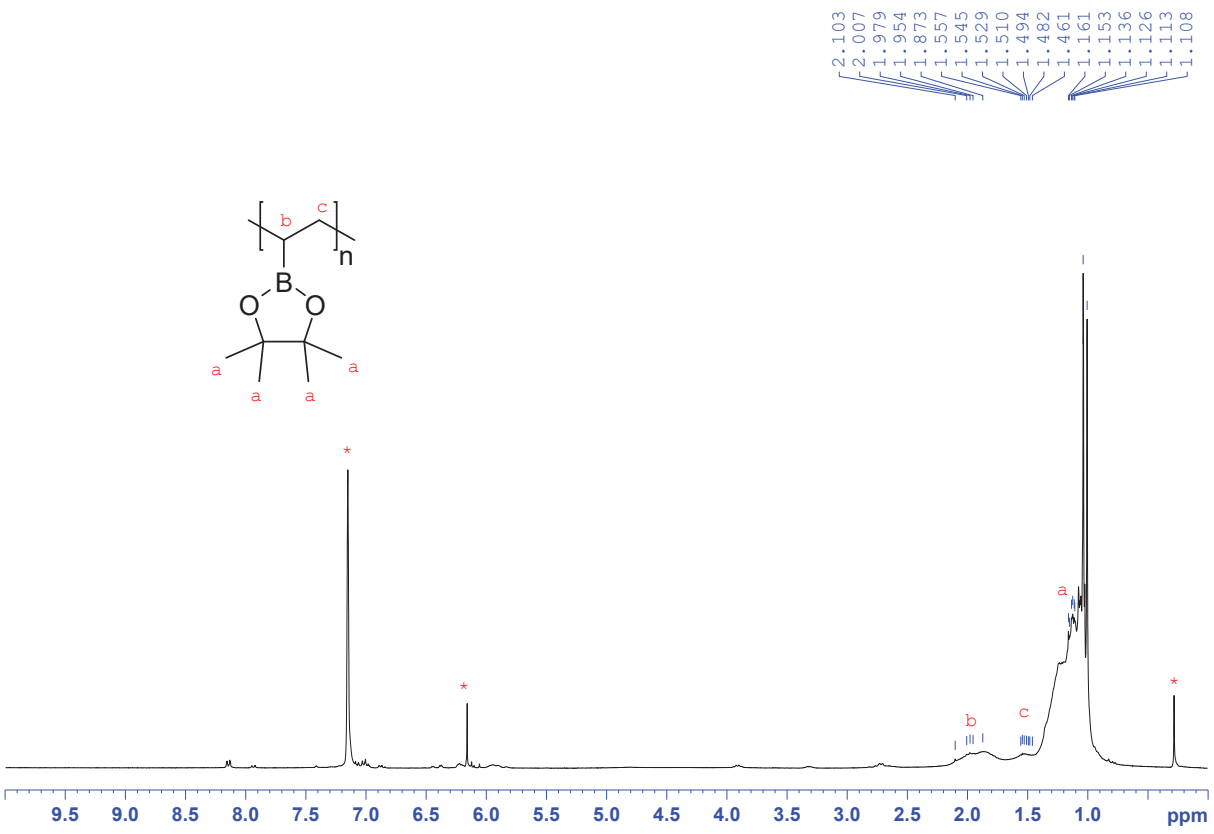

*Figure V. 107: ^{1}H NMR spectrum of poly(vinylboronic pinacolate) in C_6D_6. *C_6D_6 and residual solvents.*

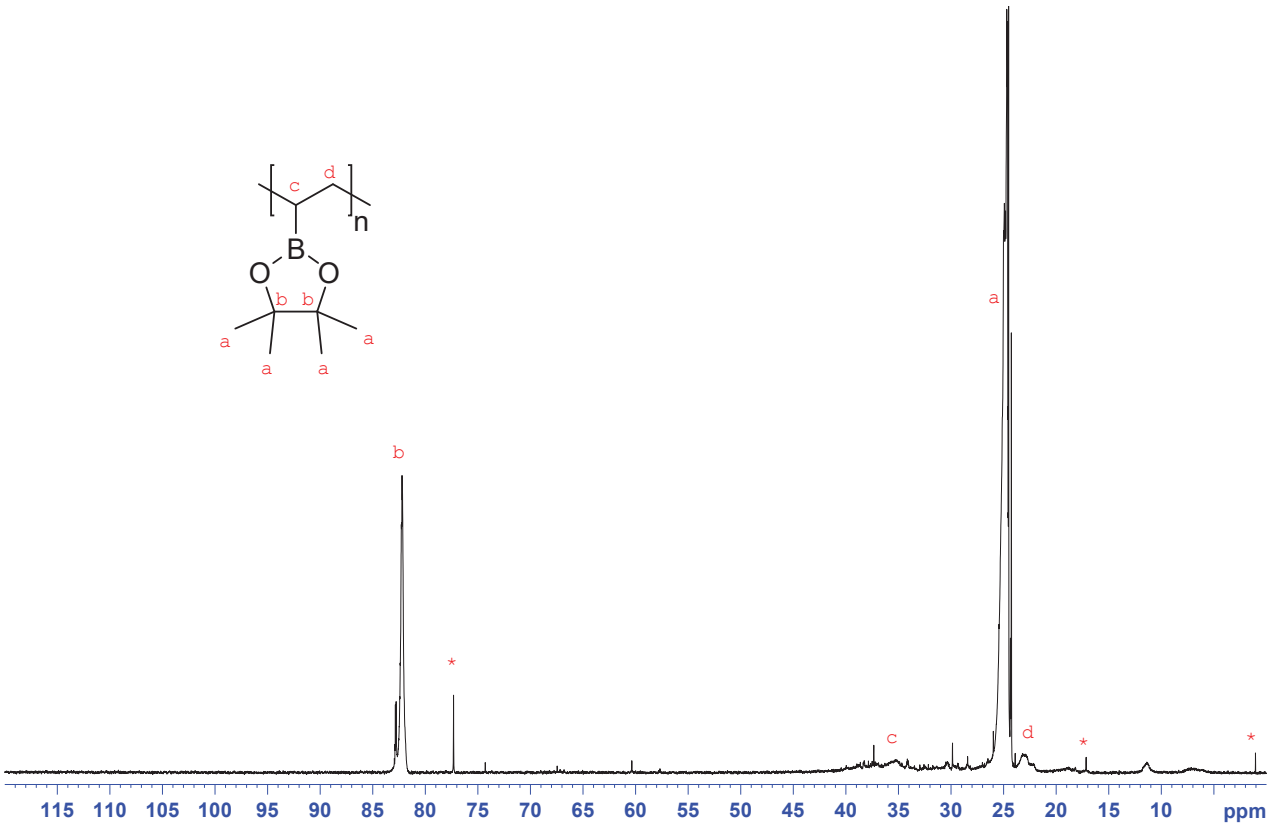

*Figure V. 108: ^{13}C NMR spectrum of poly(vinylboronic pinacolate)in C_6D_6. *C_6D_6 and residual solvents.*

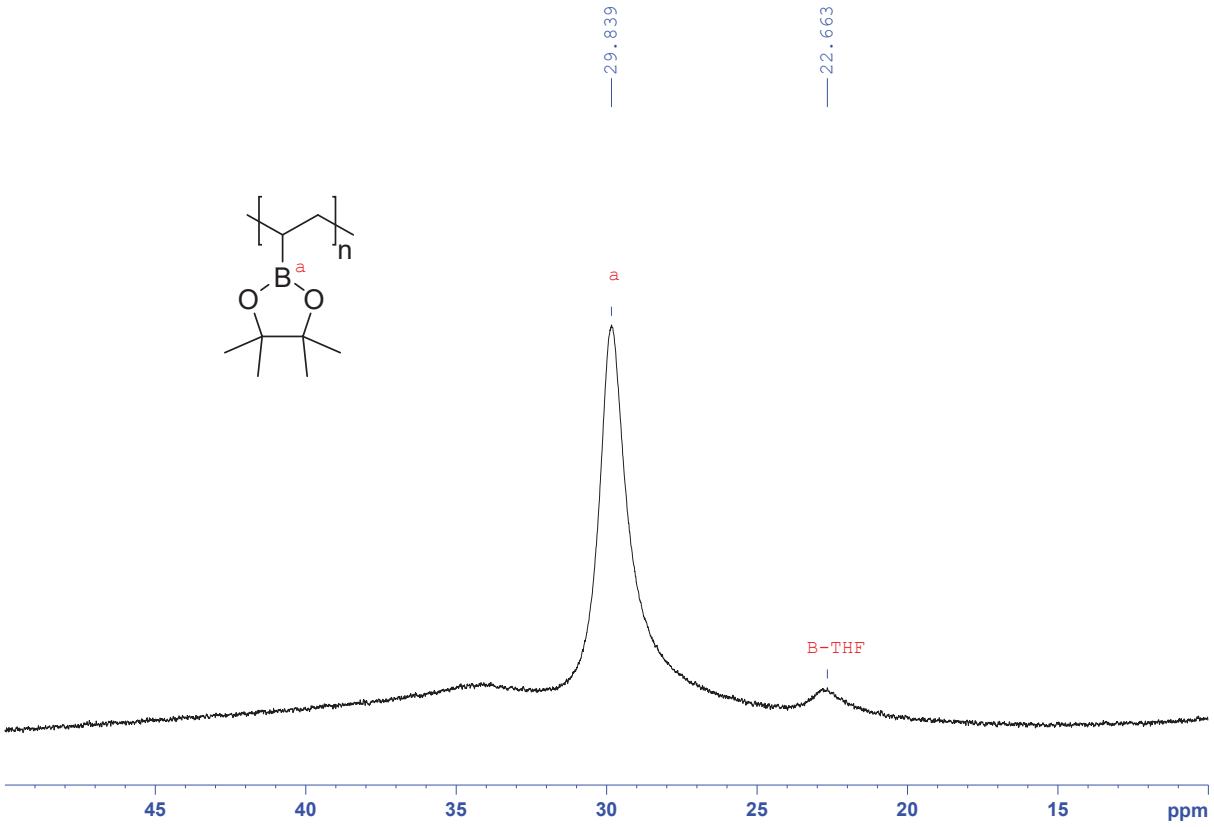

*Figure V. 109: ^{11}B NMR spectrum of poly(vinylboronic pinacolate) in C_6D_6. *C_6D_6 and residual solvents.*

Thermogravimetric analysis:

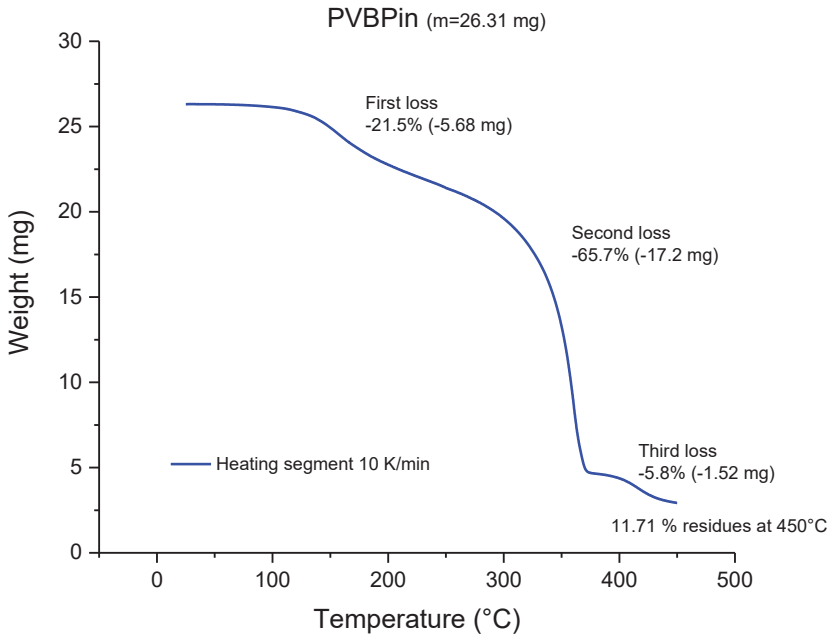

Figure V. 110: TGA thermal curve of poly(vinylboronic pinacolate) in 100 µL Alumina crucible.

Size-exclusion chromatography in THF:

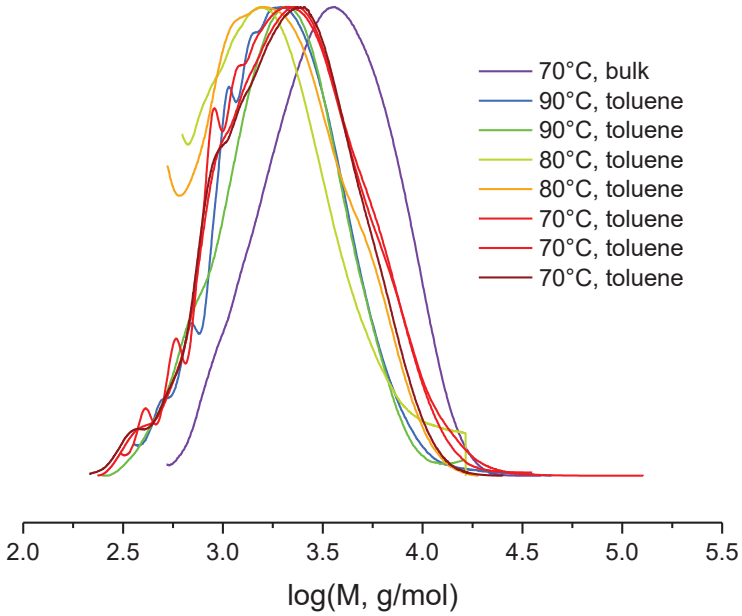

Figure V. 111 : Chromatograms of poly(vinylboronic pinacolate) synthesized using different paramaters.

D. Synthesis and characterization of copolymers from vinyl acetate and vinylboronic pinacolate

Experimental protocol:

The procedure used was the same than the one for the synthesis of the homopolymers. The monomer quantities were simply adapted depending on the ratio targeted. Yield: 71%.

^{1}H NMR (300 MHz, benzene-d_6, 25°C, δ): 5.6-5.0 (1H), 2.3-1.4 (8H), 1.3-0.8 (12H).

^{13}C NMR (400 MHz, benzene-d_6, 25°C, δ): 171.5, 83.3, 69.7, 37.2, 35.5, 32.5, 25.2, 21.

^{11}B NMR (300 MHz, benzene-d_6, 25°C, δ): 22.7.

NMR spectroscopies:

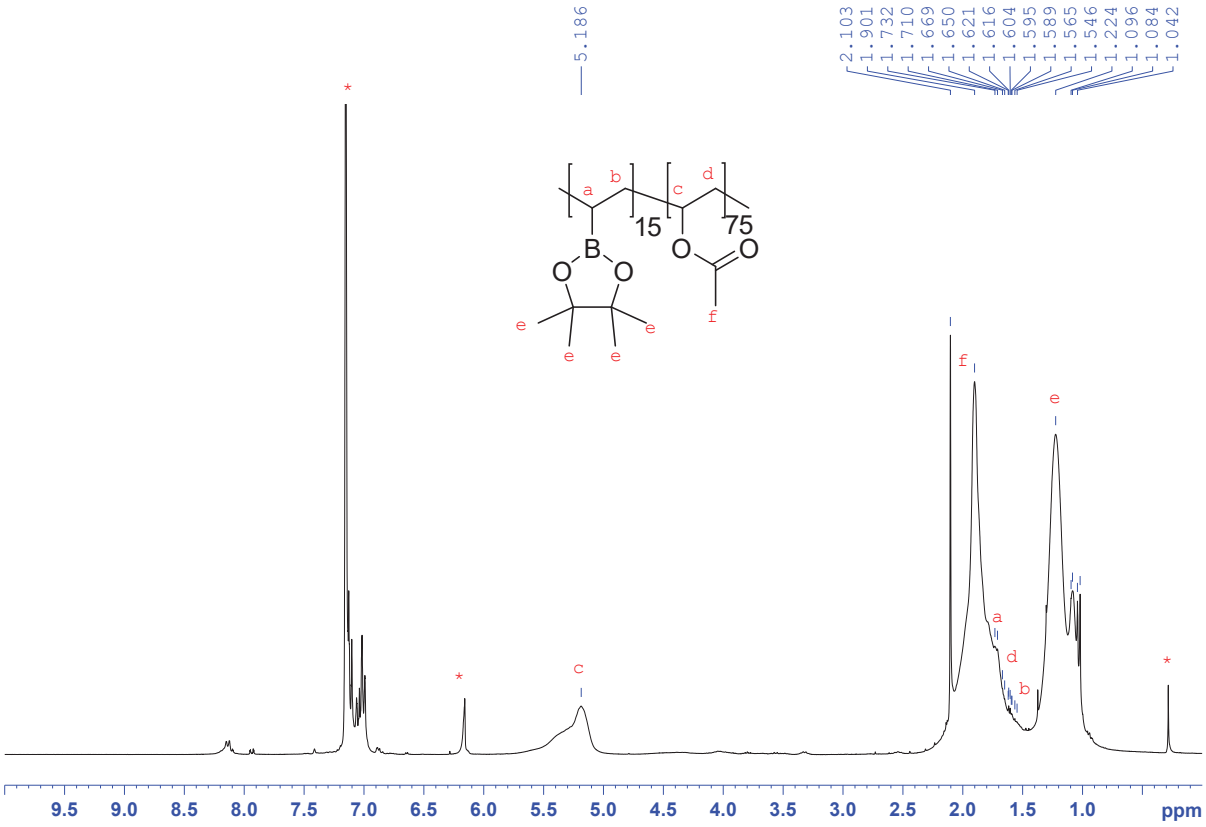

*Figure V. 112: ^{1}H NMR spectrum of poly(vinylboronic pinacolate-co-vinyl acetate) with 15 mol % of 4-vinylboronic pinacolate in the copolymer in C_6D_6. *C_6D_6 and residual solvents.*

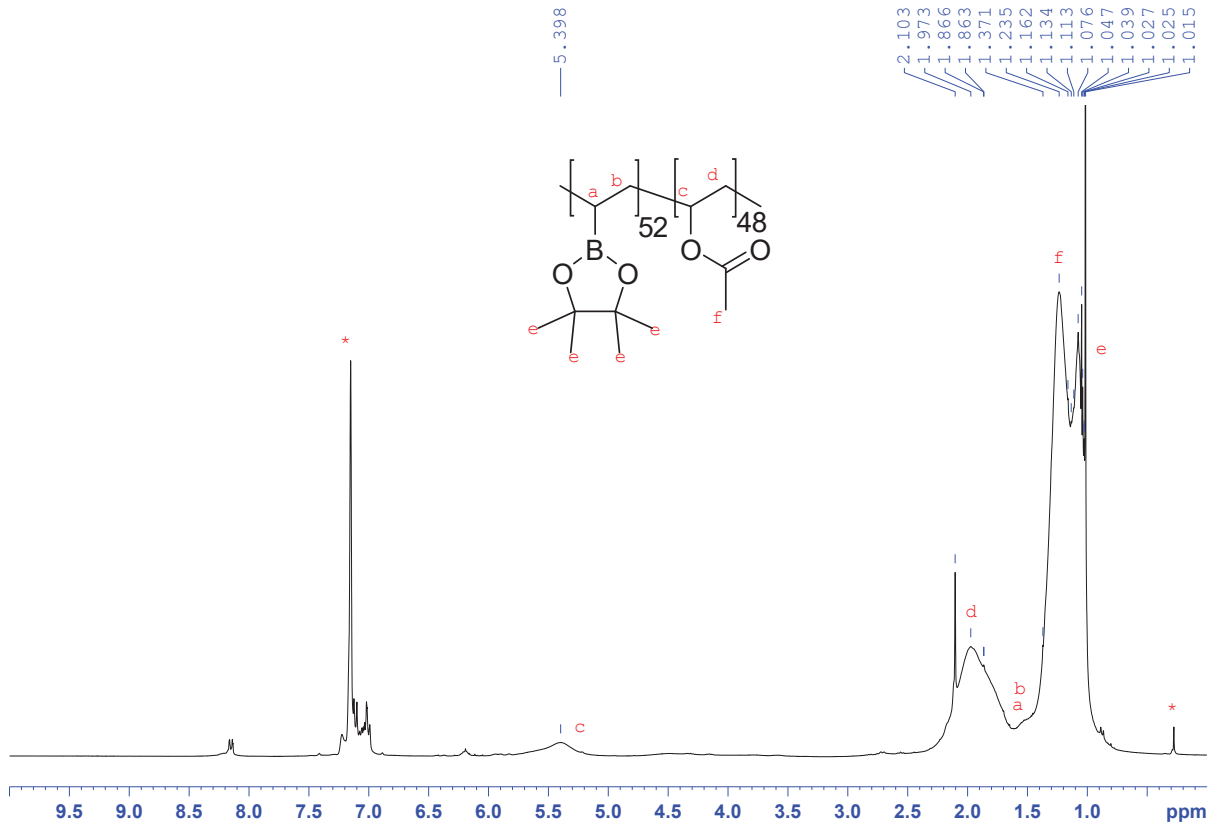

*Figure V. 113: ^{1}H NMR spectrum of poly(vinylboronic pinacolate-co-vinyl acetate) with 52 mol % of 4-vinylboronic pinacolate in the copolymer in C_6D_6. *C_6D_6 and residual solvents.*

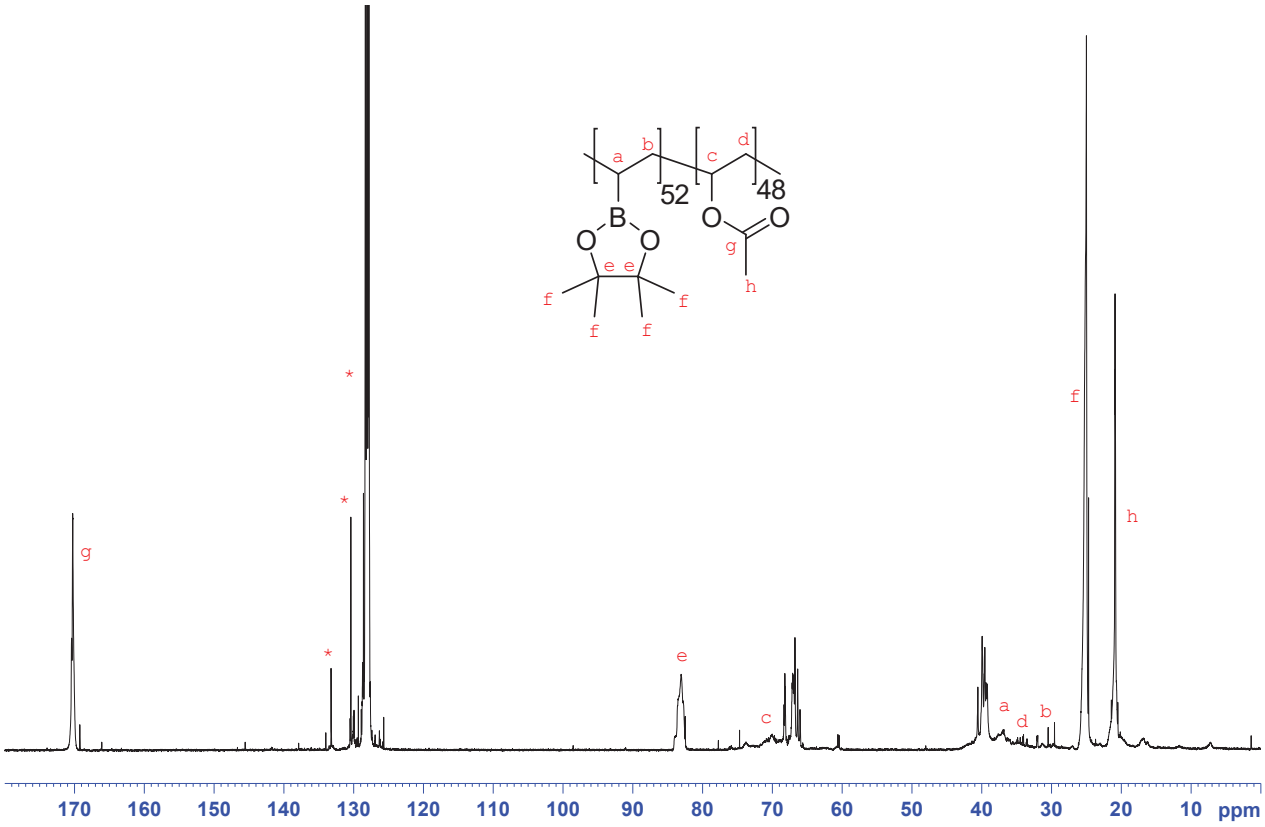

*Figure V. 114: ^{13}C NMR spectrum of poly(vinylboronic pinacolate-co-vinyl acetate) with 52 mol % of 4-vinylboronic pinacolate in the copolymer in C_6D_6. *C_6D_6 and residual solvents.*

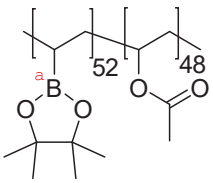

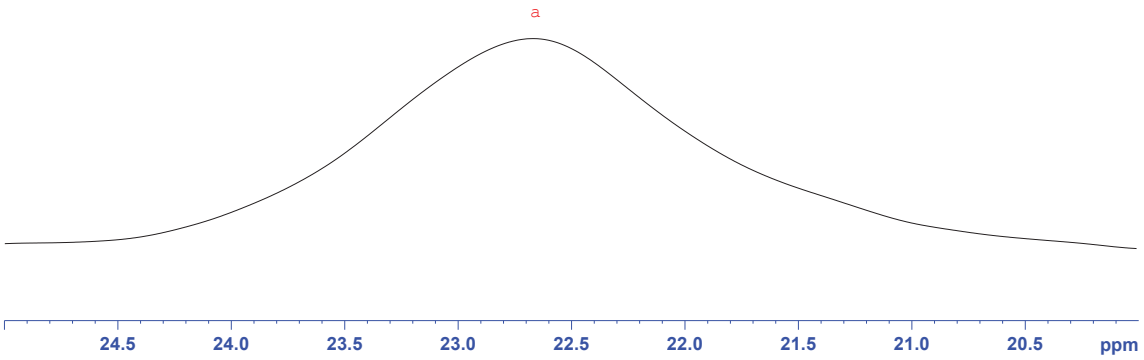

*Figure V. 115: ^{11}B NMR spectrum of poly(vinylboronic pinacolate-co-vinyl acetate) with 52 mol % of 4-vinylboronic pinacolate in the copolymer in C_6D_6. *C_6D_6 and residual solvents.*

Differential scanning calorimetry measurements:

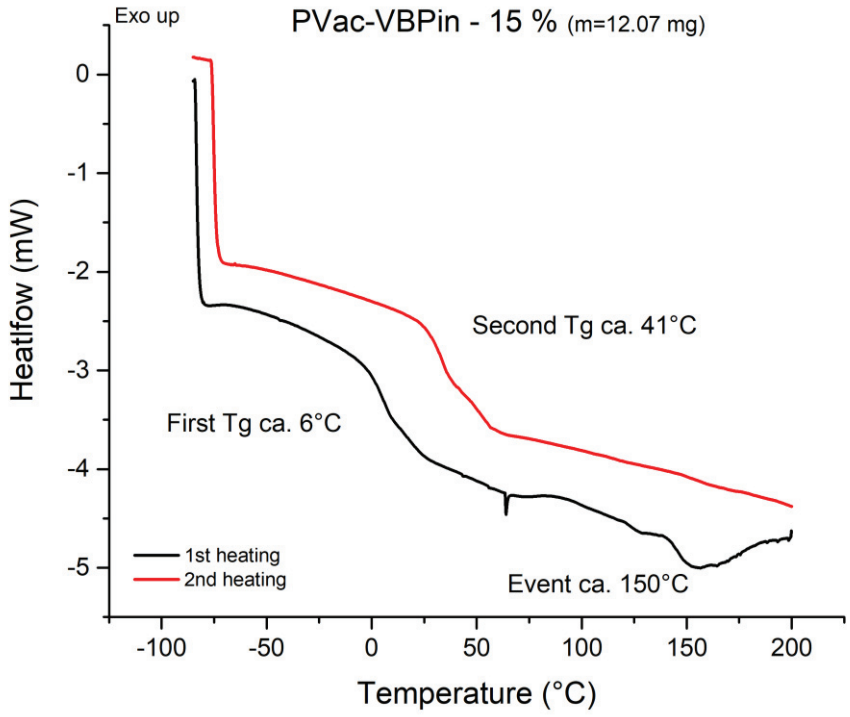

Figure V. 116: DSC thermograms of poly(4-vinylboronic pinacolate-co-vinyl acetate) containing 15 mol % of VBPin in 40 µL opened aluminum pans.

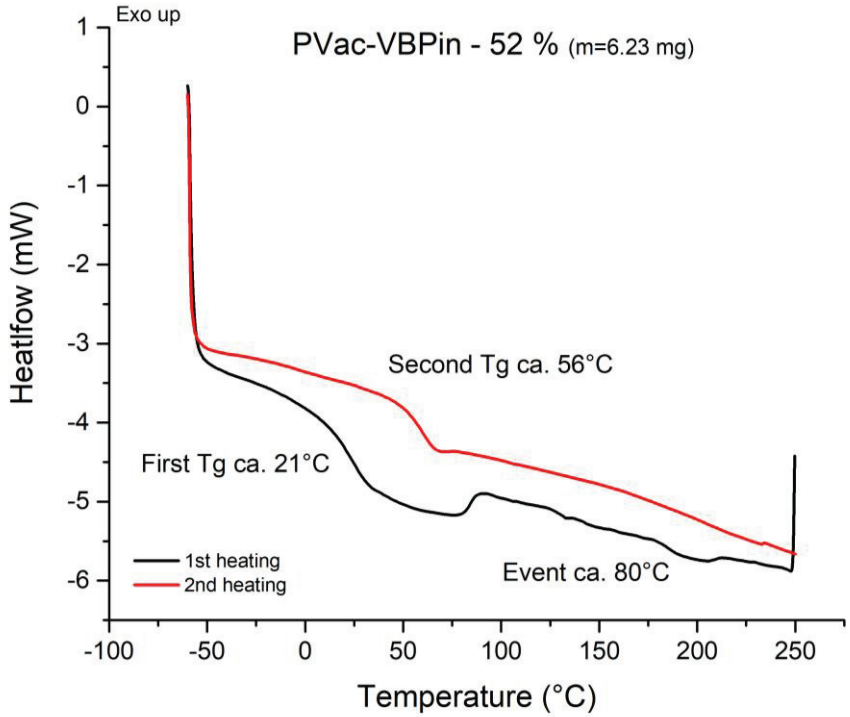

Figure V. 117: DSC thermograms of poly(4-vinylphenylboronic pinacolate-co-vinyl acetate) containing 52 mol % of VBPin in 40 µL opened aluminum pans.

Thermogravimetric analysis:

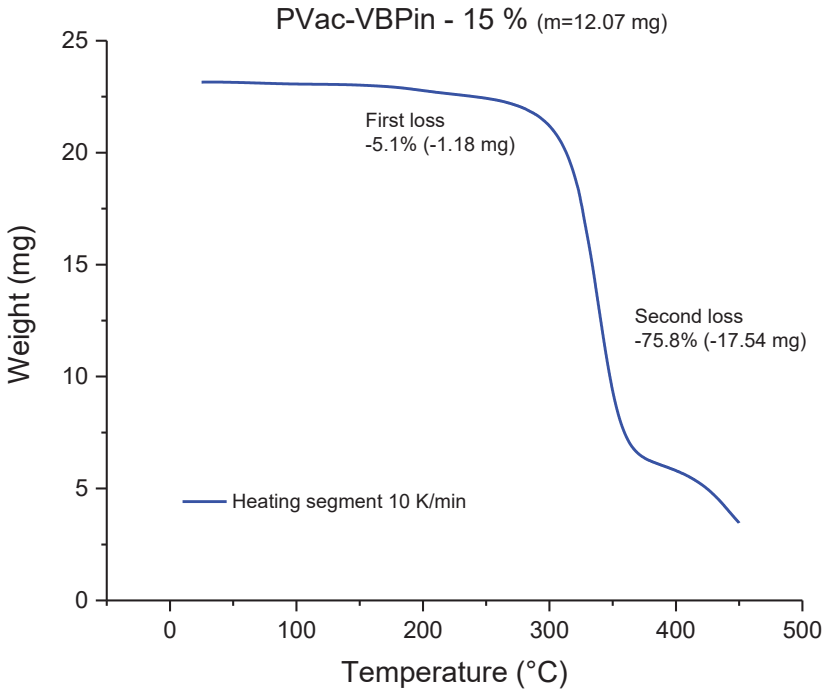

Figure V. 118: TGA thermal curve of poly(vinylboronic pinacolate-co-vinyl acetate) containing 15 mol % of VBPin in 100 µL alumina crucible.

Size-exclusion chromatography in THF :

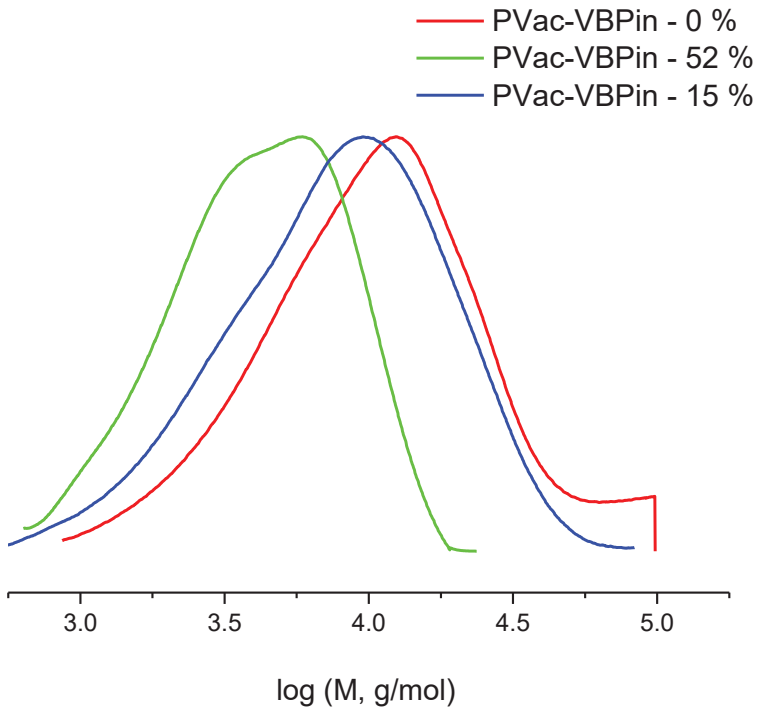

Figure V. 119: Chromatograms of copolymers from vinyl acetate and vinylboronic pinacolate at different ratios.

E. Synthesis and characterization of copolymers from vinylboronic pinacolate and ethylene

Experimental protocol:

Caution: polymerizations involve high pressure and explosives gas.

An intermediate 1.5 L tank filled with ethylene was used to charge the reactor. The tank was cooled down to -20°C to liquefy ethylene at 35 bars. Then, when thermodynamic equilibrium was reached, the intermediate tank was isolated and heated to reach up to 300 bars of ethylene pressure. In a Schlenk tube was introduced the desired quantity of benzoyl peroxide, vinylboronic pinacolate protected by one molar equivalent of THF and dimethyl carbonate as solvent in the case of polymerization in solution. Then the solution was introduced into the reactor through the injection sas. Afterward, ethylene was added until the desire pressure (200 bars). For polymerization in supercritical CO_2, the tank was once again cooled down to -20°C to liquefy CO_2 at 35 bars and, when thermodynamic equilibrium was reached, it was isolated and heating up to 300 bar to have CO_2 in supercritical state. The CO_2 is added after ethylene in the reactor autoclave. After 4 hours of polymerization under stirring (500 rpm) at 70°C, the reactor was slowly cooled down and degassed and the polymer was dried under vacuum in the case of solution polymerization.

^{1}H NMR (300 MHz, benzene-d_6, 25°C, δ): 1.49 (2H), 1.36 (2H), 1.35 (2H), 1.15 (1H), 1.11 (12H).

^{11}B NMR (300 MHz, benzene-d_6, 25°C, δ): 32.

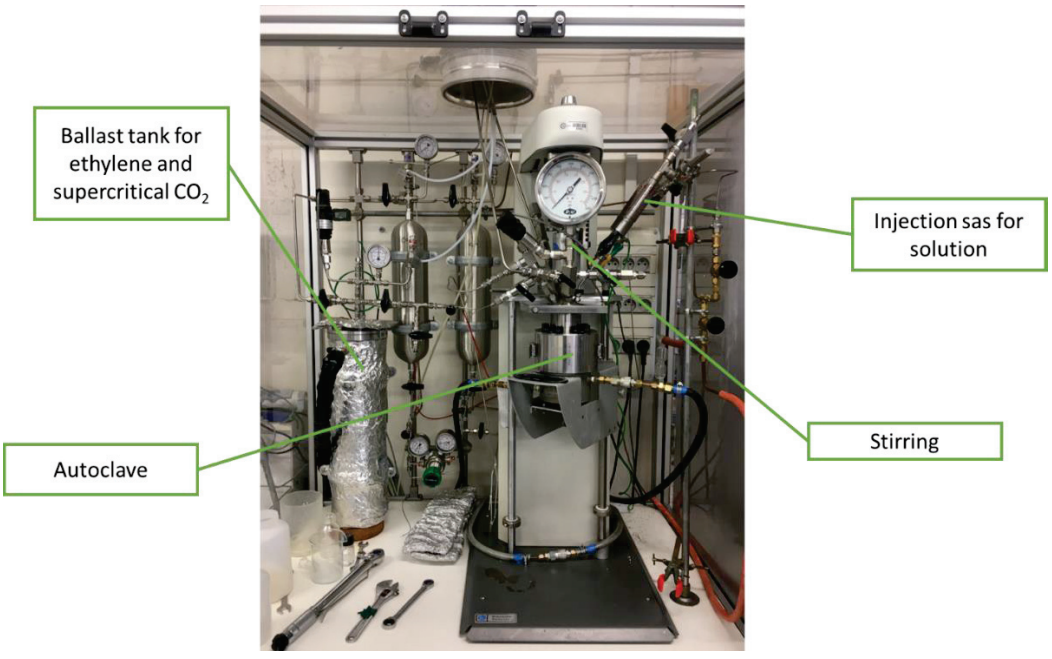

Figure V. 120: High-pressure reactor used for the copolymerization with ethylene.

NMR spectroscopies:

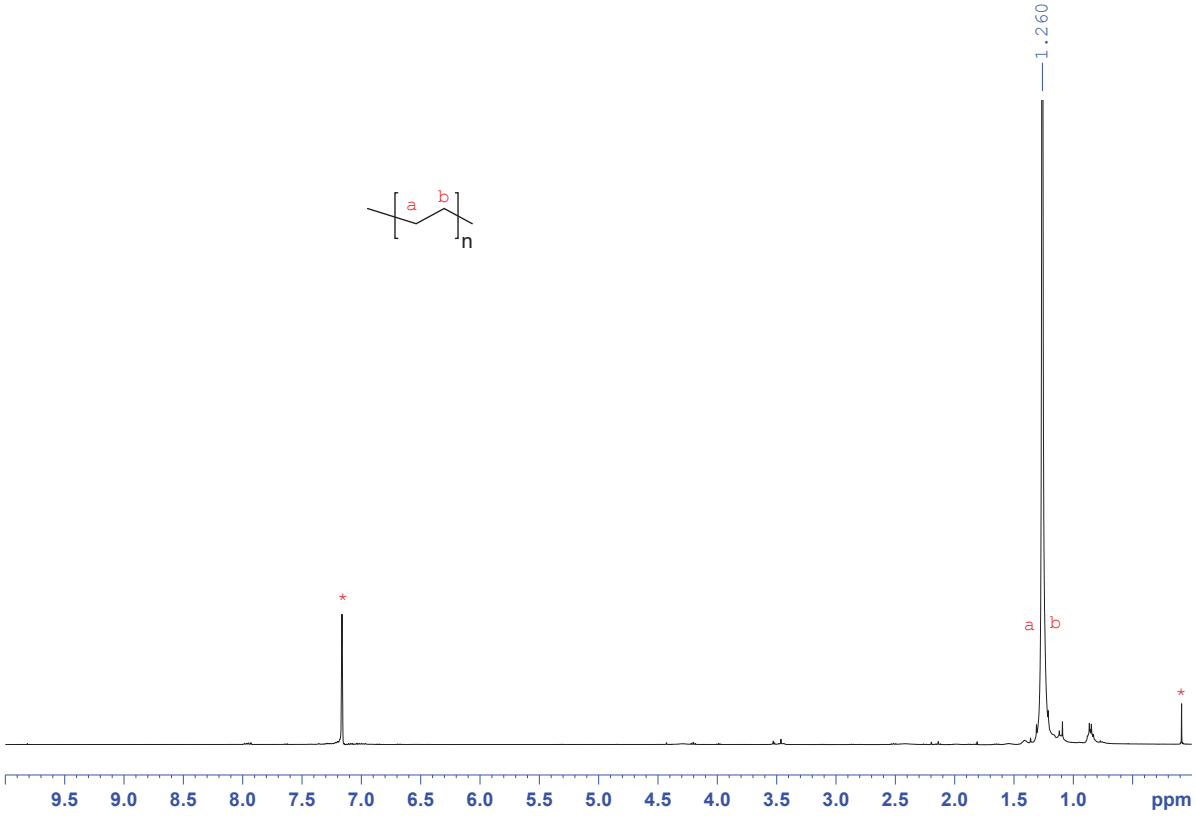

*Figure V. 121: ^{1}H NMR spectrum of poly(ethylene) in C_6D_6/TCE. *C_6D_6 and residual solvents.*

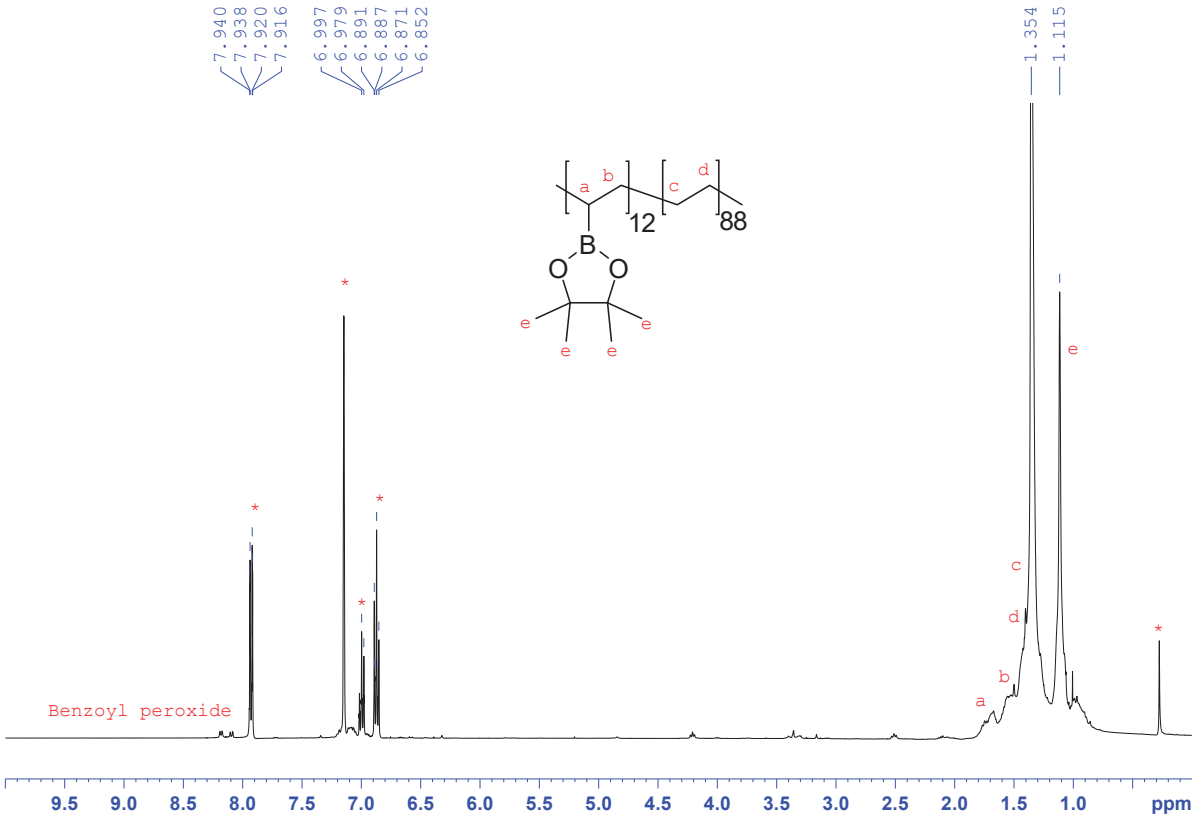

*Figure V. 122: ^{1}H NMR spectrum of poly(ethylene-co-vinylboronic pinacolate) synthesized in dimethyl carbonate in C_6D_6/TCE. *C_6D_6 and residual solvents.*

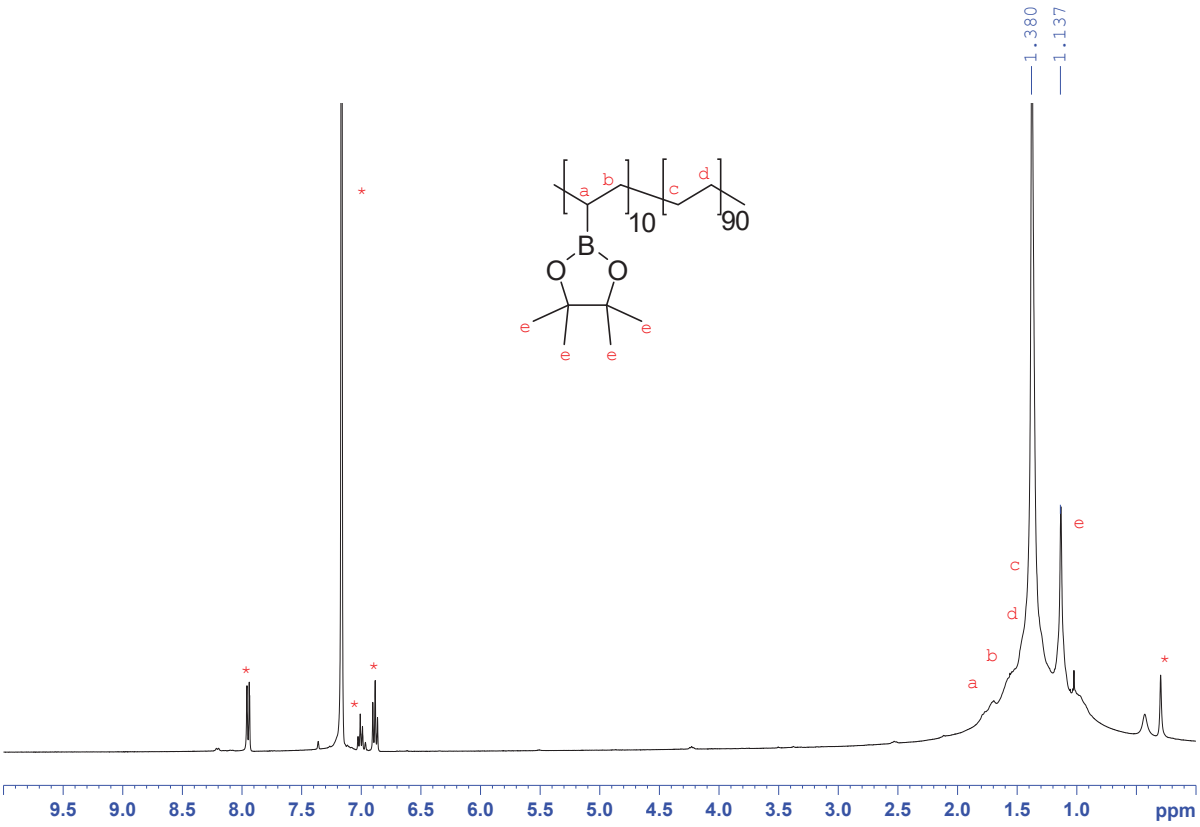

*Figure V. 123: ^{1}H NMR spectrum of poly(ethylene-co-vinylboronic pinacolate) synthesized in supercritical CO_2 in C_6D_6/TCE. *C_6D_6 and residual solvents.*

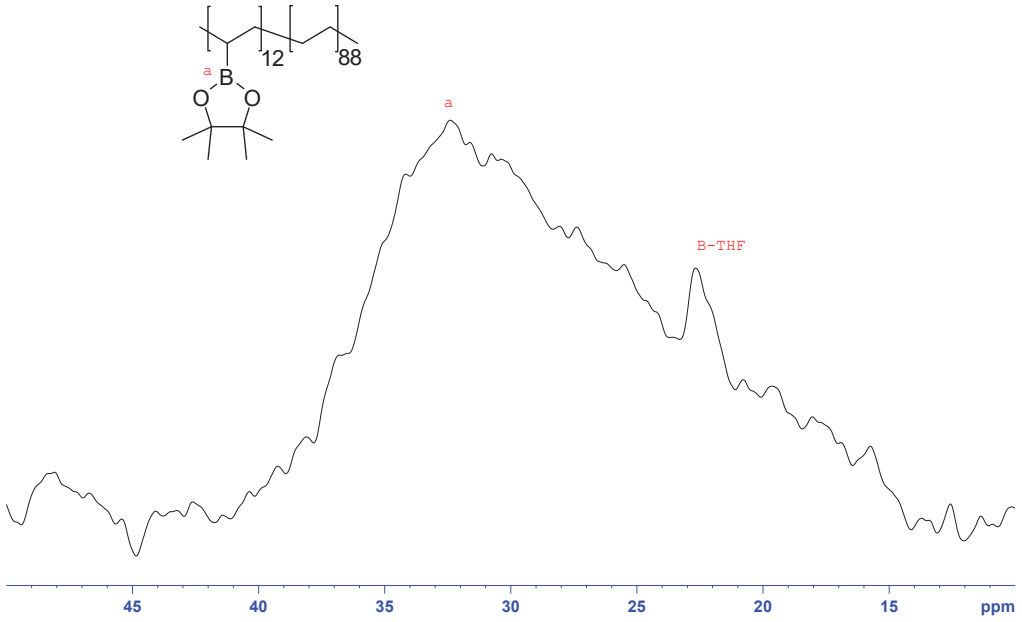

Figure V. 124: ^{11}B NMR spectrum of poly(ethylene-co-vinylboronic pinacolate) synthesized in dimethyl carbonate in C_6D_6/TCE.

F. Functionalization of polybutadiene

a. Data on the native polybutadiene

Before any trial of functionalization of polybutadiene, the commercial polybutadiene from Sigma Aldrich was analyzed from several methods of characterization to anticipate its behavior. The polymer is sold as a high molecular weight polybutadiene with $M_w \approx 200\,000$ g/mol.

NMR spectroscopies:

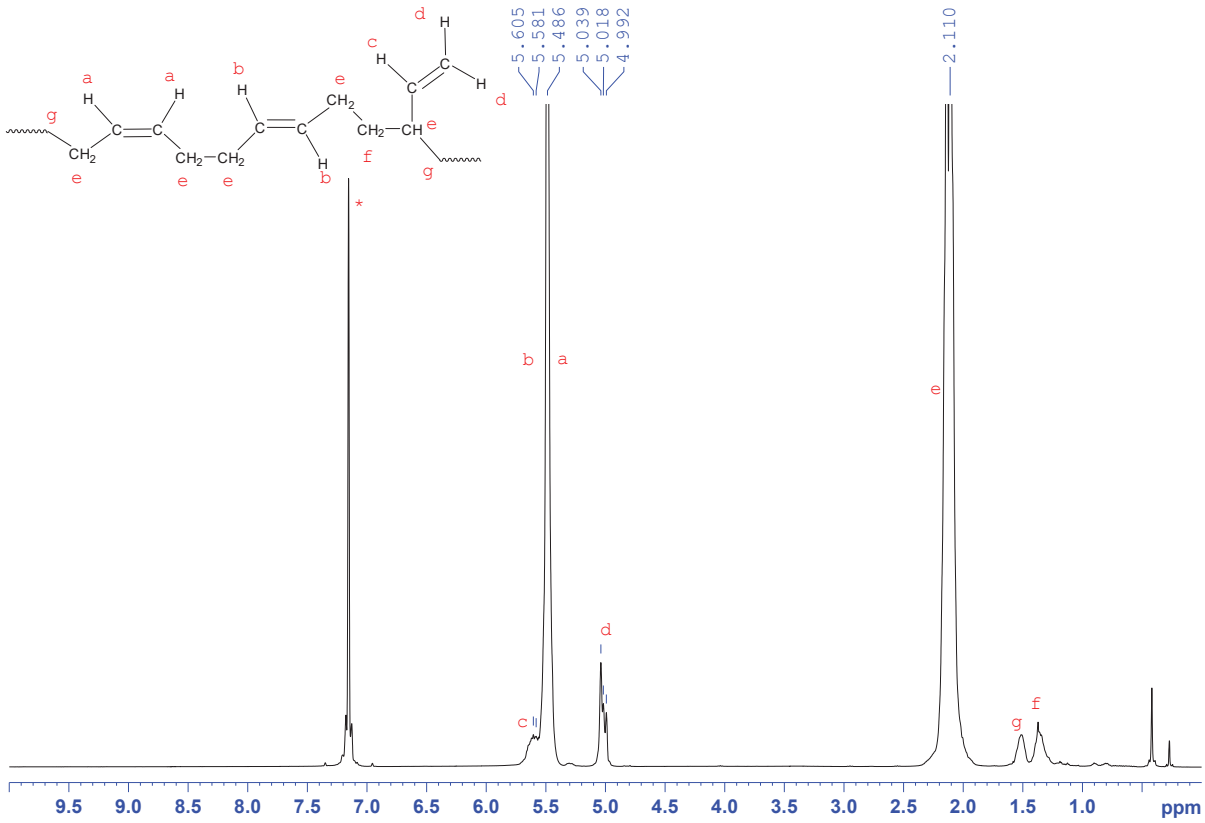

*Figure V. 125: ^{1}H NMR spectrum of commercial polybutadiene in C_6D_6. *C_6D_6 and residual solvents.*

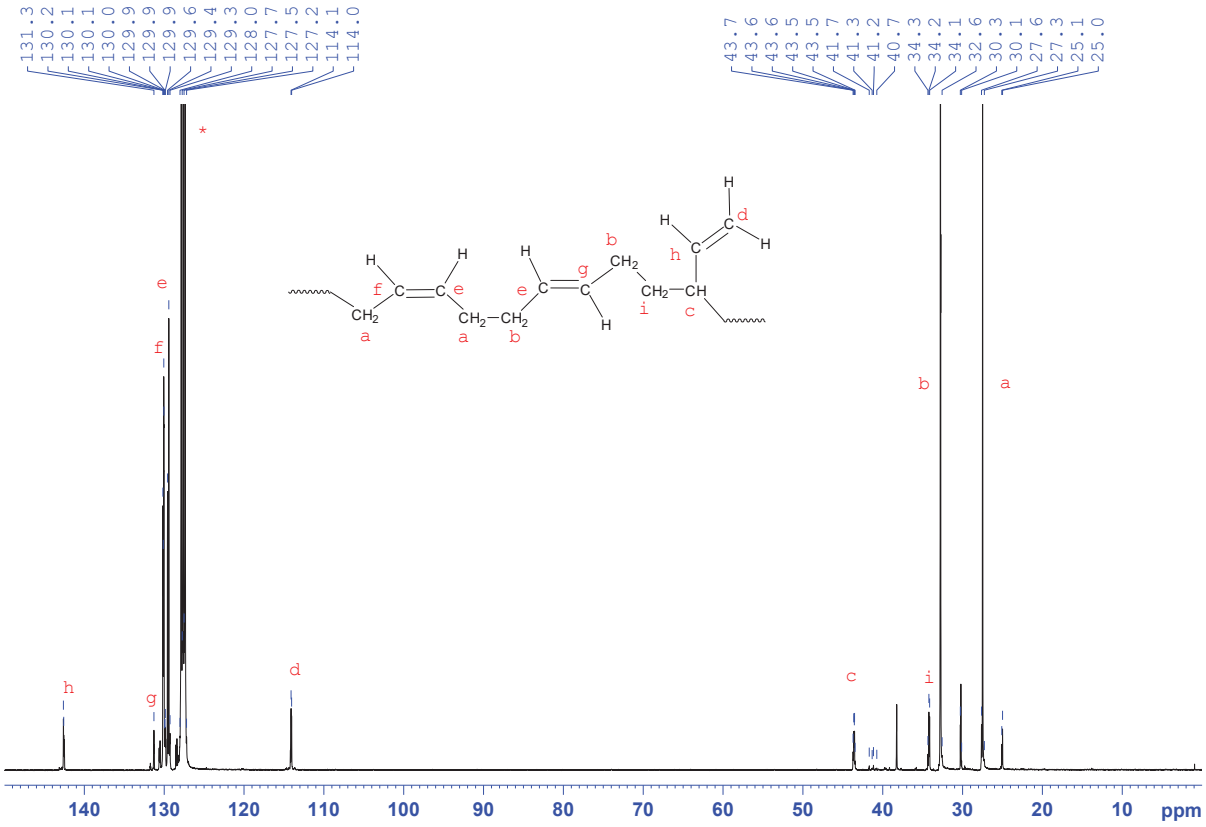

*Figure V. 126: ^{13}C NMR spectrum of commercial polybutadiene in C_6D_6. *C_6D_6 and residual solvents*

Differential scanning calorimetry measurements:

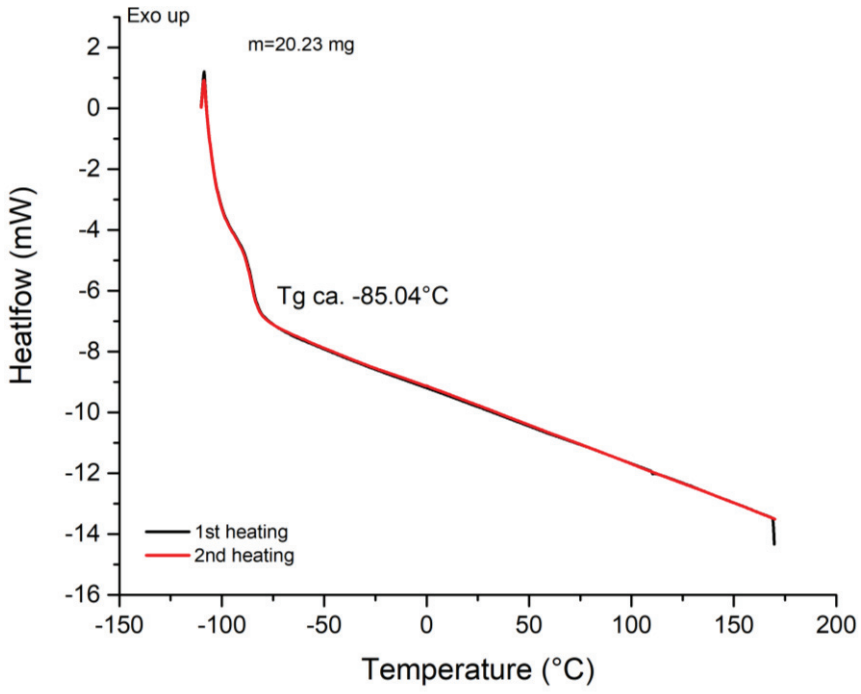

Figure V. 127: DSC thermograms of the commercial polybutadiene in 40 µL opened aluminum pans.

Rheology experiments:

As we got interested in the mechanical behavior of the modified polybutadiene, we first monitored the response of native polybutadiene to temperature using an 8 mm plan-plan geometry equipped with a Pelletier cell.

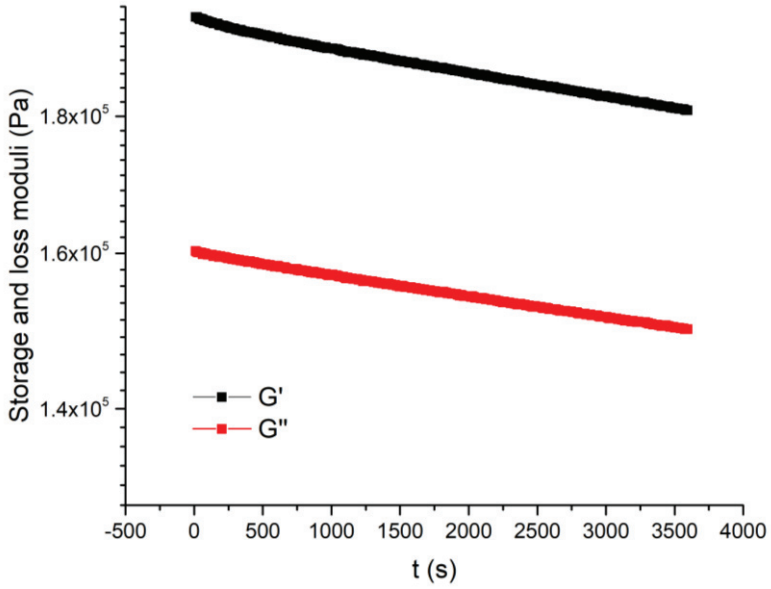

Figure V. 128: Monitoring of the storage and loss moduli during oscillation time at 110°C for the native polybutadiene.

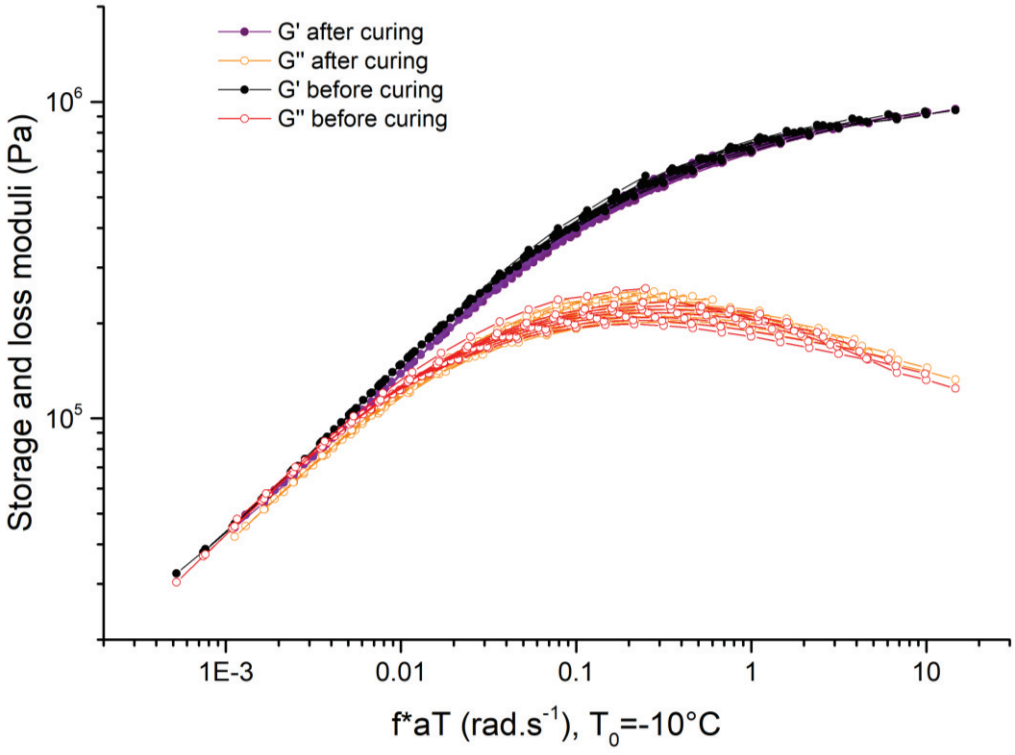

Figure V. 129: Comparison of the time-temperature superposition of the frequency sweeps before and after curing at 110°C on native polybutadiene, referenced at -10°C.

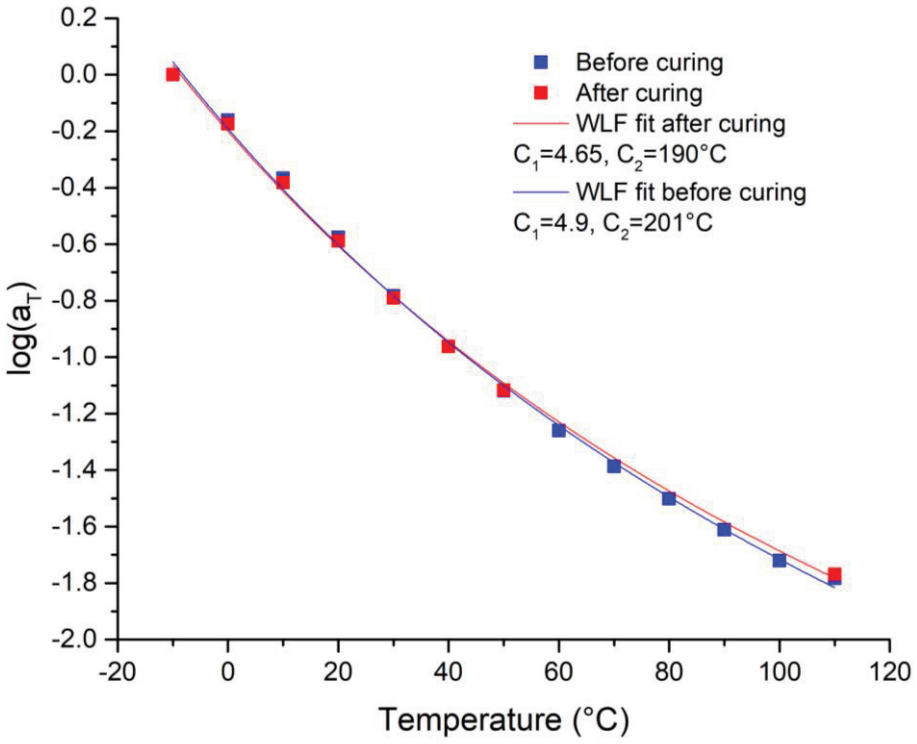

Figure V. 130: Comparison of WLF profiles before and after curing at 110°C of the native polybutadiene.

b. Functionalization of polybutadiene *via* copper catalysis

Experimental procedure:

The objective was to functionalize 30 % mol of double bonds of the polybutadiene.

1 g (5.54 mmol of double bonds to be functionalized) of polybutadiene is dried during several hours by solvent evaporation cycles and is dissolved in a first schlenk tube in 10 mL of dried toluene. In a second schlenk tube, t-BuOK (31.1 mg, 0.28 mmol, 5 mol %) is dried under vacuum at 80°C during 5 hours. Then, CuCl(I) (13.7 mg, 0.14 mmol, 2.5 mol %) and 1,2-bis(dicyclohexylphosphino)ethane (117.06 mg, 0.28 mol, 5 mol %) are added to this second schlenk *via* the glovebox and 5 mL of dried toluene was added to this catalyst solution. The solution is mixed for 3 minutes. Then HBPin (1.92 mL, 13.2 mmol, 2.2 mol equivalent) was added to the catalyst solution. The mix was stirred for another 1 minute and is added to the polybutadiene solution by cannula. The reaction is performed during several hours at ambient temperature.

NMR spectroscopies:

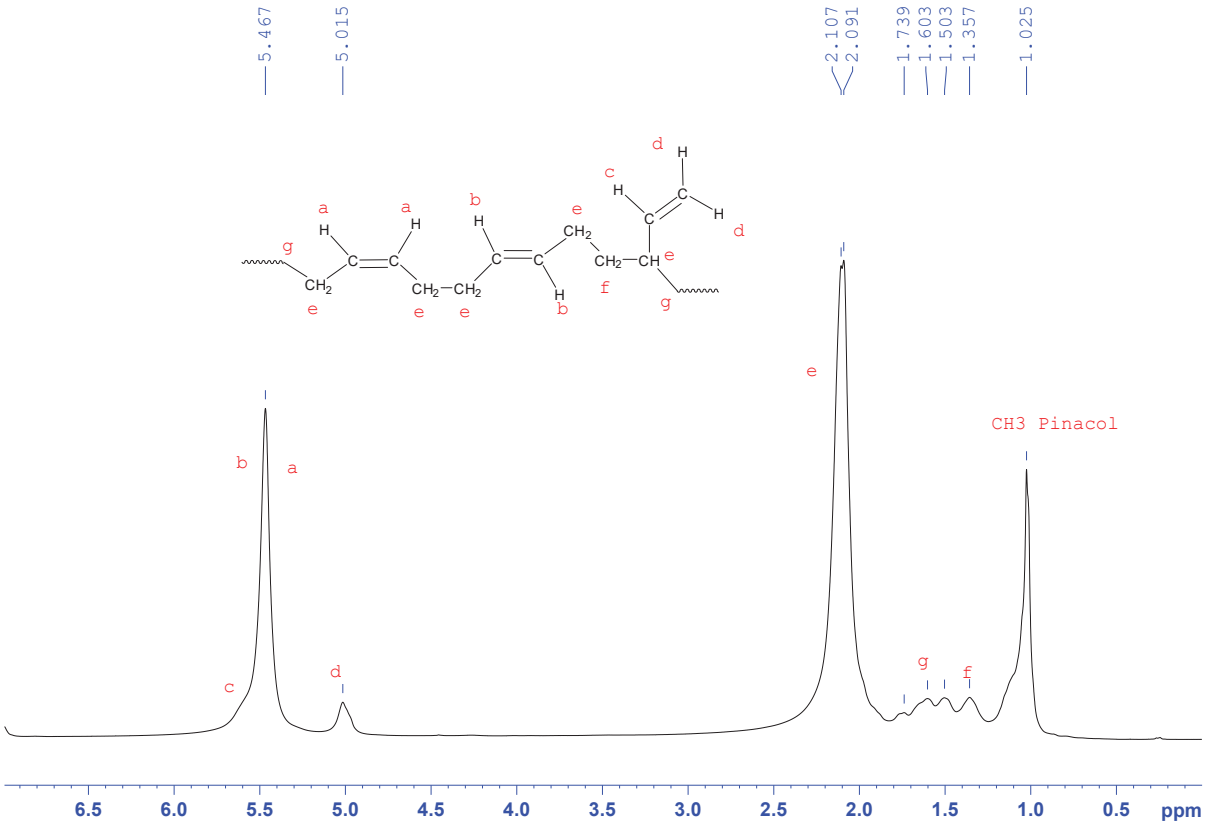

*Figure V. 131: ^{1}H NMR spectrum of modified polybutadiene by copper catalysis in C_6D_6. *C_6D_6 and residual solvents*

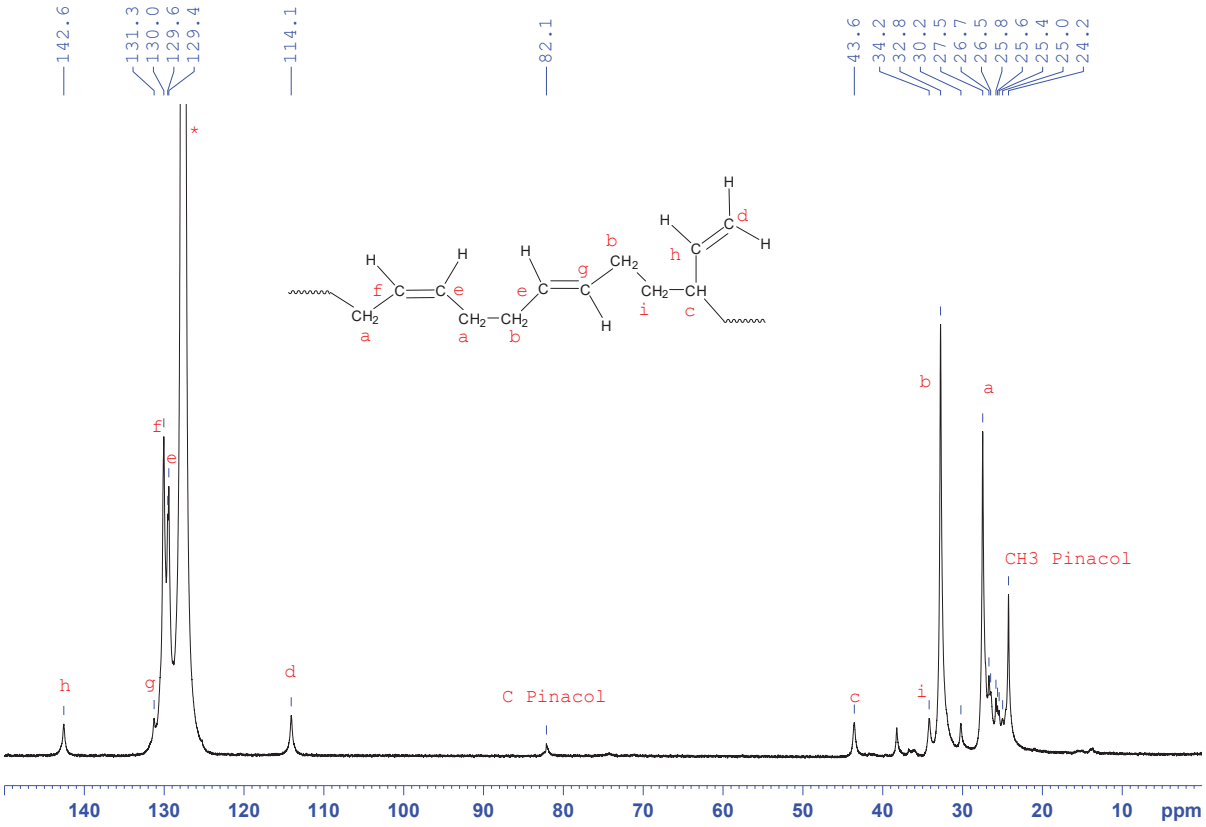

*Figure V. 132: ^{13}C NMR spectrum of modified polybutadiene by copper catalysis in C_6D_6. *C_6D_6 and residual solvents*

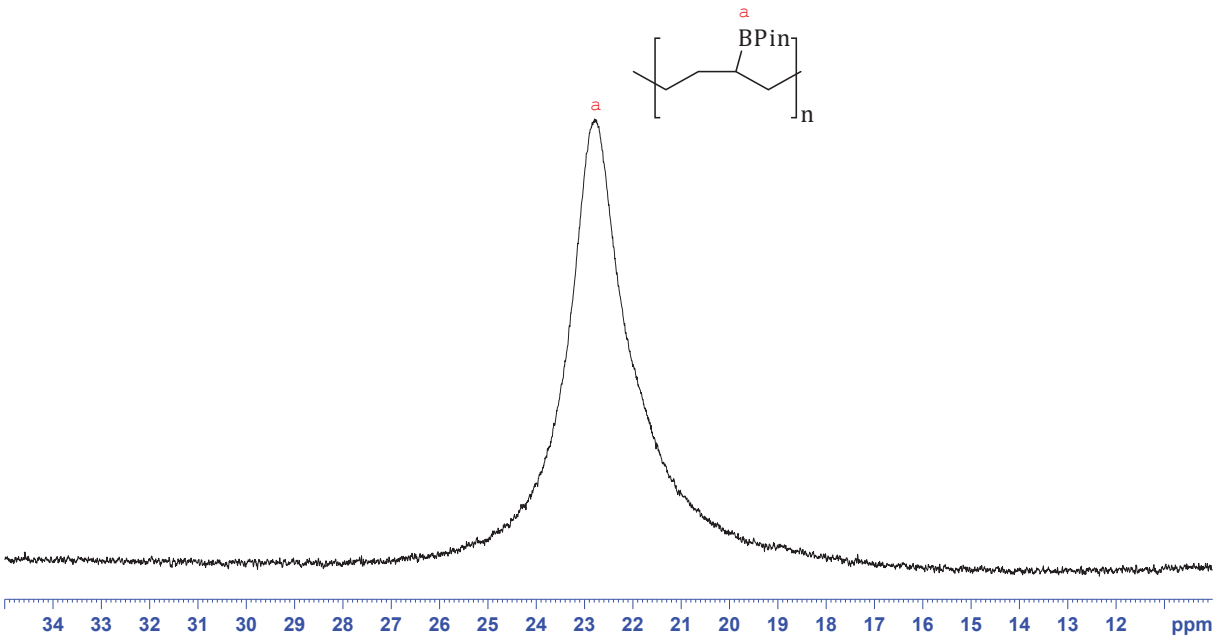

*Figure V. 133: ^{11}B NMR spectrum of modified polybutadiene by copper catalysis in C_6D_6. *C_6D_6 and residual solvents*

Thermogravimetric analysis:

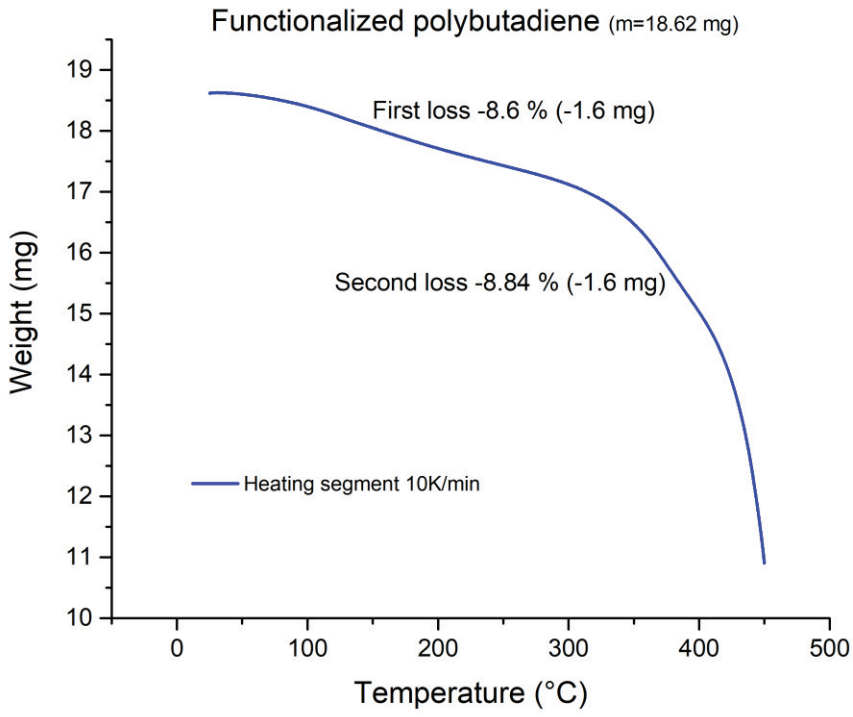

Figure V. 134: TGA thermal curve of the modified polybutadiene by copper catalysis in 100 µL alumina crucible.

c. Functionalization of polybutadiene *via* iron catalysis

Experimental procedure:

The objective was to functionalize 30 % mol of double bonds of the polybutadiene.

1 g (5.54 mmol of double bonds to be functionalized) of polybutadiene is dried during several hours by solvent evaporation cycles and is dissolved in a first schlenk tube in 30 mL of dried THF. In a second schlenk, the catalyst solution is prepared by reaction between iPrBIP Iron catalyst (84.1 mg, 2.5 % mol) in 3 mL of THF and MeMgBr (0.14 mL, 3.0 M in Et_2O, 3.0 molar equivalents compared to iron catalyst). The solution is going from blue to purple after the addition of the Grignard solution. 0.1 mL of HBPin is adding in the catalyst solution while 0.86 mL is added to the polymer solution (total of 0.96 mL, 6.65 mmol, 1.2 molar equivalents). The catalyst solution is tcosferred in the first schlenk *via* cannula technique and the reaction is continued for 24 h at ambient temperature.

NMR spectroscopies:

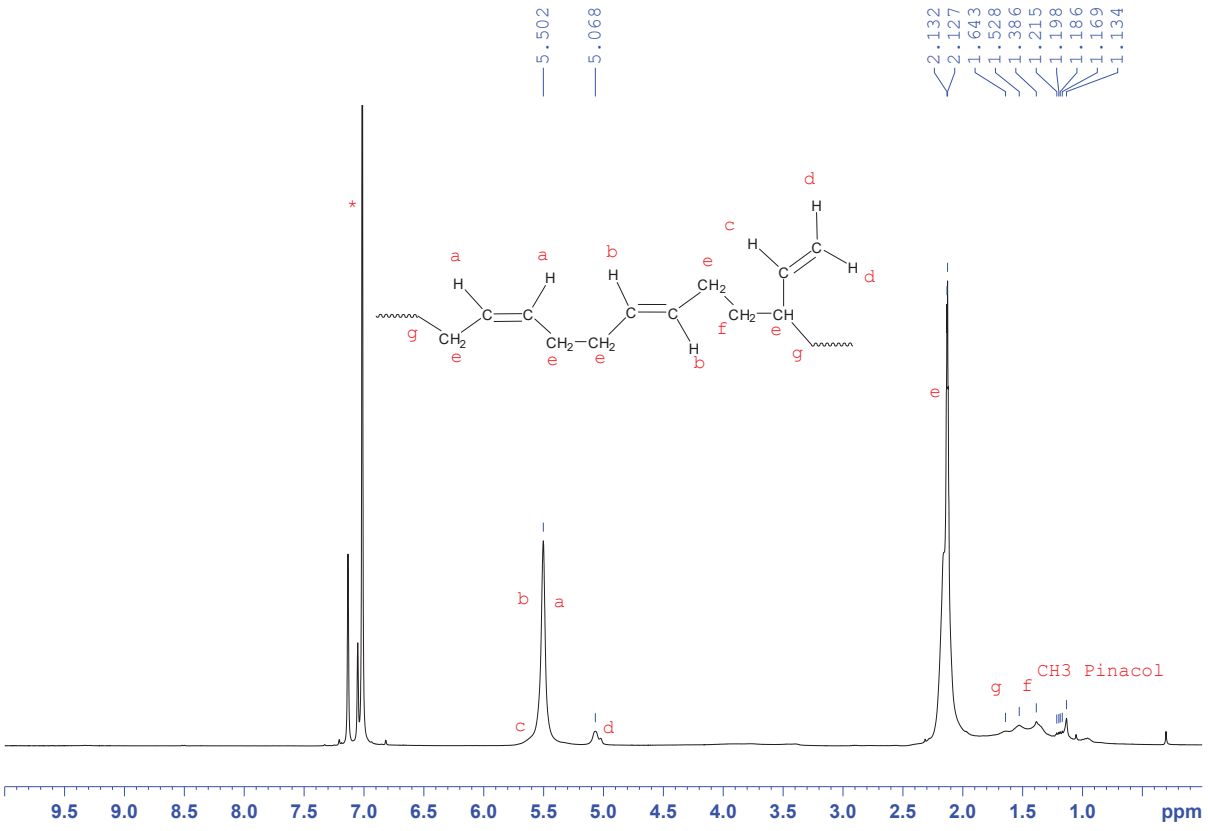

*Figure V. 135: ^1H NMR spectrum of modified polybutadiene by iron catalysis in C_6D_6. *C_6D_6 and residual solvents*

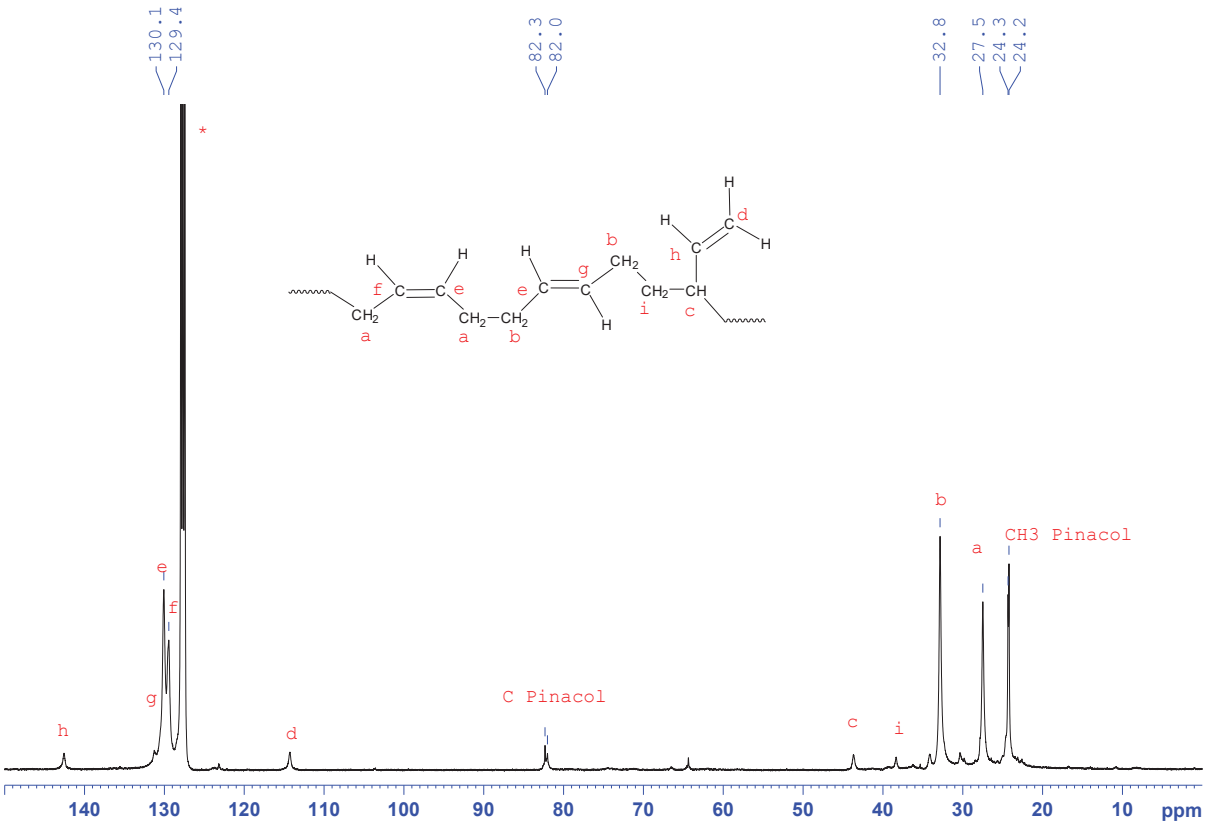

*Figure V. 136: ^{13}C NMR spectrum of modified polybutadiene by iron catalysis in C_6D_6. *C_6D_6 and residual solvents*

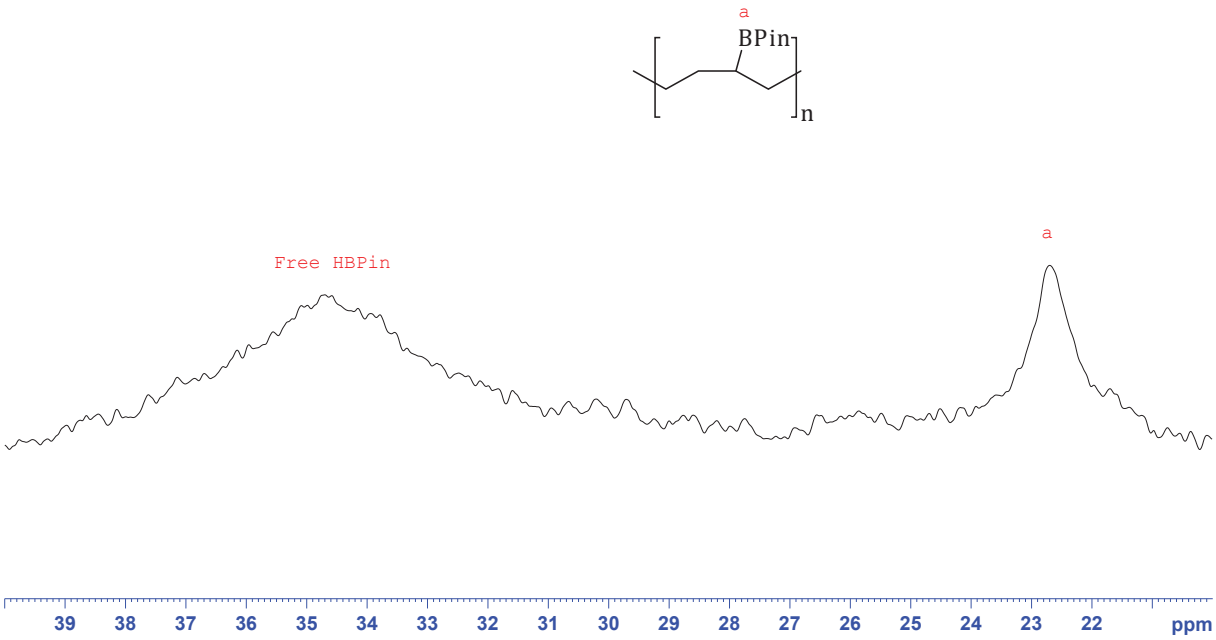

*Figure V. 137: ^{11}B NMR spectrum of modified polybutadiene by iron catalysis in C_6D_6. *C_6D_6 and residual solvents*

Thermogravimetric analysis:

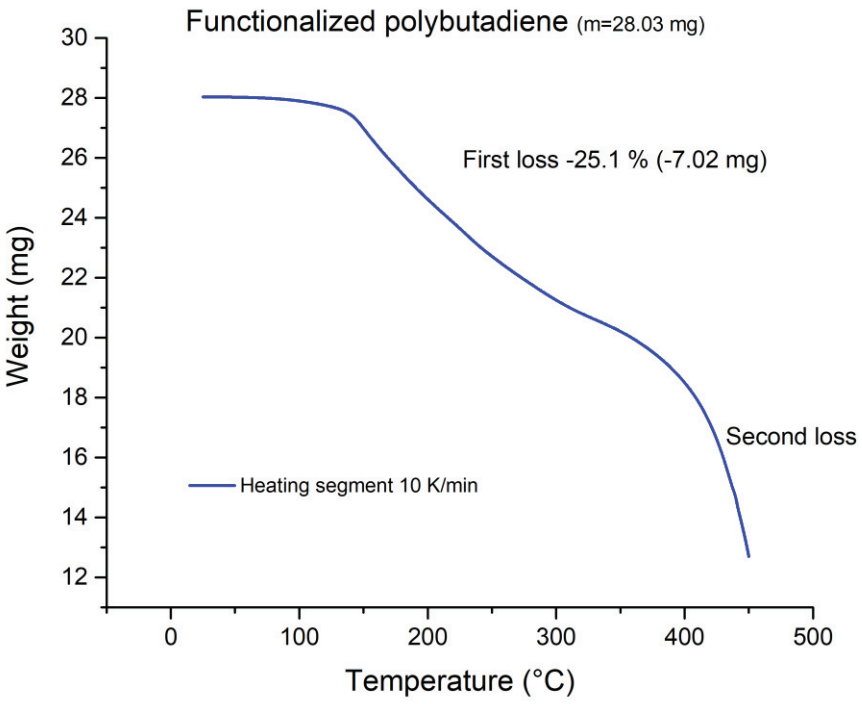

Figure V. 138: TGA thermal curve of modified polybutadiene by iron catalysis in 100 µL alumina crucible.

V. References

[1] D. Wu, A. Chen, and C. Johnson, "An improved diffusion-ordered spectroscopy experiment incorporating bipolar-gradient pulses," *J. Magn. Reson.*, vol. 115, pp. 260–264, **1995**.

[2] Y. Zhao and D. G. Truhlar, "The M06 suite of density functionals for main group thermochemistry, thermochemical kinetics, noncovalent interactions, excited states , and tcosition elements: two new functionals and systematic testing of four M06-class functionals and 12 other functions," *Theor. Chem. Acc.*, vol. 120, pp. 215–241, **2008**.

[3] F. Weigend and R. Ahlrichs, "Balanced basis sets of split valence, triple zeta valence and quadruple zeta valence quality for H to Rn: Design and assessment of accuracy," *Phys. Chem. Chem. Phys.*, vol. 7, pp. 3297–3305, **2005**.

[4] A. V Marenich, C. J. Cramer, and D. G. Truhlar, "Universal Solvation Model Based on the Generalized Born Approximation with Asymmetric Descreening," *J. Chem. Theory Comput.*, vol. 5, pp. 2447–2464, **2009**.

[5] M. J. Frisch *et al.*, "Gaussian 09." Gaussian, Inc., Wallingford CT, **2016**.

[6] A. J. J. Lennox and G. C. Lloyd-Jones, "Preparation of Organotrifluoroborate Salts : Precipitation-Driven Equilibrium under Non-Etching Conditions," *Angew. Chemie Int. Ed.*, vol. 51, pp. 9385–9388, **2012**.

[7] Z. Gan, A. Okui, Y. Kawashita, and M. Hayashi, "Convenient Synthesis of Linear-extended Bipyridines Involving a Central Phenyl Linking Group," *Chem. Lett.*, vol. 37, no. 12, pp. 1302–1303, **2008**.

[8] M. Kwok Wai Choi, H. He Song, and P. H. Toy, "Direct Radical Polymerization of 4-Styryldiphenylphosphine: Preparation of Polystyrene Polymers," *J. Org. Chem.*, vol. 68, no. 17, pp. 9831–9834, **2003**.